ISSN 0021-9673

VOL. 683 NO. 1 OCTOBER 14, 1994

3rd Int. Symp. on Hyphenated Techniques in Chromatography Antwerp, February 22–25, 1994

JOURNAL OF CHROMATOGRAPHY A

INCLUDING ELECTROPHORESIS AND OTHER SEPARATION METHODS

SYMPOSIUM VOLUMES

ELSEVIER

JOURNAL OF CHROMATOGRAPHY A

INCLUDING ELECTROPHORESIS AND OTHER SEPARATION METHODS

Scope. The *Journal of Chromatography A* publishes papers on all aspects of **chromatography, electrophoresis** and related methods. Contributions consist mainly of research papers dealing with chromatographic theory, instrumental developments and their applications. In the *Symposium volumes*, which are under separate editorship, proceedings of symposia on chromatography, electrophoresis and related methods are published. *Journal of Chromatography B: Biomedical Applications* —This journal, which is under separate editorship, deals with the following aspects: developments in and applications of chromatographic and electrophoretic techniques related to clinical diagnosis or alterations during medical treatment; screening and profiling of body fluids or tissues related to the analysis of active substances and to metabolic disorders; drug level monitoring and pharmacokinetic studies; clinical toxicology; forensic medicine; veterinary medicine; occupational medicine; results from basic medical research with direct consequences in clinical practice.

Submission of Papers. The preferred medium of submission is on disk with accompanying manuscript (see *Electronic manuscripts* in the Instructions to Authors, which can be obtained from the publisher, Elsevier Science B.V., P.O. Box 330, 1000 AH Amsterdam, Netherlands). Manuscripts (in English; *four* copies are required) should be submitted to: Editorial Office of *Journal of Chromatography A*, P.O. Box 681, 1000 AR Amsterdam, Netherlands, Telefax (+31-20) 5862 304, or to: The Editor of *Journal of Chromatography B: Biomedical Applications*, P.O. Box 681, 1000 AR Amsterdam, Netherlands. Review articles are invited or proposed in writing to the Editors who welcome suggestions for subjects. An outline of the proposed review should first be forwarded to the Editors for preliminary discussion prior to preparation. Submission of an article is understood to imply that the article is original and unpublished and is not being considered for publication elsewhere. For copyright regulations, see below.

Publication information. *Journal of Chromatography A* (ISSN 0021-9673): for 1995 Vols. 683–714 are scheduled for publication. *Journal of Chromatography B: Biomedical Applications* (ISSN 0378-4347): for 1995 Vols. 663–674 are scheduled for publication. Subscription prices for *Journal of Chromatography A*, *Journal of Chromatography B: Biomedical Applications* or a combined subscription are available upon request from the publisher. Subscriptions are accepted on a prepaid basis only and are entered on a calendar year basis. Issues are sent by surface mail except to the following countries where air delivery via SAL is ensured: Argentina, Australia, Brazil, Canada, China, Hong Kong, India, Israel, Japan, Malaysia, Mexico, New Zealand, Pakistan, Singapore, South Africa, South Korea, Taiwan, Thailand, USA. For all other countries airmail rates are available upon request. Claims for missing issues must be made within six months of our publication (mailing) date. Please address all your requests regarding orders and subscription queries to: Elsevier Science B.V., Journal Department, P.O. Box 211, 1000 AE Amsterdam, Netherlands. Tel.: (+31-20) 5803 642; Fax: (+31-20) 5803 598. Customers in the USA and Canada wishing information on this and other Elsevier journals, please contact Journal Information Center, Elsevier Science Inc., 655 Avenue of the Americas, New York, NY 10010, USA, Tel. (+1-212) 633 3750, Telefax (+1-212) 633 3764.

Abstracts/Contents Lists published in Analytical Abstracts, Biochemical Abstracts, Biological Abstracts, Chemical Abstracts, Chemical Titles, Chromatography Abstracts, Current Awareness in Biological Sciences (CABS), Current Contents/Life Sciences, Current Contents/Physical, Chemical & Earth Sciences, Deep-Sea Research/Part B: Oceanographic Literature Review, Excerpta Medica, Index Medicus, Mass Spectrometry Bulletin, PASCAL-CNRS, Referativnyi Zhurnal, Research Alert and Science Citation Index.

US Mailing Notice. *Journal of Chromatography A* (ISSN 0021-9673) is published weekly (total 52 issues) by Elsevier Science B.V., (Sara Burgerhartstraat 25, P.O. Box 211, 1000 AE Amsterdam, Netherlands). Annual subscription price in the USA US$ 5389.00 (US$ price valid in North, Central and South America only) including air speed delivery. Second class postage paid at Jamaica, NY 11431. **USA POSTMASTERS**: Send address changes to *Journal of Chromatography A*, Publications Expediting, Inc., 200 Meacham Avenue, Elmont, NY 11003. Airfreight and mailing in the USA by Publications Expediting.

See inside back cover for Publication Schedule, Information for Authors and information on Advertisements.

0021-9673/94/$07.00

Printed in the Netherlands

For Contents see p. VII.

Chiral HPLC Column

Application Guide for Chiral HPLC Column Selection

SECOND EDITION!

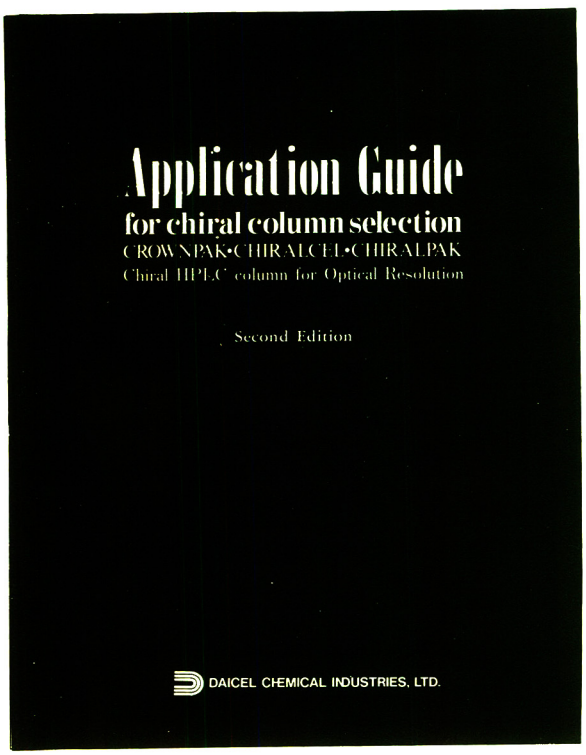

GREEN BOOK

The 112-page green book contains chromatographic resolutions of over 350 chiral separations, cross-indexed by chemical compound class, structure, and the type of chiral column respectively. This book also lists chromatographic data together with analytical conditions and structural information. A quick reference guide for column selection from a wide range of DAICEL chiral HPLC columns is included.

To request this book, please let us know by fax or mail.

DAICEL CHEMICAL INDUSTRIES, LTD.

AMERICA

CHIRAL TECHNOLOGIES, INC.

730 Springdale Drive, P.O. Box 564, Exton, PA 19341
Phone: +1-215-594-2100
Facsimile: +1-215-594-2325

EUROPE

DAICEL (EUROPA) GmbH

Oststr. 22
D-40211 Düsseldorf, Germany
Phone: +49-211-369848
Facsimile: +49-211-364429

ASIA/OCEANIA

DAICEL CHEMICAL INDUSTRIES, LTD.
CHIRAL CHEMICALS NDD
8-1, Kasumigaseki 3-chome,
Chiyoda-ku, Tokyo 100, JAPAN
Phone: +81-3-3507-3151
Facsimile: +81-3-3507-3193

ANALYTICAL BIOTECHNOLOGY

Proceedings of the 4th International Symposium on Analytical Methods, Systems and Strategies in Biotechnology (ANABIOTEC '92), Noordwijkerhout, The Netherlands, 21-23 September 1992

Edited by **C. van Dijk**

Previously published as part of the 1993 subscription to the journals *Analytica Chimica Acta* and *Journal of Biotechnology*

ANABIOTEC '92 focused on the further integration of biotechnology and analytical chemistry. The results of this symposium clearly demonstrated that a substantial progress could be reported in the application of both conventional and new analytical techniques, the latter essentially based on natural analytical tools such as biomolecules. The main themes covered during this meeting are fermentation monitoring, chromatography, instrumental analysis, biosensors and bioanalysis.

A selection of the contents.
Preface.
Process Control. Monitoring and control of recombinant protein production (K. Schügerl *et al.*). Rapid and quantitative analysis of bioprocesses using pyrolysis mass spectrometry and neural networks: application to indole production (R. Goodacre, D.B. Kell). Characterization of a sampling unit based on tangential flow filtration for on-line bioprocess monitoring (T. Buttler, L. Gorton, G. Marko-Varga). Automated monitoring of biotechnological processes using on-line ultrafiltration and column liquid chromatography (N.C. Van de Merbel *et al.*). On-line monitoring of penicillin V during penicillin fermentations: a comparison of two different methods based on flow-injection analysis (M. Carlsen *et al.*). Development of an on-line method for the monitoring of vicinal diketones and their precursors in beer fermentation (C. Mathis *et al.*). Monitoring of fermentation by infrared spectrometry. Alcoholic and lactic fermentations (D. Picque *et al.*).
Chromatography and other Separation Techniques. Chromatographic analysis of biopolymers distribution in "poly-hemoglobin", an intermolecularly crosslinked hemoglobin solution (J. Simoni, G. Simoni, M. Feola). Application of multivariate mathematical-statistical methods for the comparison of the retention behaviour of porous graphitized carbon and octadecylsilica columns (E. Forgács, T. Cserháti, B. Bordás).
Antibodies. Catalytic antibodies: new developments (R. Hilhorst).
Biosensors. Measurements of nitric oxide in biological materials using a porphyrinic microsensor (T. Malinski *et al.*). Reusable fiber-optic-based immunosensor for rapid detection of imazethapyr herbicide (R.B. Wong, N. Anis, M.E. Eldefrawi). Biosensor monitoring of blood lactate during open-heart surgery (M. Kyröläinen *et al.*).
Instrumental Techniques. Introduction to the dielectric estimation of cellular biomass in real time, with special emphasis on measurements at high volume fractions (C.L. Davey *et al.*). Spectral analysis of interactions between proteins and dye ligands (J. Hubble, A.G. Mayes, R. Eisenthal).
Enzymatic Analysis. Preservation of shelf life of enzyme based analytical systems using a combination of sugars, sugar alcohols and cationic polymers or zinc ions (T.D. Gibson, J.N. Hulbert, J.R. Woodward).
Colloidal Carbon Particles. Colloidal carbon particles as a new label for rapid immunochemical test methods: Quantitative computer image analysis of results (A. van Amerongen *et al.*). Author Index.

© 1993 208 pages Hardbound
Price: Dfl. 265.00 (US $ 151.50)
ISBN 0-444-81640-2

ORDER INFORMATION
For USA and Canada
ELSEVIER SCIENCE INC.
P.O. Box 945
Madison Square Station
New York, NY 10160-0757
Fax: (212) 633 3880
In all other countries
ELSEVIER SCIENCE B.V.
P.O. Box 330
1000 AH Amsterdam
The Netherlands
Fax: (+31-20) 5862 845
US$ prices are valid only for the USA & Canada and are subject to exchange rate fluctuations; in all other countries the Dutch guilder price (Dfl.) is definitive. Customers in the European Union should add the appropriate VAT rate applicable in their country to the price(s). Books are sent postfree if prepaid.

ELSEVIER SCIENCE B.V.

JOURNAL OF CHROMATOGRAPHY A

VOL. 683 (1994)

JOURNAL OF CHROMATOGRAPHY A

INCLUDING ELECTROPHORESIS AND OTHER SEPARATION METHODS

SYMPOSIUM VOLUMES

ELSEVIER

Amsterdam — Lausanne — New York — Oxford — Shannon — Tokyo

J. Chromatogr. A, Vol. 683 (1994)

0021-9673/94/$07.00

Printed in the Netherlands

SYMPOSIUM ISSUE

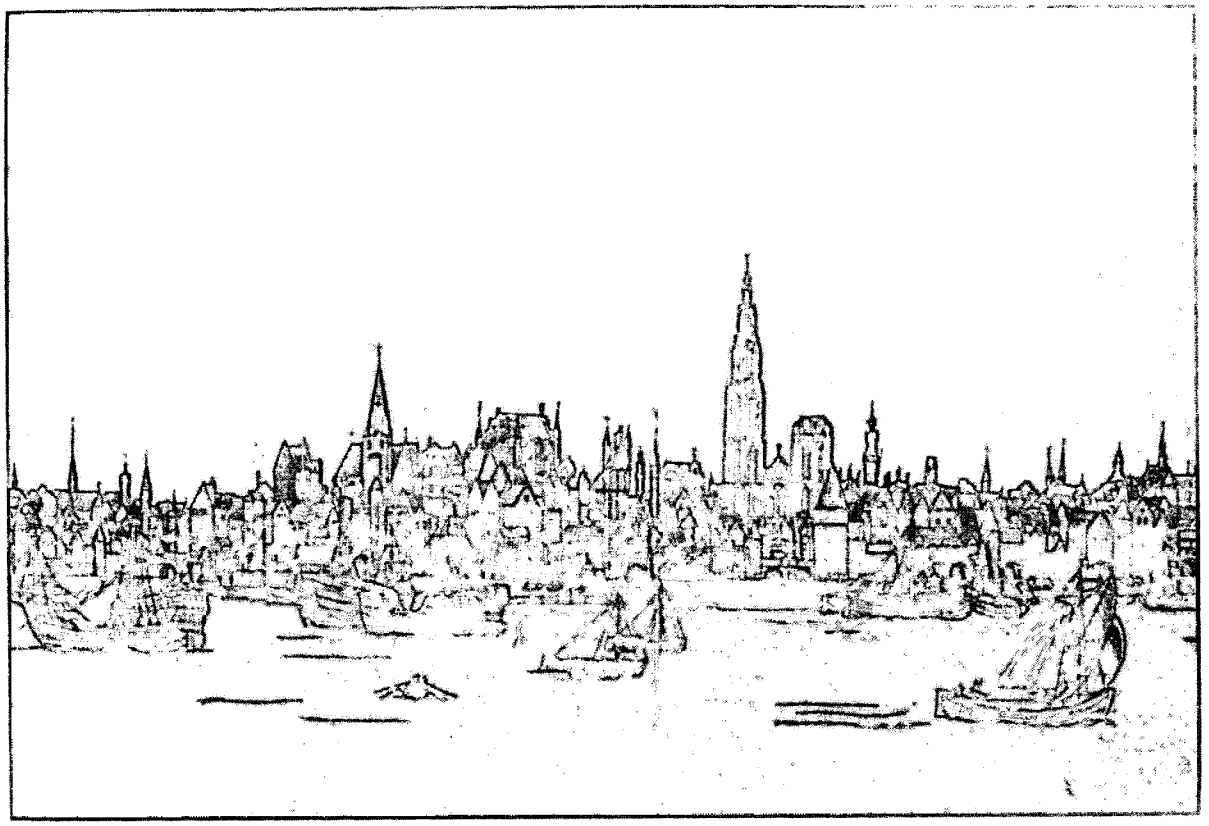

THIRD INTERNATIONAL SYMPOSIUM ON HYPHENATED TECHNIQUES IN CHROMATOGRAPHY

Antwerp (Belgium), February 22–25, 1994

Guest Editor

R. SMITS

(Antwerp)

VOL. 683, NO. 1 JOURNAL OF CHROMATOGRAPHY A OCTOBER 15, 1994

CONTENTS

3RD INTERNATIONAL SYMPOSIUM ON HYPHENATED TECHNIQUES IN CHROMATOGRAPHY, ANTWERP, FEBRUARY 22–25, 1994

TECHNIQUES

LIPIDS AND RELATED COMPOUNDS

SILICIUM COMPOUNDS

PESTICIDES AND PHARMACEUTICALS

FUELS

SPECIATION AND ORGANO COMPOUNDS

ELSEVIER

Journal of Chromatography A, 683 (1994) 1

JOURNAL OF CHROMATOGRAPHY A

Preface

The *Third International Symposium on Hyphenated Techniques in Chromatography — Hyphenated Chromatographic Analyzers* (HTC 3) was again held at the University of Antwerp (UIA) on February 22–25, 1994. HTC 3 was attended by about 240 participants from 20 different countries, mostly from Western Europe and the USA; 34 companies exhibited instruments and supplies.

The symposium was preceded by six workshops on: supercritical fluid fractionation–supercritical fluid extraction–supercritical fluid chromatography; liquid chromatography–diode array detection for method validation in the pharmaceutical industry; techniques for the introduction of large volumes of liquid into gas chromatography — a key to coupled techniques; a short course on high-performance liquid chromatography–mass spectrometry; volatile organic compound analysis by thermal desorption–capillary gas chromatography–mass spectrometry; and troubleshooting high-performance liquid chromatography systems.

The HTC 3 symposium was organized by the Working Party on Chromatography of the Royal Flemish Chemical Society (KVCV). Valuable financial support was offered by the Nationaal Fonds voor Wetenschappelijk Onderzoek (NFWO, Brussels) and by an important number of sponsoring companies. The organizing committee [K.D. Bartle, H.J. Cortes, R. Senten (secretary), R. Smits (chairman) and P. Van hee (treasurer)] was aided by an advisory international scientific committee consisting of F. Adams (chairman), K.D. Bartle, H.J. Cortes, C.A. Cramers, K. Grob, D.L. Massart, P. Sandra and D. Westerlund.

During the symposium, 38 lectures and 55 posters covered the most important fundamental aspects, instrumental developments and applications of the various hyphenated chromatographic techniques and of hyphenated chromatographic analyzers. As in the previous meeting, the main topics of the three sessions were: hyphenated supercritical fluid, gas and liquid chromatography. Excellent reviews on the state-of-the-art of hyphenating different techniques were presented by Adams, Bartle, Brinkman, Cortes, Cramers, Donard, Ebdon, Esmans, Fell, Frank, Janssen, Karlsson, Massart, Rocca, Sandra, Sanz-Medel, Taylor and Widmer.

The HTC 3 symposium showed the growing importance of hyphenated chromatographic techniques and analyzers in research and routine analysis of industrial, environmental, pharmaceutical, food and biological samples. These themes will again be treated during the *Fourth International Symposium on Hyphenated Techniques in Chromatography — Hyphenated Chromatographic Analyzers* (HTC 4) which will be held in the St. John's Congress Centre of Bruges (Belgium) on February 6–9, 1996.

Antwerp (Belgium)

Robert Smits
Symposium Chairman

SSDI 0021-9673(94)00747-O

ELSEVIER

Journal of Chromatography A, 683 (1994) 3–8

JOURNAL OF CHROMATOGRAPHY A

Effect of spectral resolution, detector linearity and chromatographic resolution on peak purity calculations

Richard W. Andrews*, Harold Richardson

Waters Chromatography Division, Millipore Corp., 34 Maple Street, Milford, MA 01757, USA

Abstract

The detection of inhomogeneity in chromatographic peaks is one of the principal benefits of photodiode array detection for HPLC. The peak homogeneity can be estimated by comparing the angles between the vector representations of the instantaneous spectrum and the peak apex spectrum, and the instantaneous spectrum and the spectral noise. When the spectral or purity angle exceeds the noise angle, the peak is not homogeneous because the differences between the instantaneous spectra and the apex spectrum cannot be explained by statistical variation of the apex spectrum. In this paper, we consider the impact of detector linearity and slit width on the purity (homogeneity) measurements of a separation of a series of compounds related to vanillin. The peak purity angle, i.e., the spectral contrast of spectra within a chromatographic peak, varies with the maximum absorbance. At small maximum absorbances (less than 0.1 AU), the variation in purity angle is dominated by system noise. At large maximum absorbances (greater than 0.5 AU), the variation in purity angle is dominated by the photometric uncertainty. The smallest measurable purity angle for a homogeneous peak is inversely proportional to the slit width and spectral bandpass of the polychrometer of the photodiode array detector.

1. Introduction

The principal benefits of photodiode array detection (PDA) in high-performance liquid chromatography include confirmation of peak identity by comparison with reference spectra [1] and detection of co-elution of compounds which have different UV–Vis absorbance spectra [2,3]. The application of PDA to the validation of pharmaceutical analyses has recently been reviewed [4].

Several measures of spectral dissimilarity have been proposed to aid in the recognition of co-elution. These include comparison of absorbance ratios at one or more pairs of wavelengths [5], monitoring changes in the absorbance-weighted average wavelength [6], overlaying spectra taken on the upslope, apex and downslope of the peak [7], and computing the angle (or its sine and/or cosine) between the n-dimensional vector representations of the spectra to be compared [8,9]. The purity angle, i.e., the angle between the n-dimensional representations, has several advantages which include: (a) all of the wavelengths contribute to the spectral comparisons, (b) the spectral noise can also be represented as a noise vector which allows the use of hypothesis testing for the significance of differences in purity angle and (c) the angle is a linear function of the difference between spectra while the sine (dissimilarity index) and cosine (similarity index) are non-linear. Library matching of UV–Vis

* Corresponding author.

0021-9673/94/$07.00
SSDI 0021-9673(94)00407-Z

spectra, i.e., comparison of stored spectra of authentic materials with apex spectra is commonly performed by applying the same algorithms [4].

The spectral bandpass, linear dynamic range, stray light, and noise define the performance of spectrophotometers. When operated as an HPLC detector, the time constant, speed of spectral acquisition, flow cell path length, and flow cell dispersion are additional critical performance characteristics. The relationship between spectral bandpass, linear dynamic range and noise is complex; the most significant challenge to photodiode array detector design is to maximize the linear dynamic range and spectral fidelity by minimizing spectral bandpass while simultaneously maintaining a high energy throughput to minimize noise. The resolution of PDA can be described by reporting the number of nm/diode by dividing the spectral range of the polychrometer by the number of diodes or by reporting the spectral bandpass of the polychrometer. The spectral bandpass of the polychrometer may exceed the nominal diode resolution of the instrument. However, no additional information is provided by the excess diodes.

Although several authors have commented on the limited information content of UV–Vis absorbance spectra [10,11] there are no reports describing the relationship between spectral bandpass of PDA spectrophotometers and the spectral differences which can be measured. Ryan [12] and Ebel and Mueck [13] noted the necessity of collecting spectra which have good signal-to-noise ratio and are within the linear dynamic range of PDA. The fundamental assumption of all of the methods of spectral comparison is that the absorbances of all of the components are strictly additive and that Beer's law is obeyed at all of the wavelengths selected for comparison. Special care must be exercised in the low UV where molar absorptivities are generally large and the absorbance can exceed the linear dynamic range of PDA [6].

The collection of a blank injection as a source of data for estimating the system noise for inclusion in purity and homogeneity calculations was recommended by Ebel and Mueck [13]. The noise models which have been included in purity calculations have assumed that the noise is constant over the entire absorbance range. While this assumption is convenient, it is true only when the absorbance values are small, i.e., less than 0.4 AU. When the absorbance exceeds that value, the principal noise source changes from a fixed noise, typically the read noise of the diode array, to shot and/or source flicker noise. The relative uncertainty in absorbance follows the familiar photometric error curve which has a broad minimum at ca. 0.5 AU because the principal noise source changes as absorbance increases and less energy reaches the PDA system. Comparisons of spectra with absorbance values that are greater than 1 AU will be limited by the uncertainty in the absorbance values. Ebel and Mueck did recommend that absorbance values be limited to less than 1 AU, but did not discuss the rationale for such a limit [13].

In this paper we consider the impact of spectral bandpass, detector linearity, and the photometric error curve on peak purity measurements for the separation of vanillin and several related compounds. We demonstrate that the photometric error curve correlates the observed spectral contrast angle with the noise-to-signal ratio.

2. Experimental

2.1. Chemicals and reagents

The mobile phase was a 88:12 (v/v) mixture of 1.0% (v/v) H_3PO_4 in water and HPLC-grade acetonitrile (both obtained from Fisher Scientific, Boston, MA, USA) pumped at 1.0 ml/min at ambient temperature. The water was purified with a Milli-Q™ system (Millipore, Bedford, MA, USA). Stock solutions (1 mg/ml) of vanillin, ethyl vanillin, *m*-anisic acid, and 4-hydroxy-3-methoxy benzoic acid (vanillic acid) in methanol were prepared and serially diluted with mobile phase. Vanillin and the related compounds were obtained from Sigma (St. Louis, MO, USA). The column used was a 150 × 3.9

mm C_{18} NovaPak™ column obtained from the Waters Chromatography Division of Millipore (Milford, MA, USA). The column was operated at ambient temperature. A typical separation is shown in Fig. 1.

2.2. Instrumentation

The chromatograph used in this study consisted of a Model W600 solvent-delivery system, Model 715 Ultra WISP™ and Model 996 photodiode array detector, all obtained from Waters. A Millennium 2010™ data system, also obtained from Waters, was used for control of the chromatograph and acquisition of the data.

2.3. Data processing and procedures

Samples of 25 μl were injected unless otherwise noted. The detector was operated with the following parameters: wavelength range: 195–400 nm; sampling rate: 2 points/s; resolution: 1.2 nm, i.e., no diode bunching; slit width: 50 μm, unless otherwise noted.

The PDA data were processed using Millennium 2010 software which supports the use of a derived channel which contains the largest instantaneous absorbance value for each data point over a user-defined wavelength range, the maxplot. The principal peak purity calculations were performed on the maxplot (200–400 nm) channel. Quantitation was performed on both the maxplot channel and the 290 nm extracted channel.

Results of peak purity, peak area and peak height measurements were exported to Microsoft Excel™ (Microsoft Corp., Redmond, WA, USA) for further processing and to SigmaPlot™ (Jandel Corp., San Rafael, CA, USA) or TableCurve™ (Jandel) for curve fitting and/or plotting.

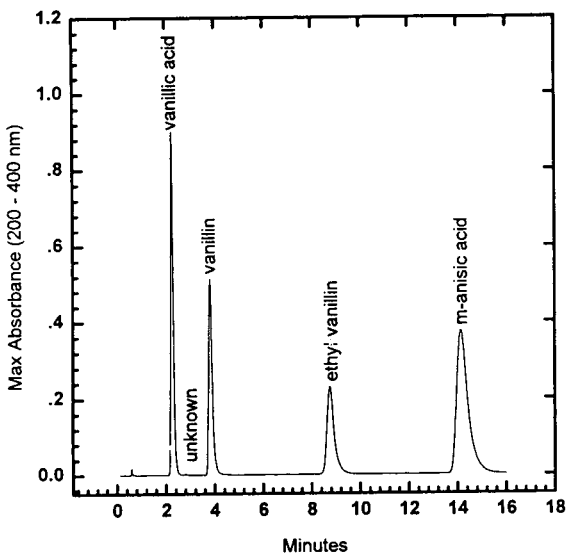

Fig. 1. Typical separation of vanillin, ethyl vanillin, vanillic acid and *m*-anisic acid, maxplot channel (200–400 nm), 25-μl injection containing 40 μg of each component.

3. Results and discussion

3.1. Detector linearity

The linear dynamic range of photometric detectors can be measured by determining the value at which the measured absorbance is 5% less than the value predicted by extrapolating a linear calibration curve which passes through the origin [14]. Dorschel et al. [15] proposed a less subjective test of linearity, i.e., that the instantaneous slope of the calibration curve be constant. We have described a more general approach to determining the goodness of fit of various chromatographic calibration models; the residuals from the regression equation should be randomly distributed over the range of calibrants [16]. The advantage of this approach is that it is applicable to all calibration models and that the residual distribution can be submitted to significance testing through the χ^2 test [17].

A series of samples containing from 1 to 100 μg/25 μl were injected, in triplicate, into the chromatograph. The maxplot (maximum instantaneous absorbance from 200 to 400 nm) and 290 nm chromatograms were extracted from the PDA data. Vanillic acid was the analyte which eluted first and had the largest peak height; its peak absorbance for the 100 μg injection was 2.2 AU. Fig. 2 shows a plot of the distribution of

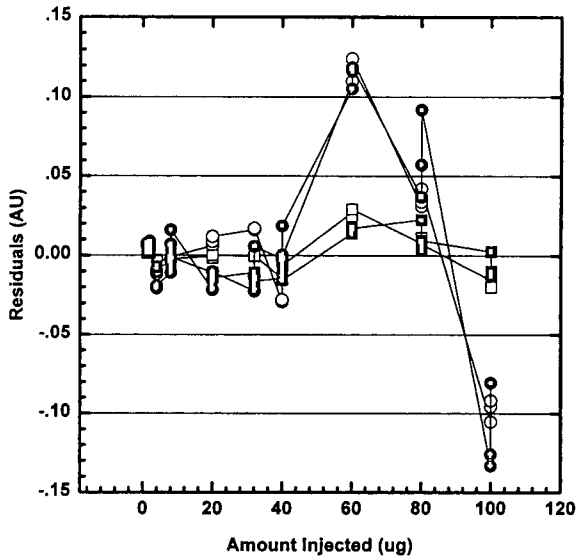

Fig. 2. Residual plots from vanillic acid calibration. ○ = Maxplot, 50-μm slit; □ = 290 nm, 50-μm slit; ● = maxplot, 150-μm slit; ■ = 290 nm, 150-μm slit.

residuals from a linear regression (zero intercept) for both the maxplot and 290 nm channels. The experiment was repeated with a 150-μm slit. Fig. 2 also shows the residual plots for that experiment. In both cases, the distribution of the residuals shows no obvious pattern, and the calibration curves are linear.

The maxplot calibration data for vanillic acid was fitted to an apparent stray light model, $A_{obs} = \log_{10}[(1+s)/(10^{-\epsilon bC}+s)]$, where s is the fractional stray light, ϵ is the molar absorptivity, b is the path length and C is the molar concentration. The apparent stray light was 0.2% and 0.1% for the detector operated with the 50-μm and 150-μm slits, respectively. These values of apparent stray light correspond to an upper limit of the linear dynamic range (as defined by the ASTM procedure E685-79 [14]) in excess of 2.2 AU.

3.2. Photometric error curve

Because the noise of photometric absorbance detectors is relatively constant over several orders of magnitude, most noise measurements are performed under conditions corresponding to the chromatographic baseline. For PDA, this means that the charge measured at the individual diodes is large and can be read with good precision and accuracy. We have examined the variation of noise, which was measured in accordance with the ASTM procedure E685-79 [14], as a function of wavelength. If the energy spectrum is normalized by the maximum energy of the deuterium lamp, i.e., 232 nm, an apparent absorbance scale can be calculated from $A = \log_{10}$ (1/transmittance). Fig. 3 shows a plot of the observed noise vs. the apparent absorbance; it also contains a plot of the noise/signal ratio for the same data set. The relative uncertainty in absorbance measurements is given by

$$s_A/A = 0.434 s_T/T \log T$$

where s_A is the standard deviation of the absorbance, A is the absorbance, s_T is the standard deviation of the transmittance and T is the transmittance. The standard deviation of the transmittance can be treated as the sum of terms corresponding to fixed noise and shot noise

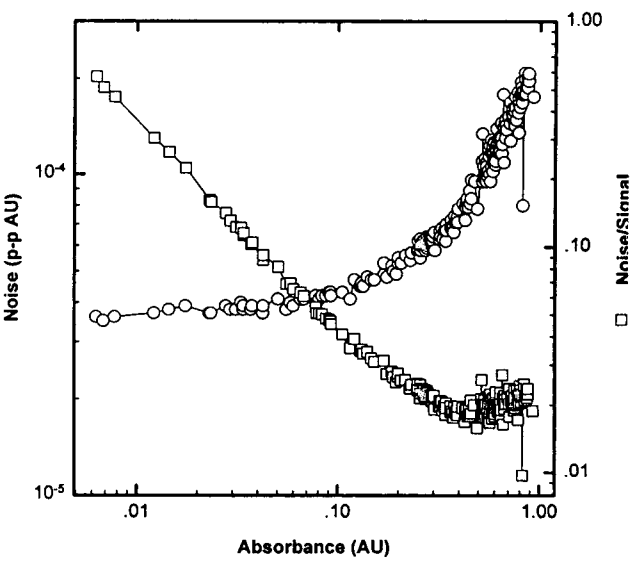

Fig. 3. Photometric error plots. ○ = Peak-to-peak noise, AU; □ = noise/signal ratio.

limited cases, i.e., $s_T = k_1 + k_2(T^2 + T)^{1/2}$. The noise/signal vs. apparent absorbance curve was fitted to this equation and the residuals showed a random distribution. The minimum in this observed photometric error curve occurs at 0.5 AU and is about 2%. Consequently, uncertainty in the absorbance measurement will become significant for absorbance values greater than 0.5 AU. When the absorbance is less than 0.5 AU, the baseline noise will be the principal source of uncertainty. The most reliable comparisons of spectra will be performed at an absorbance corresponding to the minimum of the photometric error curve.

It should be noted that the photometric error curve predicts an increase in the relative uncertainty in absorbance which limits the confidence in spectral comparisons at an absorbance value which is one fourth of the upper limit of the linear dynamic range of the detector. Fortunately, the minimum in the photometric error curve is broad, and the relative uncertainty in absorbance does not change dramatically from 0.1 to 0.8 AU.

3.3. Peak purity (spectral homogeneity) measurements

We examined the variation in the purity angle for each of the peaks observed in the chromatograms used to measure the linear dynamic range of PDA. The results of those measurements for the vanillic acid and vanillin peaks are shown in Fig. 4. The curves in Fig. 4 are based on a combined fixed and shot noise model of the photometric error curve and have randomly distributed residuals.

Each plot of purity angle vs. maximum absorbance displays a minimum; for the 50 μm slit, that minimum occurs at 0.5 AU and a purity angle of 0.4°. When the 150-μm slit was used, the minimum occurred at 0.3 AU and 0.6°. The effect of increasing the slit width was to decrease the dynamic range of spectral homogeneity measurements.

The minima occurred at absorbance values much smaller than the upper limit of the linear dynamic range of the detector (greater than 2.2 AU). The maximum error in absorbance associated with the apparent stray light values of 0.2% and 0.1% corresponds to 0.3% and 0.2% at the minima of the peak purity curves which demonstrates that the comparison of spectra is limited by photometric uncertainty, not detector linearity.

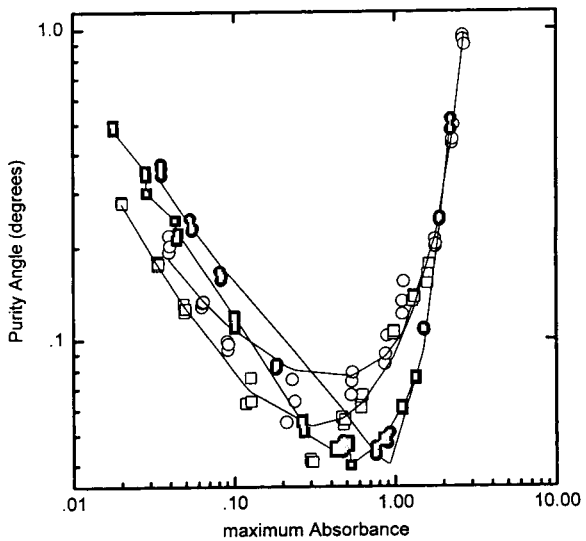

Fig. 4. Peak purity plots for vanillic acid and vanillin. ● = Vanillic acid, 50-μm slit; ■ = vanillin, 50-μm slit; ○ = vanillic acid, 150-μm slit; □ = vanillin, 150-μm slit.

4. Conclusions

Sensitive detection of spectral inhomogeneity within chromatographic peaks requires the use of the smallest spectral bandpass that the detector can support and limiting the maximum absorbance over the entire wavelength range used for comparing spectra to a value which corresponds to the minimum of the plot of purity angle vs. maximum absorbance. The use of a larger slit width, i.e., degrading spectral resolution, shifts the minimum of the purity angle vs. maximum absorbance curve to smaller values of absorbance and higher purity angles and decreases the PDA sensitivity to spectral inhomogeneity within a peak.

Acknowledgements

The authors gratefully recognize the assistance of two of our colleagues at the Waters Chromatography Division of the Millipore Corp. Harold Coderre for providing the noise and energy spectra and Mark Gorenstein for helpful discussions of spectral homogeneity.

References

[1] E.I. Mender, R. Schaubhut, C.E. Mender and D.J. Vonderschmitt, *J. Chromatogr.*, 419 (1987) 135–154.
[2] H.K. Chan and G.P. Carr, *J. Pharm. Biomed. Anal.*, 8 (1990) 271–217.
[3] B.B. Seaton, B. Clark and A.F. Fell, *Anal. Proc.*, 23 (1986) 4224–427.
[4] J.B. Castledine and A.F. Fell, *J. Pharm. Biomed. Anal.*, 11 (1993) 1–13.
[5] J.B. Castledine, A.F. Fell, R Modin and B. Sellberg, *J. Pharm. Biomed. Anal.*, 9 (1991) 619–624.
[6] T. Alfredson and T. Sheehan, *J. Chromatogr. Sci.*, 24 (1986) 473–482.
[7] J.C. Miller, S.A. George and B.G. Willis, *Science*, 218 (1982) 241–246.
[8] T.L. Sheehan, M. Adaskaveg and J.L. Excoffier, *Am. Lab.*, May (1989) 66–74.
[9] G. Cameron, P.E. Jackson and M.V. Gorenstein, *Chem. Aust.*, 60 (1993) 288–289.
[10] G.W. Schieffer, *J. Chromatogr.*, 319 (1989) 387–91.
[11] D. Wickham, in D. Parriott, (Editor), *A Practical Guide to HPLC Detection*, Academic Press, New York, 1993, Ch. 4, pp. 67–109.
[12] T.W. Ryan, *J. Liq. Chromatogr.*, 16 (1993) 315–329.
[13] S. Ebel and W. Mueck, *Chromatographia*, 25 (1988) 1075–1086.
[14] *ASTM Standards in Chromatography*, ASTM, Philadelphia, PA, 1989, method E685-79, pp. 687–693.
[15] C.A. Dorschel, J.L. Ekmanis, J.E. Oberholtzer, F.V. Warren, Jr. and B.A. Bidlingmeyer, *Anal. Chem.*, 61 (1989) 951A–968A.
[16] H. Richardson and R.W. Andrews, presented at the *1992 Pittsburgh Conference and Exposition, New Orleans, March 9–12, 1992*, abstract 598.
[17] J.H. Zar, *Biostatistical Analysis*, Prentiss Hall, Des Moines, IA, 2nd ed., 1984, pp. 278–283.

ELSEVIER

Journal of Chromatography A, 683 (1994) 9–19

JOURNAL OF CHROMATOGRAPHY A

High-performance liquid chromatography–mass spectrometry (pneumatically assisted electrospray) of hydroxy polycyclic aromatic hydrocarbons

M.T. Galceran*, E. Moyano

Departament de Química Analítica, Universitat de Barcelona, Diagonal 647, 08028 Barcelona, Spain

Abstract

Electrospray (ES) in both positive and negative ionization mode and coupling high-performance liquid chromatography (HPLC) to mass spectrometry (MS) for the characterization of hydroxy polycyclic aromatic hydrocarbons (hydroxy-PAHs) are studied in this work. A series of reference hydroxy-PAHs were separated on a reversed-phase column and their ES spectra were analyzed in both ionization modes. $[M + H]^+$ and $[M - H]^-$ were obtained for positive and negative ES. Reduction of quinones was also observed in negative ES. Suitable masses for single-ion monitoring were used in HPLC–MS analysis. Flow injection of solute standards in isocratic mode and LC analyses in gradient mode using methanol–formic acid/ammonium formate 10 m*M*, pH 3 as eluent were performed.

1. Introduction

Electrospray ionization mass spectrometry (ES-MS), since its introduction in the early 1980s [1,2] has emerged as a technique for the analysis of a variety of compounds ranging from high-molecular-mass biopolymers to metal ions [3–7]. The studies of Fenn and co-workers [1,2,4,8] demonstrated the potential of ES ionization as an interface for capillary liquid chromatography (LC)–MS. Henion and co-workers [9–11], using a modification of the ES method which they called ion spray (IS), where the nebulization of the liquid effluent is assisted by a turbulent gas (nitrogen) flow, have also described a number of applications of this technique for the detection of many analytes of biological and pharmaceutical interest. Smith and co-workers [12–14] using ES as the interface for capillary electrophoresis were able to demonstrate the suitability of ES for the detection of bioorganic ionic analytes.

The capabilities of the spray methods have created also a high interest in the mechanism by which the gas-phase analyte ions are produced. It has been found empirically that the best analytical results are obtained for compounds that are ionic in solution (i.e., preformed ions). Such species include metal salts, organic salts, and compounds (e.g., peptides and proteins) which can be ionized [3–7]. The latter species are typically observed as protonated, or otherwise positively ionized molecules such as sodium adducts in positive-ion mode and as the deprotonated molecules or as molecular adduct anions in negative-ion mode.

There are two important stages in the pro-

* Corresponding author.

0021-9673/94/$07.00
SSDI 0021-9673(94)00480-W

duction of gas-phase ions: the production of the charged droplets and the production of gas-phase ions from the charged droplets. The mechanism by which the droplets are charged is assumed to be electrophoretic [15–17], although the electrospray process may also involve electrochemical reactions at the metal–liquid interface of the ES capillary tip [18–20].

The production of gas-phase ions from the charged droplets can be produced as the result of a large electrical field applied to the surface of the liquid [21–24]. When the electrical field exceeds a critical value the solute ions escape ("evaporate") from the liquid phase into the gas phase. Also ionization in the gas phase can take place via reactions identical to those occurring in chemical ionization sources. Since ions and neutral molecules are formed close together at the atmospheric pressure source, many ion/molecule collisions occur.

Few data are available on LC–MS of hydroxy polycyclic aromatic hydrocarbons (hydroxy-PAHs). Ionization of neutral, relatively non-polar compounds, such as PAHs was inefficient [19], but ES can be used in the analysis of hydroxy-PAHs because of their functional groups. Here we discuss the applicability of ES with both positive and negative ionization to the analysis of hydroxy-PAHs, developing the MS conditions suitable for the identification of these products. Calibration conditions for low-molecular-mass compounds were established. The hydroxy-PAH spectra were interpreted using the mechanisms described in the literature and coupling LC with MS was studied.

2. Experimental

2.1. Reagents

The compounds studied were 5-hydroxyindole (5-HI), 1-indanol (1-HI), 2-hydroxy-1,4-naphthoquinone (2-H-1,4-NQ), 9-hydroxyfluorene (9-HFL), 9-hydroxyphenantrene (9-HF) and 2-hydroxy-9-fluorenone (2-H-9-FLO) and were provided by Aldrich (Milwaukee, WI, USA). LC solvents, methanol (HPLC grade; Merck, Darmstadt, Germany) and water purified with a Culligan system were used. All solvents were degassed in an ultrasonic bath for 15 min.

A stock solution of the compounds was prepared containing 1 mg ml^{-1} of each in methanol. The 100 μg ml^{-1} solutions in mobile phase were obtained by dilution of appropriate volumes of this stock solution.

2.2. Instruments and procedures

MS was performed using a VG Quattro (FISON Instruments, VG Biotech, Altrincham, UK) triple quadrupole mass spectrometer equipped with an ES interface, which was assisted pneumatically, with nitrogen at a flow-rate of 10 l h^{-1}. Drying nitrogen was heated to 80°C and introduced into the capillary region at a flow-rate of 200 l h^{-1}. The electrospray needle was held at a potential of +3.8 kV and −3.2 kV relative to the potential at the counter electrode for positive and negative modes respectively. The focus potential was 60 V.

For data acquisition the mass spectrometer operated over the mass range m/z 10.0–600.0 in centroid mode at a cycle time of 2.00 s and at inter scan time of 0.10 s. Ion intensity was optimized using the mobile phase ion clusters, and calibrations were performed with these clusters in positive mode and NaI (2 μl ml^{-1} in mobile phase) in negative mode. To improve cluster formation a drying nitrogen flow of 50 l h^{-1} and a focus potential of 40 V were used.

Flow injection analysis (FIA) was used using methanol–formic acid/ammonium formiate 10 mM (pH 3) (55:45) at 35 μl min^{-1} was performed in an HPLC system with two Phoenix 20 (Carlo Erba, Milan, Italy) syringe pumps, a master (A) and a slave (B) pump. A ODS-Hypersil C_{18} (5 μm particle size, 100 × 1 mm I.D.) reversed-phase column (Shandon Scientific, Cheshire, UK) was used for hydroxy-PAH LC separation; in this case the mobile phase was run in the gradient mode. Mixtures of standards were prepared in mobile phase and 10-μl aliquots were injected in the FIA mode and 200 nl were injected in the chromatographic mode.

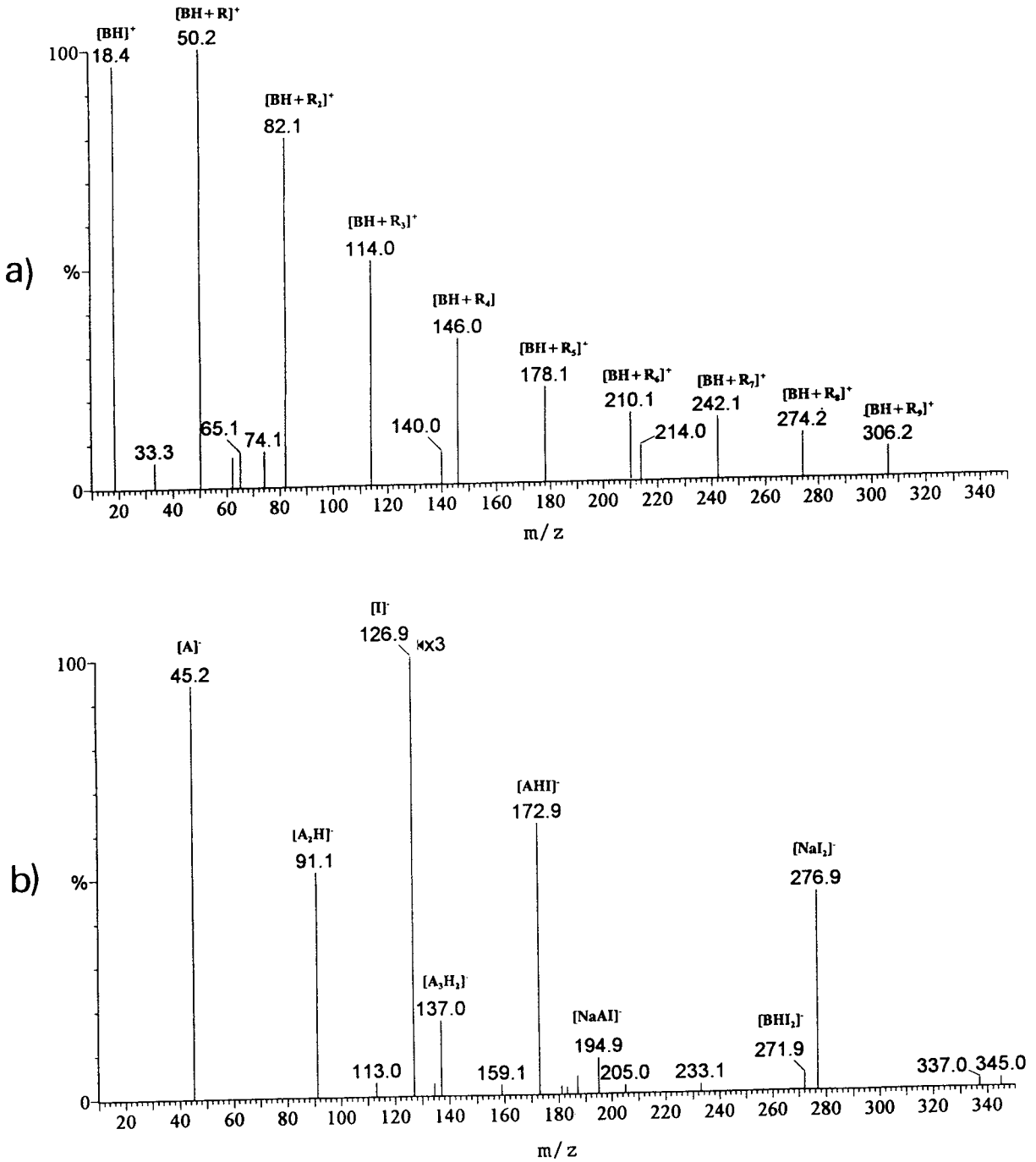

Fig. 1. ES spectra of (a) mobile phase in positive ionization and (b) NaI in negative ionization. A = $HCOO^-$; B = NH_3; R = CH_3OH.

3. Result and discussion

3.1. Calibration

One of the problems associated with "soft" ionization techniques like IS and thermospray (TSP), is that common MS reference compounds, such as perfluorokerosene (PFK), cannot be used to calibrate the mass spectrometer. Poly(ethylene glycol)s (PEGs) and poly(propylene glycol)s (PPGs) were therefore studied as reference standards [25–28]. Unfortunately, PEG and PPG mixtures are not the most suitable candidates for reference compounds, since they cause rapid contamination of the ion source due to the deposition of non-volatile material [29,30]. In addition, it is often difficult to identify individual PEG and PPG

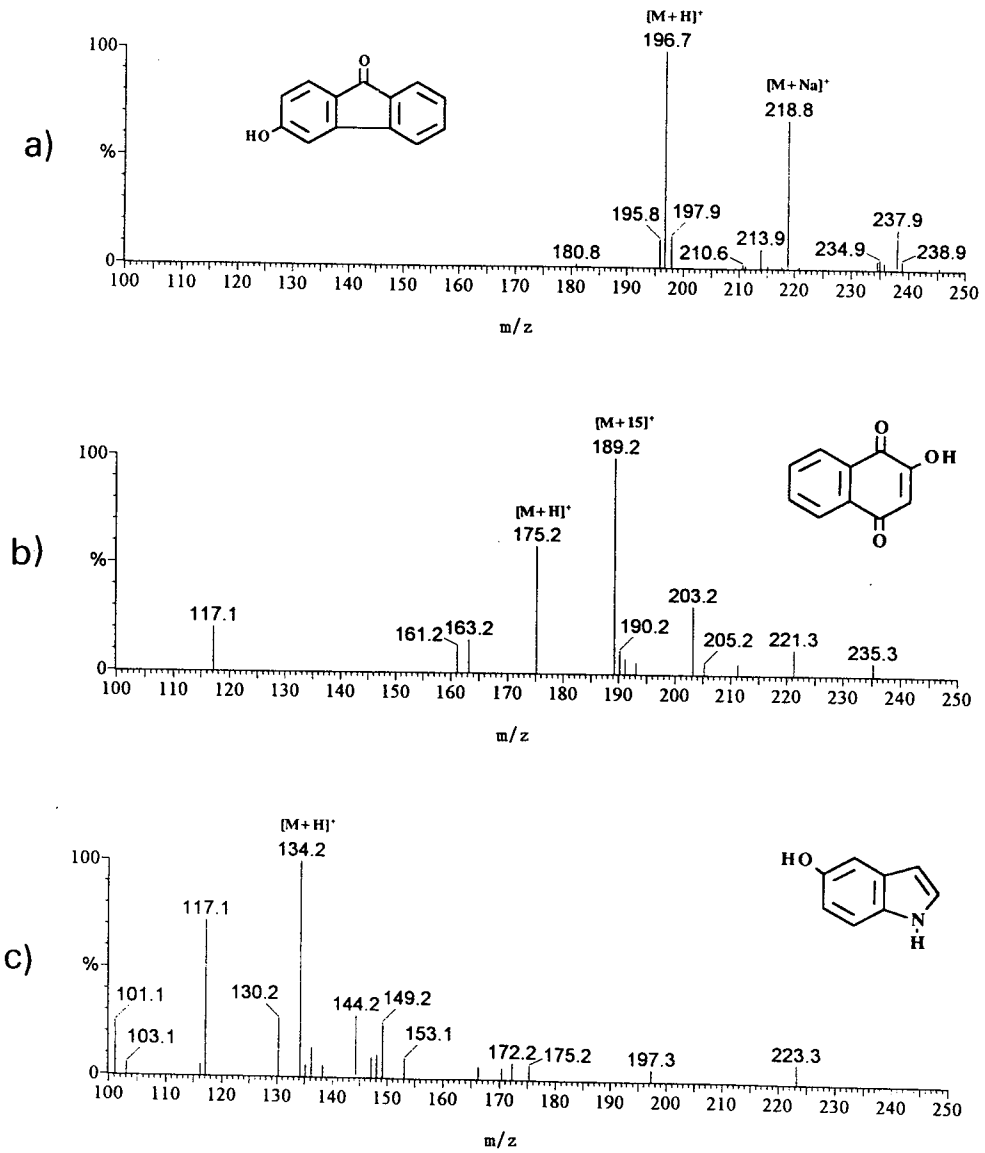

Fig. 2. Positive-ion ES ionization mass spectra of (a) 2-H-9-FLO (M_r = 196), (b) 2-H-1,4-NQ (M_r = 174) and (c) 5-HI (M_r = 133).

oligomer peaks in the complex spectra obtained with the mixtures used to cover the entire mass range.

Cesium iodide cluster ions $[Cs_nI_{n-1}]^+$, and other alkali metal halide salts, are routinely used as mass calibration standards in fast atom bombardment (FAB) and liquid secondary ion (LSI) MS. Anacleto et al. [31] reported, however, that cesium iodide was difficult to remove completely from the ES ionization source, and provided a source of contamination that hindered the ES process. There is a clear need for a more universal calibration method in ES.

An alternative approach to calibration for LC–MS is to use the mobile phase itself. It has been shown that acetic acid–ammonia cluster ions $[(CH_3COOH)_x + (NH_3)_4 + NH_4]^+$ can be generated under certain conditions in TSP ionization to provide a convenient mass calibration over the mass range m/z 100–1000 [29–31].

In positive ES, calibration was performed using the mobile phase ions. Fig. 1a shows the spectrum obtained for the calibration in which the ammonium–methanol cluster ions predominate.

The spectrum shown in Fig. 1b was obtained by FIA of NaI and the $[Na_nI_{n+1}]^-$ ion series is observed. In addition satellite peaks at lower masses are also observed for each of the $[Na_nI_{n+1}]^-$ clusters. These satellite peaks corresponded to a progressive replacement of iodide (127 u) by the formiate anion ($HCOO^-$; 45 u) of the mobile phase. Sodium iodide as calibrant has the advantage that both sodium and iodine are monoisotopic. Formic cluster ions were also used for calibration purposes.

3.2. Mechanisms of ionization

Organic compounds introduced into the source as sample components can be ionized in a variety of ways. Proton addition to form $[M + H]^+$ and proton loss to form $[M - H]^-$ are common routes of ionization for gas-phase bases and gas-phase acids, respectively [32,33].

The general reaction to form $[M + H]^+$ occurs whenever M is a stronger gas-phase base than AH and can be written as:

$$M + AH \rightarrow [M + H]^+ + A^-$$

So α-β-unsaturated ketones (2-H-9-FLO and 2-H-1,4-NQ) and amines (5-HI) are stronger gas-phase bases than methanol and formic acid, and their mass spectra (Fig. 2) are dominated by abundant $[M + H]^+$ species and some $[M + NH_4]^+$ and $[M + Na]^+$ species. Because sodium was not introduced into the reference mixture, the $[M + Na]^+$ could come from contamination of the samples, the solvents, or the glassware.

Both 9-HFL and 1-HI are hydroxy non-aromatic compounds and their acidity and probably their proton affinities are low. Both of them gave the $[M - 17]^+$ ion in positive electrospray as base peak (Fig. 3). This fragmentation is similar to that obtained when positive chemical ionization with methane as reagent gas was used (Fig. 4). The $[M + H]^+$ ions obtained from cyclic alcohols are unstable and the loss of H_2O is the most probable path of fragmentation [34].

Electrochemical oxidation reaction may be occurring at the metal–liquid interphase of the capillary tip. The actual oxidation reaction(s) depend on the electrical potential at given locations of the metal–liquid interface and on the electrochemical oxidation potential for the given reaction(s). Oxidation may explain the ion m/z 181 in the spectrum of the 9-HFL (Fig. 3a), which corresponds to the protonation of the oxidation product (Scheme 1a).

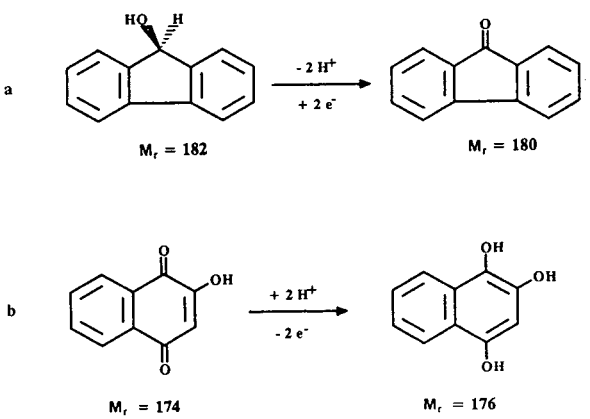

Scheme 1. Electrochemical reactions of (a) 9-HFL and (b) 2-H-1,4-NQ.

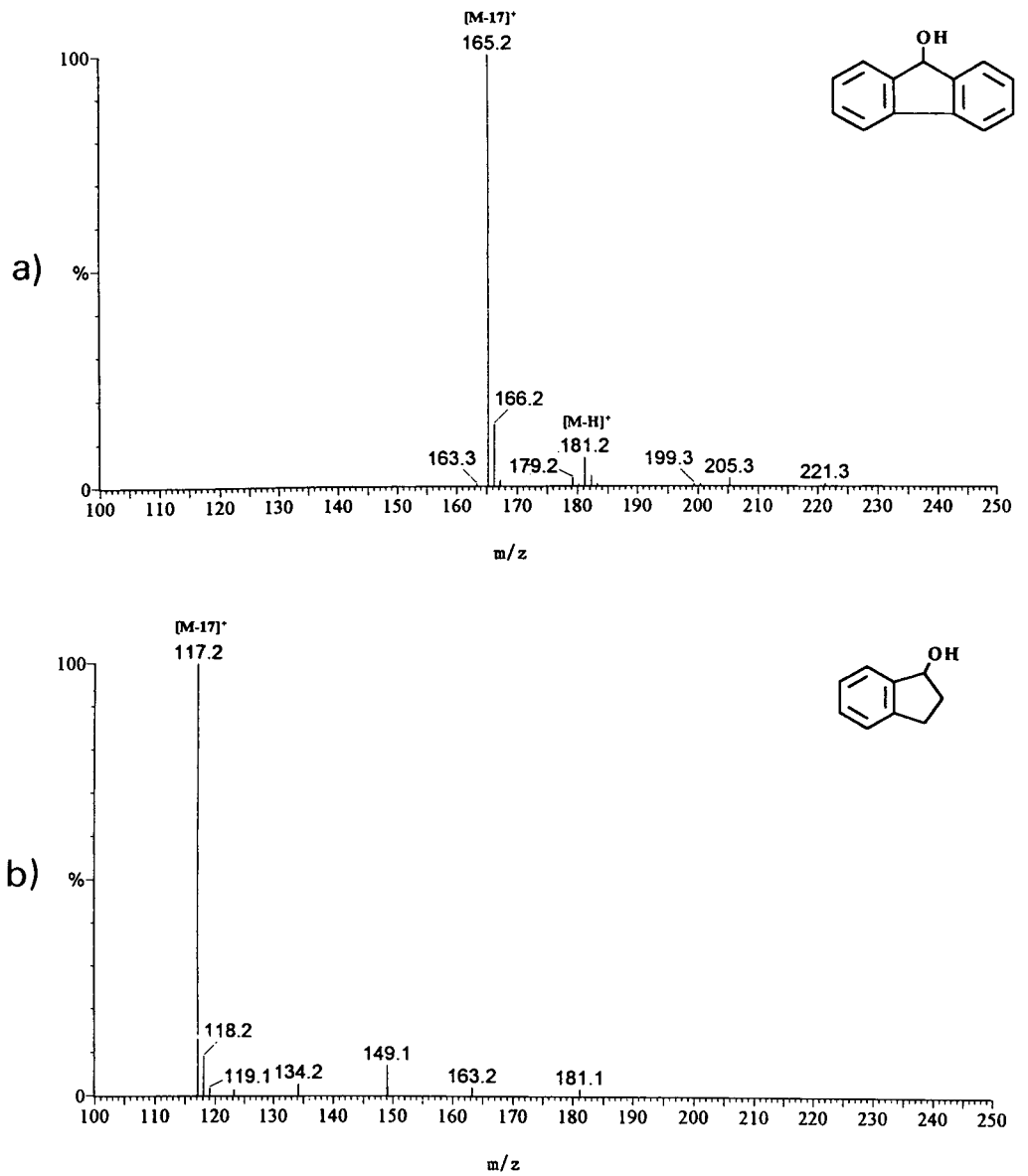

Fig. 3. Positive-ion ES ionization mass spectra of (a) 9-HFL ($M_r = 182$) and (b) 1-HI ($M_r = 134$).

For the 2-H-1,4-NQ the $[M + 15]^+$ ion (m/z 189) (Fig. 2a) presumably arises from oxidation of the phenol to a ketone, followed by the addition of CH_3.

In negative ES the reduction of quinone group for the 2-H-1,4-NQ can be observed (Fig. 5a). The $[M + H]^-$ (m/z 175) could be the reduction product (Scheme 1b).

As has been mentioned proton loss $[M - H]^-$ is a common route of ionization for gas-phase acids in negative ES if ions of sufficient basicity are present. The general reaction is:

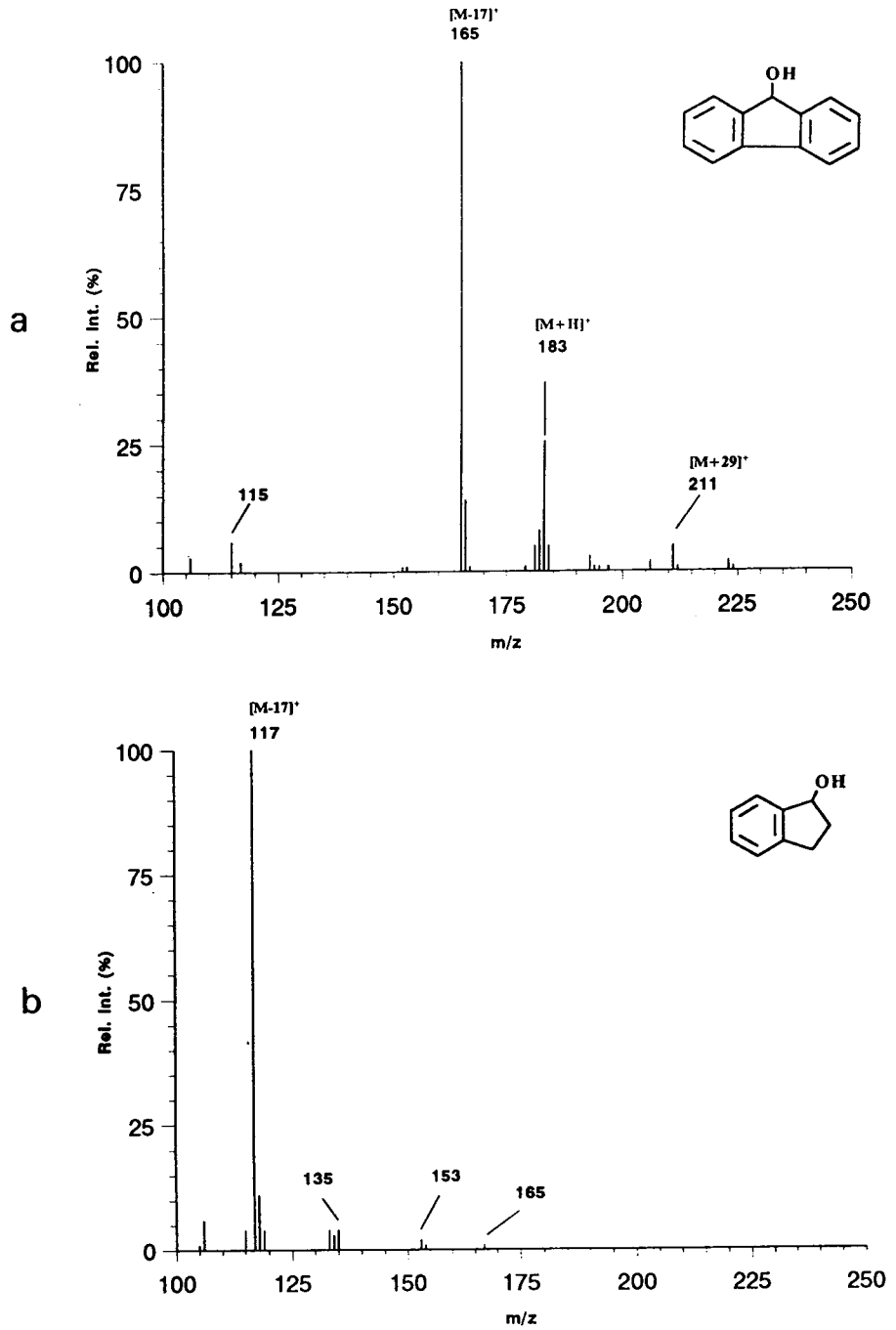

Fig. 4. Positive chemical ionization mass spectra, with methane as reagent gas, of (a) 9-HFL (M_r = 182) and (b) 1-HI (M_r = 134).

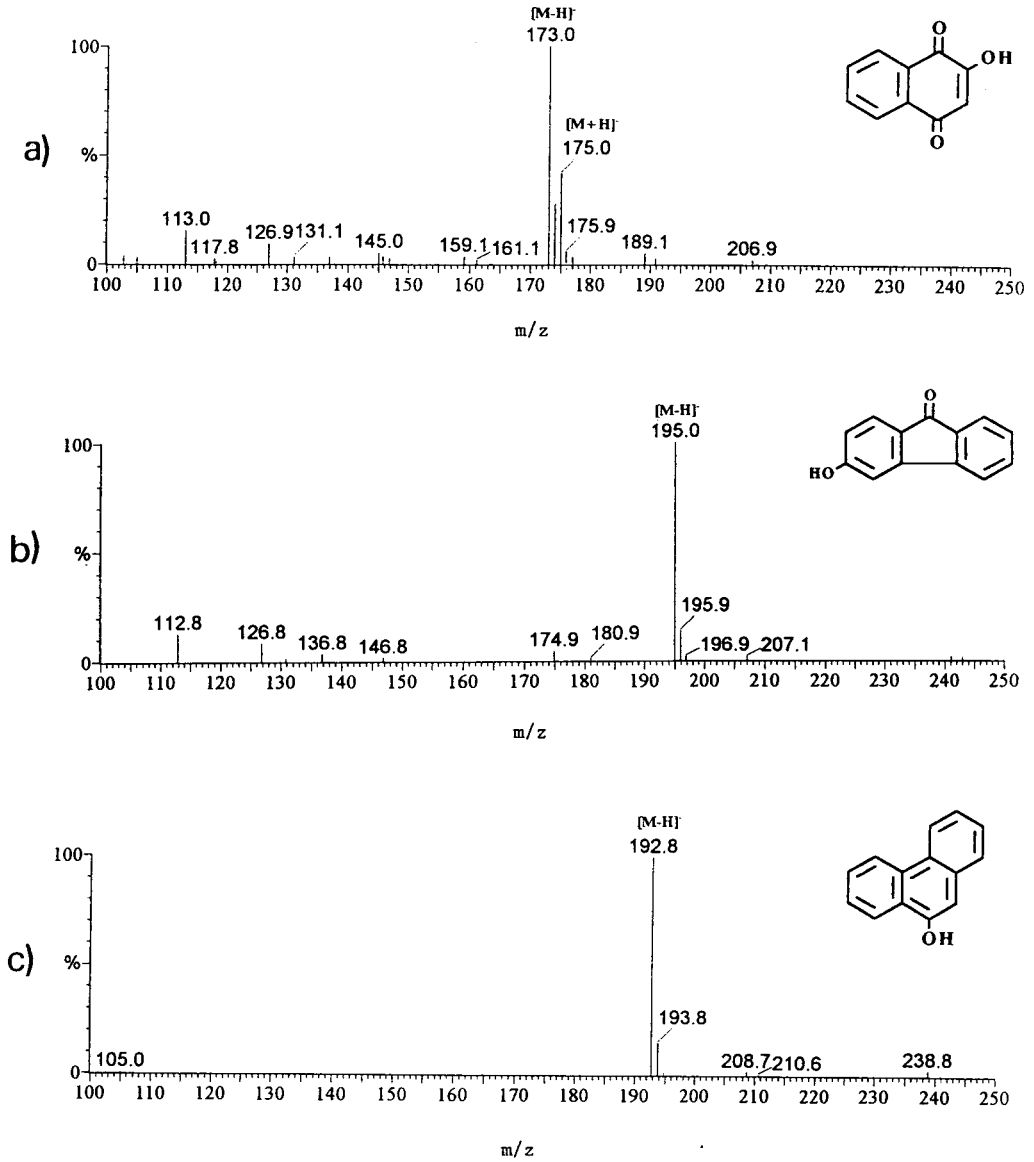

Fig. 5. Negative-ion ES ionization mass spectra of (a) 2-H-1,4-NQ ($M_r = 174$), (b) 2-H-9-FLO ($M_r = 196$) and (c) 9-HF ($M_r = 194$).

$$M + A \rightarrow [M - H]^- + [AH]^+$$

and will occur whenever A is a stronger acid than M. Dissociation constants for organic compounds in different solvents have hardly any relevance for gas-phase work. When a formic stream is vaporized through the ES source $[HCOO]^-$ ions are formed. If a gas-phase acid is introduced, ionization to $[M - H]^-$ occurs if M is a stronger gas-phase acid than HCOOH. Moreover, non-aromatic alcohols (9-HFL, 1-HI) and some phenols (5-HI) are weaker than formic acid, and do not ionize under these conditions. Fig. 5 shows the negative ES spectra for 2-H-1,4-

NQ, 2-H-9-FLO and 9-HF which are dominated by the $[M-H]^-$ ion.

3.3. HPLC–MS

Few studies are available on the separation of these compounds by HPLC, only some naphthols have been separated using C_8 column with acetonitrile–acetic buffer as mobile phase and UV detector [35]. A synthetic mixture of the six hydroxy-PAHs was prepared and used for HPLC on a C_{18} reversed-phase column. Satisfactory separation and well shaped peaks for the aromatic compounds were only obtained at low pH. The system was run in the gradient mode at 35 μl min^{-1}. Solvent A was methanol and solvent B was formic acid–ammonium formiate 10 m*M* (pH 3). The gradient was: 45% A from 0 to 10 min, a linear increase to 60% A from 10 to 25 min and isocratic elution at this composition for 5 min. The chromatogram obtained using UV detection is given in Fig. 6. Low resolution between 1-HI and 2-H-1,4-NQ can be observed and coelution of 9-HFL and 2-H-9-FLO occurred.

Poor resolution can be avoided using a specific detection method such as MS using the hydroxy-PAHs spectra to select the monitoring masses for each compound. In positive ES single-ion monitoring (SIM) of $[M+H]^+$ ion at *m/z* 197 and *m/z* 134 for the 2-H-9-FLO and 5-HI respectively, the $[M-17]^+$ fragment ion at *m/z* 165 and *m/z* 117 for the hydroxy non-aromatic com-

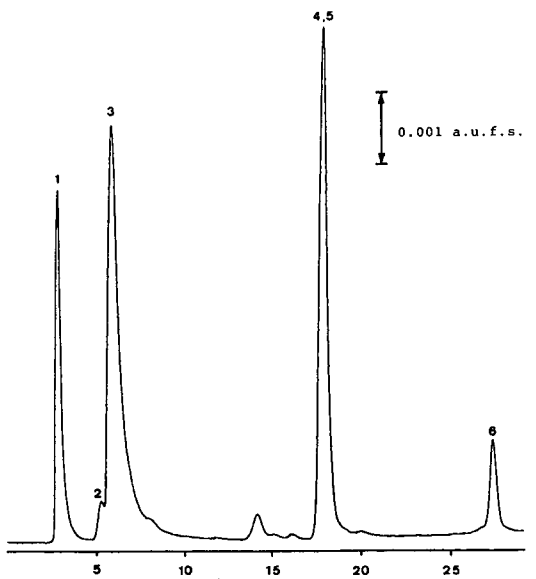

Fig. 6. HPLC–MS analysis of hydroxy-PAHs with UV detector (280 nm). Components in the mixture were (1) 5-HI, (2) 2-H-1,4-NQ, (3) 1-HI, (4) 9-HFL, (5) 2-H-9-FLO and (6) 9-HF.

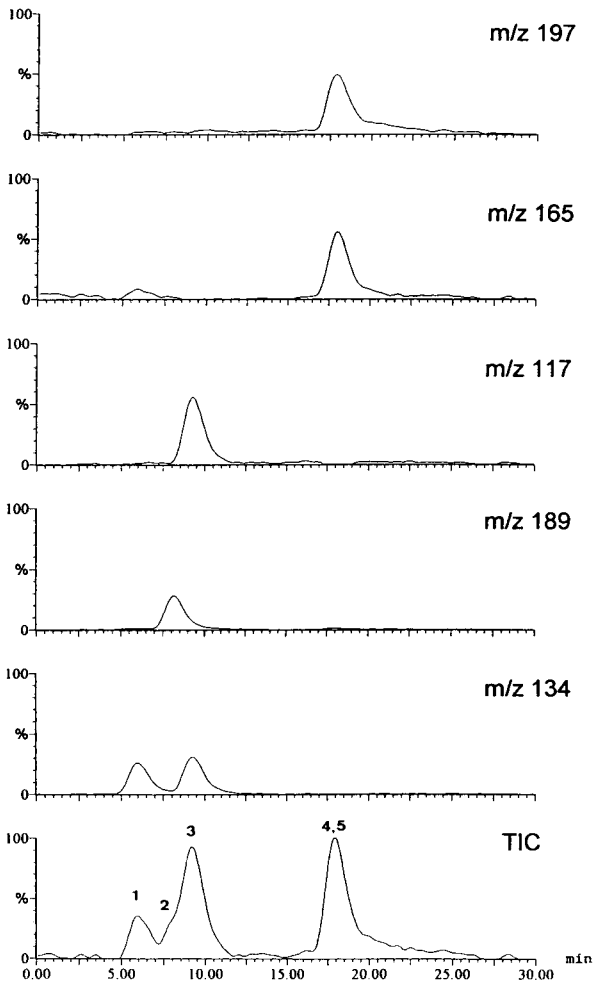

Fig. 7. HPLC–MS analysis in positive electrospray ionization of hydroxy-PAHs. The lower trace is the TIC obtained by summing all ions above. Components in the mixture were (1) 5-HI, (2) 2-H-1,4-NQ, (3) 1-HI, (4) 9-HFL and (5) 2-H-9-FLO.

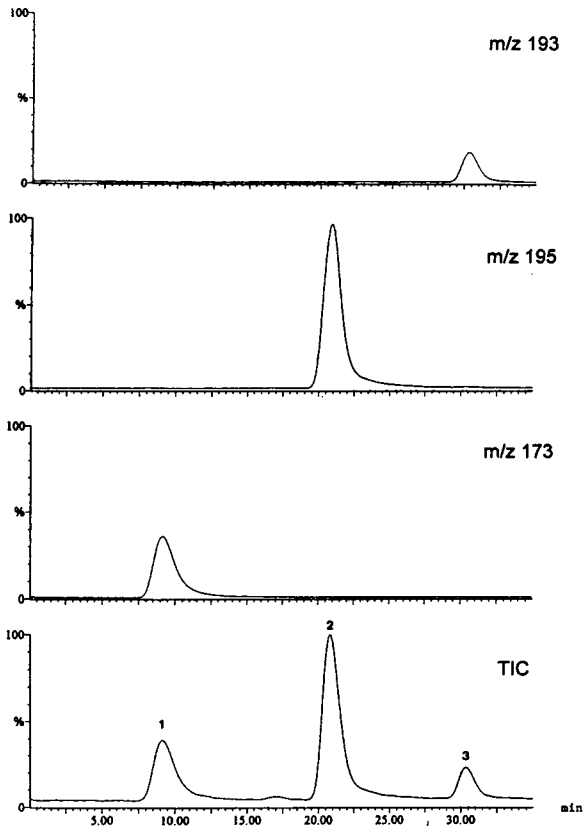

Fig. 8. HPLC–MS analysis in negative electrospray ionization of hydroxy-PAHs. The lower trace is the TIC obtained by summing all ions above. Components in the mixture were (1) 2-H-1,4-NQ, (2) 2-H-9-FLO and (3) 9-HF.

pounds (9-HFL, 1-HI) and $[M + 15]^+$ ion at m/z 189 for the 2-H-1,4-NQ were used. The reconstructed ion liquid chromatograms for each mass and the total ion chromatogram (TIC) are given in Fig. 7, showing that quantification at the 50-ng level is possible.

In negative ES the $[M - H]^-$ ion was monitored for each hydroxy aromatic compound 9-HF, 2-H-9-FLO and 2-H-1,4-NQ. The reconstructed-ion liquid chromatograms are shown in Fig. 8.

Negative ES showed lower background current and the response in negative ES was 15-fold that for the 2-H-9-FLO and 2-H-1,4-NQ than positive ES which would lead to improved sensitivity.

References

[1] M. Yamashita and J.B. Fenn, *J. Phys. Chem.*, 88 (1984) 4451.
[2] M. Yamashita and J.B. Fenn, *J. Phys. Chem.*, 88 (1984) 4471.
[3] J.B. Fenn, M. Mann, C.K. Meng, S.K. Wong and C.M. Whitehouse, *Science*, 246 (1989) 64.
[4] J.B. Fenn, M. Mann, C.K. Meng and S.K. Wong, *Mass Spectrom. Rev.*, 9 (1990) 37.
[5] R.D. Smith, J.A. Loo, C.G. Edmonds, C.J. Barinaga and H.R. Udseth, *Anal. Chem.*, 62 (1990) 882.
[6] E.C. Huang, T. Wachs, J.J. Conboy and J.D. Henion, *Anal. Chem.*, 62 (1990) 713A.
[7] M. Mann, *Org. Mass Spectrom.*, 25 (1990) 575
[8] C.M. Whitehouse, R.N. Dreyer, M. Yamashita and J.B. Fenn, *Anal. Chem.*, 57 (1985) 675.
[9] A.P. Bruins, T.R. Covey and J.D. Henion, *Anal. Chem.*, 59 (1987) 2642.
[10] T.R. Covey, R.F. Bonner, B.I. Shusham and J.D. Hennion, *Rapid Commun. Mass Spectrom.*, 2 (1988) 249.
[11] E.C. Huang and J.D. Henion, *J. Am. Soc. Mass Spectrom.*, 1 (1990) 158.
[12] J.A. Olivares, J.A. Nguyer, C.R. Yonker and R.D. Smith, *Anal. Chem.*, 59 (1987) 1230.
[13] R.D. Smith, J.A. Olivares, N.T. Nguyen and H.R. Udseth, *Anal. Chem.*, 60 (1988) 436.
[14] H.R. Udseth, J.A. Loo and R.D. Smith, *Anal. Chem.*, 60 (1988) 1948.
[15] I. Hayati, A.I. Bailey and T.F. Tadros, *J. Colloid Interface Sci.*, 117 (1987) 205.
[16] I. Hayati, A.I. Bailey and T.F. Tadros, *J. Colloid Interface Sci.*, 117 (1987) 222.
[17] R.J. Pfeifer and C.D. Hendricks, *AIAA J.*, 6 (1968) 496
[18] M.G. Ikonomou, A.T. Blades and P. Kebarle, *Anal. Chem.*, 63 (1991) 1989.
[19] G.J. Van Berkel, S.A. McLuckey and G.L. Glish, *Anal. Chem.*, 63 (1991) 2064.
[20] G.J. Van Berkel, S.A. McLuckey and G.L. Glish, *Anal. Chem.*, 64 (1992) 1586.
[21] J.V. Iribarne and B.A. Thomson, *J. Chem. Phys.*, 64 (1976) 2287.
[22] B.A. Thomson and J.V. Iribarne, *J. Chem. Phys.*, 71 (1979) 4451.
[23] B.A. Thomson, J.V. Iribarne and P.J. Dziedzic, *Anal. Chem.*, 54 (1982) 2219.
[24] J.V. Iribarne, P.J. Dziedzic and B.A. Thomson, *Int. J. Mass Spectrom. Ion Phys.*, 50 (1983) 331.
[25] M. Hemling, presented at the *38th ASMS Conference on Mass Spectrometry and Allied Topics, Tucson, AZ, June 1990.*
[26] B.D. Musselman, R.B. Tamura, R.B. Cody and D.B. Kassel, presented at the *39th ASMS Conference on Mass Spectrometry and Allied Topics, Nashville, TN, May 1991.*

[27] R.B. Cody, J. Tamura and B.D. Musselman, *Anal. Chem.*, 64 (1992) 1561.
[28] M.A. Baldwin and Langley, *Org. Mass Spectrom.*, 22 (1987) 561.
[29] C.E.M. Heeremanns, R.A.M. van der Hoeven, W.M.A. Niessen and J. van der Greef, *Org. Mass Spectrom.*, 24 (1989) 109.
[30] S.J. Stont and A.R. da Cunha, *Org. Mass Spectrom.*, 25 (1990) 187.
[31] J.F. Anacleto, R.K. Boyd, S. Pleasance, P.G. Sim and P. Thibault, presented at the *39th ASMS Conference on Mass Spectrometry and Allied Topics, Nashville, TN, May 1991.*
[32] E.C. Horning, M.G. Horning, D.I. Carroll, I. Dzidic and R.N. Stillwell, *Anal. Chem.*, 45 (1973) 936.
[33] D.I. Carroll, I. Dzidic, R.N. Stillwell, M.G. Horning and E.C. Horning, *Anal. Chem.*, 46 (1974) 706.
[34] I. Dzidic and J.A. McCloskey, *J. Am. Chem. Soc.*, 93 (1971) 4955.
[35] G.K. Chao and J.C. Suatoni, *J. Chromatogr. Sci.*, 20 (1982) 436.

ELSEVIER

Journal of Chromatography A, 683 (1994) 21–29

JOURNAL OF CHROMATOGRAPHY A

Determination of chlorophenols in drinking water samples at the subnanogram per millilitre level by gas chromatography with atomic emission detection

M.I. Turnes, I. Rodriguez, M.C. Mejuto, R. Cela*

Departamento de Química Analítica, Nutrición y Bromatología, Universidad de Santiago de Compostela, 15706 Santiago de Compostela, Spain

Abstract

The use of an atomic emission detector following a process of preconcentration of drinking water samples by a factor of 1500:1 allows the highly selective determination of chlorophenols present in samples below the maximum limit of 0.5 ng/ml set by international regulations. The preconcentration of the samples is carried out using 0.25-g commercial graphitized carbon cartridges without the need for sample derivatization prior to solid-phase extraction.

1. Introduction

Scientific interest in recent years has focused on the determination of trace levels of organic pollutants in natural waters and industrial effluents. The US Environmental Protection Agency [1] has drawn up a list of eleven phenolic compounds considered major pollutants. Chlorophenols are among the most toxic and carcinogenic of these.

In 1982 the European Community adopted the EC Priority Pollutants List that has been subsequently expanded and updated. Among the eleven phenols considered by EPA, only chlorophenols are in the EC list, although the maximum admissible concentration of phenols in water used for consumption has been set at 0.5 ng/ml [2].

For the individual compounds, EC regulations do not specify mandatory analytical methods. However, with the current analytical methods it is not possible to measure directly the phenols in drinking waters at the stipulated levels. This had led to the development of several analytical procedures making use of preconcentration and derivatization processes. Prior derivatization (esterification with acetic anhydride and treatments with alkylating reagents such as diazomethane or methyl iodide and with halogen-containing reagents such as pentafluorobenzyl bromide, pentafluorobenzoyl chloride and heptafluorobutyric anhydride of phenols prevents adsorption problems and improves peak shape and detectability, in most cases enhancing liquid- or solid-phase extraction recoveries [3–5]. For sample concentration, several workers have used liquid–liquid extraction with organic solvents [6–8]. As an alternative, solid-phase extraction processes have been examined, using different adsorbent materials, such as resins [9,10], a variety of bonded reversed phases [11–13] and graphitized carbon materials [14–16].

* Corresponding author.

0021-9673/94/$07.00
SSDI 0021-9673(94)00510-G

When dealing with waste-water samples, HPLC gives excellent results, but for drinking water gas chromatography (GC) is preferred [17,18]. However, when large volumes of water have to be processed to obtain high concentration factors, the final extracts tend to be rich in multiple organic compounds, producing chromatograms that are difficult to assess, when a non-specific detection method flame ionization detection (FID) is used and even with much more selective detectors such as the electron-capture detector. For this kind of sample GC–MS is often recommended [19], using targeted ^{13}C-labelled chlorophenols as internal standards. Up to 5 l of water sample can be concentrated by solid-phase extraction (SPE) after conversion of phenols into their acetates to avoid the low breakthrough volumes often exhibited by polar compounds in C_{18} cartridges.

In 1989 the first commercial instrument for atomic emission detection (AED) [20] was put on the market. GC–AED is a powerful tool when the species of interest contain some element that is not common to the other compounds of the matrix [21–24], as it allows for the specific determination of that particular element.

In this work, we studied the capability of CG–AED to detect and determine chlorophenols in drinking waters by carrying out a preconcentration process on SPE graphitized carbon cartridges. The proposed procedure has the inherent advantages of selectivity of detection for chlorinated compounds coupled with high sensitivity. This, together with the high degree of preconcentration obtained by graphitized carbon SPE cartridges, allows the necessary sensitivity levels to be reached to carry out the determination of these compounds within the legal limits that have been established without the need for sample derivatization and a specialized internal standard.

2. Experimental

2.1. Reagents

The reagents used (methanol, dichloromethane, formic acid) (Merck, Darmstadt, Germany) were of the maximum purity available. In the preconcentration process, commercial cartridges of graphitized carbon black, Supelclean, ENVI-Carb SPE of 0.25 g (Supelco, Bellafonte, PA, USA) and octadecyl (C_{18})-bonded silica Mega Bond Elut (Varian, Sunnyvale, CA, USA) and Environmental Sep-Pak Plus (Millipore–Waters, Milford, MA, USA) cartridges were used.

Standards of the different chlorophenols to be determined, 2-chlorophenol (2CP), 2,4-dichlorophenol (24DCP), 4-chloro-3-methylphenol (4C3MP), 2,4,6-trichlorophenol (246TCP) and pentachlorophenol (PCP), were supplied by Merck and Aldrich (Milwaukee, WI, USA). Stock standard solutions (4.0 mg/ml) were prepared of each separately in methanol. From these solutions, kept in a dark, refrigerated environment, the corresponding working standard solutions to be used in spiking samples were obtained by dilution with methanol. Those to be used as calibrants were dissolved in dichlorometane –methanol (90:10, v/v), 0.25 *M* in formic acid.

2.2. Apparatus

The analyses were carried out using a Hewlett-Packard (Avondale, PA, USA) Model 5890 Series II gas chromatograph, equipped with a split–splitless injection port and a microwave-induced plasma atomic emission detector (Hewlett-Packard Model 5921A). All the system was controlled by a CG–ECD Chemstation (HP 35920A). A Scientific Glass Engineering (Ringwood, Victoria, Australia) BP-5 (50 m × 0.32 mm I.D.) methylphenylsilicone capillary column, 1 μm film thickness, was used in all experiments. Helium (99.9999%) was used as the carrier gas. The quantification of peaks was carried out by bracketing standards. The optimum parameters for the determination of the compounds under study are shown in Table 1.

2.3. Sample preparation

Before processing the water samples, the cartridge must be conditioned. First, it is washed with 5 ml of dichloromethane–methanol (80:20, v/v), 2 ml of methanol and 15 ml of a 10 g/l

Table 1
CG–AED conditions for the separation of chlorophenols.

GC parameters	
Injection port	Split–splitless
Purge time on	200 s
Injection port temperature	250°C
Injection volume	2 μl
Column head pressure	135 kPa
Split flow	6.4 ml/min
Over temperature programme	
Initial temperature	80°C
Rate	15°C/min
Final temperature	250°C
Final time	10 min
AED parameters	
Transfer line temperature	260°C
Cavity block temperature	260°C
Wavelengths	Chlorine 480.192 nm
	Carbon 495.724 nm
Helium make-up flow	44.4 ml/min
Ferrule purge	28 ml/min
Spectrometer purge flow	2 l/min (N_2)
Solvent vent beginning	2.5 min
Solvent vent end	7.2 min
Reagent gas	Oxygen

solution of ascorbic acid in HCl-acidified ultrapure water at pH 2. This acidic treatment, described by Di Corcia and Marchetti [25], is necessary to reduce the quinone groups to hydroquinone, which are less reactive. The presence of these quinone groups as impurities in the carbon surface may cause irreversible adsorption of certain compounds, including some of the phenols studied in this work.

The drinking water samples or the spiked samples are forced through the cartridge at a flow-rate of 10–15 ml/min with the help of vacuum membrane pumps. The cartridge is then washed with 7 ml of HCl-acidified ultrapure water (pH3), rinsing slowly. After large volumes of water have been flushed through, shrinking of the sorbent bed may occur. When this happens, before the washing stage, the upper polypropylene frit is pressed against the bed. This helps by the elimination of the water and makes the eluent system more effective, as it flushes through the carbon bed more homogeneously [26]. Finally, 1 ml of methanol is flushed through very slowly in order to eliminate the residual water. Dry air is blown through the cartridge for 5 min with the same pumps as used for the suction of the samples.

The cartridge is eluted with 8 ml of a 0.25 *M* formic acid solution in dichloromethane–methanol (90:10, v/v). This final extract is concentrated on a Turbo Vap II concentration workstation (Zymark) by means of a 55 kPa nitrogen current and a 30°C water-bath until it reaches a final volume of ca. 0.5 ml. To ensure repeatable results, it is diluted to exactly 1 ml. The extract is then ready to be injected into the GC–AED system.

3. Results and discussion

Under the working conditions described in Table 1, the separation of the five chlorophenols under study is very good. Fig. 1 show the chlorine (479.53-nm line) and carbon (495.71-nm line) traces of a sample of 500 ml of ultrapure water (Milli-Q water), spiked with the five compounds under study at a level of ca. 2 ng/ml each, when submitted to the whole experimental procedure described. In the chromatogram monitored at the chlorine line (Fig. 1a) there were only five peaks corresponding to the five phenols added. The signal corresponding to the carbon emission line (Fig. 1b) produces a chromatogram relatively more complicated with a large number of peaks. In this case, accurate quantification of the species under study is possible except for 2-chlorophenol and 4-chloro-3-methylphenol, which overlap other small peaks. In Fig. 1 it is also evident that the chromatographic conditions used can be modified to speed up the analysis, provided that AED is used and that no other di-, tri- or tetrachlorophenols could be expected to be present in the samples. However, the conditions in Table 1 were finally adopted to ensure that the 2CP peak did not fall into the solvent vent time-window.

Obviously, the situation with a surface or drinking water sample is much more difficult. The chromotograms in Fig. 2 correspond to the analysis of 1-l tap water samples. In Fig. 2a the chlorine traces for the unspiked sample and a sample spiked with the five species (1–2 ng/ml

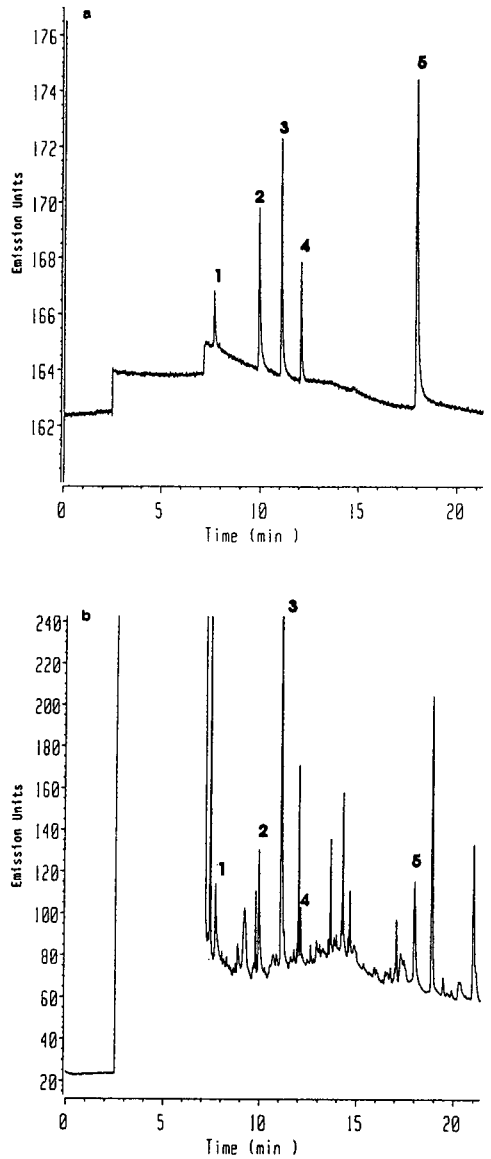

Fig. 1. Chromatograms for the Cl479-nm and C496-nm emission lines of a chlorophenol standard solution analysed by the proposed procedure. (a) Trace of chlorine line; (b) trace of carbon line. Peaks: 1 = 2CP (3.2 ng/ml); 2 = 24DCP (3.2 ng/ml); 3 = 4C3MCP (6.4 ng/ml); 4 = 246 TCP (1.6 ng/ml); 5 = PCP (9.9 ng/ml). For operating conditions, see Table 1.

each) have been superimposed to show the differences more clearly. Fig. 2b depicts the carbon trace for the unspiked sample and Fig. 2c the chromatogram obtained when analysing the spiked sample but using FID. The advantages of using AED become clear from the comparison of these chromatograms.

Under the conditions described under Experimental, the quantification limits (signal-to-noise ratio = 10) in water samples were 2CP 0.12, 24DCP 0.08, 4C3MP 0.15, 246TCP 0.07 and PCP 0.48 ng/ml. Therefore, the proposed procedure allows for the accurate quantification of the five species on an individual basis below the limits stipulated by the international regulations. On the other hand, calibration graphs for all five species show good linearity in the range 0.1–10 μg/ml, provided that consistent inertness of the chromatographic system is ensured. However, we found that the column degraded rapidly when routine injections of extracts were carried out. As it is very difficult to find appropriate internal standards that match adequately the inertness differences in the system for all the species considered, it is advisable to use the bracketing standard technique for quantitative measurements.

3.1. Sample preparation and extract concentration

There have been many studies of the use of the solid–liquid extraction technique (SPE) for the concentration of aqueous phenol samples. In fact, chlorophenols have been used as model compounds in many SPE studies [27–29]. Most of these studies were focused on the use of two types of adsorbents: C_{18}-bonded silica and graphitized carbon black materials.

Although the aim of this work was to develop a procedure capable of quantifying chlorophenols at concentrations under 0.5 ng/ml without the need for any derivatization step, some data were obtained comparing the efficiency and some practical aspects of the two adsorbents in concentrating aqueous samples of chlorophenols. Table 2 shows the recoveries of the five chlorophenols with both types of sorbents. The data in Table 2 are the averages of four independent experiments measured in duplicate. With GCB cartridges, experiments with sample volumes of 2 l were also carried out. Although the recoveries

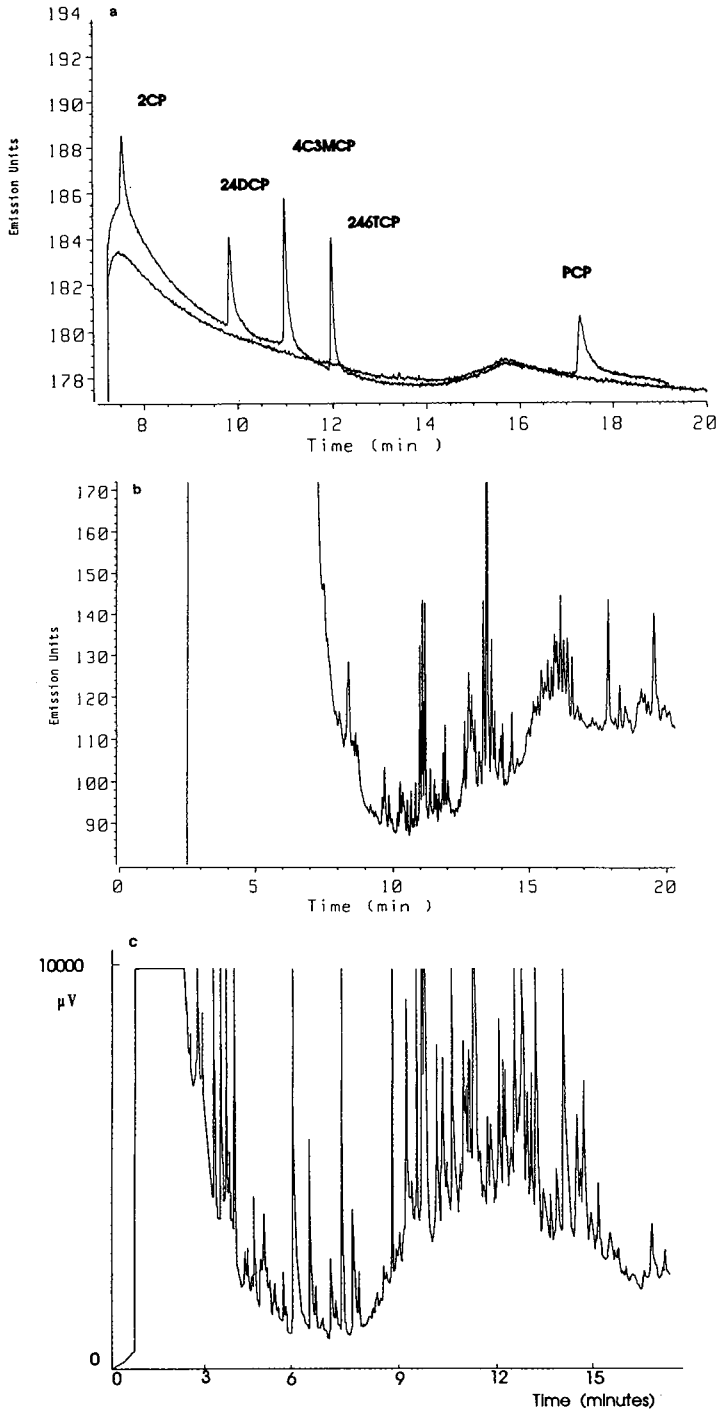

Fig. 2. Chromatograms of a tap water sample. (a) Superimposed traces of chlorine line for an unspiked sample (lower trace) and a spiked sample (upper trace). (b) Carbon trace for the unspiked sample. (c) FID trace for the spiked sample. Peaks as in Fig. 1; operating conditions as in Table 1.

Table 2
Recoveries of the chlorophenols using graphitized carbon black and C_{18} cartridges.

Compound	Concentration range in samples (ng/ml)	Recovery (%)[a]				
		GCB cartridges			C_{18} cartridges	
		Sample volume (ml)			Sample volume (ml)	
		500	1000	1500	250	500
2CP	1–3	70 ± 7	87 ± 14	73 ± 9	40 ± 5	37 ± 8
24DCPO	0.5–3	100 ± 4	107 ± 17	97 ± 10	107 ± 14	96 ± 4
4C-3MCP	0.5–6	88 ± 1	87 ± 12	92 ± 9	80 ± 12	114 ± 13
246TCP	0.2–1.5	83 ± 3	97 ± 12	97 ± 10	86 ± 6	89 ± 15
PCP	0.5–20	76 ± 9	95 ± 18	100 ± 14	48[b]	nd[c]

[a] Values corrected for evaporation losses.
[b] Only two measurements were carried out.
[c] Not detected.

obtained were not significantly lower than those shown in Table 2, greater variability in the results was found. Hence 1.5 l of sample were considered a practical limit for the proposed procedure. We also examined the recovery for various chlorophenol concentrations in sample volumes of 1.5 l, and found no noticeable differences in the recoveries and repeatability. However, the data in Table 2 show poor precision of the measurements. This can be attributed mainly to the evaporative concentration stage.

As cartridge eluates have to be concentrated under a nitrogen flow at a temperature similar to that found in the laboratory, we proceeded to evaluate the possible losses that this process might entail. These losses were measured by preparing a standard solution of the five phenols studied in the same solvent as used to extract the carbon cartridges. Aliquots of 8 ml of this solution were concentrated until a final volume of ca. 0.5 ml was reached, then diluted to 1 ml and injected into the chromatograph. The results suggested that substantial evaporation losses (30–40 ± 10%) occur for all the species considered. Other similar evaporation control experiments (with the same evaporation device) carried in our laboratory [30], which among others included the same species here considered but dissolved in hexame, did not show noticeable losses except for 2-chlorophenol. Therefore, evaporation losses cannot be attributed to defective running of the evaporation device and the solvent used must have a critical role in the observed losses. Although the losses, being almost constant for all the species, can be compensated for at the time of calculating chlorophenol concentrations in the samples, it is evident from Table 2 that the variability of evaporation losses determines the variance of the final results. Evaporation losses are clearly the weakest aspect of the proposed procedure and will need to be improved.

Another point in Table 2 is to appreciate that once corrected for evaporative losses, all the species studied except 2-chlorophenol shows recoveries higher than 90% with GCB cartridges. For 2-chlorophenol we checked that no breakthrough took place under the described conditions, by using two cartridges in series. Although we have no clear explanation for the observed virtually constant losses of 2-chlorophenol, this can be attributed also to evaporation losses. According to Borra et al. [15], drastic losses of 2-chlorophenol occur when evaporating solutions that had been made alkaline.

Regarding the C_{18} data in Table 2, another practical aspect has to be considered. Here the aqueous samples containing chlorophenols were

acidified with 0.1 *M* HCl until they reached a pH of ca. 2.5–3, before passing through the C_{18} cartridges. Cartridge elution was carried out using a hexane–ethanol (79:21) azeotrope. Under these conditions, complete recoveries for 24DCP, 4C3MP and 246TCP were obtained, provided that the sample volume did not exceed 500 ml, in which case breakthrough occurred, making the recoveries much poorer. The low recovery of 2CP has to be attributed to the low breakthrough volumes that have been shown [10] for monochlorophenols. On the other hand, the low recovery of PCP can be justified by the relatively high pH of samples. Complete recovery of PCP can be obtained by acidifying the samples to below pH $\approx$ 2. However, when highly

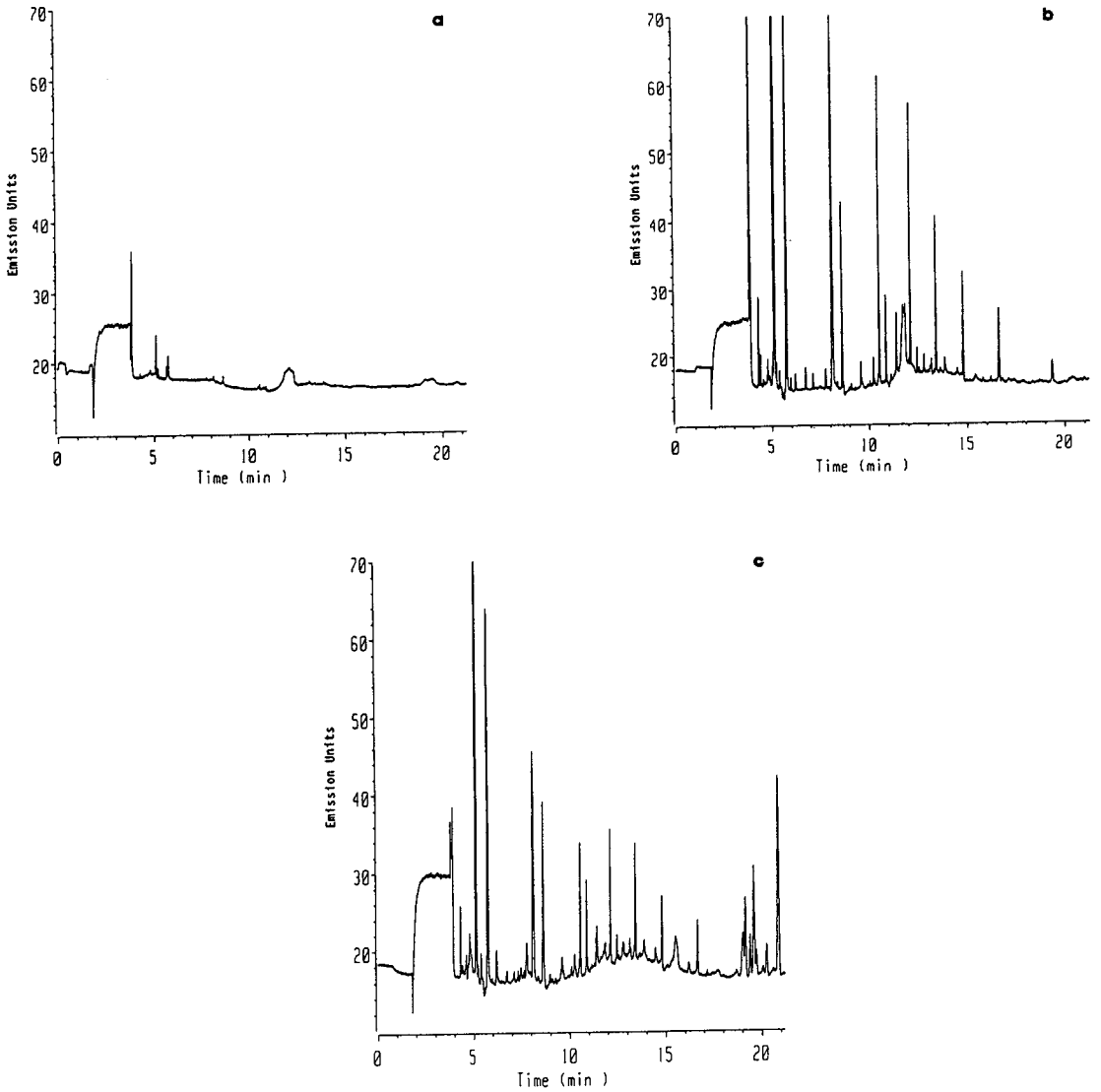

Fig. 3. Chromatograms for the Si252-nm emission line of (a) a solvent injection, (b) an acidified sample of Milli-Q water flushed through a Mega Bond Elut C_{18} cartridge and (c) the same type of sample flushed through a Sep-Pak Plus C_{18} cartridge. All the chromatograms were obtained using the same operating conditions (see Table 1).

acidic samples are concentrated in C_{18} cartridges appreciable amounts of silica can be dissolved. In fact, we have sometimes observed that concentrated extracts of samples acidified to pH 1.5–2 and stored in a refrigerator for several weeks develop a fine, white, cloudy precipitate. Also, we have observed previously that the inertness of the column and injection port quickly degrades when repeated injections of these types of extracts were carried out. In Fig. 3 AED traces corresponding to the silicon emission line for a blank (solvent) (Fig. 3a) and an acidic sample concentrated by means of C_{18} Mega Bond Elut (Fig. 3b) and Sep-Pak Plus (Fig. 3c) cartridges can be compared. It is evident that the silicon signals in the sample chromatograms cannot be attributed to column bleeding. The conclusion was that the proper pH control necessary to ensure good recoveries of PCP with C_{18} cartridges would have adverse effects on the inertness of the chromatographic system and column lifetime. When using GCB cartridges it is obvious that this effect cannot arise and pH control of the samples is not a critical factor regarding the retention of chlorophenols, making its use advantageous instead of C_{18} cartridges.

4. Conclusions

With the quantification limits obtained, the reported method allows the determination of chlorophenols in drinking water samples at levels below 0.5 ng/ml without derivatization. It is of little use to monitor the chromatograms obtained using the carbon emission line in AED or to use FID. However, the chromatogram obtained from the chlorine emission line clearly reveals the presence of the peaks corresponding to chlorophenols. The concentration of the extracts results in losses that are higher than those in the solid-phase extraction process with GCB cartridges and leads to most of the variability found in the results. Hence, improvements to this stage of the analytical process are necessary in order to obtain full benefits of the proposed procedure.

Acknowledgement

This work was supported by the Spanish Interministerial Commission for Science and Technology (project PB92-0372).

References

[1] L.H. Keith (Editor), *Compilation of Sampling Analysis Methods*, US Environmental Protection Agency, Boca Raton, FL, 1991, pp. 389–486.
[2] *Directica 80/77/CEE 15-7-1990; Diario Oficial de las Comunidades Europeas 30-8-1990*, European Community, Brussels, 1990.
[3] J. Drozd, *Chemical Derivatization in Gas Chromatography*, Elsevier, Amsterdam, 1981, Section 5.1, pp. 84–91.
[4] W. Fresenius, K.E. Quentin and W. Schneider (Editors), *Water Analysis*, Springer, Berlin, 1988, Section 4.2, pp. 555–558.
[5] J. Hajslova, V. Kocourek, I. Zemanova, F. Pudil and J. Davidek, *J. Chromatogr.*, 439 (1988) 307–316.
[6] R.T. Coutts, E.E. Hargesheuner and F.M. Pasutto, *J. Chromatogr.*, 179 (1979) 291–299.
[7] J. Knuutinen, *J. Chromatogr.*, 209 (1981) 446–450.
[8] N.D. Bedding, A.E. McIntyre, J.N. Lester and R. Perry, *J. Chromatogr. Sci.*, 26 (1988) 597–605.
[9] B. Gawdik, B.H. Czerwinska, *J. Chromatogr.*, 509 (1990) 135–140.
[10] L. Schmidt, J.J. Sun, J. Fritz, D.F. Hagen, C.G. Markell and E.E. Wisted, *J. Chromatogr.*, 641 (1993) 57–61.
[11] C.E. Werkhoven-Goewie, U.A.T. Brinkman and R.W. Frei, *Anal. Chem.*, 53 (1981) 2072–2080.
[12] L. Renberg and K. Lindstrom, *J. Chromatogr.*, 214 (1981) 327–334.
[13] S.A. Schuette, R.E. Smith, L.R. Holdan and J.A. Graham, *Anal. Chim. Acta*, 236 (1990) 141–144.
[14] T.A. Bellar and W.L. Budde, *Anal. Chem.*, 60 (1988) 2076–2083.
[15] C. Borra, A. Di Corcia, M. Marchetti and R. Samperi, *Anal. Chem.*, 58 (1986) 2048–2052.
[16] A. Di Corcia, S. Marchese and R. Samperi, *J. Chromatogr.*, 642 (1993) 163–174.
[17] R.L. Grob, *Chromatographic Analysis of the Environment*, Marcel Dekker, New York, 1983.
[18] B.K. Afghan and A.S.Y. Chau, *Analysis of Trace Organics in the Aquatic Environment*, CRC Press, Boca Ratou, FL, 1991, pp. 131–140.
[19] R. Soniassy, P. Sandra and C. Schlett, *Water Analysis. Organic Micorpollutants*, Hewlett-Packard, Waldbronn, 1994, Ch. 6.
[20] R.L. Firor, *Am. Lab.*, 21 (1989) 40–48.

[21] H. Uchida, A. Berthodt and J.D. Winefordner, *Analyst*, 115 (1990) 933–937.
[22] K.-C. Ting and P. Kho, *J. Assoc. Off. Anal. Chem.*, 74 (1991) 991–998.
[23] R. Lobinski, W.R. Dirkx, M. Ceulemans and F. Adams, *Anal. Chem.*, 64 (1992) 159–165.
[24] R. Lobinski, F. Adams, *Trends Anal. Chem.*, 12 (1993) 41–49.
[25] A. Di Corcia and M. Marchetti, *Anal. Chem.*, 63 (1991) 580–585.
[26] A. Di Corcia, S. Marchese and R. Samperi, *J. Chromatogr.*, 642 (1993) 175–184.
[27] E. Forgacs, T. Cserhati and B. Bordas, *Chromatographia*, 36 (1993) 19–26.
[28] G. Marko-Varga and D. Barcelo, *Chromatographia*, 34 (1992) 146–154.
[29] V. Coquart and M.C. Hennion, *J. Chromatogr.*, 600 (1992) 195–201.
[30] C. Casais and R. Cela, unpublished results.

ELSEVIER

Journal of Chromatography A, 683 (1994) 31–44

JOURNAL OF CHROMATOGRAPHY A

High-performance liquid chromatography of phenolic aldehydes with highly selective fluorimetric detection by means of postcolumn photochemical derivatization

M. Lores, C.M. García, R. Cela*

Departamento de Química Analítica, Nutrición y Bromatología, Facultad de Química, Universidad de Santiago de Compostela, Avda. de las Ciencias s/n, 15706 Santiago de Compostela, Spain

Abstract

Postcolumn photochemical derivatization was used in the HPLC with fluorimetric detection of polyphenolic aldehydes in samples which also have present phenolic acids at higher concentrations. This is the most common situation in many food and agricultural samples. Phenolic aldehyde photoproducts give highly sensitive fluorescent signals whereas for some phenolic acids with native fluorescence this property disappears as a consequence of the photoreaction. Individual parameters for each polyphenolic photoproduct (excitation and emission wavelength) were investigated, which allowed the resolution of complex mixtures to be optimized. The selectivity can be improved even further by means of time-programmed changes in the excitation/emission wavelength pairs in the fluorescence detector during the chromatographic elution.

1. Introduction

The term "phenolic" or "polyphenol" can be defined chemically as a substance that possesses an aromatic ring bearing one or more hydroxyl substituents, including functional derivatives (esters, methyl ethers, glycosides, etc.) [1]. Phenolic compounds are closely related to the sensory and nutritional quality of fresh and processed plant foods and their analytical control have been of growing interest in recent years because many phenolic compounds in foods seem to have inhibitory effects on mutagenesis and carcinogenesis [2]. The role of such compounds in oenology has been widely demonstrated [3,4]. They affect the quality of wines, in both positive and negative ways.

The determination of such compounds is usually carried out by separation by gradient high-performance liquid chromatography (HPLC) with UV detection [5], although there have been some studies using electrochemical [6–8] and fluorimetric detection [9,10].

In recent years, photochemical postcolumn derivatization had led to improvements in selectivity and sensitivity in the detection of several types of compounds. The advantages of using this type of postcolumn reactor have now been clearly demonstrated [11–17]. Several papers [18–20] have described simple techniques for the construction of these reactors, which are also available commercially [21]. Cela et al. [22] have published data about the applicability of a lab-

* Corresponding author.

0021-9673/94/$07.00
SSDI 0021-9673(94)00519-F

oratory-made photochemical reactor to improve the UV detection and identification possibilities of a large number of polyphenolic species separated by HPLC. These results suggest that many of these species undergo photochemical changes that can be used to improve detectability not only UV absorption [22] but also by fluorimetric and electrochemical methods [23].

In most food and agricultural derived materials, phenolic acids appear in a high concentrations in comparison with phenolic aldehydes. The absorption spectra of both phenolic families are very similar. Normally, the determination of the aldehydes is strongly hampered by overlapping acid peaks when the chromatographic system cannot resolve completely the mixtures in natural samples, which is the most common situation. However, the fluorescence response of phenolic aldehydes generally increases after photochemical reaction, whereas most phenolic acids show the opposite behaviour. Therefore, by optimizing the individual parameters of each type of compound in the fluorimetric detector, this effect can be used to detect and determine aldehydes selectively in the presence of relatively large amounts of acids.

In this paper, the results of such a study covering 36 polyphenolic species (22 phenolic acids and 14 phenolic aldehydes) are presented.

2. Experimental

All of the standards of the 36 polyphenolic species (22 acids and 14 aldehydes) used in this study were of purity 97% from Merck (Darmstadt, Germany) and Fluka (Buchs, Switzerland). All solutions were prepared in methanol (HPLC grade, Merck)–water [purified with a (Milli-Q Millipore, Milford, MA, USA)] (1:1) in the 10–100 ppm range. Fluorescence spectra of all the standards were measured by means of a Kontron (Zurich, Switzerland) Model SFM23 spectrofluorimeter, sweeping the spectral region between 20 and 30 nm over the absorption maximum wavelength and 700 nm.

Methanol and HPLC-grade water both containing 0.5% formic acid (95%; Merck) were used as solvents in gradient elution. As we have already shown [22], formic acid run better than acetic acid and other acids when photochemical derivatization has to be carried out. Mixtures of the species studied were eluted using the multisegmented gradient depicted in Table 1; the retention times and capacity factors of the polyphenolic compounds are given in Table 2. The injection volume was always 15 μl, except for 10 μl when the flow-injection analysis (FIA) mode was used. All UV chromatograms were recorded over the range 230–450 nm with 2.0-nm resolution.

The experimental set-up consisted of a pump (Waters–Millipore Model 600), a universal injector (Waters Model U6K), a reversed-phase chromatographic column (Waters Novapack C_{18}, 15 cm × 3.9 mm I.D.; 4 μm) and a second injection valve (Model 7010; Rheodyne, Cotati, CA, USA) fitted with a 10-μl loop for injections in the FIA mode, a laboratory made photoreactor and a pair of detectors in series.

Diode-array (Waters Model 990+) and fluorescence programmable (PU4027, Philips, Cam-

Table 1
Gradient programme used for the elution of complex mixtures of polyphenolic compounds (A = water; B = methanol)

Time (min)	Flow-rate (ml/min)	A (%)	B (%)	Curve[a]
0	1.00	95	5	–
5	1.00	95	5	10
20	1.00	70	30	9
30	1.00	60	40	9
40	1.00	55	45	9
50	1.00	50	50	9

[a] Numbers of gradient curves correspond to pre-programmed gradient profiles on the Waters M600 pump.

Table 2
Retention times and capacity factors of the polyphenolic standards under the elution conditions described under Experimental

No.	Compound	t_R (min)[a]	k'
1	3,4,5-Trihydroxybenzoic (gallic) acid	2.94	1.16
2	2,4,6-Trihydroxybenzoic (protocatechuic) acid	3.19	1.35
3	2,6-Dihydroxybenzoic (γ-resorcylic) acid	4.55	2.35
4	3,4-Dihydroxibenzoic acid	5.18	2.81
5	3,5-Dihydroxybenzoic (α-resorcylic) acid	6.26	3.60
6	3,4-Dihydroxybenzaldehyde (protocatechualdehyde)	7.52	4.53
7	4-Hydroxybenzoic acid	9.02	5.63
8	2,5-Dihydroxybenzoic (gentisic) acid	9.9	6.28
9	2,5-Dihydroxybenzaldehyde	10.82	6.96
10	4-Hydroxybenzaldehyde	11.59	7.52
11	3-Hydroxybenzoic acid	12.67	8.32
12	3-Hydroxybenzaldehyde	12.97	8.54
13	2,4-Dihydroxybenzoic (β-resorcylic) acid	14.3	9.51
14	4-Hydroxy-3-methoxybenzoic (vanillic) acid	16.63	11.23
15	2,6-Dimethoxybenzoic acid	21.47	14.79
16	2-Hydroxybenzaldehyde (salicylaldehyde)	21.47	14.79
17	3,4-Dihydroxycinnamic (caffeic) acid	22.64	15.65
18	4-Hydroxy-3-methoxybenzaldehyde (vanillin)	23.51	16.29
19	3-Hydroxy-4-methoxybenzaldehyde (isovanillin)	25.66	17.87
20	4-Hydroxy-3,5-dimethoxybenzoic (syringic) acid	28.81	20.18
21	2-Hydroxy-3-methoxybenzaldehyde (*o*-vanillin)	30.29	21.27
22	3,5-Dimethoxy-4-hydroxybenzaldehyde	30.94	21.75
23	4-Hydroxycinnamic (*p*-coumaric) acid	30.94	21.75
24	3-Hydroxycinnamic (*m*-coumaric) acid	32.67	23.02
25	4-Hydroxy-3-methoxycinnamic (ferulic) acid	33.24	23.44
26	3-Methoxybenzaldehyde (*m*-anisaldehyde)	33.47	23.61
27	3,4-Dimethoxybenzaldehyde (veratraldehyde)	33.47	23.61
28	3,4-Dimethoxybenzoic (veratric) acid	33.59	23.70
29	2,4-Dimethoxybenzoic acid	33.59	23.70
30	3,5-Diemthoxy-4-hydroxycinnamic (sinapic) acid	34.59	24.43
31	2-Hydroxycinnamic (*o*-coumaric) acid	34.59	24.43
32	3,4,5-Trimethoxybenzaldehyde	35.59	25.17
33	2,4-Dimethoxybenzaldehyde	37.3	26.43
34	3,5-Dimethoxybenzaldehyde	38.81	27.54
35	3,5-Dimethoxybenzoic acid	39.45	28.01
36	3,4,5-Trimethoxycinnamic acid	40.83	29.02

[a] Dead time for column (t_0) = 1.36 min.

bridge, UK) having independent data acquisition and control systems. The specific conditions for each analysis are specified in Section 3 or in the figure captions. A complete scheme of this experimental device has been published elsewhere [22,23], and it is reproduced in Fig. 1.

The 6 m × 0.3 mm I.D. PTFE (Supelco, Bellefonte, PA, USA) tubing knitted coil photoreactor was constructed according the method of Poulsen et al. [20] as described elsewhere [22]. The knitted coil photoreactor was placed inside a mirror prism which allowed good light reflection and efficient air-cooling ventilation.

3. Results and discussion

3.1. Preliminary experiments

As a first step, the absorption and fluorescence spectra of all the compounds under study were measured. In Fig. 2a and b the spectra for

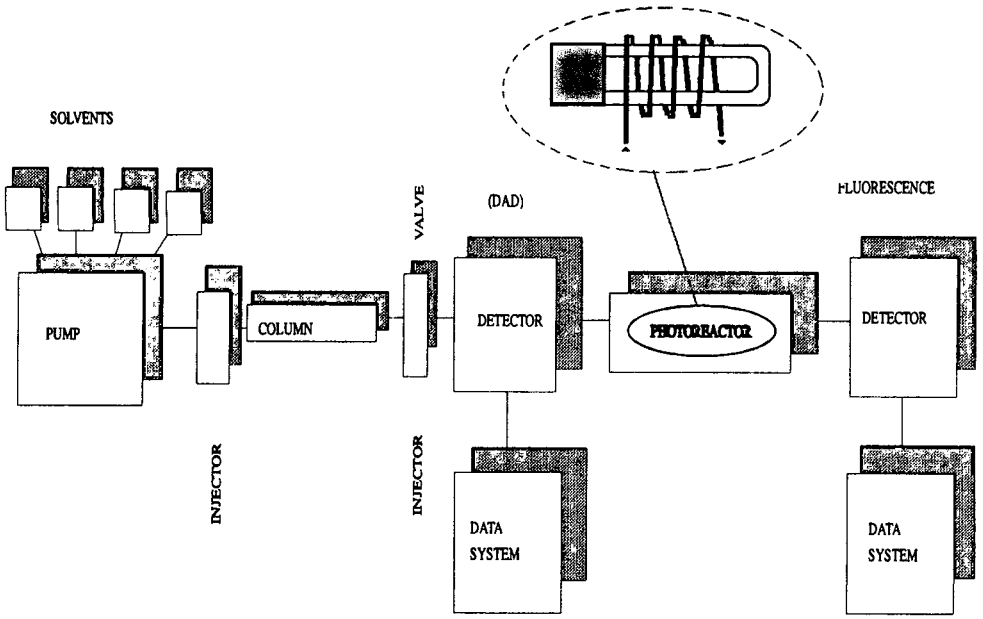

Fig. 1. Scheme of the experimental device with detail of the lamp shape.

salicylaldehyde (taken as a typical example in order to depict the complete process) are shown.

The next step was to determine each individual compound in the FIA mode, connecting the pump to the photoreactor and the fluorescence detector (Fig. 2c). The carrier was water–methanol (70:30) at a constant flow-rate of 1 ml/min. Higher proportions of methanol should be avoided because interferences appear in some spectral regions.

Each standard was injected four times, as can be seen in Fig. 2c. In the first two injections the photoreactor was turned off and in the last two injections it was turned on. This process was repeated for each excitation/emission maxima pairs for standards having more than one excitation/emission pair. Some of the species studied, seven acids (gallic, 3-hydroxybenzoic, 2,4,6-tridroxybenzoic, 4-hydroxycinnamic, 2,6-dihydroxybenzoic, *m*-coumaric and caffeic) and two aldehydes (2,5- and 3,5-dihydroxybenzaldehyde) neither showed native fluorescence nor acquired it after undergoing the photoreaction. Four different patterns were observed for the remaining compounds: some fluorescent species lost this property; others with no natural fluorescence acquired it; and the remaining showed both negative and positive changes in their original fluorescence intensity. The results obtained in this step are summarized in Table 3, showing only those excitation and emission wavelengths for which more significant changes were observed.

It must be emphasized that the lamp power plays a very important role in the photoreaction of phenolic species. As far as we know, all commercial photoreactors mount 8-W low-pressure mercury tube lamps. Although some commercial devices mount the knitted coil in front of the lamp [24], often the knitted coil is fitted around the tube lamp in order to exploit the maximum lamp radiation and minimize the coil length. The laboratory-made photoreactor used in all the experiments described in this paper has an Osram HSN10/Uafr lamp (Perez Antolin, Santiago, Spain) having a nominal power of 10 W with the shape depicted in Fig. 1. Also laboratory-made knitted coils were used used in all instances. However, when the knitted coil has to be replaced with a new one, we have occasionally encountered significant differences in the results obtained. In these instances the new coil

was discarded and a new one fitted in order to guarantee consistent performance of the photoreactor. In an attempt to avoid coil-to-coil variations we decided to try a commercial knitted tubing coil (Astec 89502; Tecknokroma, Barcelona, Spain), but it cannot be fitted over the lamp owing to its inner hole size. In fact, this knitted reactor only allows the use of the nar-

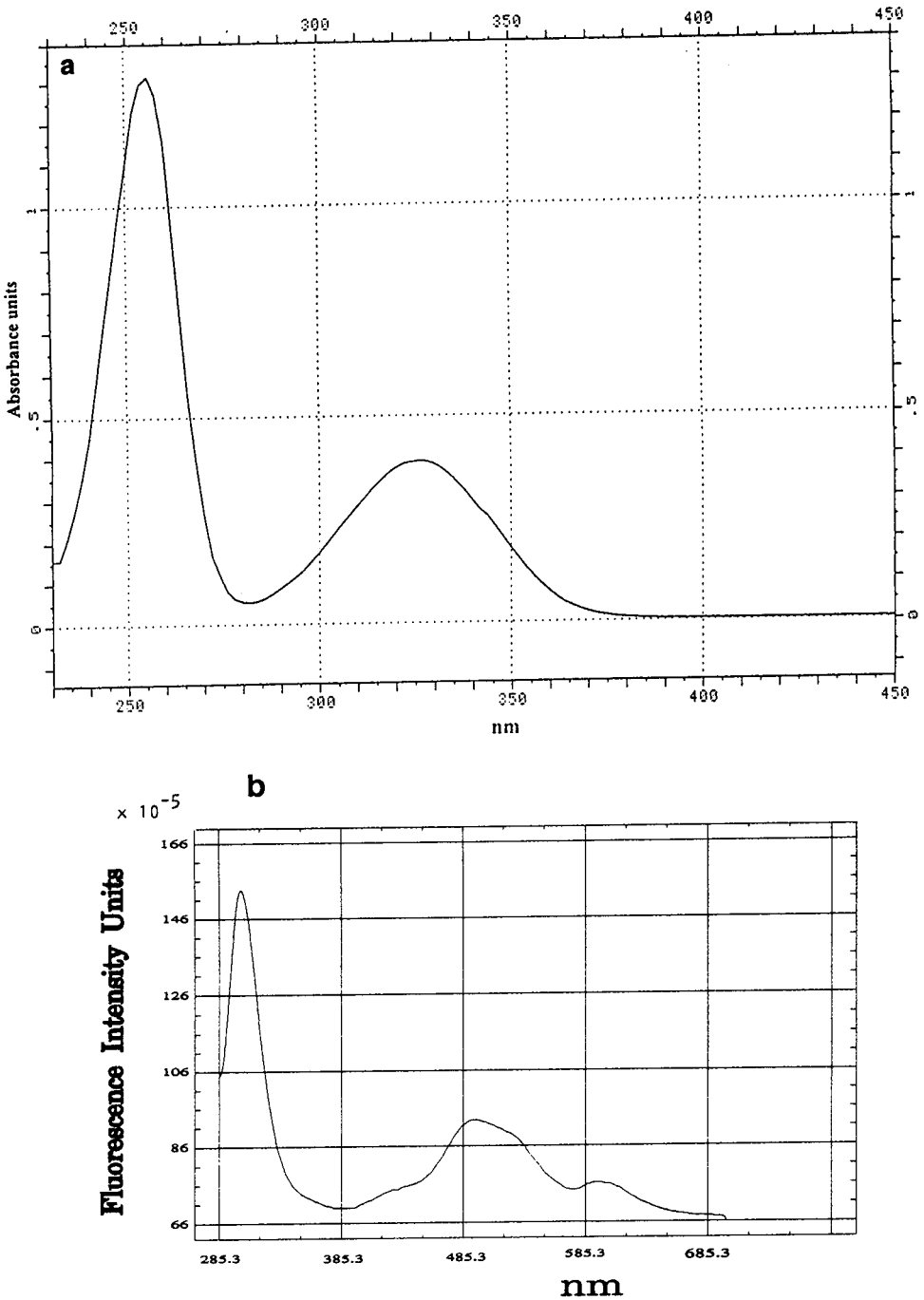

Fig. 2. *(Continued on p. 36)*

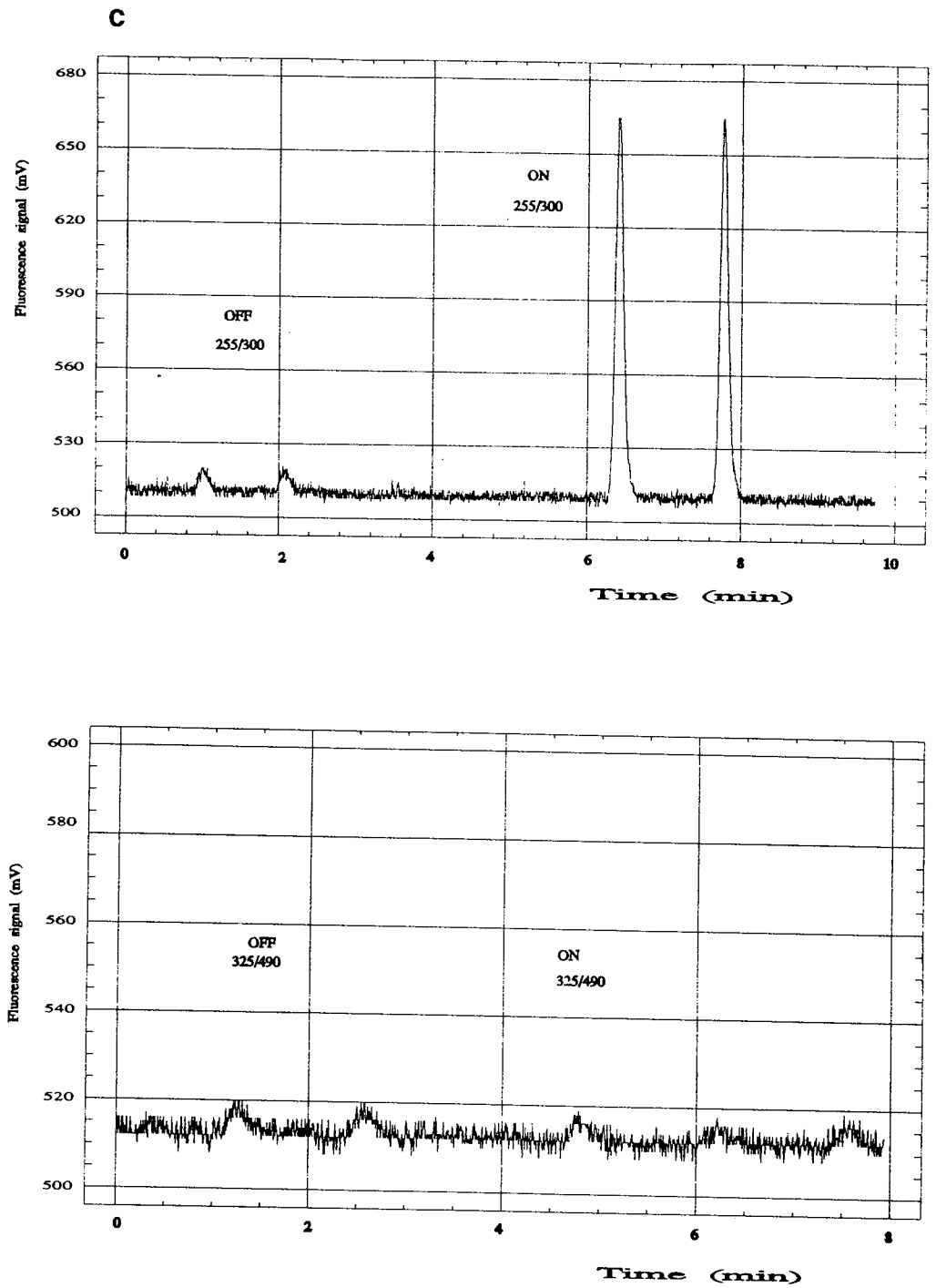

Fig. 2. Example of the steps followed in the analysis of polyphenolic standards 2-hydroxybenzaldehyde (salicylaldehyde). (a) Absorption spectrum; (b) emission spectrum; (c) fluorescence recordings obtained in the FIA mode turning the photoreactor 'on'/'off'. Mobile phase, water–methanol (70:30); flow-rate, 1 ml/min; wavelength pairs as shown in (c).

Table 3
Effect of the postcolumn photochemical reactor (PCR) on the fluorescence behaviour of the studied phenolic compounds

Compound	λ_{ex} (nm)	λ_{em} (nm)	Fluorescence response[a]
3,4,5-Trihydroxybenzoic (gallic) acid	275	345	□
2,4,6-Trihydroxybenzoic (protocatechuic) acid	290	326	□
2,6-Dihydroxybenzoic (γ-resorcylic) acid	245	392	↓
3,4-Dihydroxibenzoic acid	260	344	↓
3,5-Dihydroxybenzoic (α-resorcylic) acid	250	388	↓
3,4-Dihydroxybenzaldehyde (protocatechualdehyde)	280	311	+
4-Hydroxybenzoic acid	255	320	↓
2,5-Dihydroxybenzoic (gentisic) acid	335	439	↓
2,5-Dihydroxybenzaldehyde	235	330	□
4-Hydroxybenzaldehyde	280	310	↑
3-Hydroxybenzoic acid	240	349	□
3-Hydroxybenzaldehyde	255	302	↑
2,4-Dihydroxybenzoic (β resorcylic) acid	260	384	↓
4-Hydroxy-3-methoxybenzoic (vanillic) acid	260	351	↓
2,6-Dimethoxybenzoic acid	280	376	↓
2-Hydroxybenzaldehyde (salicylaldehyde)	255	300	↑
3,4-Dihydroxycinnamic (caffeic) acid	245	426	□
4-Hydroxy-3-methoxybenzaldehyde (vanillin)	280	313	+
3-Hydroxy-4-methoxybenzaldehyde (isovanillin)	275	312	↑
4-Hydroxy-3,5-dimethoxybenzoic (syringic) acid	275	359	↓
2-Hydroxy-3-methoxybenzaldehyde (o-vanillin)	265	313	↑
3,5-Dimethoxy-4-hydroxybenzaldehyde	270	464	−
4-Hydroxycinnamic (p-coumaric) acid	310	406	□
3-Hydroxycinnamic (m-coumaric) acid	280	405	□
4-Hydroxy-3-methoxycinnamic (ferulic) acid	295	432	↓
3-Methoxybenzaldehyde (m-anisaldehyde)	227	296	↑
3,4-Dimethoxybenzaldehyde (vertraldehyde)	235	308	↑
3,4-Dimethoxybenzoic (veratric) acid	260	349	↓
2,4-Dimethoxybenzoic acid	255	339	↓
3,5-Dimethoxy-4-hydroxycinnamic (sinapic) acid	325	430	−
2-Hydroxycinnamic (o-coumaric) acid	275	439	−
3,4,5-Trimethoxybenzaldehyde	285	438	−
2,4-Dimethoxybenzaldehyde	235	339	+
3,5-Dimethoxybenzaldehyde	310	418	□
3,5-Dimethoxybenzoic acid	255	361	−
3,4,5-Trimethoxycinnamic acid	300	435	−

[a] ↓ = The fluorescence detector signal decreases under PCR action; ↑ = the fluorescence detector signal increases under PCR's action; + = non-fluorescence compound that acquires this property by PCR action; − = fluorescence compound that loses this property under PCR action; □ = non-fluorescent compound or photoproduct.

rower 8-W tube lamps, so we decided to change the lamp also, mounting a General Electric G8T5. With this new photoreaction device a series of experiments were carried out showing that the photoreactions do not take place at all for most of the compounds studied. The conclusion was that at least a 10-W lamp is needed in order to obtain the results described in this paper, although we are currently investigating this effect in more detail in connection with the photochemical mechanisms involved in polyphenol photoreactions.

3.2. *Spectral characteristics of the photoproducts*

The spectral data obtained from pure compounds without connecting the photoreactor

could be used to find the optimum detection conditions only if the compounds to be analysed show native fluorescence. The chromatogram depicted in Fig. 3 corresponds to the gradient elution of a 50 μg/ml each of the 36 species under study in a mixture showing that most of the species do not give any fluorescence signal. This result is not surprising because it is well known [25–27] that electron-withdrawing substituents (such as COOH and COH) in the aromatic ring tend to decrease fluorescence. However, the data in Table 3 indicate that the fluorescence characteristics of the photoproducts could be used for detection purposes. Moreover, if the spectral characteristics of the acid and aldehyde photoproducts are sufficiently different, a selective procedure to detect aldehydes in the presence of acids could be developed. In any case, it is clear that the spectral characteristics of these photoproducts of unknown nature have to be recorded in order to optimize the detector settings. However, keeping in mind that the system must operate in HPLC, it is clear that one must choose a limited number of excitation/emission pairs that can be programmed into the detector.

In Table 3 it can be seen that no excitation/emission pair can be selected as a general solution. Therefore, it was decided to register several emission spectra, fixing the excitation wavelengths in a broad range (230–320 nm) around the absorption maximum of each photoproduct.

Fig. 4a shows the absorption spectrum of the salicylaldehyde photoproduct and Fig. 4b its emission spectrum. It should be noted that some of these photoproducts are unstable and also have different photoreaction kinetics, which implies a large influence of the flow-rate [22]. This means that emission scans cannot be registered from a single injection of the compound with stopped flow when the chromatographic band reaches the detector cell. Hence, once the working flow-rate is fixed, the emission spectra have to be registered by means of several successive injections, keeping the absorption wavelength fixed at the selected value with the postcolumn photochemical reactor in the 'on' position. These injection series produce a group of ten ASCII data files for each species, which, once adequately formatted for the SURFER program (Golden Software, Golden, CO, USA), allow one to obtain a three-dimensional view or contour plot of the emission spectrum as depicted in Fig. 4b.

From a comparison of all the registered alde-

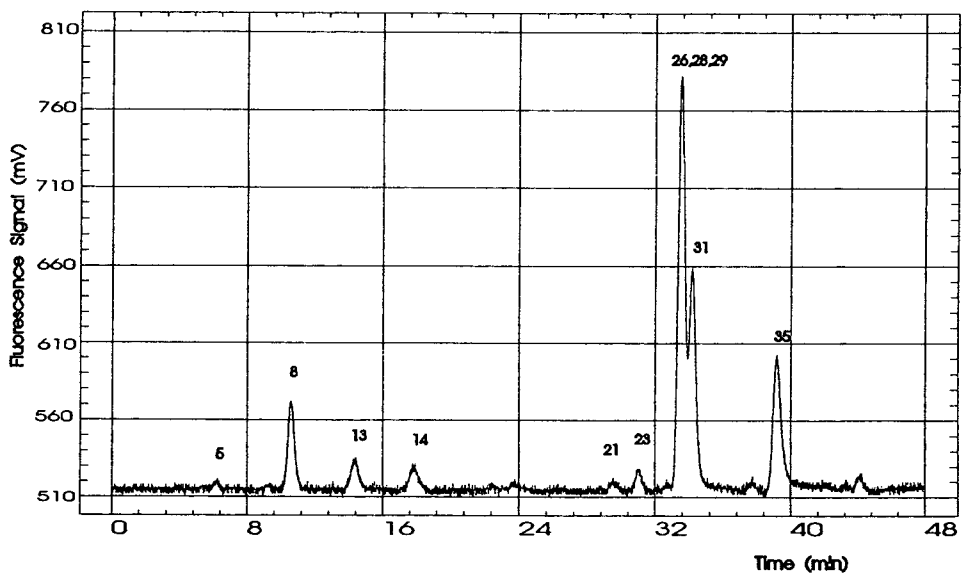

Fig. 3. Fluorescence chromatogram of a mixture of 36 polyphenolic compounds (50 μg/ml each) with photoreactor in 'off' position. Gradient conditions in Table 1. $\lambda_{ex} = 270$ nm; $\lambda_{em} = 310$ nm.

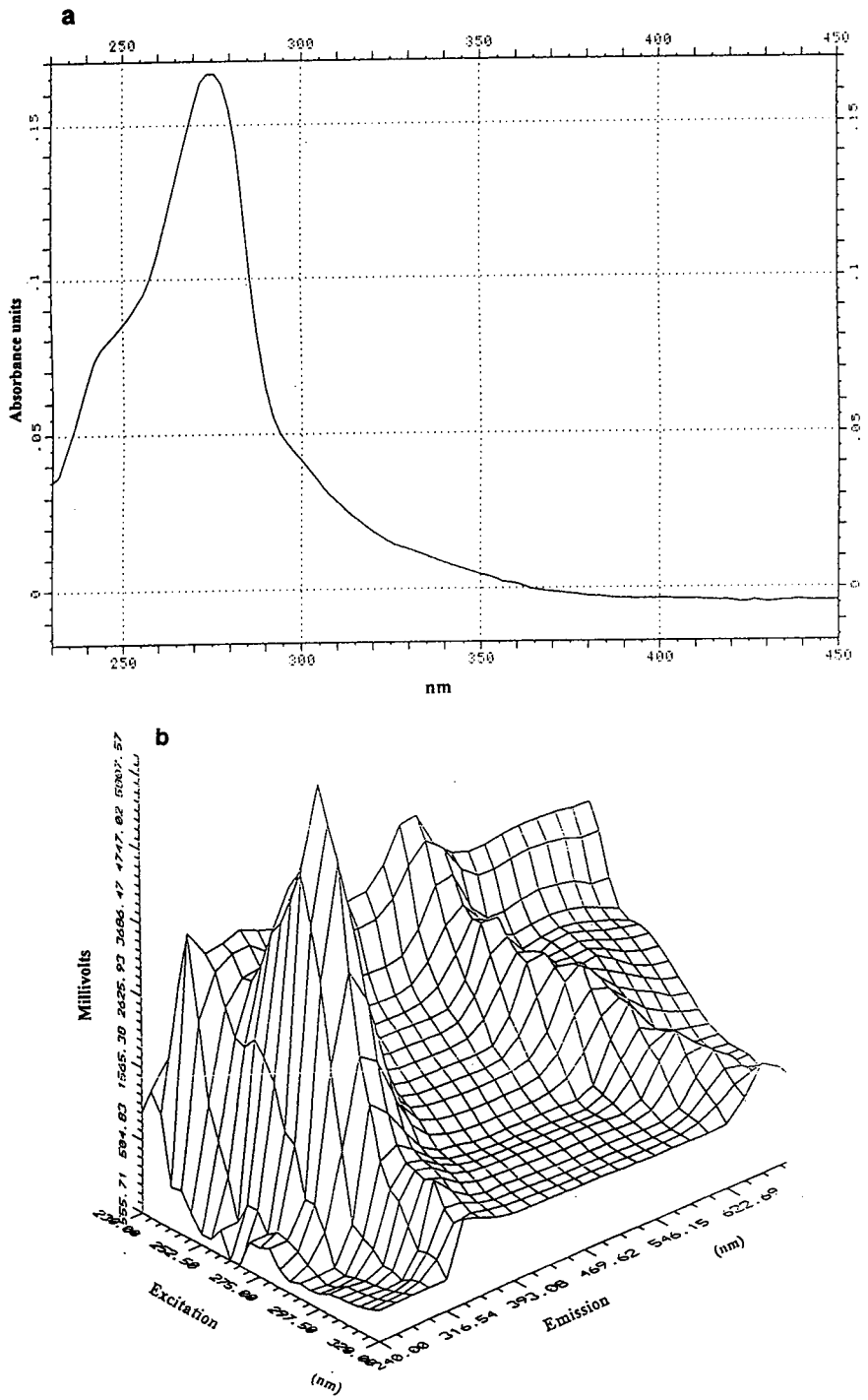

Fig. 4. Example of the steps followed in the analysis of polyphenolic photoproducts: 2-hydroxybenzaldehyde (salicylaldehyde) photoproducts. (a) Absorption spectrum; (b) experimentally reconstructed scanning emission spectrum.

hyde and acid photoproduct fluorescence spectra, it was decided that 270/310 nm is the most convenient excitation/emission wavelength pair. This pair permits the very sensitive detection of all the polyphenolic aldehydes studied except for those not photoreacting, such as 2,5-dihydroxybenzaldehyde and 3,5-dimethoxybenzaldehyde. Most of the polyphenolic acids considered do not interfere under these operating conditions, with the exception of 2,6-dimethoxybenzoic, syringic, 4-hydroxycinnamic, veratric, ferulic, 2,4-dimethoxybenzoic, *o*-coumaric and sinapic acids, which give fluorescence signals and overlap some of the aldehyde peaks.

Fig. 5 shows the UV chromatogram for the mixture of 36 polyphenolic compounds at a 50 μg/ml concentration of each. In this instance the concentration levels of polyphenolic acids and aldehydes are similar. However, it is evident that for mixtures where the concentration level of each species approaches those in real food and agricultural samples (e.g., wines), the aldehyde peaks could not be integrated owing to overlapping of the acid peaks.

The chromatogram in Fig. 3 corresponds to the same injection as depicted in Fig. 5 when the signal of the fluorescence detector was monitored with the photoreactor 'off'.

Fig. 6 shows the fluorescence chromatogram for a similar mixture with an aldehyde concentration level of 10 μg/ml each. In this instance, only the aldehyde peaks (and the above-mentioned interfering acids, of course) appear with an excellent signal-to-noise ratio. The more critical region in the chromatogram is that in the range 31–35 min. In this region ten compounds of the complex mixture eluted. In the UV chromatograms only five peaks can be distin-

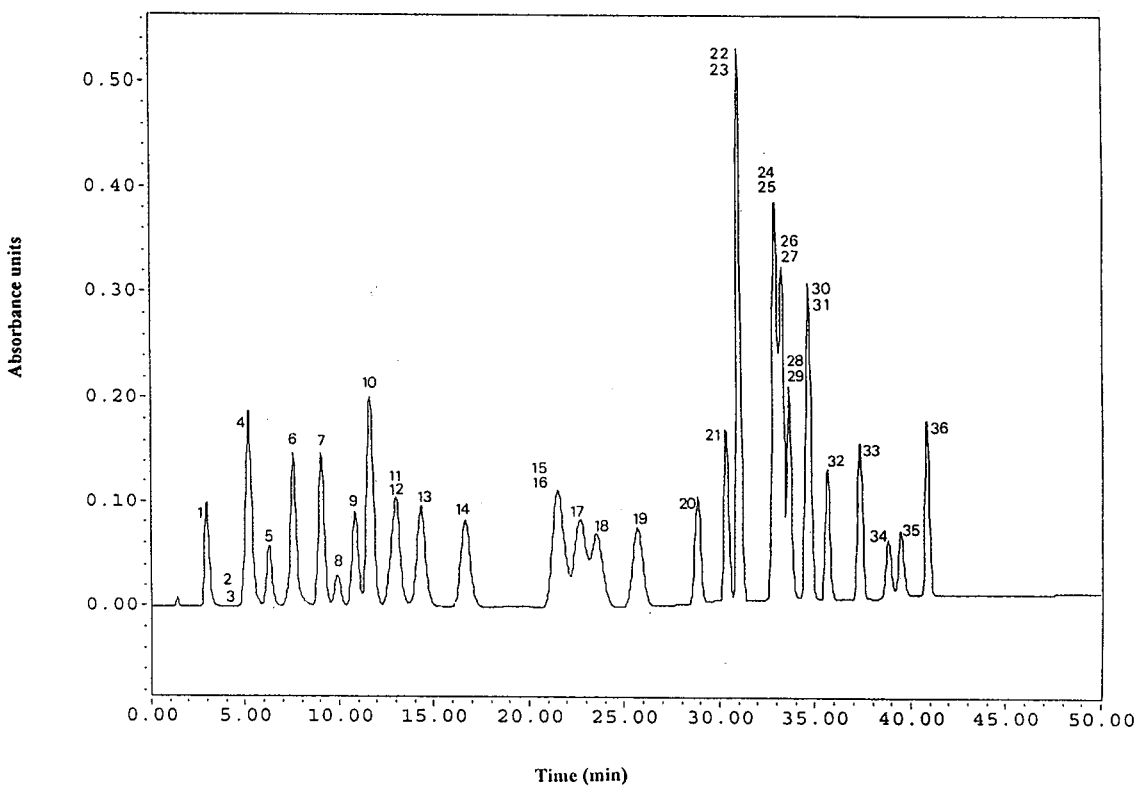

Fig. 5. UV chromatogram of a mixture of 36 polyphenolic compounds (50 μg/ml each) with photoreactor in 'off' position. Gradient conditions in Table 1. $\lambda_{ref} = 280$ nm; resolution = 2 nm.

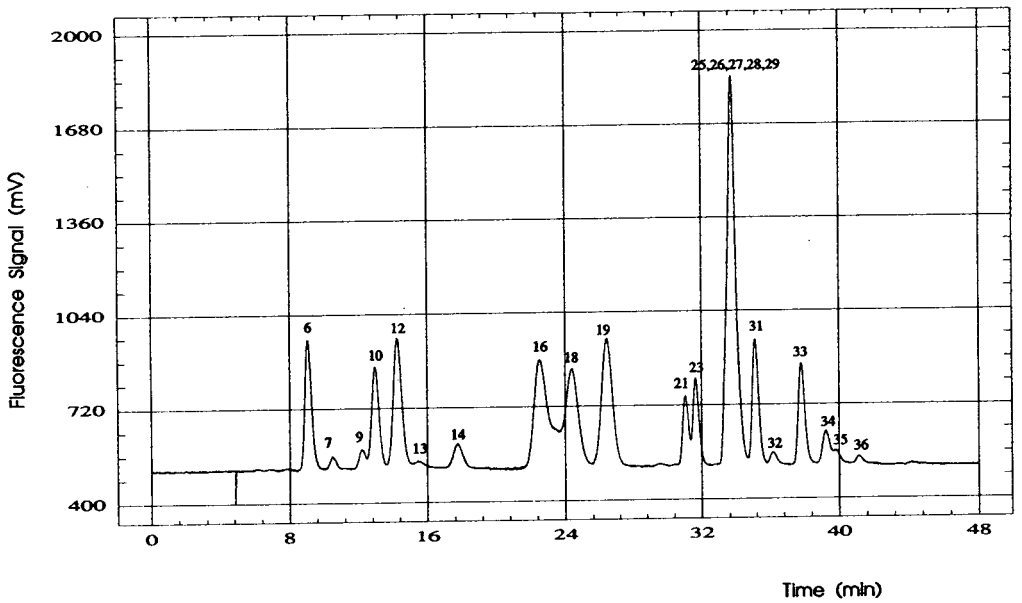

Fig. 6. Fluorescence chromatogram of mixture of 36 polyphenolic compounds (10 μg/ml each) with photoreactor in 'on' position. Gradient conditions in Table 1. $\lambda_{ex} = 270$ nm; $\lambda_{em} = 310$ nm.

Table 4
Absorption and emission maxima for phenolic aldehydes and the interfering acid photoproducts

Photoproduct of:	λ_{abs} (max.) (nm)	λ_{em} (max.) (nm)
3,4-Dihydroxybenzaldehyde (protocatechualdehyde)	232/282	321
2,5-Dihydroxybenzaldehyde	294	350
4-Hydroxybenzaldehyde	232/276	310
3-Hydroxybenzaldehyde	274	306
2,6-Dimethoxybenzoic acid	255	260
2-Hydroxybenzaldehyde (salicylaldehyde)	277	310
4-Hydroxy-3-methoxybenzaldehyde (vanillin)	234/280	312
3-Hydroxy-4-methoxybenzaldehyde (isovanillin)	234/278	316
4-Hydroxy-3,5-dimethoxybenzoic (syringic) acid	275	400
2-Hydroxy-3-methoxybenzaldehyde (*o*-vanillin)	278	313
3,5-Dimethoxy-4-hydroxybenzaldehyde	232/276	340
4-Hydroxycinnamic (*p*-coumaric) acid	280	354
4-Hydroxy-3-methoxycinnamic (ferulic) acid	235/280	354
3,4-Dimethoxybenzoic (veratric) acid	260/290	374
3-Methoxybenzaldehyde (*m*-anisaldehyde)	243/277	305
3,4-Dimethoxybenzaldehyde (veratraldehyde)	234/278	302
2,4-Dimethoxybenzoic acid	255/339	300
3,5-Dimethoxy-4-hydroxycinnamic (sinapic) acid	240/325	270
2-Hydroxycinnamic (*o*-coumaric) acid	275	316
3,4,5-Trimethoxybenzaldehyde	236/274	335
2,4-Dimethoxybenzaldehyde	234/276	310
3,5-Dimethoxybenzaldehyde	236/274	335

guished. Several attempts to develop a gradient curve, allowing a better separation of this region, led to the conclusion that more powerful separation techniques (e.g., multi-dimensional LC) are needed to resolve this group of very similar compounds; seven of them are 3- or 4-methoxy-substituted and the other three are structural isomers. In the fluorescence chromatogram an enormous peak appears in this region. In this peak, ferulic acid, veratric acid, veratraldehyde, *m*-anisaldehyde and 2,4-dimethoxibenzoic overlapped. If the aim of the separation process, as in this instance, is the selective detection of the aldehydes, it is possible to avoid the interference of the overlapping acids in this peak by means of an adequate programming of the excitation/emission pairs. The data in Table 4 show that careful selection of the absorption/emission pairs could help to minimize the signal of the acids in the 31–35-min band.

The chromatogram in Fig. 7 shows the result of an injection of the same mixture but programming the detector to change the excitation/emission pair from 270/310 nm to 240/305 nm at 32.5 min, returning to 270/310 nm at 35 mins. In this instance no signal of the acids was obtained in the 33–35-min band, thus allowing a more accurate integration of the aldehyde peaks.

From Fig. 7 it is evident that low detection limits for phenolic aldehydes can be achieved by the proposed procedure. The data in Table 5 show the absolute detection limits obtained for all the compounds studied showing an enhanced fluorescence signal when submitted to photochemical derivatization. Also, repeatability data for five successive injections of 5 μl of a standard mixture of these compounds with a concentration of 0.1 μg/ml each are included in Table 5. It can be seen that except for those compounds for which the concentration levels are very close to

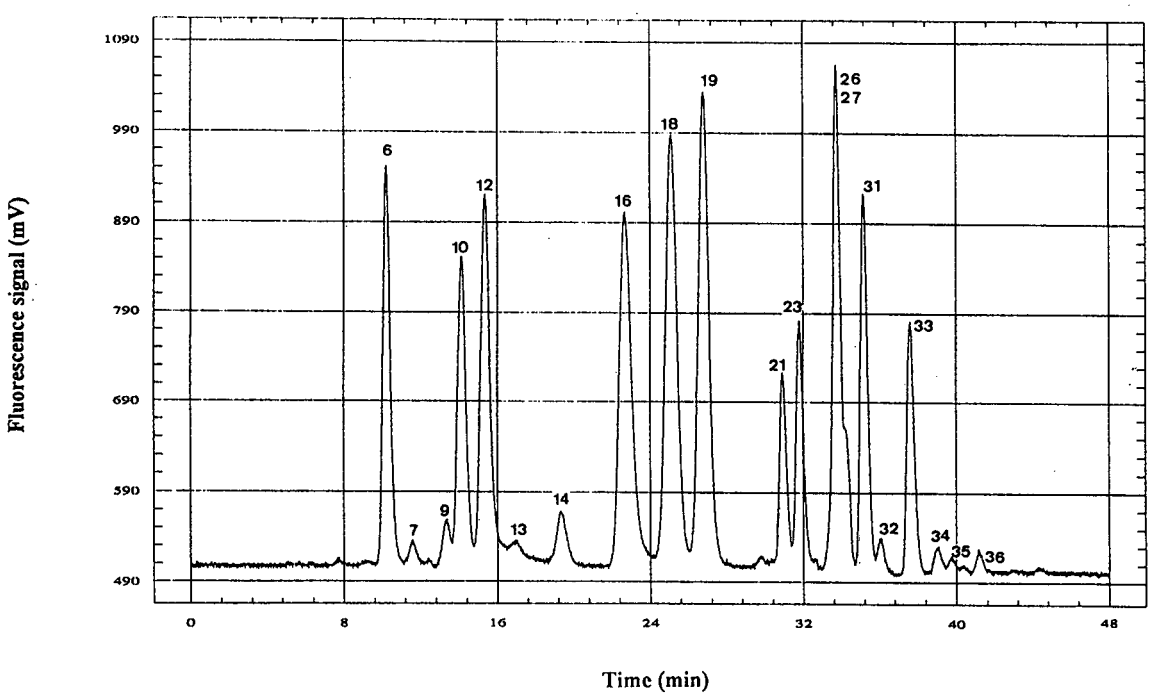

Fig. 7. Fluorescence time-programmed chromatogram of a mixture of 36 polyphenolic compounds (10 μg/ml each) with photoreactor in 'on' position. Gradient conditions in Table 1. Wavelength programme: 0–32.5 min, $\lambda_{ex} = 270$ nm, $\lambda_{em} = 310$ nm; 32.5–35 min, $\lambda_{ex} = 240$ nm, $\lambda_{em} = 305$ nm; 35–50 min, $\lambda_{ex} = 270$ nm, $\lambda_{em} = 310$ nm.

Table 5
Absolute limits of detection (signal-to-noise ratio = 3), peak height (mV) and relative standard deviation (R.S.D.) of the peak height for the species producing signals in the fluorescence detector under the action of the photochemical reactor

Compound	Limit of detection (ng)	Peak height (*)[a]	R.S.D. (%)
3,4-Dihydroxybenzaldehyde (protocatechualdehyde)	1.2	83	15
4-Hydroxybenzoic acid	10.0	4	42
2,5-Dihydroxybenzaldehyde	3.3	16	29
4-Hydroxbenzaldehyde	0.8	119	10
3-Hydroxybenzaldehyde	0.7	135	7
2,4-Dihydroxybenzoic (β-resorcylic) acid	10.0	4	35
4-Hydroxy-3-methoxybenzoic (vanillic) acid	5.0	7	35
2-Hydroxybenzaldehyde (salicylaldehyde)	0.6	151	3
4-Hydroxy-3-methoxybenzaldehyde (vanillin)	0.8	123	4
3-Hydroxy-4-methoxybenzaldehyde (iosvanillin)	0.8	129	4
2-Hydroxy-3-methoxybenzaldehyde (*o*-vanillin)	2.5	10	12
4-Hydroxycinnamic (*p*-coumaric) acid	2.0	19	19
4-Hydroxy-3-methoxycinnamic (ferulic) acid	2.0	25	16
3-Methoxybenzaldehyde (*m*-anisaldehyde)	0.6	185	8
3,4-Dimethoxybenzaldehyde (veratraldehyde)	0.5	446	6
3,4-Dimethoxybenzoic (veratric) acid	0.5		
2,4-Dimethoxybenzoic acid	0.5		
2-Hydroxycinnamic (*o*-coumaric) acid	0.6	158	9
3,4,5-Trimethoxybenzaldehyde	10.0	5	20
2,4-Dimethoxybenzaldehyde	1.0	107	3
3,5-Dimethoxybenzaldehyde	2.4	11	52
3,5-Dimethoxybenzoic acid	5	8	48
3,4,5-Trimethxoycinnamic acid	10.0	4	50

[a] Average from five chromatograms.

their detection limits, the relative standard deviations obtained are satisfactory for quantitative purposes.

On the other hand, the photoreaction mechanisms for the considered compounds are still obscure. Taking into account the variety of compounds considered here, probably no unique mechanism could be responsible for the behaviour exhibited by all the species. Apparently several mechanisms could take place as a function of the lamp power. Although some data have appeared in the literature regarding the photochemistry of cinnamic acids [28] and we have made several attempts to elucidate the nature of some photoproducts by means of LC–MS and GC–MS, so far we can draw no reliable conclusions about the photoreaction mechanisms.

4. Conclusions

The opposite behaviour in the fluorescence response of phenolic aldehydes and acids after undergoing photochemical reactions can be exploited to improve the selectivity and sensitivity in the fluorimetric detection of the former group. Moreover, programming different pairs of excitation/emission wavelengths throughout the analysis time, interferences from the acids can be avoided, thus improving the selectivity of the aldehyde detection even further. Further research is in progress in order to elucidate the photoreaction mechanisms taking place for each species or group of compounds and to establish the effect of the lamp power on these mechanisms and the kinetics of photoreactions. Once having this knowledge, it will be possible to

exploit fully the analytical possibilities of the proposed technique.

Acknowledgement

This work was supported by the Spanish Interministerial Commission for Science and Technology (project PB92-0372).

References

[1] J.B. Harborne, in J.B. Harborne (Editor), *Methods in Plant Biochemistry*, Vol. 1, Academic Press, London, 1989, pp. 1–28.
[2] Ch. Ho, Ch. Y. Lee and M. Huang (Editors), *Phenolic Compounds in Food and The Effects on Health I*, American Chemical Society, Washington, DC, 1992.
[3] J. Ribereau-Gayon, E. Peynaud and P. Sudraud, *Sciences et Techniques du Vin*, Vol. 1, Dunod, Paris, 1976.
[4] V.L. Singleton and P. Esau, *Phenolic Substances in Grapes and Wines and Their Significance*, Academic Press, New York, 1969.
[5] C. Barroso, R. Cela and J.A. Perez-Bustamante, *Chromatographia*, 17 (1983) 249–252.
[6] D.A. Roston and P.T. Kissinger, *Anal. Chem.*, 53 (1981) 1695–1699.
[7] S. Mahler, P.A. Edwards and M.G. Chisholm, *J. Agric. Food Chem.*, 36 (1988) 946–951.
[8] P.J. Woodring, J.M. Underberg and H. Lingeman, *J. Agric. Food Chem.*, 38 (1990) 729–732.
[9] Y. Ohkura, K. Ohtsubo, K. Zaitsu and K. Kohashi, *Anal. Chim. Acta*, 99 (1978) 317–324.
[10] M. Nakanura, M. Toda and H. Saito, *Anal Chim. Acta*, 134 (1982) 39–45.
[11] H. Jansen and R.W. Frei, in K. Zech and R.W. Frei (Editors), *Selective Sample Handling and Detection in HPLC, Part B*, Elsevier, Amsterdam, 1989, Ch. V.
[12] J.R. Poulsen and J.W. Birks, in J.W. Birks (Editor), *Chemiluminescence and Photochemical Reaction Detection in Chromatography*, VCH, New York, 1989, Ch. VI.
[13] I.S. Krull, C.M. Selavska, M. Lockabaugh and W.R. Childress, *LC · GC Int.*, 2 (1989) 28–39.
[14] G.J. de Jong, U.A.Th. Brinkman and R.W. Frei, in H. Lingeman and W.J.M. Underberg (Editors), *Detection-Oriented Derivatization Techniques in Liquid Chromatography*, Marcel Dekker, New York, 1990, Ch. IV.
[15] P.J. Twitchett, P.L. Williams and A.C. Moffat, *J. Chromatogr.*, 149 (1978) 683–691.
[16] A.H.M.T. Scholten and R.W. Frei, *J. Chromatogr.*, 176 (1979) 349–357.
[17] A.H.M. Scholten, P.L.M. Welling, U.A.Th. Brinkman and R.W. Frei, *J. Chromatogr.*, 199 (1980) 239–248.
[18] H. Engelhardt and H.D. Neue, *Chromatographia*, 15 (1982) 403–408.
[19] C.M. Selavska, K.S. Jiao and I.S. Krull, *Anal. Chem.*, 59 (1987) 2221–2224.
[20] J.R. Poulsen, K.S. Birks, M.S. Gandelman and J.W. Birks, *Chromatographia*, 12 (1986) 231–234.
[21] K. Blau, in K. Blau and J. Halket (Editors), *Handbook of Derivatives for Chromatography*, Wiley, 1993, Ch. XV.
[22] R. Cela, M. Lores and C.M. Garcia, *J. Chromatogr.*, 626 (1992) 117–126.
[23] R. Cela and M. Lores, *Book of Abstracts of HTC2, Section Chromatography*, KVCV, Antwerp 1992, C15.
[24] *Supelco Rep.* 12, No. 4 (1993), 6–7.
[25] E.P. Crowell and Ch.J. Varsel, *Anal. Chem.*, 35 (1963) 189–192.
[26] E.L. Wehry, in G.G. Guibault (Editor), *Practical Fluorescence*, Marcel Dekker, New York, 1990, Ch. III.
[27] J.W. Birks, in J.W. Birks (Editor), *Chemiluminescence and Photochemical Reaction Detection in Chromatography*, VCH, New York, 1989, Ch. I.
[28] R.B. Cundall and A. Gilbert, in A. Maccoll and L. Tedder (Editors), *Photochemistry*, Nelson, London, 1970, Ch. VIII.

ELSEVIER

Journal of Chromatography A, 683 (1994) 45–50

JOURNAL OF CHROMATOGRAPHY A

Real-time controlled multidimensional gas chromatography with electronic pressure control: application to chlorobiphenyl analysis

Erkki Sippola*[,a], Kimmo Himberg[b], Frank David[c], Pat Sandra[d]

[a]*VTT Chemical Technology, P.O. Box 1401, FIN-02044 VTT, Espoo, Finland*

[b]*National Bureau of Investigation, Crime Laboratory, Suvilahdenkatu 10 A, FIN-00580 Helsinki, Finland*

[c]*Research Institute for Chromatography, Kennedypark 20, B-8500 Kortrijk, Belgium*

[d]*Laboratory of Organic Chemistry, University of Ghent, Krijgslaan 281 (S4), B-9000 Ghent, Belgium*

Abstract

Multidimensional gas chromatography was applied to the quantitative determination of planar chlorobiphenyls (PCBs) in commercial PCB mixtures. The instrumental setup is based on real-time controlled column switching in which the heartcuts are elucidated through retention indices calculated by linear extrapolation from the retention times of *n*-alkanes as reference compounds. Electronic pressure control providing pressure programming was used to adjust the pressure at the injector and at the mid-point of the column tandem.

1. Introduction

The high resolving power of multidimensional gas chromatography (MDGC) is based on the large peak capacity, n_c, which results from the transfer of an unresolved fraction from the first column to a second column of different selectivity [1]. The resolving power of an MDGC system resembles the selectivity of gas chromatography–low resolution mass spectrometry [2].

Selectivity in MDGC is inversely proportional to the width of the fraction transferred to the second column [3,4]. Thus, the peak capacity in conventional MDGC is often significantly less than optimum due to the relatively broad heartcuts needed to eliminate small variations in absolute retention times of peaks to be transferred. Real world samples can cause harmful inaccuracies in absolute retention times like for example by the occurrence of large and small peaks. Also aging of the first column reduces reproducibility of retention times. Regular calibrations are therefore needed in conventional MDGC to ensure precise heartcuts.

A computer method based on indices (I) instead of on retention times has recently been developed to overcome these problems and to enable reliable quantitation while exploiting all the selectivity a multidimensional high-resolution gas chromatograph can offer [5]. In this system reference compounds, e.g. *n*-alkanes, are co-injected with the sample. Absolute retention times of the reference compounds are used to predict the retention times of the compounds to be heartcut. This is achieved by real-time extrapolation of the time scale using retention

* Corresponding author.

SSDI 0021-9673(94)00406-Y

indices. The details of the technique are described in Ref. [5].

Tuning of an MDGC system for a particular application is a time-consuming procedure: the pressure balance between the first column and the mid-point of the column tandem is critical and very much dependent on the dimensions of the columns applied and thus needs careful adjusting. Moreover the use of temperature programming strongly affects the pressure balance. Even flow-controlled systems fail in compensating the changes in mid-point pressure caused by a temperature gradient.

Electronic pressure control (EPC), which nowadays is available on modern GC instrumentation, was applied to program and thus to optimize the inlet pressure and the mid-point pressure during temperature programming.

Chlorobiphenyls (PCBs) are a complex group of 209 congeneric compounds, several tens of which have become environmental pollutants [6,7]. Their congener specific separation is known to be a demanding task even for high-resolution chromatographic systems [8,9]. In this contribution the system described above was applied to the separation of the most toxic coplanar chlorobiphenyl congeners from commercial PCB mixtures.

2. Experimental

A single-oven HP 5890 Series II gas chromatograph (Hewlett-Packard, Avondale, PA, USA) was modified to the multidimensional mode by an SGE Column Switching System (Scientific Glass Engineering, Ringwood, Victoria, Australia). The data system was an HP 3365 Series II ChemStation. A schematic illustration of the instrument is presented in Fig. 1.

Real-time control of the heartcutting was accomplished by a tailor-made computer program, FERRET (Fractionation by Estimation of Retention through Real-time Extrapolation of the Timescale, VTT, Espoo, Finland) [5]. Connection between the gas chromatograph and personal computer (HP Vectra 486/33N, Hewlett-Packard) was made via a DT-2802 chromatography board (Data Translation, Marlboro, MA, USA).

The pressures for column inlet and mid-point of the column tandem were controlled by two EPC units: a back pressure regulated unit was used for the splitless injector, which was operated under constant pressure mode. The mid-point pressure was controlled by a forward pressure regulated EPC unit of a cool on-column injector.

A capillary column, 25 m × 0.20 mm I.D. Ultra-1 (Hewlett-Packard), coated with a 0.11-μm film of methyl silicone was used as first column. The final separation was carried out on a 30 m × 0.18 mm I.D. capillary column coated with 0.25-μm home-synthesized polycarbonate stationary phase [10].

Retention times of the reference compounds were monitored by a flame ionization detector. The separation in the second column was recorded by an electron capture detector.

The temperatures of injector and detectors were 300 and 320°C, respectively, in all runs. Splitless time for 1-μl injections was adjusted to 1 min. Helium was used as the carrier gas. Initial inlet pressure and the pressure at the mid-point of the columns were 0.420 and 0.305 MPa at 80°C producing 25 and 42 cm/s linear carrier gas velocity on the first and second column, respectively.

The column oven temperature was programmed at 6°C/min to 270°C after a 1-min isothermal part at the initial temperature of 80°C. All heartcuts were made during this gradient. The fractions were collected in a cold trap situated at the inlet of the second column. A negative temperature gradient of 20°C/min was carried out in order to cool the columns down to 180°C, the temperature at which the fractions were re-injected into the second column. A second separation was done under a program rate of 8°C/min to the final temperature (300°C). The retention time of the last eluting analyte in the second column was ca. 53 min after sample introduction.

Alkanes having even carbon numbers and ranging from dodecane to hexacosane used as reference compounds for retention index calcula-

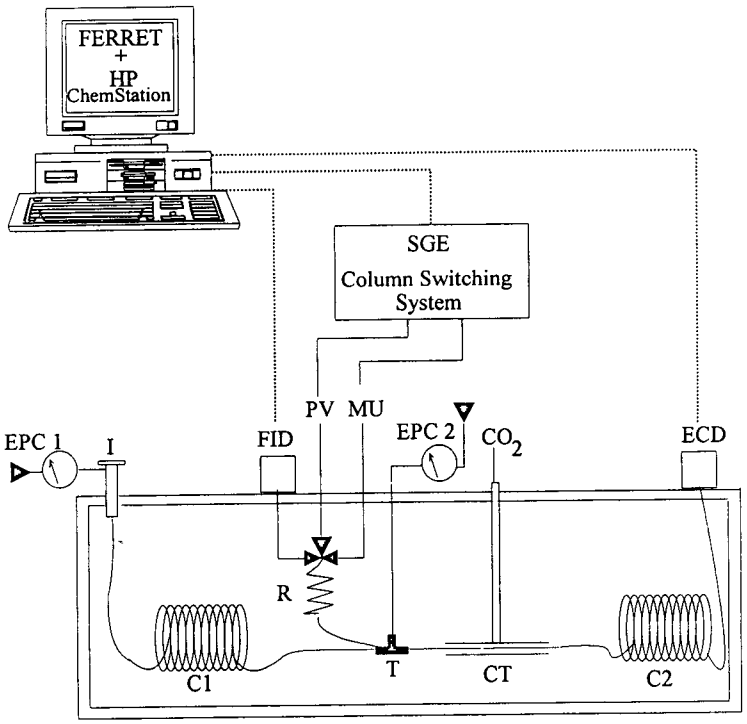

Fig. 1. Key parts of the multidimensional gas chromatograph used in the present study: EPC = electronic pressure control unit; I = injector; C1 and C2 = first and second capillary column; FID = flame ionization (monitor) detector; PV = pneumatic valve; MU = helium make up gas; R = capillary flow restrictor; T = coupling T-piece for the outlet of the first column, inlet of the second column and the restrictor capillary; CT = cold trap with liquid CO_2 cooling; ECD = electron capture (main) detector. Solid lines indicate gas tubings and dotted lines data cables.

tions were purchased from Alltech (Laarne, Belgium). Standard solutions (10 ng/μl) of non-*ortho* chlorinated 3,3′,4,4′-tetrachloro-, 3,3′,4,4′,5-pentachloro-, 3,3′,4,4′,5,5′-hexachlorobiphenyl and mono-*ortho* chlorinated 2,3,3′,4,4′-pentachlorobiphenyl (IUPAC nos. 77, 126, 169 and 105, respectively) were purchased from Dr. Ehrenstorfer (Augsburg, Germany). A 10 ng/μl solution of 1,2,3,4-tetrachloronaphthalene used as internal standard and PCB mixtures Aroclor 1242, 1248 and 1260, all in 100 ng/μl concentration were purchased from the same source. All samples were dissolved in nanograde quality 2,2,4-trimethyl pentane (Rathburn, Walkerburn, UK).

Four calibration mixtures containing 1, 10, 100 and 1000 pg/μl of each congener were prepared from the individual PCB stock solutions. Tetrachloronaphthalene was added as an internal standard to the calibration mixtures and the Aroclor solutions giving a concentration of 1000 pg/μl. Finally, a mixture of *n*-alkanes was added into all solutions as retention index markers giving a concentration level of 10 ng/μl per component.

3. Results

Traditionally the pressure balancing in MDGC is, more or less, searching for a good compromise between the optimum pressures at different temperatures. MDGC instruments from different manufacturers slightly differ in details but the basic principle is the same in all cases: heartcuts producing a total transfer of the fractions throughout the temperature range require balancing of the system at the highest temperature used in the current application. This is a

Table 1
Retention indices in index units (i.u.) and heartcut widths of the planar chlorobiphenyls and the internal standard 1,2,3,4-tetrachloronaphthalene (TCN)

Compound	Interpolated I (i.u.)	Extrapolated I (i.u.)	Peak width (s)	Heartcut width (s)
TCN	1919.75	1910.14	10.2	14
PCB-77	2122.67	2112.78	9.7	12
PCB-105	2250.31	2245.64	9.4	12
PCB-126	2324.83	2313.25	9.6	12
PCB-169	2506.19	2497.53	9.0	12

Interpolated retention indices were calculated as originally published by Van den Dool *et al.* [11]. Extrapolated indices were calculated on the basis of the last two *n*-alkanes preciding each analyte [5]

drawback as the optimal carrier gas flow-rate in the first column usually requires the smallest possible backpressure at the mid-point. This problem can be overcome if pressure programming is applied.

The inlet pressure (0.420 MPa) was first chosen to give a relatively high flow-rate in the second column. The pressure at the mid-point was monitored by EPC readout while the vent line of the on-column injector was plugged. The mid-point pressure was recorded during a slow temperature program. An almost linear pressure increase of 0.020 MPa was observed through the temperature gradient. The mid-point pressure was then adjusted at initial temperature to give a total transfer of the heartcut. The change in pressure during the temperature gradient was taken into account in the final mid-point pressure program: 0.305 MPa (1 min), $8.0 \cdot 10^{-4}$ MPa/min to 0.325 MPa, the final pressure.

Retention indices of the congeners to be heartcut and the heartcut widths were first determined by running a semi-quantitative ca. 10 ppm PCB mixture also containing the *n*-alkanes as reference compounds. Peak widths defined as 6σ were estimated as an average of the widths in three runs. The heartcut widths were chosen to be ca. 1.2 times the corresponding peak width due to slight tailing most probably caused by the T-piece of the SGE system. As the widths of heartcuts were very narrow, the delay for a solute to elute from the T-piece to monitor detector, 1 s, was also taken into consideration. The obtained index values calculated by the linear extrapolation method [5] and the heartcut widths are given in Table 1.

Table 2
Concentrations of planar chlorobiphenyls and their relative standard deviations (R.S.D.) in Aroclor mixtures on the basis of four determinations expressed as % (w/w)/R.S.D. (%); results of the present study are compared with literature values [12,13]

		PCB-77	PCB-105	PCB-126	PCB-169
Aroclor 1242	Present study	0.31/0.32	0.19/1.1	0.0077/5.0	– [a]
	Ref. [12]	0.50	0.33	–	–
	Ref. [13]	0.25	0.43	0.0037	–
Aroclor 1248	Present study	0.31/0.48	1.0/0.50	0.01/0.48	–
	Ref. [12]	0.30	0.55	–	–
	Ref. [13]	0.40	1.0	0.011	–
Aroclor 1260	Present study	0.024/1.7	0.07/1.0	0.0096/1.2	–
	Ref. [12]	–	0.08	–	0.05
	Ref. [13]	0.0038	0.045	0.0004	–

[a] Not observed.

A multipoint calibration containing four concentration levels in the range of 1–1000 pg/μl was made for all analytes on the basis of duplicate injections at each concentration level. Correlation coefficients of 1.000 were obtained in each case. Measured concentrations of toxic

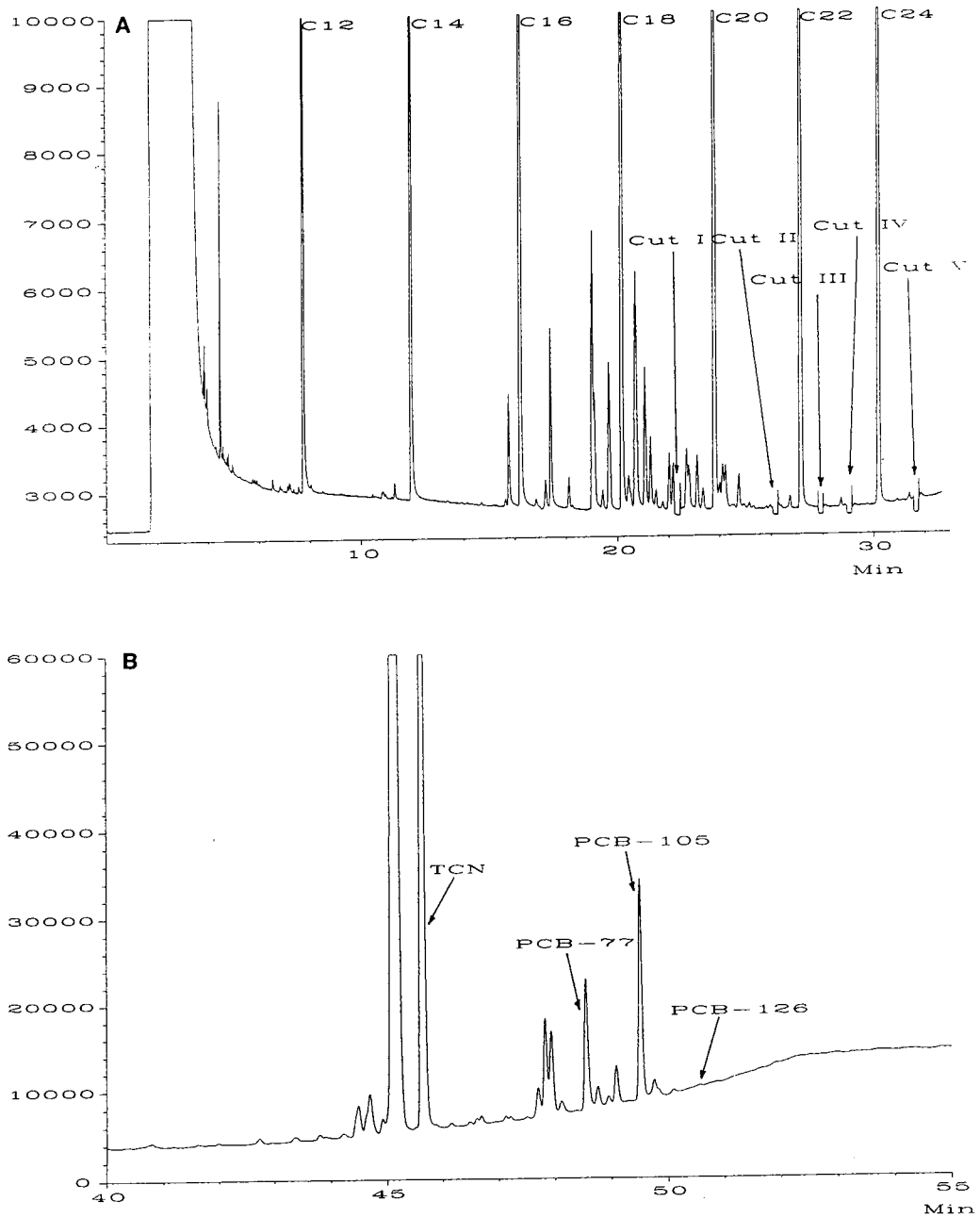

Fig. 2. Chromatograms illustrating the separation of coplanar chlorobiphenyls from Arochlor 1242 in the first (A) and second (B) column. *y*-Axis represents detector response in abundance units.

chlorobiphenyl congeners as averages of four injections are given in Table 2. Relative standard deviations (Table 2) were less than 5% for all determinations. Chromatograms illustrating the separation in the first and the second column are presented in Fig. 2. The results of the present study are well compatible with those published in Refs. [12,13] considering that some batch-to-batch variation in the composition of chlorobiphenyls is commonly known to exist. Small deviations can also be caused by the different selectivity of the polycarbonate column compared to more conventional stationary phases.

4. Discussion

Multidimensional gas chromatography utilizing real-time controlled column switching has been shown to be applicable for complex samples. The system does not need regular calibrations in order to have repeatable and reproducible heartcuts, i.e. very narrow heartcuts maximizing selectivity of the system, can be used without the danger of loosing parts of the analytes. The repeatability ($n = 47$) of retention times and retention indices was 0.15 and 0.015%, respectively. Electronic pressure control seems to be a very promising tool for multidimensional gas chromatography. For example in this study, the instrumental setup was twice dismantled and rebuilt using the original chromatographic method containing pressure settings. No recalibrations or test runs were required which was proved by running known test samples. Pressure balancing could even be automated providing an instrument with the same user-friendly characteristics as a classical gas chromatograph.

In addition to the high selectivity, the system also provides reliable compound identification as retention parameters are drawn from two columns with different characteristics. The presence of the analyte peak at the second detector indicates that the compound has a retention index in the first column within a narrow I window (in this case ca. 13 index units) corresponding to the width of the heartcut. On the other hand the absolute retention time of the analyte peak in the second column of different selectivity and calculated from the re-injection from the cold trap is an independent variable. Thus, even if the analyte peak has not been observed at the monitor detector two independent retention variables are obtained and their combination used as the basis for the compound identification is analogous to the more traditional application of two-channel gas chromatography utilizing two parallel columns of different selectivity.

Acknowledgements

The Research Institute for Chromatography, Kortrijk, Belgium, is thanked for donation of the polycarbonate column.

References

[1] J.C. Giddings, in H.J. Cortes (Editor), *Multidimensional Chromatography*, Marcel Dekker, New York, 1990, Ch. 1, p. 1.
[2] J.F.K. Huber, E. Kenndler and G. Reich, *J. Chromatogr.*, 172 (1979) 15.
[3] J.F.K. Huber, E. Kenndler and W. Nyiry, *J. Chromatogr.*, 247 (1982) 211.
[4] G. Schomburg, H. Husmann and E. Hübinger, *J. High Resolut. Chromatogr. Chromatogr. Commun.*, 8 (1985) 395.
[5] K. Himberg, E. Sippola, F. David and P. Sandra, *J. High Resolut. Chromatogr.*, 16 (1993) 645.
[6] K.C. Jones, *Sci. Total Environ.*, 68 (1988) 141.
[7] V.A. McFarland and J.U. Clarke, *Environ. Health Perspect.*, 81 (1989) 225.
[8] J. Boer and Q.T. Dao, *Int. J. Environ. Anal. Chem.*, 43 (1991) 245.
[9] N. Kannan, D.E. Schulz-Bull, G. Petrick and J.C. Duinker, *Int. J. Environ. Anal. Chem.*, 47 (1992) 201.
[10] P. Sandra, F. David, E. Sippola and E. Benickà, in preparation.
[11] H. van den Dool and P.D. Gratz, *J. Chromatogr.*, 11 (1963) 463.
[12] J.C. Duinker, D.E. Schulz and G. Petrick, *Anal. Chem.*, 60 (1988) 478.
[13] B. Larsen, S. Bøwadt and S. Facchetti, *Int. J. Environ. Anal. Chem.*, 47 (1992) 147.

ELSEVIER

Journal of Chromatography A, 683 (1994) 51–58

JOURNAL OF CHROMATOGRAPHY A

Speciation of butyltin compounds in sediments using gas chromatography interfaced with quartz furnace atomic absorption spectrometry

W.M.R. Dirkx, M.B. de la Calle, M. Ceulemans, F.C. Adams*

Department of Chemistry, Universitaire Instelling Antwerpen (UIA), Universiteitsplein 1, 2610 Wilrijk, Belgium

Abstract

A method is presented for the determination of tri- and dibutyltin in sediments by gas chromatography–quartz furnace atomic absorption spectrometry. The compounds are released from the matrix by the action of acetic acid and extracted into hexane after formation of an extractable complex with diethyldithiocarbamic acid (DDTC). Pentylmagnesium bromide is used to derivatize the non-volatile organotin–carbamate complexes. A detection limit of 2.5 ng/g (as Sn) can be achieved. The optimization of the different parameters is discussed and the accuracy of the method was validated by the analysis of two certified reference materials. A first approach was made to determine tri- and dimethyltin compounds forming extractable complexes with NaDDTC under pH controlled conditions.

1. Introduction

Organotin compounds comprise one of the most thoroughly studied groups of organometallic chemicals in terms of their uses and applications as insecticides, fungicides, bactericides, stabilizers of polyvinyl chloride (PVC) plastics and autifouling agents. The deletereous effects of tributyltin (TBT) leached from antifouling paints into the marine environment have been the subject of extensive studies in recent years. The recognition of the toxicity of these compounds has led to environmental legislation restricting their use in a number of countries [1,2].

Soils and sediments are the main source of trace elements that enter the food chain and the main receptor of contaminants from anthropogenic activities. In the particular case of organotin compounds, several researchers have shown that butyltin compounds readily sorb onto suspended particulate matter and sediments [3,4].

To evaluate environmental risks, and in order to measure and speciate low levels of butyltins in waters and sediments, practical, reproducible and sensitive analytical methods are essential. As organotin compounds are not involved in mineralogical processes and bind to the surface of the sediment, the complete dissolution of the sediment prior to the analysis is not considered necessary. The basic approach to release organotin compounds from sediments involves acid leaching (HCl, HBr, HOAc) in aqueous or methanolic medium by sonication, stirring, shaking or Soxhlet extraction with an organic solvent.

* Corresponding author.

0021-9673/94/$07.00
SSDI 0021-9673(94)00491-Q

The formation of volatile gas chromatographable species after liberation of the organotin compounds is done either by *in situ* hydridization using $NaBH_4$ [5–7] or by Grignard derivatization after complexation of the organotin compounds with tropolone [8–10] or sodium diethyldithiocarbamate (NaDDTC). More recently, sodium tetraethylborate ($NaBEt_4$) has gained popularity as a derivatizing reagent in organometallic speciation analysis [11–13].

Gas chromatography (GC) is the most widely used separation technique in organotin speciation analysis owing to its high resolution power and the availability of sensitive detection methods such as flame photometric detection (FPD), atomic absorption spectrometry (AAS), mass spectrometry (MS) and atomic emission spectrometry (AES) [14,15].

This paper presents an optimized procedure for the speciation of TBT and dibutyltin (DBT) in sediments. It is based on acid leaching followed by extraction of the liberated compounds in hexane, using DDTC as complexing agent. The complexes are derivatized using pentylmagnesium bromide (n-PeMGBr) leading to stable and species amenable to GC. The accuracy of the method was validated by the analysis of two certified reference materials. Further, it was successfully used in a number of exercises and a certification programme organized by the Community Bureau of Reference (BCR). An attempt was made to adapt the method to the determination of trimethyltin (TMT) and dimethyltin (DMT).

2. Experimental

2.1. Reagents

Bu_3SnCl (96%), Bu_2SnCl_2 (95%), $BuSnCl_3$ (95%), Me_3SnCl (99%), Me_2SnCl_2 (97%), $MeSnCl_3$ (97%), Pr_3SnCl (98%) and n-PeNgBr (2.0 mol/l in diethyl ether) were obtained from Aldrich (Milwaukee, WI, USA) Stock standard solutions were prepared following the method described in detail elsewhere [16]. Working standard solutions were prepared by a series of dilutions of the stock standard solutions with octane.

Diethyldithiocarbamic acid (DDTC) solution was prepared by dissolving 2.25 g of sodium diethyldithiocarbamate salt (NaDDTC) (Merck, Darmstadt, Germany) in 10 ml of water. The solution of DDTC in pentane, used for sediment analysis, was obtained by shaking the aqueous solution of NaDDTC with 20 ml of 0.5 mol/l H_2SO_4 and extracting with 10 ml of pentane for 5 min.

ICN Alumina B-Super I (ICN Biomedicals, Eschwege, Germany) was used in the clean-up step for sediment samples.

All other reagents were of analytical-reagent grade. Deionized water further purified in a Milli-Q system (Millipore, El Paso, TX, USA) was used throughout.

2.2. Apparatus

A laboratory interfaced GC–AAS system described previously [16,17] consisting of a Varian Model 3700 gas chromatograph and a Perkin-Elmer Model 2380 atomic absorption spectrometer was used. The system was adapted to the use of an RSL 150 Megabore column. Chromatograms were recorded on a Spectra-Physics SP 4290 integrator in the peak-height mode. The optimum parameters used for GC and AAS are given in Table 1.

2.3. Procedure

A river scheldt sediment, sampled with a box corer mounted on the Research Vessel Belgica, was used to develop the leaching–extraction procedure. The Scheldt sediment was oven-dried on watch-glasses at 50°C, ground with an agate mortar and pestle and successively sieved with polyethylene sieves ranging from 600 to 45 μm, prior to organotin determination. Only the 63–180-μm fraction was selected for the optimization experiments.

A 1-g amount of sediment was accurately weighed and transferred into a 100-ml Pyrex erlenmeyer flask equipped with a ground-glass stopper, followed by 4 ml of deionized water, 1 ml of glacial acetic acid (96%), 1 ml of DDTC

Table 1
Optimum GC–AAS operating parameters

GC parameters	
Injection port	Wide-bore on-column liner
Injection port temperature	230°C
Injection volume	4 μl
Column	RSL 150 (15 m × 530 μm I.D., 1.2 μm film thickness)
Argon (carrier gas) flow-rate	6 ml/min
Oven program	
Initial temperature	100°C
Ramp rate	10°C/min
Final temperature	270°C
GC detector temperature	270°C
Block temperature	270°C
Interface parameters	
Transfer line	Deactivated fused silica, 530 μm I.D.
Transfer line temperature	270°C
AAS parameters	
Wavelength	286.4 nm
Light source	Sn electrodeless discharge lamp (8 W)
Slit	0.7 nm normal
Hydrogen flow-rate	350 ml/min
Air flow-rate	45 ml/min
MHS-20 furnace temperature	900°C

solution in pentane and 25 ml of hexane. The mixture was sonicated in an ultrasonic bath (Branson Model 1200) for 30 min. After phase separation, the organic phase was decanted into a 100-ml beaker. In the original erlenmeyer flask, the sediment was extracted again for 30 min with a fresh 25-ml portion of hexane with magnetic stirring. The sample was then centrifuged at 4000 *g* for 5 min (IEC Centra-CL centrifuge). The combined hexane extracts were dried over Na_2SO_4. The Na_2So_4 was rinsed twice with 10-ml portions of hexane.

The combined organic phase was then evaporated to dryness in a 50-ml erlenmeyer flask under reduced pressure at 40°C on a rotatory evaporator. Subsequently 250 μl of *n*-octane containing Pr_3SnPe as the internal standard were added, after which pentylation with 1 ml of 1 mol/l n-PeMgBr in diethyl ether was carried out; the mixture was gently agitated for 3 min. Excess Grignard reagent was destroyed by the addition of 10 ml of 0.5 mol/l H_2SO_4. The mixture was shaken for 1 min and then transferred into a capillary separating funnel. The octane layer was sampled for clean-up.

A Pasteur pipette was dry packed in successive order with glass-wool and 5 cm (±1.25 g) of Al_2O_3 B-Super I, which had been activated at 140°C for 24 h. After cooling, 5% (v/w) of water and 1 g of anhydrous sodium sulphate were added. The packing was first conditioned by passage of 5 ml of hexane–diethyl ether (9:1). The colourless eluate was evaporated to ca. 0.25 ml by means of a stream of nitrogen. This solution was then transferred into a small conical vial and was ready for analysis by GC–AAS. A scheme of the leaching–extraction procedure is shown in Fig. 1.

3. Results and discussion

3.1. Optimization of the extraction parameters

The parameters to be investigated were the extraction solvent, the influence of acetic acid

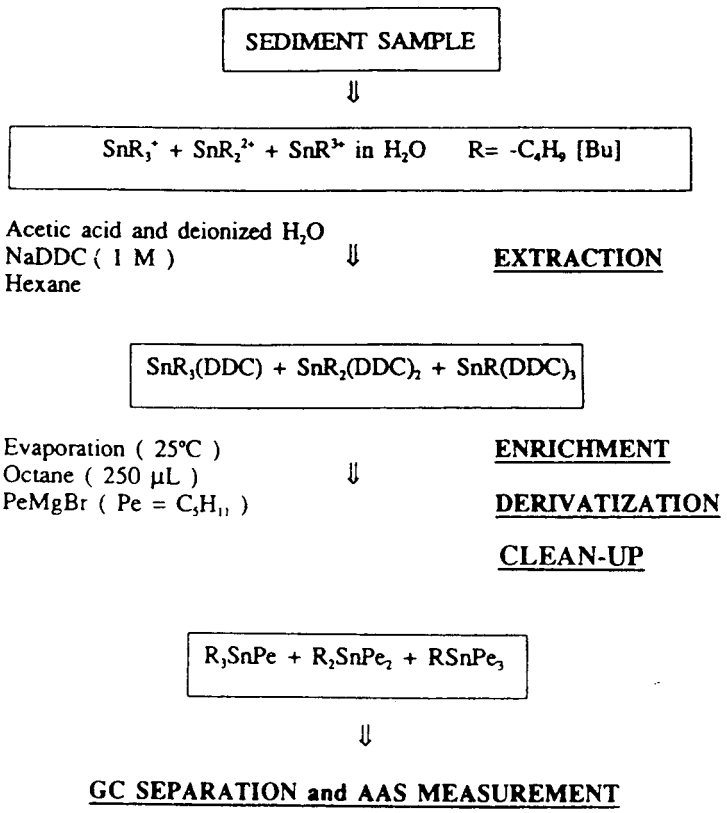

Fig. 1. Scheme of the speciation procedure for TBT and DBT determination in sediments.

and DDTC concentrations on the extraction recovery of butyltin compounds, spiking equilibrium time, the extraction time and the effect of the sediment itself.

Choice of extraction solvent

Hexane was chosen instead of other non-polar solvents such as pentane for the extraction because the latter (b.p. 36°C) was partially evaporated especially during the 30-min ultrasonic leaching–extraction step.

Organotin compounds have different properties in terms of polarity. Non-polar solvents, such as hexane, are optimum for the extraction of TBT and/or DBT, but more polar solvents seem to be necessary for the extraction of other species such as tri-, di- and monomethyltin and monobutyltin.

Chloroform and hexane–isopropyl acetate (80:20) were used as organic solvents to evaluate the possibility of increasing the extraction efficiency of the more polar organotin compounds. The use of both solvents was rejected because a certain amount of water and acetic acid were dissolved in them, remaining in the erlenmeyer flask after the evaporation of the organic solvent with the rotavapor. Under these conditions derivatization of the organotin compounds with Grignard reagents could not be carried out as these derivatizating agents decompose in the presence of small amounts of water.

Selection of the optimum amount of acetic acid

Most of the existing procedures use acids (HCl, HBr or acetic acid) to release the organotin compounds from the matrix. In this work, the best results were obtained with glacial acetic acid (96%). The variation in extraction recovery with changing acetic acid concentration

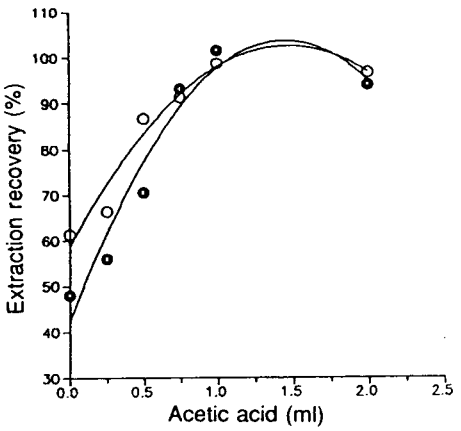

Fig. 2. Effect of the amount of acetic acid (96%) on the recovery of TBT and DBT. ○ = Bu_3Sn^+; ● = Bu_2Sn^{2+}.

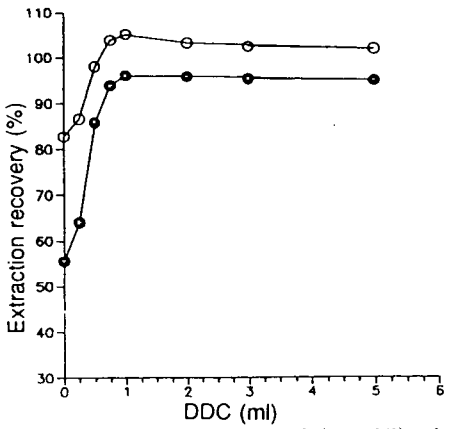

Fig. 3. Effect of the amount of DDTC (1 mol/l) solution on the extraction of TBT and DBT from sediments. ○ = Bu_3Sn^+; ● = Bu_2Sn^{2+}.

is illustrated in Fig. 2. The experiments were performed with spiked concentrations of the six ionic alkyltin species of the order of 1 $\mu g\ g^{-1}$ (as Sn). Apart from the variable amount of acetic acid, the normal analytical procedure was used. From Fig. 2 it can be seen that 1 ml of the concentrated acetic acid per gram of sediment is sufficient to liberate all DBT and TBT from the sediment surface within 60 min.

Selection of the optimum amount of DDTC

When 4 ml of Milli-Q-purified water and 1 ml of glacial acetic acid were added to the sediment sample, the measured pH in the mixture was ca. 2.0. Under these acidic conditions the aqueous NaDDTC solution cannot be used because of its known instability in acidic media. To overcome this problem, the acid form of NaDDTC, which is soluble in the organic solvent, needs to be used. Therefore, the daily prepared aqueous solution of NaDDTC (1 mol/l) was shaken with 10 ml of pentane and 20 ml of a 0.5 mol/l H_2SO_4 solution to obtain a solution of the carbamic acid (DDTC) in pentane, to be used in the leaching extraction procedure.

Fig. 3 shows the recovery of TBT and DBT from sediment as a function of the DDTC concentration. Both species showed optimum recoveries with 1 ml of 1 mol/l DDTC solution. When larger volumes (5–10 ml) of DDTC solution were added, the recoveries obtained for dimethyltin and monobutyltin increased up to 70 and 20%, respectively. However, simultaneously a decrease in the recoveries of TBT and DBT was observed. The extraction recoveries for TMT and MMT did not increase. Therefore, 1 ml of a 1 mol/l DDTC solution in pentane was used in subsequent work.

Effect of extraction time

An extraction time of 10 min provided a recovery of 75% for the butyltin species. To obtain higher recoveries the extraction time should be increased, and a maximum was reached at about 60 min (2×30 min), which kept the overall leaching–extraction procedure time reasonably short for practical use.

Spiking equilibrium time

Spiking experiments may present many problems that are not always faced in an appropriate way. One of the major problems is that the compounds naturally present and the spiked compounds are usually not in the same chemical form and are not bound to the sample (especially in solid samples) in the same way. Therefore, the results obtained from spiking experiments may not completely reflect the amount of organotin extracted from real sediment samples.

For this study, two series of spiked sediment samples were prepared, one series with an

Table 2
Extraction recoveries (%) of TBT and DBT in a spiked sediment after different equilibrium times ($n = 4$)

Species	15 min	24 h
Bu_3Sn^+	93 ± 5	87 ± 5
Bu_2Sn^{2+}	93 ± 5	80 ± 6

equilibrium time of 15 min and the other series with an equilibrium time of 24 h in the dark. The extraction recoveries obtained are shown in Table 2. For tributyltin only a different of 6% could be noted, whereas for dibutyltin the difference was twice as large. Despite this small difference, an equilibrium time of 15 min after spiking was used in further application studies.

Influence of sediment composition

After optimization of the above-mentioned parameters, different kinds of sediments were spiked with organotins and the effect of the kind of sediment on the extraction efficiency was studied. The sediments used were sediment sampled in Lake Maggiore, Italy, and certified reference materials estuarine sediment (CRM 277), lake sediment (CRM 280) and river sediment (CRM 320). Blank determinations showed that all sediments were free from butyltin except that sampled in Lake Maggiore, which contained both DBT and TBT. Some differences, up to 15%, were found in the recovery of TBT and DBT for the different sediments. Therefore, it is wise to control and/or to re-optimize all parameters when analysing an unknown sediment matrix.

3.2. Analytical characteristics of the leaching extraction procedure

Precision and recovery efficiency

Recovery and/or speciation of analytes from a complex matrix such as sediment are often difficult to assess and interpret. A common approach consists in the addition of a known amount of the analyte to the matrix of interest, allowing time for equilibration and then subjecting the spiked material to the analytical procedure.

An aqueous working standard solution (containing all six butyl- and methyltin species) was added to the river Scheldt sediment (63–189 μm) leading to concentrations of about 5 $\mu g/g^{-1}$ as Sn for each species. Analyses were conducted as mentioned above.

An estimate of the reproducibility of the optimized method for TBT and DBT speciation in sediments was obtained by analysing six replicates. The reproducibility of the entire procedure was estimated as ca. 5 % (relative standard deviation). The extraction recoveries were 95% and 103% for TBT and DBT, respectively.

Accuracy

The accuracy of the procedure was validated by the analysis of certified PACS-1 sediment (National Research Council of Canada). The results obtained for TBT and DBT in PACS-1 are given in Table 3. MBT cannot be determined

Table 3
TBT and DBT determinations in CRM 462 and PACS-1

Sample	Butyltin species	Result	Certified value
BCR CRM 462	Bu_3Sn^+	64.8 ± 7.7[a]	70.5 ± 13.2[a]
	Bu_2Sn^{2+}	127.6 ± 7.2[a]	128.0 ± 16.0[a]
PACS-1	Bu_3Sn^+	1.24 ± 0.09[b]	1.21 ± 0.24[b]
	Bu_2Sn^{2+}	1.53 ± 0.17[b]	1.14 ± 0.20[b]
	$BuSn^{3+}$	–	0.28 ± 0.17[b]

[a] Concentrations in ng/g as compound (±95% confidence interval).
[b] Concentrations in $\mu g/g$ as Sn (±95% confidence interval).

using this method. The results for TBT are in good agreement with the certified value, whereas for DBT the amount found in PACS-1 is higher but not significantly different from the certified DBT value. The method was also applied in a certification campaign organized by the BCR on coastal sediment CRM 462; the results obtained applying the described procedure for TBT and DBT agree well with the certified value within the 95% confidence interval, as can be seen from Table 3. Fig. 4 shows a chromatogram for a sample of CRM 462 sediment.

Detection limit

The detection limit of the method depends on the amount of sediment used for extraction and the final volume injected into the GC–QFAAS system. Starting from the analysis of 1 g of sediment, and assuming an injection of 4 μl of extract into the GC–QFAAS system, ionic butyltin compounds in the sediment can be detected at levels down to ca. 2.5 ng/g as Sn.

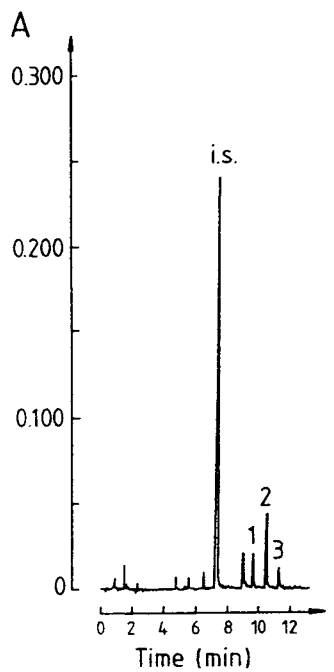

Fig. 4. GC–AAS of a sample of CRM 462 sediment. Peaks: 1 = Bu_3Sn^+; 2 = Bu_2Sn^{2+}; 3 = $BuSn^{3+}$; i.s. = internal standard (Pr_3SnPe). *A* = Detector response.

3.3. Determination of trimethyltin and dimethyltin

Different studies were carried out in order to test the possibility of extracting not only TBT and DBT, but also methylated compounds such as TMT and DMT.

The extraction of organotin compounds in hexane by complexation with NaDDTC has been successfully applied by Dirkx et al. [16] to the determination of these compounds in water. The simultaneous extraction of methyl- and butyltin species was possible by adjusting the pH of the sample to pH 5.

Adjusting the pH of the sediment slurry to pH 4.5–5.0 by adding appropriate amounts of powdered sodium acetate, after the leaching step and before the addition of NaDDTC, resulted in increases in the extraction efficiency for TMT (90%) and DMT (60%). NaDDTC solution in water could be used in these experiments because it is stable enough at this pH. However, under these conditions the recovery of TBT and DBT decreased considerably. Such a decrease in the recovery of the butylated species is not attributable to the non-desorption of the compounds from the matrix, because the leaching conditions were not modified with respect to the procedure proposed for DBT and TBT determination.

When TBT and DBT were first extracted following the previously described optimized procedure and after separation of the organic phase the pH of the remaining sediment was adjusted to pH 4.5–5, the recovery of DMT was 70% but only 40% of the spiked TMT was recovered.

On the basis of these promising results, further experiments will be carried out with different complexing agents and organic solvents in order to determine the four species simultaneously.

4. Conclusions

A reproducible method has been developed for the determination of di- and tributyltin present in sediments. The low detection limit

achieved, 2.5 ng/g, makes it suitable for the determination of these species in the environment, where butylated organotin compounds are released by anthropogenic activities. The feasiblity of DDTC as a complexing agent for the determination of both TBT and DBT without pH control and of NaDDTC for TMT and DMT at pH 4.5–5 has been demonstrated. The accuracy of the method has been tested through the analysis of certified materials, CRM 462 and PACS-1, with good agreement between the certified value and the results obtained with the proposed method. Method development for the determination of the methyltin compounds is of great interest for the clarification of biological processes, so far not completely understood.

Acknowledgements

Research grants by the Spanish Education Ministry and NFWO, Belgium, to M.B. de la Calle and M. Ceulemans, respectively, are gratefully acknowledged.

References

[1] R.J. Huggett, M.A. Unger, P.F. Seligman and A.O. Valkirs, *Environ. Sci. Technol.*, 26 (1992) 232.
[2] L. Ebdon, K. Evans and S. Hill, *Sci. Total Environ.*, 83 (1989) 63.
[3] P.H. Dowson, J.M. Bubb and J.N. Lester, *Appl. Organomet. Chem.*, 7 (1993) 623.
[4] L. Randall and J.H. Weber, *Sci. Total Environ.*, 57 (1986) 191.
[5] V. Desauziers, F. Leguille, R. Lavigne, M. Astruc and R. Pinel, *Appl. Organomet. Chem.*, 3 (1989) 469.
[6] C.L. Matthias, S.J. Bushong, L.W. Hall, J.M. Bellama and F.E. Brinckman, *Appl. Organomet. Chem.*, 2 (1988) 547.
[7] Ph. Quevauviller and O.F.X. Donard, *Appl. Organomet. Chem.*, 4 (1990) 353.
[8] I. Tolosa, J.M. Bayona, J. Albaiges, L.F. Alencastro and J. Taradellas, *Fresenius' J. Anal. Chem.*, 339 (1991) 646.
[9] K. Fent and M.D. Muller, *Environ. Sci. Technol.*, 25 (1991) 489.
[10] Y.K. Chau, S. Zhang and R.J. Maguire, *Analyst*, 117 (1992) 1161.
[11] S. Rapsomanikis, O.F.X. Donard and J.H. Weber, *Anal. Chem.*, 58 (1986) 35.
[12] M. Ceulemans, R. Łobiński, W.M.R. Dirkx and F.C. Adams, *Fresenius' J. Anal. Chem.*, 347 (1993) 256.
[13] Y. Cai, S. Rapsomanikis and M.O. Andreae, *Anal., Chim. Acta*, 274 (1993) 243.
[14] O.F.X. Donard, *Trends Anal. Chem.*, 11 (1992) 17.
[15] Y.K. Chau, *Analyst*, 117 (1992) 571.
[16] W.M.R. Dirkx, W.E. Van Mol, R.J.A. Van Cleuvenbergen and F.C. Adams, *Fresenius' Z. Anal. Chem.*, 335 (1989) 769.
[17] W.M.R. Dirkx, R. Łobiński and F.C. Adams, *Anal. Sci.*, 9 (1993) 273.

ELSEVIER

Journal of Chromatography A, 683 (1994) 59–65

JOURNAL OF CHROMATOGRAPHY A

High-performance liquid chromatography separation and light-scattering detection of phospholipids from cooked beef

Maria Fiorenza Caboni*, Simonetta Menotta, Giovanni Lercker

Istituto di Industrie Agrarie, Università di Bologna, Via S. Giacomo 7, 40126 Bologna, Italy

Abstract

A sensitive high-performance liquid chromatography (HPLC) method for the separation and quantitative analysis of major phospholipids (PLs) in biological systems is described. PLs were purified by solid-phase extraction with an amino (NH_2) phase. Separation of PLs was carried out on an HPLC silica gel column, with a mobile phase consisting of chloroform, methanol and ammonium hydroxide, and detection was performed with a light-scattering evaporative detector. HPLC analysis of PLs extracted from ground beef cooked under different conditions and capillary gas chromatography of the fatty acid methyl esters showed that cooking treatments did not have a significant effect on the PL composition and fatty acid contents of the single PLs in ground beef.

1. Introduction

Phospholipids (PLs) are ubiquitous constituents of all living tissues, since they are one of the main structural and functional components of cell membranes. PLs are, therefore, present in all foodstuffs and, because of their emulsifying properties, they can exert profound effects during food processing. PLs play an important role in governing the quality of meat during cooking and processing [1–3] and they are important flavour precursors because of their high content of long-chain polyunsaturated fatty acids. Fatty acids are important precursors of beef flavor since they are the primary source of carbonyl compounds upon heating [4,5]. In general, the more unsaturated fatty acids are the most susceptible to oxidation, giving a greater rate of oxidation [6]. Hornstein et al. [7] observed that upon exposure to atmosphere, PLs extracted from pork and beef muscles developed rancid off flavours much faster than neutral fats. This high susceptibility of PLs to oxidation is attributed to their high concentration of polyunsaturated fatty acids [8].

Numerous HPLC methods have been described for the separation of PLs. With a few exceptions [9–12], silica gel has been frequently used as the stationary phase. With respect to the mobile phase, different mixtures have been utilized; *n*-hexane–2-propanol–water [13–15], acetonitrile–methanol–water [16,17] or chloroform–methanol–ammonium hydroxide [18–20].

However, detection of PLs has been a major problem. Due to the absence of a specific absorption peak for lipids, UV detection does not allow a quantitative estimation of these compounds and refractive index detection is not compatible with gradient elution. The light-scattering (LS) evaporative detector, on the other

* Corresponding author.

0021-9673/94/$07.00
SSDI 0021-9673(94)00505-4

hand, allows detection of non-volatile substances with a very good sensitivity level and, moreover, it is compatible with all gradient elution. In fact, PL quantities ranging from 0.25 and 4 μg have been detected by LS detection [20].

The objective of this work is to develop an HPLC method for separation and quantitative analysis of PLs in biological systems. An application of this method was performed on ground beef subjected to different cooking treatments, in order to determine the PL composition and the fatty acid composition of the major PLs.

2. Experimental

2.1. Reagents and standards

All chemicals were purchased from Carlo Erba (Milan, Italy). Methanol and chloroform were HPLC grade; ammonium hydroxyde (30%), *n*-hexane, diethyl ether and acetic acid were analytical grade. Freshly deionized and distilled water was used. Fatty acid methyl ester standards (FAMEs) were obtained from Sigma (St. Louis, MO, USA).

PL standards were from Sigma: L-α-phosphatidylethanolamine (PE) from bovine brain, L-α-phosphatidylcholine (PC) from bovine liver, L-α-phosphatidyl–L-serine (PS) from bovine brain, sphingomyelin (Sph) from bovine brain, L-α-phosphatidylinositol (PI) from soybean, L-α-phosphatidyl D,L-glycerol (PG) from egg yolk lecitin.

Silica column regeneration solution was purchased from Supelco (Bellefonte, PA, USA).

2.2. Sample preparation

Patties (120 g) were prepared from ground beef purchased in a local supermarket (Bologna, Italy). These patties were then subjected to the following treatments: boiling, roasting in an oven, microwave heating, barbecue cooking style, roasting over a metal plate without oil (MP), and a combination of roasting and microwave heating. The microwave oven was a Model Sfornatutto Combi 7 plus, Dé Longhi (Treviso, Italy). Cooking was performed on both sides of the patties (half time per side). Cooking times and conditions are given in Table 1; temperatures were measured at the surface of the patties. All samples were compared against a raw patty (control).

2.3. Lipid extraction and separation

Total lipids were extracted from 30 g of patty, using the procedure described by Folch et al. [21]. A 250-mg amount of lipids was then dissolved in 250 μl of chloroform and applied to a Bond Elut (500 mg size) column with amino (NH_2) bonded phase (Varian, Harbor City, CA, USA), which was previously conditioned with hexane. The elution was carried out by adding 2.5 ml of a chloroform–isopropanol mixture (2:1, v/v) (two times), 2.5 ml of a 2% (v/v) solution of acetic acid–diethyl ether (two times) and 1 ml of methanol (four times) [22]. The

Table 1
Cooking times and temperatures for six cooking treatments

Cooking treatments	Cooking time (min)	Cooking conditions
BO	20	100°C
R	30	225°C
M	6	1000 W[a]
BA	18	200°C
MP	15	180°C
COMB	10	225°C + 1000 W[a]

Abbreviations: BO = boiling; R = roasting in an oven; M = microwave heating; BA = barbecue cooking style; MP = roasting over a metal plate without oil; COMB = combination roasting–microwave heating.
[a] Power of microwave heating.

methanolic fraction, which contained the PLs, was then diluted 10 times and analyzed by HPLC.

2.4. Fatty acid methyl ester preparation

The major phospholipids in the beef samples, i.e. PE and PC, were recovered by the HPLC three-way side vent valve from Scientific System (State College, PA, USA) and were transmethylated directly with 2 *M* KOH, according to Christopherson and Glass [23]. FAMEs were then analyzed by capillary gas chromatography (cGC).

2.5. Calibration of standard curves

Standard curves for HPLC analysis were run with the commercial standards of PC, PE, PS, PI, PG and Sph. Solutions contained 0.25–4 μg of PL and were injected in an increasing concentration order, in each run. Three replicates were run for each concentration. Regression analyses were done using the quadratic function $y = (a + bx)^2$.

2.6. High-performance liquid chromatography

The HPLC system comprised the following components: ERC degasser, Erma (Tokyo, Japan); Rheodyne injector Model 7125 (Cotati, CA, USA); Knauer pump Model 64 (Berlin, Germany); Autochrom gradient controller M-300 (Milford, MO, USA); Sedere light-scattering evaporative detector Sedex Model 45 (Vitry sur Seine, France). The HPLC system was equipped with an on-line filter (Rheodyne). The HPLC columns were LiChrosorb 60, 10 μm (25 cm × 4.6 μm I.D.) Wellington House (Macclesfield, UK) and Spherisorb Si 10 μm (25 cm × 4.6 mm I.D.) Phase Separations (Deeside, UK). The chromatograms were recorded with a Spectra-Physics 4290 integrator (San Jose, CA, USA). The LS detector was set at 60°C of evaporation temperature and at 2 atm of pressure of nebulization gas (compressed air) (1 atm = 101 325 Pa).

A methanolic ammonium hydroxide gradient in chloroform was chosen as eluent system because of its low viscosity and good solvent properties [18,19]. After optimization, the following binary gradient was utilized: (A) chloroform–methanol–ammonium hydroxide 30% (80:19.5:0.5, v/v) and (B) chloroform–methanol–water–ammonium hydroxide 30% (60:34:5.5:0.5, v/v). The flow-rate was 1.5 ml/min. The solvent program is shown in Table 2.

Table 2
HPLC solvent program for a binary gradient

Time (min)	A (%)	B (%)
0	100	0
8	45	55
15	40	60
20	40	60
35	100	0

A = chloroform–methanol–ammonium hydroxide 30% (80:19.5:0.5, v/v); B = chloroform–methanol–water–ammonium hydroxide 30% (60:34:5.5:0.5, v/v).

The time required for returning to the starting conditions and for column equilibration (15 min) was observed, in order to avoid significant variations in the retention volumes.

2.7. Capillary gas chromatography

cGC analysis were performed using a Carlo Erba 4260 gas chromatograph (Rodano, Milan, Italy) equipped with split injector and flame ionization detector. The cGC column was a 25 m fused-silica capillary column (0.25 mm I.D. and 0.25 μm film thickness) coated with cyanopropyl methyl silicone from Quadrex (New Haven, CT, USA). The oven temperature program was from 150 to 240°C at a rate of 3°C/min. Injector and detector temperatures were both set at 260°C. The helium carrier gas flow-rate was 2 ml/min, with a split ratio of 1:30. cGC chromatograms were recorded with a Spectra-Physics 4290 integrator.

3. Results and discussion

Calibration curves for each of the PL standards were run with concentrations ranging from

0.25 to 4 μg of PLs and exponential curves were obtained according to the equation $y = (a + bx)^2$. The quadratic regression constants (a, b) and the correlation coefficients (r^2) for each PL calibration curve are given in Table 3, for which the statistic curve fit F was found to be significant at a 0.01% level. Malton [24] has found a linear response for the calibration curves, but using considerably larger amounts of PLs. The minimum quantifiable amount of PL was 100 ng, except for the case of Sph in which 250 ng was the minimum quantitated. In fact, Sph gives two bands as reported by some authors [20,25,26]. For quantitative purposes, the Sph content was calculated from the sum of two peaks. The method described here, therefore, is sensitive enough to quantify the PL levels present in biological systems.

Fig. 1 shows a HPLC trace of a 15-min analysis of a mixture of PL standards. Once the adequacy of this method was established, some considerations were made with respect to the HPLC column, which was packed with a silica phase and used with an aqueous eluent. Silica phase columns are able to give optimum separation of PL mixtures [27,28], besides being relatively inexpensive. Moreover, according to Vanderdeelen et al. [29], the irregular phase seems to be more suitable for this type of analysis than the spheric configuration; thereby, an irregular phase column was used in this work. However, a strong decay of the column properties was observed after 2 months of continuous use. It was possible to delay the column removal for a week, by immersing the column in a commercial regenerating liquid overnight. Despite these difficulties, the total cost of the analysis was still affordable due to both the low cost of the column and the relatively high number of analyses that could be run. On the other hand, solid-phase extraction (SPE) columns with a NH_2 bonded phase gave an optimal purification of the PL fraction with a 99% recovery.

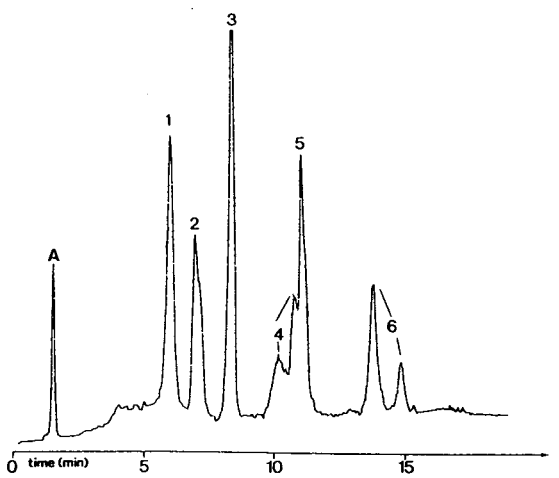

Fig. 1. HPLC trace of phospholipid standards. Peaks: A = free fatty acids; 1 = PG; 2 = PE; 3 = PI; 4 = PS; 5 = PC; 6 = Sph.

Table 3
Quadratic regression constants (a, b) and correlation coefficients (r^2) for phosopholipid calibration curves

PL	a	b	r^2
PC	501.514	554.701	0.9737
PE	444.424	570.524	0.9811
PS	628.386	428.922	0.9333
PI	478.605	727.641	0.9879
PG	329.380	562.413	0.9748
Sph	459.484	565.489	0.9764

Abbreviations: PC = phosphatidylcholine; PE = phosphatidylethanolamine; PS = phosphatidylserine; PI = phosphatidylinositol; PG = phosphatidylglycerol; Sph = sphingomyelin

This methodology was then applied to study the effect of different cooking treatments in the PL composition of ground beef, from a qualitative and quantitative point of view. Many authors have already reported the PL composition of bovine muscle from a biological standpoint [24,30], rather than from a food technology aspect. Since this work analyses lipids in foods, instead of lipids in an specific muscle or organ, a direct comparison with those data would not be valid.

Fig. 2 shows the HPLC trace of roasted ground beef, where a good peak separation of the main PLs was obtained.

Table 4 reports the PL concentrations in ground beef samples (expressed in mg/g of fat). Traces of PS and PG were also found (data not

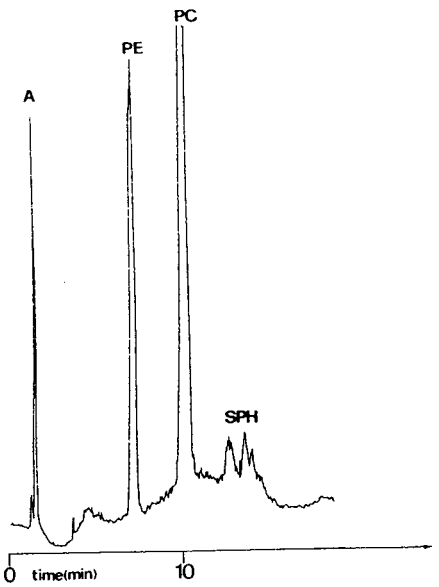

Fig. 2. HPLC trace of phospholipids from roasted ground beef. A = Free fatty acids.

shown). In general, cooking treatments produced small variations in the PL content. On the other hand, Sph decreased uniformly in all cooked samples; this might be due to a weaker interaction between Sph and the cellular membrane so that part of the Sph is lost with some fat during cooking.

With respect to the FAME preparation, transmethylation was carried out using the method by Christopherson and Glass [23], since its application to PLs has been also confirmed by other authors [31,32]. Although other methodologies have been suggested for this purpose [33], the method followed in this study was used because of the fast sample preparation at room temperature and the quantitative validity of the results.

Table 4
Effect of cooking treatments on the phospholipid contents in ground beef (expressed in mg/g of fat)

Treatment	PC	PE	Sph	Total
RM	15.36	11.36	9.36	36.08
BO	15.84	16.8	7.76	40.4
R	17.36	15.44	8.16	40.96
M	17.44	15.2	7.92	40.56
BA	17.68	18.8	7.2	43.68
MP	14.24	11.52	6.48	32.24
COMB	16.96	13.28	6.64	36.88

Abbreviations as in Tables 1 and 3.

FAMEs were identified by comparison with a cGC trace of a standard mixture of FAMEs and confirmation was with a fractionation by silver ion TLC [34], which separated the different methyl esters by degree of unsaturation, and with a further cGC analysis of the fractions. Identification was in agreement with previous papers [35,36]. Results from Table 5 and 6 show little variations in the FAME content of the PLs of cooked beef samples. No increase was observed in the amount of *trans* fatty acids, except in the case of C16:1. Changes in the polyunsaturated fatty acids content could have been expected due to an oxidation process which takes place during cooking; however, no differences were noticed in the PLs of raw and the cooked patties in this respect.

The analytical procedures given in this work allow rapid (total run of 35 min, included restoring of the initial conditions), accurate and sensitive analysis from animal tissues. The SPE method allows the separation of PLs from other types of lipid and a quantitative concentration of minor amounts of PLs for further HPLC analysis.

The type of detector used in this investigation was a light-scattering one, which is based on the nebulization of the eluate of the HPLC column by evaporation of the mobile phase. Detection is carried out by measuring the amount of light scattered by the solid particles that are left after evaporation of the mobile phase.

The high sensitivity of the LS detector used in this investigation permits detection and quantification of small amounts of PLs. This innovative model of detector selects by split the more homogeneous and minute particles of the nebulized solute, so that interaction is avoided among the larger droplets that have not been completely evaporated. Moreover, this detector has a more accurate control of the temperature and of the evaporation pressure than the previous models. These parameters along with the cell geometry have a direct influence on both the nebulization

Table 5
Effect of cooking treatments on FAME content (%) in ground phosphatidycholine

Treatment	Fatty acids %																		
	14:0	15.0	16.0	16:1t	16:1	17:0	17:1	18:0	18:1t	18:1	18:2	18:3	20:1	20:3	20:4	20:5	22:4	22:5	22:6	others
RM	0.7	0.3	24.0	0.2	2.1	0.7	0.7	10.0	0.6	30.9	22.6	1.2	0.5	0.7	3.1	0.3	0.2	0.6	0.1	0.5
BO	0.1	0.3	20.5	0.7	1.3	0.5	0.8	7.1	0.6	27.4	29.4	1.0	0.2	1.6	5.3	0.5	0.4	1.4	0.4	0.6
R	0.1	0.2	21.9	0.6	1.3	0.5	0.5	7.3	0.8	27.7	28.9	0.9	tr	1.5	4.5	0.8	0.3	0.9	0.2	0.5
M	0.1	0.2	23.0	0.7	1.3	0.5	0.5	7.7	0.8	29.3	25.4	1.0	tr	1.6	4.8	0.9	0.3	1.0	0.2	0.5
BA	0.2	0.3	22.9	0.7	1.5	0.5	0.7	7.1	0.4	27.4	28.5	0.2	tr	1.4	4.6	0.4	0.7	1.3	0.2	0.6
MP	0.2	0.3	23.2	0.6	1.3	0.5	0.6	7.2	0.5	27.3	28.3	0.8	0.2	1.1	4.4	0.3	0.4	0.8	tr	0.5
COMB	0.2	0.3	23.1	0.7	1.5	0.6	0.9	7.3	0.6	26.6	28.0	1.0	0.2	1.5	4.8	0.4	0.5	1.1	0.2	0.6

t = *trans*; tr = trace; RM = raw; other abbreviations as in Table 1.

Table 6
Effect of cooking treatments on FAME content (%) in ground beef phosphatidylethanolamine

Treatment	Fatty acids %															
	16:0	16:1	17:0	17:1	18:0	18:1t	18:1	18:2	18:3*n*6	18:3*n*3	20:1	20:3	20:4	20:5	22:4	22:5	22:6
RM	3.2	0.6	0.2	0.2	18.9	0.2	15.8	26.9	tr	0.5	0.2	3.2	22.5	1.2	2.0	3.8	0.8
BO	1.7	0.6	0.3	0.3	18.7	0.8	15.1	28.2	0.1	0.7	0.5	3.3	22.7	1.4	1.8	3.3	0.6
R	2.0	0.8	0.2	0.2	20.4	0.5	15.7	31.1	0.2	0.7	0.4	3.5	19.5	1.0	1.1	2.3	0.4
M	5.4	1.0	0.3	3.2	20.7	0.9	14.5	29.5	0.2	0.8	0.2	3.4	24.3	1.6	2.0	4.3	0.4
BA	2.0	0.7	0.3	0.6	24.0	0.3	12.4	21.9	0.2	1.0	0.4	2.5	25.0	1.4	1.8	3.5	2.0
MP	3.2	1.1	0.6	1.3	17.6	0.1	13.5	26.7	0.1	1.2	0.3	2.2	25.1	0.8	1.3	3.7	1.0
COMB	2.9	0.7	0.4	0.2	19.5	0.1	14.5	27.1	0.1	0.7	0.2	4.4	22.2	1.3	2.0	3.2	0.5

Abbreviations as in Table 5.

homogeneity and the evaporation velocity, therefore affecting directly the sensitivity and repeatability of the instrument. Due to these improvements, more precise quantifications are achieved, thus reducing respectively the effects of underestimation and overestimation of the amounts of major and minor component of the mixture, respectively.

On the other hand, all types of solvent gradient can be utilized with the LS detector. However, the solvent mixture should be prepared only with very volatile acid or bases in the absence of buffers.

A good recovery of the single PLs is achieved by using the split valve, allowing further analysis of the FAMEs by cGC.

With respect to the analysis of the ground beef samples, it can be concluded that no differences were observed in the FAME contents of the PLs, despite the different cooking methods used. Moreover, it seems that lipids in foods are much more protected than those from model systems, which are generally used to simplify complex events that occur in nature. As demonstrated by previous investigations, other nutrients present in foods have a protective effect on fatty substances [37] and when lipids are constituents of an organized biological structure, this "protection" phenomenon is more evident.

References

[1] D.S. Mottram and R.A. Edwards, *J. Sci. Food Agric. Sci.*, 38 (1983) 517.
[2] B.R. Wilson, A.M. Pearson and B.F. Shortland, *J. Agric. Food Chem.*, 24 (1976) 1311.
[3] J.D. Keller and J.E. Kinsella, *J. Food Sci.*, 38 (1973) 1200.

[4] E. Selke, W.K. Rohwedder and H.J. Dutton, *J. Am. Oil Chem. Soc.*, 54 (1977) 62.
[5] E. Selke, W.K. Rohwedder and H.J. Dutton, *J. Am. Oil Chem. Soc.*, 57 (1983) 75.
[6] H.Y. Gokolp, H.W. Ockerman, R.F. Plimpton and W.J. Harper, *J. Food Sci.*, 48 (1983) 259.
[7] I. Hornstein, P.F. Crowe and M.J. Heimberg, *J. Food Sci.*, 26 (1961) 581.
[8] D.K. Larick, B.E. Turner, R.M. Kock and J.D. Crouse, *J. Food Sci.*, 54 (1983) 521.
[9] N. Sotirhos, C. Thorngren and J. Herslof, *J. Chromatogr.*, 331 (1985) 313.
[10] M.V. Bell, *Lipids*, 24 (1989) 585.
[11] J.M. Samet, M. Friedman and D.C. Henke, *Anal. Biochem.*, 182 (1989) 32.
[12] K. Shimbo, *Agric. Biol. Chem.*, 50 (1986) 2463.
[13] P. Van Der Meen, J. Vanderdeelen, M. Huys and L. Baert, *J. Chromatogr.*, 447 (1988) 436.
[14] W.W. Christie, *J. Lipid Res.*, 26 (1984) 507.
[15] W.W. Christie, *J. Chromatogr.*, 361 (1986) 369.
[16] H.P. Nissen and H.W. Kreysel, *J. Chromatogr.*, 276 (1983) 190.
[17] W.J. Hurst and R.A. Martin, *J. Am. Oil Chem. Soc.*, 61 (1984) 1462.
[18] A. Stolyhwo, M. Martin and G. Guiochon, *J. Liq. Chromatogr.*, 10 (1987) 1237.
[19] W.L. Erdahl, A. Stolyhwo and O.S. Privett, *J. Am. Oil Chem. Soc.*, 50 (1973) 513.
[20] J. Becart, C. Chevalier and J.P. Biesse, *J. High Resolut. Chromatogr. Chromatogr. Commun.*, 13 (1990) 126.
[21] J. Folch, M. Lees and G.H.S. Stanley, *J. Biol. Chem.*, 226 (1957) 479.
[22] M. Kaluzny, L. Duncan, M. Merritt and D. Epps, *Lipids Res.*, 26 (1985) 135.
[23] S.W. Christopherson and R.L. Glass, *J. Dairy Sci.*, 52 (1969) 1289.
[24] S.L. Malton, *J. Am. Oil Chem. Soc.*, 69 (1992) 784.
[25] W.W. Christie, *J. Lipid Res.*, 142 (1985) 507.
[26] W.M.A. Hax and W.S.M. Geurts Van Kessel, *J. Chromatogr.*, 142 (1977) 735.
[27] W.W. Christie, *Z. Lebensm.-Unters.-Forsch.*, 181 (1985) 171.
[28] W.W. Christie, *HPLC and Lipids*, Pergamon Press, Oxford, 1987, p. 272.
[29] J. Vanderdeelen, M. Huys and L. Baert, *J. Am. Oil Chem. Soc.*, 67 (1990) 815.
[30] Y.K. Yeo and L.A. Horrocks, *Food Chem.*, 28 (1988) 197.
[31] R.J. Maxwell and W.N. Marmer, *Lipids*, 18 (1983) 543.
[32] R.J. Crackel, D.J. Buckley, A. Asghar, J.I. Gray and A.M. Booren, *J. Food Sci.*, 53 (1988) 1220.
[33] K. Eder, A.M. Reichlmar-Lais and M. Kirchgessner, *J. Chromatogr.*, 607 (1992) 55.
[34] D. Gegiou and M. Georguli, *J. Am. Oil Chem. Soc.*, 60 (1983) 815.
[35] L.S. Melton, *Food Technol.*, 37 (1983) 239.
[36] H.G. Brown, L.S. Melton, M.J. Riemann and W.R. Bakus, *J. Anim. Sci.*, 48 (1979) 338.
[37] M.F. Caboni, C. Mirri, T. Gallina Toschi, G. Lercker and P. Capella, in J. Velisěk (Editor), *Proceedings of Chemical Reaction in Foods II, FECS Event No. 174, Prague, 23-25 Sept. 1992*, pag. 176.

ELSEVIER

Journal of Chromatography A, 683 (1994) 67–74

JOURNAL OF CHROMATOGRAPHY A

Multi-residue screening and confirmatory analysis of anabolic steroids in urine by gas chromatography coupled with tandem mass spectrometry

G. Van Vyncht,*[a,b] P. Gaspar[a], E. DePauw[b], G. Maghuin-Rogister[a]

[a]*Laboratory of Analysis of Foodstuffs of Animal Origin, Faculty of Veterinary Medicine, University of Liège, B-42, Sart Tilman, 4000 Liège, Belgium*

[b]*Mass Spectrometry Centre, Chemistry Department, University of Liège, B-6, Sart Tilman, 4000 Liège, Belgium*

Abstract

The diversity of substances used illegally as growth promoters in meat production requires the development of multi-analyte methods of analysis involving a sample pretreatment step that is as rapid and as easy as possible, followed by a specific and sensitive determination of several residues within the same run. A general strategy for the screening and confirmatory analysis of fifteen artificial anabolic compounds in urine samples is described. It is based on solid-phase extraction on C_{18} Empore discs and amino-bonded columns followed, after derivatization (trimethylsilyl or methyloxime-trimethylsilyl derivatives), by gas chromatography coupled with collisionally activated dissociation tandem mass spectrometry.

1. Introduction

All over the world, and particularly in the European Community (EC), the attention of consumers is increasingly focused on chemical compounds generating residues in foodstuffs of animal origin. Public health authorities and the agrofood industries are faced with many difficulties in satisfying consumers and exportation market demands regarding the quality of meat and the safety and control of such residues. The detection of artificial anabolic agents illegally used as growth promoters in industrial farming is considered as a priority in the EC.

The diversity of substances used illegally as growth promoters in meat production has made it essential to develop a multi-residue strategy of analysis, involving a rapid and easy sample pretreatment followed by a specific and sensitive determination of several residues in the same run.

The official techniques used until now for these controls present many drawbacks. On the one hand, the immunological screening methods, radio- [1] and enzyme immunoassays [2], are very sensitive but, in most instances, are mono-residue tests. Moreover, the cross-reactivity properties of the antibodies [3] used in these tests with structural analogues of the controlled residue preclude an unambiguous identification of the compound in the complex matrix of a biological sample. As a consequence, positive results have to be validated by other, more reliable, analytical methods. The confirmatory

* Corresponding author.

0021-9673/94/$07.00
SSDI 0021-9673(94)00358-G

analysis techniques most often used are thin-layer chromatography [4] and low-resolution mass spectrometry coupled with gas chromatography [5]. To reach acceptable detection limits (μg/kg or ppb levels), they require extensive purification of the biosample (HPLC and/or multi-step column chromatography) before the analytical determination itself. Moreover, these efficient purifications are selective and do not allow multi-residue detection within the same chromatographic run.

The technique of determination that appears to be the most powerful for the analysis of anabolic steroid residues is collisionally activated dissociation tandem mass spectrometry (CAD-MS–MS) in the multiple reaction monitoring mode (MRM), coupled with gas chromatography.

The mass spectrometer used in our laboratory is a VG-AutoSpecQ ("EBEQQ" hybrid instrument), which allows the CAD mode of MS–MS to be used. It involves the selection of a precursor ion (formed in the ion source) in the sector part (EBE) of the mass spectrometer, its fragmentation in the quadrupolar collision cell (energetic collision with a gas such as air, helium or argon), followed by the determination of the mass to charge ratio (m/z) of the product ions by the last quadrupolar analyser. In this way, it is possible to monitor transitions from selected precursor ions to particular product ions (MRM mode), the first part of the instrument thus being considered as a physical mass filter that will avoid a major part of the biological matrix interferences to be analysed by the second analyser.

This is a very selective method that can be used with simple pretreatment of purification of the biosample. It is sensitive enough to reach the detection limits in the ppb range and also permits the determination of several residues within the same chromatographic run.

The aim of this study was to develop a general strategy for the screening and confirmatory analysis of artificial anabolic compounds in urine samples of animal origin. This paper describes the development of a rapid procedure for the detection of these residues, involving solid-phase extraction on C_{18} Empore discs and amino (NH_2)-bonded columns for sample pretreatment of large volumes of urine (30 ml), followed by gas chromatography coupled with tandem mass spectrometry for determination. The target compounds selected in this study were artificial and naturally occurring anabolic compounds commonly but illegally used in industrial farming.

2. Experimental

2.1. Material and reagents

All the solvents were of analytical-reagent grade from Merck (Darmstadt, Germany). β-Glucuronidase–arylsulphatase from *Helix pomatia* was obtained from Boehringer (Mannheim, Germany), N-methyl-N-trimethylsilyltrifluoroacetamide (MSTFA), N,N-bistrimethylsilyltrifluoroacetamide (BSTFA) and dry pyridine from Macherey–Nagel (Düren, Germany), iodotrimethylsilane (TMSI) from Aldrich (Brussels, Belgium), dithioerythritol (DTE) from Sigma (Deisenhofen, Germany) and methoxylamine hydrochloride from Supelco (Bellefonte, PA, USA).

Standards of steroids (see Fig. 1) were as follows. β-nortestosterone (nandrolone, 17β-hydroxy-4-estren-3-one), methylboldenone (17-methyl-1,4-androstadien-17β-ol-3-one), methyltestosterone (17-hydroxy-17-methylandrost-4-en-3-one), boldenone (1,4-androstadien-17β-ol-3-one), α-testosterone (17α-hydroxyandrost-4-en-3-one), β-testosterone (17β-hydroxyandrost-4-en-3-one), chlorotestosterone (clostebol, 4-chloro-17β-hydroxyandrost-4-en-3-one), chlorotestosterone acetate, *trans*-diethylstilbestrol [*trans*-DES; 4,4′-(1,2-diethyl-1,2-ethenediyl)bisphenol], ethinylestradiol [17α-ethinyl-1,3,5(10)-estratriene-3,17β-diol), α-estradiol [estra-1,3,5(10)-treine-3,17α-diol] and β-estradiol [estra-1,3,5(10)-treine-3,17β-diol] were obtained from Sigma (Deisenhofen, Germany). α-Trenbolone (17α-hydroxy-19-norandrosta-4,9,11-trien-3-one) and β-trenbolone (17β-hydroxy-19-norandrosta-4,9,11-trien-3-one) were

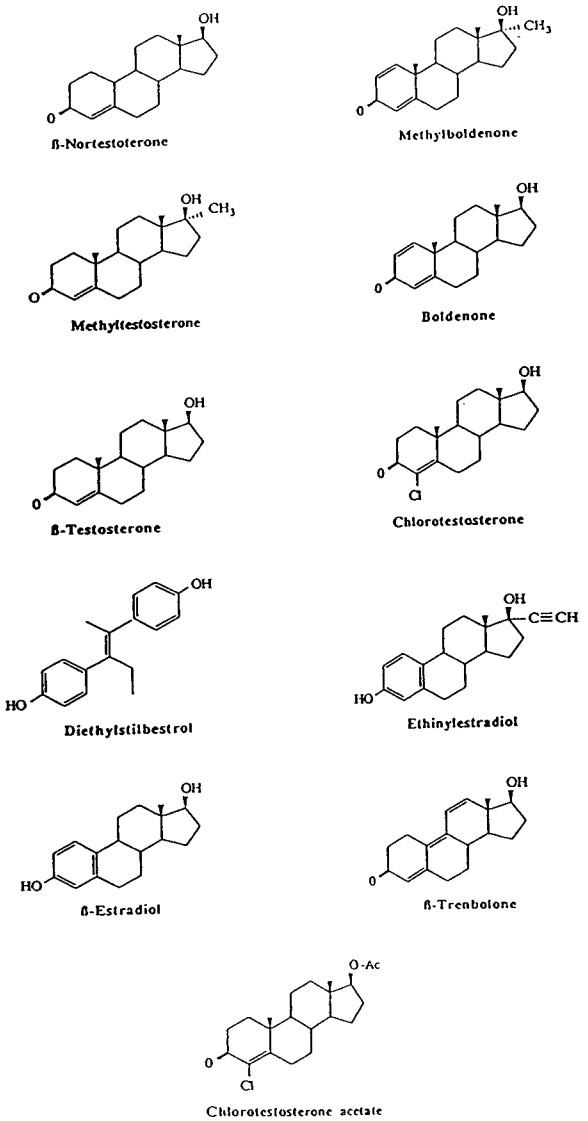

Fig. 1. Structures of the target anabolic compounds.

gifts from Roussel Uclaf (Romainville, France). α-nortestosterone (17α-hydroxy-4-estren-3-one) was a gift from CER (Marloie, Belgium).

Solid-phase Empore (3M) octadecyl-bonded Bakerbone discs (47 mm) and a Bakerbond Speamino (NH_2-bonded column (200 mg, 3 ml) were obtained from J.T. Baker (Deventer, Netherlands).

A DB-5 fused-silica capillary GC column (Ultra-2; 20 m × 0.2 mm I.D., 0.33-μm film thickness) was supplied by Hewlett-Packard (Avondale, PA, USA).

2.2. Apparatus

The extraction apparatus was composed of a Vac Elut SPS24 vacuum manifold from Varian (Brussels, Belgium) for Empore discs and a Baker Van Elut for disposable columns. An HP-5890 Series II gas chromatograph and an HP-7673 automatic injector were supplied by Hewlett-Packard. The tandem mass spectrometer used was a VG AutoSpecQ (VG Analytical, Manchester, UK).

2.3. Hydrolysis of conjugated steroids

Blank, fortified (2,5 and 10 ng/ml) and incurred urine samples (30 ml) were adjusted to pH 4.6 with 3 *M* sodium acetate buffer. They were hydrolysed at 60°C for 3 h with 75 μl of β-glucuronidase–arylsulphatase digestive juice from *Helix pomatia*.

2.4. Solid-phase extraction of steroids

The hydrolysed urine samples were centrifuged at 2000 *g* for 10 min at room temperature. The supernatant was extracted on a C_{18} Empore disc (47 mm) under a depression of 0.4 bar. The discs were preconditioned with ethyl acetate (10 ml), methanol (10 ml) and water purified with a Milli-Q system (2 × 10 ml). The sample was then applied to the extraction disc. The washing sequence consisted of 5 ml of methanol–water (55:45, v/v) and 5 ml of hexane. The disc was dried under vacuum (0.15 bar depression) for 10 min and the steroids were eluted with 3 × 5 ml of ethyl acetate. This extract was dried under a stream of nitrogen in a water-bath at 40°C. The dry residue was dissolved in 1 ml of ethyl acetate and applied to a Bakerbond column (200 mg) under a depression of 0.2 bar. The columns were preconditioned with 3 × 2 ml of ethyl acetate. The steroids were collected and further eluted with 500 μl of ethyl acetate.

2.5. Derivatization procedures

Trimethylsilylation

The extracts were evaporated to dryness at 40°C under a stream of nitrogen and derivatized with 50 μl of MSTFA–TMSI–DTE (100:10:5) at 60°C for 30 mins [7].

Methyloxime/trimethylsilyl ether (MO/TMS) derivatization

The extracts were evaporated to dryness at 40°C under a stream of nitrogen and derivatized with 100 μl of methoxylamine hydrochloride in dry pyridine solution (20 mg/ml) at 60°C for 1 h. Pyridine was evaporated to dryness under a stream of nitrogen (40°C) and trimethylsilylation was performed with 50 μl of BSTFA (60°C, 30 min) [7–9].

2.6. Gas chromatography

The temperature of the GC column oven was initially 120°C for 1 min, then increased at 15°C/min to 240°C and subsequently at 5°C/min to 300°C, the final temperature being maintained for 9 min. The carrier gas has helium (grade N_{60}) with a column head pressure of 100 mbar and a flow-rate of 1 ml/min. A 1-μl volume of the derivatization mixture was injected in the splitless mode; the injector and transfer line temperatures were 300°C.

2.7. Tandem mass spectrometry

The positive electron impact mode (EI^+) was applied with an electron energy of 70 eV and a trap current of 200 μA. The source temperature was 190°C. The collision gas used for CAD was air at a pressure of 10^{-6} mbar and with a collision energy of 30 eV. The resolution (at 10% of valley) of the sector part of the hybrid instrument (VG-AutoSpecQ) for the MRM mode was 100 and the quadrupole span was 0.5 mass unit. The dwell time for each transition was 80 ms.

3. Results

3.1. Solid-phase extraction recoveries

The recoveries of the extraction procedure (Empore disc and amino-bonded column) for several anabolic steroids were determined for 30-ml urine samples, using tritiated standards. The samples were spiked with tritiated steroids before hydrolysis and the complete extraction procedure was performed for each compound separately. The final extract (in ethyl acetate) was evaporated to dryness under a stream of nitrogen and the dry residue was dissolved in 200 μl of methanol. A 4-mol volume of scintillation liquid (EcoScint A from National Diagnostics) was added and the radioactivity of the extract was measured using a Beckman LS5000CE liquid scintillation counter. The extraction recoveries obtained are given in Table 1.

3.2. Derivatization procedures

The fastest and most sensitive derivatization technique was trimethylsilylation, using MSTFA–TMSI–DTE. This method allows the derivatization of the alcohol functions and, moreover, the enolization and trimethylsilylation of the ketone function of the 3-keto-steroids [6,7].

Unfortunately, trenbolone, one of the androgenic steroids tested, generates numerous isomers using this derivatization mode [7–9], owing to its three conjugated double bonds. One solution to this problem was to block the A-ring of trenbolone to form a 3-methyloxime group, and further derivatize the 17-alcohol function with a trimethylsilylating agent (BSTFA). In this way, only one peak was observed under the GC conditions used. The other 3-keto-steroids could also be MO-TMS derivatized (see Table 2), but for methyltestosterone we could not reach a detection limit below 10 ppb (in the MRM mode), owing to its poor MO-TMS derivatization efficiency under the conditions used.

Fig. 2 presents, as examples, the EI^+ full-scan ion spectra of the enol–TMS–TMS ether derivative of nortestosterone and of the MO-TMS derivative of trenbolone.

Table 1
Recoveries of tritiated anabolic steroids in spiked urine samples (30 ml) by the solid-phase extraction procedure

Compound	Mean recovery (%) ($n = 5$)	Standard deviation (%)
β-Nortestosterone	96	3
Methyltestosterone	95	4
β-Trenbolone	89	5
Ethinylestradiol	98	3
Diethylstilbestrol	87	6
β-Estradiol	98	2
Testosterone	94	5
α-Trenbolone	91	4

3.3. Tandem mass spectrometry

Different tandem mass spectrometric modes of analysis were tested (daughter and parent ion spectra, constant neutral loss scanning and multiple reaction monitoring) in both the first field-free region and collision quadrupole, using these derivatives. Only the MRM mode using the quadrupole collision cell air pressure 10^{-6} mbar;

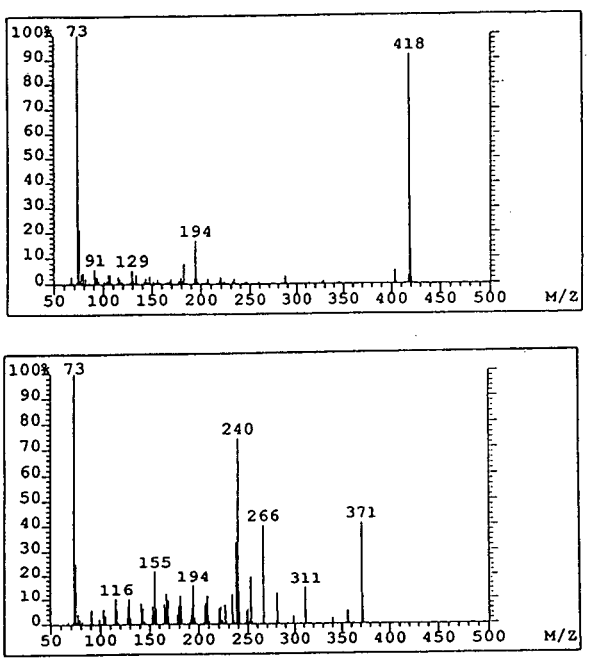

Fig. 2. Electron impact full-scan spectra of the enol–TMS–TMS ether derivative of 19-nortestosterone (m/z 418) and of the MO-TMS derivative of trenbolone (m/z 371).

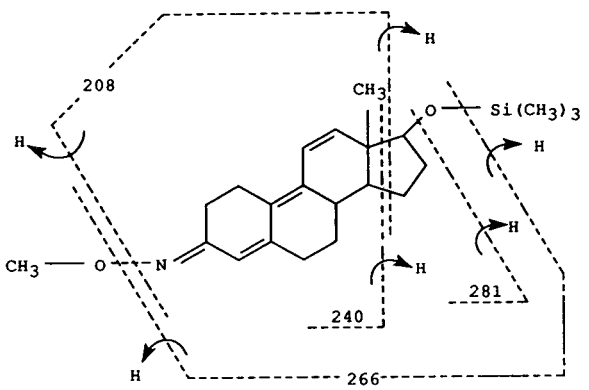

Fig. 3. Tandem mass spectrometric fragmentation (CAD) scheme for the molecular ion (m/z 371) of the MO-TMS derivative of trenbolone. Air pressure, 10^{-6} mbar; collision energy, 30 eV.

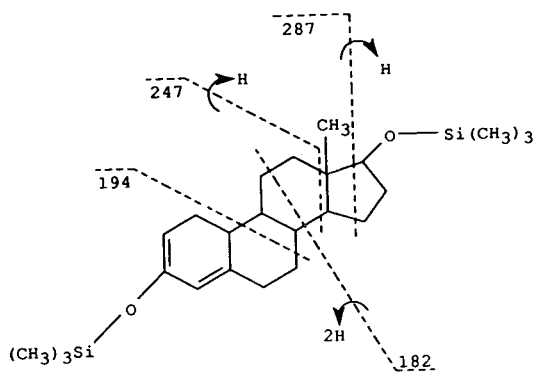

Fig. 4. Tandem mass spectrometric fragmentation (CAD) scheme for the molecular ion (m/z 418) of the enol–TMS–TMS ether derivative of nortestosterone. Air pressure, 10^{-6} mbar; collision energy, 30 eV.

Table 2
Most sensitive transitions monitored [CAD with air (10^{-6} mbar), collision energy 30 eV] and detection limits for each target compound, relative to their derivatization mode

Steroid	Derivatization mode	Retention time (min) (min:s)	Transition monitored (m/z)	Relative intensity (%)	Approximate detection limit (ppb)
α/β-Nortestosterone	TMS	13:10/13:40	418–287	60	0.5
			418–259	25	1
			418–247	20	1
			418–194	100	0.2
			418–182	25	1
	MO-TMS	13:20/13:50	375–344	45	1
			375–295	40	1
			375–254	100	0.5
Boldenone	TMS	14:00	430–415	50	0.5
			430–325	25	1
			430–299	10	2
			430–206	100	0.2
	MO-TMS	14:30	387–356	100	0.5
			387–266	40	1
			387–120	50	1
Methylboldenone	TMS	15:00	444–339	30	1.5
			444–299	25	1.5
			444–206	100	0.5
	MO-TMS	15:30	401–370	100	0.5
			401–280	85	1
α/β-Testosterone	TMS	13:30/14:10	432–417	50	0.5
			432–327	100	0.2
			432–301	60	0.5
			432–208	75	0.5
	MO-TMS	13:40/14:20	389–268	70	1
			389–153	80	1
			389–125	100	0.5
Methyltestosterone	TMS	15:10	446–356	10	0.5
			446–301	100	0.1
α/β-Trenbolone	MO-TMS	14:00/14:50	371–281	65	1
			371–266	90	0.5
			371–240	100	0.5
Chlorotestosterone	TMS	16:50	466–431	70	1
			466–335	100	0.5
			466–230	25	2
	MO-TMS	17:10	423–266	100	0.5
			423–240	25	2
			423–208	20	2.5
Chlorotestosterone acetate	TMS	17:50	436–401	75	1
			436–432	50	1
			436–230	100	0.5
	MO-TMS	18:20	393–302	20	2.5
			393–266	25	2
			393–171	100	0.5
α/β-Estradiol	TMS	13:40/14:10	416–326	20	1
			416–285	100	0.2
			416–232	25	1
Ethinylestradiol	TMS	15:30	440–425	100	0.5
			440–285	60	1
			440–196	30	1.5
trans-Diethylstilbestrol	TMS	11:00	412–397	70	1
			412–383	100	0.5
			412–217	55	1

collision energy 30 eV), allowed to reach ppb (μg/kg) detection limits in multi-residue analysis, as other modes required residue levels over 10 ppb.

The CAD-MS–MS fragmentation schemes proposed, as examples, for the MO-TMS derivative of trenbolone and for the enol–TMS–TMS ether derivative of nortestosterone, under the described conditions, are presented in Figs. 3 and 4, respectively [9,10].

The detection limits reached under these conditions are summarized in Table 2 for each compound and relative to the derivative used. All of them range from 0.1 to 2 ppb, allowing the monitoring of such residues in urine samples (decision level of 2 ppb for artificial anabolic compounds). Another advantageous point is that, for all the target residues tested, one of the three mentioned transitions is more sensitive with detection limits below 0.5 ppb. The monitoring of this unique transition per target residue allows the screening of up to fifteen anabolic compounds during the same chromatographic run.

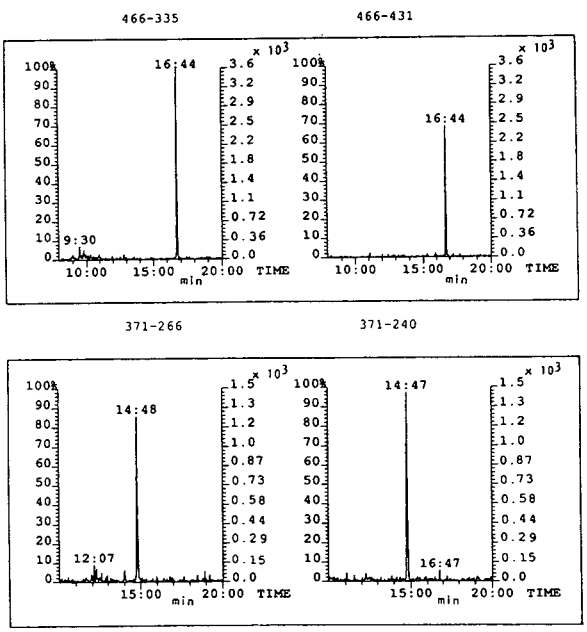

Fig. 5. GC–MS–MS for a 2 ppb spiked urine sample, for two transitions of the enol–TMS–TMS ether derivative of chlorotestosterone (m/z 466–431/466–335) and two transitions of the MO-TMS derivative of trenbolone (m/z 371–266/371–240). Collision cell air pressure, 10^{-6} mbar; collision energy, 30 eV.

As an example, Fig. 5 shows the GC–MS–MS traces obtained for a 2 ppb spiked urine sample, for two transitions of the enol–TMS–TMS ether derivative of chlorotestosterone (m/z 466–431/466–335) and two transitions of the MO-TMS derivative of trenbolone (m/z 371–240/371–266). The chemical background observed in these low-resolution MS–MS analyses is much lower than in the chromatograms obtained in the low- or medium-resolution single-ion monitoring mode (SIR), in which it is impossible to interpret data in the ppb range without further purification of the urine sample.

4. Discussion

The method developed here, requiring minimal sample preparation, allows, on the same extract, both screening and/or confirmation for multi-residue analysis of anabolic compounds. If ambiguities still remain, the switch, using the same protocol, from TMS to MO-TMS derivatives brings a further confirmation step for 3-keto-steroids. The MO-TMS derivatization mode is necessary for the detection of trenbolone owing to its isomerization during TMS derivatization. Such an MS–MS method could be implemented on cheaper tandem mass spectrometric quadrupolar instruments.

A parallel approach using high-resolution mass spectrometry (HR-MS with resolution >5000) in the single-ion recording (SIR) mode gives the same detection limit for individual compounds. The simultaneous detection of several anabolic steroid residues would imply an acquisition based on voltage SIR. In this instance, the available mass range is only 10% of the nominal mass fixed at the magnet. The narrowness of this mass range does not allow a multi-residue strategy of analysis.

Work is in progress on the direct determination (without derivatization) of extracts using HPLC coupled with electrospray ionization at the inlet to the MS instrument.

Acknowledgements

We thank the Belgian Institute of Veterinary Meat Inspection (IEV; Institut d'Expertise Vétérinaire) for financial support. We also thank Roussel Uclaf (Romainville, France) and CER (Marloie, Belgium) for gifts of reference compounds.

References

[1] M.L. Scippo, P. Gaspar, G. Degand, F. Brose and G. Maghuin-Rogister, P. Delahaut and J.P. Willemart, *Anal. Chim. Acta*, 275 (1993) 57.
[2] G. Degand, P. Shmitz and G. Maghuin-Rogister, *J. Chromatogr.*, 489 (1989) 235.
[3] P. Gaspar and G. Maghuin-Rogister, *J. Chromatogr.*, 328 (1985) 413.
[4] F. Smets, H. DeBrabander, P. Bloom and G. Pottie, *J. Planar Chromatogr.*, 4 (1991) 208.
[5] E. Daeseleire, A.De Guesquière and C. Van Peteghem, *J. Chromatogr.*, 562 (1991) 673.
[6] E. Houghton, L. Grainger, M.C. Dumasia and P. Teale, *Org. Mass Spectrom.*, 27 (1992) 1061.
[7] K. Blau and G.S. King (Editors), *Handbook of Derivatives for Chromatography*, Heyden, London, 1977, Ch. 2–6.
[8] D. deBoer, M.E. Gainza Bernal, R.D. van Ooyen and R.A.A. Maes, *Biol. Mass Spectrom.*, 20 (1991) 459.
[9] B. Spranger and M. Metzler, *J. Chromatogr.*, 564 (1991) 485.
[10] K.L. Busch, G.L. Glish and S.A. McLuckey, *MS/MS —Techniques and Applications of Tandem Mass Spectrometry*, VCH, New York, 1988, Ch. 3–5.

ELSEVIER

Journal of Chromatography A, 683 (1994) 75–85

JOURNAL OF CHROMATOGRAPHY A

Identification of thermal oxidation products of cholesteryl acetate

Renzo Bortolomeazzi[a], Lorena Pizzale[a], Lanfranco S. Conte[a], Giovanni Lercker*[,b]

[a]*Dipartimento di Scienze degli Alimenti, Università di Udine, via Marangoni 97, 33100 Udine, Italy*

[b]*Istituto di Industrie Agrarie, Università di Bologna, via S. Giacomo 7, 40126 Bologna, Italy*

Abstract

The polar products separated by solid-phase extraction from the peroxidation mixture of cholesteryl acetate, were investigated. The oxidation products were identified by comparing GC retention times as well as the mass spectra against those of available or synthesized standards. The main oxidation products where 7β-chydroperoxicholesteryl acetate, 7α-hydroperoxicholesteryl acetate, 7-ketocholesteryl acetate, the α and β isomers of 7-hydroxycholesteryl acetate, the α- and β-epoxy isomers in 5,6 position and several derivatives from the loss of groups (especially the acetic and/or hydroxyl groups in the form of acetic acid and water).

1. Introduction

The fact that a number of cholesterol oxidation products are highly toxic [1–4] explains the many detailed studies dealing with their identification [1,5] and formation mechanisms over the last fifteen years. Many analytical problems encountered in determining cholesterol's oxidation mechanisms via the identification of oxidation products are linked to the presence of an hydroxyl group in position 3, that interacts via a polar effect with both the chromatographic materials and substrate components. The present study reports and discusses the identification of the thermal oxidation products of cholesteryl acetate (CA), a molecule in which the importance of the polarity of the –OH group in position 3 is practically nullified, thereby resulting in a polarity similar to that of a fatty acid methyl ester. This approach makes it possible to exploit both the analytical procedure using the experimental conditions adopted in previous studies [6–10] for separations and molecular structure identification.

2. Experimental

2.1. Materials and reagents

Cholesterol, CA (>99%), 5,6α-epoxycholestanol (5,6α-epox), 5,6β-epoxycholestanol (5,6β-epox), 7α-hydroxycholesterol (7α-OH), 7β-hydroxycholesterol (7β-OH), 4β-hydroxycholesterol (4β-OH), 7-ketocholesteryl acetate (7-KA) and 7-keto-3,5-cholestadiene (7-KDA) were supplied by Steraloids (Wilton, NH, USA). The reagents and solvents (analytical or HPLC grade) were supplied by Carlo Erba (Milan, Italy). The solid-phase extraction (SPE) columns (Bond Elut, Analytichem International, Varian, CA, USA) were packed with 500 mg silica.

* Corresponding author.

0021-9673/94/$07.00
SSDI 0021-9673(94)00656-3

2.2. Preparation of 3β-acetyl derivatives of 7α-OH (7α-OHA), 7β-OH (7β-OHA), 5,6α-epox (5,6α-epoxA) and 5,6β-epox (5,6β-epoxA)

Single standard compound was acetylated with pyridine–acetic anhydride (1:1, v/v), for 12 h (epoxides) or 1–2 h (hydroxides) at room temperature. Preparative HPLC and GC–ion-trap detector (ITD) MS were carried out for purification and identification of the 3β-acetyl derivatives.

2.3. CA thermal peroxidation

A 0.5-g amount of CA was oven-heated at 160°C for 90 min, in a 20-ml PTFE-sealed screw cap container.

2.4. SPE collection of cholesteryl acetate oxidation products (CAOPs)

The cholesteryl acetate peroxidized was dissolved in 2 ml of *n*-hexane and loaded onto a

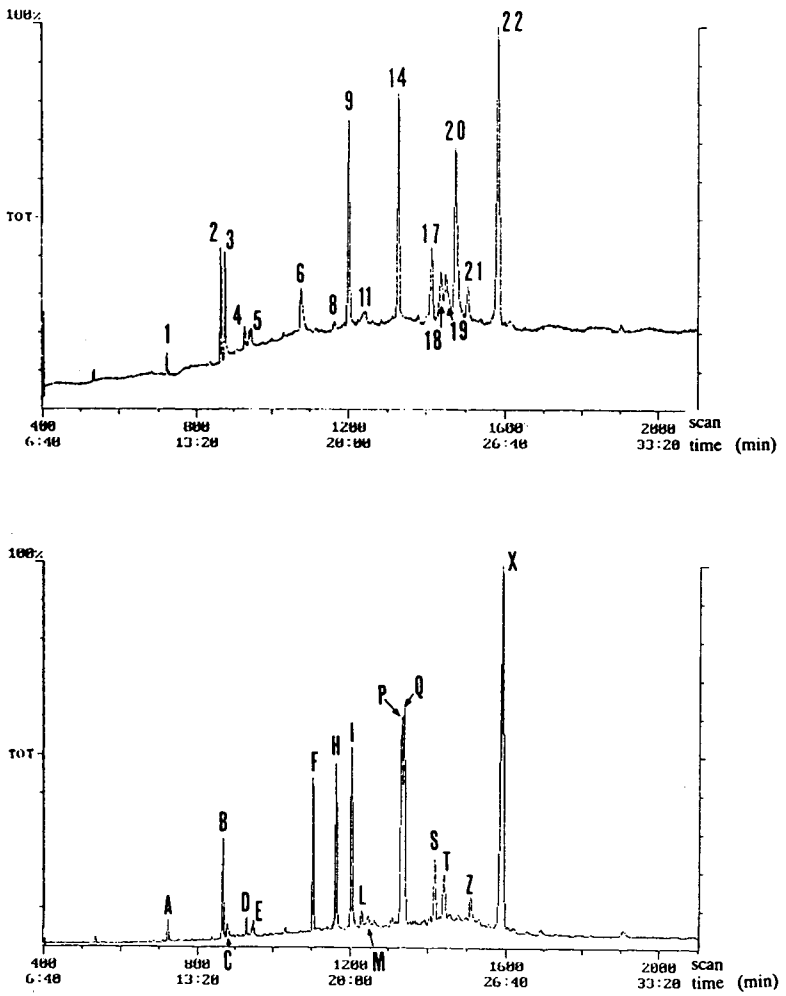

Fig. 1. GC–ITD-MS reconstructed chromatograms of SPE polar fraction: directly injected (top) and injected after TMS derivatization (bottom). Component identification is reported in Table 1.

SPE column preconditioned with 5 ml of *n*-hexane. The column was then eluted with 4 ml of *n*-hexane–diethyl ether (95:5, v/v), 5 ml of chloroform–methanol (1:1, v/v) and 5 ml of methanol.

The second fraction which contained the CA thermal oxidation products was then analyzed by GC–ITD-MS both directly and after silanization.

2.5. Trimethylsilyl ether (TMS) preparation

The samples were silylated with about 0.1 ml of pyridine–hexamethyldisilazane–trimethylchlorosilane (5:2:1, (v/v/v) [11] for 30 min at room temperature, in a desiccator. After drying by evaporation under nitrogen flow, samples were re-dissolved in 30–50 μl of benzene.

2.6. GC–ITD-MS

The capillary gas chromatograph was a Varian 3400 coupled to a Varian Saturn ion-trap detector utilized in the electron impact (EI) mode; the fused-silica column was a DB-5 type (5% phenylmethyl) (J&W, Folsom, CA, USA), with

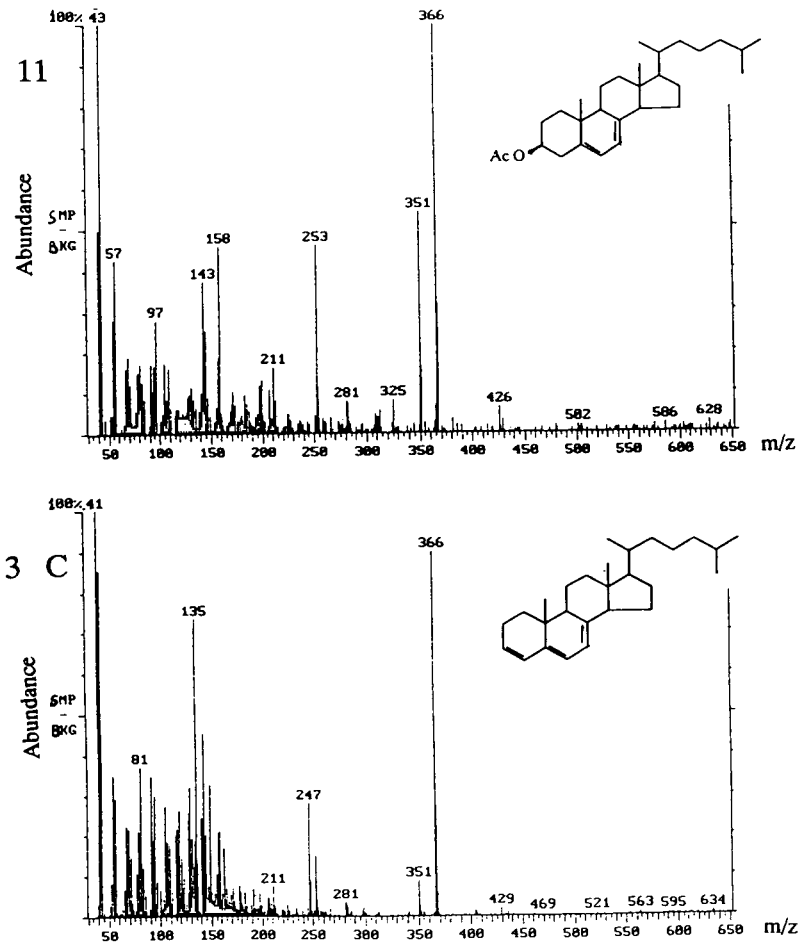

Fig. 2. Mass spectrum of 5,7-cholestadienyl-3β-acetate (11, M) (top): fragments at *m/z* 426 and 366 correspond to the molecular ion (M^+) and the loss of acetic acid, respectively. Mass spectrum of 3,5,7-cholestatriene (3, C) (tentative) (bottom). Mass spectrum of GC background was substracted (sample – background, SMP – BKG) from mass spectra.

dimensions 30 m × 0.255 mm I.D. and 0.25 μm film thickness. Oven temperature was programmed from 220 to 300°C at a rate of 5°C/min. Injection was in the split mode (1:50 ratio) at a 1 ml/min flow-rate with helium as carrier gas; the injector, transfer line and manifold temperatures were 300, 300 and 220°C, respectively. The filament emission current was 10 μA.

3. Results and discussion

The GC–ITD-MS traces (Fig. 1) were recorded by analyzing the mixture of polar components after SPE collection and purification; these components were examined immediately (Fig. 1, top) and after derivatization by silylation of all –OH groups (Fig. 1, bottom). From the

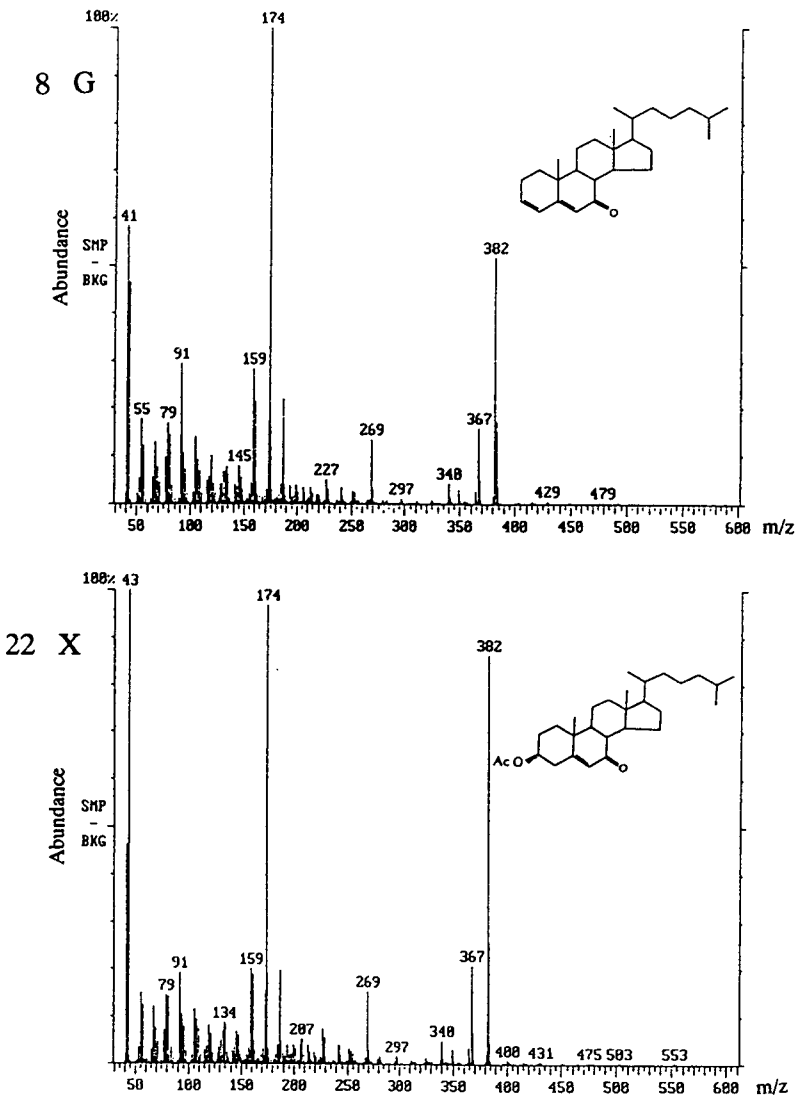

Fig. 3. Mass spectra of 7-keto-3,5-cholestadiene (8, G) (top) and 7-keto-cholesteryl-3β-acetate (22, X) (bottom). Fragment at m/z 382 correspond to the loss of acetic acid (60 u) from molecular ion; fragment at m/z 174 correspond to the elimination of the upper rings (and side chain, except for one methylene group) from the m/z 382 fragment. Mass spectrum of GC background was substracted (sample – background, SMP – BKG) from mass spectra.

found substances, 1-A, 2-B, 3-C, 4-D, 5-E, 11-M, 14-P, 18-T, 17-S and 21-Z are common to both traces.

Fig. 2 shows the mass spectra of components 3 (C) and 11 (M) from Fig. 1; Fig. 3 the mass spectra of components 8 (G) and 22 (X); Figs. 4 and 5 the spectra of components 14 (P) and 17 (S) respectively; Fig. 6 the mass spectra of components 18 (T) and 21 (Z); Fig. 7 the mass spectrum of component 19 (H, as TMS) and Fig. 8 the mass spectrum of component 20 (Q, as TMS).

The mass spectra of components 6, F and 9 (I) correspond to those of cholesterol, CA and TMS cholesterol, respectively.

Table 1 shows the identification for the components in Fig. 1. All main components were determined by comparing GC responses as well

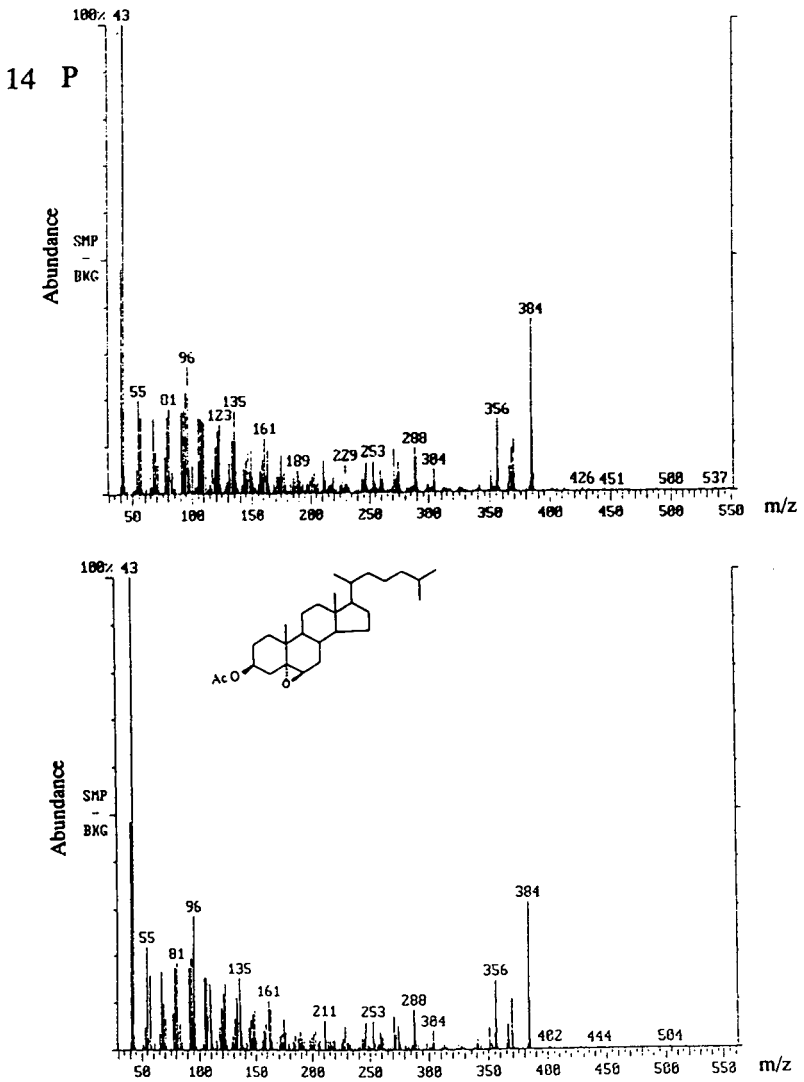

Fig. 4. Mass spectra of 5,6β-epoxy-cholesteryl-3β-acetate (14, P) (top) and corresponding standard (bottom). Fragment at m/z 384 correspond to the loss of acetic acid (60 u) from the molecular ion. Mass spectrum of GC background was substracted (sample – background, SMP – BKG) from mass spectra.

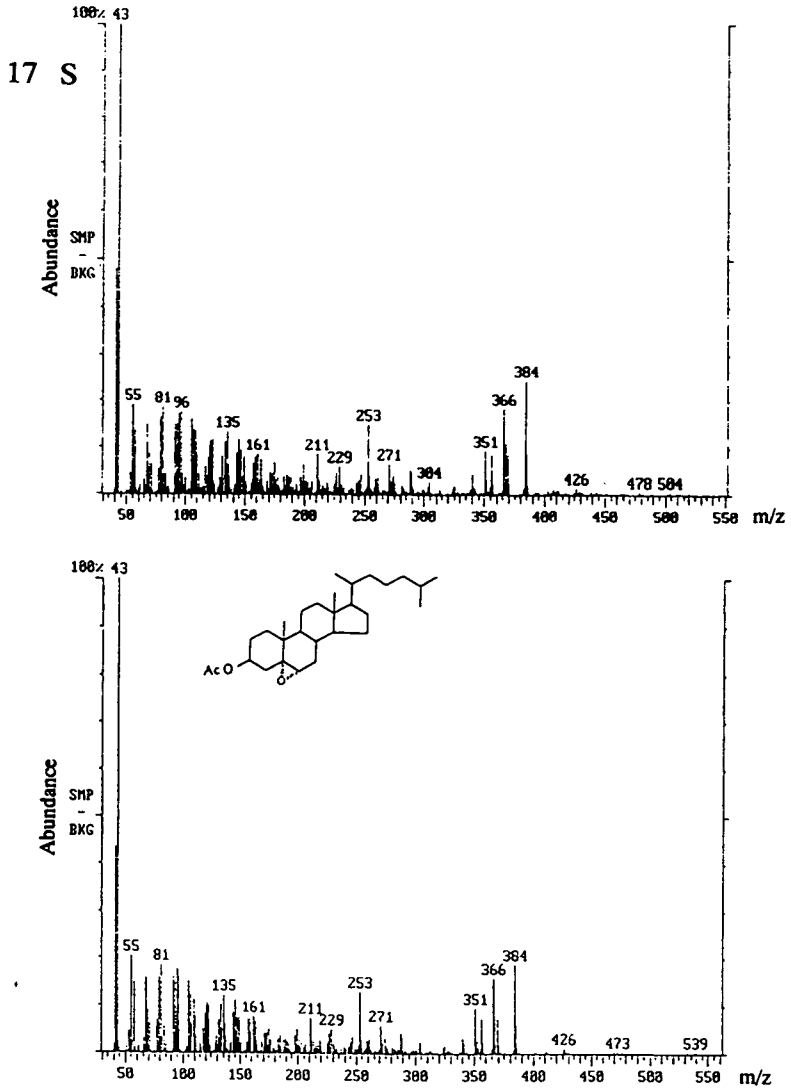

Fig. 5. Mass spectra of 5,6α-epoxy-cholesteryl-3β-acetate (17, S) (top) and corresponding standard (bottom). Fragment at m/z 384 correspond to the loss of acetic acid (60 u) from the molecular ion. Mass spectrum of GC background was substracted (sample – background, SMP – BKG) from mass spectra.

as the mass spectra against those of the standards and of synthesized substances. The identification of some components are tentative, on the basis of GC retention times and mass spectrum interpretation.

The mass spectrum of component 11 (M) (Fig. 2, top) is similar to that of cholesteryl acetate except that it has 2 atomic mass units (u) less, suggesting an additional unsaturation besides the one in position 5,6. The same fragments can also be seen in component 3 (C) (Fig. 2, bottom); the retention time and the quantitative difference in their ratios at m/z 43 and 41 (probably linked to the presence or absence of the acetyl group) suggest for component 3 (C) the structure of a steroid hydrocarbon with three unsaturations (in

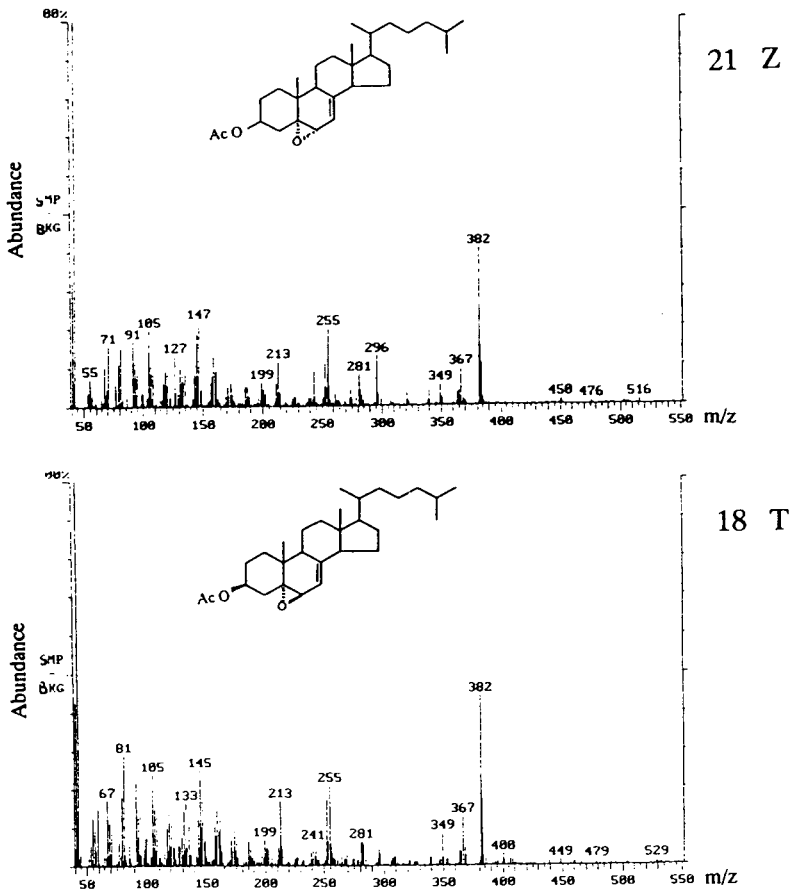

Fig. 6. Mass spectra of 5,6β-epoxy-7-cholestenyl-3β-acetate (18, T) (tentative) (bottom) and 5,6α-epoxy-7-cholestenyl 3β-acetate (21, Z) (tentative) (top). Mass spectrum of GC background was substracted (sample – background, SMP – BKG) from mass spectra.

3,4, in 5,6 and in 7,8), which are likely derived from the CA hydroxide compounds via the loss of H_2O and acetic acid. Component 11 (M) could thus be considered as an intermediate of component 3 (C) since it shows, via its mass spectrum, a structure with a molecular weight of 426, which confirms the presence of the acetyl group (characteristic loss of 60 u). The same holds true for component 8 (G) whose mass spectrum (Fig. 3, top) is very similar to that of 7-KA (Fig. 3, bottom; peaks 22 and X), and which is identical to that of its corresponding standard. The mass spectra of 8 (G) and 22 (X) are quite similar except for the smaller fragment at m/z 43. This indicates the absence of the acetyl group, a fact confirmed by the shorter retention time.

Figs. 4 and 5 show the mass spectra of the two 5,6-epoxyacetate isomers: β-epox (Fig. 4, top; peaks 14 and P) and α-epox (Fig. 5, bottom; peaks 17 and S); their retention times and mass spectra are identical to those of the corresponding standards. Fig. 6 shows the mass spectra of components 18 (T) and 21 (Z) from Fig. 1. The fact that the distribution of fragments with high values of m/z is the same as that of the two identified epoxides (Fig. 4) with 2 u less, suggests that these are epoxy derivatives (position 5,6) which have another, easily eliminated group. These two substances are probably gener-

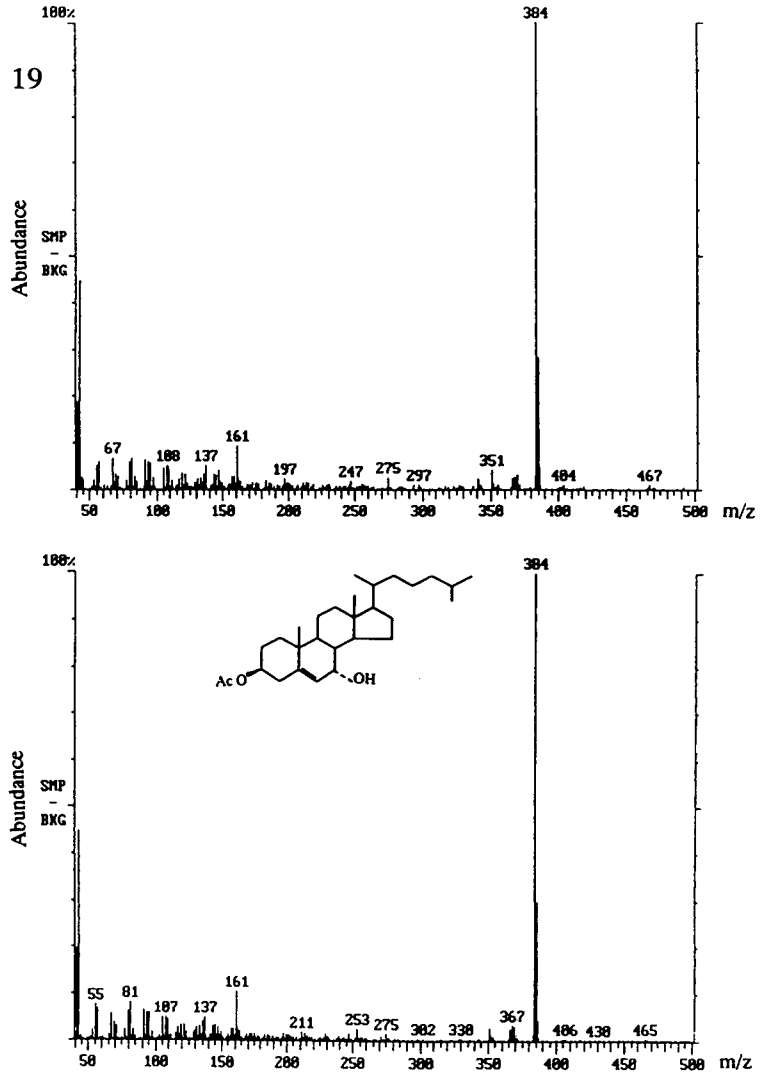

Fig. 7. Mass spectra of 7α-hydroxycholesteryl-3β-acetate (19; H, as TMS) (top) and corresponding standard (bottom). Fragment at m/z 384 correspond to the loss of acetic acid (60 u) from the molecular ion. Mass spectrum of GC background was substracted (sample − background, SMP − BKG) from mass spectra.

ated from the 5,6-epoxy-7-hydroxy-cholesteryl 3β-acetates, which were found in other research [12], by dehydration in 7,8 position of 7β-OHA-epoxide and 7α-OHA-epoxide, respectively.

The mass spectra of components 19 (H) and 20 (Q) are shown in Figs. 7 and 8. They exhibit the same characteristics (retention time and mass spectra) as 7α-OHA (peak 19), 7β-OHA (peak 20), [7α-OTMSA (H) and 7β-OTMSA (Q)].

The component 3 (C) is found in small amounts after silanization of peroxidation mixture (Fig. 1, bottom), since it is probably produced by the direct degradation of hydroxides which are, in this case, mostly stable in the form

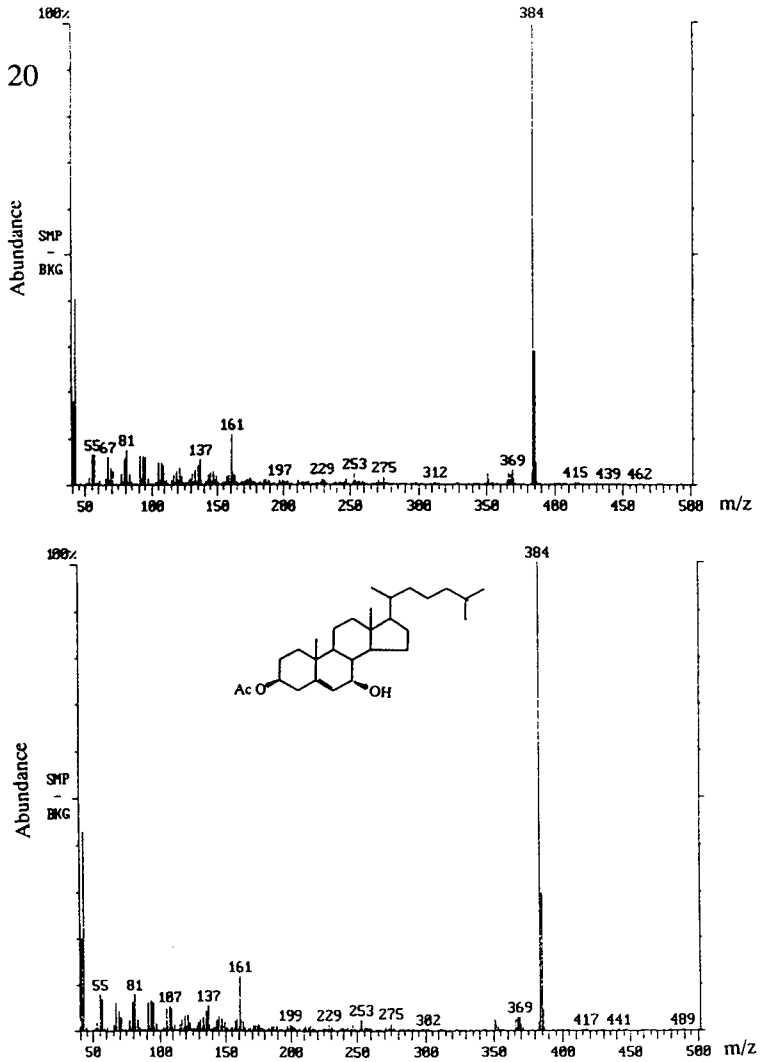

Fig. 8. Mass spectra of 7β-hydroxycholesteryl-3β-acetate (20; Q, as TMS) (top) and corresponding standard (bottom). Fragment at m/z 384 correspond to the loss of acetic acid (60 u) from the molecular ion. Mass spectrum of GC background was substracted (sample – background, SMP – BKG) from mass spectra.

of TMS derivatives. Therefore, previous identifications, as well as other data, could be confirmed from the resulting products of silanization.

Fig. 9 shows the identified products and their structures. Note the main components of the CA oxidation products, except for 7β-OOHA and 7α-OOHA, are 7-KA, 7β-OHA, 7α-OHA, 5,6β-epoxA and 5,6α-epoxA. Although SPE fractionation distinguishes well between polar and non-polar products, it cannot be ruled out that CA (peak 9) and cholesterol (peak 6) derive from the starting substrate; the former as residue and the latter as polar impurity. When CA is peroxidized, like methyl oleate, isolable hydro-

Table 1
Main thermo-oxidation products of cholesteryl acetate

GC peak (Fig. 1)	Name	Identification
1	Unknown	
2 (A)	Unknown	
3 (C)	3,5,7-Cholestatriene	Tentative
4 (D)	Unknown	
5 (E)	Unknown	
6	5-Cholesten-3β-ol (cholesterol)	t_R, MS
8 (G)	3,5-Cholestadien-7-one	t_R, MS
9 (I)	5-Cholesten-3β-acetate (CA)	t_R, MS
11 (M)	5,7-Cholestadien-3β-acetate	Tentative
14 (P)	5,6β-Epoxycholestan-3β-acetate	t_R, MS
17 (S)	5,6α-Epoxycholestan-3β-acetate	t_R, MS
18 (T)	5,6β-Epoxy-7-cholesten-3β-acetate	Tentative
19	5-Cholesten-7α-ol-3β-acetate	t_R, MS
20	5-Cholesten-7β-ol-3β-acetate	t_R, MS
21 (Z)	5,6α-Epoxy-7-cholesten-3β-acetate	Tentative
22 (X)	5-Cholesten-7-oxo-3β-acetate	t_R, MS
F	3β-Trimethylsilyloxy-5-cholestene	t_R, MS
H	7α-Trimethylsilyloxy-5-cholesten-3β-acetate	t_R, MS
L	Unknown	
Q	7β-Trimethylsilyloxy-5-cholesten-3β-acetate	t_R, MS

Identification carried out by mass spectrum interpretation (tentative) or by retention time (t_R) and mass spectrum (MS) comparison with those of standard availables or synthesized.

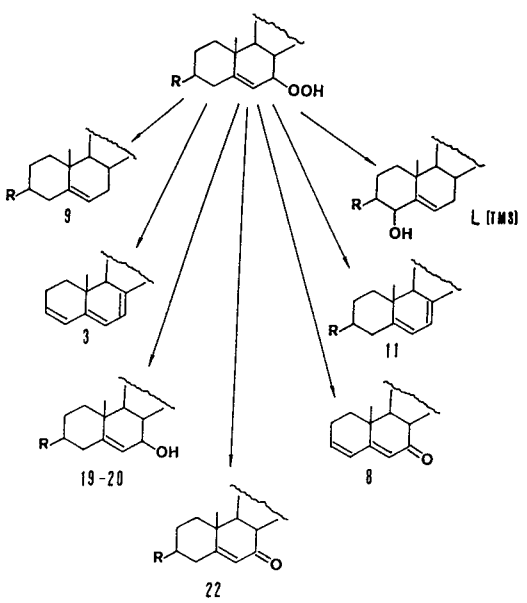

Fig. 9. Structures of the identified products

peroxides are formed [13]; these, in turn, give rise both directly or not to all the identified products [12].

Acknowledgements

This study was supported by the National Research Council of Italy, Special Project "Raisa", Sub-project 4 Paper No. 1778.

References

[1] L.L. Smith, *Cholesterol Autoxidation*, Plenum Press, New York, London, 1981.
[2] G. Maerker, *J. Am. Oil Chem. Soc.*, 64 (1987) 388.
[3] T. Gallina Toschi and M.F. Caboni, *Ital. J. Food Sci.*, 4 (1992) 223.
[4] S. Bosinger, W. Luf and E. Brandl, *Int. Dairy J.*, 3 (1993) 1.

[5] L.L. Smith, in C. Vigo-Pelfrey (Editor), *Membrane Lipid Oxidation*, Vol. I, Liposome Technology, Menlo Park, CA, 1991, p. 129.
[6] G. Lercker, in C. Galli and E. Fedeli (Editors), *Fat Production and Consumption*, Plenum, 1987, p. 269.
[7] R. Bortolomeazzi, L. Pizzale and G. Lercker, *J. Chromatogr.*, 626 (1992) 109.
[8] R. Bortolomeazzi, L. Pizzale and G. Lercker, *Chromatographia*, 36 (1993) 61.
[9] G. Lercker, in F. Ursini and E. Cadenas (Editors), *Dietary Lipids, Antioxidants and the Prevention of Atherosclerosis (Workshop)*, CLEUP Univ. Publ., Asolo, Italy, 1992, p. 103.
[10] G. Lercker, R. Bortolomeazzi and S. Moret, in P. Sandra (Editor), *Proceedings of 15th International Symposium on Capillary Chromatography, Riva del Garda, 23–27 May 1993*, Huethig, Heidelberg, p. 1243.
[11] C.C. Sweeley, R. Bentley, M. Makita and W.E. Wells, *J. Am. Chem. Soc.*, 85 (1963) 2497.
[12] G. Lercker, R. Bortolomeazzi, L. Pizzale and S. Vichi, in preparation.
[13] R. Bortolomeazzi, L. Pizzale, S. Vichi and G. Lercker, *Chromatographia*, in press.

ELSEVIER

Journal of Chromatography A, 683 (1994) 87–94

JOURNAL OF CHROMATOGRAPHY A

First results in trace identification of allelochemicals and pheromones by combining gas chromatography–mass spectrometry and direct deposition gas chromatography–Fourier transform infrared spectrometry

J. Auger*, S. Ferary

IBEAS URA CNRS 1298 and SAVIT, Université F. Rabelais, Parc de Grandmont, 37200 Tours, France

Abstract

The advantages of a combining GC–MS and direct deposition GC–Fourier transform IR spectrometry at the same level of sensitivity are demonstrated using an apolar capillary column. This technique was applied to allelochemicals and pheromones present in minute concentrations. The identification of *Allium* volatiles and of the leek-moth male pheromones is described.

1. Introduction

In complex mixtures of volatiles, identification by gas chromatographic (GC) means alone via retention times requires a knowledge of the compounds to be identified. In many instances of extracts of environmental and food samples, the identity of the major components (priority pollutants, for instance) is known but some extracts contain unknown minor compounds at low levels. Nevertheless, identification of these minor components can be of considerable interest.

In the ecological chemistry of insects, this problem is much more widespread because semiochemicals (allelochemicals and pheromones) are often present in very low concentrations biological matrices containing numerous aboundant and unknown substances. Further, these substances have a wide range of chemical diversity.

To succeed in these complex identifications, structural elucidation can be achieved through the use of coupled techniques such as GC–MS, the most commonly applied technique, MS is the method of choice owing to its high sensitivity and selectivity. However, despite its strengths, MS is not sufficient alone for univocal identification. For example, structural isomers often are not differentiated by MS and a complementary technique such as GC–Fourier transform (FT) IR spectrometry the most generally useful alternative, is needed.

Until a few years ago, it was not possible to combine the two coupled techniques GC–MS

* Corresponding author.

0021-9673/94/$07.00
SSDI 0021-9673(94)00436-D

and GC–IR at the same level of performance owing to the relatively low sensitivity of the conventional light-pipe based interfaces. With this gas cell system, as for GC–MS interfaces, the spectrum is measured in real time as each component eluates, so that each measurement can be performed without trapping the eluates. Identified spectra can usually be obtained only from amounts in the 1–50 ng range depending on to the absorbance of the compounds. The only way to lower the detection limits to the MS range (10–100 pg) is to trap each separated compound by freezing, which is achieved through the use of matrix isolation or direct deposition techniques.

In the matrix isolation interface, argon is added to the GC eluates and the mixture is condensed on a moving metal substrate cooled to 12 K. Each solute is trapped in an argon matrix as the carrier gas is pumped off and deposited as a trace whose width can be as small as 0.3 min; this technique increases tenfold the intensity of IR spectra compared with the intensity obtained with a light-pipe (1 mm I.D.) interface. The low temperature also decreases IR band widths, which leads to an enhancement of sensitivity and specificity relative to the gas-phase interface. Further, as each component is retained on the substrate, the signal-to-noise ratio of the spectra can be increased by subsequent scanning of the eluates [1].

In the new direct deposition interface from Bio-Rad, pure column effluent is condensed on a moving ZnSe window transparent to IR radiation and cooled to 77 K. The width of the spots can be reduced to about 0.1 mm and the eluates can be scanned immediately by means of FT-IR microscopy. With this interface, the detection limits of routine real-time GC–IR have been reported to be less than 100 pg [2] and in practice the potential applicability of direct deposition GC–IR has been evaluated in environmental analysis [3,4].

In view of these advantages, it might be very useful to combine direct deposition GC–IR and GC–MS for (i) the characterization of allelochemicals responsible for insect–plant relationships (possible biopesticides) and of insect pheromones and (ii) confirmatory analyses of xenobiotics in minute concentrations. We describe here the example of *Allium* volatiles attractive to the leek-moth, a specific pest of *Allium* species, and we have identified and determined leek-moth male pheromones.

2. Experimental

2.1. Instrumentation

Gas chromatography–mass spectrometry

Chromatographic separations were performed using a Hewlett-Packard (Palo Alto, CA, USA) HP5890 II instrument with a split–splitless injector and a fused-silica capillary column (20 m × 0.22 mm I.D.) with an HP1 methylsilicone film (film thickness 0.33 μm). The conditions were as follows: injector temperature, 200°C; oven temperature programme, 70°C for 5 min, then increased at 2°C/min to 280°C; carrier gas, helium; column flow-rate, 1.0 ml/min; splitting ratio, 1:30, or splitless; injection volume, 1 μl in all experiments.

Total ion chromatograms (TIC) and mass spectra were recorded using a Hewlett-Packard HP 5898 "mass engine" with an HP UX workstation in the electron impact ionization mode at 70 eV. The transfer line was maintained at 100°C, the source temperature at 200°C and the quadrupole temperature at 100°C.

Gas chromatography–IR spectrometry

GC separations were performed using exactly the same instrument and the conditions as for GC–MS, except for the flow-rate, which can be lowered to optimize the deposition, and sometimes a delay was added before temperature programme to better the solvent separate.

The Gram–Schmidt reconstructed chromatograms (GSC), the functional group chromatograms (FGC) and the IR spectra were recorded using a Bio-Rad Digilab (Cambridge, MA, USA) FTS 45A spectrometer equipped with a Digilab Tracer direct deposition interface con-

taining its own nitrogen-cooled MCT detector and with an SPC 3200 data system for data acquisition and instrument control. The transfer line was maintained at 250°C and real-time spectra were obtained by addition of four scans, with a resolution of 8 cm^{-1}.

These two coupled techniques were used here in parallel fashion and usually the runs were not simultaneous.

2.2. Sample preparation

Pheromonal extracts

The leek moth, *Acrolepiopsis assectella* (Acrolepiidae), possesses coremata or hair-pencils that are concealed when at rest in an abdominal pocket, which opens to the exterior laterally between the eight and ninth abdominal segments. These organs are extruded during sexual behaviour when the male, attracted by the sexual pheromones of calling females, approaches and flutters its wings a few millimetres from the female. Male pheromones emitted in this fashion provoke the adoption of the acceptance posture by the calling female and thus have an aphrodisiac role.

Through pressure on the abdomen of virgin males aged from 4 to 6 days, the opening of the pocket containing the hair-pencil becomes visible. With fine forceps the hair-pencils were removed, still retracted within the epithelium of the pocket. Using this method 300 hair-pencils were removed in the middle of the photophase and immediately immersed in 0.5 ml of hexane and kept at −20°C.

Allium volatiles

Allium vineale odour was emitted by cutting green leaves in a closed glass vessel (1 l) at room temperature. Headspace volatiles were trapped for 1 hr (flow-rate 250 ml/min) on a glass cartridge (20 mm × 4 mm I.D.) containing 30 mg of Tenax GC (Alltech, Deerfield, IL, USA) (60–80 mesh) directly connected to a Gilian (Wayne, NJ, USA) LFS 113 pump [5]. The trapped volatiles were eluted from the cartridge with 1 ml of peroxide-free diethyl ether (analytical-reagent grade) and immediately analysed.

Materials

Hydrocarbons used as reference compounds were obtained from Aldrich (Milwaukee, WI, USA).

3. Results and discussion

3.1. Pheromonal extracts

For the leek-moth hair-pencil extract, the TIC and the FGC between 2800 and 3000 cm^{-1} both show nine peaks (Fig. 1). The IR and mass spectra indicate a structure based on a linear saturated hydrocarbon from $C_{16}H_{34}$ to $C_{23}H_{48}$ for the peaks 1, 2, 3, 4, 5, 6, 8 and 9 (see, e.g. the spectra of peak 2, Fig. 2). Any doubt remaining as to the existence of branched isomers is lifted by the observation of the regular decrease in the ratio of the intensity of the IR asymmetric stretch bands CH_3 at 2950 cm^{-1} versus CH_2 at 2930 cm^{-1}. The identification of peak 7 is in progress.

Each injection corresponds approximately to a male equivalent and the abundance of these *n*-alkanes can be estimated as hexadecane = 4 ng, heptadecane = 400 ng, octadecane = 10 ng, nonadecane = 200 ng, eicosane = 4 ng, heneicosane = 200 ng, docosane = 4 ng and tricosane = 30 ng.

Among the compounds of this series, only four *n*-alkanes provoked as many responses of a sexual nature in virgin females as did the male extract. These are the three *n*-alkanes with the odd number of carbon atoms, heptadecane, nonadecane and heneicosane, which are the most abundant, and also hexadecane, which is less abundant, as are the other compounds with an even number of carbon atoms. This is the first case of *n*-alkanes in which the male pheromonal role has been clearly demonstrated [6].

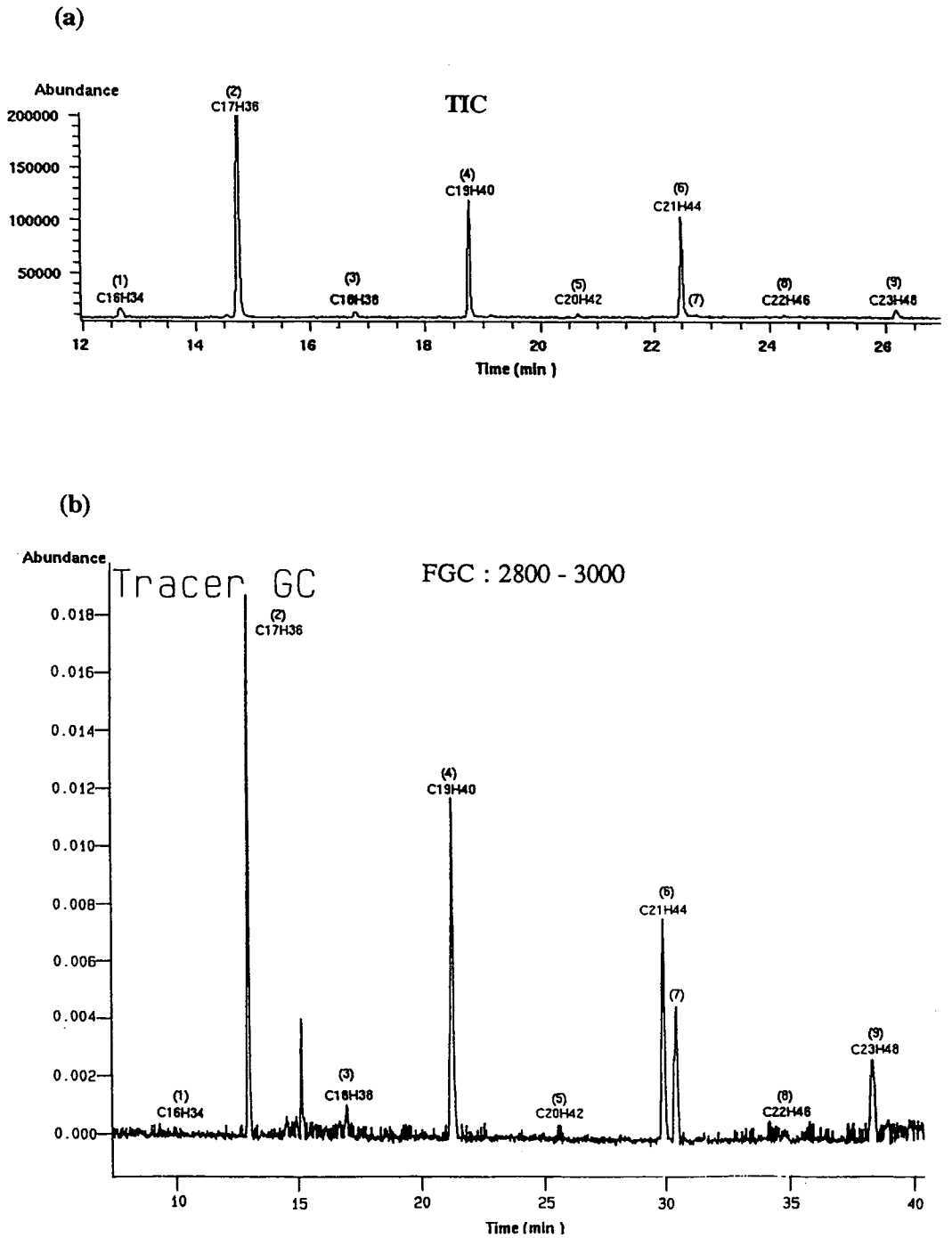

Fig. 1. (a) Total ion chromatogram and (b) functional group chromatogram (2800–3000 cm^{-1}) of pheromonal extract of the leek-moth male. For conditions, see Experimental.

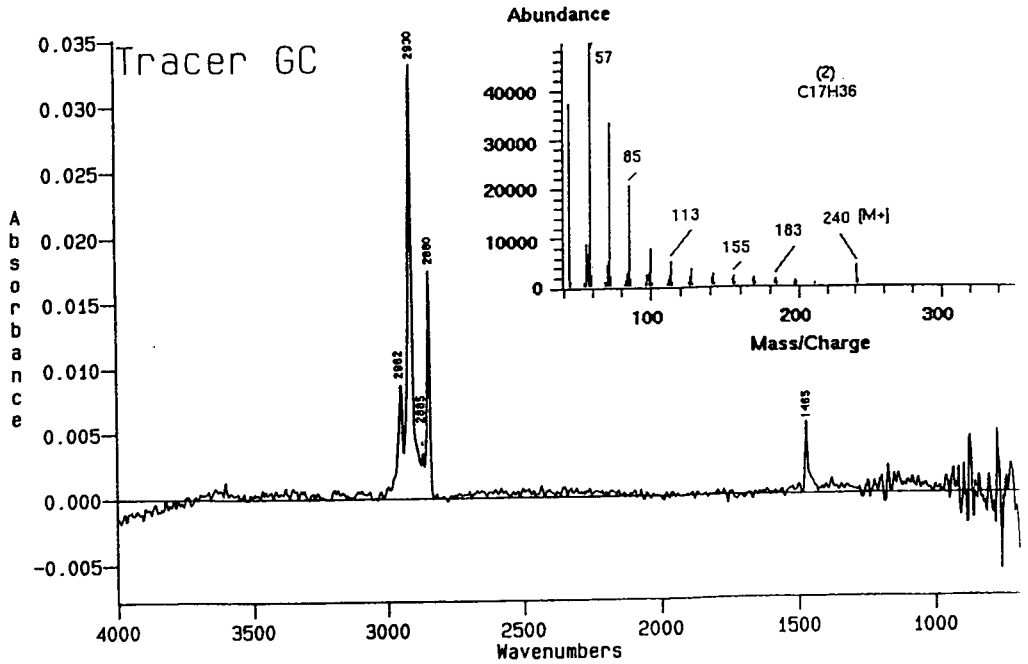

Fig. 2. IR and mass spectra of compound 2 in the pheromonal extract of the leek-moth. See Fig. 1.

3.2. *Allium* volatiles

The *Allium* odours are all attractive for the leek-moth and they contain mainly sulfur volatiles with four moieties, methyl, propyl (specified to leek, *A. Porrum*), allyl (specific to garlic, *A. sativum*) and 1-propenyl (specific to onion, *A. cepta*) [7]. Wild *Allium* species contain all these thio moieties in various proportions, depending on the species, and were screened in our laboratory.

For example, the TIC and GSC of *A. vineale* volatiles show mainly disulfides (Fig. 3). These disulfides exist as different structural isomers, e.g., compounds 1 and 3. Their mass spectra are not very different (same M^+ at 146) and are compatible with dipropenyl disulfides (diallyl disulfide according to an MS library search). Their IR spectra show the same characteristic allylic bands but the spectrum of 3 has some others that can be attributed to —CH_3 (deformation) for 2850 and 2940 cm^{-1}, to C—CH_3 (deformation) for 1340 and 1445 cm^{-1} and to —CH=CH— (out-of-plane deformation) for 925 and 950 cm^{-1} (Fig. 4). It is concluded that 1 is diallyl disulfide and 3 is allyl-1-propenyl disulfide.

All the disulfides identified in *A. vineale* are more or less attractive for the leek-moth, tested in an olfactometer [7].

From these examples it can be seen that direct deposition GC–IR is very useful for qualitative analysis of compounds at trace levels. This technique produces excellent spectroscopic information and is best suited for non-routine analysis where positive identification of compounds is required. The information obtained is complementary to the information obtained from GC–MS.

The linking of GC–MS with GC–IR at the same level of sensitivity appears to be the way to the future in chemical ecology and the combination of GC–MS and direct deposition GC–FT-IR is especially promising.

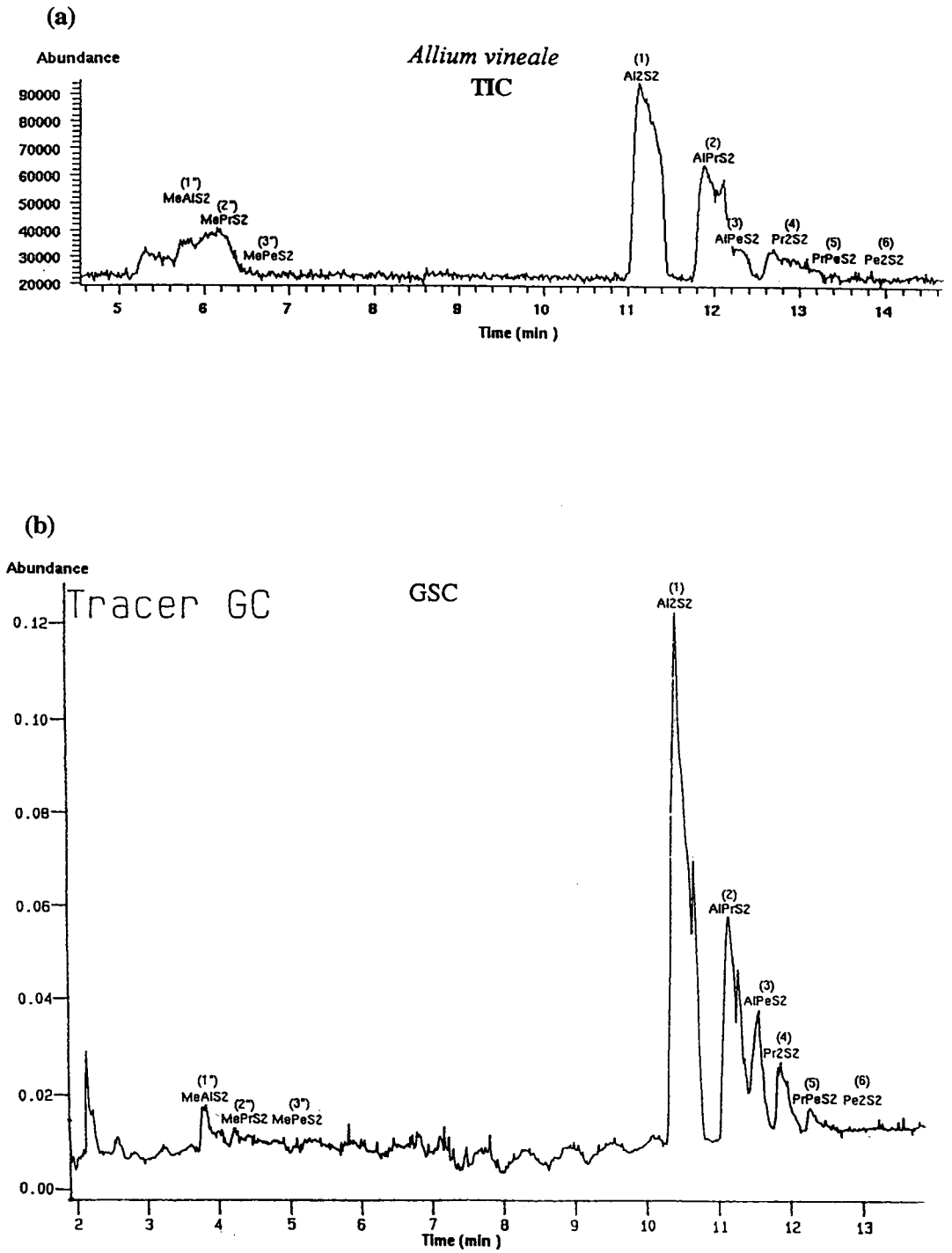

Fig. 3. (a) Total ion chromatogram and (b) Gram–Schmidt reconstructed chromatogram of *Allium vineale* trapped volatiles. For conditions, see Experimental.

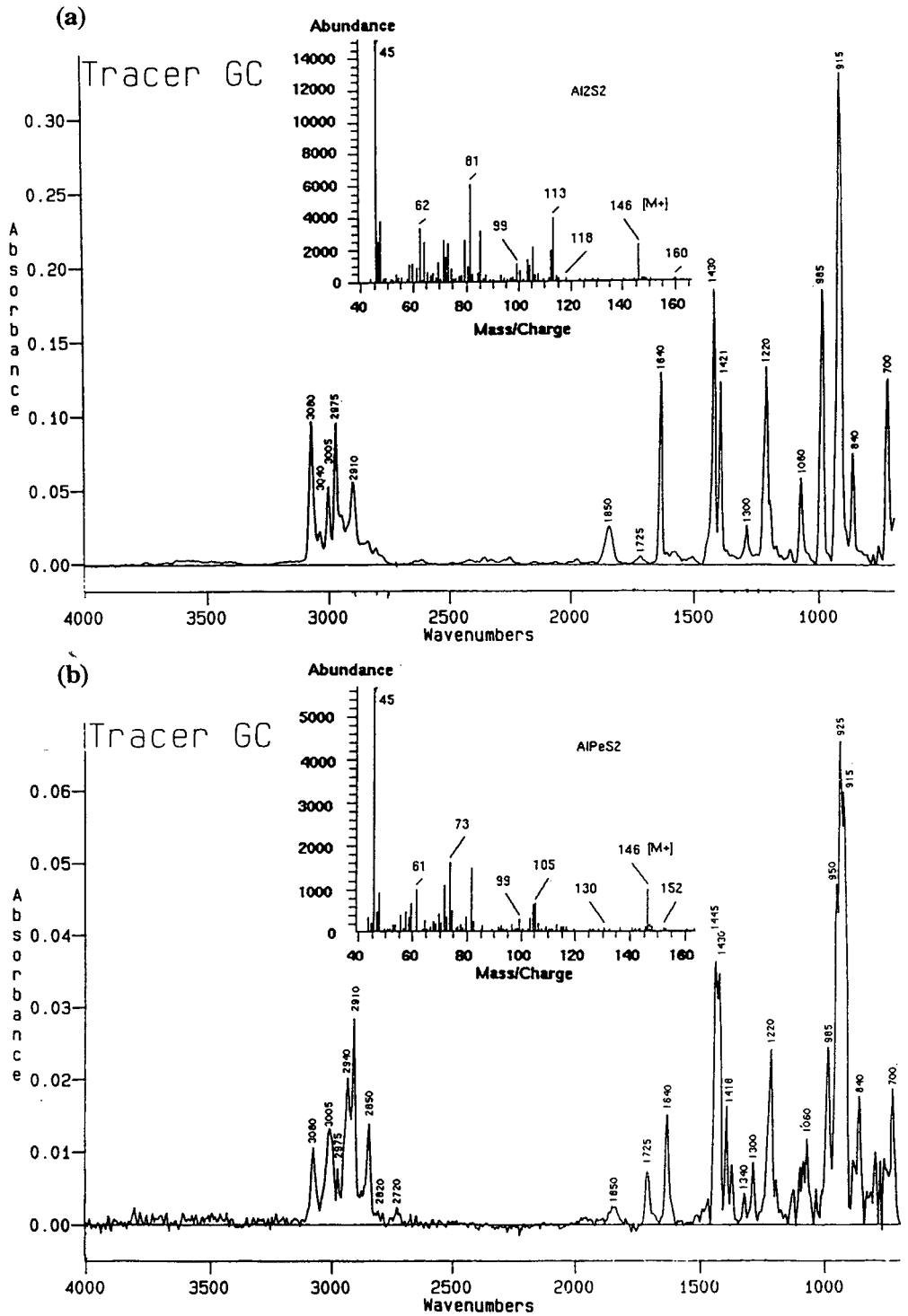

Fig. 4. IR and mass spectra of examples of *Allium* volatiles: (a) diallyl disulfide; (b) allyl 1-propenyl disulfide.

Acknowledgements

We thank Dr. E. Thibout for supplying the leek-moth hair-pencils and Dr. J. Boscher for supplying the *Allium vineale* leaves, and we gratefully acknowledge support from the Région Centre (financial assistance of S. Ferary for Ph.D. Thesis).

References

[1] P.R. Griffiths, S.L. Pentoney, Jr., A. Giorgetti and K.M. Shafer, *Anal. Chem.*, 58 (1986) 1349.
[2] S. Bourne, A.M. Haefner, K.L. Norton and P.R. Griffiths, *Anal. Chem.* 62 (1990) 2448.
[3] T. Visser and M.J. Vredenbregt, *Vibr. Spectrosc.*, 1 (1990) 205.
[4] T. Visser and M.J. Vredenbregt, A.P.J.M. de Jong, L.A. Van Ginkel, H.J. Van Rossum and R.W. Stephany, *Anal. Chim. Acta*, 275 (1993) 205.
[5] A. Tangerman, *J. Chromatogr.* 366 (1986) 205.
[6] E. Thibout, S. Ferary and J. Auger, *J. Chem. Ecol.*, 20 (1994) 1571.
[7] C. Lecomte, E. Thibout and J. Auger, *Phytophaga*, 1 (1987) 105.

ELSEVIER

Journal of Chromatography A, 683 (1994) 95–104

JOURNAL OF CHROMATOGRAPHY A

On-line liquid chromatography–gas chromatography for the analysis of free and esterified sterols in vegetable oil methyl esters used as diesel fuel substitutes

Christina Plank*, Eberhard Lorbeer

Institute of Organic Chemistry, University of Vienna, Währingerstrasse 38, A-1090 Vienna, Austria

Abstract

An on-line LC–GC method for the analysis of free and esterified sterols in vegetable oil methyl esters has been set up. Qualitative and quantitative information about this important group of minor components is provided without saponification and off-line pre-separation. Prior to analysis the free sterols are silylated with N-methyl-N-trimethylsilyltrifluoracetamide; betulinol is used as an internal standard. Using concurrent eluent evaporation with the loop-type interface for eluent transfer, transfer temperature and transfer efficiency are carefully optimized. The concentration of the free sterols as well as their qualitative and quantitative composition and the concentration of the sterol esters are determined in five different types of vegetable oil methyl esters. The recovery of the LC–GC procedure and the reproducibility of the quantitative results are evaluated.

1. Introduction

The introduction of quality standards for vegetable oil methyl esters, obtained by alkali-catalyzed transesterification of vegetable oils with methanol, is gaining in importance due to their increased use as diesel fuel substitutes and as technical products. In Austria standards for the quality of rapeseed oil methyl ester used as diesel fuel substitute have been introduced by the standard ÖNORM C 1190 [1] and also several other countries are elaborating standard specifications for these new kinds of oleochemical products. The amounts of the most important organic minor components (mono-, di- and triacylglycerols as well as free glycerol) have been limited by this standardization, since their presence in the fuel causes serious problems through formation of engine deposits and hazardous emissions.

In the production of vegetable oil methyl esters, the sterols as main constituents of the unsaponifiable matter of most vegetable oils remain in the fatty acid methyl ester phase, and are recovered both as free sterols and as esterified sterols in the transesterification product. The influence of the sterols on the technical properties of vegetable oil methyl esters is still not precisely understood, but their presence may influence the combustion characteristics, the storage properties, low-temperature behaviour characteristics and other physical and chemical properties in various ways. Sterol content and composition can also be criteria to distinguish

* Corresponding author.

0021-9673/94/$07.00
SSDI 0021-9673(94)00393-N

between products of different degree of purification or between different types of vegetable oil methyl esters.

Conventional methods for the analysis of the sterol fraction in oils and fats comprise saponification of the triglycerides, extraction of the unsaponifiables, pre-separation by preparative thin-layer chromatography [2–4], chromatography on silica gel columns [5,6], or by off-line HPLC [7], and finally gas chromatographic analysis.

In 1989, Grob et al. described an on-line LC–GC method for the direct determination of minor components in edible oils and fats avoiding saponification [8]. The sterols and related compounds as well as their fatty acid esters were isolated from the rest of the sample, primarily from the triglycerides, by HPLC and transferred on-line to GC. Recently this LC–GC method was modified, replacing the esterification of the free sterols with pivalic acid by trimethylsilylation [9]. A variation of the conventional methods for the analysis of sterols in oils and fats, substituting saponification by transesterification and isolation and pre-separation by on-line LC–GC, was proposed by Biedermann et al. [10].

Recently, we described a method for the direct determination of sterols in vegetable oil methyl esters by capillary GC [11]. In this work, an on-line LC–GC method for the rapid and reliable determination of free and esterified sterols in vegetable oil methyl esters is presented. In contrast to conventional methods for the analysis of the sterol fraction in fats and fat derivatives [4], analysis is carried out without saponification and any off-line pre-separation. Trimethylsilylation of the free sterols prior to analysis allows the determination of the concentration and composition of the free sterols as well as of the concentration of the sterol esters in a single LC–GC run. Transfer temperature and transfer efficiency, the most important parameters for correct solvent transfer and reliable quantitation using concurrent eluent evaporation with the loop-type interface, are optimized. Qualitative and quantitative determination of free and esterified sterols is carried out in five different types of vegetable oil methyl esters. The reproducibility of the quantitative results and the recovery of the LC–GC procedure is evaluated.

2. Experimental

2.1. Chemicals

The reference substances used in this study, stigmasterol, cholesteryl oleate, cholesteryl palmitate, cholesteryl stearate, and betulinol were purchased from Sigma (Deisenhofen, Germany) and were at least 97% pure. MSTFA (N-methyl-N-trimethylsilyltrifluoroacetamide) was obtained from Fluka (Buchs, Switzerland). Analytical grade pyridine and *n*-hexane were supplied by Loba Feinchemie (Fischamend, Austria). *n*-Hexane, dichloromethane and acetonitrile in LiChrosolv quality (Merck, Darmstadt, Germany) were used as LC eluents.

2.2. Preparation of samples and standard solutions

Stock solutions of stigmasterol (0.55 mg/ml), cholesteryl stearate (0.72 mg/ml), and betulinol (5.11 mg/ml) in pyridine were used to prepare the standard solutions. The concentrations of the reference substances in the standard solutions varied between 0.3 μg/ml and 6.1 μg/ml for stigmasterol and between 0.4 μg/ml and 8.0 μg/ml for cholesteryl stearate; the concentration of betulinol as internal standard was 5.7 μg/ml in all standard solutions. Appropriate amounts of the stock solutions of stigmasterol and cholesteryl stearate and 10 μl of the betulinol stock solution were transferred to 10 ml screw-cap vials.

For preparation of samples, betulinol stock solution (10 μl containing 51.1 μg betulinol) was added as internal standard to 20.0–30.0 mg of vegetable oil methyl ester in a 10 ml screw-cap vial.

In order to silylate the hydroxyl groups of the free sterols, N-methyl-N-trimethylsilyltrifluoroacetamide (50 μl) was added to the standard and to the sample material. After shaking briefly, the

capped vials were heated at 70°C for 15 min. The silylated mixtures were dissolved in *n*-hexane and diluted to 10 ml.

2.3. Instrumentation

LC–GC analyses were carried out on the Dualchrom 3000 (Carlo Erba, Milan, Italy). The LC system consisted of a Phoenix 30 syringe pump, a pneumatic six-port valve with a 10 μl loop, a pneumatic ten-port valve with the LC separation column, and a variable wavelength detector (MicroUVIS 20). The GC was equipped with a flame ionization detector and with an automated valve system for the interfaces and for the solvent vapor exit. Acquisition of data from both the UV detector and the FID was performed with a Chrom-Card (Fisons Instruments, Milan, Italy) in combination with an IBM compatible personal computer.

2.4. LC pre-separation

In order to simplify peak identification in the subsequent gas chromatogram, the large amounts of fatty acid methyl esters were separated from the sterols by LC pre-separation. A 100 × 2 mm I.D. LC column packed with 5-μm silica (Spherisorb S5W; Phase Separation, Deeside, Clywd, UK) was used with *n*-hexane–dichloromethane–acetonitrile (79.9:20:0.1, v/v/v) as mobile phase at a flow rate of 350 μl/min. Volumes of 10 μl were injected through a Valco six-port valve; detection was carried out at 220 nm. The LC column was backflushed with 1 ml of dichloromethane–acetonitrile (95:5, v/v), followed by mobile phase, 3 min after transfer of the LC fraction to the GC system. The backflush valve returned to stand-by 10 min later.

2.5. LC–GC transfer and GC analysis

Since the elution temperatures of silylated sterols and sterol esters were above 260°C, concurrent eluent evaporation [12,13] with the loop-type interface [14] was the transfer technique of choice. GC separation was carried out on a 12 m × 0.32 mm I.D. fused-silica capillary column coated with a 0.1-μm film of 5% phenyl polydimethylsiloxane (DB-5; J and W Scientific, Folsom, CA, USA), connected in series with a 4 m × 0.53 mm I.D. uncoated, deactivated fused-silica pre-column (Carlo Erba), a 3 m × 0.32 mm I.D. retaining pre-column coated with DB-5 of 0.1 μm film thickness, and an early vapor exit by means of glass press-fit connection.

Carrier gas inlet pressure behind the flow regulator was 250 kPa and the regulated flow-rate was 1.2 ml/min at 40°C (hydrogen). Detector temperature was 370°C.

The transfer of a 1000 μl fraction started 2.67 min after LC injection by switching the sample valve and the carrier gas valve, and by opening the solvent vapor exit. The content of the 1000 μl sample loop containing the silylated sterols and the sterol esters was transferred to the GC column at an oven temperature of 130°C under conditions of concurrent eluent evaporation.

When the pressure had dropped by 100 kPa after transfer was complete, and a delay of 20 s had passed, sample and carrier gas valves automatically returned to "stand-by". The solvent vapor exit was switched to a high resistance (1 m × 75 μm fused-silica capillary) 55 s after the pressure drop, leaving a small purge flow. After 8 min at an initial temperature of 130°C, the GC oven was heated at 30°/min to 260°C, then at 3°/min to 270°C, and finally at 15°/min to 345°C (held for 7 min). Transfer of 1000 μl took 4.5 min. Total LC–GC run time was 33 min, with 5 min cooling.

3. Results and discussion

3.1. Optimization of transfer temperature

Using fully concurrent eluent evaporation with the loop-type interface for eluent transfer, special attention must be paid to the transfer temperature, i.e. the GC column temperature during transfer. The transfer temperature must be at least equal to the eluent boiling point corrected for carrier gas inlet pressure, to produce an eluent vapor pressure that keeps the liquid out of the GC column. Too low transfer temperatures

result in flooding of the GC column by the LC eluent and consequently, in broad, deformed peaks. Transfer temperatures, exceeding the minimum required column temperature to a great extent, have the drawback that peak broadening and losses through the vapor exit affect solutes of up to unnecessarily high elution temperatures.

For the mobile phase used and an inlet pressure of 250 kPa, a transfer temperature of about 110°C is optimal according to Grob and co-workers [13,15]. Based on the guidelines given in those references, transfer temperature was optimized experimentally by repeated transfer of LC fractions of an rapeseed oil methyl ester (RME) sample at transfer temperatures from 100°C to 160°C. Fig. 1 shows the peak shapes of silylated sterols and betulinol and of the sterol esters observed after transfer at different column temperatures.

A transfer temperature of 100°C creates a vapor pressure in the GC column which is lower than the carrier gas inlet pressure. As a consequence, the eluent flows into the GC column resulting in extremely large initial peak widths, peak broadening and peak deformation. At a GC column temperature of 160°C, the trimethylsilyl derivatives of the sterols exhibit already a considerable vapor pressure and are partially lost through the early vapor exit during the transfer. The resulting peak areas are too small and peaks are broadened due to large initial peak widths.

A transfer temperature of 130°C was found to be optimal for the analysis of free and esterified sterols with the conditions used. The peak areas correspond to the actual amounts of substances and also the peak shapes are satisfactory. The "splitting" of the sterol ester peaks is due to overlapping of esters with different C_{18}-fatty acid residues and not to insufficient transfer.

The time required for the transfer (corresponding to the width of the solvent peak) does not show clear correlation with the transfer temperature. Transfer of 1000 μl at a carrier gas inlet pressure of 250 kPa at GC column temperatures between 90°C and 160°C took from 4.5 min to 6 min.

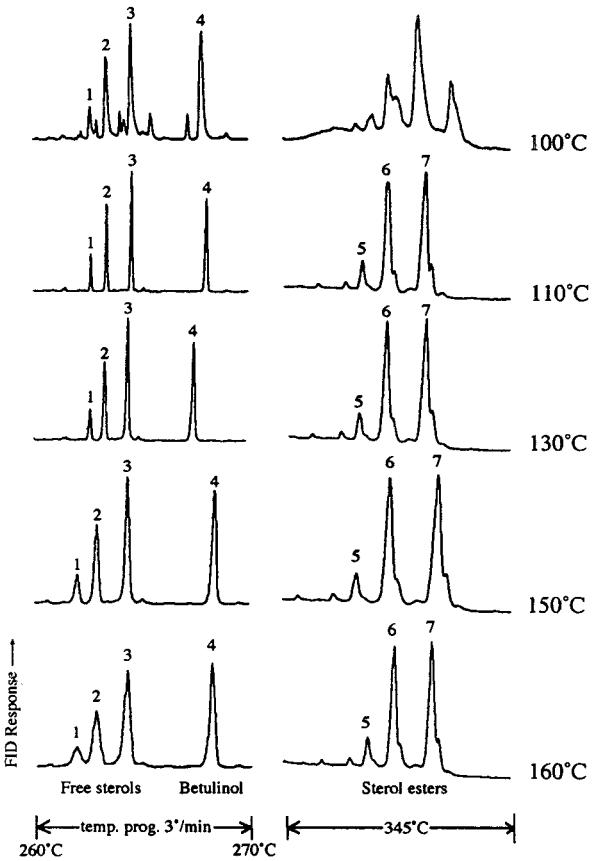

Fig. 1. Peak shapes observed after transfer to the GC system at varying transfer temperatures. 1000-μl fractions were introduced into the GC system via a loop-type interface at a maximum applied inlet pressure of 250 kPa. Eluent: *n*-hexane–dichloromethane–acetonitrile (79.9:20:0.1, v/v/v). GC column: 12 m × 0.32 mm I.D. fused-silica capillary column coated with DB-5 (0.1 μm film thickness), equipped with a 4 m × 0.53 mm I.D. uncoated pre-column, a 3 m × 0.32 mm I.D. retaining pre-column and an early vapor exit. Peak assignment: 1 = brassicasterol; 2 = campesterol; 3 = β-sitosterol; 4 = betulinol, I.S.; 5,6,7 = sterol esters.

3.2. Optimization of transfer efficiency

For the approximate determination of the fraction window, silylated stigmasterol and cholesteryl stearate were injected to LC and detected at 220 nm. With the phase system used, silylated sterols and sterol esters show lower retention than fatty acid methyl esters. Sterol

trimethylsilyl ethers as well as fatty acid steryl esters exhibit poor UV absorption and are not eluted exactly at the same time. At the transfer time, when the sample loop is decoupled from the LC flow path by switching the sample valve from the "stand-by" to the "transfer" position, the major part of the fatty acid methyl esters should not have reached the sample loop, whereas the sterols and sterol esters remain there completely. Transfer efficiency, i.e. the proportion of solute material injected to LC that is recovered by GC, was optimized to come close to 100% by adjustment of the transfer time. Losses by incomplete transfer, by degradation in the LC column or by leaks were carefully avoided to ensure that the transferred fraction contained all material of interest.

In order to determine the fraction window exactly, LC fractions of an RME sample were transferred to the GC with slight variations of the transfer time. As a reference, the same sample volume as injected into the LC was directly introduced into the GC by loop injection without pre-separation (10 μl loop mounted in the sample valve; Fig. 2). Completeness of transfer was checked by comparison of the peak areas obtained by LC–GC transfer and by loop injection. In Table 1, the transfer efficiencies for β-sitosterol and for the sum of the sterol esters are given for different transfer times. With the conditions used, 2.67 min after LC injection turned out to be the optimum transfer time.

Table 1
Efficiency of LC–GC transfer at different transfer times

Transfer time (min)	Transfer efficiency (%)[a]	
	β-Sitosterol	Sterol esters
2.33	94	96
2.50	98	107
2.67	100	104

[a] Percentages refer to peak areas obtained by loop injection as 100%.

An LC chromatogram of silylated rapeseed oil methyl ester is shown in Fig. 3. The fraction window of interest (indicated by the hatched area) lasted from the dead time of the LC column to the beginning of the fatty acid methyl ester peaks and had a volume of 650 μl. Since high accuracy of the analysis was essential and no interfering signals were observed, the fraction

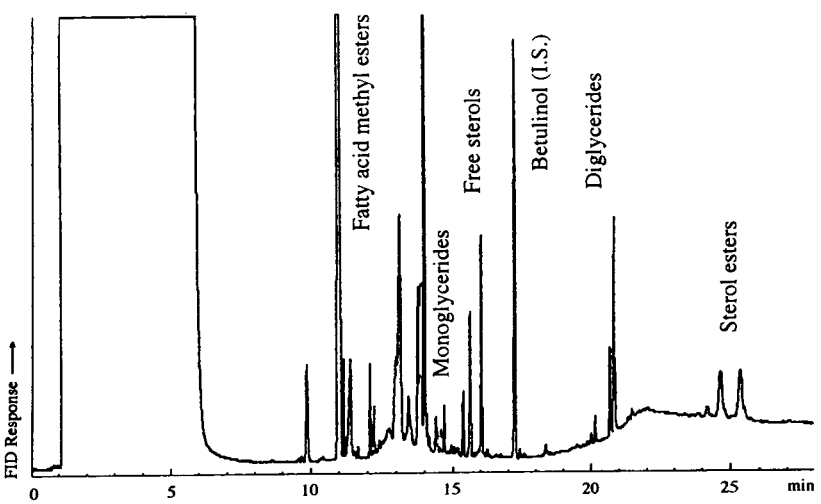

Fig. 2. Gas chromatogram of silylated rapeseed oil methyl ester obtained by large-volume loop injection without LC pre-separation. Betulinol was added as internal standard. GC column: as in Fig. 1. GC temperature programme: 130°C (8 min), at 30°C/min to 260°C, at 3°C/min to 270°C, at 15°C/min to 345°C (7 min).

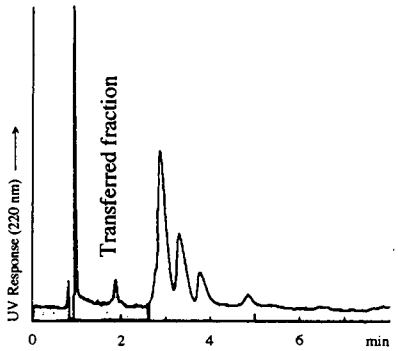

Fig. 3. Liquid chromatogram of silylated rapeseed oil methyl ester. The fraction indicated was transferred to the GC system and contained the TMS-derivatives of the free sterols and betulinol, as well as the sterol esters. LC column: 100 × 2 mm I.D. Spherisorb S5W silica. Mobile phase: as in Fig. 1. Flow-rate: 350 μl/min. Injected volume: 10 μl. Detection: 220 nm.

volume was extended to 1000 μl. As a consequence, LC retention times had not to be precisely controlled.

3.3. Qualitative analysis

An LC–GC–FID chromatogram of a rapeseed oil methyl ester fraction containing free sterols, the internal standard betulinol (as TMS derivatives) and the sterols esters is shown in Fig. 4. The group of the originally free sterols is eluted first, with the peaks of β-sitosterol, campesterol and brassicasterol clearly dominating. In addition, cholesterol, stigmasterol, and Δ^5-avenasterol could be identified by analyses of samples spiked with reference substances and by comparison with literature data [4,16,17]. Then follows the peak of betulinol, which appeared to be a suitable internal standard eluting between the groups of the originally free sterols and the sterol esters. Finally, the esterified sterols form a multiplet of peaks. Due to insufficient resolution and the lack of commercially available standard material, the individual sterol ester peaks could not be reliably identified. Tentative identifications were, however, made, as the pattern of the free sterols was repeated with some changes in the quantity ratios.

3.4. Calibration

For the quantitative determination of the free and esterified sterols in vegetable oil methyl esters, a calibration with stigmasterol and cholesteryl stearate as reference substances was carried out. As already noted [11] for a reliable gas chromatographic determination of free and es-

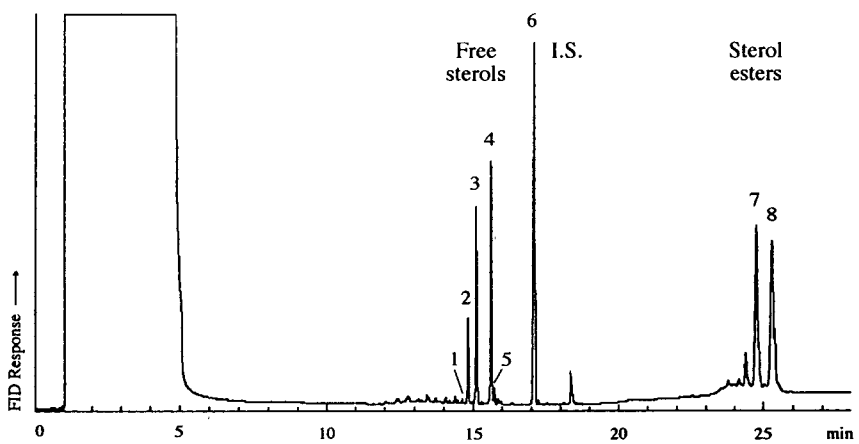

Fig. 4. Gas chromatogram of the rapeseed oil methyl ester fraction shown in Fig. 2. Conditions as in Fig. 1, 2, 3. Peak assignment: 1 = cholesterol; 2 = brassicasterol; 3 = campesterol; 4 = β-sitosterol; 5 = Δ^5-avenasterol; 6 = betulinol I.S.; 7 = campesteryl-C_{18}-esters; 8 = β-sitosteryl-C_{18}-esters.

terified sterols a calibration of the response factors is necessary. Especially for the high-boiling sterol esters, thermal degradation on the GC column results in substantial deviations of the response factors from unity. In LC–GC analysis, LC pre-separation and the LC–GC transfer can show additional influence on the peak sizes of the solutes of interest. For these reasons, external calibration and the addition of an internal standard are inevitable.

Standard solutions containing known amounts of the reference substances (stigmasterol and cholesteryl stearate) and the internal standard (betulinol) were analyzed three times each by LC–GC, in order to determine the ratio A_c:A_{st} (peak area of component (A_c):peak area of internal standard (A_{st})). Using the phase systems and the conditions mentioned above, the following calibration functions have been obtained: W_c:$W_{st} = (1.13 \pm 0.02) \cdot A_c$:$A_{st}$ for stigmasterol; W_c:$W_{st} = (1.65 \pm 0.03) \cdot A_c$:$A_{st}$ for cholesteryl stearate (W_c, weight of component; W_{st}, weight of internal standard). Good linearity of the calibration functions was observed (stigmasterol: standard error = 0.025, $n = 6$, $r^2 = 0.996$; cholesteryl stearate: standard error = 0.032, $n = 6$, $r^2 = 0.996$) within the concentration range of interest (10–2500 ppm for free sterols; 15–3200 ppm for sterol esters).

The concentrations of all free sterols were calculated based on the internal standard betulinol, using the response factor determined for stigmasterol. The sterol esters were quantified analogously using the response factor obtained for cholesteryl stearate.

3.5. Quantitative analysis

The concentration of the free sterols, as well as their qualitative and quantitative composition, and the total concentration of the sterol esters were determined by on-line LC–GC in five different vegetable oil methyl esters. Due to insufficient resolution, quantitation of the individual sterol ester species was not possible. The total concentrations of free sterols and sterol esters in rapeseed oil methyl ester (RME), sunflower oil methyl ester (SFME 1), high oleic sunflower oil methyl ester (SFME 2), soybean oil methyl ester (SBME) and used frying oil methyl ester (UFME) are given in Table 2. Rapeseed oil methyl ester shows the highest content of free and esterified sterols followed by used frying oil methyl ester, which contains a great proportion of transesterified rapeseed oil, also indicated by the relatively high content of brassicasterol.

The compositions of the free sterols in the analyzed vegetable oil methyl ester samples were calculated based on the concentrations of the individual free sterols related to the total amount of free sterols and are given in Table 3. Like in vegetable oils, the sterol composition is more characteristic of a certain type of vegetable oil methyl ester than the fatty acid composition. β-Sitosterol represents the main component of the free sterols in all vegetable oil methyl esters considered. Brassicasterol was only present in rapeseed oil methyl ester and used frying oil methyl ester. A relative content of Δ^7-stigmastenol of more than 10% is typical of sunflower oil methyl esters. Only in used frying oil methyl

Table 2
Total concentration of free sterols and sterol esters in different vegetable oil methyl esters ($n = 4$)

	Concentration (weight%)				
	RME	SFME1	SFME2	SBME	UFME
Free sterols	0.33	0.25	0.25	0.20	0.25
Sterol esters	0.73	0.18	0.15	0.15	0.50

Abbreviations: RME, rapeseed oil methyl ester; SFME 1, sunflower oil methyl ester; SFME 2, high oleic sunflower oil methyl ester; SBME, soybean oil methyl ester; UFME, used frying oil methyl ester.

Table 3
Composition of the free sterols in different vegetable oil methyl esters ($n = 4$)

	Composition (% of the free sterols)				
	RME	SFME1	SFME2	SBME	UFME
Cholesterol	1.7	1.0	<0.1	0.7	12.6
Brassicasterol	12.7	<0.1	<0.1	<0.1	6.7
Campesterol	34.2	9.5	8.6	22.8	22.7
Stigmasterol	0.5	7.5	8.6	18.6	3.4
β-Sitosterol	49.2	61.6	66.6	53.1	47.9
Δ^5-Avenasterol	1.7	4.3	3.9	1.8	1.5
Δ^7-Stigmastenol	<0.1	14.7	11.5	2.7	5.0
Δ^7-Avenasterol	<0.1	1.3	0.8	0.3	0.2

Abbreviations as in Table 2.

ester was cholesterol found to any considerable extent.

3.6. Recovery and reproducibility of results

For the evaluation of the recovery of the LC–GC procedure, a reference sample and a spiked RME sample containing known amounts of standard substances were analyzed four times. The reference sample contained a mixture of silylated sterols, cholesteryl palmitate and cholesteryl oleate at concentrations typical of authentic vegetable oil methyl ester samples. Distilled rapeseed oil methyl ester (not containing any sterols) was spiked with the standard substances mentioned. By comparison of the quantitative results obtained by LC–GC analysis of the reference sample and the spiked RME sample with the actual concentrations of the standard substances, the percentage recoveries were calculated. As shown in Table 4, the recovery of the LC–GC analysis is excellent for all solutes of interest.

In order to check the precision of the method, an RME sample was prepared and injected five times into the LC–GC. The quantitative results obtained for β-sitosterol as major component of the free sterols, for the total free sterols, and for the total sterol esters are given in Table 5.

As an additional test for reproducibility, five samples of an RME specimen were prepared and analyzed by LC–GC following the procedure outlined above. The results are summarized in Table 6.

The data in Tables 5 and 6 indicate the excellent reproducibility of the outlined method. Besides the errors resulting from repeated injection, further inaccuracies might be caused by sample weighing, the addition of the internal standard, and by possible insufficiency of the

Table 4
Average recovery of the LC–GC procedure for free sterols and sterol esters ($n = 4$)

	Concentration (μg/ml)	Recovery (%)	
		Reference sample	Spiked RME sample
Free sterols	0.15	100	96
Cholesteryl palmitate	0.15	110	109
Cholesteryl oleate	0.25	105	102

Table 5
Concentrations of free β-sitosterol, of total free sterols, and of total sterol esters in RME, obtained by consecutive injections into LC—GC ($n = 5$)

Analysis	Concentration (weight%) in RME		
	β-Sitosterol	Free sterols	Sterol esters
1	0.120	0.253	0.568
2	0.119	0.254	0.577
3	0.120	0.256	0.581
4	0.120	0.255	0.588
5	0.117	0.250	0.593
Mean	0.119	0.254	0.582
Standard deviation	0.001	0.002	0.009
Standard deviation (%)	0.92	0.82	1.52

derivatization. Comparison of the data in Tables 5 and 6 shows that the contribution of these errors to the total standard deviation is small.

4. Conclusion

The proposed LC–GC method provides qualitative and quantitative information about free and esterified sterols in vegetable oil methyl esters. Advantageous in comparison to conventional techniques involving saponification and off-line pre-separation are the simple preparation of samples, the extremely short analysis time and the possibility of complete automation. Peak identification is easy due to the absence of interfering components. The excellent recovery and reproducibility of quantitative results allow reliable qualitative and quantitative determination of free and esterified sterols in these new kinds of oleochemical products.

Acknowledgement

Financial support by the Austrian Federal Ministry of Agriculture and Forestry and by the

Table 6
Concentrations of free β-sitosterol, of total free sterols, and of total sterol esters, obtained by repeated complete analyses of the same RME sample ($n = 5$)

Analysis	Concentration (weight%) in RME		
	β-Sitosterol	Free sterols	Sterol esters
1	0.118	0.254	0.571
2	0.122	0.260	0.576
3	0.122	0.257	0.570
4	0.124	0.261	0.594
5	0.120	0.256	0.588
Mean	0.121	0.258	0.580
Standard deviation	0.002	0.003	0.010
Standard deviation (%)	1.57	1.00	1.66

Vienna Chamber of Commerce is gratefully acknowledged.

References

[1] *ÖNORM C 1190: Fuels - Diesel Engines, Rape Seed Oil Methyl Ester; Requirements*, Österrreichisches Normungsinstitut, Vienna, Austria, 1991.
[2] E. Homberg, *Fat Sci. Technol.*, 89 (1987) 215.
[3] M. Arens, H. Fiebig and E. Homberg, *Fat Sci. Technol.*, 92 (1990) 189.
[4] German Society of Fat Sciences (Editor), *German Standard Methods for the Analysis of Fats and Other Lipids*, F-III 1 (91), Wissenschaftliche Verlagsgesellschaft mbH, Stuttgart, 1991.
[5] R.E. Worthington and H.L. Hitchcock, *J. Am. Oil Chem. Soc.*, 61 (1984) 1085.
[6] P. Horstmann and A. Montag, *Fette-Seifen-Anstrichm.*, 88 (1986) 262.
[7] M.C. Iatrides, J. Artaud and M. Derbesy, *Analusis*, 12 (1984) 205.
[8] K. Grob, M. Lanfranchi and C. Mariani, *J. Chromatogr.*, 471 (1989) 397.
[9] A. Artho, K. Grob and C. Mariani, *Fat Sci. Technol.*, 95 (1993) 176.
[10] M. Biedermann, K. Grob and C. Mariani, *Fat Sci. Technol.*, 95 (1993) 127.
[11] Ch. Plank and E. Lorbeer, *J. High Resolut. Chromatogr.*, 16 (1993) 483.
[12] K. Grob, B. Schilling and Ch. Walder, *J. High Resolut. Chromatogr. Chromatogr. Commun.*, 9 (1986) 95.
[13] K. Grob, *On-Line Coupled LC–GC*, Hüthig, Heidelberg, 1991.
[14] K. Grob and J.-M. Stoll, *J. High Resolut. Chromatogr. Chromatogr. Commun.*, 9 (1986) 518.
[15] K. Grob and Th. Läubli, *J. High Resolut. Chromatogr. Chromatogr. Commun.*, 10 (1987) 435.
[16] T. Itoh. K. Yoshida, T. Yatsu, T. Tamura and T. Matsumoto, *J. Am. Oil Chem. Soc.*, 56 (1981) 545.
[17] G. Lognay, F. Lacoste, M. Marlier, F. Mordret, C. Auge, R. Raoux, P.J. Wagstaffe, A. Boenke and M. Severin, *Fat Sci. Technol.*, 95 (1993) 98.

ELSEVIER

Journal of Chromatography A, 683 (1994) 105–113

JOURNAL OF CHROMATOGRAPHY A

Supercritical fluid chromatography–mass spectrometry and matrix-assisted laser-desorption ionisation mass spectrometry of cyclic siloxanes in technical silicone oils and silicone rubbers

U. Just[a,*], F. Mellor[b], F. Keidel[a]

[a]*Bundesanstalt für Materialforschung und -prüfung (BAM), Unter den Eichen 87, D-12205 Berlin, Germany*
[b]*E. Merck, Frankfurter Strasse 250, D-64271 Darmstadt, Germany*

Abstract

Supercritical fluid chromatography in combination with mass spectrometry is used for determining cyclic siloxanes beside linear methyl and hydroxyl "end-capped" siloxanes. Electron impact ionisation and chemical ionisation techniques are utilized for identifying cyclic siloxanes in technical silicone oils and silicone rubber. Ammonia as reagent gas is preferred in the higher-molecular-mass range. Matrix-assisted laser-desorption ionisation mass spectrometry can be useful as a supplementary method for characterizing smaller amounts of both cyclic and linear siloxanes as well as silanols in the higher-molecular-mass range.

1. Introduction

Siloxanes have widely been used over the past 40 years. Methylsiloxanes, especially polydimethylsiloxanes (PDMSs), make up a major part of organo-silicon compounds. Silicone oils (low-molecular-mass PDMSs) are the basic materials for most silicone additives and silicone rubbers. Desired properties of silicone oils are a great range of fluidity, a low freezing point and low temperature dependence of viscosity. Therefore the preparation requires inhibition of cyclic siloxane formation or augmentation of linear "end-capped" siloxanes in final products [1].

Gel permeation chromatography and ^{29}Si NMR spectrometry may give information about the average molecular mass, but they cannot provide the resolution required to determine the amount of cyclic siloxanes in technical silicone oils [2]. By means of high-temperature gas chromatography substances of high molecular mass do not elute or they elute with great peak broadening. Supercritical fluid chromatography (SFC) has proven to be a method of choice for analysing cyclic siloxanes in technical silicone oils [3,4]. It is possible to couple SFC with mass spectrometry (MS), too [5–11]. We used this combination to determine cyclic siloxanes as well as linear methyl and hydroxyl "end-capped" species in technical silicone oils.

Other techniques used are direct exposure probe (DEP) and matrix-assisted laser-desorption ionisation (MALDI) MS which complements SFC in characterising siloxanes [12,13].

* Corresponding author.

0021-9673/94/$07.00
SSDI 0021-9673(94)00342-7

2. Experimental

2.1. SFC

Equipment: SFC 602-D (Dionex); injector: pneumatic time-programmable switching valve (Valco), internal volume 0.5 μl, injection time: 1 s; samples were dissolved in toluene; retention gap: 1 m × 50 μm uncoated fused silica; column: 10 m × 50 μm fused silica, SB-Methyl-100; detection: flame ionization detection (FID) (350–380°C), integral or frit restrictor, MS (see Section 2.2)

Programmes: (a) Synchronized linear temperature and density programme; initial temperature: 100°C, hold for 10 min, then increase with a ramp rate of 0.6°C/min to 150°C; initial density: 0.2 g/ml, hold for 10 min, then increase with a ramp rate of 0.0065 g/ml to 0.6 g/ml. (b) Isothermal "asymptotic" pressure programme: temperature: 120°C; initial pressure: 10 MPa, increase with a ramp rate of 2 MPa/min to 16 MPa, then with a ramp rate of 1 MPa/min to 22 MPa, then with 0.5 MPa/min to 28 MPa, with 0.25 MPa/min to 34 MPa, and then with 0.12 MPA/min to 40 MPa, hold for 20 min. (c) "Fast" synchronized linear temperature and pressure programme: initial temperature: 120°C, increase with a ramp rate of 1.5°C/min to 150°C, hold for 40 min; initial pressure: 10 MPa, increase with a ramp rate of 1.5 MPa/min to 40 MPa, hold for 40 min.

2.2. MS

Equipment: SSQ 700 (Finnigan MAT), mass range 10–4000 u, emission current 200 μA, electron multiplier −1500 V, scan time 1 s; SFC–MS interface: option for Finnigan SSQ 700 with transfer line, flange and heater assembly [14]; temperature of the transfer line: 120°C; SFC–MS restrictor: 1 m uncoated 50 μm I.D. fused-silica tubing with a 2 cm frit (Dionex); restrictor temperature: 260°C, by controlling the heater tip via the MS software; ion source temperature: 170°C (chemical ionisation, CI), 150°C (electron impact ionisation, EI); manifold heater temperature: 70°C; initial CO_2 velocity at 10 MPa and 120°C about 2 cm/s; manifold pressure: $1.6 \cdot 10^{-6}$ Torr (1 Torr = 133.322 Pa); manifold pressure with ammonia: $2.1 \cdot 10^{-6}$ Torr; manifold pressure with ammonia (and with 35 MPa CO_2 pressure/145°C in SFC system): $1.4 \cdot 10^{-5}$ Torr; spectra: EI mode, tuning automatically with perfluorotributylamine (FC-43) in the range 50–650 u, from 650–1400 u tuning manually via insertion probe, manual change of resolution (molecular mass range > 1500 u) intensifies peak masses; CI mode with methane, isobutane and ammonia as reagent gases, ammonia was preferred in the high molecular mass range; DEP: Finnigan MAT DEP system; voltage: 0 to 10 V d.c.; output current: 0 to 1350 mA; initial current: 25 mA, hold for 0.4 min; increase with a ramp rate of 40 mA/min to 300 mA, hold for 10 min.

2.3. MALDI-MS

Equipment: Kratos Kompact MALDI III, positive ion mode, reflectron time-of-flight, 20 kV accelerating voltage; matrix: dihydroxybenzoic acid (10 mg/ml in acetone); samples: 5 μl in 1 ml acetone.

2.4. Materials and reagents

The supercritical CO_2 was SFC grade (Scott). The silicone rubber was laboratory tubing material. Specially prepared substances to identify linear siloxanes were provided by Dr. U. Scheim, Institute of Organic Chemistry, TU Dresden, Germany. Technical silicone oils were obtained from Merck and Chemiewerk Nünchritz, Germany.

The molecular masses of linear siloxanes exhibit the general formula M_2D_n or $Si(CH_3)_3$–O–$[Si(CH_3)_2$–O–$]_nSi(CH_3)_3$; the general formula of the corresponding cyclic siloxanes is D_m, where M is $(CH_3)_3Si$–$O_{0.5}$, D the monomer unit $Si(CH_3)_2$–O–and m and n the degree of polymerisation, where $m = n + 2$.

3. Results and discussion

EI mass fragmentation is the first technique to try for any sample that can be vaporized into the mass spectrometer. For siloxanes containing only

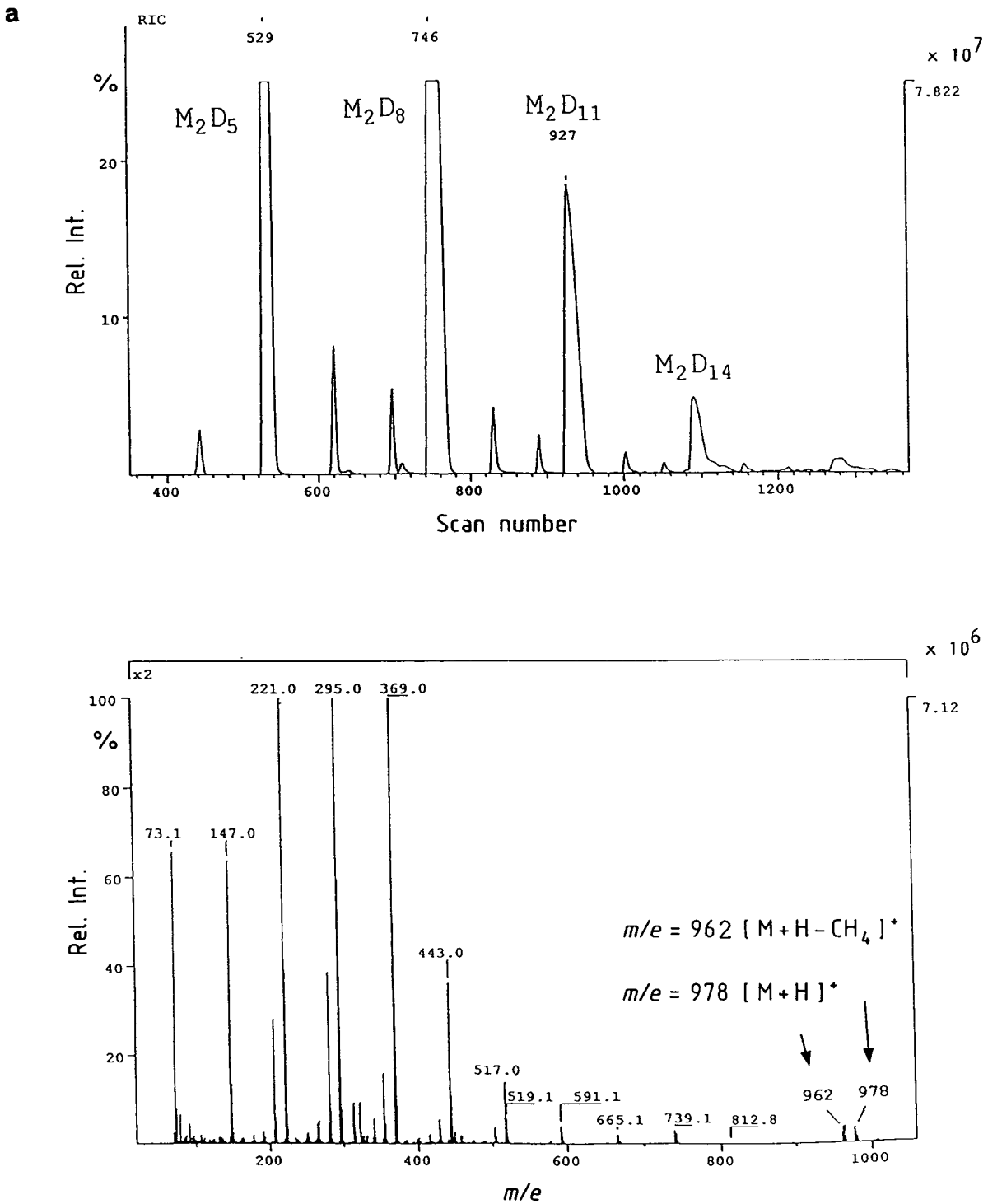

Fig. 1. *(Continued on p. 108)*

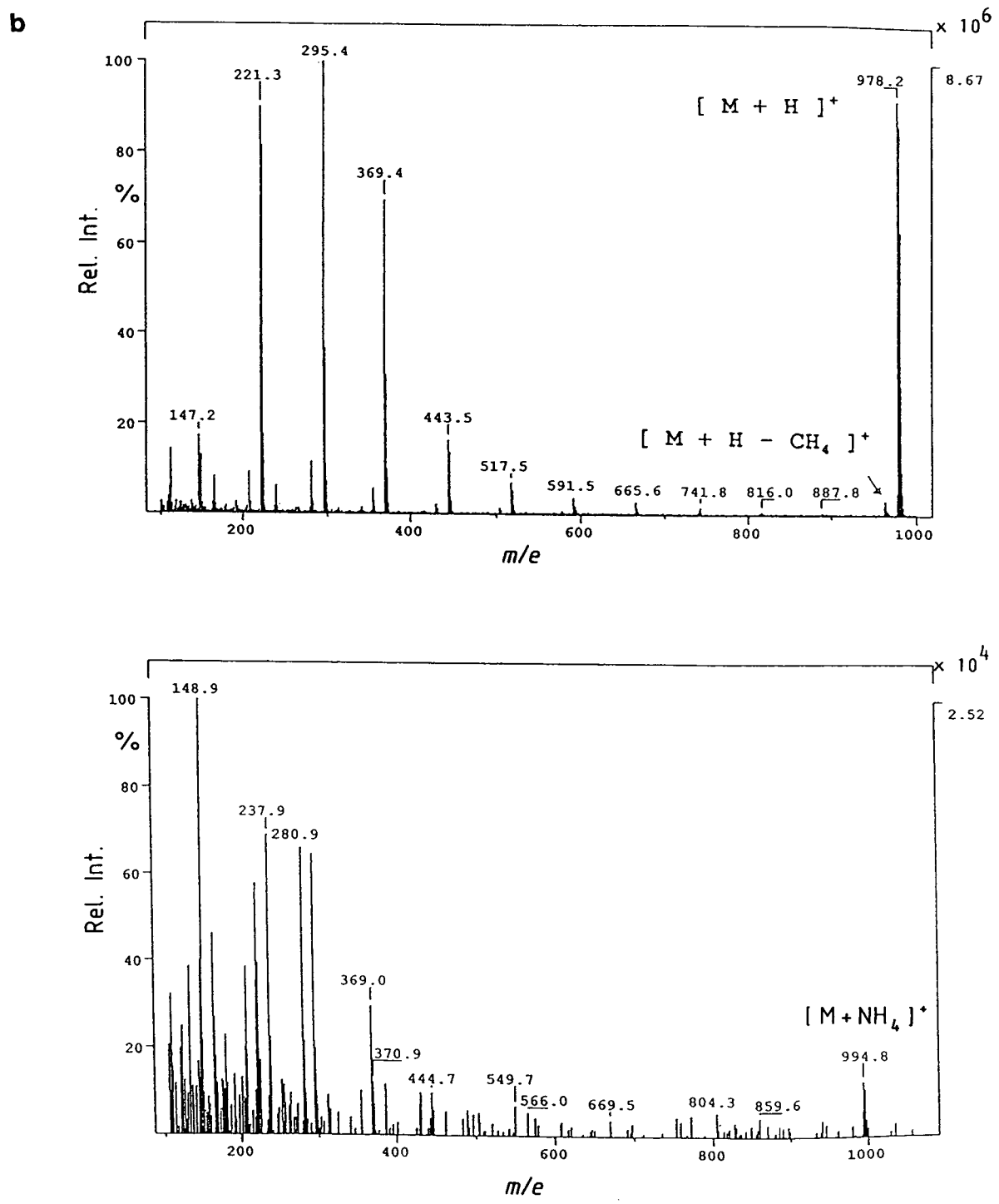

Fig. 1. (a) SFC–MS chromatogram of a mixture of mainly linear PDMS (top); CI (CH_4) mass spectrum of M_2D_{11} (bottom). (b) CI (iso-C_4H_{10}) mass spectrum of M_2D_{11} (top), CI (NH_3) mass spectrum (bottom).

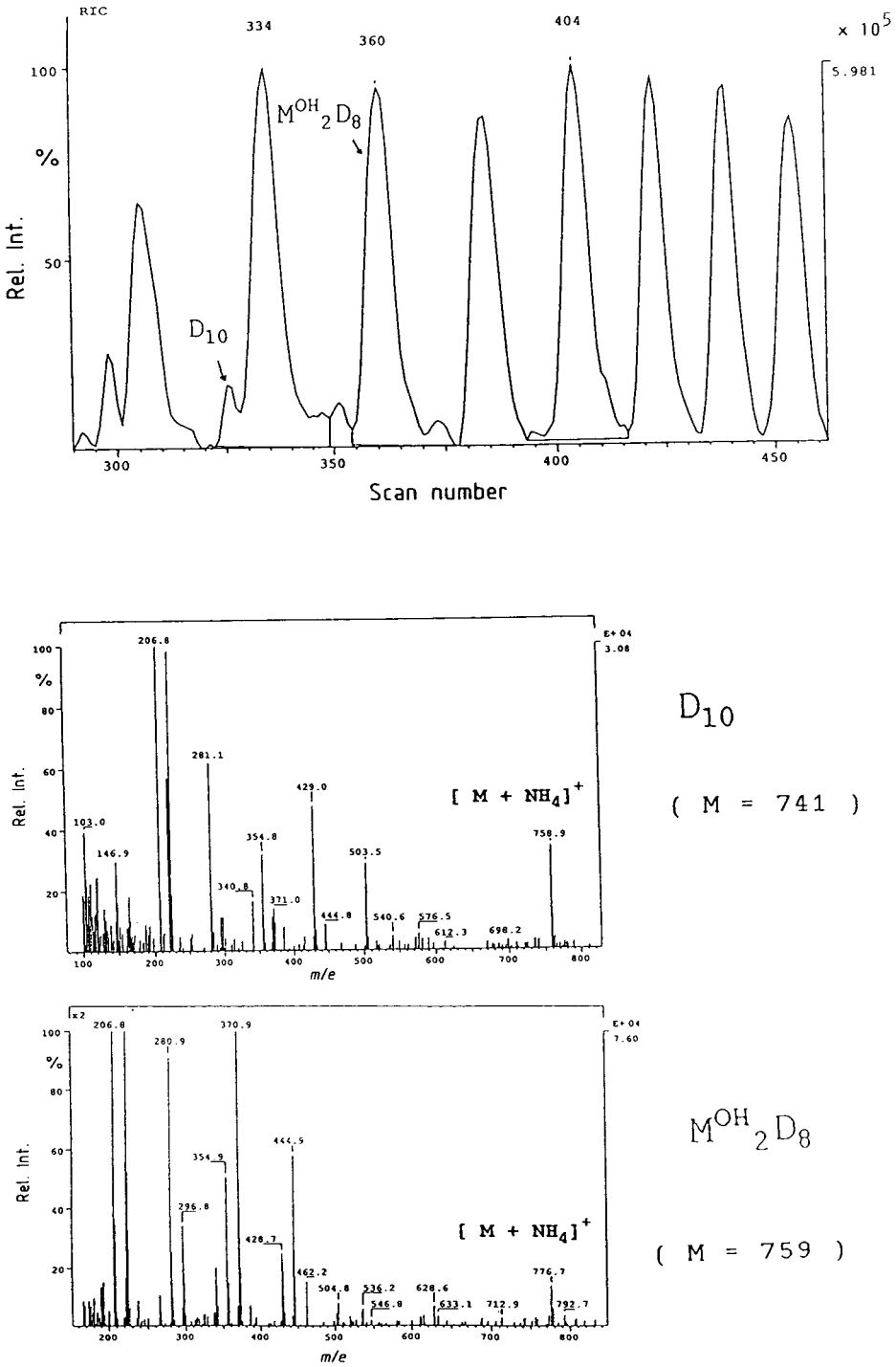

Fig. 2. SFC–MS chromatogram of a silanol sample containing methyl end-capped and cyclic siloxanes (top); CI (NH_3) mass spectra of D_{10} (middle) and $M_2^{OH}D_8$ (bottom).

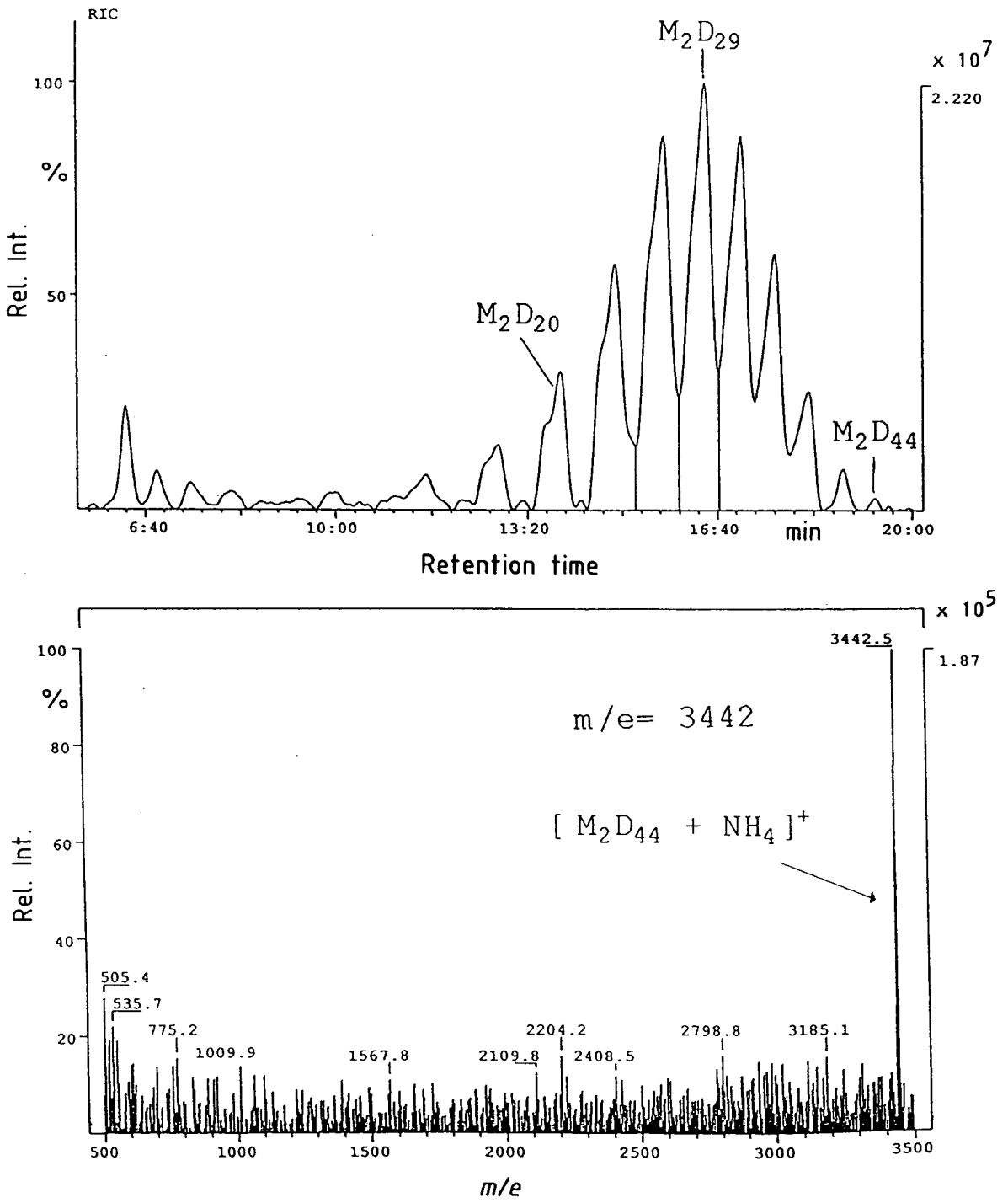

Fig. 3. SFC–MS chromatogram of a siloxane mixture with linear methyl end-capped components (top); CI (NH_3) mass spectrum of M_2D_{44} (bottom).

few silicon atoms, EI is informative. When the chain length increases, EI does not provide information on the complete molecule anymore, but it gives clues helping to identify the repeat unit from characteristic ions [15]. By coupling SFC with MS using SFC method b, a slow isothermal "asymptotic" pressure programme, we got normal EI mass spectra with intensive fragmentation (molecular mass difference 74 u). Molecular ions could not be observed, but cleavage of a methyl group from the molecules, e.g. octacyclosiloxane (D_8) losing CH_3. Library searchable spectra were obtained up to M_2D_4 or D_6.

Our first CI experiments were done with methane as the reagent gas. We analyzed the same sample used in the previous EI experiments consisting of mainly linear PDMSs. Fig. 1a (top) shows the SFC chromatogram of this oil and (bottom) the mass spectrum of a linear component in this siloxane mixture with its molecular mass of 977 u. The mass spectrum indicates the $(M+H)^+$ peak m/z 978 in this case of M_2D_{11}; it is significant in the relation to the isotope cluster of the silicon-containing ions. Some fragmentation takes place, and the mass spectrum shows the molecular ions losing methane ($=16$ u), m/z 962, too. When the molecular masses of the compounds increase, no molecular or quasimolecular ions can be obtained with methane as reagent gas.

Softer ionization media are isobutane (C_4H_{10}) or ammonia (NH_3) [16]. With isobutane mass spectra can be obtained which show the $(M+H)^+$ ion; if ammonia is used as reagent gas the mass spectra show the $(M+NH_4)^+$ ion (Fig. 1b). In the latter case not much fragmentation can be observed even in high-molecular-mass range. In the low-molecular-mass range a triplet structure occurs with ammonia as reagent gas. Quasimolecular ions are formed either by hydrogen or ammonium ion addition, then losing methane. Thus, ions can be observed at $M+18$ and $M+2$ $(18-16)$, and also at $M+1$ and $M-15$.

With ammonia as reagent gas, Si–OH components can be identified, too. Fig. 2 shows a silicone oil which contains cyclic and linear siloxanes, the linear ones "end-capped" either with methyl or hydroxyl end groups. Interesting is the chromatographic retention of these species. The cyclic siloxane D_{10} is followed by M_2D_8 in the retention time scale; $M_2^{OH}D_8$, however, elutes later, at nearly the same retention time as the retention time of M_2D_9. Fig. 2 (bottom) shows the mass spectra (CI with ammonia as reagent gas) of D_{10} and $M_2^{OH}D_8$.

With ammonia as reagent gas cyclic and linear siloxanes are distinguishable in the mass spectra; in the EI mode this cannot be achieved because water is ejected from the linear diols after the methyl loss. Thus, in the EI mode cyclic siloxanes and silanol-ended linear ones show the same ions [15].

By coupling SFC with MS, we were able to get well defined "reference substances", siloxane mixtures specially prepared for this purpose. Using SFC program c we determined for example the linear component M_2D_{44} in such a siloxane mixture. The signal-to-noise ratio of the molecular ion $(M+NH_4)^+$ was about 5 (Fig. 3).

SFC is a method of choice to determine the amount of cyclic components of technical

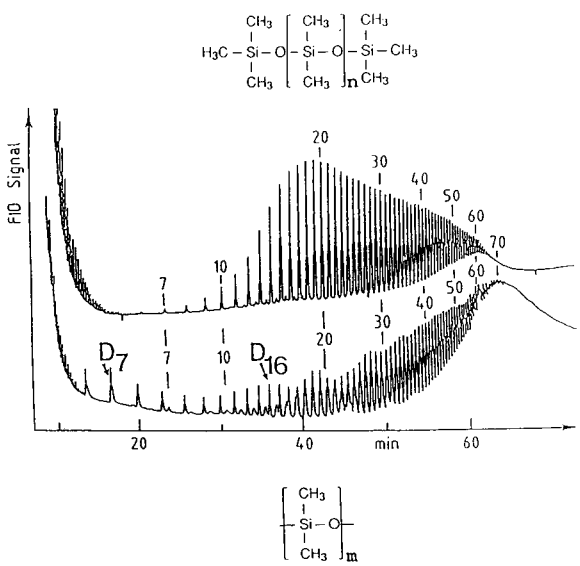

Fig. 4. SFC–FID chromatograms of a silicone oil with mainly linear components (top curve) and an oil with cyclic siloxane components (bottom curve).

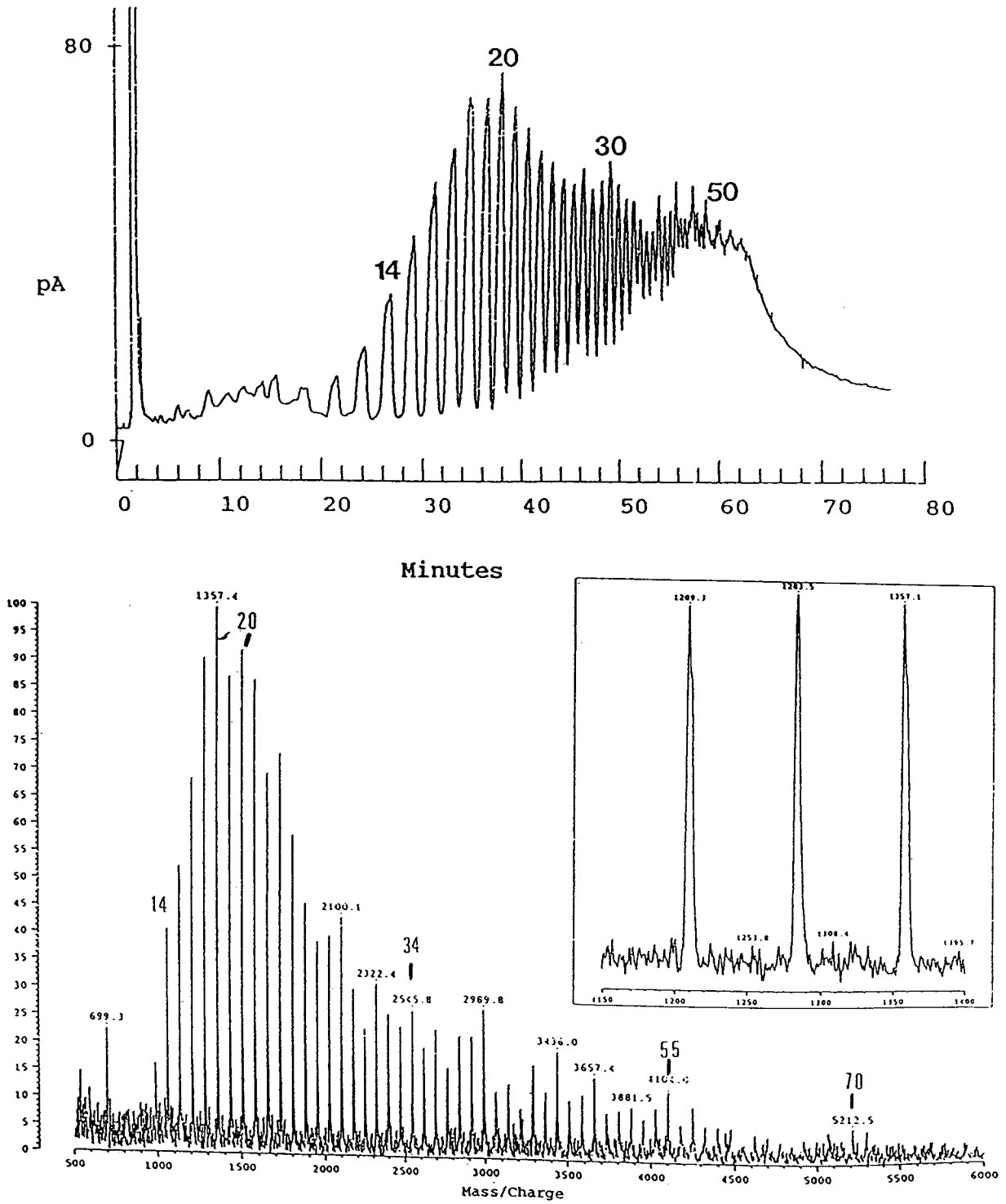

Fig. 5. SFC–FID chromatogram of cyclic siloxanes in silicone rubber, extracted with hexane (top); MALDI-MS spectrum (bottom), expanded plot shows molecular mass difference 74 u.

silicone oils in the low-molecular-mass range, important for the quality of the oils. Thus SFC can lead to a sufficient resolution in functionality and molar mass. Fig. 4 exhibits the SFC chromatograms of an oil consisting of mainly linear components (top) and of a silicone oil with a larger amount of cyclic components in the lower-molecular-mass range (bottom).

Using hexane we extracted cyclic siloxanes from silicone rubber, laboratory tubing material. The amount of extractable components by an 8-h Soxhlet extraction had been 2%. We analyzed the extract first by SFC. The molecular mass distribution of this extract is depicted in Fig. 5 (top). Additionally to coupling SFC with MS we also tried to use DEP as a screening method. Only a qualitative overview could be obtained showing that the components are cyclosiloxanes. DEP does not seem to be useful for quantitative measurements.

A faster and easier method used for characterising siloxanes in a qualitative manner is MALDI-MS. This method is based on the principle that the dissolved specimen is mixed with a matrix and then crystallizes. The specimen is desorbed and ionized by laser incidence. The molecular mass is determined by the time-of-flight (TOF). MALDI-MS may be used as a supplementary method to SFC of siloxanes. In the molecular mass range below 1000 u SFC has clear advantages; MALDI-MS does not provide for indication of smaller siloxane molecules in this range. On the other hand, the resolution in the higher-molecular-mass range is more pronounced than in SFC, as Fig. 5 shows. It is very difficult to identify traces of cyclosiloxanes with higher molecular masses by SFC–MS. The MS equipment used is also limited to the mass range of 4000 u. But with MALDI-MS we are able to determine cyclic and linear components with even higher molecular masses; nevertheless, the problem of discrimination remains in the lower-molecular-mass range. Thus, it is not yet possible to use MALDI-MS for quantitative data, but in a qualitative manner MALDI-MS may be used as a supplementary method to SFC–MS in the higher-molecular-mass range.

Further work is done by us to separate completely cyclic and linear components in technical silicone oils by "critical chromatography" (chromatography at the critical point of adsorption where the species are separated not by molecular mass but by functionality) and then analyse the separated compounds in a second dimension by SFC–MS and MALDI-MS.

References

[1] E.G. Rochow, *Einführung in die Chemie der Silicone*, Verlag Chemie, Weinheim, 1952.

[2] B. Hagenhoff, A. Benninghoven, H. Bathel and W. Zoller, *Anal. Chem.*, 63 (1991) 2466.

[3] *Technical Note TN 26*, Dionex, Sunnyvale, CA, 1992.

[4] U. Just, F. Mellor and F. Keidel, *Fresenius' J. Anal. Chem.*, 348 (1994) 745–748.

[5] R.D. Smith, J.C. Fjeldsted and M.L. Lee, *J. Chromatogr.*, 247 (1982) 231.

[6] R.D. Smith, W.D. Felix, J.C. Fjeldsted and M.L. Lee, *Anal. Chem.*, 54 (1982) 1883.

[7] B.W. Wright, H.T. Kalinoski, H.R. Udseth and R.D. Smith, *J. High Resolut. Chromatogr. Chromatogr. Commun.*, 9 (1986) 145.

[8] R.D. Smith, H.T. Kalinoski and H.R. Udseth, *Mass Spectrom. Rev.*, 6 (1987) 445–496.

[9] D.L. Pinkston and D.J. Bowling, in K. Jinno (Editor), *Hyphenated Techniques in Supercritical Fluid Chromatography and Extraction (Journal of Chromatography Library*, Vol. 53), Elsevier, Amsterdam, 1992, pp. 25–46.

[10] D.L. Pinkston, G.D. Owens, J.L. Burkes, T.E. Delaney, D.S. Millington and D.A. Maltby, *Anal. Chem.*, 60 (1988) 962–966.

[11] A. Cary, *SSQ 70 Application Data Sheet No. 37*, Finnigan MAT, San Jose, CA, 1988.

[12] M. Karas and F. Hillenkamp, *Anal. Chem.*, 60 (1988) 2299.

[13] U. Bahr, A. Deppe, M. Karas, F. Hillenkamp and U. Giessmann, *Anal. Chem.*, 64 (1992) 2866–2869.

[14] *TSQ 70 Service Manual, 70 Series SFC Option Operator's Manual*, Finnigan MAT, San Jose, CA, 1989.

[15] J.A. Moore, in A.L. Smith (Editor), *The Analytical Chemistry of Silicones*, Wiley, New York, 1991, pp. 426–428.

[16] A. Harrison (Editor), *Chemical Ionization Mass Spectrometry*, CRC Press, Boca Raton, FL, 1983.

ELSEVIER

Journal of Chromatography A, 683 (1994) 115–124

JOURNAL OF CHROMATOGRAPHY A

Pyrolysis–gas chromatography–mass spectrometry of poly(dialkylsilylenes)

Marianne Blazsó

Research Laboratory for Inorganic Chemistry, Hungarian Academy of Sciences, Budaörsi út 45, H-1112 Budapest, Hungary

Abstract

A series of silylene copolymers with di-*n*-alkyl substituent groups varying from dimethyl to di-*n*-hexyl were pyrolysed in an analytical pyrolyser coupled to a capillary GC–MS system. The thermal decomposition of the silylene copolymers begins at about 200°C and proceeds via cyclic oligomer formation. The pyrolysis at 300°C of those copolymers which contain dimethylsilylene units lead to tetracycles and pentacycles, but those which have ethyl or longer alkyl substituents decompose exclusively to tetracycles. The copolymer composition and structure were evaluated from the pyrolysis product distribution data. Mass spectra and GC retention indices were obtained on several di-*n*-alkylsilylene cyclotetramers and cyclopentamers.

1. Introduction

On line pyrolysis–gas chromatography–mass spectrometry (Py–GC–MS) is successfully used for studying thermal decomposition processes in polymers [1,2]. Pyrolysis of macromolecular chains leads mostly to gaseous and volatile products, their nature and amount being related to the chemical structure of the polymer and the pyrolysis temperature. The pyrolysis mechanism is often found to be analogous for polymers of the same type [3]. Relatively mild pyrolysis, around the temperature at which decomposition begins, yields oligomeric volatile species or relatively large fragments in many instances. The large thermal fragments usually preserve the original chemical structure of the macromolecule, hence information on the monomer sequences of copolymers could also be obtained using these coupled techniques [4].

The thermal decomposition mechanism of poly(dimethyl-, poly(methylalkyl- and poly(methylphenylsilylenes) has been described previously [5]. Cyclic tetramer and pentamer formation proved to be the initial thermal decomposition mechanism for poly(methylalkylsilylenes) at 300–400°C.

The aim of this work was to relate the pyrolysis mechanism of poly(di-*n*-alkylsilylenes) with that of poly(dimethyl- and poly(methylalkylsilylenes) and to characterize the monomer distribution in a series of copolymers synthesized from two different di-*n*-alkylsilylene monomers. For these purposes qualitative and quantitative analysis of the initial thermal de-

0021-9673/94/$07.00
SSDI 0021-9673(94)00357-F

composition products of a series of copolymers were performed.

2. Experimental

2.1. Materials

The copolymer samples were obtained from polymerization of a mixture of di-*n*-alkyldichlorosilanes in toluene with sodium under reflux, as described by Menescal and West [6].

2.2. Pyrolysis–GC–MS

Rapid pyrolyses were performed at 300°C for 10 s in a Chemical Data System Pyroprobe 120 equipped with a platinum coil and quartz sample tube interfaced either to a Hewlett-Packard Model 5880 A gas chromatograph with a flame ionization detector or to a Hewlett-Packard Model 5985 B gas chromatograph–mass spectrometer. The sample mass was about 100–200 μg. Helium carrier gas at a flow-rate of 20 ml/min purged the pyrolysis chamber held at 250°C; it was split in a ratio of 1:20 before being introduced into the fused-silica capillary column (25 m × 0.2 mm I.D.) coated with 0.33-μm dimethylsiloxane bonded phase (Hewlett-Packard U-1). A temperature programme was applied to the GC oven from 50 to 300°C at a rate of 6°C/min. The GC–MS interface was held at 300°C. The mass spectrometer was operated at 70 eV.

The temperature-programmed retention indices were determined using the *n*-alkane series of polyethylene (BDH, Poole, UK) pryolysate together with dotriacontane and hexatriacontane standards (PolyScience, Evanston, IL, USA).

3. Results and discussion

Typical pyrolysis gas chromatograms (pyrograms) are shown in Fig. 1. The pyrograms of copolymers containing dimethylsilylene units exhibited considerably more products than those of copolymers which contained only diethyl- or longer di-*n*-alkylsilylene units. The main peaks of the pyrograms proved to be oligocyclosilanes. The di-*n*-alkylsilylene copolymers which lack methyl groups decomposed exclusively to cyclotetramers, whereas copolymers containing dimethylsilylene monomers gave cyclopentamers in addition to cyclotetramers. The composition of these cyclooligomeric molecules corresponds to the possible combinations of the monomers. The pyrolysis products are listed in Table 1.

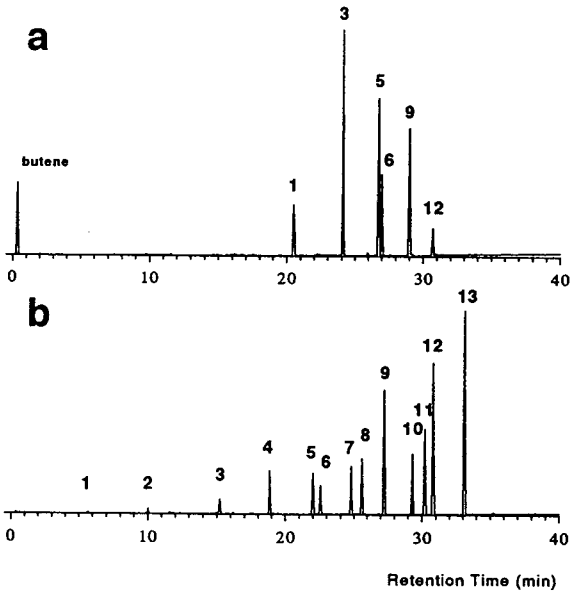

Fig. 1. Pyrograms obtained on a temperature-programmed U-1 capillary column. (a) Poly(diethylsilylene-co-di-*n*-butylsilylene); (b) poly(dimethylsilylene-co-di-*n*-butylsilylene). Peak numbers refer to the products in Table 1.

3.1. GC–MS analysis of the pyrolysis products

The identification of the pyrolysis products is based on their electron impact (EI) mass spectra, which exhibit abundant molecular ions. Typical spectra are shown in Figs. 2 and 3.

Table 1
Pyrolysis products of copolymers $(R_2Si)_n(R'_2Si)_m$

Peak No.	-cyclotetrasilane	-cyclopentasilane
1	Octa-R'-	
2		Decamethyl-
3	Hexa-R'-di-R-	
4		Octamethyldi-R-
5	1,1,2,2-Tetra-R'-tetra-R-	
6	1,1,3,3-Tetra-R'-tetra-R-	
7		1,1,2,2-Tetra-R-hexamethyl-
8		1,1,3,3-Tetra-R-hexamethyl-
9	Di-R'-hexa-R-	
10		1,1,2,2-Teatramethylhexa-R-
11		1,1,3,3-Tetramethylhexa-R-
12	Octa-R-	
13		Dimethylocta-R-

R = *n*-Propyl, *n*-butyl, *n*-pentyl, -*n*-hexyl; R' = methyl-, ethyl-, *n*-propyl, *n*-butyl, *n*-pentyl.

In the mass spectra of tetracycles even-mass number ions indicate 1-alkene elimination. The ions at *m/z* 344, 288, 232 and 176 correspond to the elimination of one to four 1-butene molecules from a tetramethyltetra-*n*-butylcyclotetrasilane molecule in the spectra shown in Fig. 2. Fig. 2 also shows that the spectra of the isomers are very similar. However, the trimelthylsilyl ion at *m/z* 73 is less abundant from the isomer of longer retention time. Taking into consideration that trimethylsilyl ion most probably originates from tetramethyldisilyl dyad, peak 6 is assigned to 1,1,3,3-tetramethyl-2,2,4,4-tetra-*n*-butylcyclotetrasilane. This is in accordance with GC retention data, which predict a longer retention time for the isomer of more elongated shape [7]. The isomeric peaks 7–8 and 10–11 were assigned similarly.

In the mass spectra of cyclopentasilanes the abundant even-mass ions originate from the cleavage of the ring. The spectra of octamethyldi-*n*-alkylcyclopentasilanes show abundant ions at *m/z* 188 and 202 (Fig. 3), which are probably due to Si_4Me_5H and Si_4Me_6 ions. A similar fragmentation may take place in hexamethyltetra-*n*-alkylcyclopentasilanes (Fig. 4) accompanied by 1-alkene elimination, resulting in Si_4Me_4RH ions at *m/z* 230, 244 and 258 in the spectra of these pentacycles with R = *n*-butyl, *n*-pentyl and *n*-hexyl, respectively.

3.2. GC retention indices of the pyrolysis products

Several quasi-homologous series can be distinguished among the oligocyclosilanes obtained by pyrolysis of the copolymers, in which the members differ in the length of the di-*n*-alkyl substituents. The temperature-programmed retention indices of the pyrolysis products of the copolymers measured on a methylsiloxane GC phase are listed in Table 2.

The molecules of homosubstituted cyclotetrasilanes form a series in which the length of all eight alkyl substituents are varied alike from methyl to *n*-hexyl; therefore, a regular change in their retention indices is expected as a function of their molecular mass. However, from the plot of these data in Fig. 5, an irregularity is observed regarding the points for methyl- and ethyl-substituted cyclotetrasilanes, indicating that some retention-determinating factor (ring conformation [8] or coverage of the silicon atoms by the substituents) is different for these molecules. Octamethylcyclotetrasilane has a lower and

Table 2
Temperature programmed retention indices (I_{PT}) of cyclooligosilanes

Substituent	I_{PT}	Substituent	I_{PT}
Cyclotetrasilanes			
Octamethyl-	1229	Octaethyl-	2071
Octapropyl-	2341	Octabutyl-	2769
Octapentyl-	3222	Octahexyl-	3685
Hexamethyldibutyl-	1726	Hexaethyldipropyl-	2159
-pentyl-	1894	-butyl-	2292
-hexyl-	2073	-pentyl-	2452
		-hexyl-	2619
Hexapropyldibutyl-	2453	Hexabutyldipentyl-	2914
-pentyl-	2591	-hexyl-	3030
-hexyl-	2745	Hexapentyldihexyl-	3353
1,1,2,2-Tetramethyltetrabutyl-	2134	1,1,2,2-Tetraethyltetrapropyl-	2230
-pentyl-	2438	-butyl-	2473
-hexyl-	2759	-pentyl-	2758
		-hexyl-	3053
1,1,3,3-Tetramethyltetrabutyl-	2176	1,1,3,3-Tetraethyltetrapropyl-	2240
-pentyl-	2500	-butyl-	2496
-hexyl-	2832	-pentyl-	2795
		-hexyl-	3103
1,1,2,2-Tetrapropyltetrabutyl-	2577	1,1,2,2-Tetrabutyltetrapentyl	3021
-pentyl-	2828	-hexyl-	3263
-hexyl-	3105	-pentyltetrahexyl-	3461
1,1,3,3-Tetrapropyltetrabutyl-	2580	1,1,3,3-Tetrabutyltetrapentyl	3045
-pentyl-	2838	-hexyl-	3278
-hexyl-	3122	-pentyltetrahexyl-	3465
Dimethylhexabutyl-	2496	Diethylhexapropyl-	2294
-pentyl-	2918	-butyl-	2637
-hexyl-	3302	-pentyl-	3026
		-hexyl-	3415
Dipropylhexabutyl-	2671	Dibutylhexapentyl-	3148
-pentyl-	3036	-hexyl-	3481
-hexyl-	3450	Dipentylhexahexyl-	3565
Cyclopentasilanes			
Decamethyl-	1475	Octamethyldibutyl-	1954
Octamethyldipentyl-	2122	-hexyl-	2298
1,1,2,2,3,3-Hexamethyltetrabutyl-	2336	1,1,2,2,4,4-Hexamethyltetrabutyl-	2400
-pentyl-	2627	-pentyl-	2719
-hexyl-	2920	-hexyl-	3016
1,1,2,2-Tetramethylhexabutyl-	2675	1,1,3,3-Tetramethylhexabutyl-	2748
-pentyl-	3053	-pentyl-	3143
-hexyl-	3412	-hexyl-	3528
Dimethyloctabutyl-	2969	Dimethyloctapentyl-	3399
-hexyl-	3781		

octaethylcyclotetrasilane a higher retention index than expected from their molecular masses.

Figs. 6 and 7 show that the retention index increment of a methylene group (*i.e.*, the slope of the lines connecting two neighbouring points) is lowered as the number of the longer sub-

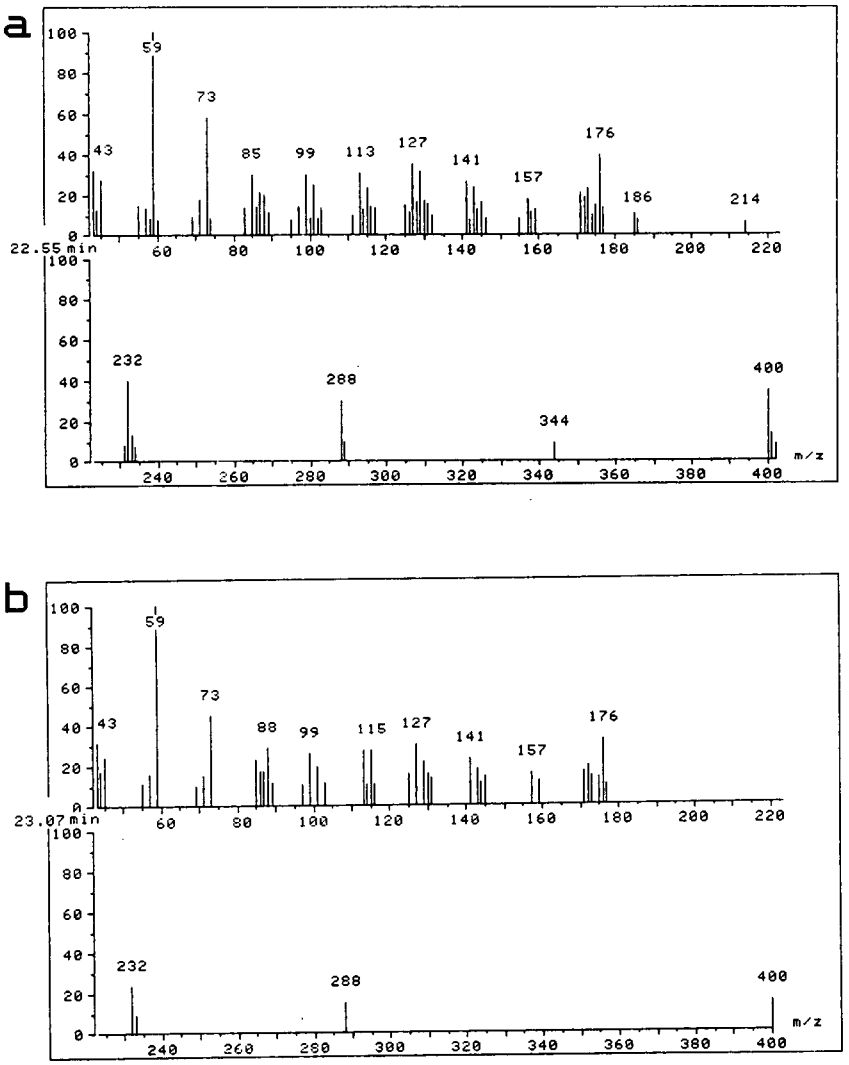

Fig. 2. Mass spectra of (a) 1,1,2,2-tetramethyl-3,3,4,4-tetra-*n*-butyl- and (b) 1,1,3,3-tetramethyl-2,2,4,4-tetra-*n*-butyl-cyclotetrasilane.

stituents or the substituent length is increased in the molecule of cyclotetrasilanes. Moreover, the retention indices of hexaethylcyclotetrasilanes are relatively higher than expected from the general trend of the other values. In Fig. 6 the points for the 1,1,2,2-tetramethyl isomers are connected with a full line and those for the 1,1,3,3-tetramethyl isomers with a dashed line among the points of tetramethyltetra-*n*-alkyl-cyclotetrasilanes.

3.3. Copolymer characterization by pyrolysis product distribution

The areas of the peaks detected by flame ionization detection (FID) were transformed into relative molar amounts using relative response factors [9]. The peak areas of the total ion GC–MS pyrograms may also be considered as an approximation for relative molar amounts. The quantitative data obtained by the two kinds

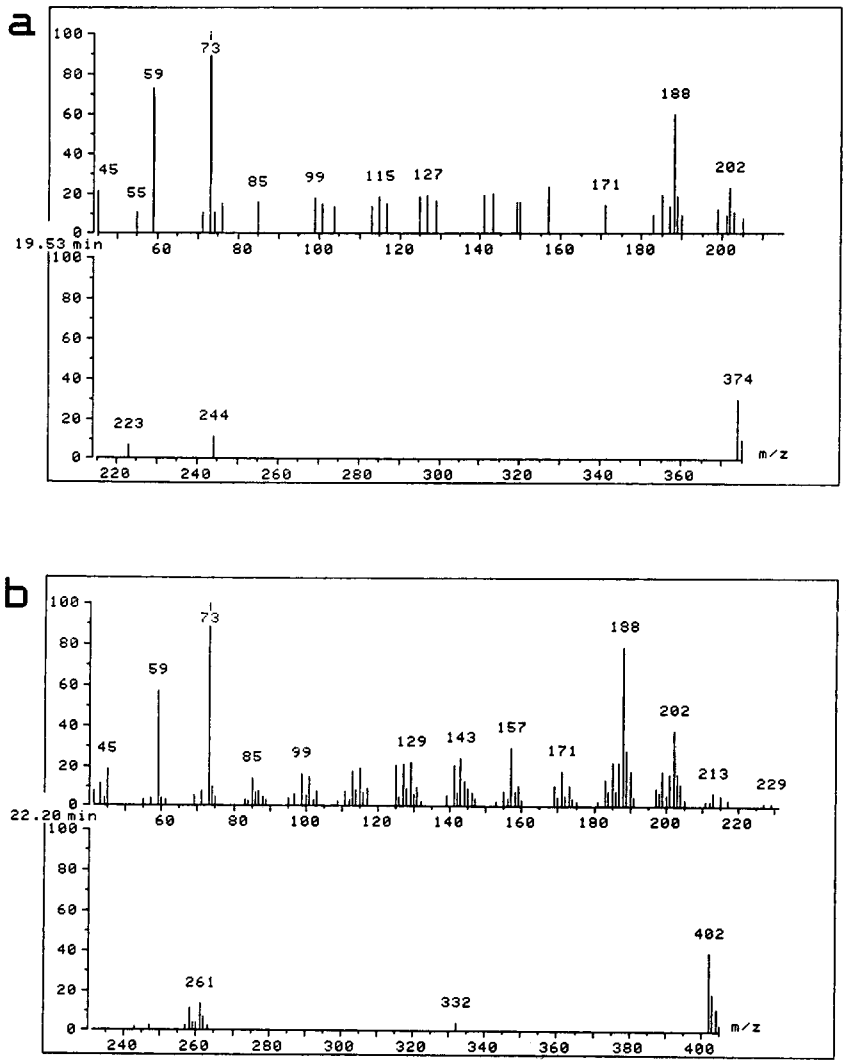

Fig. 3. Mass spectra of (a) octamethydi-*n*-butyl- and (b) octamethyldi-*n*-pentylcyclopentasilane.

of detection are shown for di-*n*-propyldiethylsilylene (sample 13) and di-*n*-pentyldimethylsilylene (sample 9) copolymers in Table 3. Product amounts were also calculated assuming a random monomer distribution in the copolymer and are given in Table 3 for comparison.

Summing separately the molar amounts of the different di-*n*-alkylsilylene units occurring in the different cyclosilanes, the ratio of the sums gives the copolymer composition. The molar ratios (n/m values) of the two monomers evaluated in this way are given in Table 4. Table 4 shows a fairly good agreement with the copolymer compositions obtained from NMR spectra of copolymer solutions [6] for most of the samples. However, huge deviations occur for the di-*n*-hexylsilyl-containing copolymers, owing to the loss of part of the low-volatility products (having retention indices above 3300). The deviations could be decreased by increasing the temperature of the interface between the pyrolyser and the gas chromatograph.

A number characterization of the monomer

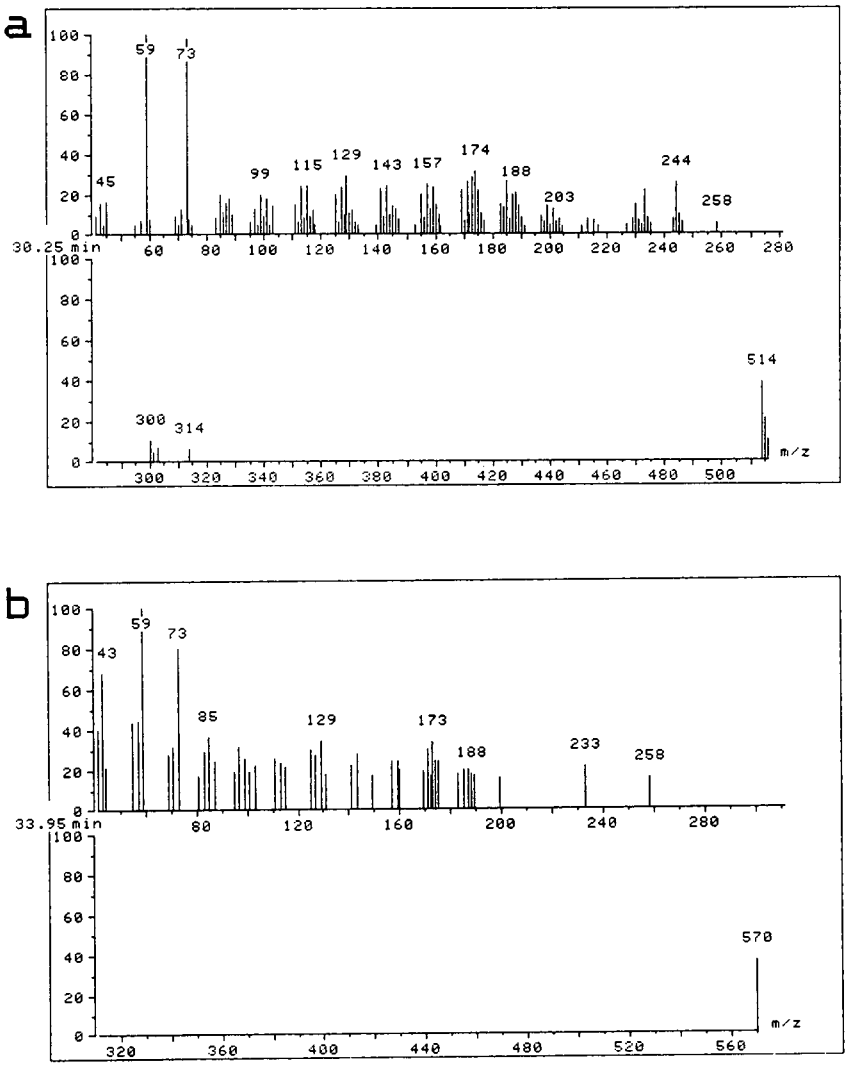

Fig. 4. Mass spectra of (a) hexamethyltetra-*n*-pentyl- and (b) hexamethyltetra-*n*-hexylcyclopentasilane.

distribution along the copolymer chain is available by counting the relative occurrence of the three possible disilylene dyads in the pyrolysate cyclosilanes. The relative occurrences of the three kinds of dyads are given in Table 5 together with the deviations to the values calculated for a random copolymer structure. According to these data, most of the samples investigated have random copolymer structures. Table 5 even demonstrates that reliable information may be obtained on the copolymer structure by pyrolysis–GC also when part of the low-volatility pyrolysis products are lost.

4. Conclusions

This Py–GC–MS investigation of di-*n*-alkylsilylene copolymers revealed that a thermal decomposition mechanism leading to cyclic

Table 3
Pyrolysis product distribution of some copolymers $(R_2Si)_n(R'_2Si)_m$

Sample No.[a]	Method[b]	Cyclotetramers (mol %)						Cyclopentamers (mol %)						
		1	3	5	6	9	12	2	4	7	8	10	11	13
9 (l)	FID	0.8	11.0	14.9	4.2	9.6	3.5	1.3	13.4	8.3	8.2	8.7	7.1	8.9
	MS	0.1	9.3	10.3	5.6	11.8	6.3	1.3	14.5	9.7	10.3	7.5	8.0	5.3
	Calc.	2.8	11.1	10.9	5.5	10.7	2.6	1.8	9.1	8.9	8.9	8.7	8.7	8.6
9 (h)	FID	0.4	9.1	20.2	5.1	18.2	10.4	0.8	5.1	4.1	4.5	6.7	7.8	7.6
	Calc.	2.0	11.1	15.1	7.6	20.7	6.9	0.5	3.4	4.6	4.6	6.3	6.3	8.6
13	FID	8.6	28.1	25.3	10.9	21.5	5.5	0	0	0	0	0	0	0
	MS	7.1	29.9	23.9	12.8	22.0	4.5	0	0	0	0	0	0	0
	Calc.	8.6	29.1	24.6	12.3	20.9	3.9							

[a] Sample numbers refer to those given in Table 4; (l) and (h) = low- and high-molecular-mass fraction, respectively.
[b] Source of quantitative evaluation: FID = flame ionization detection; MS = mass spectrometric total ion; calc. = calculated values for a random copolymer structure.

pentamers takes place only with polysilanes containing methyl substituents. According to the pyrolysis product distributions, the relative amount of pentamers to tetramers is considerably higher in the pyrolysate of the low-molecular-mass fraction of the investigated copolymer samples (Table 3). These observations suggest that the pentacycle formation may be a backbiting process occurring from the terminus of the macromolecular chain. The results can be explained if the backbiting decomposition to pentacycles is prevented by the presence of longer

Table 4
Composition of copolymers $(R_2Si)_n(R'_2Si)_m$

Sample No.[a]	R	R'	n/m[b]		
			Py	^{29}Si NMR	^{1}H NMR
1	*n*-Hexyl	*n*-Pentyl	0.39	–	–
2	*n*-Hexyl	*n*-Butyl	0.58	–	0.84
3	*n*-Hexyl	*n*-Propyl	0.66	0.75	–
4	*n*-Hexyl	Ethyl	0.60	1.16	1.11
5 (l)	*n*-Hexyl	Methyl	0.20	–	0.32
5 (h)			0.72	1.18	1.33
6	*n*-Pentyl	*n*-Butyl	0.82	–	0.89
7	*n*-Pentyl	*n*-Propyl	0.89	0.96	0.98
8	*n*-Pentyl	Ethyl	0.86	0.90	0.81
9 (l)	*n*-Pentyl	Methyl	0.98	–	0.89
9 (h)			1.36	–	1.30
10	*n*-Butyl	*n*-Propyl	1.46	1.50	1.45
11	*n*-Butyl	Ethyl	0.79	0.80	0.87
12 (l)	*n*-Butyl	Methyl	0.89	–	0.79
12 (h)			2.27	–	2.19
13	*n*-Propyl	Ethyl	0.87	0.83	0.79

[a] (l) = Low- and (h) = high-molecular-mass fraction.
[b] Py = Measured by pyrolysis; NMR = measured by NMR spectroscopy [6].

Table 5
Relative occurrence of dyads in copolymers $(R_2Si)_n(R'_2Si)_m$

Sample No.[a]	R	R′	Relative molar amounts[b]					
			$(R_2Si)_2$		$(R_2Si)(R'_2Si)$		$(R'_2Si)_2$	
1	*n*-Hexyl	*n*-Pentyl	51	0	41	+1	8	0
2	*n*-Hexyl	*n*-Butyl	41	+1	44	−3	15	+1
3	*n*-Hexyl	*n*-Propyl	38	+2	44	−4	18	+2
4	*n*-Hexyl	Ethyl	38	−1	49	+2	13	−1
5 (l)	*n*-Hexyl	Methyl	69	0	28	0	2	−1
5 (h)			33	−1	50	+1	17	−1
6	*n*-Pentyl	*n*-Butyl	32	+2	45	−4	22	+2
7	*n*-Pentyl	*n*-Propyl	28	0	50	0	22	0
8	*n*-Pentyl	Ethyl	30	+1	48	−2	22	+1
9 (l)	*n*-Pentyl	Methyl	24	−1	51	+1	26	0
9 (h)			18	0	49	0	33	0
10	*n*-Butyl	*n*-Propyl	17	0	48	0	35	0
11	*n*-Butyl	Ethyl	32	+1	48	−1	20	+1
12 (l)	*n*-Butyl	Methyl	26	−2	54	+4	26	−2
12 (h)			8	−1	45	+2	47	−1
13	*n*-Propyl	Ethyl	28	−1	51	+1	21	−1

[a] (l) = Low- and (h) = high-molecular-mass fraction.
[b] Values in the second columns are deviations of found values from values calculated for a random copolymer structure.

n-alkyl groups on the silicon atoms. Some other mechanism, as yet not clear, must then be invoked to explain the formation of tetracycles at higher temperature.

The qualitative and quantitative analysis of the volatile products applying pyrolysis–GC–MS resulted in useful information about the copolymer composition and structure. In addition, GC retention data revealed differences between the retention index increments of methyl, ethyl and longer *n*-alkyl substituents of cyclotetra- and cyclopentasilanes.

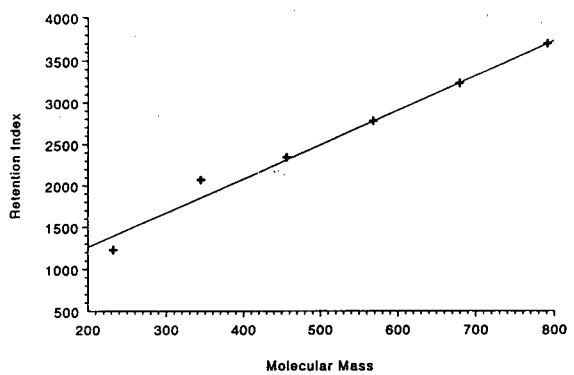

Fig. 5. Temperature-programmed retention indices of octamethyl-, -ethyl-, -*n*-propyl-, -*n*-butyl-, -*n*-pentyl- and -*n*-hexylcyclotetrasilane plotted against their molecular masses.

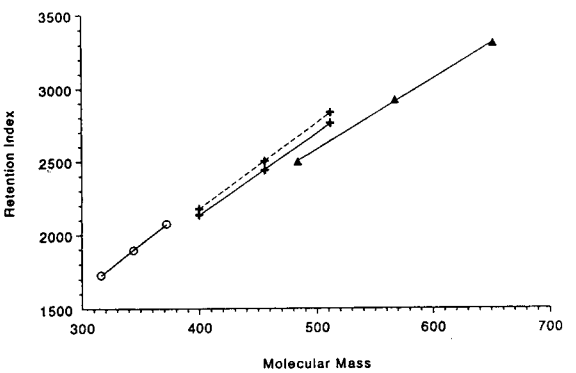

Fig. 6. Temperature-programmed retention indices of (○) hexamethyldi-, (+) tetramethyltetra- and (▲) dimethylhexa-*n*-butyl-, -*n*-pentyl- and -*n*-hexylcyclotetrasilane.

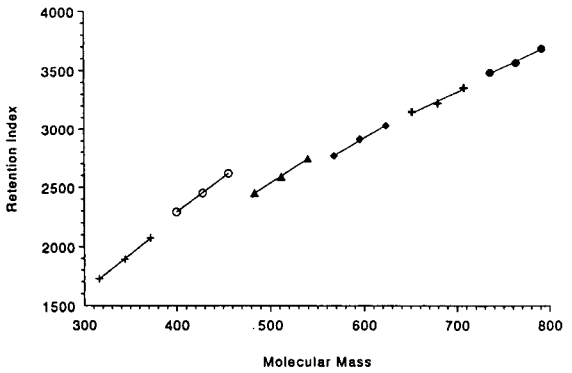

Fig. 7. Temperature-programmed retention indices of (+) hexamethyl-, (○) hexaethyl-, (▲) hexa-*n*-propyl-, (◆) hexa-*n*-butyl-, (+) hexa-*n*-pentyl- and (○) hexa-*n*-hexyl-di-*n*-butyl-, -di-*n*-pentyl- and -di-*n*-hexylcyclotetrasilane.

Acknowledgements

This work was supported by the Hungarian National Research Fund (OTKA), under contract No. 3078. The gift of the polymer samples from Professor Robert West and Rogerio Menescal, University of Wisconsin, Madison, WI, USA, is gratefully acknowledged.

References

[1] W.J. Irwin, in J. Cazes (Editor), *Analytical Pyrolysis —A Comprehensive Guide (Chromatographic Science Series*, Vol. 22), Marcel Dekker, New York 1982, Ch. 6.
[2] S.A. Liebman and E.J. Levy (Editors), *Pyrolysis and GC in Polymer Analysis (Chromatographic Science Series*, Vol. 29), Marcel Dekker, New York, 1985.
[3] G. Montaudo, in N. Grassie (Editor), *Developments in Polymer Degradation—7*, Elsevier Applied Science, London, 1987.
[4] N. Grassie, in J. Brandrup and E.H. Immergut (Editors), *Polymer Handbook*, Wiley, New York, 1989, p. II/365.
[5] M. Blazsó, R. West and T. Székely, *J. Anal. Appl. Pyrol.*, 15 (1989) 175.
[6] R. Menescal and R. West, *Macromolecules*, in press.
[7] R.C. Crippen, *Identification of Organic Compounds with the Aid of Gas Chromatography*, McGraw-Hill, New York, 1973, Ch. 5.
[8] V.S. Mastryukov, S.A. Strelkov, L.V. Vilkov, M. Kolonits, B. Rozsondai, H.G. Schuster and E. Hengge, *J. Mol. Struct.*, 238 (1990) 433.
[9] J.C. Strenberg, W.S. Gallaway and D.L.T. Jones, in N. Brenner, J.E. Callen and M.D. Weiss (Editors), *Gas Chromatography*, Academic Press, New York, 1962, p. 246.

ELSEVIER

Journal of Chromatography A, 683 (1994) 125–139

JOURNAL OF CHROMATOGRAPHY A

Effects of parameters on supercritical fluid extraction of triazines from soil by use of multiple linear regression

E.G. van der Velde*, M.R. Ramlal, A.C. van Beuzekom, R. Hoogerbrugge

Laboratory of Organic-Analytical Chemistry, National Institute of Public Health and Environmental Protection (RIVM), P.O. Box 1, 3720 BA Bilthoven, Netherlands

Abstract

The effects of various parameters on supercritical fluid extraction (SFE) of triazines from soil were studied with an experimental design, based on multiple linear regression. The SFE was performed using a multi-extraction unit with simultaneous extraction of eight samples. Different types of soil samples were spiked with a series of five triazines with different polarities.

The developed design was a compromise of various objectives like the relative importance of the different parameters, the total amount of experiments and instrumental limitations. Eleven series of experiments using different conditions were performed, resulting in a data set of over 200 data. Regression analysis was applied to evaluate the data set of each individual triazine component. Furthermore, the influence of the different parameters was tested, resulting in a limitation of the original parameter set as well as a combination of some parameters to avoid interactions. The influence of the pressure on the recovery appeared to be very important, recoveries increased with increasing pressures. The influence of the modifier was also essential, only when it was added directly to the extraction cell, and the effect is increasing with component polarity. The effects of the temperature and extraction time were slightly negative and not significant, whereas a small effect of the type of soil was observed. Two other models, combining the whole data set for all triazines, were applied resulting in a more pronounced effect of the individual parameters.

Multiple linear regression appeared to be a useful tool to study the effects of the many parameters in SFE, in order to reduce the number of experiments, to facilitate the evaluation of data and to distinguish possible interactions between several parameters.

1. Introduction

In the past few years, supercritical fluid extraction (SFE) has received widespread attention in the field of analysis of organic contaminants in environmental samples. After many qualitative applications, SFE is now ready to prove its potential advantages as a quantitative and fast alternative for conventional extraction techniques such as liquid–liquid and Soxhlet extraction. Recent reviews have shown its applicability for a wide range of analytes in all kinds of matrices [1–5].

The advantages of SFE are the high efficiency and selectivity, the short extraction times, the simple concentration steps and the reduction in toxic and environmentally hazardous solvents. However, some advantages of SFE still have to be proved, like the ability to reduce the cost per

* Corresponding author.

0021-9673/94/$07.00
SSDI 0021-9673(94)00536-I

analysis and on-line coupling with chromatographic techniques in routine analysis.

A challenge in SFE is the choice in and optimization of extraction parameters. Important parameters are pressure, temperature, amount and type of modifier, extraction time and cell volume. The extraction efficiency is directly depending on the solubility of the analytes in the fluid, which is determined by the density (pressure and temperature) and the vapour pressure of the analytes (temperature), and on the modifier. The modifier can be premixed with the fluid or added directly to the extraction cell. In the first case the modifier will increase the solubility of the analytes in the fluid, whereas in the second case the displacement of the analytes from the matrix active sites is facilitated [2]. It is suggested that a better wetting of the sample will enhance the accessibility of the analytes. The variability of the pressure and temperature will be determined by the supercritical point of the fluid, with or without addition of modifier, and by instrumental limitations. The extraction time determines, in combination with the restrictor dimensions and the cell volume, the total amount of supercritical fluid passing the cell.

In many publications, these extraction conditions are established empirically, due to a lack of solubility data of analytes in the supercritical fluids, especially when modifiers are added. Because of the complexity of the extraction process and the multitude of parameters, a solution is to use a statistical approach to reduce the number of experiments, to facilitate the interpretation of the data and to distinguish the possible interactions between several parameters. In most cases, a relatively simple approach is chosen starting with the two or three most important parameters in two settings, resulting in a 2^2 or 2^3 factorial design [6,7]. Ho and Tang [7] describe a 2^3 factorial design for three parameters (pressure, temperature and extraction time) at two levels (low and high) for the determination of polycyclic aromatic hydrocarbons (PAHs) and organochlorine pesticides from cartridges. The result was used as the initial condition for a variable-size simplex optimization. Because only three parameters were varied, at the end it was necessary to add a modifier to improve recoveries for the heavier PAHs. Lopez-Avila et al. [8] applied a model with seven variables (pressure, temperature, moisture, cell volume, sample size, extraction time, modifier volume) at two levels (low and high) to determine group differences between the low and high values. Finally, 1/16th of the full design (8 experiments) is performed, so only a ranking of main effects and no statistical significance were reported.

In this study, a statistical approach of parameter settings using multiple linear regression is presented, primarily to show the effects of extraction parameters in SFE of triazines from soil. Secondly, the SFE instrument was only available during a short time period and therefore all experiments had to be planned beforehand, because GC analyses were performed afterwards. An experimental design offers the opportunity to make a plan for experiments, based on expert knowledge on the importance of the parameters.

1.1. Experimental design

For the design of the experiments the following arguments had to be considered.

(1) The main objective of the study was to establish the effects of a number of parameters on the SFE of triazines from soil. These are both the SFE parameters mentioned above and the types of soil.

(2) The relative importance of the parameters may differ considerably. Some are of crucial importance, as stated above, others are only incorporated because their influence could not be excluded beforehand.

(3) Series contain seven or eight experiments with equal instrumental settings.

(4) The reproducibility was expected to be large ($>10\%$), so interpretation of individual experiments would be difficult.

The difference in importance of the parameters is in contradiction with the most commonly used experimental designs which are symmetrical in the parameters. Therefore, instead of the conventional symmetrical designs another

Table 1
Parameter settings in experimental design

Parameter	Degrees of freedom	Settings
Pressure (MPa)	1	20, 25, 30, 50
Temperature (°C)	1	50, 70, 80, 90, 100
Extraction time (min)	1	30, 35, 40, 60, 70
Type of modifier	2[a]	MeOH, mixed CO_2–MeOH, mixed CO_2–acetone
Amount of modifier (μl)	1	100, 200, 300, 1000
Cell volume (ml)	1	3.5, 10
Amount of triazines (μl)	1	(25), 50, 100, (200), (250), (300), (400)[b]
Type of soil	2	Sand, peat, clay

[a]Only addition of MeOH used in model evaluation.
[b]Amounts of modifier used for linearity experiment only are given in parentheses.

strategy was chosen. On the basis of experimental knowledge and literature on SFE, a first concept of the design was made. The design was modified to optimize the statistical properties using multiple linear regression and simulated and measured data for SFE of triazines.

Finally, an experimental design was chosen based on ten parameters (and a constant), which is a compromise between the various objectives of this study. In Table 1 an overview is given of these parameters and the settings, whereby the more important parameters are included in all experiments.

2. Experimental

2.1. Samples

Three types of blank soil with different contents of organic carbon were used, namely sand, peat and clay, with 0.3, 3.3 and 6.8% organic carbon, respectively. In addition, field samples were collected at different time intervals after treatment with atrazine from two locations, Bergeijk (code B1A/B and B2A/B) and Laren (code L1A/B and L2A/B), both in the Netherlands.

All soils were dried at 40°C, passed through a 2.8-mm sieve and were subsequently homogenized in a ball mill. The blank soils were used for spiking experiments with triazines, i.e. simazine, atrazine, terbuthylazine and the metabolites desisopropylatrazine and desethylatrazine at concentrations of 30–170 μg/kg of soil for each component. Individual soil samples were spiked by adding a standard solution of triazines to the extraction cell, containing a subsample of the soil.

2.2. Standard materials

Highly pure standard materials (purity >98%) of simazine, atrazine, terbuthylazine, desisopropylatrazine and desethylatrazine were obtained from C.N. Schmidt (Amsterdam, Netherlands). Methanol was HPLC grade (J.T. Baker, Deventer, Netherlands) and ethyl acetate and acetone were nanograde (Promochem, Wesel, Germany).

CO_2 was SFE/SFC grade (Air Products & Chemicals, Waddinxveen, Netherlands).

2.3. Supercritical fluid extraction

Supercritical fluid extractions were performed on a Dionex (Salt Lake City, UT, USA) SFE-703 multi-extraction instrument, suitable for the simultaneous extraction of eight samples, with a SFE-703M co-solvent addition module, made available by Dionex Breda (Breda, Netherlands). The specific experimental conditions as extraction temperature, pressure, cell volume, extraction times etc., for the different experi-

ments are given in the tables. Some parameters were not varied due to instrumental or other limitations, e.g. the type of supercritical fluid, restrictor dimensions, cell geometry and the collection device. Furthermore, the instrument only allowed dynamic and no static extractions.

Fused-silica restrictors in stainless-steel tubing with a controlled flow of 250 ml/min (gaseous CO_2) were used at temperatures of 180°C. The samples were collected in 10-ml vials with 5 ml ethyl acetate with a known concentration of internal standards [desmethrin and polychlorinated biphenyl (PCB) 171]. The vials, equipped with an inner tube, were cooled to°5C.

Exactly weighed soil samples (of about 6 g for 3.5-ml cells and 14 g for 10-ml cells) were put into the extraction cell, at one side filled with a thin layer of quartz sand to prevent clogging of the system. Cells were completely filled and stamped to achieve homogeneous packing, which is important to prevent dead volumes and channelling. In the spiking experiments, a small volume of triazines in acetone was added dispersed over the soil in the extraction cell. Next, the cell was purged with a nitrogen flow during 20 min to allow the solvent to evaporate, this preventing the spiking solvent to act as modifier. Modifiers were added either directly to the extraction cell, or premixed with CO_2 by the co-solvent pump. Finally, SFE extracts were thoroughly mixed and were subjected to GC analysis.

2.4. Analysis

A Carlo Erba HRGC 5300 gas chromatograph with nitrogen–phosphorus detection (NPD) system and splitless injector, equipped with a A200S autosampler (all Carlo Erba, Milan, Italy) and using a DB5 column (30 m × 0.32 mm I.D.; 0.25 μm; J & W Scientific, Folsom, CA, USA), was used for the quantitative analysis of the triazines. After injection of 3 μl and a splitless time of 45 s, the temperature programme consisted of an initial temperature of 80°C, 2 min hold, programmed to 170°C at 25°C/min, 8 min hold, then at 2°C/min to 190°C and at 15°C/min to the final temperature of 270°C and held for 15 min. The injector temperature was 220°C and detector temperature was 300°C. A GC–electron-capture detection (ECD) system consisting of an HP 5890 gas chromatograph, equipped with an HP 7673a autosampler and interfaced to an HP 3365 Chemstation (Hewlett-Packard, Palo Alto, CA, USA) using an Ultra 1 column (50 m × 0.25 mm I.D.; film thickness $d_f = 0.5$ μm; Hewlett-Packard) for confirmation. Quantification was performed by comparison with an external standard mixture, using desmethrin (GC–NPD) and PCB 171 (GC–ECD) as internal standards. Lower limits of determination for each component were 4 μg/kg, using the conditions specified above for sample preparation and analysis.

2.5. Statistical method

A linear model is used to describe the influence of the parameters on the recovery of the triazines. The model contains a constant (p_{11}) and the influence of 10 parameters ($p_1 \ldots p_{10}$):

$\boldsymbol{p} = p_1, p_2, \ldots p_{11}$ (p_{11} is the constant).

Then every experiment has 10 parameter settings described as:

$\boldsymbol{x} = x_1, x_2, \ldots x_{11}$ ($x_{11} = 1$).

The linear model, $M(\boldsymbol{x}, \boldsymbol{p})$, then reads:

$$M(\boldsymbol{x},\boldsymbol{p}) = p_1x_1 + p_2x_2 + \ldots p_{10}x_{10} + p_{11}$$

Some of the parameters in this model, like the various types of soil, have only two possible settings which are 1 for the soil type corresponding with the sample and 0 for the other soils. The settings of other parameters like pressure, temperature and extraction time have a continuum of possible settings. The linear model used does not incorporate terms of higher order like x_1^2 and interactions like x_1x_2. The incorporation of all these terms is not possible because then the number of terms would exceed the number of experiments.

In designing the experiments, the accuracy of the parameters of interest was calculated using simulated data, with the linear model both for the complete data set as for two subsets, which

contained only the first 35% and 70% of the data points (in case some experiments might be excluded for time reasons). Then, mutations in the designed parameter settings were applied to improve the accuracy of the important parameters both for the total data set as for the subsets. The information from the subsets was used to change the order in which the experiments were planned.

The linear model is calculated separately for each of the components analysed. The estimates of the parameters (p) and their standard deviation are calculated using (unweighed) multiple linear regression [9].

3. Results and discussion

The final experimental set up is consisting of eleven series of seven or eight simultaneous extractions, based on ten parameters with different settings (Table 1). The temperature is varied from 50 to 100°C, while the maximum pressure ranged from 20 to 50 MPa, because of instrumental limitations. The extraction time was chosen between 30 min for the 3.5-ml cell (only seven cells were available) and 70 min for the 10-ml cell. In all experiments different amounts of modifier were tested, methanol was added directly to the cell or CO_2 was premixed with methanol or acetone. From previous experiments on another SFE instrument (Carlo Erba SFC 3000), the initial conditions were established. From several collection solvents, the trapping efficiency of ethyl acetate proved to be the best. Further, it was shown that especially the use of a modifier is very important to increase the solubility of the triazines in CO_2. The best results were obtained with methanol. These results are in agreement with other SFE data on triazines in soil [10,11] and were used as initial conditions in this study. In two series the repeatability and linearity of the instrument and the supercritical fluid extraction were tested. The influence of the parameters was tested on different types of soil (sand, clay and peat) spiked with triazines and on field samples.

In Table 2, an overview is given of all series of experiments with the specific extraction conditions for pressure, temperature, extraction time, cell volume, amount and type of modifier, spike volume and the type of soil. The results are given as a percentage of recovery for recovery experiments and for field samples a concentration is calculated. Results below determination limits (LOD; 4 μg/kg for 10-ml cells and 9 μg/kg for 3.5-ml cells) are marked with an $<$. In the model calculation, these results have been given the value zero. A number of experiments was not successful, due to plugging and imperfections in the collection device, and is marked with an a. These experimental data were not incorporated in the linear model. In Fig. 1a, a typical GC–NPD chromatogram of triazines spiked on peat soil is given. This chromatogram shows that no matrix disturbances are present using SFE as extraction technique.

3.1. Repeatability and linearity

The study has been designed for evaluation with a model incorporating all relevant parameters, instead of comparisons between pairs of experiments to study single parameters. Two exceptions on this general idea were made deliberately: the repeatability and the linearity.

Therefore, two series of experiments were incorporated to study these items explicitly. In series 3 (Table 2), seven identical experiments were performed and in series 5, nearly identical experiments were performed with variation in the amount of added triazine standards. Calibration curves for all triazines have correlation coefficients of 0.981 and better.

In Table 3, the averages and standard deviation of the recoveries are shown for series 3 and 5. The average recovery of series 3 ranged from 9 to 66% with standard deviations of 7 to 21%, whereas series 5 ranged from 92 to 99% with standard deviations of 5 to 11% for the different triazines. Recoveries for series 5 were good, with moderate standard deviations for intra-series variations. Apparently, extraction conditions of series 5 were more close to the optimum. In addition, results may be influenced by the type of soil, clay (series 3) versus sand (series 5). It is

Table 2
Results of SFE of triazines in experimental design (recoveries (%) and concentrations (μg/kg) of triazines by selected conditions)

Series/ experiment No.	Soil type	Spike (μl)	Cell volume (ml)	Modifier	Pressure (MPa)	Tempera-ture (°C)	Extraction time (min)	Triazines in recoveries (%)/concentrations (μg/kg)				
								Desisopropyl-atrazine	Desethyl-atrazine	Simazine	Atrazine	Terbuthyl-azine
1.1	Clay	100	3.5	100 μl MeOH	20	50	40	<	8%	17%	60%	55%
1.2	Clay	100		200 μl MeOH				<	27%	80%	79%	59%
1.3	Clay	100		300 μl MeOH				27%	54%	78%	52%	39%
1.4	Sand	–		100 μl MeOH				[a]	[a]	[a]	[a]	[a]
1.5	Sand	100		100 μl MeOH				<	<	<	<	<
1.6	Peat	100		100 μl MeOH				<	<	8%	10%	9%
1.7	Field B1B	–		100 μl MeOH				[a]	[a]	[a]	[a]	[a]
2.1	Clay	–	10	300 μl MeOH	20	70	60	[a]	[a]	[a]	[a]	[a]
2.2	Clay	50		300 μl MeOH				<	25%	31%	41%	39%
2.3	Clay	50		1 ml MeOH				34%	31%	44%	41%	40%
2.4	Sand	50		300 μl MeOH				34%	25%	101%	100%	96%
2.5	Sand	50		1 ml MeOH				82%	58%	73%	74%	64%
2.6	Field B1B	–		300 μl MeOH				<	<	<	26 μg/kg	<
2.7	Field B1B	–		1 ml MeOH				[a]	[a]	[a]	[a]	[a]
2.8	Sand	50		300 μl MeOH				[a]	[a]	[a]	[a]	[a]
3.1	Clay	50	3.5	100 μl MeOH	25	50	30	11%	26%	45%	74%	76%
3.2	Clay	50		100 μl MeOH				5%	37%	59%	58%	60%
3.3	Clay	50		100 μl MeOH				<	<	36%	55%	56%
3.4	Clay	50		100 μl MeOH				<	47%	68%	73%	72%
3.5	Clay	50		100 μl MeOH				<	12%	17%	64%	62%
3.6	Clay	50		100 μl MeOH				6%	39%	43%	68%	65%
3.7	Clay	50		100 μl MeOH				43%	60%	81%	73%	70%
4.1	Clay	–	10	300 μl MeOH	50	50	70	<	<	<	<	<
4.2	Clay	50		300 μl MeOH				<	58%	56%	56%	52%
4.3	Sand	–		300 μl MeOH				<	<	<	<	<
4.4	Sand	50		300 μl MeOH				107%	111%	113%	105%	105%

4.5	Peat	–		300 μl MeOH				<	<	<	<	<
4.6	Peat	50		300 μl MeOH				40%	115%	120%	108%	98%
4.7	Field B1B	–		300 μl MeOH				<	<	<	29 μg/kg	<
4.8	Field B1B	50		300 μl MeOH				91%	92%	84%	62%	80%
5.1	Sand	25	3.5	300 μl MeOH	30	70	35	90%	[a]	99%	97%	95%
5.2	Sand	50		300 μl MeOH				[a]	[a]	[a]	[a]	[a]
5.3	Sand	100		300 μl MeOH				93%	84%	96%	91%	89%
5.4	Sand	200		300 μl MeOH				109%	102%	103%	99%	95%
5.5	Sand	250		300 μl MeOH				87%	87%	102%	100%	96%
5.6	Sand	300		300 μl MeOH				92%	86%	89%	84%	84%
5.7	Sand	400		300 μl MeOH				113%	102%	103%	98%	93%
6.1	Clay	–	10	CO_2–MeOH (90:10)	30	80	70	<	<	<	<	<
6.2	Clay	50		CO_2–MeOH (90:10)				<	<	<	<	<
6.3	Sand	–		CO_2–MeOH (90:10)				<	<	<	<	<
6.4	Sand	50		CO_2–MeOH (90:10)				<	<	16%	57%	69%
6.5	Peat	–		CO_2–MeOH (90:10)				<	<	<	<	<
6.6	Peat	50		CO_2–MeOH (90:10)				<	<	31%	49%	53%
6.7	Field B1B	–		CO_2–MeOH (90:10)				<	<	<	9 μg/kg	<
6.8	Quartz	–		CO_2–MeOH (90:10)				<	<	<	<	<
7.1	Clay	–	3.5	CO_2–MeOH (95:5)	25	90	30	<	<	<	<	<
7.2	Clay	50		CO_2–MeOH (95:5)				<	<	<	<	<
7.3	Sand	–		CO_2–MeOH (95:5)				<	<	<	<	<
7.4	Sand	50		CO_2–MeOH (95:5)				<	<	7%	47%	73%
7.5	Peat	–		CO_2–MeOH (95:5)				<	<	<	<	<
7.6	Peat	50		CO_2–MeOH (95:5)				<	17%	58%	89%	94%
7.7	Field B1B	–		CO_2–MeOH (95:5)				<	<	<	12 μg/kg	<
8.1	Field B1B	–	10	300 μl MeOH	20	50	60	<	<	<	50 μg/kg	<
8.2	Field L1B	–		300 μl MeOH				<	<	<	41 μg/kg	<
8.3	Field L1A	–		300 μl MeOH				<	<	<	59 μg/kg	<
8.4	Field L2A	–		300 μl MeOH				<	<	<	48 μg/kg	<
8.5	Field L2B	–		300 μl MeOH				<	<	<	41 μg/kg	<
8.6	Field B1A	–		300 μl MeOH				<	<	<	30 μg/kg	<
8.7	Field B2B	–		300 μl MeOH				<	<	<	37 μg/kg	<
8.8	Field B2A	–		300 μl MeOH				<	<	<	22 μg/kg	<

(Continued on p. 132)

Table 2 *(continued)*

Series/ experiment No.	Soil type	Spike (μl)	Cell volume (ml)	Modifier	Pressure (MPa)	Temperature (°C)	Extraction time (min)	Triazines in recoveries (%)/concentrations (μg/kg)				
								Desisopropyl-atrazine	Desethyl-atrazine	Simazine	Atrazine	Terbuthyl-azine
9.1	Clay	–	3.5	100 μl MeOH	30	100	30	<	<	<	<	<
9.2	Clay	50		100 μl MeOH				<	<	22%	48%	56%
9.3	Sand	–		100 μl MeOH				<	<	<	<	<
9.4	Sand	50		100 μl MeOH				<	<	<	43%	57%
9.5	Peat	–		100 μl MeOH				<	<	<	<	<
9.6	Peat	50		100 μl MeOH				12%	32%	92%	111%	104%
9.7	Field B1B	–		100 μl MeOH				<	<	<	28 μg/kg	<
10.1	Clay	–	10	CO_2–acetone (90:10)	30	100	70	<	<	<	<	<
10.2	Clay	50		CO_2–acetone (90:10)				<	<	<	<	<
10.3	Clay	50		CO_2–acetone (90:10)				<	<	<	25%	29%
10.4	Sand	–		CO_2–acetone (90:10)				<	<	<	<	<
10.5	Sand	50		CO_2–acetone (90:10)				<	<	23%	46%	55%
10.6	Peat	–		CO_2–acetone (90:10)				<	<	<	<	<
10.7	Peat	50		CO_2–acetone (90:10)				<	<	37%	57%	67%
10.8	Field B1B	–		CO_2–acetone (90:10)				<	<	<	17 μg/kg	<
11.1	Clay	–	3.5	CO_2–acetone (90:10)	20	70	30	<	<	<	<	<
11.2	Clay	50		CO_2–acetone (90:10)				<	<	<	<	<
11.3	Sand	–		CO_2–acetone (90:10)				<	<	<	<	<
11.4	Sand	50		CO_2–acetone (90:10)				<	<	<	55%	82%
11.5	Peat	50		CO_2–acetone (90:10)				<	<	14%	68%	95%
11.6	Field B1B	–		CO_2–acetone (90:10)				<	<	<	<	<
11.7	Field L1B	–		CO_2–acetone (90:10)				<	<	<	<	<

Spike concentration: ca. 10 μg triazine component/ml. < = LOD: 4 μg/kg for 3.5-ml cell and 9 μg/kg for 10-ml cell.

[a] Experiment failed.

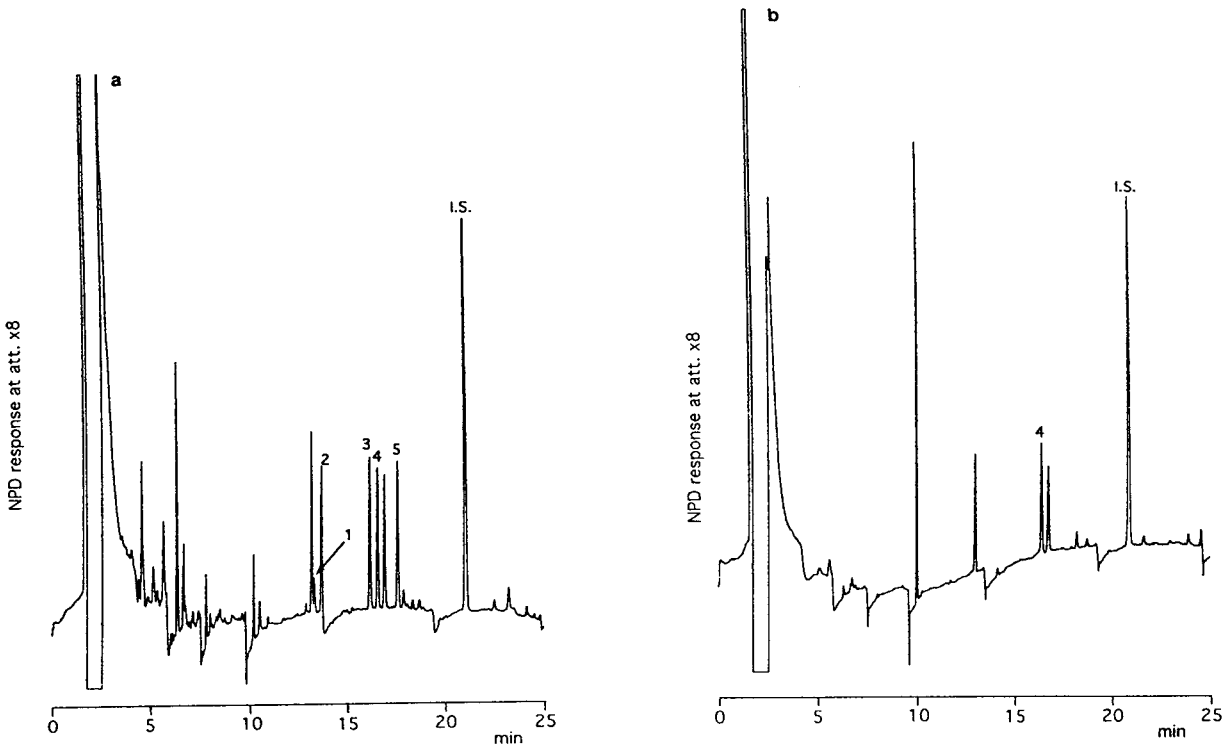

Fig. 1. GC–NPD chromatograms of (a) triazines spiked on peat soil and (b) atrazine in a field sample treated with atrazine. Peaks: 1 = desisopropylatrazine; 2 = desethylatrazine; 3 = simazine; 4 = atrazine; 5 = terbuthylazine; I.S. = internal standard. For chromatographic conditions see Experimental.

known that clay, with a higher content of organic carbon and another absorptive nature, will cause more irreversible binding of organic components than sand.

3.2. Linear model

The linear model could be applied on about 40 successful (recovery) experiments and was pri-

Table 3
Repeatability and linearity of SFE experiments

Repeatability/ linearity	Desisopropyl-atrazine	Desethyl-atrazine	Simazine	Atrazine	Terbuthyl-azine
Repeatability (series 3)					
Average (%)	9	32	50	66	66
S.D. (%)	15	21	21	8	7
R.S.D. (%)	165	65	43	12	11
Linearity (series 5)					
Average (%)	97	92	99	95	92
S.D. (%)	11	9	5	6	5
R.S.D. (%)	11	10	5	6	5

marily calculated using all ten parameters. The results showed that the addition of premixed modifier, both methanol and acetone, had only a small amount of relevant data points and had no significant effect and therefore, these parameters were excluded from the model.

Of the remaining parameters both the amount of modifier and the volume of the cell appeared to have a significant effect. However, the combination of these two parameters as the amount of modifier added per ml of cell volume seems logical. Therefore the quotient of the amount of modifier and the cell volume was introduced as an independent parameter in the linear model. With this new factor, the quality of the model improved and both the significant influence of the original parameters (amount of modifier and cell volume) vanished.

The coefficients resulting from the model calculation and the standard errors in these coefficients are shown in Table 4. The value of each coefficient can be interpreted as the effect that is calculated when the setting of the corresponding parameter is changed from the minimum into the maximum value. The standard error is the estimated standard deviation of this effect. The effect is expected to be proportional at smaller changes of the parameter settings, since it is a linear model.

3.3. *Effects of parameters*

From Table 4 can be concluded that the influence of the pressure on the recovery is very important. Recoveries increase when the pressure is increased in the range from 15 to 50 MPa. The amount of modifier added to the cell with respect to the volume of the cell is another important parameter. This influence however is not equal for all components, but increases with increasing component polarity. The influence of the temperature is small and negative. The negative contribution would, in combination with the positive contribution by an increase in pressure, point to a positive effect of an increase in density.

The influence of the amount of spike is significant for the first two components only. This effect may be artificially caused by the fact that a small amount of spike might not be detected at all ($<$LOD) and therefore a value of zero is included into the data set, while by a higher spike concentration and a similar recovery the real value (>0) can be used.

Variations in the recovery caused by type of soil (compared to sand) vary between -23 and 28%. These effects are relatively small compared to the effects of changing some other extraction parameters. Surprisingly, the effect is positive for the different triazines in peat, while a decrease in recovery should be expected on behalf of the better binding of the analytes to the soil matrices with higher contents of organic carbon in comparison with sand, as was seen for clay [12].

The effect of enlarging the extraction time is calculated by using the extraction time divided by the cell volume as the descriptive parameter. For all components a small (non-significant) negative effect is found. This suggests that the extraction time can be reduced without losing recovery.

The calculated values for the constant represent the predicted recovery when all parameter values are set to zero. For these non-optimal settings hardly any recovery is predicted for the more polar components —the metabolites desisopropylatrazine and desethylatrazine— increasing to a recovery of nearly 60% for the non-polar ones.

The residual standard deviations (difference between the experimental recoveries and the recoveries from the linear model) range between 15 and 25%. Comparing these standard deviations with the linearity experiment above, the latter appeared to be smaller. This is not surprising since the linearity was studied in a single series of experiments and using the same type of soil. So, inter-series variations and possible model imperfections are excluded.

Concluding, starting from these effects of the individual parameters to optimize the extraction parameters for triazines from soil, extractions have to be performed at maximum pressure (50 MPa), maximum addition of methanol as modifier (100 μl/ml cell volume), minimum tempera-

Table 4
Maximum effect of different parameters on the recoveries of individual triazines on basis of linear model

Parameter	Desisopropylatrazine		Desethylatrazine		Simazine		Atrazine		Terbuthylazine	
	Coefficient	Standard error	Coefficient	Standard error	Coefficient	Standard error	Coefficient	Standard error	Coefficient	Standard error
Constant	1	13	−3	12	14	19	48	19	65	20
Clay (1 = clay, 0 = sand or peat)	−21	6	−2	6	−4	9	−13	9	−23	10
Peat (1 = peat, 0 = sand or clay)	−16	9	7	8	28	12	28	13	23	13
Pressure (0 = 15 MPa, 1 = 50 MPa)	68	15	101	13	76	21	47	22	36	23
Temperature (0 = 31°C, 1 = 100°C)	−16	11	−42	10	−33	15	−28	16	−25	17
Spike volume (1 = 400 μl)	45	18	42	19	10	27	3	28	3	29
Extraction time/cell volume (0 = 6 min/ml, 1 = 11 min/ml)	−22	12	−15	12	−12	18	−9	19	−13	19
Modifier/cell volume (1 = 100 μl/ml)	107	15	100	15	128	22	77	23	49	24
Residual standard deviation	16.1		14.7		23.4		24.1		25.4	

See text. Residual standard deviation is the difference between the experimental recoveries and the recoveries from the linear model.

ture (50°C) and probably a lower extraction time, within the range of extraction conditions of this model. A test of these conditions has to be performed in a closer investigation.

3.4. Combined models

The results in Table 4 show a large amount of similarity between the models of the triazines studied. This in combination with the molecular familiarity between the triazines led to an attempt to describe the recoveries of all components using one model. An exception was made for both the constants and the influence of the amount of modifier/cell volume since these parameters show a large variation in effect between the different components. The result of this combined analysis is shown in Table 5. Note that the standard errors in the other coefficients decreased by more than a factor of two, due to the larger amount of data points in the model with respect to the separate models. The residual standard deviations are hardly changed while the number of overall model parameters is reduced from 40 to 16.

The application of a linear model without interactions is not a priori justified. To check the effect of non-linearities, the quadratic terms of both pressure and amount of modifier/cell volume were added to the model. These parameters had no significant influence. The separate effects of pressure and modifier/cell volume are the most important, therefore the interaction is determined. Introducing a combined effect of pressure and modifier/cell volume, the significance of the separate parameters disappears. This implies, that an increase of both parameters simultaneously will have an influence on extraction results, which is even larger than the effect predicted by the linear model.

Although no significant non-linear effects were found, the linear model has some intrinsic limitations since non-realistic recoveries below 0 and above 100% can be predicted easily. An elegant alternative is the use of a transformation which has these limits as asymptotic values. The application of some transformations is discussed by

Table 5
Effect of the parameters on the recovery of the triazines using a combined linear and a sigmoid model

Parameter	Combined linear model		Sigmoid model
	Coefficient	Standard error	Coefficient
Constant desisopropylatrazine	−4	9	−45
Constant desethylatrazine	7	9	−12
Constant simazine	23	9	5
Constant atrazine	46	9	56
Constant terbuthylazine	53	9	66
Clay (1 = clay, 0 = sand or peat)	−12	4	−21
Peat (1 = peat, 0 = sand or clay)	14	5	35
Pressure (0 = 15 MPa, 1 = 50 MPa)	65	9	144
Temperature (0 = 31°C, 1 = 100°C)	−28	6	−71
Spike volume (1 = 400 μl)	20	11	30
Extraction time/cell volume (0 = 6 min/ml, 1 = 11 min/ml)	−14	7	−37
Modifier/cell volume desisopropylatrazine (1 = 100 μl/ml)	84	11	149
Modifier/cell volume desethylatrazine (1 = 100 μl/ml)	74	11	113
Modifier/cell volume simazine (1 = 100 μl/ml)	75	11	198
Modifier/cell volume atrazine (1 = 100 μl/ml)	42	11	63
Modifier/cell volume terbuthylazine (1 = 100 μl/ml)	26	11	32
Residual standard deviation	21.5		19.9

Bourguignon et al. [13] to describe the effect of pH on HPLC retention.

In this paper a first attempt was made using the sigmoid function $S(y)$ for the transformation.

$$S(y) = [1 + \exp(-4y)]^{-1}$$

The results of the linear model, $M(\boldsymbol{x},\boldsymbol{p})$, were introduced in the sigmoid function. In order to enable a comparison with the linear model the sigmoid model $M_S(\boldsymbol{x},\boldsymbol{p})$ was scaled as:

$$M_S(\boldsymbol{x},\boldsymbol{p}) = S[M(\boldsymbol{x},\boldsymbol{p})/100 - 0.5]100$$

The division and multiplication with 100 were necessary since all recoveries are expressed in percentages. A characteristic of the transformation is that values near 50% are not changed. The effects of most parameters are slightly larger compared with the results from the linear combined model. This indicates that for recoveries near 50% the influence of the parameters is larger than the calculated value from the linear model. Near the limits of 0 and 100% the influence of the parameters will be (much) smaller.

Concluding, the results of these two models confirm the effects obtained by the original linear model, the effects are larger and the errors are smaller. It delivers an interesting complementation, but no replacement of the linear model.

3.5. Field samples

In the series of experiments some field samples have been involved, which have been treated with atrazine. In Table 6, the atrazine concentrations for sample B1B (location Bergeijk; pitcode 1; second sampling), extracted eight times under different conditions, are shown. From this results can be seen, as for the spiked samples, that the concentrations are strongly varying with the extraction conditions from <9 to 50 μg/kg soil. Especially, the extractions with premixed modifiers score much lower than with modifier added directly to the extraction cell. The atrazine concentrations were corrected for recoveries as predicted by the linear model, resulting in a best estimation of the atrazine concentration of 41 μg/kg for this field sample. In combination with the average recovery of 61%, the variation in results is in agreement with the error predicted by the linear model. In Fig. 1b, a chromatogram of a field sample with atrazine is shown.

In Table 7, an overview is given for all field

Table 6
Atrazine in a field sample (B1B) using different SFE conditions

Series/ experiment No.	Cell volume (ml)	Modifier	Pressure (MPa)	Temperature (°C)	Extraction time (min)	Atrazine (μg/kg) determined	Atrazine[a] (μg/kg) after correction
2.6	10	300 μl MeOH	20	70	60	26	42
4.7	10	300 μl MeOH	50	50	70	29	27
6.7	10	CO_2–MeOH (90:10)	30	80	70	9	19
7.7	3.5	CO_2–MeOH (95:5)	25	90	30	12	37
8.1	10	300 μl MeOH	20	50	60	50	71
9.7	3.5	100 μl MeOH	30	100	30	28	49
10.8	10	CO_2–acetone (90:10)	30	100	70	17	44
11.6	3.5	CO_2–acetone (90:10)	20	70	30	<9	<26
				Average (7 experiments)		25	41
				S.D.		14	17
				R.S.D. (%)		56	40

[a]Corrections were calculated with the predicted recoveries according to the linear model.

Table 7
Atriazine concentrations (μg/kg) in field samples (series 8)

Sample code	Location	Sampling June 1991		Sampling October 1991	
		LLE	SFE	LLE	SFE
		June 1991	April 1992	October 1991	April 1992
B1A/B1B	Bergeijk	110	30	40	50
B2A/B2B	Bergeijk	100	22	63	37
L1A/L1B	Laren	100	59	33	41
L2A/L2B	Laren	130	48	50	41

Concentrations are not corrected for recovery and dry mass.

samples, which are collected at two locations (Bergeijk and Laren) at two pits (code 1 and 2) in two time periods (code A and B) after treatment with atrazine, in comparison with the results from conventional solvent extraction. Because the period of analysis is different for both techniques, only qualitative explanations can be given. The LLE concentrations, directly after treatment, are the highest, while four months later they are reduced with more than 50% by breakdown —although no metabolites could be determined— or irreversible binding to the matrix. The SFE of the first and second collection show comparable results, independent if samples are taken directly after treatment or later (and samples were stored in the laboratory in the dark at 4°C), and these values are in agreement with the results from the second solvent extraction.

4. Conclusions

The effects of various parameters on SFE of triazines from soil were tested using an experimental design, based on multiple linear regression. The model was adapted to exclude non contributing parameters and to combine some parameters to avoid interactions.

Two important parameters on the SFE efficiency were found, the pressure and the amount of modifier with respect to the cell volume. The recovery is increasing with increasing pressures, at the same time a small negative contribution was found for the temperature, both pointing towards a positive effect of an increase in density. The influence of the modifier is also essential, but only when it was added directly to the extraction cell and the effect is increasing with component polarity. Small effects were found for the type of soil and the extraction time. Residual standard deviations of the linear model range between 15 and 25%, whereas the intra-series repeatabilities are moderate (standard deviation of 5 to 11%), if optimal extraction conditions are chosen.

Starting from these effects of the individual parameters, extraction of triazines from soil can be optimized. Extractions have to be performed at maximum pressure (50 MPa), maximum addition of methanol as modifier (100 μl/ml cell volume), minimum temperature (50°C) and probably a shorter extraction time, within the range of extraction conditions of this model.

Two other models were tested, which make one data set for all triazines and apply a sigmoid transformation. The results of these two models give a more pronounced effect of the individual parameters.

A series of field samples, treated with atrazine, were involved in the experiments. The atrazine concentration can be determined with an error, which is in agreement with the error predicted by the linear model and further, SFE yields comparable results with solvent extractions.

Concluding, a dedicated experimental design and application of multiple linear regression

enabled a study of the effects of the individual parameters in supercritical fluid extraction. It is possible to reduce the number of experiments, to facilitate the evaluation of data and to distinguish possible interactions between several parameters.

Acknowledgement

Dionex Breda is acknowledged for their loan of the instrument and further equipment.

References

[1] S.B. Hawthorne, *Anal. Chem.*, 62 (1990) 633A–642A.
[2] S.B. Hawthorne, D.J. Miller, M.D. Burford, J.J. Langenfeld, S. Eckert-Tilotta and P.K. Louie, *J. Chromatogr.*, 642 (1993) 301–317.
[3] V. Camel, A. Tambuté and M. Caude, *J. Chromatogr.*, 642 (1993) 263–281.
[4] R.W. Vannoort, J.P. Chervet, H. Lingeman, G.J. de Jong and U.A.Th. Brinkman, *J. Chromatogr.*, 505 (1990) 45–77.
[5] T. Greibrokk, *J. Chromatogr.*, 626 (1992) 33–40
[6] M.K.L. Bicking, *J. Chromatogr. Sci.*, 30 (1992) 358–360.
[7] J.S. Ho and P.H. Tang, *J. Chromatogr. Sci.*, 30 (1992) 344–350.
[8] V. Lopez-Avila, N.S. Dodhiwala and W.F. Beckeret, *J. Chromatogr. Sci.*, 28 (1990) 468–476.
[9] D.L. Massart, B.G.M. VandeGinste, S.N. Deming, Y. Michotte and L. Kaufman, *Chemometrics —a Textbook*, Elsevier, Amsterdam, 1988.
[10] V. Janda, G. Steenbeke and P. Sandra, *J. Chromatogr.*, 479 (1989) 200–205.
[11] R.L. Firor, in P. Sandra (Editor), *Proceedings of the 11th Symposium on Capillary Chromatography, Monterey, 1990*, Huethig Verlag, Heidelberg, 1990, pp. 625–638.
[12] E.G. van der Velde, W. de Haan and A.K.D. Liem, *J. Chromatogr.*, 626 (1992) 135–143.
[13] B. Bourguignon, F. Marcenac, H.R. Keller, P.F. de Aguiar and D.L. Massart, *J. Chromatogr.*, 628 (1993) 171–189.

ELSEVIER

Journal of Chromatography A, 683 (1994) 141–149

JOURNAL OF CHROMATOGRAPHY A

Structural elucidation and trace analysis with combined hyphenated chromatographic and mass spectrometric methods Potential of using hybrid sector mass spectrometry–time-of-flight mass spectrometry for pesticide analysis

Stefan Schütz[a,*], Hans E. Hummel[a], Alexander Duhr[b], Hermann Wollnik[b]

[a]*Department of Biological and Biotechnical Plant Protection, Institute of Phytopathology and Applied Zoology, Justus Liebig University, Ludwigstrasse 21b, 35390 Giessen, Germany*

[b]*Second Physical Institute, Justus Liebig University, Heinrich Buff Ring 58, 35392 Giessen, Germany*

Abstract

The development of methods for analysis of triazines and their hydroxy metabolites in humic soil samples with combined chromatographic and mass spectrometric techniques is described. A two-way approach was used for separating interfering humic substances and for performing structural elucidation of the herbicide traces. Humic soil samples were extracted by supercritical fluid extraction and analysed both by HPLC–particle beam MS and a new MS–MS method. The new MS–MS unit is of the tandem-sector field-time-of-flight-MS type.

1. Introduction

Herbicides are widely used in agriculture and are subject to differing registration policies in several countries within the European Union (EU). Important is the group of triazine herbicides, some members of which are moderately toxic and environmentally persistent for several months. These triazines are readily soluble in water. Their leaching from cropland into subsoil water can be considerable. Therefore, one compound of this group (atrazine) is not permitted for use at all in Germany and others (terbuthylazine) are restricted in water protection areas. In order to confirm abuse of those compounds, metabolite concentrations in the soil have to be determined.

In our department (Biological and Biotechnical Plant Protection) triazines and their metabolites are usually quantified in leaching water and soil samples with a previously described LC method coupled with UV detection [1] or with GC–MS methods [2,3].

GC–MS is a common and sensitive method for the determination of triazines and their nonpolar metabolites [2,3]. However, the polar hydroxy metabolites must also be detected in order to confirm illegal application of triazines [4,5]. HPLC separation techniques are convenient for determining polar hydroxytriazines [6].

With LC and MS detection, triazines can be determined via direct liquid introduction (DLI) [7], thermospray (TSP) in "filament on" or

* Corresponding author.

0021-9673/94/$07.00
SSDI 0021-9673(94)00611-3

"filament off" modes [8–14], particle beam (PB) [12–17] or with an atmospheric pressure ionisation (API) [18] interface. Although triazines have been extensively studied [1–18], few data on analysis of hydroxytriazines in soil with high humic acid content are available.

In less complex samples, the use of tandem mass spectrometry (MS–MS) permits rapid analysis of specific compounds without the need for chromatographic separation [19,20]. In more complex samples like humic soils the necessary chromatographic effort can be reduced significantly. The overall limit of detection is usually higher in this approach, but the improved signal-to-noise ratio in the secondary mass spectrum facilitates structural elucidation. Although environmentally important compounds have been studied [19–30], few data on MS–MS examinations of pesticides in soil have been reported.

In this study, it was our aim to develop an analysis method for hydroxytriazines in complex soil samples. We combined modern methods of analysis for achieving fast and reliable results. This goal was approached from two different ends of the analytical chain. On one hand we developed a short procedure for extraction and separation of triazines from humic soil by supercritical fluid extraction (SFE) and on the other hand we tried to achieve structural elucidation of preseparated hydroxytriazines by using a MS–MS method.

SFE is a technique used to extract non-polar substances preferably from semi-solid samples with an unnoxious solvent [31,32]. Supercritical CO_2 is usually employed as the extraction solvent of choice, with varying solvent strength depending on applied pressure, temperature and modifiers added.

In an attempt to extract atrazine of medium polarity [33] and its polar hydroxy metabolites in the same process, application of high pressure (50 MPa) and addition of 10% methanol as a modifier is necessary. When compared to conventional extraction [34] and static SFE methods [35] the use of the principle of "fractionated extraction" [36] in a dynamic extraction mode results in a considerable gain of extraction selectivity. Co-extraction of humic acids is suppressed significantly under these conditions. Therefore, usually applied clean-up procedures like gel permeation chromatography [37] and solid-phase extraction [38] can be circumvented at considerable savings in time and cost.

The hybrid tandem mass spectrometer consists of a double-focusing sector field mass spectrometry (BE-MS) system, a collision cell working with surface-induced dissociation (SID) and serving as a detector for the first MS system, and a time-of-flight (TOF) MS system [39–43].

2. Experimental

2.1. Reagents

High-purity gases He (99.999%) and CO_2 (SFC grade) were obtained from Messer-Griesheim (Düsseldorf, Germany), water from a Milli-Q system (Millipore, Bedford, MA, USA). HPLC-grade methanol, acetonitrile, analytical-reagent grade ammonium acetate, and analytical-reagent grade perfluorotributylamine (PFTBA) were obtained from Merck (Darmstadt, Germany) and triazines and their hydroxy metabolites from Riedel-de Haen (Seelze, Germany).

2.2. Sample handling

Stock solutions of the triazine herbicides and their hydroxy metabolites were prepared by dissolving 25 mg of each compound in 50 ml methanol. From these solutions mixed standard solutions were prepared and diluted with methanol.

Standard samples were prepared by spiking Kieselgur (Merck) with a liquid standard solution followed by vigorous mixing. Spiked soil samples containing 500, 50, 5, 2 or 0.5 μg/g of each analyte were produced from a sandy humic soil in the same way.

The spiked soil samples were stored for two days at 4°C and kept at intermediate humidity in the dark.

Moreover, real soil samples selected from pesticide degradation studies of our laboratory

(Biological and Biotechnical Plant Protection) were employed, but these results will be published elsewhere [44].

2.3. Extraction

A Dionex (Sunnyvale, CA, USA) Model SFE 703 apparatus was used to perform SFE of standard and soil samples in 10-ml sample cartridges. Conditions of the dynamic extraction of triazines and polar hydroxy metabolites from soil were as follows: flow-rate of 1 ml/min with a modifier content of 10% methanol, extraction time of 15 min and extraction pressure of 50 MPa at 40°C. The collection vessels (stainless steel) were charged with 3.5 ml methanol and fitted with heat-exchange jackets which were adjusted to ca. 20°C via a circulating-water bath during collection.

2.4. Chromatography

The liquid chromatograph consisted of a Hewlett-Packard (Palo Alto, CA, USA) Model HP 1050 pump and a Rheodyne (Cotati, CA, USA) Model 7125 injector fitted with a 20-μl sample loop. The conditions for the chromatographic separation of triazines and polar hydroxy metabolites from co-extracted humic acids were set at a flow-rate of 0.30 ml/min with an isocratic 1 m*M* ammonium acetate–acetonitrile (50:50) mobile phase on a RP18 Supersphere 200 × 2.1 mm (4 μm particle size) separation column obtained from MZ Analysentechnik (Mainz, Germany).

The PB interface from Hewlett-Packard (Model 5998 A) was used to couple the electron impact (EI) source of the mass spectrometer to the liquid chromatograph. The PB interface desolvation chamber temperature was 40°C, the helium pressure of the nebulizer was 45 p.s.i. (1 p.s.i. = 6894.76 Pa), and the capillary position of the nebulizer was optimized daily.

2.5. Mass spectrometry

The experiments were performed both on a HP 5989 quadrupole mass spectrometer with a mass range of 1000 u and on a new tandem mass spectrometer.

The hybrid tandem mass spectrometer was constructed by the Second Physical Institute [39–43]. It consists of a double focusing sector field mass spectrometer (mass range 10000 u, mass resolution 10 000), a collision cell working with SID and a TOF-MS system with a mass range above 10 000 u and an energy-limited mass resolution of 1000 (Fig. 1).

Because of differences in construction, EI sources of both mass spectrometers have to be operated under different optimum conditions.

The source temperature of the quadrupole MS was 250°C, ionisation energy 70 eV and the mass range scanned was 90–240 u in the positive ion full scan mode.

The source temperature of the tandem MS was 100°C, ionisation energy 200 eV and the mass range scanned by the primary MS was 5–300 u in the positive ion full scan mode. In the tandem mode, the first stage MS is set to transmit a specific molecular ion (parent ions/primary beam). As a matter of operation, one complete daughter ion mass spectrum is recorded within every time of flight (μs). Therefore, for TOF-MS no scanning is needed.

The energy of the primary beam is 3 keV, the potential of the SID target surface is 1.4 keV. The incident angle of colliding ions is 2° and the potential gradient across the channel plate 1 kV. The potential of the drift tube of the TOF-MS

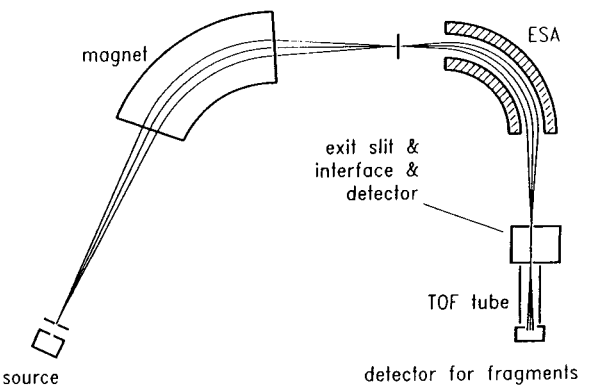

Fig. 1. Overall construction scheme of the tandem BE-MS–SID-TOF-MS.

system is 0 V, the detector potential −3 kV in order to improve the sensitivity of the channel plate. The mass scale of TOF-MS was calibrated by MS–MS measurement of the H_2O, N_2, O_2 and perfluorotributylamine signals.

3. Results and discussion

3.1. Extraction and chromatography

Recoveries of Soxhlet extractions from humic soil (2 h, methanol) were compared with recoveries of extraction from humic soil by SFE (15 min, CO_2 10% methanol).

The yields for atrazine and terbuthylazine were comparably high for both methods. Recoveries for the hydroxy metabolites on the other hand were significantly better with SFE than with Soxhlet extraction (Table 1). Moreover, SFE yields clearer extracts with up to 80% lower background of humic coextracts.

Chromatographic separations with UV detection of triazines and their metabolites require prolonged gradient programs [1]. The possibility of gaining additional structural information by a quadrupole MS or a MS–MS detector facilitates performing chromatography within a few minutes and with an isocratic program (see Fig. 3) because complete separation of every compound of the mixture is not absolutely necessary.

These simplifications both increase the lifetime of mesobore columns significantly and facilitate the optimization of PB operating conditions. The mesobore column thus may run on isocratic separation conditions. This results in a gain of sensitivity of the LC–PB-MS method when compared to a gradient program.

4. Mass spectrometry

(1) SFE extracts from soil and standard mixtures of triazines and their hydroxy metabolites were measured with LC–PB-MS in the SCAN mode. This strategy results in readily interpretable mass spectra of each component (Fig. 2). However, the sensitivity of this method in the SCAN mode is poor (5 mg/kg soil) for these compounds (Fig. 3).

Structural information of measurements with LC–PB-MS in the selected ion monitoring (SIM) mode is sometimes equivocal and is confined to target analysis, especially in the determination of structurally similar compounds like metabolites of one herbicide. The sensitivity of this method in the SIM mode is increased by a factor of 10 to ca. 0.5 mg/kg soil.

Table 1
Comparison of recoveries of SFE and Soxhlet extraction from spiked soil

Spiked (ppm, w/w)	Recovery (%)											
	SFE						Soxhlet extraction					
	T	A	OHT	OHA	OHDEA	OHDIA	T	A	OHT	OHA	OHDEA	OHDIA
0.5	91 ± 7	93 ± 9	83 ± 5	81 ± 11	80 ± 9	79 ± 17	95 ± 9	93 ± 10	53 ± 11	50 ± 7	57 ± 9	40 ± 9
2.0	95 ± 3	90 ± 5	78 ± 7	78 ± 4	70 ± 6	76 ± 2	94 ± 4	92 ± 7	50 ± 6	48 ± 10	50 ± 8	37 ± 13
5.0	88 ± 5	87 ± 4	73 ± 7	66 ± 3	81 ± 8	70 ± 8	90 ± 5	94 ± 3	48 ± 8	39 ± 7	43 ± 9	48 ± 7
Overall	91.7	90.0	78.0	75.0	77.0	75.0	93.0	93.0	50.3	45.6	50.3	41.7
Range	82–101	84–104	64–88	63–90	75–83	61–96	84–103	83–102	41–64	32–56	36–66	24–55

$n = 3$. SFE: 15 min, 1 ml/min, 10% methanol, 50 MPa. Soxhlet extraction: 2 h, 150 ml methanol. Spiked soil: sandy humic soil stored at 4°C for two days after spiking. T = Terbuthylazine; A = atrazine; OHT = hydroxyterbuthylazine; OHA = hydroxyatrazine; OHDEA = hydroxydeethylatrazine; OHDIA = hydroxydeisopropylatrazine = hydroxydeterbutylterbuthylazine.

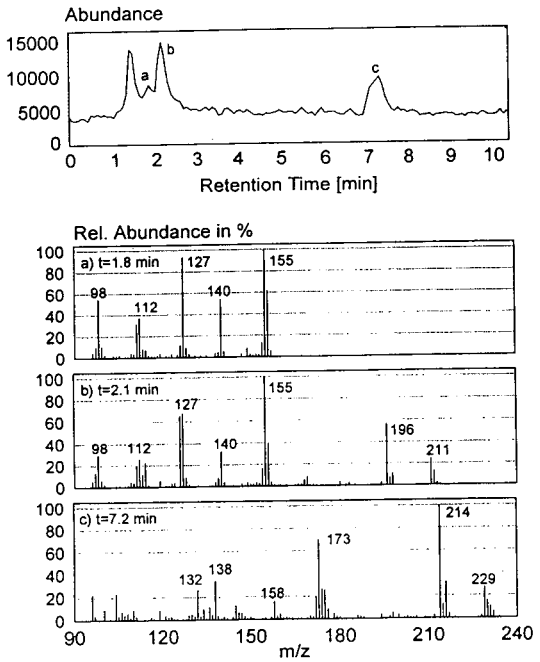

Fig. 2. (Top) Total ion chromatogram (SCAN mode) of a sample containing 20 mg/kg of (a) deterbutyl-2-hydroxyterbuthylazine (b) 2-hydroxyterbuthylazine and (c) terbuthylazine. (Bottom) Resulting mass spectra of the analysed components a–c.

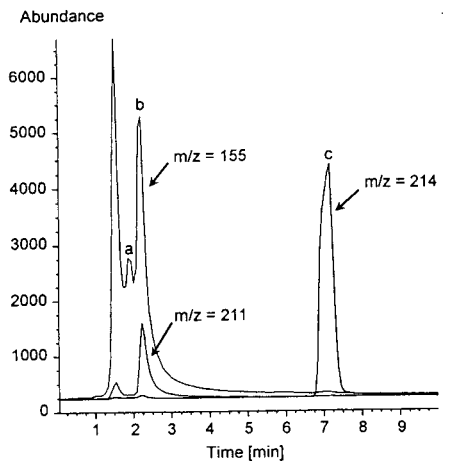

Fig. 3. Ion chromatogram (SIM mode) of a sample containing 20 mg/kg of (a) deterbutyl-2-hydroxyterbuthylazine (b) 2-hydroxyterbuthylazine and (c) terbuthylazine. Mass 155 corresponds to a or b, mass 211 to b and mass 214 to c.

The comparably high limits of detection can be explained by increasing losses of analytes with decreasing molecular mass, especially below 200 u, due to co-volatilisation with the solvent into the vacuum system during the desolvation step.

(2) Measurements with the DLI-MS–MS of triazines and their hydroxy metabolites result in reliable tandem mass spectra down to 0.2 mg/kg soil. The interpretation of the secondary mass spectra is difficult because of the low mass resolution of the second stage mass spectrometer ($M/\Delta M = 10$). In spite of this shortcoming the interpretation of these mass spectra is possible because of the similarity of their fragmentation pattern to those resulting from EI ionisation (Fig. 4). Therefore, characteristic masses appearing in EI mass spectra can be used for interpretation of SID-TOF mass spectra. This is an important advantage, because of already existing EI-MS libraries (for instance NIST, National Institute of Standards and Technology, Gaitherburg, MD, USA).

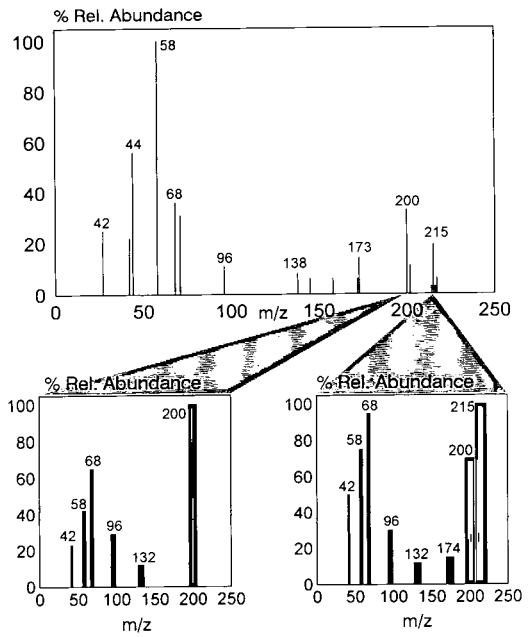

Fig. 4. Tandem mass spectra of atrazine. The primary mass spectrum is a typical EI fragmentation mass spectrum, the secondary mass spectra are SID-fragmentation mass spectra of the parents ions m/z 200 and 215. The widths of the mass bars in the secondary mass spectra correspond to the half widths of the mass peaks.

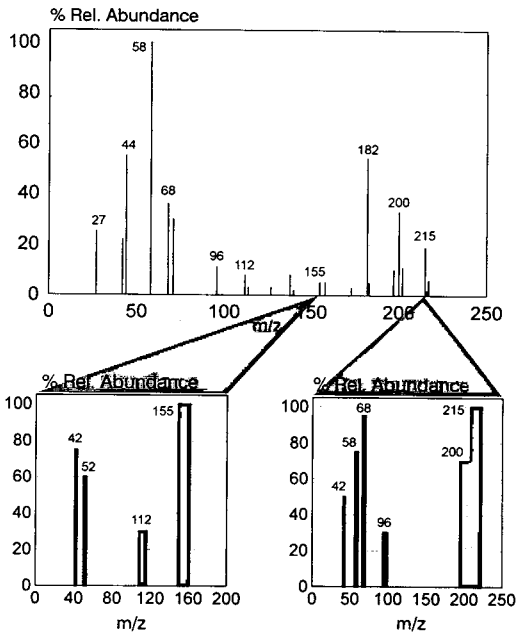

Fig. 5. Tandem mass spectra of a sample containing a surplus of atrazine and 20 ng deisopropyl-2-hydroxyatrazine. The secondary mass spectra are SID-fragmentation mass spectra of the molecular ions of atrazine (m/z 215) and its metabolite (m/z 155).

The identification of deisopropyl-2-hydroxyatrazine ($m/z = 155$) in the presence of high atrazine ($m/z = 215$) concentrations by means of the characteristic fragment with 112 amu in the secondary mass spectrum (Fig. 5) may serve as an example. The time required to get a statistically correct secondary mass spectrum of about 50 000–100 000 counts depends on the intensity of the selected parent ion in the primary spectrum. In the measurements presented this analysis time was shorter than 1 min.

Because of the so far unsatisfactory mass resolution, the main advantage of the MS–MS method, its sensitivity, is nearly leveled down, because more counts are necessary to fit a reliable mass bar into a broad peak. Moreover, useful secondary mass spectra are confined to low masses ($m/z = 20$–200) because of the difficulty of peak matching of higher masses. The theoretical mass resolution of TOF-MS is $M/\Delta M = 1000$. Therefore, understanding the process within the collision cell [45–50] is crucial for an improvement of the mass resolution of this hybrid MS–MS method. Further investigations will be discussed elsewhere.

The performances of two different methods of structure-elucidating trace analysis with MS detectors are compared (Table 2). Normally, an increase in structural information is accompanied by a decrease of sensitivity. The DLI-MS–MS method keeps the advantage of obtaining structural information in form of mass spectra similar to EI mass spectra down to a lower limit of detection (20 ng) and a significantly lower limit of quantification. Nevertheless, LC–PB-MS and DLI-MS–MS can be used complementarily because of their different preferred mass ranges (LC–PB-MS: $m/z = 200$–2000; DLI-MS–MS: $m/z = 20$–200). Other methods like LC–diode array detection (DAD) and LC–TSP-MS do not

Table 2
Comparison of LC–PB-MS and DLI-MS–MS

	LC–PB-MS (SIM)			LC–PB-MS (SCAN)			DLI-MS–MS		
	T	OHT	OHDIA	T	OHT	OHDIA	T	OHT	OHDIA
Limit of detection (ng)	50	50	100	400	400	1000	20	20	20
Limit of quantification (ng)	400	500	1200	1000	1200	2500	50	50	50
Linear range	10^3	10^3	10^3	10^2	10^2	10^2	10^2	10^2	10^2
Structural information	Target analysis			Yes, intermediate masses			Yes, low masses		

Abbreviations as in Table 1.

Table 3
Comparison of other methods for the analysis of hydroxytriazines OHT and OHA

	LC–DAD [52]	LC–TSP-MS (SCAN) [51]	DLI-MS–MS	LC–PB-MS (SIM)	LC–PB-MS (SCAN)
Limit of detection (ng)	0.2	1–2	20	50	400
Structural information	UV spectra	Molecular ion	SID mass spectra	Three selected ions	EI mass spectra

Abbreviations as in Table 1.

suffer from those limitations and are significantly more sensitive. However, the structural information obtained from those methods are poor (Table 3). Therefore, our MS–MS method appears useful as supporting tool for structural elucidation of hydroxytriazines in humic soil.

5. Conclusions

A method for structural elucidation and trace analysis with combined chromatographic (LC–MS) and mass spectrometric (MS–MS) techniques was developed to facilitate reliable determination of triazines and hydroxy metabolites in humic soil down to 0.5 mg/kg soil.

Using selective dynamic SFE yields remarkably clean extracts with good recoveries down to 0.5 mg/kg triazine and hydroxy metabolites in humic soil. This simplifies the chromatographic separation and introduction into the MS system by PB interface. Comparison of PB-quadrupole MS measurements (SCAN and SIM modes) with measurements of a hybrid MS–MS with DLI shows comparative sensitivities within 10-min runs. The advantages of the new MS–MS method, i.e. increased sensitivity and structural information, are nearly compensated due to the low mass resolution of 10 in the secondary MS system.

Comparing the performance of LC–PB-MS and the actual DLI-MS–MS method results in an advantage of the MS–MS method in analysing polar metabolites of low molecular masses and high polarities, i.e. those substances not easily analysed by LC–PB-MS with sufficient sensitivity. Moreover, the relative mass uncertainty is not as disturbing when examining low masses as opposed to high masses. In examining compounds of intermediate molecular masses, both methods can be used complementarily because of their different advantages and disadvantages. For instance, DLI-MS–MS was found to provide a rapid and comprehensive survey of metabolites present without HPLC losses, while LC–MS succeeded in resolving isobaric species present [53].

Both strategies are not really routine methods, MS–MS less than LC–MS. Most analysed real soil samples with herbicide residues result from application according to good agricultural practice. Therefore, an additional preconcentration step will be necessary for obtaining reliable quantitative results in most cases of metabolite analysis, where the metabolite concentration is smaller than the parent compound. Nevertheless, the described methods are successfully used to confirm LC–DAD results of soil analysis from field trials [44]. If it is possible to increase the mass resolution of the second stage MS to $M/\Delta M = 100$ to 1000, the hybrid MS–MS method will be at least 10- to 100-fold more sensitive while yielding secondary mass spectra for reliable structure elucidation.

Moreover, because of the construction of the hybrid MS–MS system with a TOF-mass spectrometer as secondary MS system, every emerging daughter ion is detected with highest sensitivity. No selection of special daughter ions is necessary in this experiment for achieving best sensitivity. In contrast, MS–MS experiments working with quadrupole or sector field MS as secondary MS have to select one daughter ion (single reaction mode) in order to achieve full sensitivity [54].

Acknowledgements

Preliminary tests on the SFE instrument of Dionex are gratefully acknowledged.

The authors wish to thank the State of Hessen, and the Federal Minister for Education, and Science in Bonn, Germany, for granting the quadrupole mass spectrometer. BMFT, Jülich, Germany, provided the PB interface and DFG, Bad Godesberg, Germany, parts of the hybrid tandem mass spectrometer.

References

[1] X. Qiao, R. Düring, H.E. Hummel, *GDCh Hauptversammlung 1991*, VCH, Weinheim, 1991, p. 222.
[2] H.-J. Stan and A. Bockhorn, *Fresenius' J. Anal. Chem.*, 339 (1991) 158–165.
[3] C.E. Rostad, W.E. Pereira and T.J. Leiker, *Biomed. Environ. Mass Spectrom.*, 18 (1989) 820–827.
[4] S.U. Khan and P.B. Marriage, *J. Agric. Food Chem.*, 25 (1977) 1408.
[5] N.M.J. Vermeulen, Z. Apostolides and D.J. Potgieter, *J. Chromatogr.*, 240 (1982) 247.
[6] P. Beilstein, A.M. Cook and R. Hütter, *J. Agric. Food Chem.*, 29 (1981) 1132–1135.
[7] R.B. Geerdink, F.A. Maris, G.J. de Jong, R.W. Frei and U.A.Th. Brinkman, *J. Chromatogr.*, 394 (1987) 51–64.
[8] D. Barcelo, G. Durand, R.J. Vreeken, G.J. de Jong, H. Lingeman and U.A.Th. Brinkman, *J. Chromatogr.*, 553 (1991) 311–328.
[9] D. Barcelo, *Org. Mass Spectrom.*, 24 (1989) 219–224.
[10] D. Barcelo, *Org. Mass Spectrom.*, 24 (1989) 898–902.
[11] R.D. Voyksner, W.H. McFadden and S.A. Lammert, in J.D. Rosen (Editor), *Applications of Mass Spectrometry Techniques in Pesticide Chemistry (Analytical Symposium Series)*, Wiley, New York, 1987, Ch. 17, p. 247.
[12] R.D. Voyksner, T. Pack, C. Smith, H. Swaisgood and D. Chen, in M.A. Brown (Editor), *Liquid Chromatography/Mass Spectrometry —Applications in Agricultural, Pharmaceutical and Environmental Chemistry (ACS Symposium Series*, No. 420), American Chemical Society, Washington, DC, 1990, pp.14–39.
[13] R.D. Voyksner and C.A. Haney, *Anal. Chem.*, 57 (1985) 991–996.
[14] D. Barcelo, in M.A. Brown (Editor), *Liquid Chromatography/Mass Spectrometry —Applications in Agricultural, Pharmaceutical and Environmental Chemistry (ACS Symposium Series*, No. 420), American Chemical Society, Washington, DC, 1990, pp. 48–61.
[15] R.D. Voyksner, J.T. Bursey and E.D. Pellizari, *Anal. Chem.*, 56 (1984) 1507–1514.
[16] M.A. Brown, R.D. Stephens and I.S. Kim, *Trends Anal. Chem.*, 10 (1991) 330–336.
[17] I.S. Kim, F.I. Sasinos, R.D. Stephens, J. Wang and M.A. Brown, *Anal. Chem.*, 63 (1991) 819–823.
[18] S. Bajic, D.R. Doerge, S. Lowes and S. Preece, *Rapid Commun. Mass Spectrom.*, 6 (1992) 663–666.
[19] F.W. Mc Lafferty, in J.F.J. Todd (Editor), *Advances in Mass Spectrometry*, Wiley, New York, 1986, p. 493.
[20] R.B. Geerdink, P.G.M. Kienhuis and U.A.Th. Brinkman, *J. Chromatogr.*, 647 (1993) 329–339.
[21] T. Cairns and E.G. Siegmund, in M.A. Brown (Editor), *Liquid Chromatography/Mass Spectrometry —Applications in Agricultural, Pharmaceutical and Environmental Chemistry (ACS Symposium Series*, No. 420), American Chemical Society, Washington, DC, 1990, pp. 40–47.
[22] K.S. Chin, A. von Langenhove and C. Tanaka, *Biomed. Environ. Mass Spectrom.*, 18 (1989) 200–206.
[23] L.D. Betowski and T.L. Jones, *Environ. Sci. Technol.*, 22 (1988) 1430–1434.
[24] H.F. Schröder, *J. Chromatogr.*, 554 (1991) 251–266.
[25] T.L. Jones, L.D. Betowski and J. Yinon, in M.A. Brown (Editor), *Liquid Chromatography/Mass Spectrometry —Applications in Agricultural, Pharmaceutical and Environmental Chemistry (ACS Symposium Series*, No. 420), American Chemical Society, Washington, DC, 1990, pp. 62–74.
[26] S.V. Hummel and R.A. Yost, *Org. Mass Spectrom.*, 21 (1986) 785–791.
[27] H.F. Schröder, *Water Sci. Technol.*, 23 (1991) 339–347.
[28] H.F. Schröder, *Wasser*, 73 (1989) 111–136.
[29] D.F. Hunt, *Anal. Chem.*, 57 (1985) 525–537.
[30] L.D. Betowski, S.M. Pyle, J.M. Ballard and G.M. Shaul, *Biomed. Environ. Mass Spectrom.*, 14 (1987) 343–354.
[31] M.L. Lee and K.E. Markides (Editors), *Analytical Supercritical Fluid Chromatography and Extraction*, VCH, Weinheim, 1991.
[32] B.E. Richter, in T. Cairns and J. Sherma (Editors), *Emerging Strategies for Pesticide Analysis*, CRC Press, Boca Raton, FL, 1992, pp. 51–68.
[33] V. Jandra, G. Steenbeke and P. Sandra, *J. Chromatogr.*, 479 (1989) 200.
[34] *DFG Manual of Pesticide Residue Analysis*, Vol. 1, VCH, Weinheim, 1987.
[35] R.L. Firor, *Application Note 228-112*, Hewlett-Packard, Avondale, PA, 1990.
[36] R.M. Campbell and M.L. Lee, *Anal. Chem.*, 58 (1986) 2247.
[37] S. Schütz, A. Duhr, H.E. Hummel and H. Wollnik, *Verh. Fac. Landbouwwet. Gent*, 58 (1993) 153–164.
[38] R. Reupert and E. Plöger, *Vom Wasser*, 72 (1989) 211–233.
[39] K.L. Schey, R.G. Cooks, R. Grix and H. Wollnik, *Int. J. Mass Spectrom. Ion Proc.*, 123 (1987) 49–61.
[40] G. Li, A. Duhr and H. Wollnik, *J. Am. Soc. Mass Spectrom.*, 3 (1992) 487–482.

[41] G. Li, A. Duhr and H. Wollnik, presented at the *40th ASMS Conference on Mass Spectrometry and Allied Topics, Washington, DC, May 31–June 5, 1992*, abstracts, p. 1438.
[42] A. Duhr, S. Schütz, R. Guckert, H. Wollnik and H.E. Hummel, *Verhandl. DPG (IV)*, 28 (1993) 317.
[43] P. Stracke, A. Duhr and H. Wollnik, *Verhandl. DPG (VI)*, 28 (1993) 523.
[44] R. Düring and H.E. Hummel, in preparation.
[45] R.G. Cooks, T. Ast and Md.A. Mabud, *Int. J. Mass Spectrom. Ion Proc.*, 100 (1990) 209–265.
[46] M.E. Bier, J.C. Schwartz, K.L. Schey and R.G. Cooks, *Int. J. Mass Spectrom. Ion Proc.*, 103 (1990) 1–19.
[47] M.E. Bier, J.W. Amy, R.G Cooks, J.E.P. Syka, P. Ceja and G. Stafford, *Int. J. Mass Spectrom. Ion Proc.*, 77 (1987) 31–47.
[48] E.R. Williams, L. Fang and R.N. Zare, *Int. J. Mass Spectrom. Ion Proc.*, 123 (1993) 233–241.
[49] K.L. Schey, R.G. Cooks, A. Kraft, R. Grix and H. Wollnik, *Int. J. Mass Spectrom. Ion Proc.*, 94 (1989) 1–14.
[50] V.H. Wysocki, J.-M. Ding, J.L. Jones, J.H. Callahan and F.L. King, *J. Am. Soc. Mass Spectrom.*, 3 (1992) 27–32.
[51] G. Durand and D. Barcelo, *J. Chromatogr.*, 502 (1990) 275–286.
[52] R. Schuster, *HPLC Application 87-13*, Hewlett-Packard, Palo Alto, CA, 1987.
[53] Th.A. Baillie, *Int. J. Mass Spectrom. Ion Proc.*, 118/119 (1992) 289–314.
[54] K.L. Busch, G.L. Glish and S.A. Mc Luckey (Editors), *Mass Spectrometry/Mass Spectrometry —Techniques and Applications of Tandem Mass Spectrometry*, VCH, New York, 1988.

ELSEVIER

Journal of Chromatography A, 683 (1994) 151–155

JOURNAL OF CHROMATOGRAPHY A

On-line liquid chromatography–gas chromatography for determination of fenarimol in fruiting vegetables

Rian Rietveld, Jan Quirijns*

TNO Nutrition and Food Research, P.O. Box 360, 3700 AJ Zeist, Netherlands

Abstract

The fungicide fenarimol was determined in fruiting vegetables such as cucumbers, tomatoes and sweet peppers by an on-line LC–GC method. The sample was extracted with ethyl acetate and the extract cleaned by a LiChrosorb Si 50 HPLC column. Pre-treatment of the silica column with ethyl acetate, saturated with water, provided separation between fenarimol and matrix components and gave a reproducible retention behaviour of fenarimol. Introduction into the gas chromatograph was achieved via the loop-type interface technique. After effluent splitting, fenarimol was detected with flame ionisation detection (FID) and electron-capture detection (ECD). The linearity range of fenarimol was 0.02–0.45 mg/kg with FID. Owing to insufficient linearity ECD was used only for confirmation. The detection limit was 0.02 mg/kg, the average recovery 93% (76–110%) and the relative standard deviation 4%. The results of the LC–GC method were comparable with the present off-line method, but less toxic solvent was needed and the on-line LC–GC method was less time-intensive.

1. Introduction

Fenarimol (2,4′-dichloro-α-(pyrimidin-5-yl)-diphenylmethanol, Fig. 1) is the active ingredient of pesticide formulations such as Rubigan and Rimidin, and is used as a systemic fungicide, on fruit, vegetables and fruiting vegetables such as cucumbers, tomatoes and sweet peppers. Fenarimol decomposes rapidly in sunlight and is readily soluble in ethyl acetate.

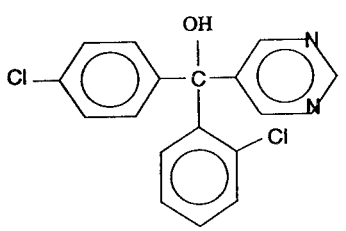

Fig. 1. Structure of fenarimol.

Several methods have been published to determine fenarimol in vegetables. Day and Decker [1] extracted it from fruit or vegetables with methanol, purified the extract by liquid–liquid partitioning with dichloromethane and an alumina column clean-up, and analysed fenarimol by gas chromatography–electron-capture detection (GC–ECD). Nejitscheva et al. [2] applied extraction with acetonitrile, filtration, liquid–liquid partitioning with chloroform, a Florisil clean-up and analysis by GC–ECD.

In our laboratory fenarimol is analysed with an off-line high-performance liquid chromatograph-

* Corresponding author.

0021-9673/94/$07.00
SSDI 0021-9673(94)00359-H

ic (HPLC) method [3]. The sample is extracted with dichloromethane–*n*-hexane, centrifuged, concentrated and cleaned on a SEP-PAK silica column. After solvent changing to methanol fenarimol is analysed via reversed-phase HPLC with ultra-violet (UV) detection. Results of this off-line method for fenarimol are: detection limit 0.02 mg/kg, average recovery 93% (82–105%), and linearity range 0.02–1.6 mg/kg.

This study describes the development of an on-line LC–GC method for the same analysis with a commercially available instrument, and is the first result of our study on the applicability of this technique in residue analysis. We expected to save time and solvent using the on-line method.

2. Experimental

2.1. Materials

Ethyl acetate (resi-analyzed) was obtained from J.T. Baker (Phillipsburg, NJ, USA) and sodium sulphate p.a. from Merck (Darmstadt, Germany). *n*-Hexane and fenarimol (C134300) were from Promochem (Wesel, Germany). Water was tap water. Standard solutions for calibration and linearity determinations were made in ethyl acetate–3% water. The eluent for HPLC was ethyl acetate–*n*-hexane–water (50:50:0.1, v/v/v).

2.2. Instrumentation

Experiments were carried out with an automated LC–GC instrument Dualchrom 3000 (Fisons, Milan, Italy), equipped with a LC-autosampler, a LC-column heater, a UV detector, two syringe pumps, as well as a 6-port and a 10-port valve (with a backflush loop) for LC. The 12.5 cm × 4.6 mm I.D. LC column was packed with LiChrosorb Si 50, 5 μm. The loop-type interface was equipped with a 500 μl loop.

The GC configuration comprised a diphenyltetramethyldisilazane-deactivated 3 m × 0.53 mm I.D. retention gap, (Interscience, Breda, Netherlands), a 3-m section of the analytical column serving as a retaining pre-column, a solvent vapour exit and a CP-Sil 5 CB analytical column, 22 m × 0.25 mm I.D., 0.4 μm film thickness (Chrompack, Middelburg, Netherlands). The effluent of the analytical column was split to a flame ionization detector (FID) and an ECD. Connections in the GC and T-pieces were of press-fit type (Interscience).

2.3. Sample preparation

A sample was homogenized in a food cutter and 50 g of subsample was blended in a beaker for 1 min with 100 ml of ethyl acetate in the presence of 25 g of sodium sulphate. The beaker with the extract was left for 5 min to clear. A portion of the organic layer was decanted in a glass-stoppered tube which could be stored in a refrigerator and 20 μl of this extract was injected onto the LC column.

2.4. Pre-treatment of the LC column

The silica gel column was pretreated with ethyl acetate–3% water at a flow-rate of 500 μl/min for two h. Then the column was stabilized with ethyl acetate–*n*-hexane–water 50:50:0.1 until the UV signal at 270 nm was stable.

2.5. LC method

The water content in the calibration solution was adjusted to that of the sample extract by addition of 3% water. 20 μl of the sample extract was injected and eluted at a flow-rate of 500 μl/min. After starting the transfer to GC, the LC column was backflushed with 1 ml ethyl of acetate–3% water, at a flow-rate of 500 μl/min, and reconditioned with mobile phase up to the next injection. The LC column heater was kept well above room temperature (35°C).

2.6. LC–GC transfer and GC method

The transfer of the LC fraction into the GC was carried out with a loop-type interface using concurrent eluent evaporation [4]. 12 min after HPLC injection, a 500-μl LC fraction was trans-

ferred into the GC at an oven temperature of 130°C.

Helium was used as the carrier gas with a constant flow-rate of 2 ml/min, measured at 25°C. During transfer the interface pressure increased to 200 kPa. The solvent vapour exit was closed 4 min after solvent evaporation had ended, the oven heated at a rate of 8°C/min to 300°C, and kept there for 5 min.

3. Results and discussion

3.1. Extraction

Ethyl acetate is a popular extraction solvent in analysis methods for residues of pesticides in all kinds of samples, such as food, fruit, vegetables, water and soil. It is moderately polar and yields good recoveries even for more polar compounds [5].

Anhydrous sodium sulphate was added during extraction to reduce the amount of free water, to realize a certain desalting effect, and to achieve disintegration of the matrix. Except if an excess of sodium sulphate is added, the extracts are saturated with water.

In order to restrict the number of additional treatments, we used the untreated extracts.

3.2. Development of the HPLC clean-up

Clean-up is necessary to separate fenarimol from interfering components and/or matrix material deteriorating the column inlet. Because of its polar structure, fenarimol may produce tailing and distorted peaks when eluted from the silica gel column [6]. Kunugi and Tabei [7,8] described a method to deactivate the silica gel with a water layer. We deactivated it with ethyl acetate–3% water before conditioning with ethyl acetate–*n*-hexane–water (50:50:0.1) until the UV signal was stable.

After each run, the column was backflushed with ethyl acetate–3% water, in order to keep the water layer on the silica intact. As shown in Fig. 2 this treatment improved the peak shape, retention characteristics were stabilized and

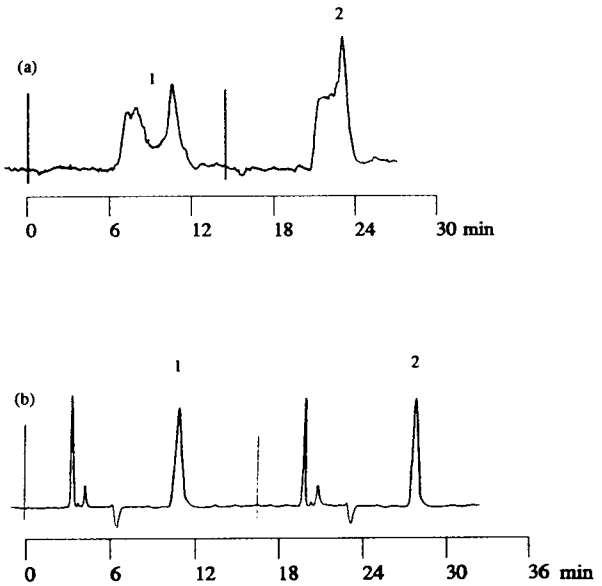

Fig. 2. HPLC chromatograms of fenarimol standard solutions before (a) and after (b) water treatment. Peak 1 is a standard solution in ethyl acetate, peak 2 is a standard solution in ethyl acetate–3% water. Eluent is *n*-hexane–ethyl acetate–water, 75:25:0 in a, 50:50:0.1 in b

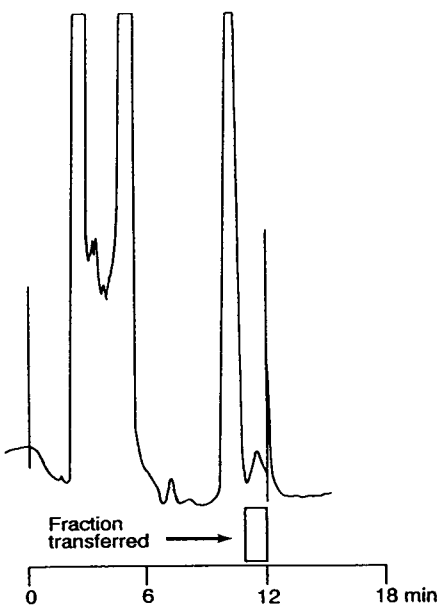

Fig. 3. HPLC chromatogram of a sample extract of sweet red peppers measured at a wavelength of 270 nm. The spike at 12 min shows the pulse caused by switching the valve to backflush.

Table 1
Sensitivity and linear range of fenarimol on three GC detectors

Detector	NPD	FID	ECD
Sensitivity in pg (S/N = 3)	250	50	10
Linear range [a] in mg/kg sample	0.1–1.5	0.02–0.45	0.019–0.11

[a] Based on a calibration solution of 0.0193 ng/μl fenarimol and 20 μl injections on the HPLC

separation between fenarimol and the matrix components improved. Peak shape was also improved by the presence of water in the extract, so we added water to the standard solution to obtain the same water influence in both solutions, instead of drying the extract, in order to restrict the number of treatments.

To avoid shifting of retention times by temperature fluctuations in the lab the LC column was kept at 35°C. Fig. 3 shows a representative HPLC chromatogram.

3.3. Development of the GC method

Fenarimol is eluted at a column temperature of around 260°C, which enables transfer by the loop-type interface. A major concern was damage of the retention gap by injecting water-containing LC-fractions. No deterioration of the retention gap or of the analytical column was observed however, after more than 50 injections of standards or extracts.

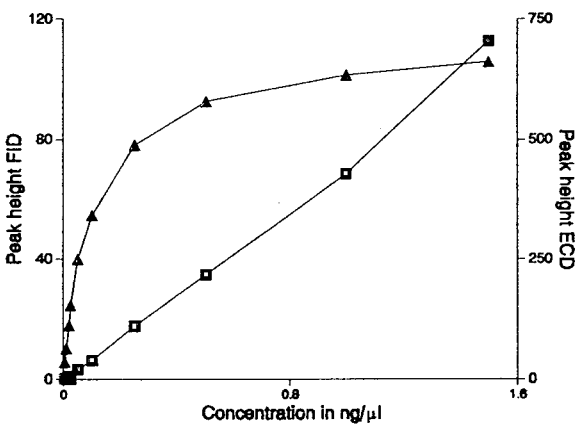

Fig. 4. Response curves of fenarimol ($n = 3$). □ = FID, ▲ = ECD.

Three detectors were tested for this method, i.e. a nitrogen–phosphorus detector (NPD), an FID and an ECD. The calibration curves were determined by injecting 10 different standard solutions in triplicate over a concentration range of 0.0052–1.54 ng/μl (the range in which the residues are found). Fig. 4 shows the response curves of the peak height of two detectors.

In spite of its broad linearity range the NPD was not suitable, because the detection limit must at least be 0.02 mg/kg, which is the content related to the "zero" tolerance. This might be solved by injecting more extract. FID was chosen because of its sufficient detection limit and good linearity. ECD was much more sensitive then NPD and FID but had a much smaller linearity range (Table 1). Therefore, ECD was used for qualitative confirmation of the fenarimol, and FID for quantitative determination.

3.4. Reproducibility

Table 2 shows the reproducibility of the instrument obtained by injecting series of a standard solution and three types of spiked samples. To

Table 2
Reproducibility (R.S.D.) of the peak heights of fenarimol for FID and ECD for various matrices ($n = 11$)

Matrix	FID	ECD
Ethyl acetate–3% water	3.5	3.9
Red sweet pepper	5.2	3.4
Tomato	5.1	3.9
Cucumber	3.2	3.3
Average	4.3	3.6

Table 3
Mean recoveries and R.S.D.s of fenarimol in fruiting vegetables ($n = 2$)

Fortification level	0.019 mg/kg		0.039 mg/kg		0.19 mg/kg	
Dectector	FID	ECD	FID	ECD	FID	ECD[a]
Red sweet pepper	89	103	89	93	92	60
Tomato	90	104	110	111	103	67
Cucumber	76	96	95	99	96	62
Average	85	101	98	101	97	63
RSD	11	6	12	10	7	7

[a] Beyond the linear range

1480 μl of ethyl acetate–3% water or extract, 20 μl of 3.86 ng/μl fenarimol in *n*-hexane was added in an autosampler vial; this corresponds to 0.1 mg/kg fenarimol in a sample. R.S.D. values of 3–5% are good, especially if it is taken into account that the reported figures also include variation upon preparing the solutions in the vials.

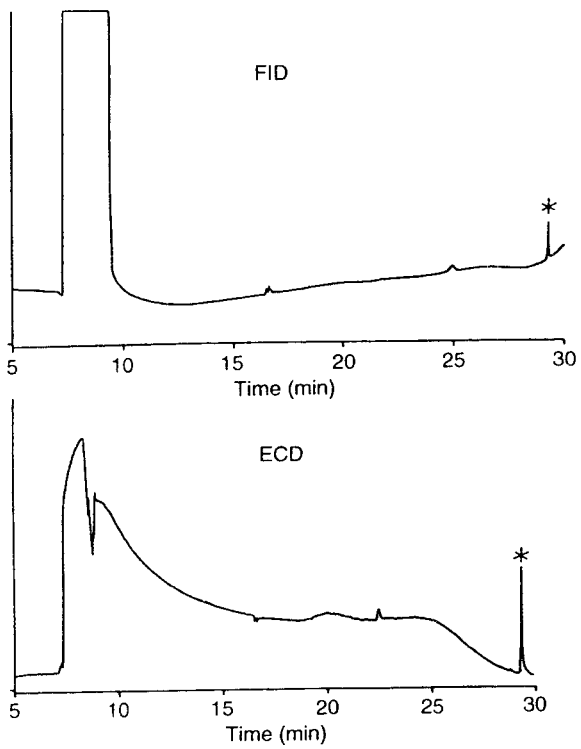

Fig. 5. Gas chromatograms of a sample extract of red sweet pepper, spiked with 0.1 mg/kg fenarimol (* = fenarimol).

Table 3 shows the recoveries carried out in duplicate by adding known amounts of fenarimol to freshly cut and homogenized samples of red sweet peppers, tomatoes and cucumbers. The recoveries were calculated against a calibration solution containing 0.0193 ng/μl fenarimol in ethyl acetate–3% water. FID and ECD chromatograms of an extract from spiked red sweet pepper are shown in Fig. 5.

Acknowledgements

René Vreuls of the Free University of Amsterdam and Pieter Jongenelen and René Leenderts of Interscience Breda are acknowledged for valuable discussions and technical assistance.

References

[1] E.W. Day and O.D. Decker, *Anal. Methods Pestic. Plant Growth Regul.*, 13 (1984) 173.
[2] A. Nejitscheva, P. Wassileva-Alexandrova and G. Marudov, *J. Chromatogr.*, 298 (1984) 508.
[3] J. Vuik, *3rd Workshop on Chemistry and Fate of Modern Pesticides*, RIVM, Bilthoven 1991, p 18.
[4] K. Grob, *On-line coupled LC–GC*, Hüthig Buch Verlag, Heidelberg, 1991.
[5] A. Andersson and H. Pålsheden, *Fresenius' J. Anal. Chem.*, 339 (1991) 365.
[6] T. Ohkuma and S. Hara, *J. Chromatogr.*, 400 (1987) 47.
[7] A. Kunugi and K.Tabei, *J. High Resolut. Chromatogr.*, 12 (1989) 59.
[8] A. Kunugi and K.Tabei, *J. High Resolut. Chromatogr.*, 12 (1989) 557.

ELSEVIER

Journal of Chromatography A, 683 (1994) 157–165

JOURNAL OF CHROMATOGRAPHY A

Determination of ethylenethiourea in water by single-step extractive derivatization and gas chromatography–negative ion chemical ionization mass spectrometry

H.D. Meiring*, A.P.J.M. de Jong

Laboratory of Organic Analytical Chemistry, National Institute of Public Health and Environmental Protection, P.O. Box 1, NL-3720 BA Bilthoven, Netherlands

Abstract

A method for the determination of ethylenethiourea (ETU) in water samples is described that involves a single-step derivatization and extraction by means of phase transfer-catalysed reaction with 3,5-bis(trifluoromethyl)benzyl bromide followed by gas chromatography–electron-capture negative ion mass spectrometric separation and detection. The reaction resulted in three ETU derivatives, identified by GC–Fourier transform spectrometry as the mono-N-substituted form and two forms substituted at the N,N′- and the N,S-positions. Quantification in the multiple-ion detection mode was performed on the abundant $[M-227]^-$ ions of the N,N′-isomer in low-level (<5 μg/l) and at the N,S-isomer in high-level samples (>5 μg/l). The limit of determination in surface water samples was 0.05 μg/l with recoveries ranging between 60 and 110%. The method was applied for confirmation purposes for the presence of ETU as analysed by HPLC with UV detection. In general, a good correlation was found between the results from both methods.

1. Introduction

Ethylenethiourea (2-imidazolidinethione; ETU) is a formulation contaminant and an environmental metabolite of ethylenebis(dithiocarbamate) fungicides (EBDCs). This group forms the most important class for controlling fungal diseases on fruits, vegetables and other agricultural crops. ETU as such is widely used as an accelerator in the production of synthetic rubber [1].

The presence of ETU in the environment or in biological tissues is of major concern, because of its known pathological effects [2]. In terms of its putative carcinogenicity, ETU was classified by the method of the International Agency for Research on Cancer (IARC) into group 2B, i.e., the compound is possibly carcinogenic to humans; sufficient animal but limited or insufficient evidence of carcinogenicity in humans is available [3,4]. Hence, reliable and rapid methods, for screening purposes, are required for the trace determination of residual ETU. In addition, the method should be sensitive, in order to meet the present norms for surface and drinking water as set by the US Environmental Protection Agency (EPA) and individual governments.

The determination of ETU is commonly performed by GC after derivatization. Onley and Yip [5] and Pease and Holt [6] described an

* Corresponding author.

0021-9673/94/$07.00
SSDI 0021-9673(94)00490-Z

extraction and subsequent alkylation method with bromobutane. The use of other types of derivatization reagents was described by Newsome [7], e.g., S-alkylation with benzyl chloride and subsequent N-acylation with trifluoroacetic anhydride; Nash [8,9] applied pentafluorobenzoylation of the S-alkylated ETU derivative and King [10], S-alkylation of ETU with *m*-trifluoromethylbenzyl chloride. All these procedures involve a multi-step derivatization/isolation method, using elevated temperatures, as a result of which decomposition of the EBDC residues present may occur. A fast, single-step extractive N-acylation of ETU with dichloroacetic anhydride was described by Singh et al. [11]. Although this derivative may dissociate in the hot GC injector, yields of about 80% were reported with detection limits in water samples down to 0.01 μg/l. GC determination of ETU after derivatization as S-butyl-ETU, S-benzyl-ETU and trifluoroacetylated ETU was optimized by Matisová et al. [12] by using capillary columns without any precleaning [12].

Although GC is still the major technique for the determination of ETU, liquid chromatographic (LC) methods are becoming more frequently used, employing UV or electrochemical detection [13,14]. Hogendoorn et al. [15] described an LC technique with column switching by means of which clean-up and concentration of ETU are performed on-line, facilitating trace level analysis in less than 10 min per sample. Combined with preconcentration of samples, a detection limit of 0.1 μg/l is achievable. LC coupled on-line with mass spectrometric (MS) detection was described by Doerge and co-workers [16,17] and Kurttio et al. [18], using particle beam and thermospray.

In our laboratory, the method described by Hogendoorn et al. [15] was used for the analysis of large series of water samples. Confirmation of the presence of ETU was conducted by LC–diode-array UV detection (DAD). For trace levels <1 μg/l, however, this technique is not sensitive enough. In view of the good results recently obtained for another group of polar pesticides (chlorophenoxy herbicides [19]), we decided to investigate the utility of a single-step extractive derivatization of ETU with a perfluorinated reagent, followed by GC–MS using the electron-capture negative ion chemical ionization (ECNICI) mode. It has been shown that the principle of extractive derivatization with a selected group of perfluorinated reagents is a fast and reliable approach for the sensitive determination of polar compounds. A wide variety of fluorinated reagents are now available that can be used in aqueous media. The advantages of the use of these types of reagents are their moderate stability towards hydrolysis in aqueous systems, improved extraction yields and the formation of stable, volatile derivatives with high electron affinities. Hence, sensitive detection systems such as GC–ECD and the more selective GC–ECNICI-MS can be applied for measurements at low levels.

This paper describes a method that was developed for the trace determination of ETU in ground and surface waters at levels down to 0.05 μg/l. Because of the large series of samples to be analysed, the procedure should be fast and simple with a minimum of sample handling. Several optimization experiments were carried our concerning both extraction and derivatization conditions, and for the selection of the derivatization reagent and the GC–MS conditions. In addition, structure elucidation was performed on the derivatives formed by GC coupled on-line with Fourier transform infrared spectrometry (GC–FT-IR). Finally, method validation was accomplished by comparison with results from the LC–UV method [15].

2. Experimental

2.1. Chemicals and reagents

Ethylenethiourea (ETU), analytical-reagent grade, was obtained from Dr. S. Ehrenstorfer (Amsterdam, Netherlands). [$^2H_7$] Bentazone (bentazone-d_7, 95 atom% deuterium) was synthesized from methyl anthranilate and isopropylsufamoyl-d_7 chloride, as described by Jacquemijns et al. [20]. Diazomethane was syn-

thesized as a saturated solution in cold diethylether, by reaction of a basic aqueous solution with N-methyl-N-nitroso-*p*-toluenesulfonamide [21]. After preparation the solution was stored at −20°C in capped tubes. Tetrahexylammoniumhydrogen sulphate ($THAHSO_4$) was obtained from Fluka (Buchs, Switzerland), pentafluorobenzyl bromide (PFB-Br) from Pierce (Rockford, IL, USA), 3,5-bis(trifluoromethyl)benzyl bromide (3,5-BTFMB-Br) from Aldrich (Bornem, Belgium), sodium hydroxide (NaOH), potassium carbonate (K_2CO_3) and dichloromethane from Merck (Darmstadt, Germany) and acetonitrile from Rathburn Chemicals (Walkerburn, UK). Demineralized water was passed through a Milli-Q reagent water system (Millipore), before use. All chemicals and reagents were used as received.

A 10 m*M* solution of $THAHSO_4$ in dichloromethane was prepared freshly each week. A 10 *M* aqueous solution of NaOH was prepared and cooled to room temperature just before use. Standard solutions of ETU and bentazone-d_7 were prepared in water at concentrations of 18 and 100 μg/l, respectively, and stored at 4°C. For the non-aqueous derivatization of ETU, a solution of 1 g/l of ETU in acetonitrile was used.

2.2. Derivatization

Methylation

To 10 μl of a standard solution of ETU in acetonitrile (1 g/l) were added 500 μl of a saturated solution of diazomethane in diethyl ether. After incubation for 5 min at room temperature, 2 μl of the solution were subjected to GC–MS with electron impact and positive ion chemical ionization.

Non-aqueous alkylation

To 10 μl of a standard solution of ETU in acetonitrile (1 g/l) were added 1 ml of acetonitrile, 50 mg of K_2CO_3 and 10 μl of the derivatization reagent (PFB-Br or 3,5-BTFMB-Br). The mixture was heated for 2 h at 90°C with occasional stirring. After cooled to room temperature, 1 μl of the solution was injected into the GC–MS system.

Phase transfer-catalysed (PTC) derivatization

To 9 ml of ground water sample (with or without sediment residues) were added 50 μl of bentazone-d_7 (100 ng/ml) and 1 ml of 10 *M* NaOH solution with continuously stirring. The mixture was centrifuged at 2500 *g* for 10 min. The clear supernatant was transferred into a clean tube with a PTFE-lined screw-cap. To the mixture were added 3 ml of $THAHSO_4$ in dichloromethane (10 m*M*) and 20 μl of 3,5-BTFMB-Br. The mixture was shaken vigorously for 30 min in a horizontal position at a rate of ca. 250 strokes/min. After phase separation, 1 μl of the clear organic layer was subjected to GC–MS analysis.

2.3. Gas chromatography–mass spectrometry

All GC–MS analyses were performed on a Hewlett-Packard HP5890 gas chromatograph directly coupled to a Finnigan MAT SSQ710 system, with a Digital 5000/25 workstation and ICIS application software. Sample separation was performed on a DB-1701 capillary column (30 m × 0.25 mm I.D., 0.15 μm film thickness) (J&W Scientific, Folsom, CA, USA). The column temperature was programmed from 50°C (held for 1 min) to 200°C at 20°C/min, followed by a second increase to 275°C at 10°C/min, and maintained isothermal at 275°C for 5 min. Samples were injected in the splitless mode (45 s sampling time) at an injector temperature of 180°C. The transfer-line temperature was maintained at 275°C. Helium was used as the carrier gas at a column head pressure of 100 kPa.

The mass spectrometer was operated in the negative ion chemical ionization (NICI) mode. Methane was used as the reagent gas at an optimized source pressure (i.e. 93 Pa CH_4, as estimated from the intensity ratio for the reagent ions $C_2H_3^+$ and $C_2H_4^{+\cdot}$ according to Drabner et al. [22]). For structure elucidation, full-scan spectra were acquired from 50 to 600 u at a rate of 1 scan/s. Quantification was performed using

Table 1
m/z values used for MID quantification of the PFB- and 3,5-BTFMB-Br ETU derivatives under ECNICI conditions

Derivative	Monosubstituted main fragment ion (m/z)	Disubstituted main fragment ion (m/z)
PFB form	101	281
3,5-BTFMB form	101	327

ECNICI with multiple-ion detection (MID) at m/z values as shown in Table 1.

2.4. Gas chromatography–Fourier transform infrared spectrometry

GC–FT-IR was used for identification of the isomeric ETU derivatives. Separations were carried out on a Carlo Erba MEGA 5160 gas chromatograph with a split–splitless injector. The gas chromatograph was equipped with a DB-17 capillary column (J&W Scientific) (15 m × 0.25 mm I.D., 0.15 μm film thickness). The injection volume was 1 μl. Helium was used as the carrier gas. The column temperature was programmed from 50°C (held for 2 min) at 10°C/min to 150°C and then at 20°C/min to 290°C, and maintained isothermal at 290°C for 5 min. The column was connected to a fused-silica transfer line of 150 μm I.D. The transfer line was guided into the FT-IR spectrometer by means of a stainless-steel tube, heated at 250°C. The spectrometer was a Digilab FTS-40 Fourier transform instrument equipped with a Digilab Tracer cryotrapping GC interface and an SPC 3200 computer for data processing. Chromatograms were processed as the Gram–Schmidt plot and as six functional group chromatograms of preselected wavenumber intervals. Spectra were recorded on-the-fly at a rate of 2 scans/s (4 scans co-added). All spectra were recorded at an optical resolution of 8 cm^{-1}.

3. Results and discussion

Preliminary experiments including methylation with diazomethane and anhydrous alkylation with PFB-Br or 3,5-BTFMB-Br were carried out to examine the ability of ETU to react in the aqueous sample with the fluorinated reagents. For this reaction, the analyte should be slightly acidic so that it can form a sufficiently stable ion pair with the catalyst for transport to the organic layer, where it can react with the reagent. For ETU, one might expect slightly acidic properties owing to its keto–thiol tautomerism [23] (Fig. 1).

Methylation of ETU with diazomethane yielded three products that were identified by their EI and PCI mass spectra as a monosubstituted form ($M_r = 116$) and two disubstituted derivatives ($M_r = 130$). Although the isomeric structure of the mono substituted ETU is not well known (N- or S-substitution), the formation of multiple derivatives was indicative of the occurrence of keto–thiol tautomerism of ETU.

Non-aqueous derivatization of ETU with 3,5-BTFMB-Br yielded the corresponding products as with methylation. GC–FTIR analysis of the mixture revealed that the C = S bond was still present in the monosubstituted derivative, indicating a reaction at the NH function. In addition, the N,N′- and N,S-substituted derivatives were also identified by GC–FTIR, the N,N′-isomer eluting earlier than the N,S-isomer (Fig. 2). NCI mass spectra of these ETU derivatives are dominated by an abundant $[M - 227]^-$ fragment ion (i.e., loss of one substituted group) at

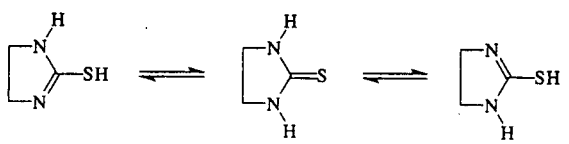

Ethylenethiourea (ETU)

Fig. 1. Proposed keto–thiol tautomerism of ETU in aqueous solutions.

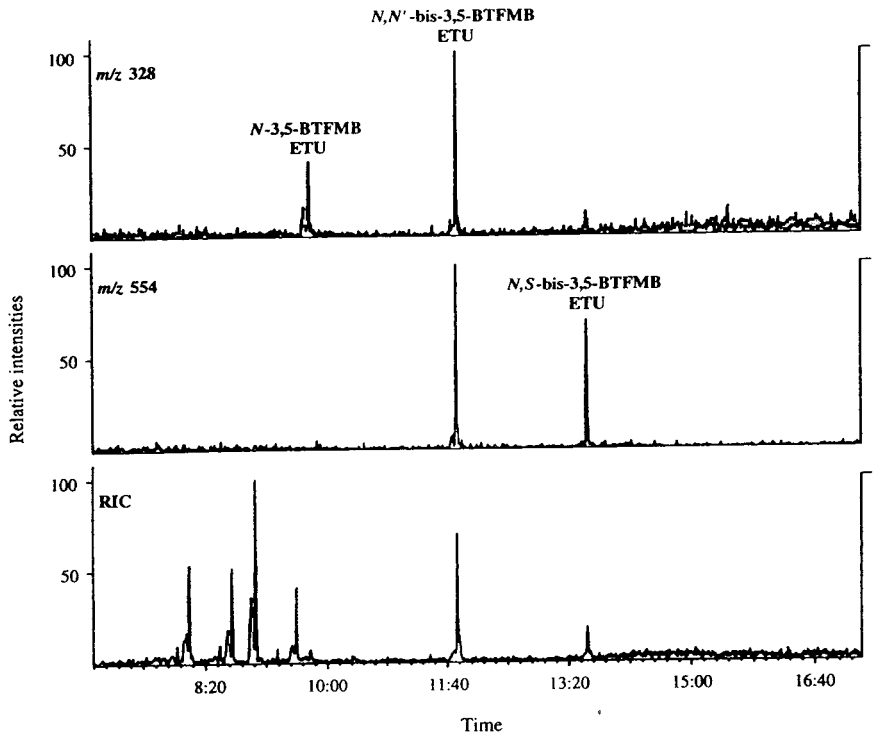

Fig. 2. Ion chromatograms (EI) of the 3,5-BTFMB-Br derivatives of ETU prepared under anhydrous conditions. GC conditions: DB-1701 fused-silica column (30 m × 0.25 mm I.D., 0.15 μm film thickness); temperature programme, 50°C (1 min) to 300°C (5 min) at 20°C/min time in min:s.

m/z 101 and 327 for the mono- and both disubstituted derivatives, respectively.

In contrast to 3,5-BTFMB-Br, the non-aqueous reaction of ETU with PFB-Br resulted in a single derivative containing two PFB groups. This was against expectation, as these reagents normally behave similarly. A corresponding difference in behaviour was also observed with the PTC derivatization of ETU. This mechanistic difference, however, was not investigated further. The NCI mass spectrum of the ETU-diPFB parallels that of the 3,5-BTFMB derivatives, by the loss of one substituent, i.e., $[M-181]^-$ at *m/z* 281.

It is obvious that the detection limit of the method will decrease when multiple ETU compounds are formed during derivatization. The most abundant 3,5-BTFMB derivative (i.e., N,N'-substituted), however, is much more sensitive in NCI than the PFB form, indicating a higher electron affinity. The formation of three derivatives can be considered as an advantage, as it provides an extra feature in compound identification. In addition to the retention time, the presence of the ETU-related satellite peaks on the chromatogram provides an unambiguous identification criterion. Because of the high chemical background in the monosubstituted ion trace (*m/z*, 101), quantification on the disubstituted derivatives (*m/z* 327) was preferred.

3.1. PTC optimization

The pH of the aqueous layer was the most important parameter affecting the reaction kinetics (Fig. 3). Clearly, a strongly alkaline medium (pH > 13) was required in order to obtain high yields. From this, ETU could be considered to

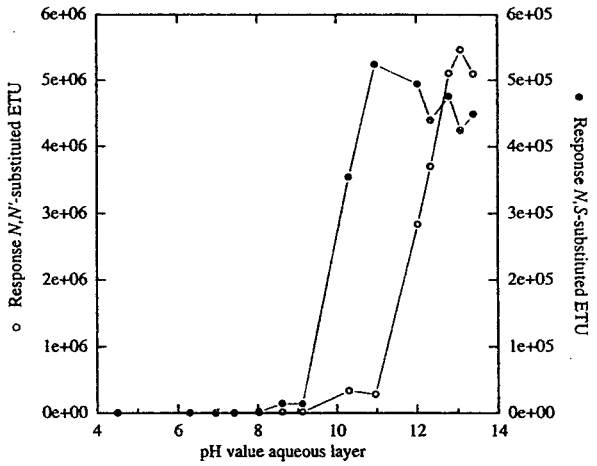

Fig. 3. Influence of the pH of the aqueous layer on the yield of the ETU derivatives. O = N,N'-Substituted; ● = N,S-substituted.

be a very weakly acidic compound. Further, the presence of a catalyst was essential, as no ETU derivative was formed in the absence of the catalyst. This indicates the similarity for the reaction with carboxylic acids. Rosenfeld and Crocco [24] did not find any pentafluorobenzyl ester for carboxylic acids, in the absence of a counter ion. This, contrasts with phenolic compounds, which can be alkylated in a similar biphasic system without a counter ion.

Experiments had revealed that no ETU was left in the aqueous layer after the PTC derivatization, indicating complete conversion of the analyte. These experiments were carried out by tenfold dilution of the aqueous layer after PTC derivatization followed by subsequent derivatization of an aliquot of this layer. As a consequence of the extreme alkaline conditions, cloudy precipitates were formed in surface samples. These precipitates were removed by centrifugation prior to the derivatization procedure.

Under the optimum conditions, the reaction proceeded rapidly and was completed within 15 min. Although the PTC extract can be analysed directly with ECNICI-MS, it is expected that GC–ECD measurements at trace levels without further clean-up procedures will be hampered by the high background.

ETU derivatives were found to be stable for at least several days when stored at room temperature. However, the derivatives were slightly sensitive to decomposition during flash heating in the hot GC injector (Fig. 4). The optimum injector temperature was 180°C. Probably, but not investigated here as such an injector was not available on the instrument used, the cold-on-column injection technique is inherently the best choice as it is expected that degradation takes place during the injection and not with the gradually increasing temperature of the GC column.

3.2. GC–analysis

Fig. 5 shows the ion traces of a blank water sample fortified with 0.13 μg/l of ETU. The ETU trace (*m/z* 327) contains several abundant background peaks that were also present when pure water (Milli-Q) samples were analysed. Consequently, the limit of determination is mainly determined by this procedural background.

The occurrence of two disubstituted derivatives of ETU with a yield ratio of ca. 10:1 (Fig. 3) permits an extension of the quantification range in unknown water samples with a constant amount of internal standard. In low-level sam-

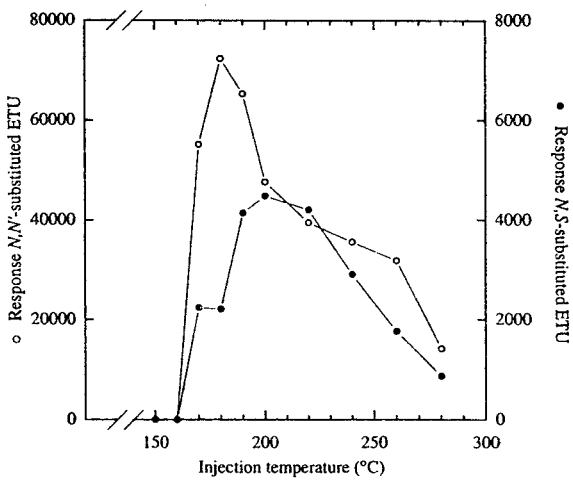

Fig. 4. Influence of the GC injection temperature on the response of the ETU derivatives. O = N,N'-Substituted; ● = N,S-substituted.

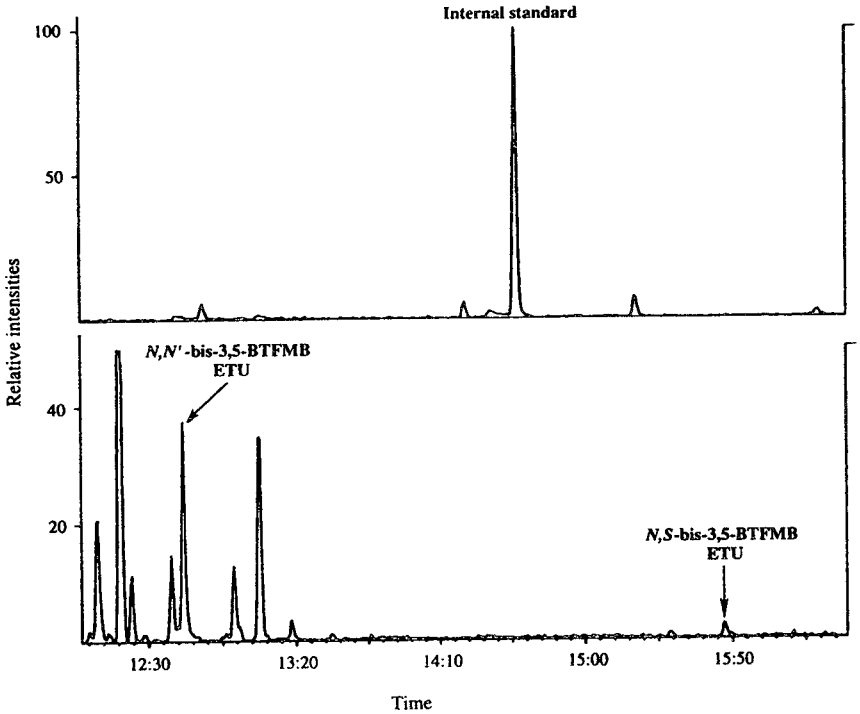

Fig. 5. Ion chromatograms obtained from a water sample fortified with 0.13 μg/l of ETU (lower trace) and the internal standard (upper trace). GC–MS conditions as described under Experimental. Time in min:s.

ples (viz., 0.05–5 μg/l of ETU) quantification can be performed on the most abundant derivative (i.e., the N,N'-substituted compound), whereas in high-level samples (>5 μg/l of ETU) the response ratio of the later eluting, minor N,S-derivative can be used. In the latter samples, the major derivative may readily reach the saturation level of the detector owing to exhausting of the population of the near thermal energy electrons in the NICI source, resulting in a deviation from linearity of the calibration graph (Fig. 6). The calibration graph for the minor derivative was found to be linear up to at least 50 μg/l of ETU.

The reproducibility and recovery of the method were satisfactory. The assay reproducibility was better than 6% (R.S.D., $n = 20$) as determined using duplicate real water samples. The overall recovery of the method was 80 ± 20% on average, as determined in fortified water samples

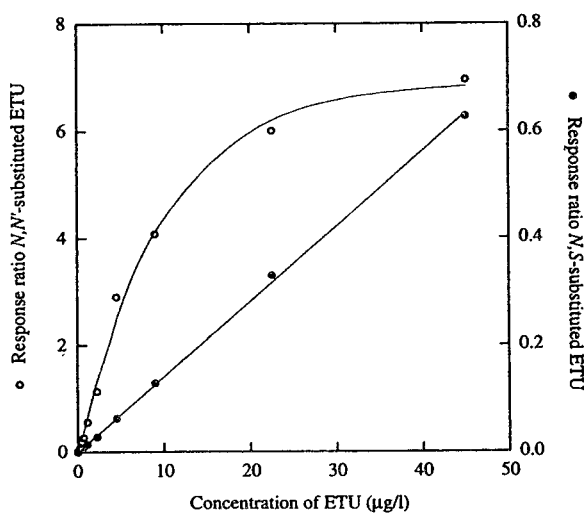

Fig. 6. Calibration graphs for the two forms of disubstituted ETU derivatives. ○ = N,N'-Substituted; ● = N,S-substituted.

in the range 0.5–10 μg/l. Recoveries of added amounts near the determination limit of the method (0.05 μg/l) varied considerably (50–110%). At this level, a slight suppression of the signal of the N,N′-derivative may occur owing to co-eluting compounds with different mass or a slight interference from compounds having the same molecular mass or fragment ions, both originating from the relatively high chemical, procedural background of the method.

3.3. Comparison GC–MS and LC–UV methods

Results of GC–MS and LC–UV analyses of different ground water samples are shown in Table 2. The table gives a random selection of results for a few hundred samples analysed in parallel. One group of results ($n = 5$) concerns false-positive results obtained by LC–UV. The relatively high levels in some samples could not be confirmed by GC–MS. A detailed inspection of the LC method revealed that sample contamination occurred from a rubber seal in the Rotavapor apparatus used for sample concentration. This conclusion is drawn from the GC–MS analysis of the original samples (levels <0.1 μg/l) and the corresponding concentrated samples (Fig. 7). Clearly, this example emphasizes the necessity of independent analysis techniques for tracing false-positive results.

As mentioned before, the comparison of some other results is hampered by the time difference between LC–UV and GC–MS analyses of such samples. Differences in results can be explained by a variable degree of decomposition that was found to occur for ETU when samples are stored for longer periods of time in the refrigerator (group II in Table 2). However, the correlation between results obtained by LC–UV (x) and GC–MS (y) was $y = 1.11x - 0.15$ with a correlation coefficient (r) of 0.989.

In conclusion, in addition to the previously described PTC derivatization of (phenoxy)carboxylic acids, this derivatization technique has

Table 2
ETU concentrations found in some ground water samples of different origins, analysed by LC–UV and GC–MS

Group	Sample No.	ETU (μg/l)		Time between analyses (days)
		LC–UV	GC–MS	
I	1289	0.65[a]	<0.10	
	1290	5.12[a]	<0.10	
	1291	0.23[a]	<0.10	
	1295	0.58[a]	<0.10	
	1299	0.33[a]	<0.10	
II	1281	0.86	0.65	8
	1282	0.22	0.22	8
	1283	0.35	0.40	8
	1287	0.79	0.48	8
	1292	0.27	0.31	13
	1293	1.03	0.75	13
	1294	1.20	0.83	13
	1296	0.31	0.13	13
	944	3.9	4.8	20
	933	1.13	1.15	28
	934	5.9	6.1	28
	1284	0.41	0.62	42
	1285	0.41	0.17	42
	1286	0.56	0.34	42
	932	0.17	0.14	106

[a] False-positive results. See text for details.

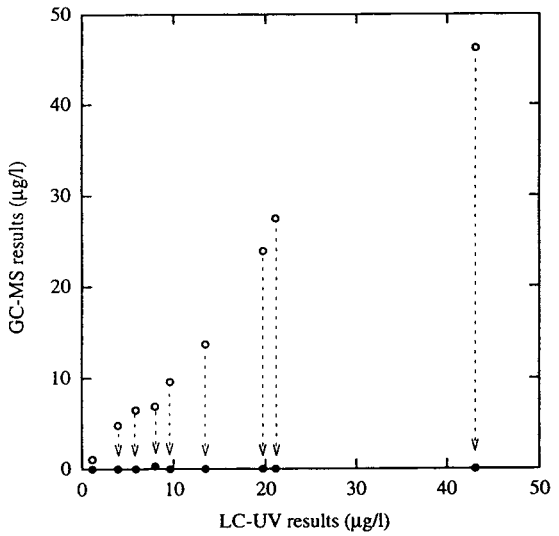

Fig. 7. Comparison of the results for ETU in water samples analysed by GC–MS and LC–UV. ○ = Water samples obtained after concentration on a Rotavapor apparatus as used in the LC–UV method; ● = corresponding original water samples.

been shown to be very useful for the determination of ETU, although it has a completely different class of functional group. The ease of sample preparation in conjunction with the high sensitivity to ECNICI mass spectrometric detection is well suited for routine target compound analysis or confirmation of ETU in surface or ground water. Although the method suffers from a severe procedural background, determination of ETU down to 0.05 μg/l can be easily achieved at unit mass resolution.

Acknowledgements

The authors are grateful to M. Jacquemijns for the synthesis of the internal standard bentazone-d_7 and to M.J. Vredenbregt for the isomeric structure elucidation of the BTFMB-ETU derivatives by GC–FT-IR. They thank W. de Graaf and M. Hack for their unflagging efforts in the LC–UV determination of ETU in many ground water samples.

References

[1] R. Engst, *Pure Appl. Chem.*, 49 (1977) 675–689.
[2] P. Kurttio, K. Savolainen, A. Naukkarinen, V-M. Kosma, L. Tuomisto, I. Penttilä and J. Jolkkonen, *Arch. Toxicol.*, 65 (1991) 381–385.
[3] IARC, *Overall Evaluations of Carcinogenicity: an Updating of IARC Monographs Volumes 1 to 42. IARC Monographs on the Evaluation of Carcinogenic Risks to Humans*, International Agency for Research on Cancer, Lyon, 1987, Suppl. 7, pp. 17–54.
[4] K.N. Woodward, A. McDonald and S. Joshi, *Carcinogenesis*, 12 (1991) 1061–1066.
[5] J.H. Onley and G. Yip, *J. Assoc. Off. Anal. Chem.*, 54 (1971) 165–169.
[6] H.L. Pease and R.F. Holt, *J. Agric. Food Chem.*, 25 (1977) 561–567.
[7] W.H. Newsome, *J. Agric. Food Chem.*, 20 (1972) 967–969.
[8] R.G. Nash, *J. Assoc. Off. Anal. Chem.*, 57 (1974) 1015–1021.
[9] R.G. Nash, *J. Assoc. Off. Anal. Chem.*, 58 (1975) 566–571.
[10] R.R. King, *J. Agric. Food Chem.*, 25 (1977) 73–75.
[11] J. Singh, W.P. Cochrane and J. Scott, *Bull. Environ. Contam. Toxicol.*, 23 (1979) 470–474.
[12] E. Matisová, J. Chovancová and T. Buzinkaiová, *J. Chromatogr.*, 286 (1984) 331–337.
[13] J. Plugmacher and W. Ebing, *Z. Lebensm.-Unters.-Forsch.*, 178 (1984) 90–92.
[14] D.R. Doerge and A.B.K. Yee, *J. Chromatogr.*, 586 (1991) 158–160.
[15] E.A. Hogendoorn, P. van Zoonen and U.A. Th. Brinkman, *Chromatographia*, 31 (1991) 285–292.
[16] D.R. Doerge and C.J. Miles, *Anal. Chem.*, 63 (1991) 1999–2001.
[17] D.R. Doerge, M.W. Burger and S. Bajic, *Anal. Chem.*, 64 (1992) 1212–1216.
[18] P. Kurttio, T. Vartiainen, K. Savolainen and S. Auriola, *J. Anal. Toxicol.*, 16 (1992) 85–87.
[19] H.D. Meiring, G. den Engelsman and A.P.J.M. de Jong, *J. Chromatogr.*, 644 (1993) 357–365.
[20] M. Jacquemijns, J.F.C. Stavenuiter and G. Zomer, *J. Labelled Compd. Radiopharm.* 28 (1990) 1229–1232.
[21] T.J. de Boer and H.J. Backer, *Org. Synth., Coll. Vol.*, 4 (1963) 250.
[22] G. Drabner, A. Poppe and H. Budzikiewicz, *Int. J. Mass Spectrom. Ion Processes*, 97 (1990) 1–33.
[23] R.T. Morrison and R.N. Boyd, *Organic Chemistry*, Allyn and Bacon, Boston, 1976, Ch. 8, pp. 261–262.
[24] J.M. Rosenfeld and J.L. Crocco, *Anal. Chem.*, 50 (1978) 701–704.

ELSEVIER

Journal of Chromatography A, 683 (1994) 167–174

JOURNAL OF CHROMATOGRAPHY A

Optimization of supercritical fluid extraction of organochlorine pesticides from real soil samples

E.G. van der Velde*, M. Dietvorst, C.P. Swart, M.R. Ramlal, P.R. Kootstra

Laboratory of Organic-Analytical Chemistry, National Institute of Public Health and Environmental Protection (RIVM), P.O. Box 1, 3720 BA Bilthoven, Netherlands

Abstract

The optimization of supercritical fluid extraction (SFE) of organochlorine pesticides from real soil samples is performed, according to a general stepwise set-up for quantitative SFE. Optimal conditions obtained from experiments with spiked samples were applied on real soil and the influence of several extraction parameters was tested to gain maximum concentrations of components in comparison with solvent extraction.

The optimal conditions achieved for spiked samples did not yield maximum concentrations for field samples. Stronger extraction conditions were necessary to overcome interactions between matrix and analytes. Longer dynamic extraction times were needed and the use of modifiers appeared to be essential for SFE of real samples. An increase in extraction pressure did not have any influence on extraction results. Comparable results were obtained for SFE and solvent extraction with an overall standard deviation between both methods of 25%.

The stepwise approach is useful in method development to visualize several aspects of SFE, such as the initial conditions, the importance of extraction parameters and the success of SFE for a specific compound–matrix combination. Possibilities in quantitative SFE are discussed, as well as restrictions in the break-through of SFE as technique for future sample pretreatment of solid samples.

1. Introduction

Several studies have shown the potential of supercritical fluid extraction (SFE) for the extraction of organic contaminants from soil. Originally, a lot of qualitative studies were reported, showing the effects of extraction at different densities on groups of components or reporting SFE of spiked samples only. Unfortunately, many studies seem to stop after the analysis of spiked samples [1–4]. More recent studies emphasize the importance of the differences between the investigations on spiked samples and field samples. In most cases, addition of modifiers or stronger extraction conditions seemed to be necessary to obtain SFE results which can be compared with conventional extraction techniques or with values of certified reference materials. Paschke et al. [5] optimized the SFE of polycyclic aromatic hydrocarbons (PAHs) and nitro-PAHs from diesel particulates with different kinds of fluids (CO_2 and $CHClF_2$) and modifiers (methanol and toluene), whereas Dankers et al. [6] improved PAH results in soil with the addition of relatively large volumes of dichloromethane. The quantitative extraction of polychlorinated biphenyls (PCBs) from river sediment was improved with supercritical

* Corresponding author.

0021-9673/94/$07.00
SSDI 0021-9673(94)00544-J

$CHClF_2$ or with methanol-modified CO_2 [7], as was also reported by Onuska and Terry [8]. In most studies, the extraction parameters were optimized varying parameter by parameter, Van der Velde et al. [9] showed the application of an experimental design in the extraction of triazines from soil.

Hawthorne et al. [10] discussed a general set-up for quantitative SFE. Basic parameters in SFE, the partitioning of the analyte in the fluid, the sweeping from the extraction cell and the collection method, can be best determined by spiking on inert material excluding matrix influences. Only the solubility of the components in the supercritical fluid is tested, as well as the extraction time and the collection device and solvent. In our previous study we concluded that the choice of the collection solvent can be very critical, especially for the more volatile components [4]. Next, recoveries were determined of spiked samples and then SFE was performed on real samples in comparison with conventional extraction techniques.

In this study, a quantitative method for SFE of organochlorine pesticides (OCPs) in real soil samples is developed using this general set-up for quantitative SFE of organic components, based on sequential optimization of extraction parameters. Experiments were started from earlier investigations of our laboratory, in which optimal conditions for SFE of PCBs and OCPs in different types of soil were determined with spiked samples [4]. Several parameters were investigated for optimization of SFE, to equal or to improve the results from solvent extractions.

Finally, the possibilities and restrictions of SFE will be discussed as technique for future pretreatment of soil samples.

2. Experimental

2.1. Samples

Soils were air dried, allowed to pass through a 2.8-mm sieve and subsequently homogenized in a ball mill. Field samples were obtained from the Dutch monitoring programme on soil, concerning soils with about 5% organic carbon used for grass land, agriculture land and orchard soil, respectively. Blank soils were characterized as sand and peat soil, with 0.3 and 3.3% organic carbon, respectively. Spiked samples were prepared just before analysis, waiting 15 min till 1 h to allow evaporation of the solvents (the evaporation time depended on the amount of solvents used) with the following components: α-hexachlorocyclohexane (α-HCH), hexachlorobenzene (HCB), β-HCH, γ-HCH, β-heptachloroepoxide (β-HEPO), 2,2-bis(p-chlorophenyl)-1,1-dichloroethene (p,p'-DDE), dieldrin, 2,2-bis(p-chlorophenyl)-1,1-dichloroethane (TDE), o,p'-DDT, p,p'-DDT and several PCBs. PCBs were from CIL (Cambridge Isotope Labs., Woburn, MA, USA), OCPs from Promochem (Wesel, Germany). Spiking levels were chosen typically between 1 and 10 ng/g of dry soil.

2.2. Extraction procedures

Solvent extraction

Aliquots of 15 g of soil were extracted two times with 40 ml of acetone during 30 min using a shaking machine. The organic layer was separated by centrifugation. The liquid fractions were mixed with 800 ml of water and a few ml of saturated sodium chloride, and were then extracted twice with 50 ml of hexane. The combined hexane fractions were dried and, after addition of internal standards (PCBs 44 and 141), concentrated in a Kuderna–Danish apparatus till 10 ml. In some cases, a clean-up is performed to remove interferences from sulphur components. All solvents used were pesticide-grade (hexane) or distilled (acetone).

Supercritical fluid extraction

Supercritical fluid extractions were performed on a Carlo Erba (Milan, Italy) SFC 3000 instrument using a double 70-ml syringe pump (SFC 300) and an SFE-30 extraction unit. Extractions were performed using constant pressure and constant temperature. Various extraction times were programmed using combinations of static and dynamic extraction conditions. The specific extraction conditions are given in the tables. Supercritical pressure was maintained inside the extraction vessel using a deactivated fused-silica

2 m × 50 μm I.D. restrictor (SGE, Austin, TX, USA), resulting in a liquid CO_2 flow of 160–180 μl/min (at 20 MPa).

Accurately weighed soil samples were brought into a 0.5-ml extraction cell, filled up at one side with a thin layer of quartz sand to prevent clogging of the system and stamped to achieve homogeneous packing. Solvent collection was performed into a 2-ml vial containing approximately 1 ml of isooctane, with a known concentration of internal standard mixture (PCBs 44 and 141). Modifier was added directly to the extraction cell, just before supercritical extraction. CO_2 was SFC grade from Air Products & Chemicals (Waddinxveen, Netherlands).

2.3. Analysis

A Hewlett-Packard (HP) 5890 gas chromatograph, equipped with an HP 7673A autosampler, an electron-capture detector, and an Ultra-2 (50 m × 0.2 mm I.D.; 0.33 μm; HP) or DB-5 (30 m × 0.25 mm I.D.; 0.25 μm; J & W Scientific, Folsom, CA, USA) column was used for chromatographic separation, interfaced to an HP 3365 Chemstation (Hewlett-Packard, Palo Alto, CA, USA). Helium was used as carrier gas (2 ml/min) and argon–methane or nitrogen as purge gas (60 ml/min). After injection of 2–4 μl, the temperature programme consisted of an initial temperature of 80°C in several steps to the final temperature of 290°C. The injector temperature was 250°C and detector temperature was 325°C. Quantification was performed by comparison with an external standard mixture, using PCBs 44 and 141 as internal standards. Limits of determination for each component were 0.5 ng/g of soil, using the conditions specified above for sample preparation and analysis.

3. Results and discussion

3.1. Optimization of extraction parameters

In earlier investigations, we determined the optimal conditions for SFE of PCBs and OCPs. Analytes were first spiked on glass beads to test the initial extraction conditions. Restrictor, pressure, extraction time and collection solvent were adapted. Next, the analytes were spiked on different types of soil and good recoveries were found (Table 1), especially for soil with high contents of organic carbon usually giving low recoveries when solvent extraction is applied, because of binding of analytes to the soil matrix [4]. In the framework of this study, extraction times were varied from 10 min static and 20 min dynamic (SFE 10/20) to 30 min dynamic extraction (SFE 30) (Table 1). For sand no effect of extraction times was found, but for peat soil a decrease in recoveries of 10 to 20% for all components was found going to longer dynamic extraction times. With respect to the identical results for sand, this cannot be an effect of the collection method. A possible explanation is the difference in kinetics of the partitioning process for components to become available from sand or from peat soil.

Starting from the optimized conditions, a first series of extraction experiments with three different field soils was performed. In Table 2, the results of the solvent extraction and SFE are given for the organochlorine pesticides (no PCBs were found), using as extraction conditions: 20 MPa, 50°C, 10 min static and 20 min dynamic extraction times and pure CO_2. In a second series, the extraction time was changed to 30 min dynamic extraction to increase recoveries.

The SFE results of the field soils are in the same order of the concentrations found after solvent extraction. In this regard it must be realized, that concentrations are not corrected for extraction recoveries. For the measured components liquid–liquid extraction recoveries ranged from 50 to 80%, whereas for SFE recoveries were between 91 and 107% (Table 1). Going to longer dynamic extraction times in SFE, a slight improvement can be seen (a further increase in dynamic extraction time did not give any better extraction results). This is in contradiction with the SFE for spiked samples. Apparently, the binding of the components to the matrix and extraction process cannot be compared for real samples and spiked samples with regard to diffusion, partitioning and kinetics.

Table 1
Recovery experiments with liquid–liquid extraction (LLE) and SFE of PCBs and OCPs on sand and peat soil ($n = 3$)

Component	Addition (ng/g)	Sand						Peat soil					
		LLE		SFE 10/20		SFE 30		LLE		SFE 10/20		SFE 30	
		Recovery (%)	S.D. (%)	Recovery (%)	S.D. (%)	Recovery (%)	S.D. (%)	Recovery (%)	S.D. (%)	Recovery (%)	S.D. (%)	Recovery (%)	S.D. (%)
α-HCH	2.3	98.3	5.3	98.4	6.7	98.6	12.5	101.0	14.0	96.4	6.8	78.3	4.4
HCB	0.9	108.0	3.0	101.6	3.7	100.4	13.3	113.0	19.0	95.9	8.4	89.7	7.5
β-HCH	3.3	110.0	4.0	103.6	0.8	102.8	14.5	157.0	11.0	112.8	14.6	97.3	5.1
γ-HCH	2.2	118.0	8.0	103.1	4.7	103.7	12.2	109.0	12.0	91.2	7.7	81.8	5.5
β-HEPO	3.2	98.5	2.9	92.1	19.3	97.4	5.6	[a]	[a]	93.9	6.6	79.1	2.1
p,p'-DDE	5.1	86.7	3.8	99.2	1.4	94.2	8.1	75.6	12.6	107.2	3.8	97.6	11.0
Dieldrin	4.8	80.5	1.7	98.3	2.4	96.7	8.7	83.1	11.9	95.6	4.6	78.2	5.8
TDE	8.2	75.9	2.8	97.5	6.1	97.8	10.5	78.9	11.3	91.3	6.8	77.1	6.4
o,p'-DDT	8.9	84.5	3.9	97.1	3.4	95.9	8.7	50.7	10.5	98.3	6.4	82.5	7.7
p,p'-DDT	10.2	91.1	6.6	93.5	7.8	93.3	17.6	64.5	10.9	103.4	9.5	111.0	42.0
PCB 28	4.5	107.0	1.0	112.4	2.2	103.5	11.3	103.0	11.0	104.9	9.8	92.5	6.4
PCB 52	3.2	89.9	2.9	96.7	3.0	97.1	11.6	59.0	8.7	94.9	6.0	78.7	5.6
PCB 101	3.9	96.9	3.1	102.7	3.1	97.9	9.6	83.8	8.4	110.5	6.7	91.4	8.1
PCB 118	2.8	90.5	4.2	109.0	4.8	99.6	7.1	98.0	13.4	102.8	8.2	89.5	9.5
PCB 138	2.8	96.5	3.7	102.7	2.5	102.4	11.2	64.2	12.5	106.7	10.2	90.1	10.8
PCB 153	4.0	89.5	6.9	102.2	1.1	94.9	7.0	57.8	13.3	99.6	6.2	85.2	9.9
Average		95.1		100.6		98.5		81.2		100.3		87.5	

SFE conditions: 20 MPa; 50°C; CO_2; extraction time 10 min static and 20 min dynamic (SFE 10/20) or 30 min dynamic (SFE 30); flow ca. 160 ml/min; collection solvent isooctane.
[a] Interference.

Modifiers with different characteristics were added directly to the extraction cell for the orchard soil to try to improve the SFE results. In Table 3, concentrations are shown after addition of toluene, acetonitrile and methanol respectively. Toluene did not gave any improvement, but rather a decrease, whereas Mulcahey and Taylor [11] reported an increase for PCBs. Both acetonitrile and methanol give an increase in concentrations, from which methanol gives the best overall results. This is in agreement with Refs. [7] and [8]. Obviously, to overcome the interactions between the analyte and the matrix, introduction of modifier is essential. To test the influence of the amount of modifier, a series of 5 to 30 μl methanol was added to the extraction cell. In Table 4, the results are shown for the orchard soil. The amount of 20 μl methanol added to the extraction cell gave the highest concentration of OCPs. This amount corresponds with a volume percentage of about 10% with respect to CO_2 on basis of the free cell volume (total cell volume minus the sample volume). Probably, concentrations decrease by using higher amounts of modifier because the fluid is no longer supercritical above this value. Addition of modifier and using a combination of static and dynamic extraction times, does not give a better extraction yield, as can be seen in the last column of Table 3. This confirms the idea that the acting of the modifier is primarily the wetting of the matrix to facilitate the accessibility of the analytes and not an increase of diffusion.

Finally, the influence of pressure was tested. Table 5 shows that an increase in pressure did not had any influence on concentrations and therefore further extractions were performed at 20 MPa to diminish co-extraction of matrix components. Second extractions were performed

Table 2
Comparison of field samples with LLE and SFE with different extraction times (concentrations are not corrected for recoveries)

Component	Grass land						Agriculture land						Orchard soil					
	LLE ($n = 4$)		SFE 10/20 ($n = 3$)		SFE 30 ($n = 3$)		LLE ($n = 4$)		SFE 10/20 ($n = 3$)		SFE 30 ($n = 3$)		LLE ($n = 2$)		SFE 10/20 ($n = 2$)		SFE 30 ($n = 2$)	
	ng/g	S.D. (ng/g)	ng/g	S.D. (ng/g)	ng/g	S.D. (ng/g)	ng/g	S.D. (ng/g)	ng/g	S.D. (ng/g)	ng/g	S.D. (ng/g)	ng/g	S.D. (ng/g)	ng/g	S.D. (ng/g)	ng/g	S.D. (ng/g)
HCB	–	–	–	–	–	–	6.4	0.1	6.0	0.6	5.8	0.4	–	–	–	–	–	–
p,p'-DDE	4.1	0.3	4.4	0.4	5.5	1.1	1.1	0.0	1.6	0.2	1.5	0.2	63.1	–	50.3	–	56.2	–
TDE	6.1	0.5	0.8	0.2	1.7	0.4	–	–	–	–	–	–	12.2	–	12.8	–	20.1	–
o,p'-DDT	2.3	0.2	3.0	0.5	4.0	1.0	0.6	0.1	1.1	0.2	1.0	0.2	44.8	–	37.7	–	43.7	–
p,p'-DDT	11.4	1.7	21.9	2.4	29.7	4.6	–	–	5.5	0.4	6.1	0.3	260.6	–	236.8	–	296.4	–

SFE conditions: 20 MPa; 50°C; CO_2; extraction time: 10 min static and 20 min dynamic (SFE 10/20) or 30 min dynamic (SFE 30); flow ca. 160 μl/min. – = Not detectable (0.5 ng/g).

Table 3
SFE with addition of different modifiers on orchard soil

Component	SFE 30						SFE 10/20	
	Modifier toluene ($n = 3$)		Modifier acetonitrile ($n = 3$)		Modifier methanol ($n = 6$)		Modifier methanol ($n = 3$)	
	ng/g	S.D. (ng/g)	ng/g	S.D. (ng/g)	ng/g	S.D. (ng/g)	ng/g	S.D. (ng/g)
p,p'-DDE	48.2	2.1	68.4	5.7	72.0	2.9	59.5	0.6
TDE	24.5	0.7	32.9	1.6	20.6	0.8	16.9	0.3
o,p'-DDT	41.3	2.4	57.2	3.9	61.8	1.5	52.5	0.9
p,p'-DDT	224	11	325	19	355	8	353	48

SFE conditions: 20 MPa; 50°C; CO_2; 20 μl modifier; flow ca. 160 μl/min.

Table 4
Influence of the amount of methanol modifier on orchard soil

Component	5 μl MeOH, 2.4%[a] (n = 3)		10 μl MeOH, 4.8%[a] (n = 3)		15 μl MeOH, 7.1%[a] (n = 3)		20 μl MeOH, 9.5%[a] (n = 6)		25 μl MeOH, 11.9%[a] (n = 3)		30 μl MeOH, 14.3%[a] (n = 3)	
	ng/g	S.D. (ng/g)	ng/g	S.D. (ng/g)	ng/g	S.D. (ng/g)	ng/g	S.D. (ng/g)	ng/g	S.D. (ng/g)	ng/g	S.D. (ng/g)
p,p'-DDE	53.9	1.1	55.9	2.3	63.3	4.7	72.0	2.9	61.3	5.2	65.3	1.0
TDE	17.1	0.5	17.1	0.4	16.6	0.5	20.6	0.8	16.3	0.6	17.3	0.2
o,p'-DDT	42.9	1.0	44.5	1.9	52.3	3.6	61.8	1.5	51.8	5.0	56.6	0.8
p,p'-DDT	250	3	261	9	311	22	355	8	315	23	344	1

SFE conditions: 20 MPa; 50°C; CO_2; 30 min dynamic; flow ca. 160-180 μl/min.
[a]% (v/v) of the modifier with respect to CO_2, on basis of free cell volume.

Table 5
Influence of extraction pressure

Component	20 MPa, density 0.791, 160–180 μl/min (n = 6)		25 MPa, density 0.841, 190–210 μl/min (n = 2)		30 MPa, density 0.880 g/ml, 230–250 μl/min (n = 2)	
	ng/g	S.D. (ng/g)	ng/g	S.D. (ng/g)	ng/g	S.D. (ng/g)
p,p'-DDE	72.0	2.9	59.3	–	70.4	–
TDE	20.6	0.8	20.5	–	24.5	–
o,p'-DDT	61.8	1.5	49.7	–	57.6	–
p,p'-DDT	355	8	329	–	383	–

SFE conditions: 50°C; CO_2; 30 min dynamic; addition of 20 μl MeOH; orchard soil.

for several experiments described above, under the same extraction conditions, and no detectable amounts of components were found.

The orchard soil was extracted six times using the final SFE conditions (20 MPa, 50°C, 30 min dynamic extractions and 20 μl methanol as modifier), in different series of experiments over a longer time period, giving good reproducibilities varying from 20.6 ± 0.8 ng/g for TDE to 355 ± 8 ng/g for *p,p'*-DDT. A typical chromatogram of SFE of OCPs in orchard soil is shown in Fig. 1.

Some random soil samples were analysed using SFE with final conditions and solvent extraction. In Fig. 2, the results of both methods are plotted. Assuming a concentration-independent relative standard deviation between both methods, a pooled standard deviation of 25% was calculated for all soils, components and concentrations. So, comparable results were obtained for SFE and solvent extraction. More soils have to be analysed to make a final comparison between liquid–liquid extraction and SFE. The reproducibility of both methods is comparable (Table 2), the time needed for sample preparation is not faster using a non-automated SFE instrument, but the use of toxic and environmentally hazardous solvents is highly reduced.

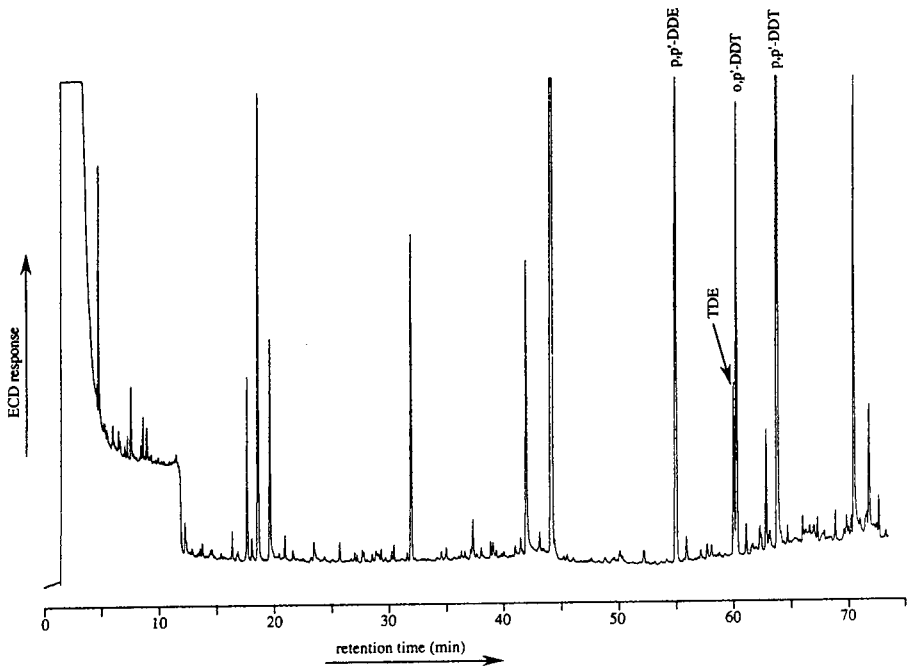

Fig. 1. GC–electron-capture detection (ECD) chromatogram of organochlorine pesticides in orchard soil using final SFE conditions. For chromatographic conditions see Experimental.

3.2. Possibilities and restrictions in quantitative SFE

The set-up of this study, using a stepwise approach for the optimization, offers several advantages. Information has been obtained about the relative importance of extraction parameters for these specific compounds, such as the solubility of the compounds by the chosen density, the transport in the SFE system and the collection method. By the next step, the spiking on the soil, the extraction of the compounds from the matrix can be studied. If no satisfactory results have been obtained in these steps, it is in principle useless to continue with SFE for this compound–matrix combination. On the other hand, it is important to avoid endless optimizations, because this process has to be repeated with the extraction of real soil samples, as described above. The SFE of real samples shows that stronger extraction conditions are necessary, because compound–matrix interactions are different for real samples, probably resulting from bound residues.

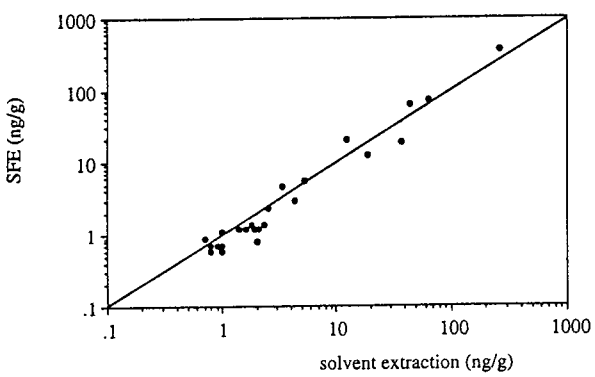

Fig. 2. Correlation of SFE with solvent extraction for several field samples and components.

A sequential as well as a statistical approach can be chosen for the optimization of extraction parameters for either spiked or real samples. The statistical approach is only appropriate, if it is known that SFE will be a suitable method for compounds and matrix. A statistical method offers the opportunity to study the effects of the different parameters with fewer experiments and to distinguish the interactions between parame-

ters [9]. In practice, the sequential approach is applied more often, especially when chemometric support is not available, and offers the opportunity to adjust parameters during the experiments, as is shown in this study. So, the choice of the approach has to be dependent on the specific SFE problem.

In overlooking our results and other publications in the field of SFE, a major breakthrough of SFE has not been reached yet, while comparable results with conventional methods have been reported. In our opinion, SFE suffers from the same problems as, for example, solvent and Soxhlet extraction. It is difficult to achieve complete extraction from solid matrices like soil, because certain fractions of compounds will irreversibly bind to the matrix. Besides, in the case of soils, every soil sample is different in composition, requiring specific optimizations and determinations of recovery. However, in conventional techniques these aspects have been accepted and endless optimizations for complete extraction yields have been dropped. In using a new technique like SFE, a solution for these problems and also higher extraction efficiencies have been expected. At this moment, SFE is not ready to offer this solution, rather than an approximation of the results of conventional techniques.

4. Conclusions

A method development for SFE of OCPs in field samples has been performed using a general stepwise approach for quantitative SFE, starting with spiking on glass beads to establish initial conditions, followed by spiking on different kinds of soil to further adapt SFE parameters. As was expected, the conditions were not directly suitable for real soil samples. The component–matrix interactions in real samples behave different with respect to spiked samples as can be seen in adaptations in extraction times and the effects of modifiers. Finally, comparable results were obtained for SFE and solvent extraction. The stepwise approach gives a deeper understanding in the parameters which are important in development of quantitative SFE. As technique, SFE is not ready yet to overcome the general problems in the extraction of soil samples.

References

[1] J.M. Wong, Q.X. Li, B.D. Hammock and J.N. Seiber, *J. Agric. Food Chem.*, 3 (1991) 1802–1807.
[2] J.R. Wheeler and M.E. McNally, *J. Chromatogr. Sci.*, 27 (1989) 534–539.
[3] M. Lohleit, R. Hillmann and K. Bächmann, *Fresenius' J. Anal. Chem.*, 339 (1991) 470–474.
[4] E.G. van der Velde, W. de Haan and A.K.D. Liem, *J. Chromatogr.*, 626 (1992) 135–143.
[5] T. Paschke, S.B. Hawthorne and D.J. Miller, *J. Chromatogr.*, 609 (1992) 333–340.
[6] J. Dankers, M. Groenenboom, L.H.A. Scholtis and C. van der Heiden, *J. Chromatogr.*, 641 (1993) 357–362.
[7] S.B. Hawthorne, J.J. Langenfeld, D.J. Miller and M.D. Burford, *Anal. Chem.*, 64 (1992) 1614–1622.
[8] F.I. Onuska and K.A. Terry, *J. High Resolut. Chromatogr.*, 12 (1989) 527–531.
[9] E.G. van der Velde, M.R. Ramlal, A.C. van Beuzekom and R. Hoogerbrugge, *J. Chromatogr. A*, 683 (1994) 125–139.
[10] S.B. Hawthorne, D.J. Miller, M.D. Burford, J.J. Langenfeld, S. Eckert-Tilotta and P.K. Louie, *J. Chromatogr.*, 642 (1993) 301–317.
[11] L.J. Mulcahey and L.T. Taylor, *Anal. Chem.*, 63 (1991) 2225–2232.

ELSEVIER

Journal of Chromatography A, 683 (1994) 175–183

JOURNAL OF CHROMATOGRAPHY A

Element-selective detection of pesticides by gas chromatography–atomic emission detection and solid-phase microextraction

Ralf Eisert[a,*], Karsten Levsen[a], Gerold Wünsch[b]

[a]*Department of Analytical Chemistry, Fraunhofer Institute of Toxicology and Aerosol Research, Nikolai-Fuchs-Strasse 1, D-30625 Hannover, Germany*

[b]*Institute of Inorganic and Analytical Chemistry, University of Hannover, Callinstrasse 9, D-30167 Hannover, Germany*

Abstract

The analysis of samples contaminated by organic compounds, especially pesticides, is an important tool of environmental monitoring. A new isolation method has been developed for the determination of pesticides in environmental water samples using solid-phase microextraction (SPME). Thus, the extraction and preconcentration steps of sample preparation are focused in a single process step. For the determination of organophosphorus pesticides using SPME extraction and preconcentration steps a GC–atomic emission detection coupling system was used. This coupling technique is a very selective analytical tool. Element-characteristic chromatograms acquired by using different element emission lines can be obtained, enhancing the selectivity of the method in environmental monitoring, and they can be used to identify even unknown compounds in environmental samples. A fused-silica fiber coated with a polymer (polydimethylsiloxane) phase is used to extract organic compounds and transfer them into a GC injector for thermal desorption and analysis. Volatile pesticides can be efficiently isolated from aqueous environmental samples, as demonstrated for organophosphorus pesticides. This method shows a precision of 8–12% (R.S.D.), depending on the compound. Furthermore, it is capable of limits of detection in the ppb and sub-ppb range. The adsorption and desorption times to carry out the optimum equilibrium and thermodesorption conditions, have been optimized. Determination of pesticides in spiked river water samples with this technique is reported and a comparison of SPME to established extraction techniques, i.e. solid-phase extraction is also carried out. The results demonstrate the suitability of the SPME approach for analysis of these polar compounds.

1. Introduction

The aim of the present work is to show the sensitivity, element-characteristic and -selective detection of compounds in environmental water samples using GC–atomic emission detection (AED) coupling. Pesticides, which are amenable to GC, can be detected using a wide spectrum of GC detection methods: i.e. flame ionization detection (FID), nitrogen–phosphorus detection (NPD), or mass spectrometry (MS). All these detection methods show extreme differences concerning their response selectivity. The element-specific AED shows a tunable detection specificity and is therefore a useful tool for elemental characterization of compounds [1].

The analysis of samples contaminated by organic compounds, especially pesticides, is an

* Corresponding author.

0021-9673/94/$07.00
SSDI 0021-9673(94)00612-1

important tool of environmental monitoring [2–5]. A new isolation method has been developed for the determination of pesticides in environmental water samples using solid-phase microextraction (SPME). Thus, the extraction and preconcentration steps of sample preparation are focused in a single process step. A fused-silica fiber coated with a polymer [polydimethylsiloxane (PDMS)] phase is used to extract organic compounds from water and transfer them into a GC injector for thermal desorption and analysis. Analytes are extracted until the partition equilibrium has been reached. After this step the fiber is directly transferred to the heated GC injector, where the adsorbed organic substances are thermally desorbed, and subsequently separated and quantified. This technique has been previously applied to substituted benzenes [6] and polar compounds, i.e. phenols [7], in water. The sample preparation step does not require the use of solvent.

The elemental characterization of pesticides in environmental water samples by solid-phase extraction (SPE) was compared with SPME. For both techniques the determination of the pesticides by GC–AED is developed, which leads to a very high selectivity of the method. Element-characteristic chromatograms are obtained from this detection technique, which show only minor matrix interferences. The isolation using SPME was first applied to the analysis of benzene, toluene, ethyl benzene and xylenes in groundwater [6]. In the new isolation technique, SPME, a fused-silica fiber was used, coated with PDMS for adsorption of the analytes (pesticides and here especially organophosphorus pesticides) from the aqueous sample. Determination of pesticides using this screening method is possible in the low ppb (w/w) range.

2. Experimental

2.1. SPME procedure

A fused-silica fiber coated with 100 μm PDMS phase was used. Vials of 5 ml were filled with 3 ml of sample for the adsorption process of the compounds from the aqueous sample using SPME. An optimized adsorption time (20 min) has been used in this study, unless stated otherwise. Thermal desorption of the pesticides has been carried out for 3 min. After this period, the liner purge of the GC injector has been closed, and the liner was purged by a helium flow. During the following 5–8 min the fiber was still kept in the liner. Possible memory effects of compounds, which may persist in the fiber for longer than 3 min under temperatures of 205°C, can be totally reduced from the fiber after such a period of time. However, no further regeneration mode for the fiber assembly was considered necessary. Several tests of a still blank value after this period have been completely negative. There is no necessity for further purification and concentration ("clean-up") before extraction and determination. GC detection of all SPME experiments was carried out using temperature program B, which is described below. See Fig. 1 and Table 1.

2.2. SPE procedure

A 1-l water sample was used for SPE. Cartridges (6 ml) were filled with 2 g of C_{18} adsorbent material (Amchro, Sulzbach-Taunus, Germany). These cartridges were first conditioned before extraction using 5 ml acetone, 5 ml methanol and 5 ml Milli-Q water. The sample was passed through the C_{18} material under vacuum at a flow of 9–10 ml/min. After drying the adsorbent, using a gentle stream of nitrogen for approximately 20 min, elution of the analytes from the SPE material was achieved using five 1-ml volumes of methanol. The combined eluent was concentrated in volume to 1 ml using a gentle stream of nitrogen. A 1-μl volume was injected for GC analysis using the temperature program A, which is described below.

2.3. Instruments

SPE

A SPE system from Supelco (Bellefonte, PA, USA) in conjunction with a supplementary dry-

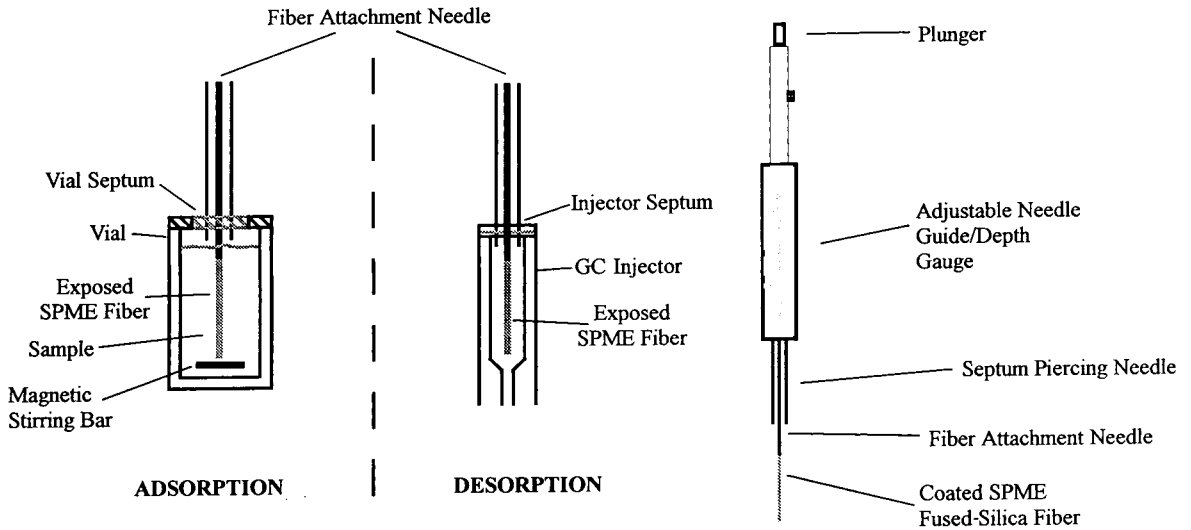

Fig. 1. Schematic description of the SPME unit and adsorption and desorption techniques.

ing unit (Visiprep and Visidry) was used in this study for the comparison experiments.

SPME

A SPME system from Supelco equipped with a fused-silica fiber coated with 100 μm PDMS phase was used for trapping the analytes from the aqueous matrix.

GC–AED

GC–AED investigations were carried out using an Hewlett-Packard atomic emission detector 5921 A and a 5890, series II, gas chromatograph. All injections were performed manually. Helium was of quality better 6.0 (both for GC separation and AED plasma) using a helium gas purification unit (VICI Valco, TX, USA). In general, the emission lines of the following elements were monitored: nitrogen (N 174.200 nm), phosphorus (P 178.079 nm), sulfur (S 181.379 nm), carbon (C 193.032 nm and C 495.724 nm), chlorine (Cl 480.192 nm), hydrogen (H 486,133 nm), bromine (Br 478.578 nm) and oxygen (O 777.302 nm). A DB-5.625 column (J & W Scientific, Fisons Instruments, Folsom, CA, USA), 30 m × 0.32 mm I.D., film thickness 0.25 μm, helium as carrier gas and a split/splitless injector were used for all investigations with the following two temperature programs: (A) 60°C for 1 min, 60–150°C at 15°C/min, 150°C for 1 min, 150–201°C at 3°C/min, 201°C for 1 min and (B) 50°C for 4 min, 50–180°C at 30°C/min, 180°C for 1 min, 180–202°C at 3°C/min, 202°C for 5 min. In general, 1 μl was injected into the GC. See Tables 2 and 3.

Table 1
Optimized conditions for SPME and analysis of organophosphorus pesticides using GC–AED

SPME Fiber	100 μm PDMS
Sample volume	3-ml water sample in 5-ml vial
Extraction temperature	Room temperature (21°C)
Extraction times	20 min
Desorption temperature	205°C
Desorption time	3 min
Injection port	split/splitless (purge delay for 3 min)
Detector (AED)	Atomic emission detector HP 5921 A
Solvent vent time (AED)	0.8–4.8 min

2.4. Materials

All pesticide standards used in this study were purchased from Promochem (Wesel, Germany)

Table 2
GC–AED operating parameters (see also Table 3)

Injector parameters	
Injection volume	1 μl or thermal desorption of the SPME fiber
Injection temperature	205°C
Injection port	split/splitless
GC parameters	
Column	DB 5.625 (30 m × 0.31 mm I.D., film thickness 0.25 μm)
Column head pressure	100 kPa He
Oven program (for SPME)	50°C (4 min hold) 50–180°C with 30°C/min 180°C (1 min hold) 180–202°C with 3°C/min 202°C (5 min hold)
Interface parameters	
Transfer line	DB 5.625 column
Transfer line temperature	250°C
Scavenger gases	
Hydrogen: 99.999% (purity)	$5 \cdot 10^5$ Pa
Oxygen: 99.995%	$2 \cdot 10^5$ Pa
Nitrogen–methane: 99.99%–99.5%	$5 \cdot 10^5$ Pa
AED parameters:	
Spectrometer purge flow	2.5 l/min nitrogen
Cavity temperature	280°C
Helium make-up flow	60 ml/min
Helium supply pressure	30 p.s.i. (207 kPa)
Cavity pressure	1.5 p.s.i. (10.35 kPa)
Column-detector coupling	Column to cavity

and Riedel-de Haën (Seelze-Hannover, Germany). They were of purity >98% and used as received. Methanol (Pestanal quality) and acetone (Pestanal quality) were also from Riedel-de Haën. Water was obtained from a Milli-Q water-purification system (Millipore, Bedford, MA, USA).

3. Results and discussion

Environmental water samples often show two types of problems during the preconcentration and extraction; first a matrix interference from non-target compounds, and second a strong adsorption effect of the matrix. Therefore, a selective preconcentration and extraction step is necessary for a specific determination in environmental analysis. SPME offers an elegant sample preparation step, which is more efficient than flushing 1-l samples through a cartridge filled with adsorbent material, i.e. 2 g C_{18} material. The adsorption equilibrium of most analytes is almost reached after 15–20 min, which is demonstrated in Fig. 2.

Linear calibration curves can be obtained for all pesticides using SPME in a concentration range of 2–200 ng/ml. This linear relationship of these compounds is shown in Table 4. Correlation coefficients are better than $r = 0.996$ for all investigated compounds. The repeatability of the injections is in the range of 8–12% (R.S.D.). For

Table 3
GC–AED operation parameters: wavelengths and plasma conditions (see also Table 2)

Measurement set	Elements	λ (nm)	Scavenger gas conditions	Filter
1	C 496	495.724	O_2	No
1	H 486	486.133	O_2	No
1	Br 478	478.578	O_2	No
1	Cl 479	480.192	O_2	No
2	N 174	174.200	O_2,H_2	No
2	S 181	181.379	O_2,H_2	No
2	C 193	193.032	O_2,H_2	No
3	O 777	777.302	N_2–CH_4 (90:10)	Vis
4	P 178	178.079	H_2, high flow	No

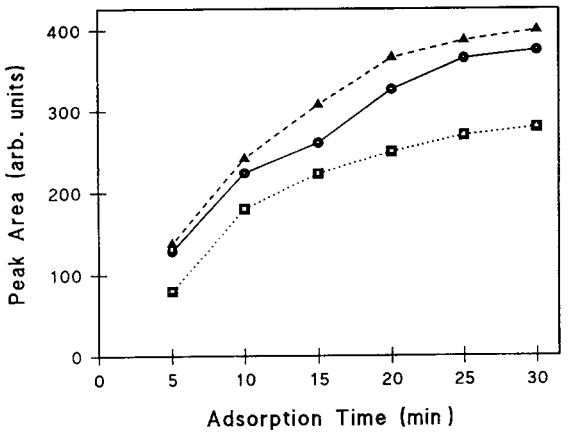

Fig. 2. The effect of varying adsorption times for SPME; optimized conditions are shown for three investigated organophosphorus compounds; equal amounts are injected; figure displays the peak area of sulfur at 181 nm versus the investigated adsorption time. ○ = Diazinon; ▲ = parathion-methyl; □ = parathion-ethyl.

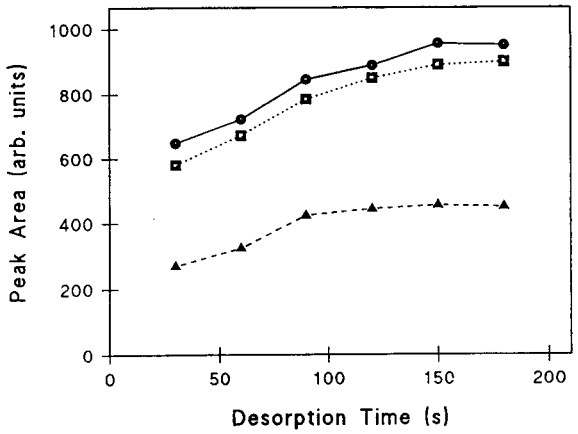

Fig. 3. The effect of varying desorption times for SPME; optimized conditions are shown for three investigated organophosphorus compounds; equal amounts are injected; figure displays the peak area of sulfur at 181 nm versus the investigated desorption time. Symbols as in Fig. 2.

the desorption of the analytes the time of the fiber exposed into the GC injector should be above 2 min, which is displayed in Fig. 3. Typical limits of detection (LODs) for all investigated compounds are between 0.5 and 5 μg/l using the emission lines of carbon (C 193 nm) and sulfur (S 181 nm), which are summarized in Table 5.

Compared to classical GC detection methods, the sensitivity is considerable poorer with AED, but AED is nevertheless much more selective. There may be interference in the emission lines of an element by an emission line of another element. Such interference can be revealed using the wavelength snapshot technique of AED. Using this three-dimensional technique an element is not characterized by only one but by all emission lines, which further enhances the selectivity. A typical example of this identification method is given in Fig. 5. The three-dimensional snapshot of bromophos-ethyl at retention time 18.46 min in a spiked surface water sample of the River Leine shows the typical three emission lines of chlorine (so-called "chlorine emission triplet"). If one of them is missing in the plot,

Table 4

Coefficients of correlation r for the calibration of six organophosphorus pesticides using SPME in Milli-Q water samples at a range of 2–200 ng/ml

Peak No.	Compound	a[a]	b[a]	r
1	Ethoprophos	−79.94	22.06	0.9998
2	Diazinon	−100.23	21.76	0.9997
3	Parathion-methyl	−14.57	10.77	0.99997
4	Parathion-ethyl	−150.74	25.78	0.9998
5	Bromophos-methyl	−170.19	24.59	0.9998
6	Bromophos-ethyl	0.29	12.43	0.9998

[a] Linear regression of type: $y = bx + a$.

Table 5
Peak assignment and limits of detection[a] of six organophosphorus pesticides using SPME and an adsorption time of 20 min; limits of detection are shown for all pesticides using the emission lines of carbon at 193 nm and sulfur at 181 nm

Peak No.	Compound	Molecular formula	Retention time (min)	Limit of detection[a], C 193 nm (μg/l water)	Limit of detection[a], S 181 nm (μg/l water)
1	Ethoprophos	$C_8H_{19}O_2PS_2$	10.98	0.5	1
2	Diazinon	$C_{12}H_{21}N_2O_3PS$	12.73	1	3
3	Parathion-methyl	$C_8H_{10}NO_5PS$	14.32	0.5	5
4	Parathion-ethyl	$C_{10}H_{14}NO_5PS$	16.06	1	3
5	Bromophos-methyl	$C_8H_8BrCl_2O_3PS$	16.58	0.5	2
6	Bromophos-ethyl	$C_{10}H_{12}BrCl_2O_3PS$	18.46	0.5	5

[a] Signal-to-noise ratio = 3.

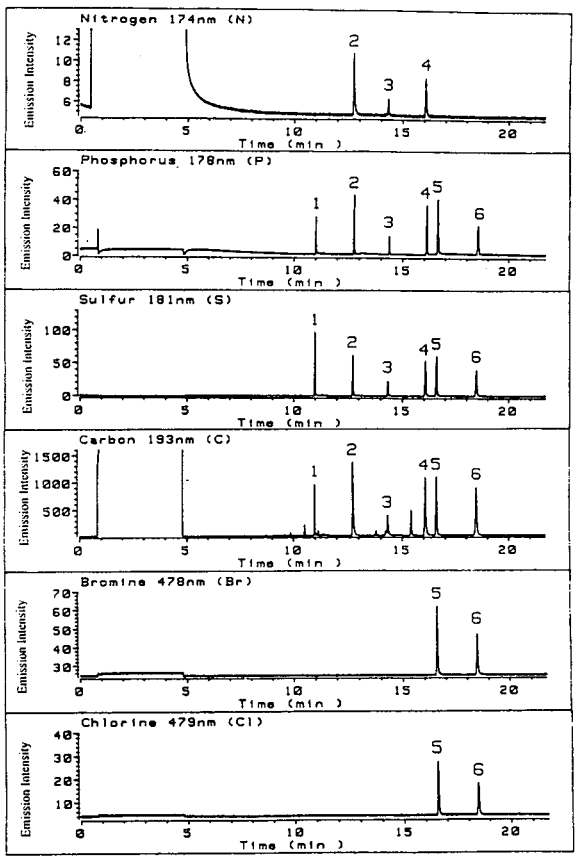

Fig. 4. Elemental characterization of a 60 ppb standard solution containing six organophosphorus pesticides [ethoprophos (1), diazinon (2), parathion-methyl (3), parathion-ethyl (4), bromophos-methyl (5) and bromophos-ethyl (6)] using SPME with a 100 μm PDMS coating; GC–AED response is shown for six different element emission lines (equal amounts of the pesticides are injected).

one can conclude that chlorine will be also missing in this compound. In the present case (see Fig. 5), chlorine could be identified, which enhances the presence of the pesticide bromophos-ethyl.

Surface water samples were taken from two rivers in Lower Saxony (Germany), the River Leine in Hannover and the River Weser in Holzminden. Suspended particles were filtered off using silanized glass wool. The samples were extracted using SPE and SPME. The chromatograms of the spiked River Leine sample (see Fig. 6), where extraction was done by the SPME technique, show less interferences of the matrix, especially of the emission line of carbon at 193 nm, as compared to the analogue determination of a spiked water sample from the River Weser (see Fig. 7 and Table 6) using the SPE technique. Thus, a chromatogram monitoring the carbon emission lines is even less selective than a chromatogram obtained by FID, as almost every matrix compound contains carbon and will thus give a response for the carbon-selective detection mode. Even more selectivity is gained if the sulfur emission line at 181 nm is monitored. From these observations, one can conclude that the SPME fiber leads to a more selective extraction of pesticides than the SPE adsorption material. The total number of non-target compound peaks, observed in a chromatogram taken in a non-specific detection mode is higher in SPE preconcentration than in SPME.

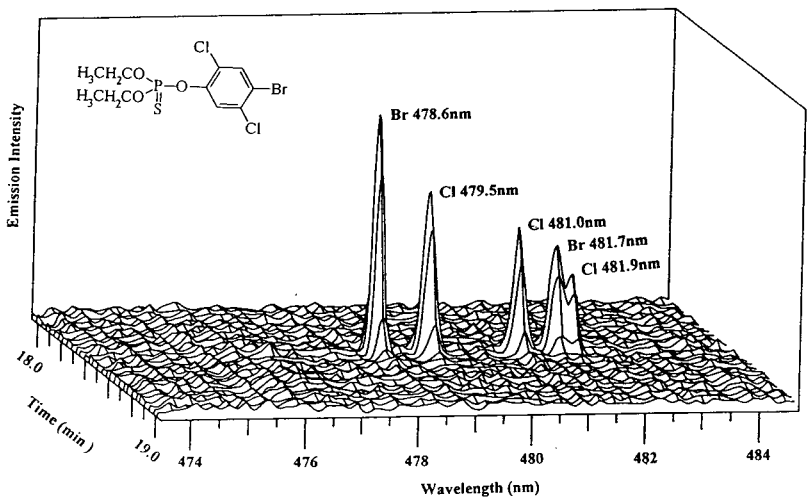

Fig. 5. Three-dimensional snapshot from the GC analysis of a spiked (60 ppb) environmental water solution (River Leine in Hannover) containing six organophosphorus pesticides using SPME (same mixture of pesticides as shown in Fig. 4); typical chlorine and bromine emission lines can be identified for the compound bromophos-ethyl at retention time 18.46 min.

4. Conclusions

The element-specific GC–AED allows a tunable specificity and is therefore a useful tool for element characterization of compounds. For instance, the presence of chlorine in a compound can be readily detected with AED in its normal operation mode (i.e. chlorine emission line Cl 479 nm) and confirmed by the wavelength snapshot technique (a small part of the emission spectra of about 50 nm; see three-dimensional snapshot of bromophos-ethyl in Fig. 5). Thus, an unknown compound in an environmental sample can be characterized as a substance which either contains the element chlorine or not. Identification of pesticides in environmental samples can be verified not only by one but by all characteristic element emission lines. The exclusion of

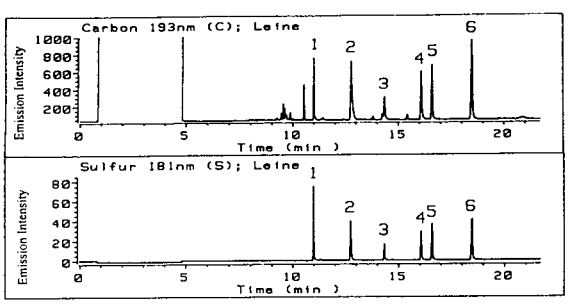

Fig. 6. Chromatogram of an environmental water sample from the River Leine in Hannover (Lower Saxony, Germany) using SPME; AED response of carbon at 193 nm and of sulfur at 181 nm is shown from obtained matrix compounds and six pesticides; sample was spiked (60 ppb) with six organophosphorus pesticides [ethoprophos (1), diazinon (2), parathion-methyl (3), parathion-ethyl (4), bromophos-methyl (5) and bromophos-ethyl (6)].

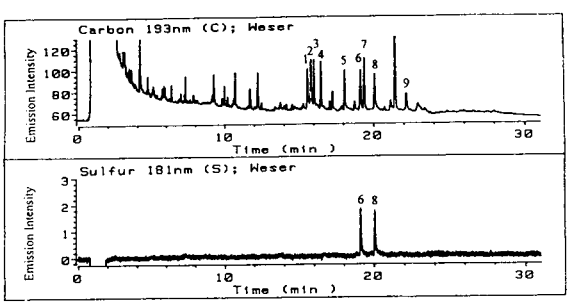

Fig. 7. Analysis of a spiked (1 ppb) environmental water sample from the River Weser in Holzminden (Lower Saxony, Germany) using SPE; AED response of carbon at 193 nm and of sulfur at 181 nm is that obtained from matrix compounds and nine pesticides [simazine (1), atrazine (2), propazine (3), terbuthylazine (4), sebuthylazine (5), metribuzin (6), vinclozolin (7), ametryn (8) and cyanazine (9)]; SPE sample preparation (C_{18} adsorbent).

Table 6
Analysis of a spiked (1 ppb) environmental water sample[a] from the River Weser in Holzminden[b] using SPE with C_{18} adsorbent material; limits of detection[c] are shown for all pesticides using the emission lines of carbon at 193 nm and sulfur at 181 nm

Peak No.	Compound	Molecular formula	Retention time (min)	Limit of detection[c], C 193 nm (pg)	Limit of detection[c], S 181 nm (pg)
1	Simazine	$C_7H_{12}ClN_5$	15.51	37	-
2	Atrazine	$C_8H_{14}ClN_5$	15.74	37	-
3	Propazine	$C_9H_{16}ClN_5$	15.94	32	-
4	Terbuthylazine	$C_9H_{16}ClN_5$	16.42	30	-
5	Sebuthylazine	$C_9H_{16}ClN_5$	18.06	34	-
6	Metribuzin	$C_8H_{14}N_4OS$	19.13	33	223
7	Vinclozolin	$C_{12}H_9Cl_2NO_3$	19.38	35	-
8	Ametryn	$C_9H_{17}N_5S$	20.07	48	300
9	Cyanazine	$C_9H_{13}ClN_6$	22.21	50	-

[a] Suspended particles of the sample are filtered off using silanised glass wool.
[b] River Weser in Holzminden (district of Lower Saxony, Germany), sampling date 9 May 1993.
[c] Limit of detection of the instrument; signal-to-noise ratio = 3.

spectral interferences is possible by observing all the characteristic element emission lines, i.e. sulfur (S 181.7 nm, S 182.0 nm and S 182.6 nm) or chlorine (Cl 479.5 nm, Cl 481.0 nm and Cl 481.9 nm). The tuning of selectivity using AED is limited due to the minimum detectable amount of a compound at different element emission lines (see Fig. 4). Environmental water samples show a wide range of disturbing matrix interferences from non-target pollutants despite some selective sample preparation steps. In these cases, additional selectivity is gained from the element-selective detection mode of GC–AED. The monitoring of sulfur at 181 nm allows a specific AED analysis of all investigated organophosphorus pesticides (see Fig. 8). The sulfur emission line was monitored, because it is much more sensitive than the phosphorus emission line, which shows always a very high specificity for these compounds. Furthermore, all matrix compounds, which interfere in the detection of carbon at 191 nm in some cases, could be

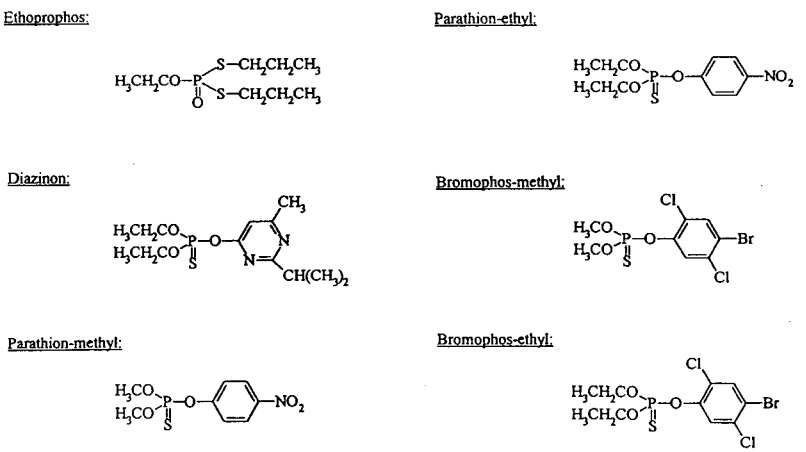

Fig. 8. Molecular structures of all investigated organophosphorus pesticides.

eliminated. In the analysis of real samples, it is suggested that the influence of non-target compounds might have been the major effect on the adsorbent material. So selectivity is most frequently gained from a detection system with a high specificity.

The selectivity of an analysis method which employs GC can be substantially enhanced when using element-specific detection such as AED, although AED is substantially less sensitive than conventional GC detectors. A MS detector would be even more specific than an AED, if pesticides have to be identified which are in the MS library. However, for unknown compounds (such as metabolites) and samples, the information gained from AED may even be superior to that from MS. Furthermore, typical element emission lines can be monitored using AED for verification of unknown compounds and for excluding interferences in the chromatogram [8,9]. Non-target substances can be separated into different compound classes, i.e. organochlorine compounds, using element-specific detection.

SPE is, in general, a useful determination technique of pesticides from aqueous matrix, where 1-l water sample spiked with 1 μg/l of each pesticide was used for extraction, as shown in Fig. 7. This leads to an enrichment factor of about 1000, if the final sample volume is 1 ml. If we compare the total amount of sample, which is necessary for the extraction and determination, SPE needs liter amounts and SPME only a few ml volume of the sample. Much more important for sample preparation steps is the time spent in using the different techniques. SPME is, however, very fast (20 min are needed for the total sample preparation up to the GC analysis step) compared to SPE, which needs about 2.5–3 h before the GC analysis can be done.

SPME is a simple, inexpensive, rapid and solvent-free sample preparation technique. Volatile pesticides can be efficiently isolated from aqueous environmental samples. This method shows a precision of 8–12% (R.S.D.), depending on the compound. Furthermore, this technique is capable of LODs in the ppb and sub-ppb range. Typical LODs for all investigated compounds are between 0.5 and 3 μg/l using AED. The adsorption and desorption times have been optimized. Typical saturation effects concerning the adsorption maximum can be observed at 15–20 min adsorption times for most pesticides. Determination of these pesticides in environmental water matrices, and in spiked river water has been shown. These samples can be detected with a high selectivity, which is gained from AED. Elements, which are only part of the target compounds and an even smaller part of non-target substances can be easily detected by their typical emission lines in these matrices and can be identified by them. The results demonstrate the suitability of the SPME approach to analysis of these polar compounds. Further investigations concerning the adsorption of different compound classes to the SPME fiber will be described by us in the future.

Acknowledgement

Financial support from the EU (Project EV5V-CT92-0061) is gratefully acknowledged.

References

[1] R. Eisert, K. Levsen and G. Wünsch, *J. Environ. Anal. Chem.*, (1994) in press.
[2] M. Cooke, D.A. Leathard, C. Webster and V. Rogerson, *J. High Resolut. Chromatogr.*, 16 (1993) 660.
[3] Z.V. Skopec, R. Clark, P.M.A. Harvey and R. Wells, *J. Chromatogr. Sci.*, 31 (1993) 445.
[4] Y. Zeng, J.A. Seeley, T.M. Dowling, P.C. Uden and M.Y. Khuhawar, *J. High Resolut. Chromatogr.*, 15 (1993) 669.
[5] O.F.X. Donard and F.M. Martin, *Trends Anal. Chem.*, 11 (1992) 17.
[6] C.L. Arthur, L.M.S. Motlagh, M.Lim, D.W. Potter and J. Pawliszyn, *Environ. Sci. Technol.*, 26 (1992) 979.
[7] K.D. Buchholz and J. Pawliszyn, *Anal. Chem.*, 66 (1994) 160.
[8] B.D. Quimby and J.J. Sullivan, *Anal. Chem.*, 62 (1990) 1027.
[9] P.C. Wylie and B.D. Quimby, *J. High Resolut. Chromatogr.*, 12 (1989) 813.

ELSEVIER

Journal of Chromatography A, 683 (1994) 185–193

JOURNAL OF CHROMATOGRAPHY A

Analysis of pesticide residues in food using gas chromatography–tandem mass spectrometry with a benchtop ion trap mass spectrometer

Steve Schachterle[a,*], Robert D. Brittain[a], John D. Mills[b]

[a]*Varian Chromatography Systems, 2700 Mitchell Drive, Walnut Creek, CA 94598, USA*

[b]*Varian, Ltd., Manor Road, Walton-on-Thames, Surrey KT12 2QF, UK*

Abstract

Recent developments on the Saturn GC–MS system offer enhanced capabilities for both the ion isolation and collision-induced dissociation steps in GC–MS–MS. With these improvements, benchtop GC–MS–MS can improve the detection limit of mass spectrometers for low-level target compounds in complex matrices. With this brief study of malathion, we demonstrate (1) excellent sensitivity, (2) wide dynamic range and (3) effective elimination of chemical background. GC–MS–MS is compared to standard GC–EI-MS and GC–CI-MS techniques for the analysis of malathion in orange extract. GC–MS–MS is the most selective and sensitive technique, virtually eliminating the background interference. Product ion mass spectra are invariant across the chromatographic peak and excellent linearity is observed over a range from 2.2 pg/μl to 2.2 ng/μl for malathion. Detection limit by GC–MS–MS was estimated at 0.5 μg/kg in the orange oil matrix ($S/N = 5$).

1. Introduction

The analysis of pesticides in food receives much attention because of concern over the possible long-term effects of exposure to even low levels of pesticides. Because analytical protocols are beginning to focus on health-based limits, detection and quantitation at extremely low levels is desirable. Following solvent extraction of a food sample, background matrix components are present at levels many times those of the target pesticides, complicating the detection of these minor components. Sample cleanup steps prior to analysis can reduce interference problems in part; capillary gas chromatography (GC) then provides a further separation step for the analysis. GC coupled to mass spectrometry (MS) can be used to achieve selective detection of target pesticide components in the presence of the complex matrix. However, the detection limits attainable are set by the levels of interfering ions from the matrix, which can obscure the signal from the target compound. Tandem mass spectrometry (MS–MS) is an approach which reduces the background due to the complex matrix by excluding all ions except the parent ion, which can then be dissociated to produce a unique product ion mass spectrum [1]. Because the number of ions which can be stored in an ion trap is limited, this reduction in background makes it possible to increase the ionization time and store more of

* Corresponding author.

0021-9673/94/$07.00
SSDI 0021-9673(94)00495-U

the desired ion, thus achieving dramatic reductions in the detection limit.

Ion-trap MS–MS offers several advantages compared to multi-sector or multi-quadrupole instruments, since the steps are carried out tandem-in-time rather than tandem-in-space [2]. Because it is not necessary to transmit the ions from one sector (or quadrupole) to another, there are no transmission losses. Also, the MS–MS efficiency is generally higher in the ion trap. In the collision-induced dissociation (CID) process in the ion trap, the translational kinetic energy of an ion is increased by coupling in external energy. As this energetic ion undergoes elastic collisions with the background gas, some of the kinetic energy will be converted to sufficient internal energy to cause fragmentation. In the ion trap, this energy is usually supplied by applying external voltages. The first workers used resonant excitation, where a single frequency matching the secular frequency of the parent ion was applied [3]. With the radio frequency (RF) trapping field held constant, difficulties arose in maintaining the excitation frequency exactly at the resonant frequency of the parent ion. The frequency had to be empirically tuned and required adjustments as the secular frequency varied with changing concentration due to space charging in the ion trap [2,4]. In order to reduce the stringent frequency requirements, subsequent approaches have applied more than one frequency through various means [5–10].

Recent developments in ion isolation in the ion trap provide very precise isolation of the parent ion and thereby lessen the requirements for selective ion excitation [11]. By modulating the RF trapping field, the secular frequency of the ion may be modulated in and out of resonance with a constant supplementary frequency applied to the endcaps. This modulated resonant excitation alleviates the strict frequency-tuning requirements previously encountered. Another approach to less selective excitation is non-resonant excitation [12], where the trapping field is rapidly changed, instantaneously increasing the kinetic energy of all ions in the trap. These recent developments in isolation and excitation greatly enhance the performance of ion-trap MS–MS. These techniques use MS–MS control parameters which are virtually independent of sample or matrix concentration and which may be calculated rather than optimized experimentally. These developments have simplified GC–MS–MS to the point that it can become a routine analytical technique. As an example, this work demonstrates the applicability of GC–MS–MS to the analysis of the pesticide malathion in orange extract.

2. Experimental

A Saturn 3 ion-trap GC–MS system (Varian, Walnut Creek, CA, USA) equipped with a Wave-Board was used for all experiments. The Wave-Board platform generates user-created, time-programmed wave forms for application to the ion-trap electrodes. For these studies, breadboard MS–MS software was used to create and insert intermediate segments between ionization and mass analysis steps in the scan function to achieve isolation and CID on stored electron impact (EI) ions from malathion (see Fig. 1). These segments were applied to both the automatic gain control (AGC) prescan and the analytical scan. Broadband isolation wave forms were applied to the endcap electrodes during and after ionization to eject unwanted ions above and below the parent ion and to selectively store a narrow range of ions around the parent ion [11]. In a two-step process, resonant ejection then removed all remaining ions below and then above the parent ion mass. The energy for CID was supplied by either non-resonant excitation [12] or modulated resonant excitation [11]. Non-resonant excitation causes an instantaneous shift in the equilibrium position of stored ions, with an accompanying increase in kinetic energy due to the restoring force of the applied fields. The modulated resonance approach applies a calculated near-resonant frequency to the endcap electrodes while the RF voltage on the ring electrode is modulated over a narrow range. With this approach, a range of resonant frequencies is effectively applied to the ions in the

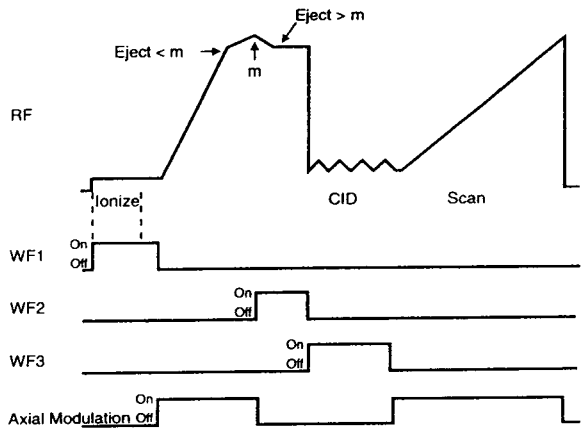

Fig. 1. Scan function showing timing of applied wave forms for modulated resonant excitation. The curve labeled RF is applied to the ring electrode. The timing diagram for the other wave forms shows when they are applied to the end caps. WF1 is an ion ejection wave form, applied during and after ionization. WF2 is a broadband ion ejection wave form, applied during ejection of masses higher than the parent mass. WF3 is a sine wave matching the secular frequency of the parent ion, applied during the CID step. The axial modulation wave form is applied during low mass ejection and also during the analytical scan.

trap. Since application of the exact resonant frequency is not required, the modulated resonant CID approach is not sensitive to shifts of secular frequency of parent ions with concentration. Thus, a greater linear dynamic range can be achieved. Whether the non-resonant or modulated resonant approach is used, the optimal excitation voltage for the CID step must be determined experimentally.

Malathion (PolyScience, Niles, IL, USA) was dissolved in methylene chloride (J.T. Baker, Phillipsburg, NJ, USA) to prepare standards over the concentration range from 2.2 pg/μl to 22 ng/μl. Two oranges were pureed and then extracted for several hours in 500 ml of methylene chloride. The entire extract was filtered into a separatory funnel. After settling, the methylene chloride phase was drawn off and evaporated to give a final solution in which 1 μl was equivalent to 5 mg of the original fruit. This final extract was then spiked with malathion at the 10 pg/μl level and at the 75 pg/μl level. Injections were 1 μl.

Capillary column: DB-5 (J & W, Folsom, CA, USA), 30 m × 0.25 mm I.D., 0.25 μm film thickness. Column program: hold at 70°C for 1 min. Ramp to 270°C at 10°C/min. Hold for 4 min. Injector: temperature-programmable, cold on-column injector (Varian SPI) with high-performance insert, programmed as follows: hold at 25°C for 0.5 min. Ramp to 260°C at 180°C/min. Hold for 21 min. Helium was used as the carrier gas at a linear velocity of approximately 35 cm/s. The transfer line was held at 260°C and the ion-trap manifold was set to 195°C. The mass spectrometer analytical scan rate was 1 s/scan.

3. Results and discussion

3.1. Full-scan and MS–MS spectra of malathion

The full-scan EI mass spectrum of malathion is shown in Fig. 2A, as are the product ion spectra resulting from CID of parent ions m/z 158 (B) or m/z 173 (C). These parent ions correspond to the ester and phosphate fragments in the malathion molecule, as shown in Fig. 3. Note that the molecular ion at m/z 330 is not observed in the full-scan EI mass spectrum; therefore the MS–MS approach for malathion requires the isolation and CID of a malathion fragment ion. The product ion spectra for the two chosen parent ions consist of a subset of fragment ions from the complete malathion mass spectrum. Thus, one can identify fragmentation pathways in MS–MS by the successive isolation and CID of different ions from the full-scan mass spectrum. After investigating the m/z 158 and m/z 173 fragment ions, we chose the m/z 173 ion for quantitative studies because it exhibited the least chemical background interference and the most intense signals.

3.2. Isolation and CID

The m/z 173 ion was isolated using a two-step process, first eliminating ions below m/z 173 then removing those ions above m/z 173 [11]. The excitation voltage near the resonant fre-

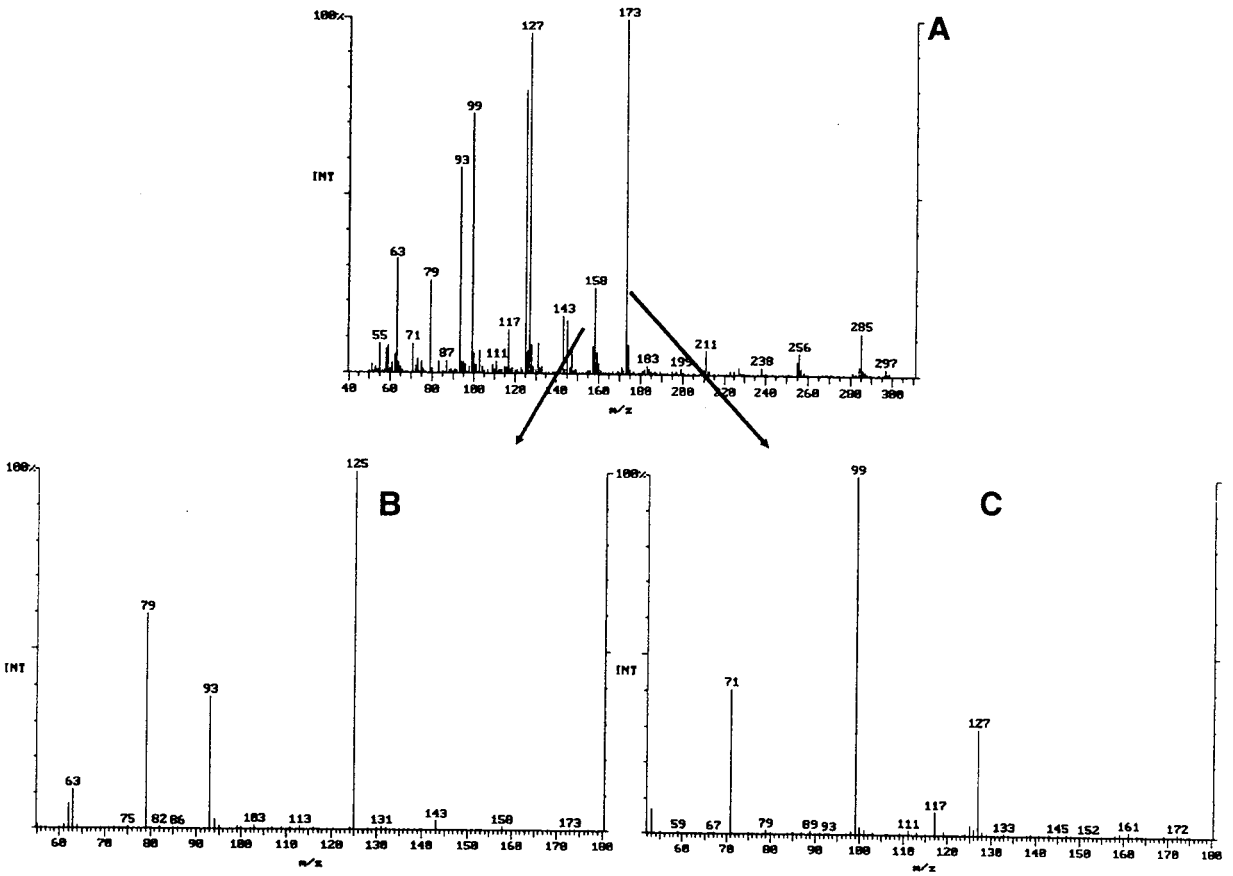

Fig. 2. EI-MS mass spectrum (A) of malathion standard with CID product ion spectra from m/z 158 (B) and m/z 173 (C) ions. Non-resonant excitation was used for CID; 40 V for 20 ms. Note that the product ions arising from m/z 158 form a distinct subset from those coming from m/z 173.

quency for m/z 173 (95 kHz) was applied for 10 ms at an amplitude of 1 V while the RF voltage was modulated over a range of ± 0.8 u, corresponding to ± 5 digital to analog converter (DAC) steps. The product ion spectrum for malathion under these conditions is shown in Fig. 4. The MS–MS process is an ion filter for the reduction of background —only those m/z 145, 127, 117 and 99 ions produced from the m/z 173 parent ion will appear in the malathion MS–MS spectrum.

The early ion-trap MS–MS approach of empirically tuning the excitation frequency exactly to the resonant frequency of the parent ion is of limited value for GC–MS–MS because the resonant frequency of parent ions varies with concentration during elution of GC peaks. Using the Wave-Board approach of modulating the RF trapping field during the excitation step, the calculated (not experimentally determined) frequency is close enough to cause dissociation. In addition, variation in resonant frequency with sample concentration does not affect the efficiency of the CID step. Also, because unit mass isolation is achieved during the isolation step, the frequency can be varied without creating unwanted product ions and the spectrum is cleaner, containing only undissociated parent ions and product ions. Fig. 4 shows the MS–MS mass spectrum from the m/z 173 parent ion of malathion at the apex and near the baseline of the chromatographic peak (1.7 ng on-column).

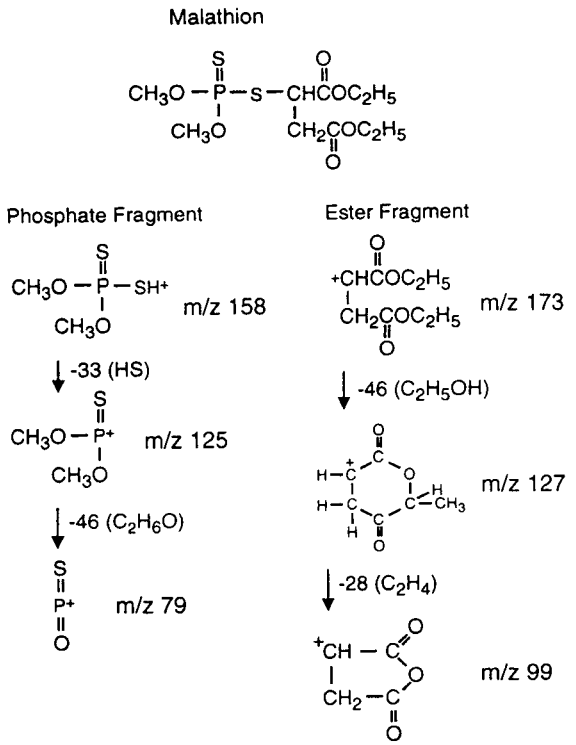

Fig. 3. Proposed fragmentation pathways for the phosphate fragment (m/z 158) and for the ester fragment (m/z 173) of malathion (M_r 330).

The ratios of the product ions are virtually identical.

3.3. Optimization of resonant and non-resonant CID

Breakdown curves show the intensity of product ions versus the applied excitation voltage. They offer a convenient means for selecting the optimum excitation voltage. The analyst might prefer to choose a CID voltage which produces primarily one product ion to achieve maximum sensitivity. Alternatively, a different voltage might be chosen so that additional product ions are present for increased confidence in identification. The breakdown curve for CID of the m/z 173 ion of malathion by modulated resonant excitation is shown in Fig. 5A. There is a wide voltage range over which the intensity of product ions is fairly constant. In a comparable breakdown curve for m/z 173 by non-resonant excitation (Fig. 5B), the maxima for the various product ions are much better defined and show less overlap. Resonant excitation at an applied voltage of 1.0 V was chosen for the quantitative aspects of this study using an excitation time of 10 ms and a modulation range of ± 0.8 u.

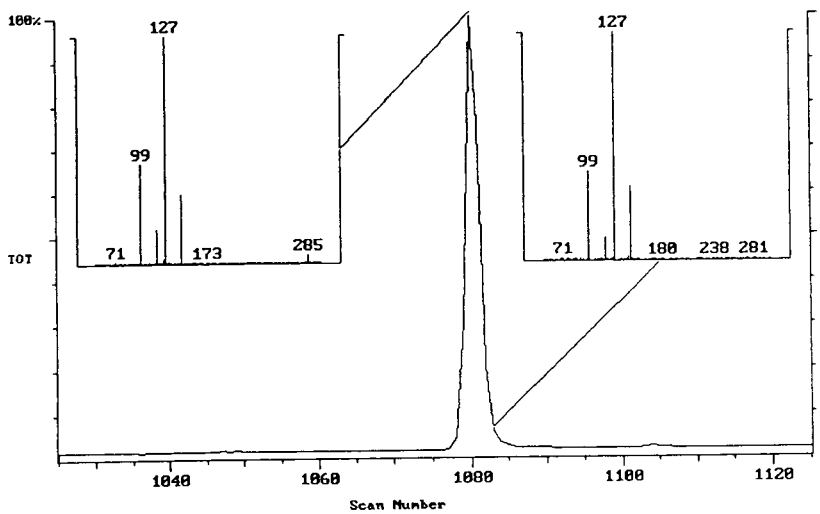

Fig. 4. CID product ion spectrum for malathion standard (1.7 ng injected) showing constant ion ratios across the chromatographic peak. Resonant excitation, 1 V for 10 ms, modulate RF ± 0.8 u at 1000 μs/DAC step.

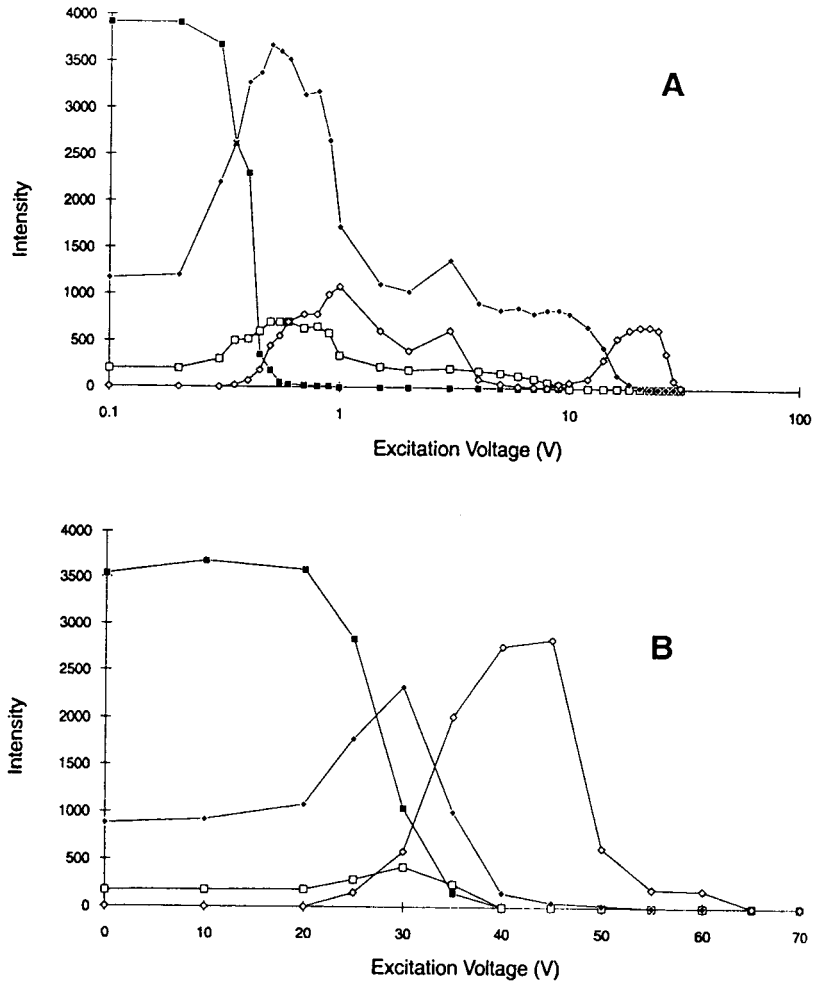

Fig. 5. Breakdown curves for malathion. (A) Resonant excitation, 5 ms, modulate ± 0.8 u at 28 μs/DAC step. (B) Non-resonant excitation, 5 ms, RF = 300. ■ = m/z 173; □ = m/z 145; ◆ = m/z 127; ◇ = m/z 99.

3.4. Linearity

To examine the linearity and dynamic range of the MS–MS approach, an external standard calibration curve was prepared based on the peak area of the quantitation ion at m/z 127 vs. concentration between 2.2 pg/μl and 22 ng/μl. The calibration curve for 11 points is linear between 2.2 pg/μl and 2.2 ng/μl with a correlation coefficient of 0.9997, a slope of 221 ± 1.4 area counts/pg and an intercept of 1960 ± 1240 area counts. This large linear range is evidence that the efficiency of the CID process does not change with analyte concentration. It also shows how well AGC maintains a constant amount of charge within the ion trap, regardless of the concentration.

3.5. Detection limit in the orange matrix

The whole-orange extract provides a rich matrix to evaluate the EI-MS, CI-MS and EI-MS–MS approaches. The results of this comparison are shown in Figs. 6–8. The spike levels for malathion were at 75 pg/μl (15 μg/kg orange) for the EI-MS and CI-MS runs, and at 10 pg/μl

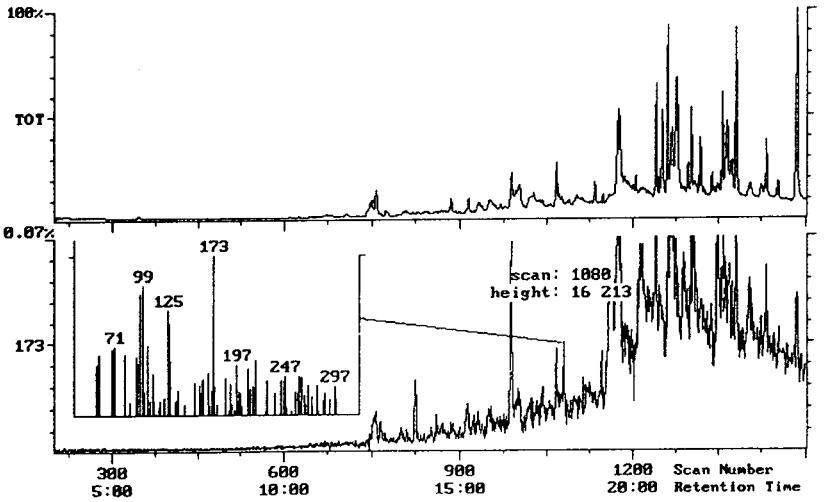

Fig. 6. Standard EI-MS chromatogram of 75 pg/μl malathion in orange extract. Top trace is total ion chromatogram, 100% = 44 221 629. Lower trace is selected ion chromatogram for m/z 173; $S/N = 5.2$. Inset mass spectrum is background subtracted. Time in min.

(2 μg/kg orange) for the EI-MS–MS run. Each figure shows the total ion current chromatogram as well as the mass chromatogram for the chosen quantitation ion. A variety of oil components coelutes with and obscures the malathion peak in standard EI-MS (Fig. 6). One qualitative measure of the level of sample contamination is the ion count for the tallest chromatographic peak, which is listed in the caption for each figure. The result for the EI-MS run is in excess of 40 000 000 counts. A conventional approach to reduce matrix interference is CI-MS when the analyte of interest is more likely to be ionized that the matrix components. As shown in Fig. 7, another advantage of CI is the appearance of the M + 1 ion at m/z 331. Significant reduction of

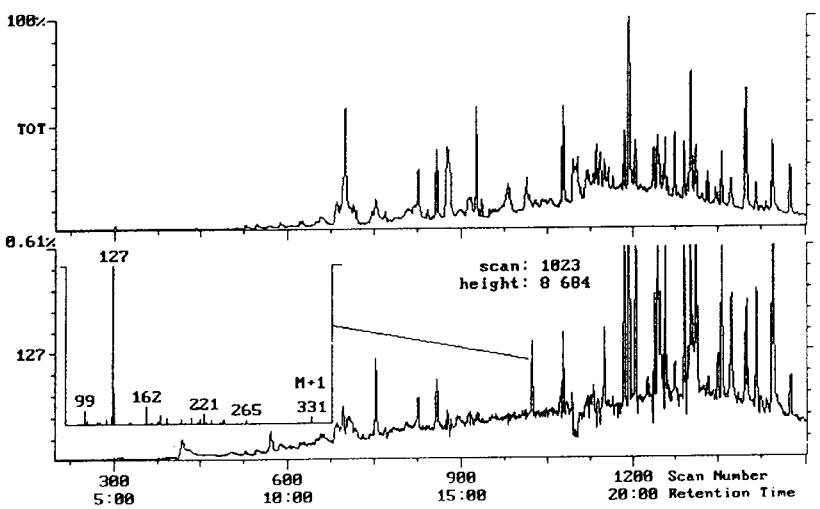

Fig. 7. CI-MS chromatogram of 75 pg/μl malathion in orange extract. Top trace is total ion chromatogram, 100% = 2 593 448. Lower trace is selected ion chromatogram for m/z 127; $S/N = 17.5$. Inset mass spectrum is background subtracted. CI reagent gas is methane. Time in min.

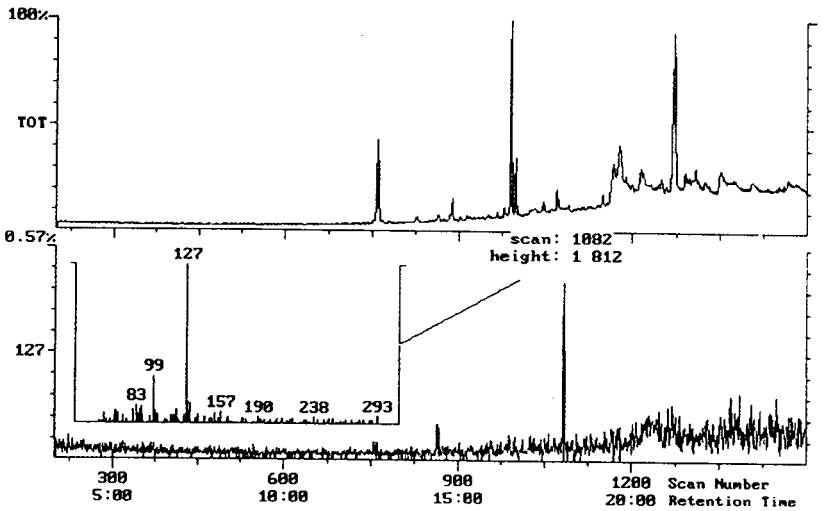

Fig. 8. MS–MS chromatogram of 10 pg/μl malathion in orange extract. Top trace is total ion chromatogram, 100% = 317 739. Lower trace is selected ion chromatogram for m/z 127; $S/N = 23.6$. Inset mass spectrum is background subtracted. CID: resonant excitation, 1 V, 10 ms, modulate ± 0.8 u at 1000 μs/DAC step. Time in min.

matrix interference was achieved for this sample with methane CI, although enough matrix components appear in the mass chromatogram to raise the detection limit. The ion count for the strongest peak is reduced to less than 3 000 000 counts. MS–MS is the most selective technique, virtually eliminating the background, and gives the best detection limit for malathion (Fig. 8). The ion count for the strongest peak in the GC–MS–MS run is reduced to about 300 000 counts, a factor of >100 less than the figure from EI-MS. Table I shows the calculated detection limits for the three techniques. Comparing the area counts for the malathion peak using each technique, MS–MS may produce a lower peak area, but also the lowest contribution from the background (noise), allowing a few pg on-column to be easily detected. Fig. 9 compares the EI-MS (A) and EI-MS–MS (B) mass spectra from the scan at the apex of malathion elution. Both runs are at the 75 pg/μl spike level, and both spectra are shown without background subtraction. Note the increase in ionization time from 185 μs in the EI-MS approach to 8196 μs in the MS–MS approach. As discussed earlier, the improved detection limit of the MS–MS technique in complex samples is a result of two factors: the increase in ionization time allowed when a narrow range of ions is stored during ionization, and the filtering effect of removing all background ions from the masses where the product ions are observed.

Table 1
Results of comparative analyses of malathion in orange extract

Technique	Injected amount (pg)	Quantitation ion	Peak area	S/N	Detection limit for $S/N = 5$ (μg/kg)
EI-MS	75[a]	173	23 786	5.2	14.5
CI-MS	75	127	12 973	17.5	4.3
EI-MS–MS	75	127	16 140	147.1	0.5

[a] 75 pg injected corresponds to 15 μg/kg of orange.

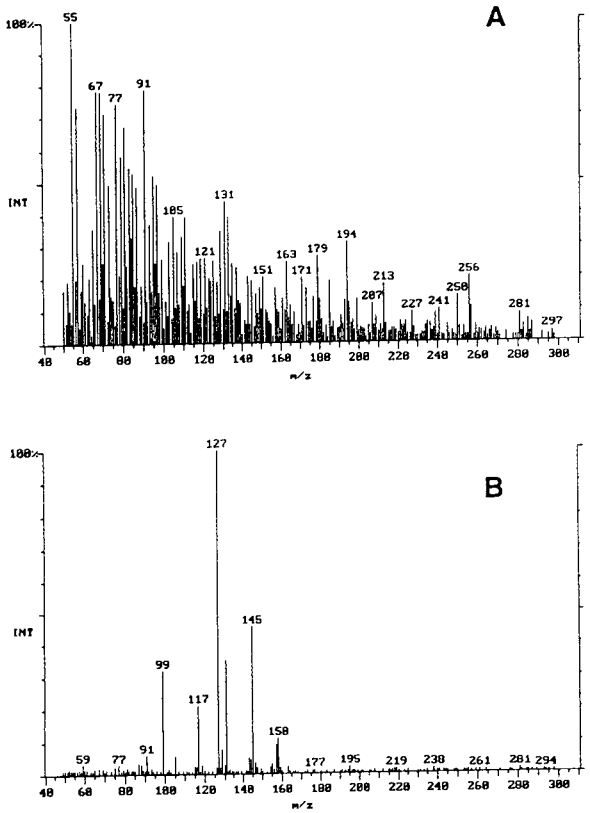

Fig. 9. MS compared with MS–MS for discrimination against chemical matrix. Mass spectra are from the apex of a chromatographic peak of 75 pg of malathion in orange extract and are not background subtracted. (A) EI-MS; ionization time calculated by AGC was 185 μs. (B) MS–MS; ionization time calculated by AGC was 8196 μs.

4. Conclusions

Using resonant methods of ion isolation and either non-resonant or modulated resonant excitation for CID, ion-trap GC–MS–MS is reliable and easy to automate, offering a convenient way to analyze target compounds in a complex sample matrix. Isolation and CID of individual fragment ions also provide fragmentation pathway information to elucidate molecular structures. GC–MS–MS was compared to two other GC–MS techniques for the analysis of malathion in orange extract. Whereas EI-MS and CI-MS are clearly viable techniques, MS–MS provides superior linear response, dynamic range, and detection limit for the analysis of malathion and should also provide a routine analytical technique for a wide variety of samples in many matrices.

References

[1] J.V. Johnson and R.A. Yost, *Anal. Chem.*, 57 (1985) 758A–768A.
[2] J.V. Johnson, R.A. Yost, P.E. Kelley and D.C. Bradford, *Anal. Chem.*, 62 (1990) 2162–2172.
[3] J.N. Louris, R.G. Cooks, J.E.P. Syka, P.E. Kelley, G.C. Stafford and J.F.J. Todd, *Anal. Chem.*, 59 (1987) 1677–1685.
[4] J.F.J. Todd, *Mass Spectrom. Rev.*, 10 (1991) 3–52.
[5] F. Vedel, M. Vedel and R.E. March, *Int. J. Mass Spectrom. Ion Processes*, 108 (1991) R11–R20.
[6] J.F.J. Todd, A.D. Penman, D.A. Thorner and R.D. Smith, *Rapid Commun. Mass Spectrom.*, 4 (1990) 108–113.
[7] S.A. McLuckey, D.E. Goeringer and G.L. Glish, *Anal. Chem.*, 64 (1992) 1455–1460.
[8] R.E. March, *Int. J. Mass Spectrom. Ion Processes*, 118 (1992) 71–135.
[9] R.K. Julian and R.G. Cooks, *Anal. Chem.*, 65 (1993) 1827–1833.
[10] G.J. van Berkel and D.E. Goeringer, *Anal. Chim. Acta*, 277 (1993) 41–54.
[11] B. Bolton, G. Wells and M. Wang, presented at the *41st ASMS Conference on Mass Spectrometry and Allied Topics, San Francisco, CA, 1993*, abstracts p. 474a.
[12] M. Wang and G. Wells, presented at the *41st ASMS Conference on Mass Spectrometry and Allied Topics, San Francisco, CA, 1993*, abstracts p. 463a.

ELSEVIER

Journal of Chromatography A, 683 (1994) 195–202

JOURNAL OF CHROMATOGRAPHY A

Comparison of derivatization procedures for the determination of diuretics in urine by gas chromatography–mass spectrometry

D. Carreras*, C. Imaz, R. Navajas, M.A. Garcia, C. Rodriguez, A.F. Rodriguez, R. Cortes

Laboratorio de Control de Dopaje, C.N.I.C.D., Consejo Superior De Deportes, C/Greco s/n, 28040 Madrid, Spain

Abstract

Three different GC–MS screening procedures, which use different ways of derivatization (methylation), are compared. In the first one, derivatization with iodomethane in acetone and a previous solid–liquid extraction is used; the second one is based on an extractive alkylation method using iodomethane in toluene (liquid–liquid extraction); and the last one is flash methylation by pyrolysis of tetraalkylammonium salts in the injector of the gas chromatograph using trimethylanilinium as the derivatization agent. The speed of the extraction, reproducibility and accuracy have been compared for 20 diuretics including the ones most often used in sports, such as bumetanide, ethacrynic acid, acetazolamide, dichlorphenamide, furosemide, hydroflumethiazide, hydrochlorothiazide and chlorthalidone; they have also been applied to the two uricosuric agents probenecid and benzbromarone.

1. Introduction

Diuretics are therapeutic agents used in the treatment of edema and hypertension resulting from cardiac or renal failure [1].

Uricosuric agents increase urinary excretion of uric acid, and hence they are effective compounds for the treatment of gout.

Diuretics and uricosuric agents are on the doping list of pharmaceutical forbidden substances indicated by the Medical Commission of the International Olympics Committee (IOC) [2].

As diuretics are drugs used to increase the volume of urine excreted by the kidneys, they are employed as doping substances first to reduce the body weight in sports with weight categories, and secondly so as not to detect other doping agents properly by reducing their concentrations in urine.

Probenecid, an uricosuric agent, is what athletes use as masking substance to reduce urinary excretion of anabolic steroids.

Diuretics are usually classified according to their pharmacological properties into four different groups: carbonic anhydrase inhibitors (such as acetazolamide and dichlorphenamide), thiazide (i.e. bendroflumethiazide, chlorothiazide and hydrochlorothiazide) and thiazide type (e.g. clopamide and chlorthalidone), loop (such as bumetanide, ethacrynic acid and furosemide), and potassium-sparing diuretics (i.e. triamterene) [3].

The detection and determination of these drugs in biological fluids is quite complex specially due to their variety of chemical structures (Fig. 1).

There are several methods available for the

* Corresponding author.

0021-9673/94/$07.00
SSDI 0021-9673(94)00657-I

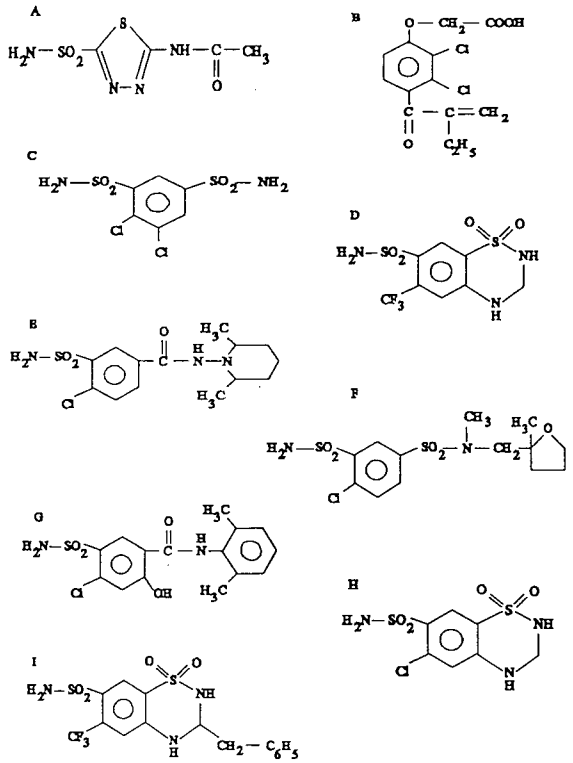

Fig. 1. Structures of diuretics. A = Acetazolamide; B = ethacrynic acid; C = dichlorphenamide; D = hydroflumethiazide; E = clopamide; F = mefruside (I.S.); G = xipamide; H = hydrochlorothiazide; I = bendroflumethizide.

determination of individual diuretics by HPLC with UV detection [4–10] and with fluorescence detection [11–14]. Screening procedures by HPLC with UV detection [15–17] and with mass spectrometry (MS) detection [18,19], have also been reported.

Gas chromatography (GC) coupled with MS is a rapid and specific technique for the determination and identification of these drugs in urine [20,21].

The polar nature of probenecid and most diuretics makes the determination of these drugs by direct GC impossible. For this reason previous derivatization is needed; such derivatization is based on methylation of the sulfonamide group and other groups containing O- or N-bonded hydrogen atoms of the diuretics.

This work describes a comparison among three different GC–MS screening procedures which use different ways of methylation, for the determination and identification of 20 diuretics and 2 uricosuric agents in spiked urine. In the first one the methyl derivatives are obtained using iodomethane in acetone in an alkaline medium [22,23], together with previous solid–liquid extraction. The second one is based on an extractive alkylation method using iodomethane in toluene and tetrahexylammonium hydrogensulphate as the phase transfer reagent, in a liquid–liquid extraction [24–26]. The last method is flash methylation by pyrolysis of tetraalkylammonium salts in the injector of the gas chromatograph using trimethylanilinium (TMA) as the derivatization agent as well as a previous solid–liquid extraction [27–29].

Positive urine samples taken from athletes are also analysed using the three derivatization procedures and are also compared.

2. Experimental

2.1. Reagents and chemicals

All reagents were of analytical grade. The reference drug samples acetazolamide, althiazide, bendroflumethiazide, benzbromarone, bumetanide, chlorothiazide, clopamide, chlorthalidone, dichlorphenamide, ethacrynic acid, furosemide, hydrochlorothiazide, hydroflumethiazide, indapamide, methyclothiazide, piretanide, probenecid, triamterene, trichlormethiazide and xipamide were from Sigma (St. Louis, MO, USA); polythiazide from Pfizer (Brussels, Belgium); mefruside was kindly provided by Bayer (Leverkusen, Germany). Methanol and acetone were obtained from Scharlau (Barcelona, Spain); nanograde toluene, silver sulphate, potassium carbonate, iodomethane and sodium hydroxide from Merck (Darmstadt, Germany); Amberlite XAD-2 and tetrahexylammonium hydrogensulphate from Serva (Heidelberg, Germany); and trimethylanilinium hydroxide from Regis (Morton Grove, IL, USA).

Table 1
Diuretics: number of methyl groups, retention times (t_R), k' values and characteristic ions with their relative abundances

Diuretic	No. of methyl groups	t_R (min)	k'	Characteristic ions, m/z (relative abundance, %)
Acetazolamide	3	3.62	0.684	249 (100), 43 (63), 108 (42), 83 (39), 264 (24)
Probenecid	1	3.90	0.814	270 (100), 135 (72), 199 (58), 271 (15), 104 (14)
Ethacrynic acid	1	4.02	0.870	261 (100), 263 (64), 243 (45), 45 (30), 316 (8)
Dichlorphenamide	4	5.15	1.39	44 (100), 253 (78), 255 (50), 108 (39), 360 (6)
Benzbromarone	1	6.29	1.92	278 (100), 438 (71), 173 (71), 440 (38), 439 (22)
Hydroflumethiazide	4	6.30	1.93	387 (100), 236 (56), 215 (54), 344 (50), 252 (46)
Chlorothiazide	3	6.55	2.05	44 (100), 248 (71), 275 (46), 169 (28), 277 (22)
Furosemide	3	6.95	2.23	81 (100), 372 (22), 96 (10), 339 (5)
Clopamide	2	6.97	2.24	111 (100), 112 (56), 127 (50), 55 (16), 139 (4)
Mefruside (I.S.)	2	7.43	2.46	85 (100)
Chlorthalidone	4	7.67	2.57	287 (100), 363 (68), 176 (63), 255 (56), 289 (32)
Bumethanide	3	7.71	2.59	406 (100), 363 (97), 254 (96), 318 (62), 196 (23)
Piretanide	3	8.40	2.91	295 (100), 296 (26), 404 (24), 266 (19), 297 (12)
Xipamide	3	8.72	3.06	276 (100), 277 (35), 168 (28), 396 (12), 233 (8)
Hydrochlorothiazide	4	9.01	3.19	353 (100), 310 (94), 218 (62), 202 (62), 288 (46)
Indapamide	3	9.01	3.19	161 (100), 132 (40), 131 (16), 407 (10)
Triamterene	6	9.15	3.26	336 (100), 322 (64), 169 (25), 309 (20), 338 (18)
Mefruside metabolite ([a])	2	9.80	3.56	99 (100), 325 (55), 327 (21), 218 (14),
Methyclothiazide	3	9.90	3.60	352 (100), 354 (51), 244 (12), 246 (4)
Trichlormethiazide	4	10.72	3.99	352 (100), 354 (45), 244 (15), 42 (15)
Polythiazide	3	11.01	4.12	352 (100), 354 (45), 244 (22), 42 (17), 246 (8)
Bendroflumethiazide	4	12.00	4.58	386 (100), 278 (25), 42 (16), 387 (15), 388 (12)
Althiazide	4	13.20	5.14	352 (100), 354 (39), 244 (22), 42 (18), 145 (11)

[a] 5-Oxomefruside.

2.2. Stock solutions

Stock solutions were prepared in methanol at a concentration of 100 μg/ml. The solutions were sealed and refrigerated at 4°C until use.

2.3. Internal standard solution

Mefruside was used as the internal standard (I.S.) and was also dissolved in methanol to 100 μg/ml.

2.4. Instrumentation

A Hewlett-Packard (HP, Palo Alto, CA, USA) Model 5890 Series II gas chromatograph connected to a Model 5971 A electron-impact (EI) mass-selective detector via a capillary direct interface was used. All chromatograms were obtained in the selected-ion mode (SIM). An HP fused-silica capillary column (25 m × 0.20 mm I.D., cross-linked 5% phenylmethylsilicone, film thickness 0.33 μm) was coupled to the ion source. The carrier gas was helium at a flow-rate of 1 ml/min and the split ratio was 10:1. The temperatures were: 280°C for the injector, 300°C for the detector, initial column temperature 230°C and final column temperature 320°C. The column temperature was increased at a rate of 35°C/min.

2.5. Analytical procedure

Procedure 1

To 5 ml of urine 10 μl of I.S. solution (100 μg/ml) was added and then the urine was passed through a Pasteur pipette (230 mm × 7 mm) containing a 20-mm plug of Amberlite XAD-2 resin. The resin was washed with 5 ml of deion-

Table 2
Comparison of the three derivatization procedures

Pharmacological properties	Diuretic	Derivatization (%)[a]		
		Iodomethane in acetone	Extractive methylation	Flash methylation
Loop	Bumetanide	51	62	100
	Ethacrynic acid	83	100	4
	Furosemide	28	19	100
	Piretanide	40	56	100
Thiazide	Althiazide	100	0	0
	Bendroflumethiazide	100	83	22
	Chlorothiazide	100	2	2
	Hydrochlorothiazide	89	100	85
	Hydroflumethiazide	57	62	100
	Methyclothiazide	100	19	0
	Polythiazide	99	100	0
	Trichlormethiazide	100	0	0
Thiazide-type	Clopamide	5	14	100
	Chlorthalidone	6	4	100
	Indapamide	35	24	100
	5-Oxomefruside[b]	100	5	70
	Xipamide	23	1	100
Carbonic anhydrase inhibitors	Acetazolamide	100	25	87
	Dichlorphenamide	98	100	57
Potassium sparing	Triamterene	100	0	50
Uricosuric agents	Benzbromarone	64	0	100
	Probenecid	48	60	100

[a] Percentages related to the highest signal (assigned the value 100) obtained for each diuretic.
[b] Metabolite of mefruside in physiological urine.

ized water, eluted with 2 ml of methanol and evaporated to dryness.

The residue was dissolved in 200 μl of acetone; then 20 μl of iodomethane and 100 mg of potassium carbonate were added. This solution was heated in a heating block at 60°C for 3 h and 4 μl of the derivative extract were injected into the GC–MS system.

Procedure 2

To 5 ml of urine in a 15-ml glass tube 10 μl of I.S. solution (100 μg/ml), 100 μl of 10 *M* sodium hydroxide, 150 μl of 0.2 *M* tetrahexylammonium and 5 ml of 0.5 *M* iodomethane solution in toluene were added. Then the urine was shaken for 20 min, centrifuged at 1500 *g* for 10 min and the organic fraction containing the methyl derivatives was transferred to another tube. The toluene fraction was washed with 3 ml of saturated silver sulphate solution, centrifuged at 1500 *g* for 10 min, decanted to another tube and taken it to dryness. The residue was dissolved in 100 μl of toluene and 4 μl of the solution were injected into the GC–MS system.

Table 3
Analytical accuracy and reproducibility of the three derivatization procedures in spiked urine ($n = 5$)

Diuretic	Iodomethane in acetone			Extractive methylation			Flash methylation		
	$\bar{x}$	S.D.	R.S.D. (%)	$\bar{x}$	S.D.	R.S.D. (%)	$\bar{x}$	S.D.	R.S.D. (%)
Acetazolamide	32.0	3.19	9.97	7.98	0.870	10.9	27.8	2.95	10.6
Althiazide	12.1	1.19	9.83	0	–	–	0	–	–
Bendroflumethiazide	335	23.1	6.89	278	25.1	9.03	73.7	7.52	10.2
Benzbromarone	23.0	1.52	6.61	0	–	–	35.9	2.98	8.30
Bumetanide	69.4	9.49	13.7	84.3	9.39	11.1	136	12.2	8.97
Clopamide	39.6	2.58	8.16	88.5	8.31	9.39	632	35.1	5.55
Chlorthalidone	29.3	2.32	7.92	19.5	2.12	10.8	488	30.9	6.33
Chlorothiazide	37.0	3.21	8.67	0.629	0.0963	15.3	0.740	0.101	13.7
Dichlorphenamide	141	17.8	12.6	144	12.5	8.68	82.1	7.61	9.27
Ethacrynic acid	184	21.0	11.4	222	21.1	9.50	8.88	0.834	9.39
Furosemide	47.9	4.89	10.2	32.5	2.49	7.66	171	12.4	7.25
Hydrochlorothiazide	150	20.1	13.4	168	15.1	8.98	143	12.9	9.02
Hydroflumethiazide	211	24.9	11.8	229	21.0	9.17	370	13.8	3.73
Indapamide	15.1	1.41	9.34	10.4	1.10	10.6	43.2	3.72	8.61
Methyclothiazide	24.8	2.60	10.5	4.74	0.491	10.3	0	–	–
Piretanide	126	11.1	8.81	176	14.2	8.07	315	22.3	7.08
Polythiazide	98.5	9.81	9.96	99.6	9.11	9.14	0	–	–
Probenecid	1006	118.9	11.82	1258	109.0	8.664	2096	162.0	7.729
Triamterene	7.19	0.891	12.4	0	–	–	359	0.482	13.4
Trichlormethiazide	0.772	0.102	14.1	0	–	–	0	–	–
Xipamide	71.3	9.30	13.0	2.48	0.293	11.8	310	24.3	7.84

The mean has been determined by the peak area ratio of the diuretic base peak to the internal standard base peak. In all cases 0.5 μg/ml of each diuretic and the internal standard have been added. Means and standard deviations have been multiplied by 1000.

Procedure 3

To 5 ml of urine 10 μl of I.S. solution (100 μg/ml) was added and then the urine was passed through a Pasteur pipette (230 mm × 7 mm) containing a 20 mm plug of Amberlite XAD-2 resin. The resin was washed with 5 ml of deionized water, eluted with 2 ml of methanol and evaporated to dryness.

The residue was dissolved in 25 μl of TMA and 1 μl of the solution was injected into the GC–MS system.

3. Results

Table 1 reports the retention time (t_R), the k' values and the characteristic ions used for the identification of diuretics methyl derivatives, as well as their relative abundances. There are several derivatives which coelute such as monomethylbenzbromarone/tetramethylhydroflumethiazide, trimethylfurosemide/dimethylclopamide, tetramethylchlorthalidone / trimethylbumetanide and tetramethylhydrochlorothiazide/trimethylindapamide.

As the diuretics which coelute show different mass spectra, their identification is possible in every case and there are no interferences from urinary endogenous material.

The results of the three different derivatization procedures described above for 20 diuretics and 2 uricosuric agents are reported in Table 2. The values in Table 2 are expressed as a percentage and related to the highest signal obtained for each diuretic. All the diuretics have been derivatized using procedure 1, but with TMA

derivatization of some diuretics (mainly thiazides) has not been achieved. Using procedure 2 some diuretics, such as triamterene and benzbromarone, have not been derivatized. In general, with this method the sensitivities found are lower than those obtained with the other methods.

In some cases no derivatization occurred with any of the three compared methods, even when concentrations in spiked urine have been increased above the limits usually found in physiological samples.

Representative chromatograms of spiked urine with a mixture of nine diuretics obtained by the three derivatization procedures are shown in Fig. 2. All the diuretics have been added at a concentration of 0.3 μg/ml except for acetazolamide and xipamide whose concentrations were 3 μg/ml.

As after administration of mefruside to humans, less than 1% of the dose has been found in the urine as an unchanged drug, it has been chosen as the internal standard in this work [30]. After ingestion of mefruside, the 5-oxomefruside appears in urine as the main metabolite.

The precision and accuracy have been measured using urine samples spiked at a concentration of 0.5 μg/ml. The samples have been extracted by the three derivatization procedures and subjected to GC–MS. The statistical results are shown in Table 3.

Figs. 3 and 4 illustrate two positive urine

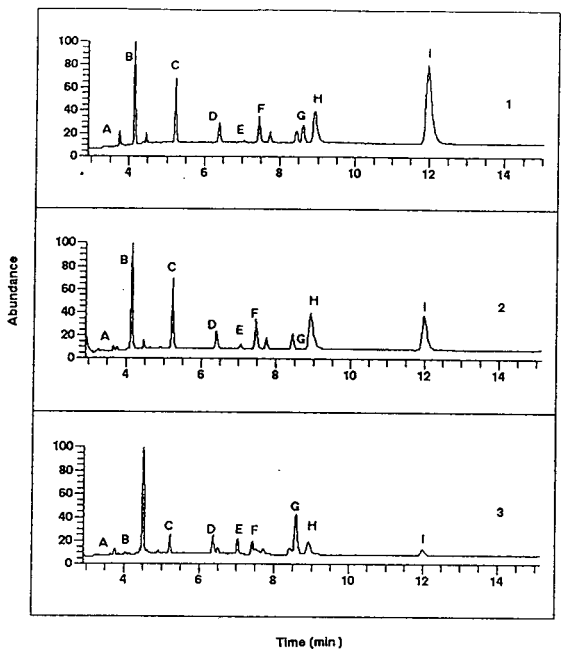

Fig. 2. Representative total ion chromatograms in spiked urine with a mixture of: A = trimethylated acetazolamide; B = monomethylated ethacrynic acid; C = tetramethylated dichlorphenamide; D = tetramethylated hydroflumethiazide; E = dimethylated clopamide; F = dimethylated mefruside (I.S.); G = trimethylated xipamide; H = tetramethylated hydrochlorothiazide; I = tetramethylated bendroflumethiazide. Chromatograms 1, 2 and 3 have been obtained using the three derivatization procedures: (1) iodomethane in acetone, (2) extractive methylation and (3) flash methylation.

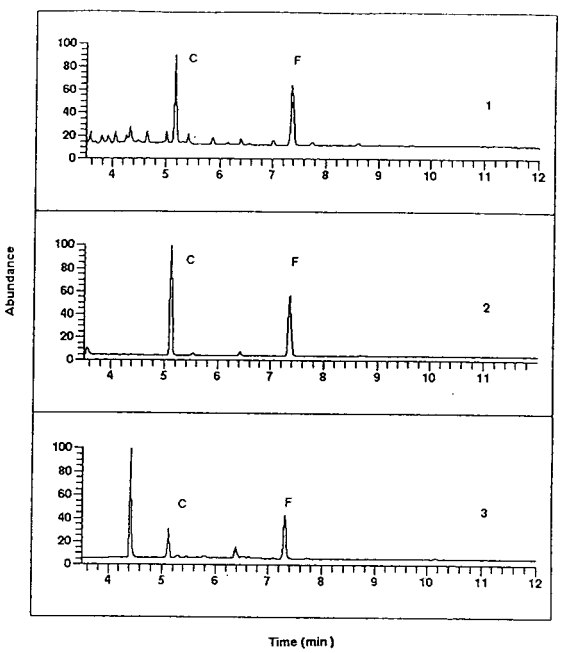

Fig. 3. Total ion chromatograms obtained from a positive urine sample containing dichlorphenamide using the three derivatization procedures: (1) iodomethane in acetone, (2) extractive methylation and (3) flah methylation. Peaks: C = tetramethylated dichlorphenamide; F = dimethylated mefruside (I.S.).

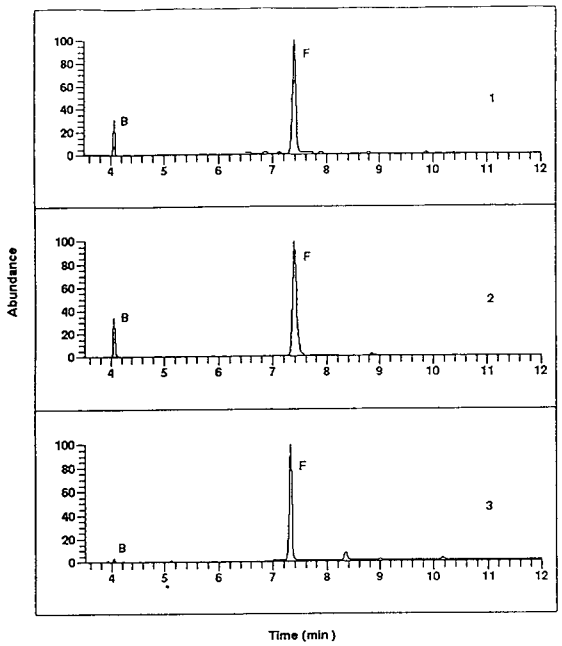

Fig. 4. Total ion chromatograms obtained from a positive urine sample containing ethacrynic acid using the three derivatization procedures: (1) iodomethane in acetone, (2) extractive methylation and (3) flash methylation. Peaks: B = monomethylated ethacrynic acid; F = dimethylated mefruside (I.S.).

samples containing dichlorphenamide and ethacrynic acid, respectively. In both cases, the signals correspond to the data in Table 2.

4. Conclusions

Screening procedures in doping analysis have to include as many drugs as possible. For this reason we propose for diuretics the derivatization using iodomethane in acetone, in a routine screening procedure. Nevertheless, the flash methylation is a reliable alternative method for a rapid confirmation in every case except for althiazide, trichlormethiazide, polithiazide and methyclothiazide. For these last two diuretics, an extractive methylation will be an alternative method; this method is not faster than flash methylation but it is faster than iodomethane in acetone.

The derivatization procedure using TMA has been applied since January 1993 to urine samples taken from athletes together with physiological samples as alternative confirmation. Over this period we have analysed about 2000 samples using iodomethane in acetone, and in more than 200 cases the flash methylation has been carried out for possible diuretics signals.

References

[1] A. Wade (Editor), *Martindale, The Extra Pharmacopeia*, Pharmaceutical Press, London, 29th ed., 1989, pp. 973–1007.
[2] *List of Doping Classes and Methods*, International Olympic Committee, Lausanne, 1991.
[3] M. Litter, *Farmacología Experimental y Clínica*, El Ateneo, Buenos Aires, 7th ed., 1988, pp. 790–830.
[4] E.T. Lin, *Clin. Liq. Chromatogr.*, 1 (1984) 115.
[5] G.K. Shiu, V.K. Prasad, J. Lin and W. Worsley, *J. Chromatogr.*, 377 (1986) 430.
[6] M. Yamazaki, Y. Ito, T. Suzuka, H. Yaginuma, S. Itoh, A. Kamada, Y. Orita, H. Nakahama, A. Nakanishi and A. Ando, *Chem. Pharm. Bull.*, 32 (1984) 2387.
[7] P.J.M. Guelen, A.M. Baars, T.B. Vree, A.J. Nijkerk and J.M. Vermeer, *J. Chromatogr.*, 181 (1980) 497.
[8] S. Guermouche, M.H. Guermouche, M. Mansouri, D. Boukhari and J. Sassard, *Analusis*, 12 (1984) 438.
[9] P.T.R. Hwang, J.R. Lang, G.C. Wood and M.C. Meyer, *J. Liq. Chromatogr.*, 8 (1985) 1465.
[10] C. Van Gulpen, A.W. Brokerhof, M. Van der Kaay, U.R. Tjaden and H. Mattie, *J. Chromatogr.*, 381 (1986) 365.
[11] K. Uchino, S. Isozaki, Y. Saitoh, F. Nakagawa, Z. Tamura and M. Tanaka, *J. Chromatogr.*, 308 (1984) 241.
[12] E.T. Lin, *Clin. Liq. Chromatogr.*, 1 (1984) 111.
[13] K.J. Swart and H. Botha, *J. Chromatogr.*, 413 (1987) 315.
[14] H. Boekens, C. Bourscheidt and R.F. Mueller, *J. Chromatogr.*, 434 (1988) 327.
[15] R.O. Fullinfaw, R.W. Burry and R.F.W. Moulds, *J. Chromatogr.*, 415 (1987) 347.
[16] S.F. Cooper, R. Massé and R. Dugal, *J. Chromatogr.*, 489 (1989) 65.
[17] F.Y. Tsai, L.F. Lui and B. Chang, *J. Pharm. Biomed. Anal.*, 9 (1991) 1069.
[18] R. Ventura, D. Fraisse, M. Becchi, O. Paisse and J. Segura, *J. Chromatogr.*, 562 (1991) 723.
[19] V. Raverdino, *J. Chromatogr.*, 554 (1991) 125.

[20] S.J. Park, H.S. Pyo, Y.J. Kim, M.S. Kim and J. Park, *J. Anal. Toxicol.*, 14 (1990) 84.
[21] A.F. Casy, *J. Pharm. Biomed. Anal.*, 5 (1987) 247.
[22] E.G. de Jong, J. Kiffers and R.A.A. Maes, *J. Pharm. Biomed. Anal.*, 7 (1989) 1617.
[23] M. Donike, presented at the *9th Workshop on Dope Analysis, Cologne, 17–22 March, 1991.*
[24] A.M. Lisi, G.J. Trout and R. Kazlauskas, *J. Chromatogr.*, 563 (1991) 257.
[25] M.K.L. Bicking and N.A. Adinolfe, *J. Chromatogr. Sci.*, 23 (1985) 348.
[26] P. Hartvig, C. Fagerlund and B.M. Emanuelsson, *J. Chromatogr.*, 228 (1982) 340.
[27] D.R. Knapp, *Handbook of Analytical Derivatization Reactions*, Wiley, New York, 1979, p. 146.
[28] G. Bruegmann, *J. Clin. Chem. Clin. Biochem.*, 19 (1981) 305–306.
[29] C. Kim, *Chromatographia*, 22 (1986) 303.
[30] H.L.J. Fleuren, C.P.W. Verwey-van Wissen and J.M. van Rossum, *J. Chromatogr.*, 182 (1980) 179.

ELSEVIER

Journal of Chromatography A, 683 (1994) 203–214

JOURNAL OF CHROMATOGRAPHY A

Simultaneous gas chromatographic–Fourier transform infrared spectroscopic–mass spectrometric analysis of synthetic fuel derived from used tire vacuum pyrolysis oil, naphtha fraction

Hooshang Pakdel*, Christian Roy

Department of Chemical Engineering, Université Laval, Ste-Foy (Québec) G1K 7P4, Canada

Abstract

Used tires were pyrolysed in a process development unit under vacuum at about 510°C and yielded 45% oil from which 27% (w/w) of a naphtha fraction (initial boiling point, IBP: 204°C) was separated. A new gas chromatographic configuration by combining infrared, mass spectrometric and flame photometric detectors to simultaneously analyze the effluent from a single capillary column injection was tested. Over 150 compounds were identified and quantified. Sulfur compounds distribution was established by sulfur-specific detection and selected ion GC–MS. Unlike petroleum, tire-derived pyrolytic naphtha is composed of highly branched chain isomeric hydrocarbons. Infrared spectroscopy as an extremely sensitive isomer-specific probe of molecular structures is described. Over 50 compounds were positively characterized by combining MS and IR data. It is shown that mass spectrometry provides superior quantitative capabilities, while infrared spectroscopy is an excellent complementary technique for simultaneous qualitative analysis of pyrolysis oils. Some of the difficulties encountered in the present application are discussed.

1. Introduction

Each year approximately 250 millions of used tires are discarded in the USA and about 24 millions in Canada. While about 20% of the used tires are recapped, most are dumped in the rural areas, which threatens the environment. Approximately one worn tire is produced per person per year in the developed countries.

Tire is principally a vulcanized rubber compound made of styrene–butadiene (SBR) polymer with about 25% styrene. Other elastomers such as natural rubber, synthetic *cis*-polyisoprene and *cis*-polybutadiene have also been used with SBR in different proportions [1]. Typically a tire is composed of 50% rubber, 27.5% carbon black, 17.5% extender oil and 5% of other ingredients.

If recycled, used tires are a source of energy and chemicals. Many processes have been described for the pyrolysis of old tires which yield oil, carbon black and gas using different heating systems and reactor configurations [1–3]. A vacuum pyrolysis unit with a design throughput capacity of 100 kg/h is available in our laboratories. The equipment has been described elsewhere [4]. Vacuum pyrolysis has several advantages due to the short gas and vapour residence time in the reactor and rather low decomposition temperature which minimizes sec-

* Corresponding author.

0021-9673/94/$07.00
SSDI 0021-9673(94)00535-H

ondary reactions. In addition, the carbon black solid residue and liquid oil are recovered separately. The oil yield is also considerably increased under vacuum compared to the atmospheric pressure conditions. The pyrolysis oil obtained under vacuum contains a significant portion of a volatile, naphtha-like fraction with an octane number similar to petroleum naphtha. Pyrolysis oil may be used directly as fuel or added to petroleum refinery feedstocks. The oil may also be used as an important source of chemicals such as benzene, toluene, xylene and limonene [5]. The non-condensable gases are used as a make-up heat source for the process and the solid char may be used either as smokeless fuel, carbon black or activated carbon [6].

In order to utilize the crude pyrolysis naphtha as refining feedstock, it is necessary to obtain comprehensive data on the physical and chemical properties of the oils. The information is important in many ways: to determine if environmentally hazardous components exist in the oil; to find out whether any nitrogen and sulfur compounds exist which need to be removed or treated before catalytic upgrading; and to establish the basic composition of the oil in order to determine the products to be refined from the oil.

Previous studies have concentrated on engineering aspects of rubber pyrolysis but detailed analyses of both the pyrolysis oil and the solid products are rarely reported. This paper reports a detailed chemical analysis of the pyrolysis oil naphtha fraction.

For a number of years, gas chromatography–mass spectrometry (GC–MS) has been accepted as the method of choice for the analysis of volatile to semi-volatile compounds. However, there are some limitations to the use of the benchtop GC–MS systems. For instance, under electron impact (EI) ionization at 70 eV, these systems often do not allow the differentiation of isomers because they lack structurally specific cleavages. In order to achieve a higher level of confidence in the identification, it is necessary to use complementary techniques which indicate the position and the nature of the substitution groups. The recent development of Fourier transform infrared (FTIR) spectroscopy and more particularly its coupling with chromatography techniques (GC–FTIR) have led to its application in the field of pollutant analysis [7,8]. Very recently, product analysis data based on GC–MS and GC–FTIR techniques enabled Dubey et al. [9] to propose a degradation mechanism for butyl rubber. Though GC–FTIR is less sensitive than GC–MS, it offers the advantage of differentiating isomers. An improved chromatographic resolution by means of programmed speed deposition and higher sensitivity than light-pipe-based GC–FTIR measurement has been achieved by a GC–matrix isolation–FTIR technique [10].

One of the main difficulties in GC separation is the complexity of sample matrices such as complex hydrocarbon mixtures derived from pyrolysis of rubber which results in peak overlap and incorrect identifications. Nitrogen- and sulfur-containing compounds in rubber pyrolysis oils are in low proportion and are difficult to identify and consequently have to be fractionated prior to analysis. Krock and Wilkins [8] have developed a multidimensional GC–FTIR–MS method to analyze complex organic pollutants. They used two GC columns in series. The multicolumn analysis can be replaced by a single column with higher resolution as discussed in this paper. Due to its high and complex isomeric hydrocarbon nature, pyrolysis naphtha is a good example to test potential applications of FTIR combined with GC and MS.

2. Experimental

The pyrolysis oil sample used in this investigation was produced from used tires in a vacuum pyrolysis process development unit (PDU). The system operated on a semicontinuous feed mode using punched cross-ply tire particles. The throughput capacity was 19 kg/h. The reactor maximum temperature and total pressure were 510°C and 33 kPa, respectively. The experiment has been identified as run H04 and the system operation has been described in detail elsewhere [4]. The process yielded 45.0%

(w/w) oil, 25.0% carbon black and 30.0% gas during the run. A pyrolytic oil sample with elemental composition of typically 88.2% carbon, 8.5% hydrogen, 1.1% nitrogen, 1.2% sulfur and 1.0% oxygen was distilled under atmospheric pressure up to 204°C to separate the naphtha fraction.

GC analysis was performed on a Hewlett-Packard HP 5890 gas chromatograph equipped with a flame photometric detection (FPD) system for sulfur analysis at 280°C and a 100 m × 0.25 mm I.D. Petrocol DH capillary column from Supelco with 0.50 μm film of bonded methyl silicone and 0.45 ml/min flow-rate and nitrogen as the make-up gas. Injection mode was split at 250°C with about 1:150 split ratio. The column was directly introduced in the FPD system for GC–FPD operation or in the ion source of a Hewlett-Packard HP 5970 series mass-selective detector for GC–MS operation. Typical MS operating conditions were as follows: transfer line 270°C, ion source 250°C, electron energy 70 eV. Data acquisition was done with HP-UX Chemstation software using a Hewlett-Packard HP-UNIX computer and NBS library data base. The mass range m/z 30–400 dalton was scanned every 1.0 s. The main objective to choose a 100-m long capillary column with a thick stationary phase (0.5 μm) was to have a high resolution and loading capacity for this particular analysis of naphtha-like volatile hydrocarbon mixture. It is not however recommended for the analysis of low-volatile mixtures. Since IR is at least a hundredfold less sensitive compared with MS, a large sample volume can be injected on a 100-m column for the IR detection without overloading the column. GC–MS analysis was successfully performed by injecting 0.8 μl of pure naphtha on a 100-m column. Maximum column head pressure was 200 kPa which only produced about 0.45 ml/min column flow-rate. Due to the low flow-rate and large pressure drop across the light-pipe this flow was insufficient for GC–FTIR–MS analysis. A pressure regulator which can control about 680 kPa should replace the existing GC pressure regulator. The required modification will be made for the future analysis. The present GC–FTIR–MS results were obtained by injecting 1-μl samples on a 30 m × 0.25 mm I.D. HP5-MS fused-silica capillary column from Hewlett-Packard with 0.25 μm film thickness. The column flow-rate was 0.9 ml/min and 1:150 split ratio.

GC–FTIR–MS operation was performed on a Bio-Rad FTS45 IR detector interfaced to the same HP gas chromatograph with a split injec-

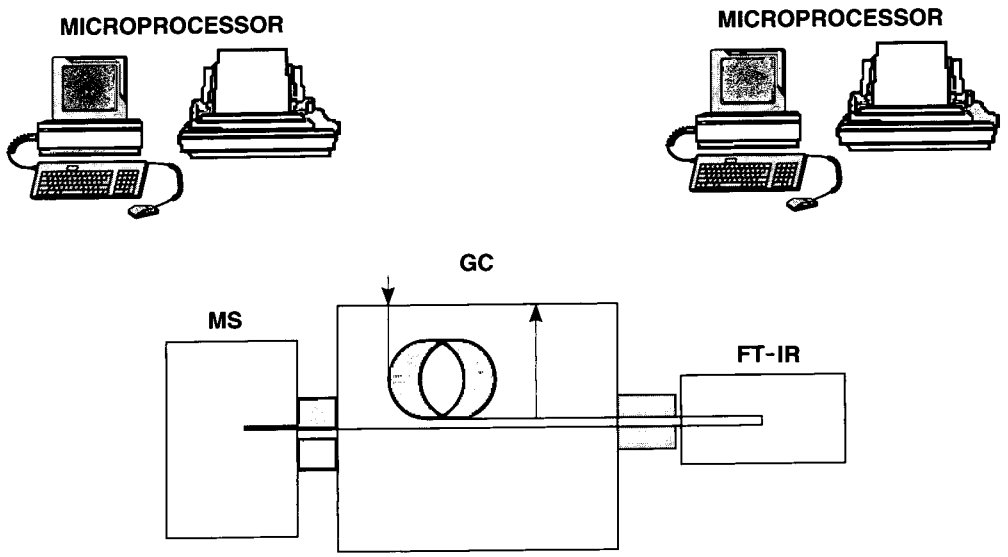

Fig. 1. Schematic diagram of simultaneous GC–FTIR–MS analyses.

tor. FTIR spectra were obtained by collecting 4 scans per scan-set using a narrow-band mercury cadmium telluride (MCT) detector with a spectral cutoff of 750 cm^{-1} and an optical resolution of 8 cm^{-1}. This corresponds to the collection of 4 spectra per second. The FTIR interface has a 10 cm × 1 mm I.D. column internally gold-coated Pyrex light pipe that was maintained at 250°C. The optics of the FTIR were purged with dried air supplied by Blaston 75-62 purge gas generator (Haverhill, MA, USA). GC oven temperature conditions were as follows:

GC–MS and GC–FPD analyses: the oven temperature was initially set at 35°C for 10 min, then programmed to 130°C at 2°C/min. Then it was programmed to 250°C at 30°C/min. It was set at 250°C for 5 min. GC–MS and GC–FPD analyses were performed separately under similar GC conditions.

GC–FTIR–MS analyses: the oven temperature was initially set at 35°C for 10 min, then programmed to 150°C at 4°C/min. Then it was programmed to 250°C at 30°C/min. It was set at 250°C for 5 min. These analyses were performed simultaneously. The experimental arrangement is shown schematically in Fig. 1. The mass-selective detector was physically located on the left side of the gas chromatograph in the standard Hewlett-Packard configuration, while the FTIR instrument was located on the right side with the front of the instrument in a reverse position to that of the gas chromatograph. Due to its short length, the light-pipe rigid-heated transfer line was temporarily modified by extending a couple of centimeters. This arrangement permitted the interface to be matched to the GC system.

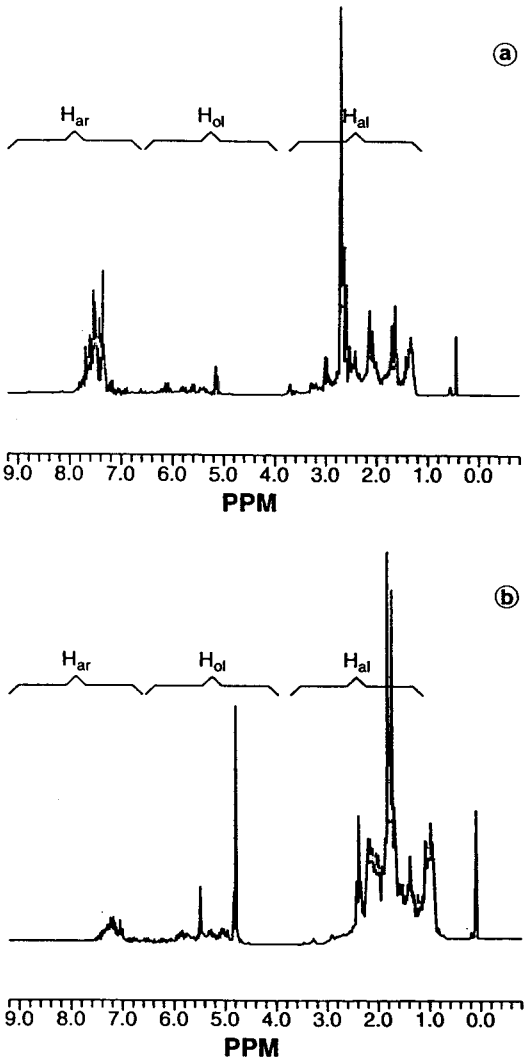

Fig. 2. 300 MHz ^1H FTNMR spectra of pyrolytic naphtha obtained at (a) 33 kPa pyrolysis pressure, (b) 13 kPa pyrolysis pressure.

3. Results and discussion

Pyrolysis oil composition depends on the pyrolysis conditions. Pyrolysis under high pressure yields higher content of high-volatile aromatic and lower content of olefinic compounds than low-pressure pyrolysis. Fig. 2 shows high-field proton FTNMR spectra of naphtha fractions recorded on a 300 MHz Brucker spectrometer. Naphtha in Fig. 2a was obtained under 33 kPa pyrolysis pressure while naphtha in Fig. 2b was obtained under 13 kPa (run H03). Fig. 2a represented 21.4% and 1.3% aromatic (H_{ar}) and olefinic (H_{ol}) protons, respectively. But Fig. 2b represented 2.7% H_{ar} and 9.3% H_{ol} protons, respectively. Volatile aromatic hydrocarbons have potential industrial applications such as solvent and octane booster for gasoline. However, a detailed characterization of pyrolytic

Table 1
Tentative characterization of pyrolytic naphtha by GC–MS

t_R (min)[a]	% (w/w)	Tentative assignment	t_R (min)[a]	% (w/w)	Tentative assignment
12.49	0.07	Acetonitrile	38.24	0.01	2,4-Heptadiene
14.28	0.025	1,4-Pentadiene	38.56	0.71	1,5-Dimethylcyclopentene
15.07	0.02	1,1-Dimethylcyclopropane	39.06	9.08	Toluene
15.85	0.02	2-Methyl-1-buten-3-yne	39.32	0.22	3-Methylthiophene
16.61	0.11	Propanenitrile	39.45	0.22	3-Methyl-1,3,5-hexatriene
17.14	0.005	Cyclopentene	39.56	0.12	Cyclopentanone
18.87	0.005	2-Methyl-2-propenenitrile	39.73	0.09	3-Methyl-2,4-hexadiene
20.01	0.035	1-Hexene	40.13	0.08	2-Methylthiophene
20.65	0.03	2-Methylpropanenitrile	40.31	0.35	Methylenecyclohexane
21.07	0.03	Hexane	40.45	0.33	2-Methyl-1,3,5-hexatriene
21.70	0.02	2-Methyl-2-pentene	40.64	0.32	5,5-Dimethyl-1,3-cyclopentadiene
21.96	0.02	3-Methyl-1,3-pentadiene	41.74	0.11	1,4-Dimethylcyclohexane
22.06	0.02	3,3-Dimethyl-1-butene	42.08	0.06	2,3-Dimethyl-1,4-hexadiene
22.21	0.025	2,3-Dimethyl-1,3-butadiene	42.63	0.08	2-Methyl-1-heptene
22.66	0.025	2-Methyl-1,3-pentadiene	43.09	0.32	1-Octene
23.04	0.10	3-Methyl-2-pentene	43.44	0.19	1,3,5-Heptatriene
24.14	0.01	4-Methyl-2-pentene	43.64	0.52	2-Methylpyridine
24.28	0.09	2-Methyl-1,3-pentadiene	44.45	0.10	3-Methylcyclohexanone
24.52	0.19	1,3-Cyclohexadiene	44.66	0.12	1,4-Dimethylcyclohexane
24.64	0.09	1,1-Dimethyl-2-methylenecyclopropane	45.12	0.07	3-Ethyl-1,4-hexadiene
24.92	0.25	1,3,5-Hexatriene	45.34	0.24	2,3,3-Trimethyl-1,4-pentadiene
25.38	0.05	2,4-Hexadiene	45.34	0.01	5-Methyl-1,3,6-Heptatriene
25.98	0.07	1,4-Hexadiene	45.95	0.19	2-Methyl-1H-pyrrole
26.06	0.06	1,1-Dimethyl-2-methylenecyclopropane	45.16	0.11	Cyclohexanone
26.17	0.14	1-Methylcyclopentene	46.90	0.38	2,3,3-Trimethyl-1,4-pentadiene
26.29	1.21	Benzene	47.07	0.21	2,3-Dimethyl-1,4-hexadiene
26.84	0.04	4,4-Dimethyl-2-pentene	47.37	0.30	3-Methyl-1,4-heptadiene
27.67	0.16	5-Methyl-1,3-cyclopentadiene	47.71	0.24	4-Ethenylcyclohexene
29.13	0.09	Bicyclo[3.1.0]hexane	47.90	0.07	Ethenylcyclohexane
30.88	0.12	1-Heptene	47.94	0.08	1-Ethenylcyclohexene
31.83	0.04	2-Heptyne	48.30	0.04	2,3-Dimethyl-2-hexene
32.13	0.16	4-Methyl-1,4-hexadiene	48.53	0.13	1-Ethylcyclohexene
32.32	0.08	1,5-Dimethylcyclopentene	48.66	0.46	3-Methylpyridine
32.53	0.07	2-Methyl-2-hexene	49.02	0.23	3-Ethylidene-1-methylcyclopentene
32.85	0.035	1-Heptene	49.27	0.06	Bicyclo[5.1.0]octane
32.23	0.06	2-Methylenebutanenitrile	49.64	1.58	Hexanenitrile
33.42	0.06	3-Methyl-2-hexene	49.86	0.13	1-Ethylcyclohexene
33.57	0.10	4,4-Dimethylcyclopentene	50.29	3.21	Ethylbenzene
34.08	0.06	4-Methyl-2-hexyne	50.46	0.20	3-Ethylthiophene
34.44	n.a.	3-Ethylcyclopentene	50.93	0.12	2,3-Dimethyl-1,4-hexadiene
34.73	0.04	Pyridine	51.05	n.a.	2,5-Dimethylthiophene
34.84	0.17	3-Methyl-1,3,5-hexatriene	51.39	13.46	*m*-Xylene
35.30	0.13	Pentenenitrile	51.65	0.24	Tetramethylmethylenecyclopropane
35.68	0.11	2,3,4-Trimethyl-2-pentene	51.75	0.12	2,3-Dimethylpyridine
35.78	0.02	2,3-Dimethyl-1,4-hexadiene	51.90	0.10	2,4-Dimethylthiophene
36.28	0.48	1H-Pyrrole	52.35	0.31	Trimethyl-1,3-cyclopentadiene
36.51	0.34	3-Methyl-1,3,5-hexatriene	52.60	0.07	1,2-Dimethylcyclohexene
36.64	0.16	4-Methylcyclohexene	52.92	0.13	Ethenylthiophene
36.87	0.13	1-Methyl-1,4-cyclohexadiene	53.05	0.17	2,3-Dimethylthiophene
37.23	0.76	Nitrile derivative	53.26	2.59	1,3,5,7-Cyclooctatetraene
37.53	0.16	1,2-Dimethyl-1,3-cyclopentadiene	53.60	0.18	3-Octen-1-yne

(Continued on p. 208)

Table 1 *(continued)*

t_R (min)[a]	% (w/w)	Tentative assignment	t_R (min)[a]	% (w/w)	Tentative assignment
53.68	0.10	Trimethylcyclopentadiene	68.76	0.04	*o*-Isopropyltoluene
53.85	3.93	*p*-Xylene	69.01	0.90	1-Propenylbenzene
54.15	0.23	2-Methylene-4-pentenenitrile	69.31	0.10	Camphene
54.45	0.01	1-Methylene-3-(1-methylethylidene)-cyclopentane	69.54	0.22	1-Methyl-2-pentylcyclohexane
			69.71	0.16	1,2,3,5-Tetramethylbenzene
54.55	0.62	1-Nonene	69.97	0.23	*m*-Propyltoluene
55.23	0.24	Trimethyl-1,3-cyclopentadiene	70.32	0.18	Diethylbenzene
55.78	0.19	Nonane	70.54	0.72	1,4-Dimethyl-2-ethylbenzene
56.03	0.15	Trimethyl-1,3-cyclopentadiene	71.47	0.12	*p*-Propyltoluene
57.14	0.01	3,5-Octadiene-2-ol	72.32	0.13	3,5-Dimethyl-1-ethylbenzene
57.31	0.56	Isopropylbenzene	72.53	0.48	*m*-Isopropyltoluene
57.41	0.01	1,2,6,6-Tetramethyl-1,3-cyclohexa-diene	72.74	0.13	2,3-Dihydro-5-methyl-1H-indene
			73.06	0.19	3,5-Dimethyl-1-ethylbenzene
57.77	0.08	1-Methyl-3-(1-methylethylidene)-cyclopentane	73.21	0.52	2-Butenylbenzene
			73.72	0.16	1,2-Dimethyl-4-ethenylbenzene
58.81	0.39	α-Ethylbenzenemethanol	74.06	0.23	2-Undecene
59.26	0.34	1-Ethenyl-2-methylbenzene	74.31	0.09	1,3-Dimethyl-2-ethenylbenzene
60.23	0.34	2,5-Dimethyl-3-methylene-1,5-heptadiene	74.65	0.08	*p*-Isobutyltoluene
			74.03	0.14	Undecane
60.40	0.56	Benzeneacetaldehyde	75.67	0.02	2,3-Dihydro-1,6-dimethyl-1H-indene
60.91	0.48	Aniline	76.03	0.10	1,2,3,5-Tetramethylbenzene
60.91	n.a.	2-Isopropylthiophene	76.33	0.40	1,2,3,5-Tetramethylbenzene
61.16	3.27	*o*-Ethyltoluene	76.65	0.02	2-Ethenyl-1,3,5-trimethylbenzene
61.42	1.71	*m*-Ethyltoluene	76.75	0.08	*o*-Propenyltoluene
61.93	1.11	1,3,5-Trimethylbenzene	76.98	0.01	1,3-Dimethyl-2-ethenylbenzene
62.48	0.20	1,4-Dimethyl-5-isopropylcyclopentene	77.94	0.12	2,3-Dihydro-5-methyl-1H-indene
62.86	0.77	Isopropenylbenzene	78.87	0.11	2,3-Dihydro-4-methyl-1H-indene
62.99	0.77	*p*-Ethyltoluene	79.11	0.26	1-Methyl-1H-indene
63.18	0.12	2,3,4-Trimethylthiophene	79.27	0.07	1-Butynylbenzene
63.90	0.14	Propenylbenzene	79.40	0.01	2-Methylbutylbenzene
64.20	1.05	α-Ethenyltoluene	79.83	0.07	1,2,3,4-Tetrahydronaphthalene
64.35	0.18	Cyclopropylbenzene	79.95	0.01	1,3-Butadienylbenzene
64.49	3.60	1,2,4-Trimethylbenzene	80.97	0.01	(2-Methyl-1-butenyl)benzene
64.79	0.49	1-Ethyl-2-pentylcyclopropane	80.31	0.01	1,2-Dihydro-2-methylnaphthalene
65.41	0.55	1,2,3,4,5-Pentamethyl-1,3-cyclopen-tadiene	81.56	0.12	Naphthalene
			82.03	0.02	2,3-Dihydro-1,2-dimethyl-1H-indene
65.53	0.10	4,5-Dimethyl-2,6-octadiene	82.52	0.05	2-Decene
65.87	0.19	Decane	82.94	0.02	2,3-Dihydro-1,3-dimethyl-1H-indene
66.11	0.01	2,5,6-Trimethyl-1,3,6-heptatriene	83.96	0.01	Benzothiazole
66.55	0.19	1,5-Dimethyl-6-methylene-spiro[2.4]-heptane	85.27	0.07	3,5-Dimethyl-1-ethyl-1H-pyrazole
			87.49	0.08	1,1-Dimethyl-1H-indene
66.72	0.01	2,5-Diethylthiophene	87.98	0.01	1,2-Dihydro-2-methylnaphthalene
67.23	1.71	1,2,3-Trimethylbenzene	88.70	0.01	1,2-Dihydro-3-methylnaphthalene
67.51	0.81	Tetramethylbenzene	90.61	0.025	1-Methylnaphthalene
68.10	0.20	4-Isopropyl-1-methylcyclohexene			
68.43	2.54	*dl*-Limonene	Total	80.19	

n.a. = Not available.
[a] Retention time, see Fig. 3.

naphtha fraction is prerequisite for its application. Vacuum pyrolysis of used tires typically yields 20–28% (w/w) of naphtha fraction.

Table 1 shows an extended list of compounds that were tentatively identified by GC–MS on a 100-m column. The compounds listed are esti-

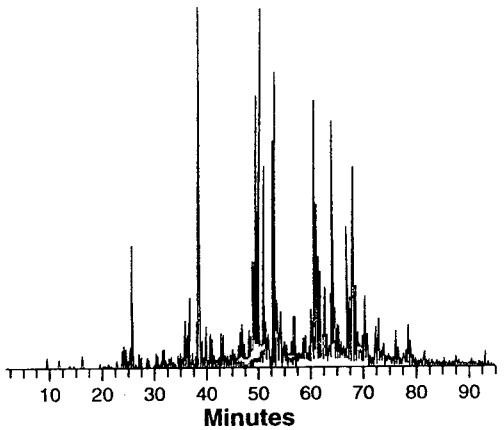

Fig. 3. Total ion chromatogram of pyrolytic naphtha.

mated to be over 80% of the total naphtha composition. Some of the results are not yet fully confirmed by GC–FTIR–MS. The total ion chromatogram is shown in Fig. 3. This chromatogram was recorded by injecting 0.8 μl of the pure sample without significantly affecting the column resolution. The sample was found extremely complex. Nevertheless, a satisfactory resolution was achieved which has motivated future GC–FTIR–MS analysis on the same column after modification of the GC flow supplier. Due to the large number of isomeric compounds (Table 1), in many cases MS failed to make unambiguous isomer-specific identification. However, Table 1 lists only the most probable isomeric structures identified by MS search file system. In close agreement with Fig. 2, Table 1 shows that the majority of compounds are substituted aromatic hydrocarbons with various isomers. Benzene, toluene, xylene, trimethylbenzene and tetramethylbenzene are the most abundant aromatic components of tire pyrolysis-derived naphtha fraction. The relative mass percentages of the individual compounds were calculated by assuming the same response factor from the peak areas of the chromatogram shown in Fig. 3. Results are presented in Table 1. Most of the volatile aliphatic and alicyclic hydrocarbons have similar GC responses near unity. Linear hydrocarbons are mainly concentrated in the first 25 min of the chromatogram (m/z 41 is the characteristic fragment ion peak) followed by benzene (m/z 78), mono-, di-, tri- and tetra-substituted benzenes (m/z 92, 91, 105 and 119, respectively) and finally indene (m/z 116) and naphthalene (m/z 128) derivatives. Substituted benzene derivatives appeared in decreasing order of abundance from mono- to tetra-substituted benzene and are depicted in selected ion chromatograms (m/z 91–119) shown in Fig. 4.

dl-Limonene is one of the most important constituents of pyrolytic naphtha with potential economic value [5]. Its concentration drastically decreased as the reactor pressure increased. Approximately 25% *dl*-limonene has been reported by this laboratory earlier under about 2.7 kPa total pressure [5]. Atmospheric pressure pyrolysis yielded practically no *dl*-limonene [11]. Moreover, the substantial proportion of mono-aromatic hydrocarbons present in the naphtha fraction suggests that this oil could become a potential feedstock for the production of aromatic solvent and BTX (benzene, toluene and xylene) or a high-octane gasoline pool (a blend of various gasolines).

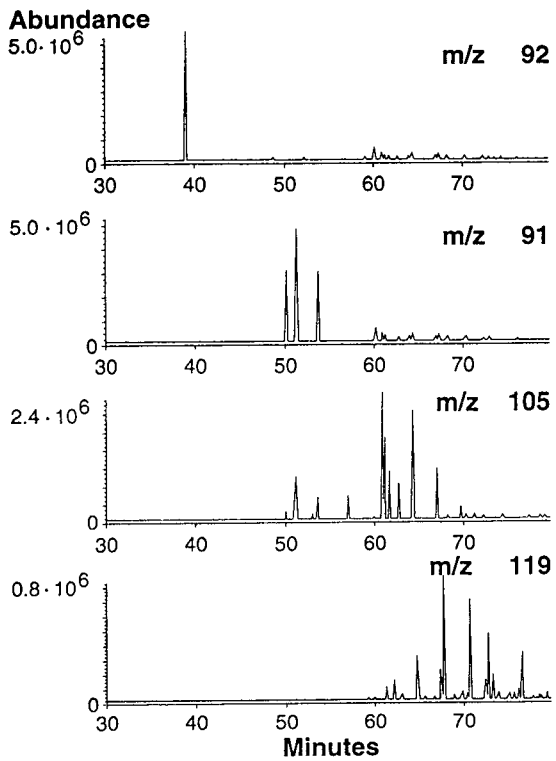

Fig. 4. Ion chromatograms of pyrolytic naphtha.

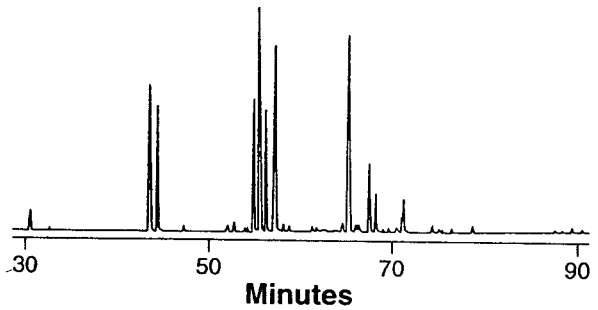

Fig. 5. Gas chromatogram of sulfur compounds in pyrolytic naphtha.

The chromatogram in Fig. 5 was recorded on the same column and conditions as Fig. 3 using sulfur-specific FPD. Fig. 6 illustrates a reconstructed selected ion chromatograms of *m/z* 97 for $(C_5H_5S)^+$, 111 for $(C_6H_7S)^+$, 125 for $(C_7H_9S)^+$ and 135 for $(C_7H_5SN)^+$ which is in good agreement with Fig. 5. Those ions are the characteristic fragment ions (or molecular ions) of methyl-, dimethyl- and ethylthiophene; trimethyl- and isopropylthiophene; *tert.*-butylthiophene and benzothiazole, respectively. Ten major peaks of Fig. 6 were identified and are listed in Table 2. GC analysis using sulfur-specific detection helped to confirm the assignments in Table 1. Those compounds are the principal pyrolysis sulfur products derived from

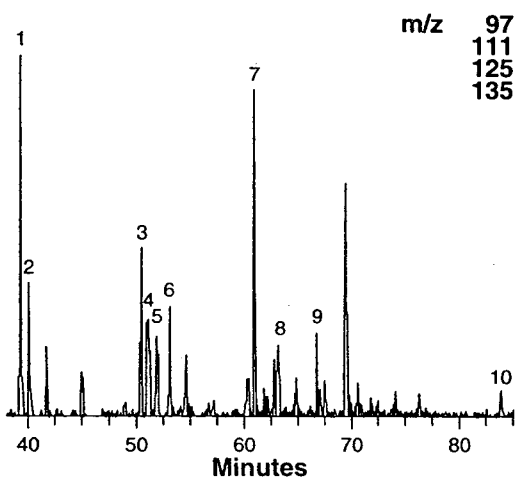

Fig. 6. Reconstructed ion chromatogram of sulfur compounds in pyrolytic naphtha.

Table 2
Sulfur compounds identified in pyrolytic naphtha

Peak No.[a]	Assignment
1	2-Methylthiophene
2	3-Methylthiophene
3	2-Ethylthiophene
4	2,5-Dimethylthiophene
5	2,4-Dimethylthiophene
6	3-Ethylthiophene
7	2,3-Dimethylthiophene
8	2-Isopropylthiophene
9	2-*tert.*-Butylthiophene
10	Benzothiazole

[a] See Fig. 6.

the vulcanization agents which have been added during the tire manufacture.

Capillary column gas chromatograms of the same oil obtained simultaneously with both IR and MS techniques are shown in Fig. 7a and b,

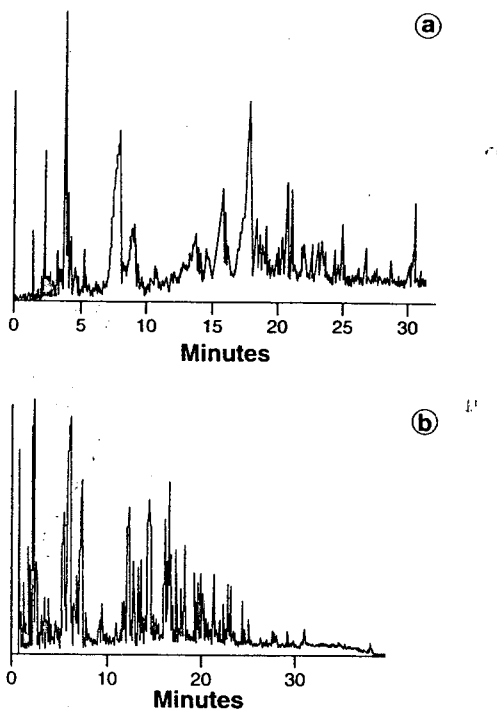

Fig. 7. Chromatograms of pyrolytic naphtha. (a) GC–FT-IR Gram–Schmidt chromatogram; (b) GC–MS total ion chromatogram.

respectively. The total ion chromatogram (Fig. 7b) was rather overloaded due to a low column loading capacity for the quantity of solution injected. The IR chromatogram in Fig. 7a shows a lower resolution compared with Fig. 7b. The chromatographic resolution can be increased if two scans are collected per scan-set at 4 cm^{-1} spectrometer resolution. Only four scans were collected at 8 cm^{-1} spectrometer resolution in this work. This experimental condition will double the file size without sacrificing the signal to noise ratio. However, most of the principal chromatographic peaks were positively identified and listed in Table 3. This example clearly illustrates the powerful and complementary nature of combined instruments. In many cases throughout the analysis where MS failed to make isomer-specific identifications, the FTIR spectra provided a positive identification of the correct compounds. However, the molecular masses from the mass spectra were equally important to establish the molecular tentative structures. MS with GC retention data or FTIR spectra alone can be used to tentatively identify many of the compounds listed in Table 1, but with far less ease and confidence than with the combined GC, MS and FTIR.

Di-, tri- and tetra-substituted benzene and ethylbenzene are the best examples which usually show quite similar isomeric mass spectra that are difficult to differentiate. These compounds are high abundant components of naphtha which have a unique IR spectra. This ability is based on specific vibrational modes associated with individual substitution patterns. The EI mass spectra of all substituted benzenes have two M^+ and $M^+ - 15$ ions as the base peaks. Therefore, usually all isomeric compounds show a similar mass spectra. FTIR on the other hand is very powerful to differentiate the isomeric structures. Figs. 8–10 illustrate MS and FTIR spectra of four pairs of typical benzene derivatives in pyrolytic naphtha. The isomeric pairs in Figs. 8a and b to 10a and b exhibit similar characteristic ions in their mass spectra which are impossible to be differentiated. On the other hand, FTIR spectra of these compounds reveal significant differences. These differences are based on ap-

Table 3
List of compounds identified by GC–FTIR–MS

t_R (min)[a]	Assignment
2.22	2-Methyl-1,5-hexadiene
2.35	Benzene
2.40	1,3-Cyclohexadiene
2.49	2-Methyl-1,4-pentadiene
2.56	1-Heptane
2.69	5-Methyl-1,4-hexadiene
3.24	1-Methylcyclohexadiene
3.47	1H-Pyrrole
3.50	1,2-Dimethyl-1,3-cyclopentadiene
3.77	Toluene
3.87	1,3,5-Heptatriene
4.09	2-Pentenenitrile
4.19	3-Octene (*trans*)
4.80	2-Methylpyridine
5.15	2,3-Dimethyl-1,4-hexadiene
6.61	Ethylbenzene
7.25	*m*-Xylene
8.25	Ethenylbenzene
8.36	*o*-Xylene
12.21	Propylbenzene
12.90	*m*-Ethyltoluene
13.35	1,3,5-Trimethylbenzene
13.94	*o*-Ethyltoluene
14.16	1-Methylethenylbenzene
14.92	1,2,4-Trimethylbenzene
15.15	2-Propenylbenzene
16.50	1,2,3-Trimethylbenzene
16.71	1,2,3,4-Tetramethylbenzene
16.98	*dl*-Limonene
17.15	1-Propenylbenzene
17.60	Indene
18.07	1-Methylpropylbenzene
18.28	Butylbenzene
18.49	3,5-Dimethyl-1-ethylbenzene
18.79	(1-Methylpropyl)benzene
18.87	3-Methylbenzonitrile
19.05	4-Methylbenzene
19.19	2,5-Diethylthiophene
19.32	1-Methyl-4-isopropylbenzene
19.45	1,2-Dimethyl-4-ethylbenzene
19.68	1-Methyl-1-propenylbenzene
19.75	*tert.*-Butylbenzene
20.00	2-Methylpropenylbenzene
20.19	1-Undecene
21.39	1,2,3,5-Tetramethylbenzene
22.15	2,3-Dihydro-5-methyl-1H-indene
22.62	3-Methyl-1H-indene
22.88	1-Methyl-1H-indene
23.07	Pentylbenzene
24.03	Naphthalene
24.28	2,3-Dihydro-1-dimethyl-1H-indene
24.60	1-Dodecene
25.71	Benzothiazole
27.15	1,1-Dimethyl-1H-indene
28.41	2-Methylnaphthalene
29.04	1-Methylnaphthalene

[a] Retention time, see Fig. 7.

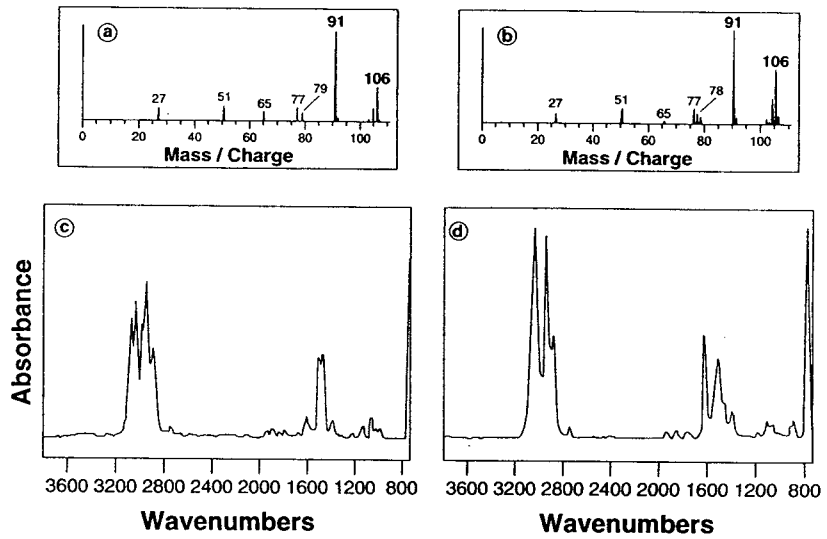

Fig. 8. MS and IR spectra of: (a, c) *o*-xylene and (b, d) *m*-xylene.

pearance or disappearance of characteristic bands or a shift to lower or higher wavelengths. Recently Smyrl et al. [12] used a single GC injection onto two capillary columns and both IR and MS analyses were performed on the separate effluents. Usually it will be very difficult to obtain similar retention time profiles in both chromatograms. The IR section requires a flow restrictor since the MS retention data will be slightly lower than IR and the spectra matching will be difficult. Interestingly, negligible retention differences were observed in this work using a single column sample injection method.

GC–FTIR–FPD was successfully tested for a standard mixture of sulfur compounds. Both MS and FTIR chromatograms showed a satisfactory

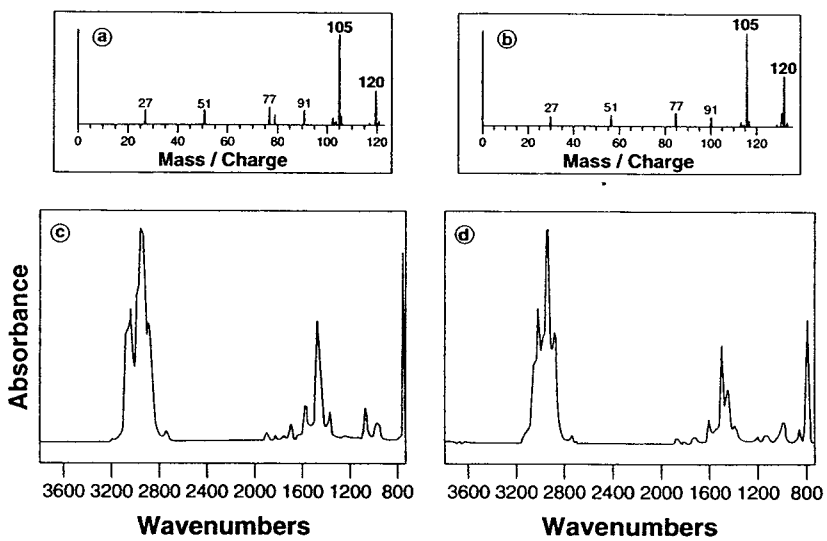

Fig. 9. MS and IR spectra of: (a, c) 1,2,3-trimethylbenzene and (b, d) 1,2,4-trimethylbenzene.

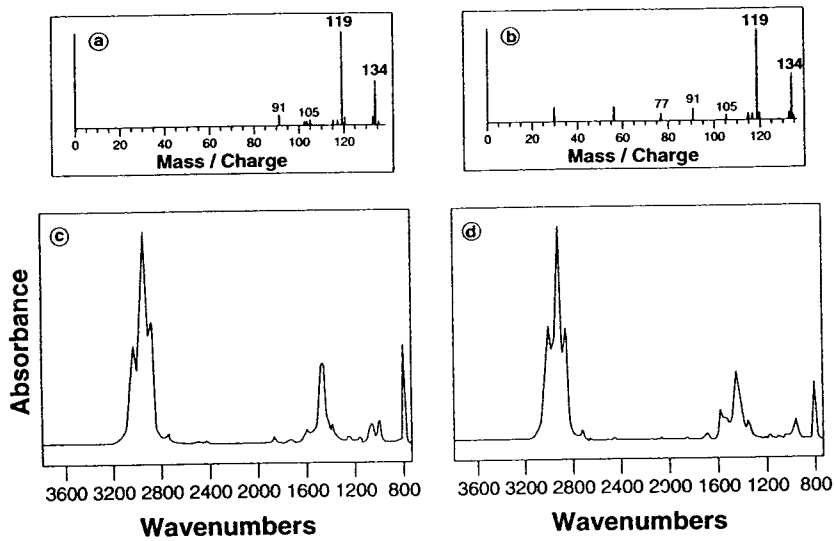

Fig. 10. MS and IR spectra of: (a, c) 1,2,3,4-tetramethylbenzene and (b, d) 1,2,3,5-tetramethybenzene.

matching retention time profile. Due to the low abundance and low GC resolution, the naphtha sulfur compounds which are listed in Table 2 could not be detected by FTIR.

Thus, it can be postulated that the higher aromatic content of the naphtha fraction analysed is associated with a relatively higher reactor pressure compared with the previous reactor configuration and conditions used [13]. However, oil composition reflects the reaction environment. It is therefore expected that a reactor can be designed and operated for specific product composition.

4. Conclusions

Used tires, when pyrolysed under vacuum, decompose to yield a complex mixture of hydrocarbon oil when analysed by GC. At 510°C and 33 kPa pressure, substituted monoaromatic hydrocarbons and their isomers were abundant in the naphtha fraction which complicated its characterization. This study has shown that a single GC injection onto a long capillary column with high loading capacity (0.5 μm stationary film thickness) and a flow-rate of about 1 ml/min enables to perform a simultaneous FTIR and MS analyses of GC effluents with matching retention times. GC–MS or GC–FTIR alone were unable for unambiguous characterization of the pyrolytic naphtha components. GC–FTIR appears, however, to be a complementary technique to GC–MS in terms of identification. Separate GC–MS and GC–FPD analyses enabled the characterization of major sulfur compounds.

References

[1] J. Dodds, W.F. Domenico, D.R. Evans, L.W. Fish, P.L. Lassahn and W.J. Toth, *Scrap Tires: A Resource and Technology Evaluation of Tire Pyrolysis and other Selected Alternate Technologies; N.T.I.S. Report No. EGG-2241*, EG & G Idaho Inc., Idaho Falls, ID, 1983.

[2] G. Crane, R.A. Elefrizt, E.L. Kay and J.R. Laman, *Rubber Chem. Technol.*, 51 (1978) 577.

[3] H. Aubin, *M.Sc. Thesis*, Universite Laval, Ste-Foy (Quebec), 1987.

[4] C. Roy, B. de Caumia, D. Blanchette, H. Pakdel, G. Couture and A.E. Schwerdtfeger, *Remediation*, submitted for publication.

[5] H. Pakdel, C. Roy, H. Aubin, G. Jean and S. Coulombe, *Environ. Sci. Technol.*, 25 (1991) 1646.

[6] C. Roy, B. Labrecque and B. de Caumia, *Resour. Conserv. Recycl.*, 4 (1990) 203.

[7] H. Budzinski, Y. Hermanage, C. Pierard, P. Garrigues and J. Bellocq, *Analusis*, 20 (1992) 155.

[8] K.A. Krock and C.L. Wilkins, *Anal. Chim. Acta*, 277 (1993) 381.
[9] V. Dubey, R.K. Shrivastava, D.N. Tripathi, R.P. Semwal, B.R. Gandhe and R. Vaidyanathaswamy, *J. Anal. Appl. Pyrol.*, 27 (1993) 207.
[10] C. Klawun, T.A. Sasaki, C.L. Wilkins, D. Carter, G. Dent, P. Jackson and J. Chalmers, *Appl. Spectrosc.*, 47 (1993) 957.
[11] P.T. Williams, S. Besler and D.T. Taylor, *Fuel*, 69 (1990) 1474.
[12] N.R. Smyrl, D.M. Hembree, Jr., W.E. Davis, D.M. Williams and J.C. Vance, *Appl. Spectrosc.*, 46 (1992) 277.
[13] S. Mirmiran, H. Pakdel and C. Roy, *J. Anal. Appl. Pyrol.*, 22 (1992) 205.

ELSEVIER

Journal of Chromatography A, 683 (1994) 215–222

JOURNAL OF CHROMATOGRAPHY A

High-performance liquid chromatography coupled off-line with capillary gas chromatography Application to the determination of the aromatics content in middle distillates

Eric Robert[a,*], Jean-Jacques Beboulene[a], Georgie Codet[a], Dan Enache[b]

[a]*Institut Français du Pétrole, 1 et 4 Avenue de Bois-Préau, 92500 Rueil Malmaison, France*

[b]*University of Ploiesti, Prahova cod 2000, Romania*

Abstract

The off-line coupling of normal-phase HPLC and capillary GC was used to determine the total aromatics content of middle distillates. Samples doped with internal standards were injected into the liquid chromatograph and the two collected fractions, saturates and aromatics, were further analysed by capillary GC. Good repeatability of the analysis was obtained for this determination on both gas oils and kerosenes and there was good agreement with other analytical methods (mass spectrometry and preparative liquid chromatography).

1. Introduction

The precise determination of the aromatics content of middle distillates (gas oils and kerosenes) is of major concern for prosses engineers. The group-type separation of hydrocarbons by liquid chromatography has been widely reported [1–3]. An HPLC method has also recently been normalized (European Committee for Standardization: ECS) that gives mono-, di- and polyaromatics contents in commercial gas oils with fairly good repeatability and reproducibility for individual and total aromatics. However, it has been stressed that this method is sample sensitive, particularly for mildly hydrotreated gas oils. This hinders the usefulness of the method for the design of hydrotreatment processes [4]. Mass spectrometry, on the other hand, needs further adaptation of the data treatment matrix to deal with kerosenes cuts.

The coupling of a gas chromatograph to a liquid chromatograph is a powerful tool for achieving a high separation efficiency and adapting a quasi-universal detector to HPLC. However, for the application in question, the choice between on-line and off-line coupling must be made. The techniques for transferring a large volume of liquid into a gas chromatograph have been extensively described [5]. The application of on-line coupling to petroleum products analysis has also been described, mainly for the identification of polycyclic aromatic compounds [6,7]. For on-line coupling, two types of interface must be considered: either a "loop-type" or an

* Corresponding author.

0021-9673/94/$07.00
SSDI 0021-9673(94)00494-T

"on-column" interface. On the one hand, the "loop-type" interface is known to produce losses of the more volatile compounds of the sample and therefore seems unsuitable for the analysis of gas oils whose initial cut point can start at 150°C. On the other hand, the "on-column" interface is not suitable for the injection of the large volumes of liquid obtained with standard HPLC columns. For these reasons, off-line coupling was chosen.

The aim of this study was to evaluate the off-line coupling of HPLC with GC to obtain an analytical "reference" method for this type of sample taking advantage of the universal response of flame ionization detection (FID).

2. Experimental

2.1. Materials

The eluent for HPLC and semi-preparative liquid chromatography were HPLC-grade *n*-pentane and HPLC-grade dichloromethane and methanol, respectively (Solvants, Documentation, Synthèses, Peypin, France), degassed with helium. As standards, triacontane (n-C_{30}) (>99%) was obtained from Aldrich (St. Quentin Fallavier, France) and *n*-ocatane (n-C_8) and *o*-xylene (both >99%) from Merck (Darmstadt, Germany).

Silica gel, 75–100 μm (100–200 mesh) (Davison Chemical, USA) and alumina gel, 60–230 μm (alumina 90, 70–230 mesh; Merck) were used as stationary phases for semi-preparative liquid chromatography.

2.2. Instruments and columns

The semi-preparative liquid chromatographic equipment consisted of an injection pump capable of delivering the eluent at a flow-rate of 2 ml/min (Model 420 pump; Kontron, Zurich, Switzerland), a calibrated injection loop of 4 ml and a stainless-steel column [110 cm × 9.53 mm (3/8 in.) O.D.]. The column was dry-filled with a bottom bed of silica (ca. 25 g) and completed with an upper bed of alumina, both activated overnight at 180°C in an oven.

The HPLC equipment consisted of a Waters (Milford, MA, USA) 600-MS solvent-delivery system equipped with a back-flush valve (Waters automated switching valve) and a UV detector (Spectromonitor 4100; LDC, Riviera Beach, FL, USA). The columns were either two aminosilica columns (as in the ECS method) or two silica columns, both obtained from Applied BioSystems (San Jose, CA, USA). These columns were 250 mm × 6.35 mm (1/4 in.) O.D. and showed a resolution for the separation of cyclohexane–*o*-xylene of 5 and 13.9, respectively, measured with one column.

The capillary GC equipment consisted of a Model 3500 gas chromatograph (Varian, Sunnyvale, CA, USA) equipped with an on-column injector and an autosampler (Varian 8035). The fused-silica capillary column was coated with a DB-1 methylsilicone stationary phase with a film thickness of 0.25 μm (60 m × 334 μm I.D.) (J&W Scientific, Rancho Cordova, CA, USA). The data acquisition and processing were performed with an HP1000 system (Hewlett-Packard, Avondale, PA, USA).

The mass spectrometer was a Kratos (Manchester, UK) MS50. The data were analysed using a modified Fitzgerald method according to ref. [8].

2.3. Procedure

For semi-preparative liquid chromatography, the eluents used were *n*-hexane for the elution of the saturates fraction and dichloromethane–methanol (9:1 v/v) for the elution of the aromatics fraction. About 2.5 g of sample, precisely weighed, were dissolved in 10 ml of *n*-hexane. The collection of the fractions was carried out on a fixed elution time basis as the method had been previously validated on a wide range of samples using refractive index (RI) and UV detectors. The solvents were carefully evaporated at room temperature under a nitrogen flow and a mass balance was made. The same type of separation using different eluents has also been described elsewhere [9].

For HPLC separation with aminosilica columns, the mobile phase (*n*-pentane) was used without further treatment. For separations with the silica columns, a set of two precolumns was installed between the pump and the injection valve in order to minimize the water content of pentane. One of the columns was filled with molecular sieve 4 Å and the other with silica activated at 180°C overnight. The eluent flow-rate was set at 1 ml/min. The samples, gas oil or kerosene, were diluted in *n*-pentane at about 20% (w/w) with addition of internal standards: n-C_8, n-C_{30} and *o*-xylene. The volume injected was 20 μl. A back-flush was applied to elute the aromatics as a single peak.

As long-chain aliphatic hydrocarbons elute close to the aromatics and long-chain substituted alkylaromatic hydrocarbons elute close to the saturates, an RI and a UV detector were used to monitor the separation. Typical chromatograms of a gas oil obtained with these detectors are shown in Fig. 1. The RI detector was first used to monitor the separation of aromatic from aliphatic compounds because both show a response on the RI detector (Fig. 1a). The UV detector was used at a wavelength of 210 nm to determine the back-flush point (Fig. 1b). The saturates fraction was collected between the retention time t_0 determined with RI detection and the back-flush time determined with UV detection; the aromatics fraction was collected with the help of the UV detector at 210 nm. Fractions of 2–4 ml were collected with concentrations of about 2000 ppm of saturates and 500 ppm of aromatics.

Further, for some analyses with correct back-flush times, the absence of monoaromatics in the collected saturates fraction was checked using UV analysis at 200 nm, a wavelength that enhances the monoaromatics response.

For capillary GC analysis, the carrier gas was helium at a pressure of 2.07 MPa (30 p.s.i.), the FID sensitivity was set to 10^{-12} A and the injection volume was 1 μl. The injector temperature was programmed from 40 to 300°C at 150°C/min and the temperature programme for elution was from 40 to 320°C at 3°C/min.

Sequences of injections including pentane injections (blank) were carried out and the integration of chromatograms was performed after subtraction of the blank. The total aromatics content was either calculated from the difference between 100% and the percentage of the saturates fraction using both internal standards (n-C_8 and n-C_{30}) or from the aromatics fraction using the *o*-xylene standard. It was observed that a repeatable and accurate determination of the saturates and aromatics contents of the fractions needs a minimum concentration level of product in the injected fraction and careful washing of the automated sampler fitted to the gas chromatograph.

3. Results and discussion

3.1. Gas oil analysis

The first step in this study was to optimize the experimental conditions. The method was evaluated with the two types of HPLC stationary phases using a well characterized gas oil (CEN17) containing about 27% (w/w) of aromatics.

It was shown that the aminosilica column requires particular attention to the back-flush time applied. However, the silica column gives a greater latitude for the choice of back-flush time owing to its much better resolution between saturates and aromatics.

Multiple samples of HPLC fractions were obtained and analysed by GC. Fig. 2 shows an example of a gas chromatogram of each fraction. The determination of the aromatics content was systematically observed to depend on the procedure used: the aromatics percentage obtained from the saturates fraction quantified using n-C_8 was greater than that obtained from the aromatics fraction quantified using *o*-xylene, which was in turn greater than that obtained from the saturates fraction quantified using n-C_{30}. Determination using the n-C_{30} internal standard was found to be unsuitable mainly owing to peak tailing. The determination using n-C_8 was considered to overestimate the aromatic content

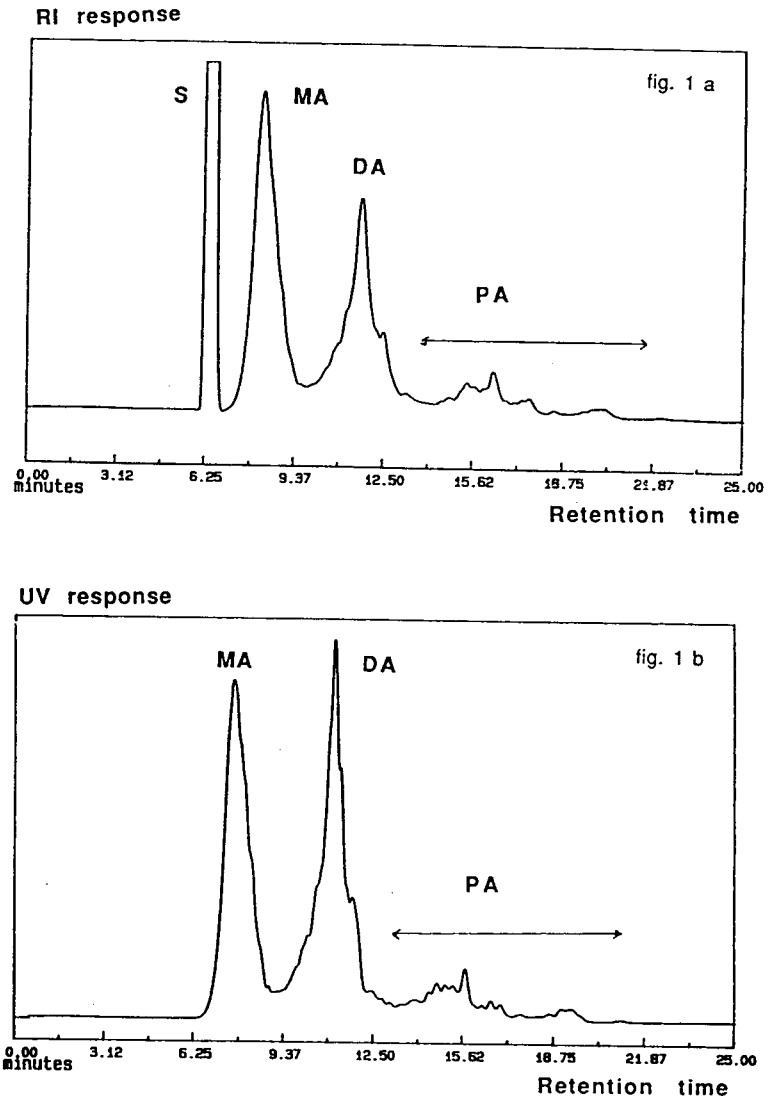

Fig. 1. Typical liquid chromatograms of a gas oil (CEN17) obtained with two aminosilica columns. (a) RI detection and (b) UV detection at 210 nm. S = saturates; MA = monoaromatics; DA = diaromatics; PA = polyaromatics.

compared with the determination using *o*-xylene, which was attributed to the presence of *n*-C_8 at low levels in the gas oil, as showed by direct GC injection of the gas oil. Consequently, only the results obtained from the HPLC aromatics fraction quantified using *o*-xylene standard were considered.

The statistical treatment of these results gave a repeatability for the total aromatics content at a level of 27% (w/w) of 3.2 and 2.6% (w/w) for the aminosilica and the silica column, respectively. The latter repeatability corresponds to a confidence interval of ±1.8% (w/w) for a single measurement. The average aromatics content of the tested gas oil was found to be 26.6 mass% (w/w) with the aminosilica column and 26.1 mass% (w/w) with the silica column. These results show a good agreement with MS measurements, i.e., 26.5 mass% (w/w) with a repeatability of 2.0%.

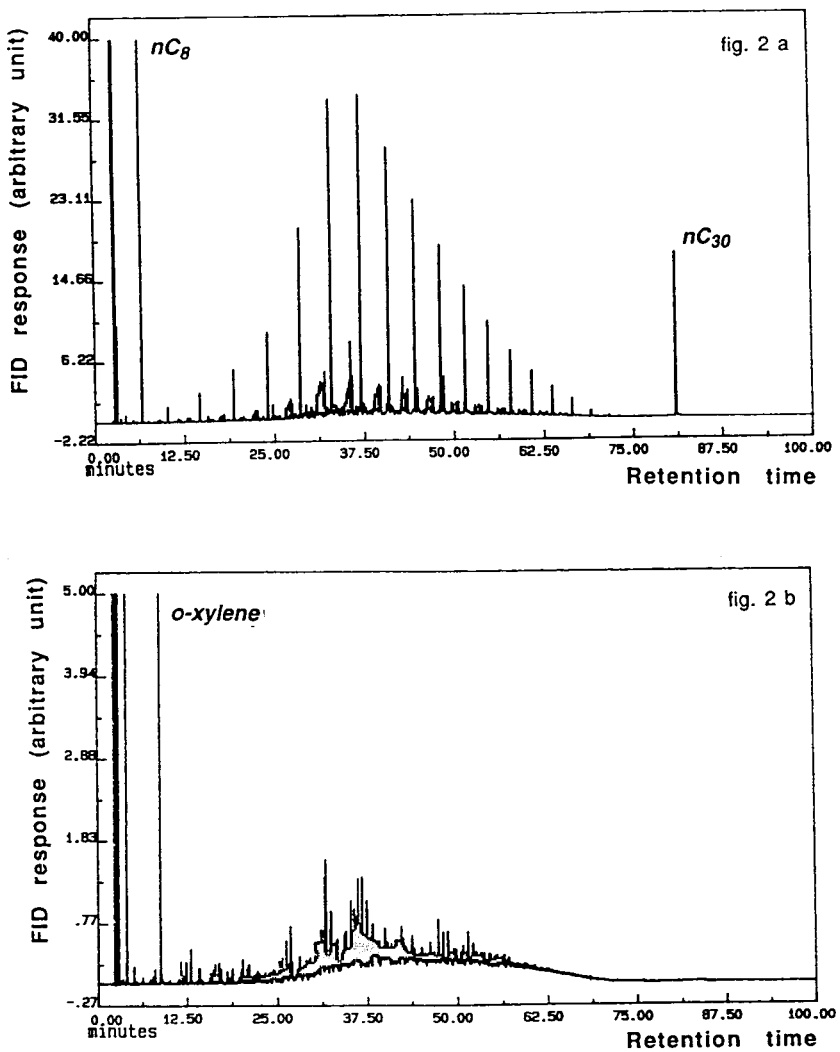

Fig. 2. Gas chromatograms of (a) the saturates and (b) the aromatics fractions of a gas oil (CEN17).

The HPLC–GC method was then used, with the aminosilica column, to determine the total aromatics content of a gas oil before and after a mild hydrotreatment. The results in Table 1 demonstrate the sample sensitivity of the ECS HPLC method and the good agreement between the HPLC–GC, MS and semi-preparative liquid chromatographic results.

The MS analysis shows that during this mild hydrotreatment a large decrease in the poly- and diaromatics content (ca. −13%, w/w) occurs whereas the monoaromatics content increases (ca. +5.5%), resulting in a decrease in the total aromatics content (ca. −7%). Results not reported in Table 1 show that after this hydrotreatment, the monoaromatics fraction contains much more C_nH_{2n-8} and C_nH_{2n-10} compounds (tetralin + indane + indene) than C_nH_{2n-6} compounds (alkylbenzenes). These C_nH_{2n-8} and C_nH_{2n-10} compounds arise from the hydrogenation of diaromatics.

The ECS HPLC method, while showing the same general trends for the three aromatic groups, does not show any significant decrease in

Table 1
HPLC–GC analysis of non-hydrotreated and mildly hydrotreated gas oils using an aminosilica HPLC column and comparison with MS, HPLC (ECS method [4]) and SA[a]

Compounds	Content (%, w/w)					
	Feed		Hydrotreated gas oil			
	MS	HPLC	MS	HPLC	HPLC–GC	SA[a]
Monoaromatics	16.4	18.5	22.0	29.4		
Diaromatics	16.5	13.2	4.6	2.9		
Polyaromatics	0.8	0.5	0.1	0.1		
Total aromatics	33.7	32.3	26.9	32.4	27.7[b]	27.5

[a] Separation of saturates and aromatics by semi-preparative LC.
[b] Average of two measurements.

the total aromatics content after hydrotreatment. It is clear from Table 1 that this is due to an overestimation of the monoaromatics content of the mildly hydrotreated gas oil. This biased result can be explained from MS analysis, which shows that *o*-xylene, the external standard for the determination of monoaromatics in the ECS method, is not well representative of the monoaromatics fraction owing to the presence of a large amount of C_nH_{2n-8} and C_nH_{2n-10} compounds in that fraction. As the differential refractive indices of tetralin and indane in *n*-heptane are ca. 0.15 compared with 0.118 for *o*-xylene (value obtained from data in ref. [10]), it is clear that the calibration with *o*-oxylene overestimates the monoaromatics content in the particular instance.

The HPLC–GC method overcomes this drawback by the use of internal standards and FID.

3.2. Kerosene analysis

The method was applied to two kerosenes, using aminosilica columns. For HPLC separation of kerosenes, the influence of the HPLC column (silica or aminosilica) on the back-flush time is much less critical as the distillation interval of these products is narrower than that of gas oils and less interferences between saturates and monoaromatics can occur.

Fig. 3 shows an example of a chromatogram for each fraction. Comparison of Fig. 3 with Fig. 2 clearly shows the influence of the distillation interval on the determination of aromatics by HPLC–GC. The narrower distillation interval of kerosenes makes the determination of the aromatics content easier as the maximum FID response for aromatics in kerosene is around 13 for ca. 14% aromatics (see Fig. 3: elution time in GC between ca. 10 and 35 min), whereas the maximum FID response for aromatics in gas oils is around 1.8 for ca. 27% aromatics (see Fig. 2: elution time in GC between ca. 10 and 75 min.). As a consequence the injected concentration of the aromatics fraction in GC for an accurate determination of the aromatics content is less critical for kerosenes than for gas oils.

The results reported in Table 2 show very good repeatability of measurements for the two samples and good agreement between aromatics content calculated from GC injection of either the saturates (using n-C_8 standard) or the aromatics fraction. It must be pointed out that these kerosene cuts had a high initial boiling point compared with commercial kerosenes. For commercial kerosenes the same problem as observed with gas oils would probably occur with the

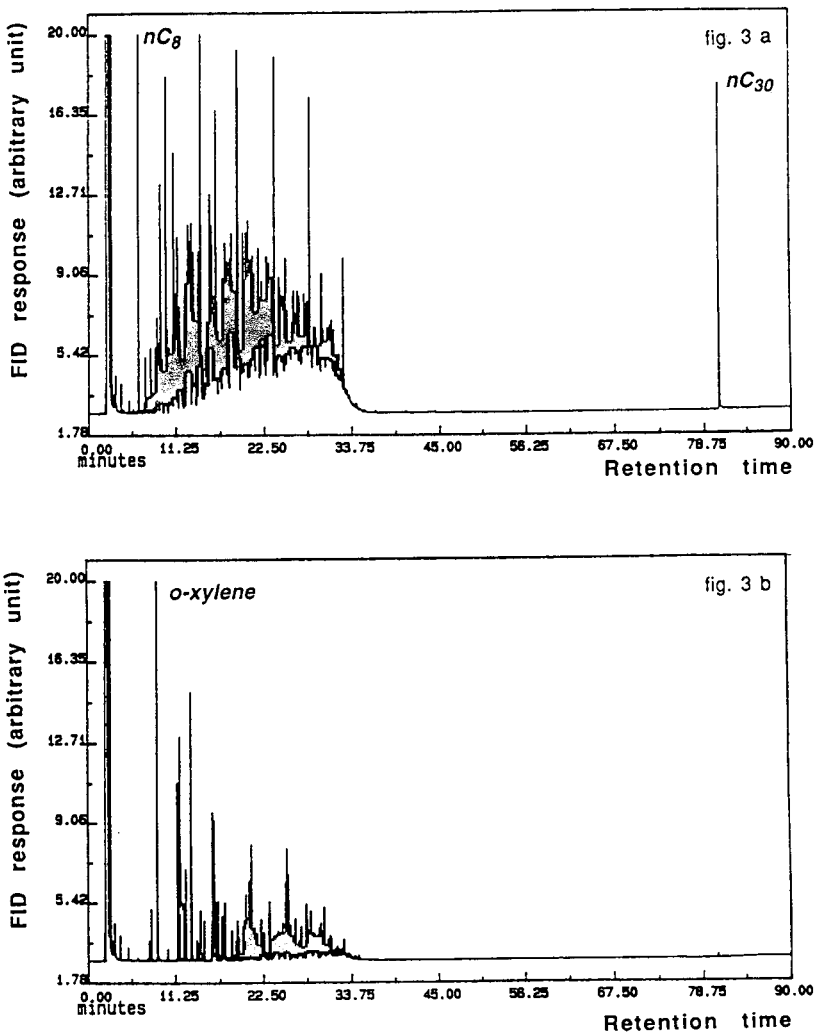

Fig. 3. Gas chromatograms of (a) the saturates and (b) the aromatics fractions of kerosene 2 (see Table 2).

determination using n-C_8 internal standard. Nevertheless, the lower final cut points of kerosenes would enable one to choose an intermediate internal standard between n-C_8 and n-C_{30} which does not interfere with the kerosene, e.g., n-C_{20}.

For the kerosene 1 samples a semi-preparative separation of saturates and aromatics was performed by liquid chromatography. The agreement between the analytical and the semi-preparative separation was very good. A comparison with the fluorescence indicator adsorption (FIAd) method [11], which gives the volume percentage, was also made and showed that, when mass percentages were calculated, taking into account the specific gravity of aromatics versus that for the whole kerosene, the FIAd method overestimates aromatics content compared with the HPLC–GC method.

On the basis of these results, we conclude that

Table 2
HPLC–GC analysis of two kerosene cuts using an aminosilica HPLC column and comparison with SA[a] and FIAd[b] methods

Method	Aromatics content			
	Kerosene 1	(b.p. 190–225°C)	Kerosene 2	(b.p. 150–250°C)
	From saturates fraction (n-C_8 internal standard)	From aromatics fraction (o-xylene internal standard)	From saturates fraction (n-C_8 internal standard)	From aromatics fraction (o-xylene internal standard)
HPLC–GC (%, w/w)	17.2, 17.0	17.3, 17.4	14.3, 14.1	14.0, 14.0
SA[a] (%, w/w)	17.1		Not measured	
FIAd[b] (%, v/v)	17.0		13.5	

[a] Separation of saturates and aromatics by semi-preparative liquid chromatography. Average of two measurements.
[b] ASTM D1319 [11].

HPLC–GC seems to be a repeatable and accurate method for the determination of the aromatics content in kerosenes and that the FIAd method probably overestimates this aromatics content. The analysis of a wider range of kerosenes will be necessary to confirm and/or generalize this point.

4. Conclusions

The off-line HPLC–GC method was evaluated for the determination of the total aromatics content in middle distillates. This method uses internal calibration and shows fairly good repeatability for both gas oils and kerosenes. We consider that this method could advantageously be used as a "reference" method for this determination in both gas oils and kerosenes. Further work is needed to determine the repeatability of the method for the whole range of aromatics content encountered in middle distillates.

Acknowledgements

We thank Dr. Anne Fafet (IFP) for the mass spectrometric analyses.

References

[1] J.C. Suatoni and R.E. Swab, *J. Chromatogr. Sci.*, 13 (1975) 361.
[2] T.V. Alfredson, *J. Chromatogr.*, 218 (1981) 715.
[3] D.J. Cookson, C.J. Rix, I.M. Shaw and B.E. Smith, *J. Chromatogr.*, 312 (1984) 237.
[4] *Minutes of CEN/TC19/WG18 Meeting*, European Committee for Standardization, Brussels, 4 June 1993.
[5] K. Grob, *On-Line Coupled LC–GC*, Hüthig, Heidelberg, 1991.
[6] I.L. Davies, K.D. Bartle, P.T. Williams and G.E. Andrews, *Anal. Chem.*, 60 (1988) 204.
[7] I.L. Davies, K.D. Bartle, G.E. Andrews and P.T. Williams, *J. Chromatogr. Sci.*, 26 (1988) 125.
[8] H. Castex, R. Boulet, J. Juguin and A. Lepinasse, *Rev. Inst. Fr. Pét.*, 38 (1983) 523.
[9] P.T. Williams, G.E. Andrews, K.D. Bartle, P. Bishop and P. Watkins, *Biomed. Environ. Mass Spectrom.*, 15 (1988) 517.
[10] R.C. Weast (Editor), *Handbook of Chemistry and Physics*, CRC Press, Cleveland, OH, 52nd ed., 1971–1972, Section C.
[11] *Manual on Hydrocarbon Analysis, 3rd ed., ASTM D1319*, American Society for Testing and Materials, Philadelphia, PA, 1977.

ELSEVIER

Journal of Chromatography A, 683 (1994) 223–231

JOURNAL OF CHROMATOGRAPHY A

Determination of organotin compounds by capillary supercritical fluid chromatography with inductively coupled plasma mass spectrometric detection

Earl Blake[a], Mark W. Raynor[a,*], David Cornell[b]

[a]*Department of Chemistry and Applied Chemistry, University of Natal, King George V Avenue, Durban 4001, South Africa*
[b]*Department of Geology, University of Natal, King George V Avenue, Durban 4001, South Africa*

Abstract

Supercritical fluid chromatography with inductively coupled plasma mass spectrometric detection is a new technique being developed for the analysis of organometallic compounds. A new interface has been developed for coupling the two instruments and this has been evaluated in terms of the restrictor temperature. The effect of concentration of analyte on peak intensity has been evaluated and reasons for the observed behaviour have been proposed.

1. Introduction

Organotin compounds are used extensively as biocides and in marine anti-fouling paints and as these compounds are continuously released into the marine environment they accumulate in sediments, marine organisms and water [1,2]. Many of these compounds are toxic to aquatic life such as shell fish and can accumulate through the food chain to cause damage to other species as well. The compounds most important in this respect are the short-chain organotin compounds such as methyl-, ethyl-, propyl- and butyltin compounds and more specifically the tetra- and trialkyltin compounds [3]. These compounds are also capable of forming breakdown products which may or may not be toxic to aquatic life [1]. In the case of butyltin compounds tetrabutyltin will decay in the presence of small amounts of ultraviolet light to form tributyltin chloride which in turn decays to dibutyltin dichloride and eventually butyltin trichloride before decaying completely to inorganic tin. A characteristic of this decay is that toxicity generally increases with the number of alkyl chains with greatest toxicity being from tributyltin chloride [1].

There has recently been much interest in the analysis of organotin species in the environment and the methods employed have included GC with atomic absorption spectrometry (AAS) and atomic emission spectrometry (AES) as detectors and HPLC with mass spectrometric (MS) detection [4–10]. Later work has concentrated on linking GC with plasma MS detectors such as microwave-induced plasma (MIP) MS [11] and inductively coupled plasma (ICP) MS [12]. Within the past two years a method that has been shown to be amenable to the analysis of these organotin compounds is supercritical fluid chromatography (SFC) with ICP-MS detection. This

* Corresponding author.

0021-9673/94/$07.00
SSDI 0021-9673(94)00479-S

method has been shown to allow speciation of organotin compounds using SFC and detection of these compounds at very low detection limits using ICP-MS [13,14]. The main advantage of this method is its ability to analyse involatile and thermally labile compounds thus eliminating the need for derivatisation to compounds more suitable for GC. Moreover, the use of high-pressure programmes can reduce the analysis time to less than 5 min. If a modifier is added to the mobile phase then it is possible to analyse many polar compounds that could not be analysed using pure CO_2 mobile phase. Compounds that are amenable to SFC should also be amenable to supercritical fluid extraction (SFE) assuming that matrix effects are not too great. This eliminates the need for extraction using potentially harmful organic solvents and possible loss or contamination of analyte during extraction. Thus, it should be possible to develop an on-line method for extraction and analysis of organometallics using SFE–SFC–ICP-MS.

The method used for linking the SFC with ICP-MS has involved a heated transfer line from the SFC and a series of Swagelok unions to connect the restrictor to the torch. A copper tube housing the restrictor was inserted into the ICP torch and the restrictor was connected to the butt connector through a three-way Swagelok. Through the third arm of the union heated argon was added as make-up gas. The principle of this interface is to heat the entire interface and the argon make-up gas and thus keep the restrictor heated at the same time. The transfer line is enclosed in heating tape and heated to the same temperature as the oven thus ensuring a constant temperature along the column [13]. The principles of this interface are good but it would appear that this interface is bulky and difficult to assemble. Moreover, once SFC has been linked to ICP-MS the only work that can be carried out is that using SFC–ICP-MS and if either instrument must be used individually it would be necessary to dismantle the interface before continuing. In addition, the work so far has made use of frit restrictors which are costly to replace if blocked or damaged and which have been shown by Pinkston and Hentschel [15] to perform inadequately at high elution pressures.

In this study a new interface has been developed and evaluated using environmentally relevant organotin compounds and a different type of restrictor has been used. The effects of the restrictor temperature and changes in the concentration have been studied. Changes in the plasma due to the mobile phase pressure program have also been studied. The ICP-MS conditions have been optimised by focusing and tuning the instrument on the element of interest. The results obtained have allowed the evaluation of ICP-MS as a detection method for SFC.

2. Experimental

2.1. Supercritical fluid chromatography

The chromatograph consisted of a Lee Scientific Series 600 GC/SFC oven, a Lee Scientific Series 600 syringe pump and a Lee Scientific Series 600 controller (Lee Scientific, Salt Lake City, USA). The pump and injection valve were cooled to approximately 7°C using a Neslab Endocal RTE 110 cooler. The mobile phase was SFC-grade CO_2 (Air Products, Allentown, USA). The capillary column was a 2 m SB-Biphenyl-30 capillary column with a 0.25-μm film thickness and the tapered restrictor was made in the laboratory from 50 μm I.D. capillary tubing (Lee Scientific) [16]. The tapered end of the restrictor was protected by a sleeve of 320-μm I.D. capillary tubing (SGE, Australia) bonded to the restrictor with polyimide resin. The gaseous restrictor flow at 15.2 MPa was measured using a bubble flow meter to be 1.5 ml/min. Injection onto the column was through a AC14UWP Valco injector with a 200-nl sample loop and a polyether ether ketone (PEEK) splitless adapter and activated using helium gas. Time-split injection was used with a 100 ms injection time.

2.2. Mass spectrometry

The ICP-MS instrument was a VG PlasmaQuad (VG Elemental, Cheshire, UK) controlled by an IBM personal computer. All acquisitions were obtained using single-ion monitoring

Table 1
Typical ICP operating conditions and MS settings

Incident power (kW)	1.35
Reflected power (W)	<5
Coolant gas flow (l/min)	14
Auxillary gas flow (l/min)	0.5
Make-up gas flow (l/min)	0.8
Intermediate pump (mbar)	$2.0 \cdot 10^{-4}$
Expansion pump (mbar)	2.4
Analyser pump (mbar)	$4.2 \cdot 10^{-6}$

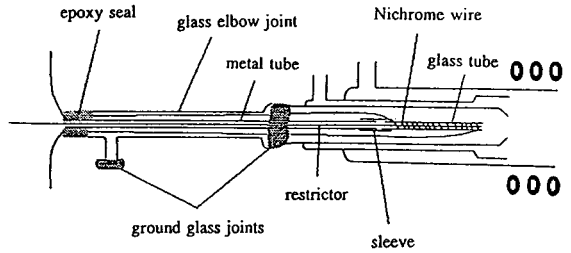

Fig. 2. Schematic diagram of the capillary SFC–ICP-MS interface design.

with 2048 channels. The dwell time per channel was altered according to the total analysis time on SFC. The operating and tuning parameters are shown in Table 1.

2.3. SFC–ICP-MS interface

The SFC–ICP-MS system is shown in Fig. 1 and details of the interface are shown in Fig. 2. The glass elbow between the nebuliser and the torch was modified to include a third arm so that the elbow resembled a T-join. A 1/16 in. (1 in. = 2.54 cm) I.D. stainless-steel tube with a fitting housing a ferrule to secure the fused-silica transfer line leading to the restrictor was placed in the end opposite the ground glass joint. A melting point tube was fitted with a heater consisting of tightly wound Nichrome wire (GM Heating, Durban, South Africa) which was bonded to the melting point tube and insulated using polyimide resin. The ends of the wire were coated with shrinksleeve to provide adequate insulation. The melting point tube was connected to the stainless-steel tube using a glass sleeve and polyimide resin. The wires from the heater were brought through the modified glass elbow to emerge where the stainless-steel tube entered the elbow. The stainless-steel tube and wires were then fixed in place using 372 epoxy which also formed a gas-tight seal. Care was taken during assembly to ensure that the stainless-steel tube and the melting point tube were kept level and straight thus ensuring that when the interface was fitted to the torch the maximum amount of sample would enter the plasma and no condensation or crystallisation would occur in the torch. The restrictor was inserted in the tubing so that the restrictor end was flush with the end of the melting point tube. The restrictor was held in place using an SGE nut and graphitised vespal ferrule on the stainless-steel tube. The restrictor was connected to the column using an SGE butt connector. The oven was placed as close as possible to the ICP to minimise the loss of chromatographic efficiency and the column was brought out of the side of the oven and con-

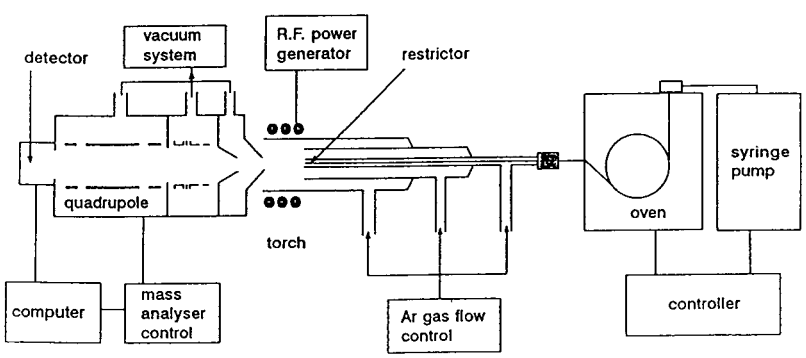

Fig. 1. Schematic diagram of the SFC–ICP-MS system. R.F. = Radio frequency.

nected to the restrictor without any heating. The length of column outside the oven was about 30 cm. As the interface was a modification of the glass elbow between the nebuliser and the torch, it could be fitted to the torch and nebuliser in the normal way. The interface was heated by connecting the wires to a GP 30-5 d.c. power supply. The temperature of the interface was varied by controlling the voltage applied to the wires.

2.4. Reagents

Tetrabutyltin (TBT) was obtained from Aldrich (Milwaukee, USA). Tributyltin chloride (TBTCl) and tetraphenyltin (TPT) were obtained from Janssen Chimica (Geel, Belgium) and triphenyltin chloride (TPTCl) was obtained from Merck (Darmstadt, Germany). The purities of the analytes were 98, 90, 97 and 98%, respectively. The solvent used for preparing solutions was dichloromethane (Holpro Lovasz, Midrand, South Africa). All solutions were prepared from stock solutions of 1000 μg/ml in each analyte.

3. Results and discussion

3.1. Interface use and assembly

The interface is relatively easy to assemble from commonly available materials and can be used with a minimum of disruption to either the SFC system or the ICP-MS instrument. As it is a modification of the elbow joint between the nebuliser and the ICP torch it can be inserted into the torch in less than a minute. Moreover, because it is attached to the nebuliser there is no need to use elaborate methods for the introduction of the heated argon make-up gas as the argon can be heated internally in the ICP-MS instrument and then follow its normal path to the torch through the nebuliser. A further advantage of this interface is that only the restrictor is heated directly and the temperature of the restrictor can be controlled rather than keeping the whole interface at high temperatures. The remainder of the transfer line was heated to 60°C by the heated argon.

The temperature of the restrictor is controlled by the voltage applied to the Nichrome wire. Although this is simple to do using a d.c. power supply with variable voltage and current, it is more difficult to measure the temperature. To obtain an idea of the temperature the interface was placed together with a thermocouple in a torch on the bench top. The voltage was then increased from 0 V in one volt increments and the temperature inside the torch next to the restrictor was noted. A period of 30 min was left between each reading to allow the temperature to equilibrate. It was found that a voltage range of 6 to 10 V gave a temperature range of about 200 to about 320°C. Although these results give a general idea of the voltage/temperature dependence, it should not be assumed that the same relationship will apply under operating conditions. Due to the difficulty of measuring the temperature of the restrictor under operating conditions it is not possible to propose a "true" voltage/temperature relationship. However, as the argon make-up gas is heated and flows over the glass tube rather than over the restrictor it is reasonable to assume that the parameters to be used under operating conditions will be similar to those used in the bench-top experiment. There are difficulties in testing this assumption as a low voltage will allow condensation of some analytes and the restrictor will block up and a high voltage could cause the glass tubing and the polyimide to melt or decompose and this in turn could seriously damage the ICP-MS instrument. However, in this study an operating range of 6 to 10 V was found to be adequate.

The interface can be considered as a modification of the ICP sample introduction system and so causes minimum disruption to this instrument. If necessary, the interface can be easily removed and replaced with the normal elbow joint to allow the ICP-MS instrument to be used individually or, for minor tests on sensitivity and other minor experiments, the interface can be left in and ICP-MS standards can be introduced with the SFC connected. This saves time and

minimises the possibility of equipment damage during disassembly.

3.2. Effect of the pressure program on the plasma

When using ICP-MS as a detection method for SFC it is necessary to monitor changes in the argon plasma as any changes may give an indication of possible interferences and the effect of the mobile phase on the plasma. To monitor the plasma the instrument was tuned on the ion at $m/z = 80$ which corresponds to the argon dimer cation. Fig. 3 shows the change in the plasma with no mobile phase flowing and with a solvent injection of dichloromethane under normal analysis conditions. With no mobile phase flowing there is no change to the plasma and only a slight negative baseline drift is observed. When mobile phase flows at the normal pressure program it can be seen that there is a distinct drop in the baseline approximately half way through the analysis. This corresponds to a pressure of about 27 MPa and is contrary to results obtained using the other interface which found a drop in the baseline at the onset of a much higher pressure ramp [14]. As the pressure ramp in this study is fairly low it can be assumed that at lower pressures the plasma will not be affected by the mobile phase but at higher pressures the mobile phase causes a damping effect on the formation of argon dimer as other side reactions occur within the plasma. The combined results indicate that as the pressure ramp increases the greater this damping effect will be. This is due to the greater flow of mobile phase at higher ramp rates. If dichloromethane solvent is injected there is a distinct negative peak in the baseline. This is the result of a side reaction in the plasma as argon reacts with the chlorine in the solvent to preferentially form ArCl and prevent argon dimer formation. After the solvent peak has been eluted and there is again a lack of chlorine the formation of dimer resumes.

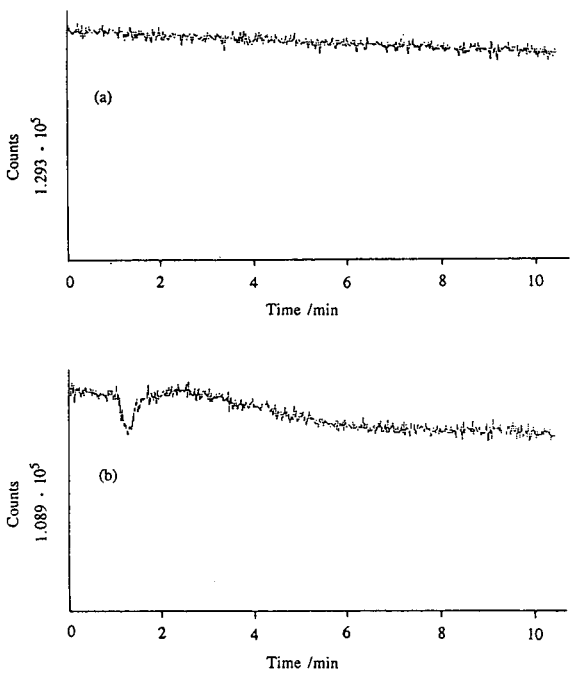

Fig. 3. SFC–ICP-MS background scan of the ion at m/z 80 with no mobile phase flowing (a) and with a dichloromethane solvent injection under normal analysis conditions (b). CO_2 programmed at 3.04 MPa/min from 12.2 MPa (hold for 30 s) to 40.5 MPa (hold for 1 min) and an isocratic temperature of 75°C.

Fig. 4 shows the effect of the mobile phase program on ArC^+ at $m/z = 52$. There is no significant change in the plasma at this charge-to-mass ratio despite a small increase in the flow of mobile phase with increased pressure from 1.5 to 3.5 ml/min. This can be ascribed to a constant increase in supply of carbon into the plasma with a constant rate of ArC^+ formation. This would

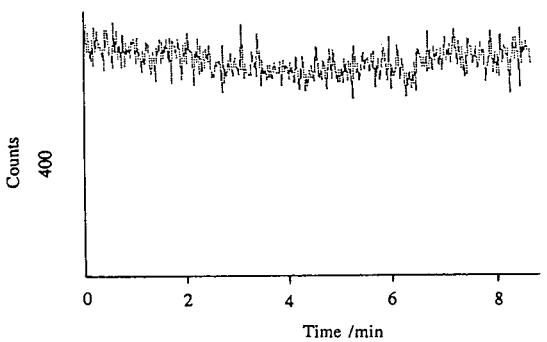

Fig. 4. The effect of mobile phase on ArC^+ at m/z 52. Mobile phase programmed from 12.2 MPa (hold for 30 s) to 40.5 MPa (hold for 1 min) at 3.04 MPa/min and an isocratic temperature of 75°C.

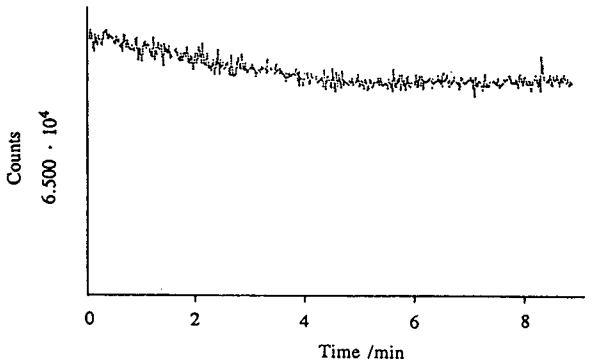

Fig. 5. The effect of mobile phase on ArO at m/z 56. Mobile phase programmed from 12.2 MPa (hold for 30 s) to 40.5 MPa (hold for 1 min) at 3.04 MPa/min and an isocratic temperature of 75°C.

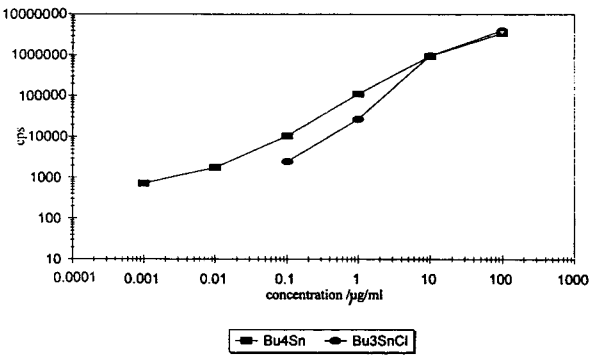

Fig. 6. A comparison of the effects of concentration on peak intensity for Bu_4Sn and Bu_3SnCl.

account for the fairly high background of this ion and should not cause any interference with the analysis. Fig. 5 shows the effect of the oxygen on the plasma by monitoring ArO. There is no significant change in the ArO present and even a slightly negative drift is observed. However, the background level is quite high compared to that of ArC^+ and this is expected as there is significantly more oxygen in the mobile phase than carbon. Moreover, as the plasma is exposed to the atmosphere there must also be some reaction with atmospheric oxygen.

3.3. Effect of the analyte concentration

The analytes initially considered were tetrabutyltin, tributyltin chloride, tetraphenyltin and triphenyltin chloride. However, it was found that triphenyltin chloride had a significant memory effect within the injector and thus interfered with the analysis at low concentrations. Thus, it was decided to limit the study of concentration dependence to tetrabutyltin and tributyltin chloride. Solutions of tetrabutyltin and tributyltin chloride ranging through 0.001, 0.01, 0.1, 1, 10 to 100 μg/ml were prepared from a stock solution of 1000 μg/ml. Each solution was analysed in triplicate and a plot of concentration versus peak intensity was made.

From the graph in Fig. 6 it can be seen that for tetrabutyltin there is a slight increase in intensity below concentrations of 0.01 μg/ml and thereafter a sharp increase in peak intensity between 0.01 and 10 μg/ml. Beyond 10 μg/ml the increase in peak intensity again begins to level off. This trend corresponds to the detector's ability to "see" the compound of interest. Below 0.01 μg/ml, although the detector can detect the Sn ion, any increase in concentration will give only marginal increase in the detector sensitivity. However, above 0.01 μg/ml each increment increase in concentration will be significantly easier for the detector to detect. Above 10 μg/ml any increase in concentration will more or less "flood" the detector and any increase in sensitivity will be marginal. Thus, it is reasonable to assume that above concentrations of about 1000 μg/ml very little increase in sensitivity will be obtained and at such high concentrations there may even be damage to the detector due to overload of the ion of interest.

Fig. 6 also shows the trend for change in peak intensity with concentration for tributyltin chloride. This is significantly different from tetrabutyltin in that the lowest concentration that can be detected is 0.1 μg/ml. The reason for this is the compounds greater polarity than tetrabutyltin. Tributyltin chloride will tend to adsorb more strongly onto any active sites in the column resulting in a certain amount of peak tailing as shown in Fig. 7. At lower concentrations the same adsorption interactions will occur as at high concentrations but as there is less analyte at the low concentration tailing becomes more relevant

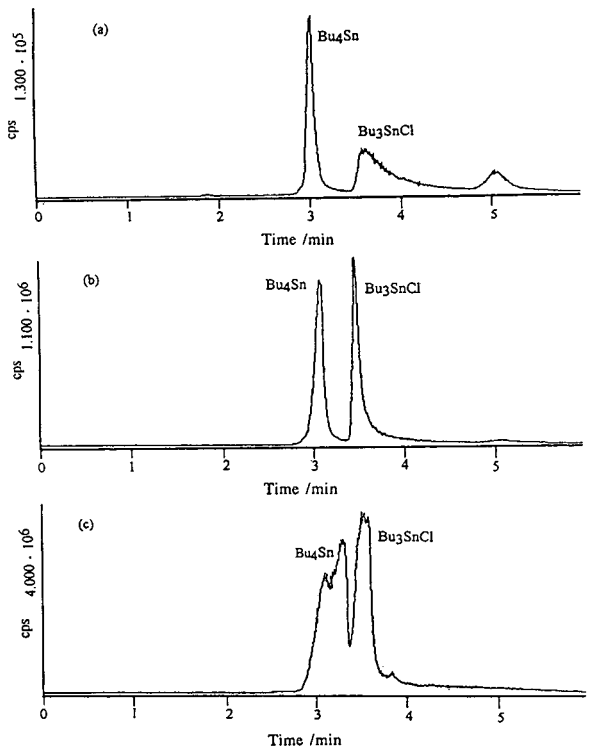

Fig. 7. Single-ion scan chromatograms of ^{120}Sn with Bu_4Sn and Bu_3SnCl concentrations of (a) 1 μg/ml, (b) 10 μg/ml and (c) 100 μg/ml. SFC Conditions: 2 m × 50 μm SB-Biphenyl-30 column, CO_2 mobile phase programmed from 12.2 MPa (hold for 30 s) to 24.3 MPa (hold for 1 min) at 3.04 MPa/min and constant temperature of 75°C. Time split injection of 100 ms and an applied voltage on the interface of 8.0 V.

resulting in a decrease in the detection limit. However, at high concentrations, although the same interactions occur and the same amount of sample adsorbs to the column, in relation to the large amount of analyte present this tailing will be less significant in relation to the peak intensity.

The comparison of the two analytes in Fig. 6 shows that below 10 μg/ml the intensity of tetrabutyltin is significantly greater than tributyltin chloride but at 10 μg/ml the two analytes converge. Above 10 μg/ml there is a slight trend for tributyltin chloride peak intensity to be greater than tetrabutyltin. In Fig. 7c it is evident that there is a change in the peak shape of tetrabutyltin as the peak broadens and begins to split. This is due to overloading of the column and interface or the ICP-MS detector. The linearity of tetrabutyltin and tributyltin chloride is over three orders of magnitude from 0.1 to 10 μg/ml. The slope of the linear range (log–log) for tetrabutyltin is 0.970 and for tributyltin chloride is 1.29.

3.4. Effect of interface temperature

To monitor the effect of the interface temperature the 10 μg/ml solution was chosen as this gave the best peak shape under the initial conditions. As stated earlier the exact temperature under operating conditions is difficult to measure and hence all results are given as a function of the applied voltage rather than temperature. At low voltage (and low temperatures of about 200°C) there is a small increase in intensity for tributyltin chloride as the applied voltage is increased but above 7 V (at about 230°C) there is a significant increase in peak intensity as applied voltage is increased. For tetrabutyltin greater increase in peak intensity occurs above 7.5 V. A comparison of these trends is made in Fig. 8 where it can be seen that the increase in peak intensity is greater for tributyltin chloride than for tetrabutyltin.

The trend in Fig. 8 can be explained in terms of the volatility of the two compounds. Tetrabutyltin is more volatile than tributyltin chloride

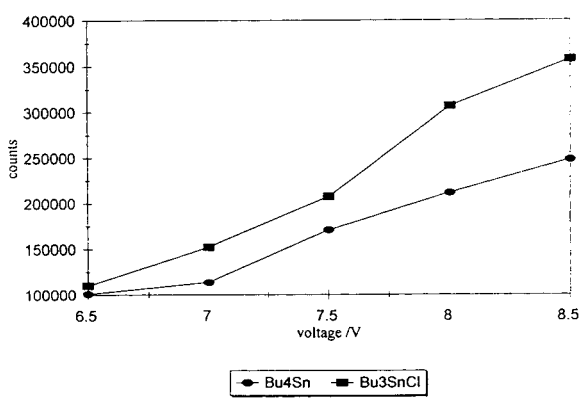

Fig. 8. A comparison of the effects of interface applied voltage on the peak intensities of Bu_3SnCl and Bu_4Sn.

and is thus less likely to condense in the restrictor than tributyltin chloride. At lower temperatures there may be some condensation of the less volatile tributyltin chloride within the restrictor due to adiabatic expansion of the mobile phase. As the temperature of the restrictor is increased both compounds will show an increase in peak intensity as the Joule–Thompson effect is more efficiently counteracted. However, as the temperature of the restrictor is increased any tributyltin chloride which may have condensed in the restrictor at low temperatures is now volatilised and the resulting increase in the amount of analyte which is transferred into the plasma accounts for the increase in peak intensity.

It was noted with reference to Fig. 8 that a plateau region (where peak intensity reaches a maximum with increasing restrictor temperature, or applied voltage) has not yet been reached for tetrabutyltin and tributyltin chloride, which indicates that detector sensitivity can still be improved. This may be achieved by changing the insulating material from polyimide to some other material capable of withstanding temperatures greater than 400°C, or by supplementing the filament heater by introducing a hot make-up flow of argon around the restrictor. This would also reduce the possibility of analyte condensation in the torch.

3.5. Detection limits and reproducibility

Triplicate 10 μg/ml mixtures of tetrabutyltin and tributyltin chloride were injected with the interface at an applied voltage of 8.5 V. The detection limits were calculated according to three times the standard deviation of the background for the triplicate injections. From previous experiments it was estimated that a time-split injection of 0.100 s corresponds to an injection of approximately 67 nl and thus a 10 μg/ml solution injected for 0.100 s will be an injection of 670 pg. The standard deviation is 27 and the sensitivity for tributyltin chloride is 3284 cps/pg. Thus, the theoretical absolute detection limit is 0.025 pg. For tetrabutyltin the sensitivity is 2287 cps/pg and the theoretical absolute detection limit is 0.035 pg. These results compare well with those obtained by Shen et al. [13] and for tributyltin chloride these results show a significant improvement. This can be seen in Fig. 6 which shows practical detection limits of 0.07 pg for tetrabutyltin and 6.7 pg for tributyltin chloride. Although tetrabutyltin was only investigated at concentrations above 0.001 μg/ml this was not the limit of detectability and hence the practical and calculated detection limits are approximately the same. However, as previously discussed, there is significant tailing on tributyltin chloride and it is doubtful that the calculated detection limit could be obtained unless a modifier was added to the mobile phase or a very well deactivated column was used. Thus, the detection limit calculated for tributyltin chloride for a 10 μg/ml solution is a statistical indication of the detection limit under ideal conditions and assuming that the peak shape would be similar to that of tetrabutyltin at all concentrations.

Optimisation of the conditions for SFC are not presented as these are not specific to the detector and will be specific for analyses of different compounds. The conditions for optimising the chromatography include pressure and density programmes and the temperature of the oven as well as the initial and final hold times and the injection time. These will all affect peak shape, resolution, selectivity and retention time but these conditions can be optimised using any suitable detector and a suitable analyte concentration. Thus, the chromatographic conditions were optimised using flame ionization detection by varying conditions of pressure and temperature and all analyses on SFC–ICP-MS were performed using these conditions. It was found that a constant temperature of 75°C was suitable for thermally labile and involatile analytes while a pressure program of 3.04 MPa/min gave the best compromise between peak shape and resolution.

4. Conclusions

The interface developed in this study is easy to assemble and use and causes minimum disrup-

tion of either SFC or ICP-MS. Analysis of the peak intensity of tetrabutyltin and tributyltin chloride with concentration shows linearity over three orders of magnitude and detection limits comparable to and even lower than those previously reported. Moreover, the design of the interface is important as it is this factor which will optimise the restrictor heating and so minimise the Joule–Thompson effect. Although the mobile phase cause changes in the plasma these do not interfere with the analysis. The low detection limits offer potential for environmental analysis and the opportunity exists to link this method with supercritical extraction and hence provide on-line extraction and analysis of environmental samples at ultra-trace levels. Poole et al. [17] have recently reported the SFC–FID analysis of a mixture of 12 organotin compounds including some polar compounds such as dibutyltin dichloride and diphenyltin dichloride using packed columns and formic acid modified carbon dioxide. As the addition of small amounts of modifier such as formic acid are unlikely to interfere with ICP-MS, this would further broaden the scope of this method. SFC with ICP-MS detection offers a fast method for analysing organometallic compounds that have not previously been amenable to chromatographic analysis. In addition low detection limits provide ultra-trace analysis of potentially harmful compounds.

Acknowledgements

The authors thank the Foundation for Research and Development, Pretoria, South Africa and the University Research Fund, University of Natal, Durban, South Africa for the financial support for this project and Stefan Nicolescu for his help with the ICP-MS work.

References

[1] J.R. Ashby and P.J. Craig, in R.M. Harrison (Editor), *Pollution: Causes, Effects and Control*, Royal Society of Chemistry, London, 2nd ed., 1990, Ch. 16.
[2] R.J. Maguire, *Environ. Sci. Technol.*, 18 (1984) 291.
[3] N.P. Vela and J.A. Caruso, *J. Anal. At. Spectom.*, 7 (1992) 971.
[4] Y.K. Chau, P.T.S. Wong and G.A. Bengert, *Anal. Chem.*, 54 (1982) 246.
[5] K.L. Jewett and F.E. Brinckmann, *J. Chromatogr. Sci.*, 19 (1981) 583.
[6] R.M. Harrison and C.N. Hewitt, *Int. J. Environ. Anal. Chem.*, 21 (1985) 89.
[7] R.C. Forster and A.G. Howard, *Anal. Proc.*, 26 (1989) 34-36.
[8] H.A. Meinema, T. Burger-Wiersma, G. Versluis-de Haan and E. Ch. Gevers, *Environ. Sci. Technol.*, 12 (1978) 288.
[9] K. Robards, P. Starr and E. Patsalides, *Analyst*, 116 (1991) 1247.
[10] O. Evans, B.J. Jacobs and A.I. Cohen, *Analyst*, 116 (1991) 15.
[11] J.M. Carey, F.A. Byrdy and J.A. Caruso, *J. Chromatogr. Sci*, 31 (1993) 332.
[12] A. Kim, S. Hill, L. Ebdon and S. Rowland, *J. High Resolut. Chromatogr.*, 15 (1992) 665.
[13] W.-L. Shen, N.P. Vela, B.S. Sheppard and J.A. Caruso, *Anal. Chem.*, 63 (1991) 1491.
[14] N.P. Vela and J.A. Caruso, *J. Anal. At. Spectrom.*, 7 (1992) 971.
[15] J.D. Pinkston and R.T. Hentschel, *J. High Resolut. Chromatogr.*, 16 (1993) 269.
[16] M.W. Raynor, K.D. Bartle, I.L. Davies, A.A. Clifford and A. Williams, *J. High Resolut. Chromatogr. Chromatogr. Commun.*, 11 (1988) 289.
[17] C.F. Poole, J.W. Oudsema and K.G. Miller, presented at the *5th Int. Symp. on Supercritical Fluid Chromatography and Extraction, Baltimore, MD, 11–14 January, 1994*, Abstracts, p. 18.

ELSEVIER

Journal of Chromatography A, 683 (1994) 233–243

JOURNAL OF CHROMATOGRAPHY A

Vesicle-mediated high-performance liquid chromatography coupled to atomic detection for speciation of toxic elements

A. Sanz-Medel*, B. Aizpun, J.M. Marchante, E. Segovia, M.L. Fernandez, E. Blanco

Department of Physical and Analytical Chemistry, University of Oviedo, Julian Claveria 8, 33006 Oviedo, Spain

Abstract

High-performance liquid chromatographic (HPLC) separation followed by element-specific detection by plasma emission or atomic absorption is shown to be a synergic combination through the use of surfactant vesicles as mobile phases for metal speciation. Several species of As, Se and Hg of environmental and toxicological concern were separated by using vesicular mobile phases of the surfactant didodecyldimethylammonium bromide (DDAB) on a C_{18} reversed-phase column which was previously modified by DDAB molecules. A mobile phase of the surfactant dihexadecyl phosphate (DHP) containing methanol was used for the speciation of butyltin compounds. The usefulness of the proposed vesicle-mediated methods has been demonstrated for the separation and determination of As species in tap water and urine and Hg species in seawater. The fundamental basis of this emerging new strategy of vesicle-mediated coupling of HPLC separation to atomic detection is also discussed.

1. Introduction

The most reliable approaches today to tackle the problem of element speciation are hybrid analytical techniques resulting from the coupling of a powerful chromatographic separation technique with atomic (specific) spectroscopic detection. In particular, inductively coupled plasma atomic emission spectrometry (ICP-AES) has been frequently used as a "specific" detection method coupled to high-performance liquid chromatography (HPLC) for metal speciation [1–4]. Conventional mobile phases for HPLC utilize organic and hydro–organic solvents and unfortunately such solvents may be detrimental to the ICP analytical performance with conventional nebulization (e.g. higher plasma background, increased unstability and noise and even eventual extinction of the plasma) [5]. Therefore, the search for alternative mobile phases for HPLC is worthwhile and may result in improved analytical characteristics of new HPLC–ICP-AES hybrid methods.

Around ten years ago aqueous micelles have been introduced as a new effective mobile phase in HPLC giving rise to micellar liquid chromatography (MLC) [6,7]. Surfactant-based organized media, such as micelles, vesicles, bile salts, etc, are able to solubilize, concentrate and organize solutes at a molecular level [7–9] and these unique properties have been shown to be very useful for HPLC separations [7]. Although the use of organized media for separations has greatly increased in recent years only normal micelles mobile phases have been investigated extensively. The use of vesicles as mobile phases

* Corresponding author.

0021-9673/94/$07.00
SSDI 0021-9673(94)00624-5

in liquid chromatography seems to have been largely neglected so far.

Single typical surfactants are amphiphilic molecules (i.e. molecules in which a non-polar hydrophobic tail is attached to a polar or hydrophilic head group) that dynamically associate in aqueous solution upon reaching the so-called critical micellar concentration (CMC) to form large spherical aggregates of colloidal dimensions termed normal micelles [8,9]. The structure of micelles is such that the hydrophilic head groups are directed toward and in contact with the aqueous solution (thus forming a polar surface), while the hydrophobic tails are directed away from the water, forming a central non-polar core.

Other surfactants possessing of two or more hydrophobic tails per monomer form bilayer in water which under sonic dispersal by ultrasonic radiation leads to closed bilayer structures like spheric bags, referred to as vesicles (schematically depicted in Fig. 1) [7,10], such as didodecyldimethylammonium bromide (DDAB) and dihexadecyl phosphate (DHP).

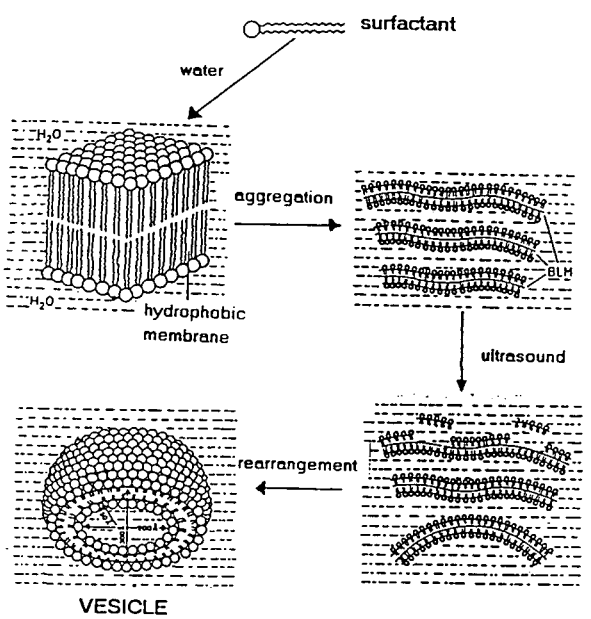

Fig. 1. Vesicle formation by ultrasonic treatment of bilayer membrane.

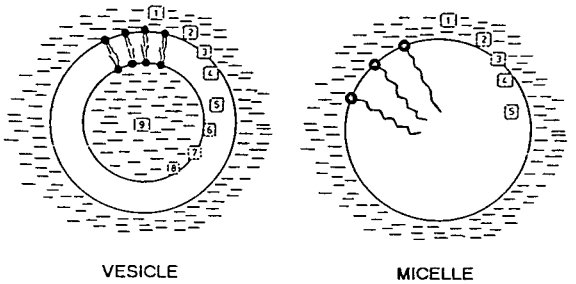

Fig. 2. Available sites for solute solubilization/interaction in vesicles and normal micelles.

It is important to recognise the chemical differences and potential between vesicles and micelles. As shown in Fig. 2 an aqueous vesicle displays nine different regions or compartments for solute localization [10]: the outer water volume (bulk volume), the hydration sphere, the outer head groups, the hydrophobic membrane close to the outer head groups and finally the similar four inner regions in the water pool direction. Micelles provide less available sites for interaction/solubilization of a given solute. In fact, localization of solute in normal micelles (Fig. 2) is restricted to the four first regions mentioned above and perhaps to a solubilization close to the hydrophobic core of the micelle [7].

Therefore, in principle, vesicles can provide a greater variety of interactions (hydrophobic, electrostatic, steric) with the solute present in the mobile phase, interactions which cannot be duplicated by any traditional pure or mixed solvent system. Moreover, the richness of possibilities in such interactions could be manipulated in order to achieve a desired separation. In fact, we have recently shown for the first time [11] that HPLC separation followed by hydride generation (HG)-ICP-AES detection can be a synergic combination for the speciation of toxic arsenic species through the use of vesicles as mobile phase.

Further work on the analytical potential and usefulness of this new strategy of vesicle-mediated HPLC separations coupled to atomic spectroscopic detection is discussed here in terms of mechanisms of separations and application to the speciation of several compounds of toxi-

cological and environmental concern derived from arsenic, mercury, tin and selenium.

2. Experimental

2.1. Instrumentation

The chromatographic system used for arsenic and mercury speciation consisted of a Knauer (Berlin, Germany) Model 6400 HPLC Pump with an attached sample injection valve equipped with a 100-μl loop.

Selenium and tin speciation studies were carried out by using an HPLC system constructed from LKB components (LKB, Bromma, Sweden), two Model 2150 HPLC pumps, a Model 2152 system controller and a Rheodyne sample injection valve (Berkeley, CA, USA) equipped with a 500-μl loop.

The analytical columns used (250 × 4.6 mm I.D.) were packed with 10-μm C_{18} bonded silica stationary phase (Spherisorb Phase Separations, Deeside, UK).

A four-channel peristaltic pump HP4 Minipuls 2 Gilson (Villiers-le-Bel, France) and a laboratory-made gas–liquid separator constituted the continuous hydride or cold vapor generator system [12].

An ultrasonic device from Sonics & Materials (CT, USA) Model VC (250 W) was used for the preparation of vesicles from surfactant solutions.

A UNICAM (Cambridge, UK) Model PU 9400X atomic absorption spectrometer, equipped with a T-shaped absorption quartz cell (12 cm × 8 mm I.D.) was used for absorption measurements of mercury vapour at 253.7 nm.

A Perkin-Elmer (CT, USA) ICP 5000 spectrometer interfaced with a microcomputer (Perkin-Elmer 3500) was used for ICP emission measurements of arsenic and tin hydrides. A computer program for transient ICP emission data acquisition and processing was written in BASIC.

A Perkin-Elmer atomic absorption spectrometer Model 3030 (EP-3030) equipped with HGA 500 furnace and AS-40 autosampler. Perkin-Elmer EDL lamp at a current of 6 mA and pyrocoated graphite tubes with a totally pyrolytic graphite L'Vov platform were used for selenium detection.

2.2. Reagents

Stock solutions (1000 mg/l of As) of arsenite was prepared by dissolving the appropriate amount of As_2O_3 (Merck, Darmstadt, Germany) in 25 ml of 0.5 *M* NaOH (Merck) solution and then diluting the solution to 1 l with 0.6 *M* HCl (Merck). Stock solutions (1000 mg/l of As) of monomethylarsonic (MMAs) and dimethylarsinic (DMAs) acids were prepared by dissolving the appropriate amount of MMAs (Carlo Erba, Milan, Italy) and DMAs (Sigma, St. Louis, MO, USA) directly in ultrapure Milli-Q water. An As(V) stock solution (1000 mg/l) was obtained from Merck.

Methylmercury stock solution (100 mg/l of Hg) was obtained by dissolving the appropriate amount of methylmercury chloride salt (Merck) in 10 ml of acetone and the solution was made up to 100 ml with ultrapure Milli-Q water. This stock solution was stored in a glass bottle at 4°C. Inorganic mercury was obtained from Merck as a 1000 mg/l Hg solution.

Monobutyltin chloride, dibutyltin chloride and tributyltin chloride (Aldrich, Milwaukee, WI, USA) stock solutions (1000 mg/l as Sn) were prepared in HPLC-grade methanol and stored at 4°C.

Stock solutions of 10 mg/l of selenocystine, selenomethionine and selenoethionine all obtained from Sigma were prepared by dissolving the appropriate amount in water. Selenite stock solution (1000 mg/l) was prepared by dissolving Na_2SeO_3 (Merck) in water and Se(VI) stock solution (1000 mg/l) was obtained from Merck.

Working standards solutions of all the compounds investigated were freshly prepared daily by diluting the stock solutions with ultrapure Milli-Q water.

The DDAB vesicular solution (10^{-2} *M*) was prepared by dissolving 0.4626 g of DDAB (Fluka, Buchs, Switzerland) in 100 ml of Milli-Q water, and sonicating this solution during 10 min with a power output of 60 W [13,14].

The DHP vesicular solution (10^{-2} *M*) was prepared by dissolving 0.5469 g of DHP (Aldrich) in 100 ml of Milli-Q water and sonicating this solution (with a power output of 60 W) during 12 min at 80°C.

Sodium borohydride solution (1%, m/v) was prepared by dissolving 1 g of $NaBH_4$ (Probus, Barcelona, Spain) in 100 ml of 0.1% (m/v) NaOH (Merck) solution. Filtration of the solution through a Whatman grade 4 filter paper before use was carried out. This solution was stored at 4°C and prepared weekly.

The mercury-selective complexing agent, 2-mercaptoethanol was obtained form Merck and used as received without further purification.

HPLC-grade methanol and acetonitrile (Romile Chemicals, Loughborough, UK) were used.

All other chemicals were of analytical reagent grade and distilled and deionized (Milli-Q system; Millipore, MA, USA) water was used throughout all the work.

2.3. Procedures

The C_{18}-bonded silica reversed-phase columns were modified by passing a total of 500 ml of a 10^{-3} *M* surfactant aqueous solutions in 50% methanol at a flow-rate of 1 ml/min. Milli-Q water was then passed through the column during 30 min at the same flow-rate.

The optimal conditions found for the chromatographic separation of the different metal species investigated are summarized in Table 1 for each element investigated. Vesicular mobile phases were prepared by dissolving the appropriate amount of surfactant in water buffered at the desired pH and containing a small amount of organic modifier, as specified in Table 1 [e.g. for Hg species separation containing 0.005% (v/v) of 2-mercaptoethanol, 5% (v/v) acetonitrile and buffered with ammonia acetate (0.01 *M*) at pH 5]. These mobile phases were degassed by ultrasonicating during 30 min prior to use.

The effluent from the column was first mixed with a 1% (v/v) HCl solution through a mixing coil and then mixed with the sodium tetrahydroborate solution for As, Se or Sn hydrides, and for mercury cold vapor generation. A continuous stream of argon carries the generated volatile species directly into the ICP injector tube [11] or into the T quartz cell of the atomic absorption spectrometer (for mercury detection) [15]: when higher sensitivity is needed and hydride generation is not effective (e.g. some selenium species) off-line detection was carried out and fractions from the HPLC eluate were collected (250 μl) in the autosampler cups and immediately analysed for selenium by atomic absorption spectrometry with electrothermal atomisation (AAS-ETA). Fig. 3 shows schematically the on-line and off-line coupling used depending on the particular element (speciation problem).

Preconcentration of mercury species from water samples was carried out using Sep-Pak C_{18} [trichloro(octadecyl)silane, chemically bonded to Porasil A] cartridges, modified with a 2-mercaptoethanol solution [15].

Table 1
Chromatographic conditions

Column	C_{18}-bonded silica, 10 μm particle size, 250 × 4.6 mm I.D. (modified with 10^{-3} *M* DDAB or 10^{-3} *M* DHP)
Temperature	Room temperature
Sample volume	100 μl (or 500 μl for Se) for As and Hg
Mobile phase	
Arsenic	0.010 *M* Sodium phosphate buffer, pH 5.75 + 0.5% methanol + 10^{-5} *M* vesicles of DDAB
Selenium	(A) 0.01 *M* Ammonium acetate buffer, pH 5 + 0.5% methanol + 10^{-4} *M* vesicles of DDAB (B) 0.2 *M* Ammonium acetate buffer, pH 7.5 + 10^{-4} *M* vesicles of DDAB
Tin.	(A) 0.1 *M* Ammonium citrate + 5% acetic acid + 10^{-5} *M* vesicles of DHP, pH 4.5 (B) Methanol; gradient (B) 50–90%
Mercury	0.01 *M* Ammonium acetate buffer + 0.005% 2-mercaptoethanol + 2 · 10^{-4} *M* vesicles of DDAB + 5% acetonitrile
Flow-rate	1.0 ml/min (or 1.5 ml/min for Hg)

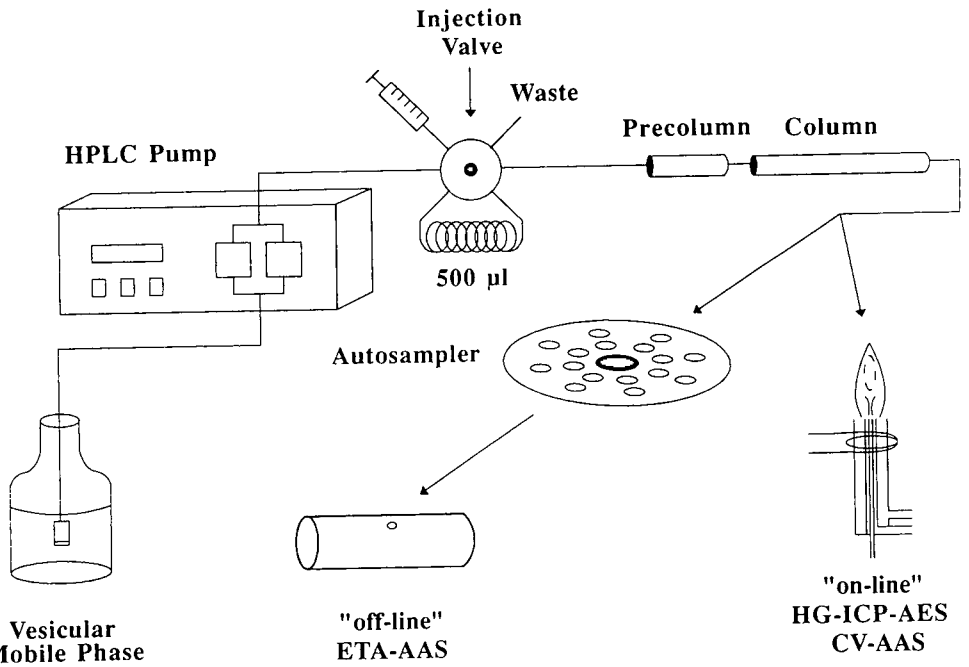

Fig. 3. Schematic diagram of the coupled HPLC–atomic detection systems for element speciation. CV = Cold vapour.

3. Results and discussion

As stated before, the obtained optimal conditions for separations of the different species have been summarized in Table 1. Optimal conditions for ICP-AES and ETA-AAS detection are given in Table 2.

3.1. Arsenic speciation

The feasibility of using vesicular mobile phases in HPLC coupled to ICP-AES was demonstrated for the first time by solving the problem of arsenic speciation [11]. As shown in Fig. 4 the more toxic arsenic species (including arseneous, arsinic, monomethylarsonic and dimethylarsinic acids), can be separated within 10 min by using a mobile phase of cationic vesicles of didodecyldimethylammonium bromide (BDDA) 10^{-5} M in phosphate buffer (pH 5.7) containing only 0.5% methanol. The column was a conventional C_{18}-bonded silica column previously modified by passing through the adequate surfactant solution (see *Procedures*). The detection was accomplished on-line by HG-ICP-AES.

The normalized detection limits observed for the different toxic species of As with this novel hybrid method were found to be below the ng level (0.5–1.2 ng of As).

The analytical potential of this vesicle-mediated hybrid technique was demonstrated by determination of toxic arsenic species in spiked samples of local tap water and human urine [11]. Satisfactory recoveries of the type illustrated in Table 3 (93–108%) were obtained for the four toxic arsenic species under investigation.

3.2. Mercury and tin speciation

This new strategy of vesicle-mediated HPLC separation coupled to on-line atomic spectroscopy detection was extended to the speciation of other elements which, as As, are able to form volatile species, e.g. mercury and tin. Experiments showed that a mobile phase consisting of cationic vesicles of DDAB ($2 \cdot 10^{-4}$ M), 0.005% 2-mercaptoethanol and 5% of acetonitrile, buf-

Table 2
Instrumental conditions

HG	
HCl^+	10% (m/v)
KI^+	0.1% (m/v)
Vesicle	$1 \cdot 10^{-3}$ *M* DDAB
$NaBH_4$	2% (m/v) (stabilized by 0.1%, m/v, NaOH)
Flow-rate	1 ml/min
Ar carrier	70 ml/min
ICP-AES	
Analytical line	193.69 nm
Radio frequency forward power	1 kW
Reflected power	<5 W
Viewing height	15 mm
CV	
$NaBH_4$	1% m/v (stabilized by 0.1% NaOH)
HCl	1% (v/v)
Flow-rate	1 ml/min
Ar carrier	Flow-rate 250 ml/min
AAS	
Wavelength	253.7 nm
Lamp current	6 mA
Slit	0.5 nm
AAS-ETA	
Wavelength	196.0 nm
Slit	0.7 nm
Intensity	6 mA
Integration time	4 s
Background	On. Deuterium
Signal processing	Integrated absorbance
Type tube	Pyrolitic graphite coated graphite with L'vov platform

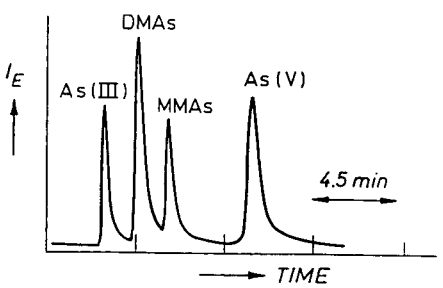

Fig. 4. Arsenic speciation by vesicle-mediated HPLC coupled to HG-ICP-AES. Experimental conditions as in Tables 1 and 2. I_E = Emission intensity (arbitrary units).

Table 3
Recoveries of arsenic species added into the tap water and human urine samples

Samples	Arsenic	Recovery (%)[a]	
		Spiked 150–250 ng/ml	Spiked 50–100 ng/ml
Tap water	As(III)	95	97
	DMAs	98	102
	MMAs	102	100
	As(V)	103	104
Human urine	As(III)	96	101
	DMAs	105	108
	MMAs	102	99
	As(V)	100	93

[a] Mean of two analyses.

fered at pH 5 with acetate, allowed the isocratic separation of Hg^{2+} and methylmercury on a C_{18} column previously modified with DDAB molecules in a similar way to that described previously. The detection limits obtained by on-line cold vapour AAS detection were 10–16 μg/l [15]. These results can be substantially improved after preconcentration of the aqueous sample in C_{18} cartridges impregnated with 2-mercaptoethanol solutions [15]. Preconcentration factors of 100 were easily achieved and with that pretreatment detection limits of 0.1–0.2 μg/l of mercury were easily achieved. The whole approach was applied to the determination of inorganic and methylmercury in spiked seawater and recoveries obtained ranged between 89 and 92% using extremely low concentrations in the toxic species (down to 5 μg/l).

Conversely, attempts to use only anionic vesicles of DHP as mobile phases for the HPLC separation of organometallic tin compounds (monobutyl-, dibutyl- and tributyltin) have been unsuccessful so far owing to the high hydrophobicity of these solutes. The separation was attempted at room temperature on a C_{18} column modified with DHP molecules under several different combinations of organic modifier (10–75% methanol), DHP ($0–6 \cdot 10^{-5}$ *M*), ammonium citrate (0.05–0.2 *M*) and acetic acid (0–

5%). The best chromatographic resolution of the various set of conditions tested was obtained using gradient elution and the separation conditions are summarized in Table 1. It is clear that the solvent strength of aqueous vesicular solutions seems to be lower than that of classical hydroorganic mobile phases [7].

In order to obtain a reasonable retention time for tributyltin on the C_{18} column modified with the surfactant, it was necessary the presence of at least 60% methanol in the mobile phase, which will probably destroy the vesicular aggregates. In fact, the retention times of butyltin species increased with surfactant concentrations in the hydro–organic mobile phase and this behavior is typical of ion-pair surfactant chromatography where the surfactant concentrations and/or conditions in the mobile phase are such that no micellar aggregates form [7]. A typical chromatogram obtained using a mobile phase containing 0.1 *M* ammonium citrate, 5% acetic acid and 10^{-5} *M* DHP and a methanol gradient 50–90% in 10 min is shown in Fig. 5.

3.3. Selenium speciation

As said before, if the attainable sensitivity of on-line conventional nebulization ICP-AES detection is not enough for speciation studies and hydride generation cannot be employed to increase this sensitivity, off-line ETA-AAS detection of the emerging fractions from the HPLC column can be called for. In fact, the utility of this atomic detector has been advantageously demonstrated for speciation of several seleno compounds which were separated by HPLC using vesicular mobile phases similar to those used for As [16].

The separation of inorganic selenium (selenite and selenate) and different selenoaminoacids (selenocistine, selenoethionine, selenomethionine) was achieved on a C_{18} column modified with molecules of the cationic surfactant DDAB with a sodium acetate gradient (0.005 to 0.2 *M*) and pH gradient (5 to 7.5) in the presence of DDAB vesicles (10^{-4} *M*) and 0.5% methanol. Fig. 6 shows the type of separation. Detection limits for these compounds were 5 μg/ml of Se.

3.4. Separation mechanisms

Once the analytical potential of vesicular-mediated HPLC separations in connection with atomic detection was demonstrated, particularly in connection with plasma detectors, we investigated the possible separation mechanisms operating in vesicular liquid chromatography. To

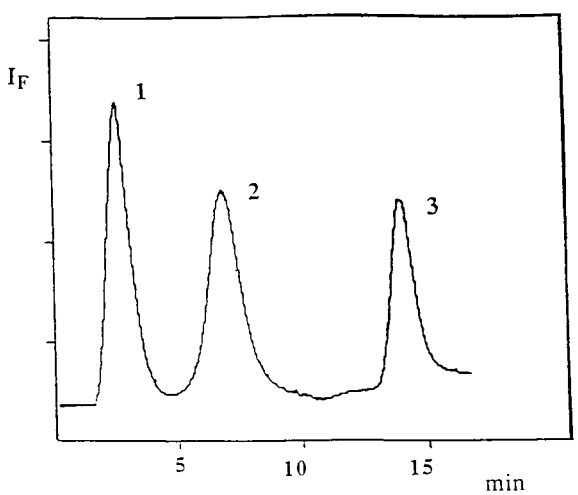

Fig. 5. Typical chromatogram showing tin speciation in water. Experimental conditions are given in Table 1. Peaks: 1 = monobutyltin; 2 = dibutyltin; 3 = tributyltin.

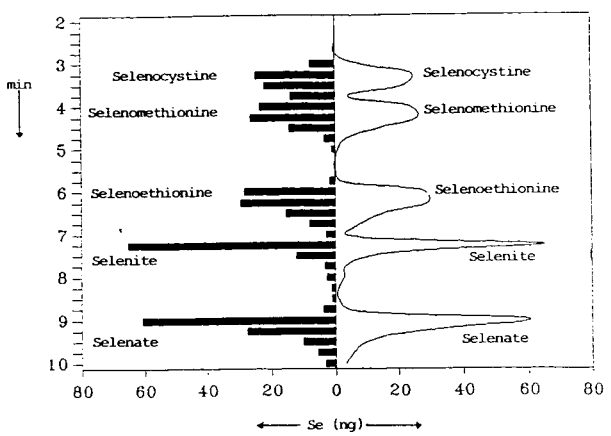

Fig. 6. Separation of inorganic selenium and different selenoaminoacids by vesicle-mediated HPLC with "off-line" ETA-AAS detection. Experimental conditions as in Tables 1 and 2.

do so the dependence of the solute retention time on the concentration of DDAB surfactant vesicles in the mobile phase was investigated for each element species. The results observed in these studies are summarised in Table 4–6 for arsenic, mercury and selenium species. The detailed observation of these results demonstrates that the effect of vesicle concentration depends on the nature of the solutes to be chromatographed. For instance, none of the retention times of any ionizable arsenic species did change at all with increasing vesicle concentration in the mobile phase (Table 4). Conversely, the retention times of hydrophobic mercury-mercaptoethanol complexes decreased with DDAB vesicles presence in the mobile phase (Table 5). However, as can be seen in Fig. 7 the retention time decrease observed with surfactant addition only takes place if monodispersed DDAB vesicles are present in the mobile phase (i.e. with previous sonicating of the surfactant solutions).

A similar effect of DDAB presence was found for the most hydrophobic selenium compounds (selenomethionine and selenoethionine) as the observed retention times decreased with DDAB presence. However, no retention time changes were observed for the ionic selenite and selenate species (Table 6).

By analogy with MLC [7,17] a vesicular mobile phase can be considered as composed of both the surfactant vesicular aggregate (pseudophase) and the aqueous bulk solvent (Fig. 8). A dissolved solute may thus distribute (a) between the bulk solvent and the (surfactant-modified) stationary phase (distribution coefficient, P_{SS}); (b) between the bulk solvent and the pseudophase (or vesicular aggregates, with distribution coefficient P_{SV}) as shown schematically in Fig. 8. Consequently, there are now two partition coefficients (P_{SS} and P_{SV}) which can influence the separation. The two defined partition coefficients have opposing effects on solute retention: as P_{SS} increases retention time increases; conversely, a high value of P_{SV} favours a decrease in retention due to increased partition into the vesicle moving with the mobile phase. The relative magnitude of both factors will depend upon the nature of solutes for a given vesicular solution and stationary phase. For instance, when charged ions of ionizable solutes such as the arsenic species (Table 4) and some selenium species (Table 6) investigated here are chromatographed with an oppositely charged vesicle-forming surfactant (DDAB) it seems that electrostatic attractions between charged solutes and the surfactant clearly predominate. To understand such interaction

Table 5
Effect of DDAB vesicle concentration on retention time

Concentration of DDAB vesicle (M)	Retention time (min)	
	Inorganic mercury	Methylmercury
0	11.33 ± 0.14	7.75 ± 0.11
10^{-5}	9.93 ± 0.13	7.38 ± 0.11
10^{-4}	9.98 ± 0.13	7.55 ± 0.11
$5 \cdot 10^{-4}$	9.92 ± 0.13	7.47 ± 0.11

Table 4
Effect of DDAB vesicle concentration on the retention times

Concentration of DDAB vesicle (M)	Retention time (min)			
	As(III)	DMAs	MMAs	As(V)
0[a]	2.82	4.55	5.96	9.80
10^{-6}	2.83	4.54	5.98	9.82
$5 \cdot 10^{-6}$	2.83	4.55	5.96	9.82
10^{-5}	2.83	4.55	5.94	9.82
10^{-4}	2.83	4.56	5.95	9.81

[a] The column behaviour was not reproducible due to the continuous DDAB desorption and release from the stationary phase in the column.

Table 6
Effect of BDDA vesicle concentration on retention times

Concentration of DDAB vesicle (M)	Retention (min)			
	Se cystine	Se methionine	Se ethionine	Selenite
0	3.2	4.1	6.1	6.5
10^{-6}	3.2	4.0	5.9	6.5
10^{-5}	2.9	3.7	5.5	6.5
10^{-4}	3.0	3.8	5.6	6.6

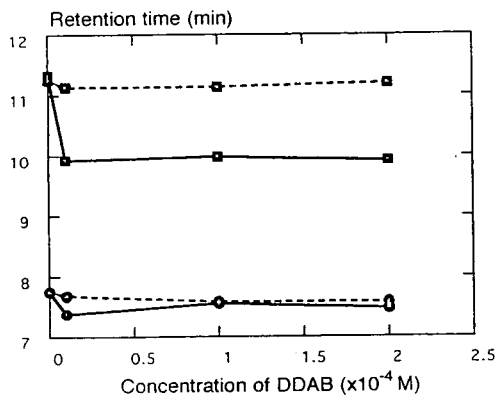

Fig. 7. Effect of DDAB concentration in the mobile phase on retention times: DDAB vesicles (solid lines), DDAB without sonicating (broken lines); □ = inorganic mercury; ○ = methylmercury.

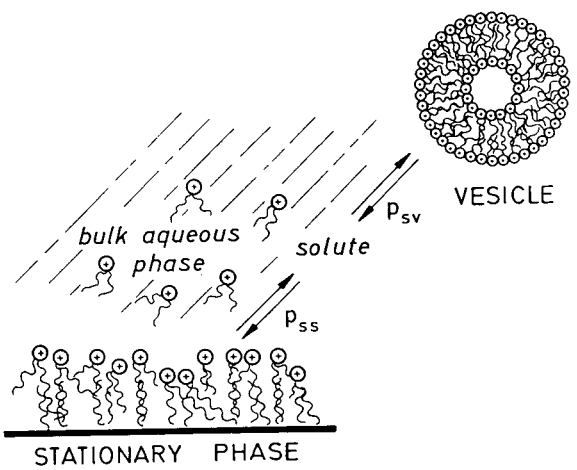

Fig. 8. Schematic representation of interactions of the solute in the aqueous bulk solvent with the (surfactant-modified) stationary phase and the (pseudophase) vesicular aggregates.

the modification of the C_{18} stationary phase by the monomers of DDAB has to be considered: as shown by Fig. 9 it is clear that during conditioning of the C_{18} column the stationary phase is modified by adsorbed surfactant molecules, preferently via its hydrophobic tails, leaving its charged groups in contact with the bulk mobile phase. In this way we may have some hydrophobic tails but also ion-exchange interactions where the solutes in the mobile phase would be attracted by the oppositely charged heads of the surfactant adsorbed to the phase. At the low vesicle concentrations used (10^{-5}–10^{-4} M) these electrostatic attractions of the stationary phase for charged solutes predominate. Thus, the mechanism of separation resembles a typical ion-exchange mechanism. Therefore the retention times observed for solutes are not related to the presence of vesicles in the mobile phase (see Table 4 for As and Table 6 for selenium).

In the case of more hydrophobic solutes, such as the neutral mercury–dimercaptoethanol complex, only hydrophobic interactions would be operative for solutes (insoluble in the aqueous phase) partitioning between the modified stationary phase (hydrophobic tails) and the vesicles. Here the presence of vesicles in the mobile phase reduced the retention times of these solutes probably because they increase the P_{SV} partition coefficient. In brief, both the stationary phase and the mobile phase characteristics can be changed by resorting to vesicles and in this way taylored separations of charged and uncharged compounds can be achieved. However, the vesicular effect on retention times is more modest than that reported in MLC [7,17] probably because the concentration of surfactant in the

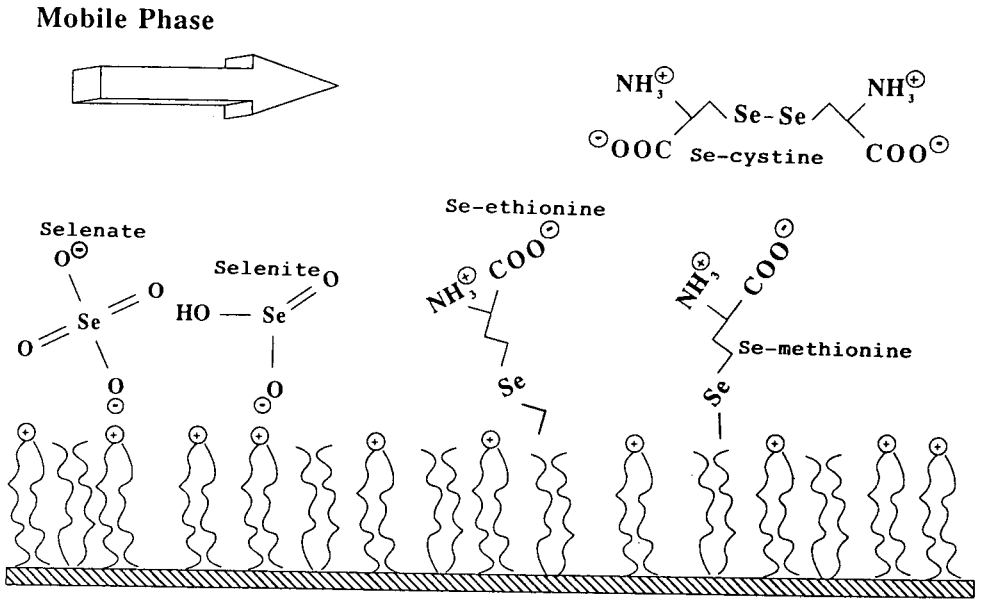

Fig. 9. Schematic representation of interactions of the selenium compounds in the aqueous bulk solvent with the (surfactant-modified) stationary phase.

mobile phase (10^{-5}–10^{-4} M) are lower than those commonly employed using micelles. In any case, no problems of viscosity were observed in all HPLC experiments with such concentrations in DDAB.

4. Conclusions

It has been demonstrated that aqueous vesicular media can be advantageously employed as mobile phases in HPLC. Although their solvent strength is lower than that of hydro–organic solvents, the vesicle-mediated HPLC procedures developed so far in our laboratory have proved to be fairly robust, chromatographic behaviour was durable and reliable and no degradation behaviour was noticed after months of daily use.

In brief, the results obtained so far indicate that vesicle-mediated HPLC separation coupled to atomic spectroscopy detection provides a competitive, low-cost, efficient and robust separation which at the same time can substantially enhance the performance of atomic spectroscopic detectors, specially plasma detectors [18]. This vesicle-enhanced hybrid techniques constitute a most useful analytical strategy to tackle the modern problem of metal speciation.

References

[1] P.C. Uden (Editor), *Element Specific Chromatographic Detection by Atomic Emissions Spectroscopy*, American Chemical Society, Washington, DC, 1992.
[2] G.E. Batley (Editor), *Trace Element Speciation: Analytical Methods and Problems*, CRC Press, Boca Raton, FL, 1989.
[3] R.M. Morrison and S. Rapsomanikis (Editors), *Environmental Analysis Using Chromatography Interfaced With Atomic Spectroscopy*, Ellis Horwood, Chichester, 1989.
[4] L. Ebdon, S. Hill and R.W. Ward, *Analyst*, 112 (1897) 1
[5] A.W. Born and F.R. Browner, *Anal. Chem.*, 54 (1982) 1402.
[6] D.W. Armstrong, *Am. Lab.*, 13 (1981) 14.
[7] W.L. Hinze and D.W. Armstrong (Editors), *Ordered Media in Chemical Separations (ACS Symposium Series*, No. 342), American Chemical Society, Washington, DC, 1987, p. 2.
[8] W.L. Hinze, in K.L. Mittal (Editor), *Solution Chemistry of Surfactants*, Vol. 1, Plenum Press, New York, 1979, p. 79.

[9] W.L. Hinze, in E. Barni and E. Pelizzetti (Editors), *Colloids and Surfactants: Fundamental and Applications*, Society Chimica Italiana, Rome, 1987, p. 167.
[10] J.H. Fuhrhop and J. Mathieu, *Angew. Chem., Int. Ed. Engl.*, 23 (1984) 100.
[11] Y.M. Liu, M.L. Fernández Sánchez, E. Blanco González and A. Sanz-Medel, *J. Anal. Atom. Spectrom.*, 8 (1993) 815.
[12] A. Menéndez García, E. Sánchez Uría and A. Sanz-Medel, *J. Anal. At. Spectrom.*, 4 (1989) 581.
[13] Y.-C.L. Lester, J.K. Hurst, M. Politi, K. Kurihara, J.H. Fendler, *J. Am. Chem. Soc.*, 105 (1983) 370.
[14] S. Lukac, *J. Am. Chem. Soc.*, 106 (1984) 4386.
[15] B. Aizpún, M.L. Fernández, E. Blanco and A. Sanz-Medel, *J. Anal. At. Spectrom.*, in press.
[16] J. Marchante Gayón, M.L. Fernández Sánchez, E. Blanco González and A. Sanz-Medel, *J. Anal. At. Spectrom.*, in preparation.
[17] D.W. Armstrong and F. Nome, *Anal. Chem.*, 53 (1981) 1662.
[18] A. Sanz-Medel, M.R. Fernández de la Campa, M.C. Valdés-Hevia, B. Aizpún Fernández and Y.M. Liu, *Talanta*, 40 (1993) 1759.

ELSEVIER

Journal of Chromatography A, 683 (1994) 245–252

JOURNAL OF CHROMATOGRAPHY A

Speciation of organomercurials in biological and environmental samples by gas chromatography with microwave-induced plasma atomic emission detection

A.M. Carro-Díaz, R.A. Lorenzo-Ferreira, R. Cela-Torrijos*

Department of Analytical Chemistry Nutrition and Food Sciences, University of Santiago de Compostela, Avda. de las Ciencias s/n, 15706 Santiago de Compostela (La Coruña), Spain

Abstract

The applicability of a commercial microwave-induced plasma atomic emission detector with capillary gas chromatography for mercury speciation in environmental samples was examined. The chromatographic conditions were optimized in order to obtain an adequate resolution of the methylmercury peak vs. interfering carbon signals. Under the proposed operational conditions, the detection limit (signal-to-noise ratio = 3) was 1.2 pg with a linear range of 1–40 ng ml^{-1} (as methylmercury in samples). Certified reference material (DORM-1) was used to evaluate the accuracy. The results of the proposed procedure were compared with those obtained by means of the usual GC method with electron-capture detection.

1. Introduction

The impact of the production and application of mercury and its compounds on the environment has increased in recent decades [1]. Methylmercury is the organomercurial compound most commonly found in aqueous environments. The ecotoxicity of this compound is well known [2] and it has been found in high concentrations in tuna, swordfish, molluscs and sediments [3].

Several highly sensitive methods have been developed for the determination and speciation of mercury in the environment. Gas chromatography with electron-capture detection (GC–ECD) has been the most widely used. Columns packed with different stationary phases [4–8] have been used, but they have all had some drawbacks on application, e.g., a small and variable response to methylmercury, peaks with tails and poor selectivity in the presence of interferences [9]. Recently, various capillary columns with polar and non-polar stationary phases have been evaluated [6,10–12]. The columns having the thickest phase and lowest polarity are the most appropriate for obtaining satisfactory separations and reproducible results.

In addition, other techniques, such as atomic spectroscopy, coupled with GC have been used. In order to improve the separation and detection of mercury compounds, they have been derivatized with sodium tetraethylborate ($NaBEt_4$), sodium tetrahydroborate ($NaBH_4$) and lithium triethylhydroborate ($LiBEt_3H$). Volatile derivatives, separated using GC, have been detected by means of atomic absorption [13–17], atomic

* Corresponding author.

0021-9673/94/$07.00
SSDI 0021-9673(94)00446-G

fluorescence [18], mass [16] or Fourier transform infrared spectrometry [19].

All the procedures proposed for the determination of organomercurial compounds highlight the need for a highly selective and sensitive detection system. Since the introduction of detection using atomic emission spectrometry combined with GC (GC–AED) [20,21], the selectivity in the speciation of organometallic compounds [22,23] has improved enormously. Not only is there high selectivity, but there is also high sensitivity and the possibility of multi-elemental analysis with a wide dynamic range. Plasma detectors that have been used for mercury speciation include the inductively coupled plasma (ICP) [24] and microwave-induced plasma (MIP) [6,25–28] types. Organomercurial compounds were converted into the iodide form [24–26] or derivatized with a Grignard reagent to obtain dialkyl derivatives [27].

In this paper we present the results of a study carried out to check the applicability of GC–AED to the direct determination of methylmercury in environmental samples.

2. Experimental

2.1. Chemicals

Methylmercury chloride (99%) was obtained from Merck (Darmstadt, Germany). A stock standard solution (1.164 mg ml^{-1} in toluene) was used to prepare the working standard solutions by dilution and to spike the samples where necessary. A 1% solution of mercury chloride (99.5%) (Merck) in toluene was used as a column-conditioning solution. Cysteine chlorohydrate (98.5%), 2-propanol, HCl, sodium sulphate (anhydrous, 99%), toluene and acetone were obtained from BDH (Poole, UK) and sodium acetate (99.5%) from Merck. Helium (99.9999%) (Carburos Metálicos, Coruña, Spain) was used as both the carrier gas and reagent gas. Oxygen and hydrogen (99.999%) (Carburos Metálicos) were used as auxiliary gases.

2.2. GC and AED instrumentation

All the experiments were carried out with Hewlett-Packard (Palo Alto, CA, USA) Model 5890 Series II gas chromatographs. For GC–ECD the instruments were equipped with a nickel-63 electron-capture detector using N55 nitrogen as the carrier and make-up gas. Data were acquired by means of a Hewlett-Packard Model 3396A integrator. For GC–AED a Hewlett-Packard Model 5921A microwave-induced plasma atomic emission spectrometer tuned at 185 nm (for mercury) and 193 nm (for carbon) was used. Data acquisition and reprocessing were carried out by means of a Hewlett-Packard Model 3592A Chemstation. The chromatographic columns tested (Hewlett-Packard) and operating conditions are summarized in Table 1.

2.3. Sample preparation

The procedure described by Hight and Corcoran [5] was used for the extraction of methylmercury from marine samples, with modifications as detailed elsewhere [29]. The procedure of Westöö [30] was used for the extraction of sediment samples, with modifications for freeze-dried sediment samples as described recently [31].

3. Results and discussion

3.1. Optimization of GC and detection conditions

The GC conditions were adapted from the parameters previously optimized for GC–ECD [10]. The effect of the injector temperature on the separation of the methylmercury peak was studied. Using the splitless mode, the temperatures tested were 150, 200 and 250°C. The column head pressure ranged between 140 and 160 kPa.

Several oven temperatures were tested with the purpose of separating the methylmercury peak from the front solvent (toluene) and concentrating the sample on the column head. The

Table 1
Optimum GC–AED parameters

Parameter	HP-1 column	HP-5 column
GC parameters		
Dimensions	25 m × 32 μm × 0.17 μm	25 m × 32 μm × 0.17 μm
Injection port	Split–splitless	Split–splitless
Injection port temperature	150°C	200°C
Split mode	Splitless	Splitless
Purge time	20 s	90 s
Splitting ratio	1:10	1:10
Septum purge	2.6 ml min^{-1}	2 ml min^{-1}
Injection volume	1.5 μl	1.5 μl
Column head pressure	140 kPa	140 kPa
Oven initial temperature	90°C	75°C
Ramp rate	–	30°C min^{-1}
Oven final temperature	–	140°C
Interface parameters		
Transfer line	HP-1 column	HP-5 column
Transfer line temperature	160°C	160°C
AED parameters		
Wavelength	185 nm (Hg), 193 nm (C)	185 nm (Hg), 193 nm (C)
Helium make-up flow-rate	60 ml min^{-1}	60 ml min^{-1}
Ferrule purge vent	20 ml min^{-1}	30 ml min^{-1}
Scavenger gases:		
Hydrogen	200 kPa	200 kPa
Oxygen	200 kPa	200 kPa
Helium supply purge	205 kPa	205 kPa
Spectrometer purge flow-rate	2 ml min^{-1} N_2	2 ml min^{-1} N_2
Solvent vent off-time	0.6–1.45 min	0.5–2.2 min
Cavity temperature	250°C	250°C

best separation was obtained for a constant temperature of 90°C with the HP-1 column. With an HP-5 column a good separation was achieved with a constant temperature of 90°C but sensitivity was improved and the analysis time was shortened by using temperature programming. The transfer line temperature must be higher than the oven temperature in order to avoid condensation, which could broaden the peak. This temperature was varied between 150 and 250°C. The optimum conditions are summarized in Table 1.

The need for the chromatographic columns to be conditioned with $HgCl_2$ to obtain satisfactory separations and reproducible results has been sufficiently confirmed [4,10]. The treatment of the HP-1 column consisted of 3–5 injections of 2–3 μl of 1% $HgCl_2$ solution in toluene. The HP-5 column underwent treatments consisting of 2–3 injections of 10 μl of 1% $HgCl_2$ solution. Both columns remained disconnected from the detector while treatment was applied, at a temperature of 90°C in the oven and in the transfer line for 12 h. The column was then reconnected to the detector, the baseline checked and a new calibration started.

The effect of the treatment was observed to be short-lived with the HP-1 column, with the sensitivity diminishing after a few hours of work. With the HP-5 column, the treatments remained efficient for over 1 week. This is to be expected when the thicknesses of the phases in the HP-5 (1.05 μm) and HP-1 (0.17 μm) columns [10] are considered.

3.2. AED optimization

The AED instrument allows the Hg emission signal to be measured at two wavelengths, 185 and 254 nm. The responses obtained for the two wavelengths were similar. However, we chose 185 nm because it allows the presence of Hg to be confirmed in the methylmercury peak by means of the emission spectrum. The equipment prevented us from using the same emission spectrum of Hg at 254 nm.

Solvent vent-off time

In order to prevent the solvent (toluene) from entering the discharge tube at high concentrations, toluene vapour was injected while monitoring the carbon emission line at 193 nm. Under the conditions described above, most of the toluene was eluted between 0.6 and 1.45 min for the HP-1 and between 0.5 and 2.2 min for the HP-5 column.

Effect of make-up gas flow-rate

In accordance with published data [32,33], it is necessary to work with a high helium make-up gas flow-rate in order to have good sensitivity for the detection of organometallic compounds. However, with Hg, a high helium make-up gas flow-rate produces a significant decrease in sensitivity [34]. In order to determine the optimum helium make-up gas flow-rate that allows the maximum sensitivity, a standard solution of 0.010 μg ml^{-1} MeHg was injected using different make-up gas flow-rates. Fig. 1 shows the variation of the peak area with the make-up gas flow-rate. Similarly, differences in the baseline and shape of the methylmercury peak were seen when the flow-rate was changed. The optimum flow-rate was established to be 60 ml min^{-1}.

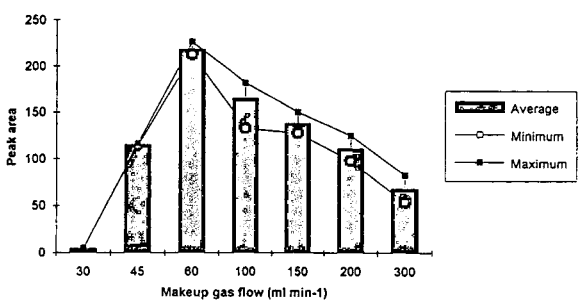

Fig. 1. Influence of the make-up gas flow-rate on the peak area of methylmercury using GC–AED.

3.3. Identification of the methylmercury peak

Although the AED system is highly selective for Hg at 185 nm, the presence of methylmercury must be confirmed by recording the emission spectrum at the peak and comparing it with the emission spectrum of Hg (Fig. 2a and b). Fig. 2a shows a chromatogram with the methylmercury peak (HP-5 column) and Fig. 2b shows the emission spectrum recorded at the apex of the methylmercury peak, showing that this peak contains Hg. The 184.9 and 194.2 nm lines correspond to Hg and the 193 nm line to the carbon background.

When methylmercury standards are injected, as shown in Fig. 2, no other peaks are recorded at 185 nm. However, when extracts of real

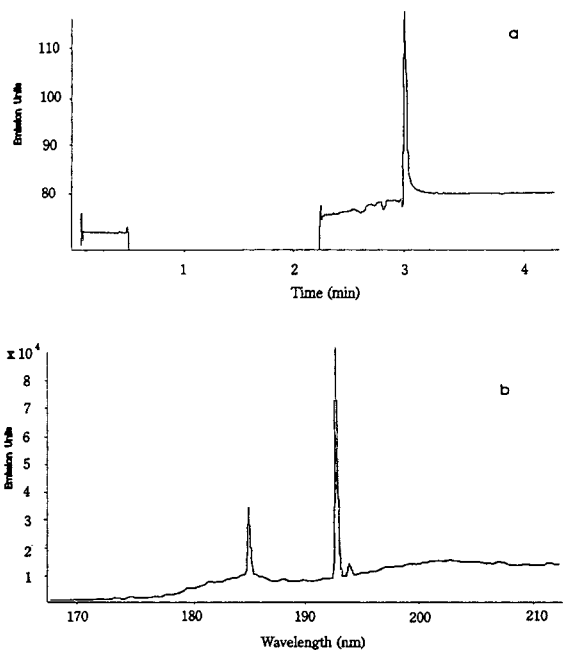

Fig. 2. Identification of the methylmercury peak. (a) Chromatogram for a standard solution in toluene (0.030 μg ml^{-1} MeHg); (b) emission spectrum recorded at the apex of the methylmercury peak.

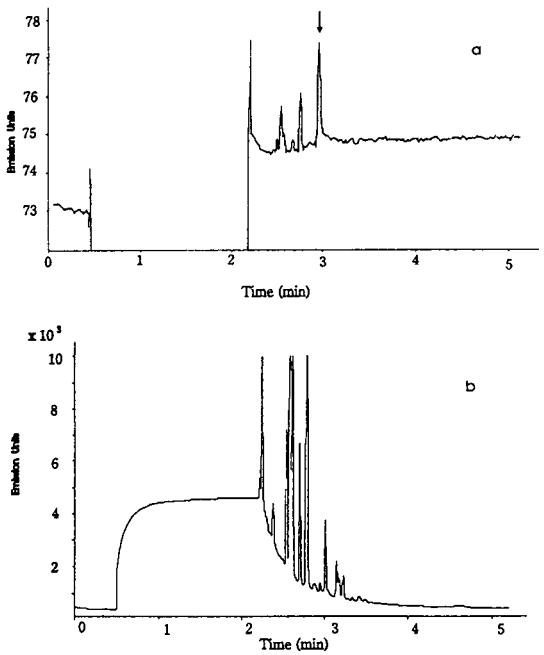

Fig. 3. Chromatograms for a clam sample using the GC–AED system. (a) 185 nm mercury line; (b) 193 nm carbon line.

samples are injected (see Fig. 3), two or more weaker peaks usually appear next to the methylmercury peak, which may lead to errors. The hypothesis that the AED system is highly selective might suggest that these peaks are due to mercury-containing species. Fig. 3b shows a chromatogram for the same sample recorded at the 193-nm carbon line. The presence of high-intensity carbon peaks at the position of the interferencing peaks in the 185-nm chromatogram can be clearly seen. The closeness of both spectral lines and the fact that the instrument cannot completely separate them explains the appearance of the small interfering peaks. In any case, the spectrum shows the absence of mercury in these peaks. Therefore, it is convenient to make a systematic check of the purity of the peaks by recording the spectra.

3.4. Calibration

Working standard solutions of 1, 5, 10, 20, 30 and 40 ng ml^{-1} MeHg were prepared for calibration from a 1.164 mg ml^{-1} MeHg stock standard solution. Each standard solution was injected three times and the results were expressed as peak area.

With the HP-1 column, a good linear response was obtained (correlation coefficient 0.990, R^2 98.10%, standard error of estimate 2.16). The detection limit (signal-to-noise ratio = 3) was 1.5 pg of methylmercury, which corresponds to a concentration of 1 ng ml^{-1} MeHg in the samples. The quantification limit (signal-to-noise ratio = 10) was 4.5 pg of methylmercury, corresponding to a concentration of 3 ng ml^{-1} MeHg in the samples.

The HP-5 column showed excellent linearity of response (correlation coefficient 0.999, R^2 99.88%, standard error of estimate 9.93). The detection limit was 1.2 pg of methylmercury, corresponding to a concentration of 0.8 ng ml^{-1} MeHg in the samples. The quantification limit was 2.6 pg of methylmercury, corresponding to a concentration of 1.7 ng ml^{-1} MeHg in the samples.

Table 2 shows a comparison of published methylmercury and mercury detection limits for different coupled techniques. The detection limit of the proposed method is low, very similar to those of other techniques, and lower than the results obtained with GC–ECD [5,10].

Table 2
Comparison of detection limits reported for the determination of methylmercury

Technique[a]	Detection limit	Ref.
GC–MIP–ICP	3 pg Hg	24
GC–MPD	1 pg Hg	28
GC–AAS	4 pg Hg	17
PT-GC–FTIR	0.15 μg Hg	19
GC–ECD	50 ng g^{-1} MeHg	10
GC–ECD	250 ng g^{-1} Hg	5
HS-GC–MIP	0.5 $\mu g\ l^{-1}$ Hg	6
cGC–CVAFD	0.6 pg Hg	35
GC–AED	1.2 pg MeHg (HP-5)	This work
	1.5 pg MeHg (HP-1)	This work

[a] MIP = Microwave induced plasma; ICP = inductively coupled plasma; MPD = microwave plasma detector; AAS = atomic absorption spectrometry; PT = programmed-temperature; HS = headspace; cGC = capillary GC; CVAFD = cold vapor atomic fluorescence detection.

3.5. Precision

In order to evaluate the precision of the HP-5 column, a series of repeated injections ($n = 11$) of 1.5 μl of 30 ng ml^{-1} MeHg standard solution were made. The relative standard derivation (R.S.D.) was 4.4%. During a similar attempt to evaluate the precision of HP-1 column, the signal decreased as the samples were injected. This can be attributed to the rapid decrease in efficiency in the treatment of the column with use, owing to the small phase thickness (0.17 μm).

3.6. Accuracy

Recovery studies were carried out using a certified reference material (DORM-1), supplied by the National Research Council of Canada, with a certified methylmercury content of 0.731 ± 0.060 μg g^{-1} Hg, and with a tuna sample obtained from the Community Bureau of Reference (BCR) during an intercalibration exercise in 1993, spiked with methylmercury.

The results are given in Table 3. The mean recovery for DORM-1 was $88.81 \pm 3.92\%$ and for tuna $84.15 \pm 8.74\%$. When the same recovery study was done using GC–ECD, the mean recovery was $88.3 \pm 2.80\%$ for DORM-1 and $90.5 \pm 4.10\%$ for tuna [36].

3.7. Analysis of environmental samples and comparison with GC–ECD

Figs. 3a, 4 and 5 show the chromatograms obtained after injecting extracts of clam and mussel samples into a GC–ECD system in comparison with the results after injection into the GC–AED system using the conditions proposed here. In both instances the same column (HP-5) was used and we used the chromatographic conditions established as optimum for each system. In general terms, for relatively clean samples, it is possible to make an accurate integration of the methylmercury peak in both systems. However, for the samples such as those in Figs. 4 and 5b, the integration of the methylmercury peak in the GC–ECD system is impossible or highly inaccurate. In both figures the theoretical position of the peak is marked on the chromatograms by an arrow. The selectivity using the

Table 3
Results of the determination of methylmercury in environmental samples by GC–AED (μg g^{-1} MeHg ± standard errors)

Sample[a]	Sample mass (g)	n	MeHg content	MeHg found		Average recovery (%)	
				GC–ECD	GC–AED	GC–ECD	GC–AED
DORM-1	0.5	10	0.785 ± 0.060	0.694 ± 0.028	0.697 ± 0.032	88.30 ± 2.80	88.81 ± 3.92
Tuna muscle 1	0.5	4	Unknown	2.859	1.599	–	–
Tuna muscle 1	0.5	7	Unknown	2.779 ± 0.131	2.581 ± 0.268	90.56 ± 4.10	84.15 ± 8.74
Sediment	0.5	2	Unknown	0.151	0.127	–	–
Cockle	0.5	4	Unknown	–	0.656 ± 0.072	–	–
Clam 1	0.5	4	Unknown	–	1.034 ± 0.108	–	–
Mussel 1	0.5	4	Unknown	0.1402 ± 0.020	0.187 ± 0.054	–	–
Tuna muscle 1	0.5	2	Unknown	3.341	4.176	–	–
Tuna muscle 2	0.5	2	Unknown	5.133	7.112	–	–
*Mussel 2	0.5	4	Unknown	0.741 ± 0.168	0.242 ± 0.027	–	–
*Mussel 3	0.5	2	Unknown	–	0.099	–	–
*Mussel 4	0.5	2	Unknown	–	0.026	–	–
*Mussel 5	0.5	2	Unknown	–	0.555	–	–
*Clam 2	0.5	2	Unknown	–	0.044	–	–
*Clam 3	0.5	2	Unknown	–	0.112	–	–
*Clam 4	0.5	2	Unknown	–	0.111	–	–

[a] Samples marked with asterisks could not be analysed using the GC–ECD system.
[b] 3.0708 μg g^{-1} MeHg added.

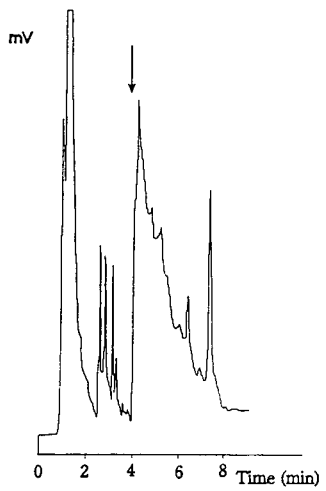

Fig. 4. Chromatogram for a clam sample using the GC–ECD system.

GC–ECD system can be improved by means of additional stages of extraction and cleaning of the samples, although clearly errors will increase during these operations. On the other hand, the GC–AED system (Figs. 3a and 5a) allows the reliable quantification of the methylmercury peak without the need to force the chromatographic separation or to apply clean-up of the samples.

Table 3 gives the results for several analyses of marine samples for methylmercury. When the same samples were analysed using both GC–ECD and GC–AED, both sets of results are given. However, several of these samples could not be analysed using the GC–ECD system owing to the presence of peaks that strongly overlapped with that of methylmercury. These samples are marked with asterisks.

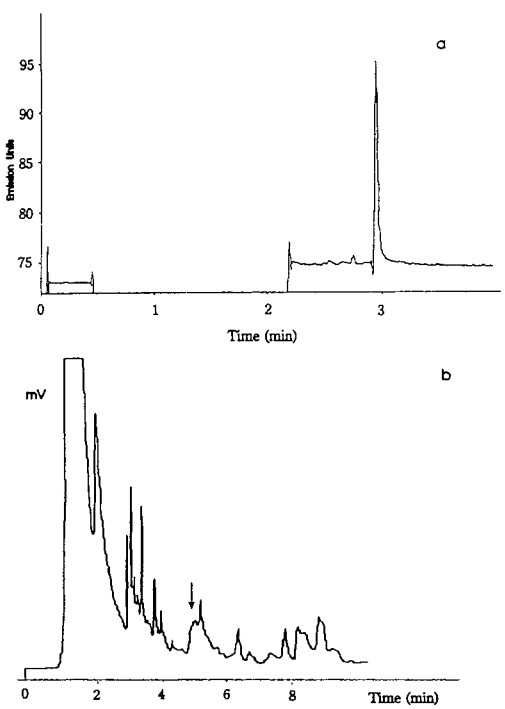

Fig. 5. Chromatograms for a mussel sample using (a) the GC–AED and (b) the GC–ECD system.

References

[1] *International Programme for Chemical Safety (ICPS), Environmental Health Criteria 101: Methylmercury*, World Health Organization, Geneva, 1990.
[2] L. Tollefson and F. Cordle, *Environ. Health Perspect.*, 68 (1986) 203–208.
[3] N.J. Yess, *J. Assoc. Off Anal. Chem. Int.*, 76 (1993) 36–38.
[4] J.E. O'Reilly, *J. Chromatogr.*, 238 (1982) 433–444.
[5] S.C. Hight and M.T. Corcoran, *J. Assoc. Off. Anal. Chem.*, 70 (1987) 24–30.
[6] P. Lansens, C. Casais, C. Meuleman and W. Baeyens, *J. Chromatogr.*, 586 (1991) 329–340.
[7] Y.H. Lee and J. Mowrer, *Anal. Chim. Acta*, 221 (1989) 259–268.
[8] M. Horvat, A.R. Byrne and K. May, *Talanta*, 37 (1990) 207–212.
[9] W. Baeyens, *Trends in Anal. Chem.*, 11 (1992) 245–254.
[10] E. Rubí, R.A. Lorenzo, C. Casais, A.M. Carro and R. Cela, *J. Chromatogr.*, 605 (1992) 69–80.
[11] C.J. Cappon and T.Y. Toribara, *LC·GC*, 4 (1986) 1012–1014.
[12] G.B. Jiang, Z.M. Ni, S.R. Wang and H.B. Han, *Fresenius' Z. Anal. Chem.*, 334 (1989) 27–30.
[13] S. Rapsomanikis, O.F. Donard and J.H. Weber, *Anal. Chem.*, 58 (1986) 35–37.
[14] S. Rapsomanikis, in R.M. Harrison and S. Rapsomanikis (Editors), *Environmental Analysis Using Chromatography Interfaced with Atomic Spectrometry*, *Ellis Horwood, Chichester*, 1989, Ch. 10.
[15] S. Rapsomanikis and P.J. Craig, *Anal. Chim. Acta*, 248 (1991) 563–567.
[16] P.J. Craig, D. Mennie, N. Ostah, O.F. Donard and F. Martin, *Analyst*, 117 (1992) 823–824.
[17] R. Fischer, R. Rapsomanikis and M.O. Andreae, *Anal. Chem.*, 65 (1993) 763–766.

[18] N.S. Bloom and W.F. Fitzgerald, *Anal. Chim. Acta*, 209 (1988) 151–161.
[19] M. Filipelli, F. Baldi, F.E. Brinckman and G.J. Olson, *Environ. Sci. Technol.*, 26 (1992) 1457–1460.
[20] B.D. Quimby and J.J. Sullivan, *Anal. Chem.*, 62 (1990) 1027–1034.
[21] J.J. Sullivan and B.D. Quimby, *Anal. Chem.*, 62 (1990) 1034–1042.
[22] R. Lobinski and F.C. Adams, *Trends in Anal. Chem.*, 12 (1993) 41–49.
[23] P.C. Uden (Editor), *Element-Specific Chromatographic Detection by Atomic Emission Spectrometry (ACS Symposium Series*, No. 479), American Chemical Society, Washington, DC, 1992, Ch. 1, p. 3.
[24] T. Kato, T. Uehiro, A. Yasuara and M. Moriya, *J. Anal. At. Spectrom.*, 7 (1992) 15–18.
[25] P. Lansens and W. Baeyens, *Anal. Chim. Acta*, 228 (1990) 93–99.
[26] P. Lansens, C. Meuleman, M. Leermakers and W. Baeyens, *Anal. Chim. Acta*, 234 (1990) 417–424.
[27] E. Bulska, D.C. Baxter and W. Frech, *Anal. Chim. Acta*, 249 (1991) 545–554.
[28] E. Bulska, H. Emteborg, D.C. Baxter, W. Frech, D. Ellingsen and Y. Thomassen, *Analyst*, 117 (1992) 657–663.
[29] R.A. Lorenzo, A. Carro, E. Rubí, C. Casais and R. Cela, *J. Assoc. Off. Anal. Chem.*, 76 (1993) 608–614.
[30] G. Westöö, *Acta Chim. Scand.*, 22 (1968) 2277–2280.
[31] A.M. Carro, R.A. Lorenzo, M.C. Casais and R. Cela, in P. Sandra and G. Devos (Editors), *Proceedings of the 15th International Symposium on Capillary Chromatography, Riva del Garda, May 1993*, Hüthig, Heidelberg, 1993, pp. 569–575.
[32] R. Lobinski, W.M.R. Drikx, M. Ceulemans and F.C. Adams, *Anal. Chem.*, 64 (1992) 159–165.
[33] Y. Liu, V. López-Ávila and M. Alcaraz, *J. High Resolut. Chromatogr.*, 16 (1993) 106–112.
[34] V. Minganti, R. De Pellegrini and R. Capelli, presented at the *15th International Symposium on Capillary Chromatography, 3rd AED Users Meeting, Hewlett-Packard: AED in Organometallic Compounds Analysis, Riva del Garda, May 1993.*
[35] N. Bloom, *Can. J. Fish. Aquat. Sci.*, 46 (1989) 1131–1140.
[36] E. Rubí, *Ph.D. Thesis*, University of Santiago de Compostela, Santiago de Compostela, 1990, pp. 176–181.

ELSEVIER

Journal of Chromatography A, 683 (1994) 253–260

JOURNAL OF CHROMATOGRAPHY A

Interfacing ion chromatography with inductively coupled plasma atomic emission spectrometry for the determination of chromium(III) and chromium(VI)

J. Prokisch*, B. Kovács, Z. Győri, J. Loch

Debrecen Agricultural University, Böszörményi út 138, P.O. Box 36, H-4032 Debrecen, Hungary

Abstract

Cr(III) and Cr(VI) can be separated and detected by ion chromatography (IC) with inductively coupled plasma atomic emission spectrometry (ICP-AES). This combined method gives reliable, reproducible results rather quickly. A measurement requires 3 min and a 50-μl sample. ICP-AES was used as an element-selective detection method for IC. Two IC techniques were compared for separation. In the first case the eluent was 7.5 m*M* potassium hydrogenphthalate and in the second case eluent changing was used. The first eluent was water; the second was 1 *M* HNO_3. The IC column was a Polispher AN anion exchanger. The Cr(VI) (CrO_4^{2-}, $Cr_2O_7^{2-}$) is retained in the column while the Cr(III) passes through without any retention. The main advantages of ICP detection are: the first (eluent) peak —which contains the Cr(III)— can be evaluated and the element selectivity and sensitivity provides reliable results. These methods were used for measuring the water-soluble Cr(III) and Cr(VI) contents of contaminated soils. The detection limits of Cr(III) and Cr(VI) are 0.25 and 0.27 μg/g, respectively.

1. Introduction

The concentration measurement of any ionic form can be particularly important in environmental samples when one ionic form (oxidation state) of the examined element is much more poisonous than the other(s). This is true in the case of chromium too.

Hexavalent chromium (CrO_4^{2-}, $Cr_2O_7^{2-}$) is very toxic and carcinogenic [1]; however, inorganic chromium(III) is essential for mammals [2]. Only atomic absorption or plasma atomic emission techniques provide information on the total amount of chromium in a test solution. This is the reason several approaches have been tried for the chromium speciation.

By means of industrial contamination through fertilization and the application of sewage sludge to arable land, a considerable quantity of chromium can get into soil and from here into surface water. In existing studies, the total amount of chromium in water, soil and plant samples was often measured with either atomic absorption spectrophotometry (AAS) or inductively coupled plasma atomic emission spectrometry (ICP-AES) in the older studies. The degree of real danger could not be determined from the data obtained with the above methods.

The oxidation states of chromium were measured separately by using one of the following approaches: (i) after organic extraction sepa-

* Corresponding author.

0021-9673/94/$07.00
SSDI 0021-9673(94)00661-X

ration of the two oxidation forms with AAS [3], (ii) with a photometer, using 1,5-diphenylcarbazide [4], (iii) by selectively volatilizing chromium species in a graphite furnace [5], (iv) by flow injection with UV detection [6], (v) by flow injection–AAS [7–9], (vi) by flow injection ICP-AES [10], (vii) by high-performance liquid chromatography (HPLC) and UV detection [11–14], (viii) by HPLC with electrochemical detection [15], (ix) by HPLC–AAS [16], (x) by HPLC–direct current plasma (DCP) [17,18], (xi) by HPLC–ICP-AES [19].

The extraction procedures are difficult. In photometric measurements there are some problems because of the effect of interfering elements (e.g. Fe(III) [20]) in the solution. The greatest sensitivity, precision, rapidity and reproducibility can be expected with the application of either flow injection (FIA) or HPLC linked to either AAS or ICP-AES instruments.

Either an acidic or a basic activated aluminium oxide, a reversed-phase C_{18} column or an ion-exchange column is used for the separation of chromium(III) and chromium(VI) in the FIA and HPLC analyses. Either AAS or ICP-AES instruments are used as an element-selective detection method. With the above-mentioned combined methods the analyses of Cr(III) and Cr(VI) can be of appropriate sensitivity.

2. Experimental

2.1. ICP-AES

A Labtam 8440M ICP-AES system with a mono- and polychromator (Labtam, Melbourne, Australia) was used. The polychromator of the ICP-AES system is a vertically mounted Paschen–Runge design with a 1-m focal length, 60 channel places and vacuum operation. The radio frequency generator is crystal controlled, operating at 27.12 MHz. A stop-flow GMK nebulizer (Labtam) is used. The following conditions were used: sample gas pressure 280 kPa; sample gas flow-rate 4.1 l/min; coolant gas pressure 140 kPa; coolant gas flow-rate 4 l/min; auxiliary gas pressure 100 kPa; auxiliary gas flow-rate 2.5 l/min; flushing gas flow-rate 1 l/min; forward power 1400 W; reflected power 5 W; ICP-AES wavelength 267.716 nm. BDH (Poole, UK) standards ($CrCl_3$ 1 mg/ml) and Reanal (Budapest, Hungary) analytical-reagent grade solid chemicals (K_2CrO_4, $K_2Cr_2O_7$) were used to prepare the calibration solutions. The IC–ICP-AES calibration curves were adjusted by measuring a high and a low standard every day.

2.2. IC

A Merck–Hitachi (E. Merck, Darmstadt, Germany) L-6200A HPLC pump with a Polyspher IC AN anion-exchange column (pre-packed column RT 100-3,2 Cat. 19815) was used in the experiments described. Two sets of conditions were applied: *Method I*: mobile phase 7.5 m*M* potassium hydrogenphthalate with 5 g/l ethylene glycol and 40 g/l 2-propanol added; flow-rate 4 ml/min; pressure 40 bar; injection volume 50 μl; measurement time 4–5 min. Retention times were 0.5 min (28 s) for Cr(III) and 2 min (119 s) for Cr(VI). *Method II*: mobile phase A, water; mobile phase B, 1 *M* HNO_3; gradient: A from 0 to 36 s, B from 36 to 120 s, followed by an abrupt change to A after 120 s; flow-rate 4 ml/min; pressure 67 bar; injected volume 50 μl; measurement time 3 min. Retention times were 0.5 min (28 s) for Cr(III) and 2 min (133 s) for Cr(VI).

All chemicals used were purchased from Reanal and were of the highest purity available. Double-distilled water was used in preparing the mobile phases.

3. Results and discussion

3.1. Optimizing of IC and ICP-AES parameters

First the IC flow-rate was optimized. Our stop-flow GMK nebulizer, a V-grove, modified Babington nebulizer, requires a relatively high flow-rate. The flow-rate–signal intensity function is a saturation curve (Fig. 1). Our aim was to reach

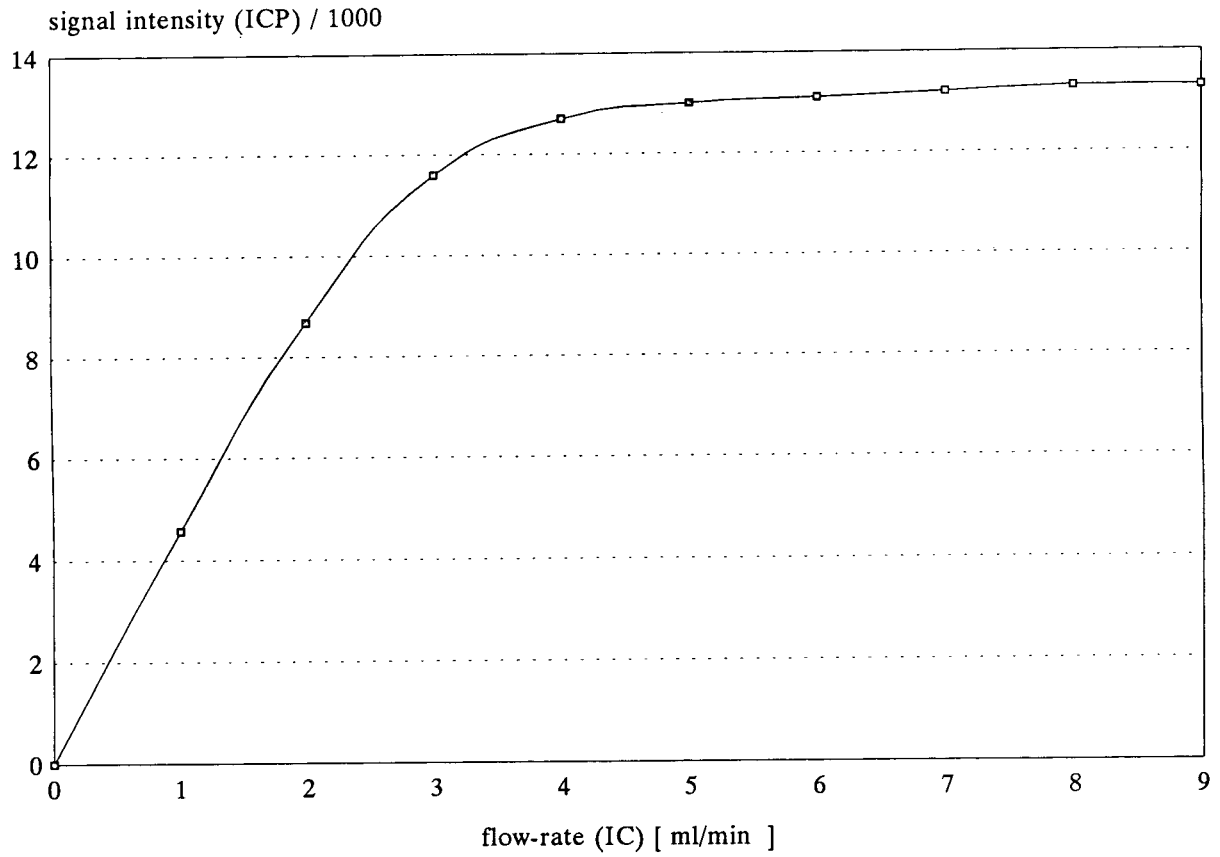

Fig. 1. Optimizing the IC flow-rate. The introduced solution was potassium hydrogenphthalate. The HPLC pump was linked to the ICP-AES system trought the stop-flow GMK nebulizer. The intensity of the ICP-AES signal was measured at 766.490 nm, on the line of potassium.

the highest intensity at the lowest flow-rate. Therefore the optimum value is 4 ml/min.

There is another way to increase the signal intensity: increasing the pressure of the sample gas. On the other hand, increasing the flow-rate of the sample gas increases the background intensity as well. The optimal pressure value is at the highest signal/background ratio, because the background equivalent concentration (BEC) is the lowest here. The pressure optimum is 280 kPa (Fig. 2).

Two separation methods were compared. The column was a Polispher AN anion-exchange column in both cases. In the first separation method the mobile phase was 7.5 m*M* potassium hydrogenphthalate. In this case the chromium(III) is in the solution peak, because it is a cation. The second peak on the chromium line is chromium(VI) (Fig. 3.) because it behaved as CrO_4^{2-} anion. There is no difference between the retention time of CrO_4^{2-} and the $Cr_2O_7^{2-}$ anions. The starting point for eluent development was the suggested eluent composition for the anion (Cl^-, NO_3^-, SO_4^{2-}, etc.) separation. This eluent contains 0.75 m*M* potassium hydrogenphthalate, 5 g/l ethylene glycol and 40 g/l 2-propanol. Using this eluent, the retention time for chromium(VI) was more than 50 min. Increasing the concentration of potassium hydrogenphthalate decreased the retention time. Our aim was to obtain a short separation time (3–5 min). The selected eluent (7.5 m*M* potassium hydro-

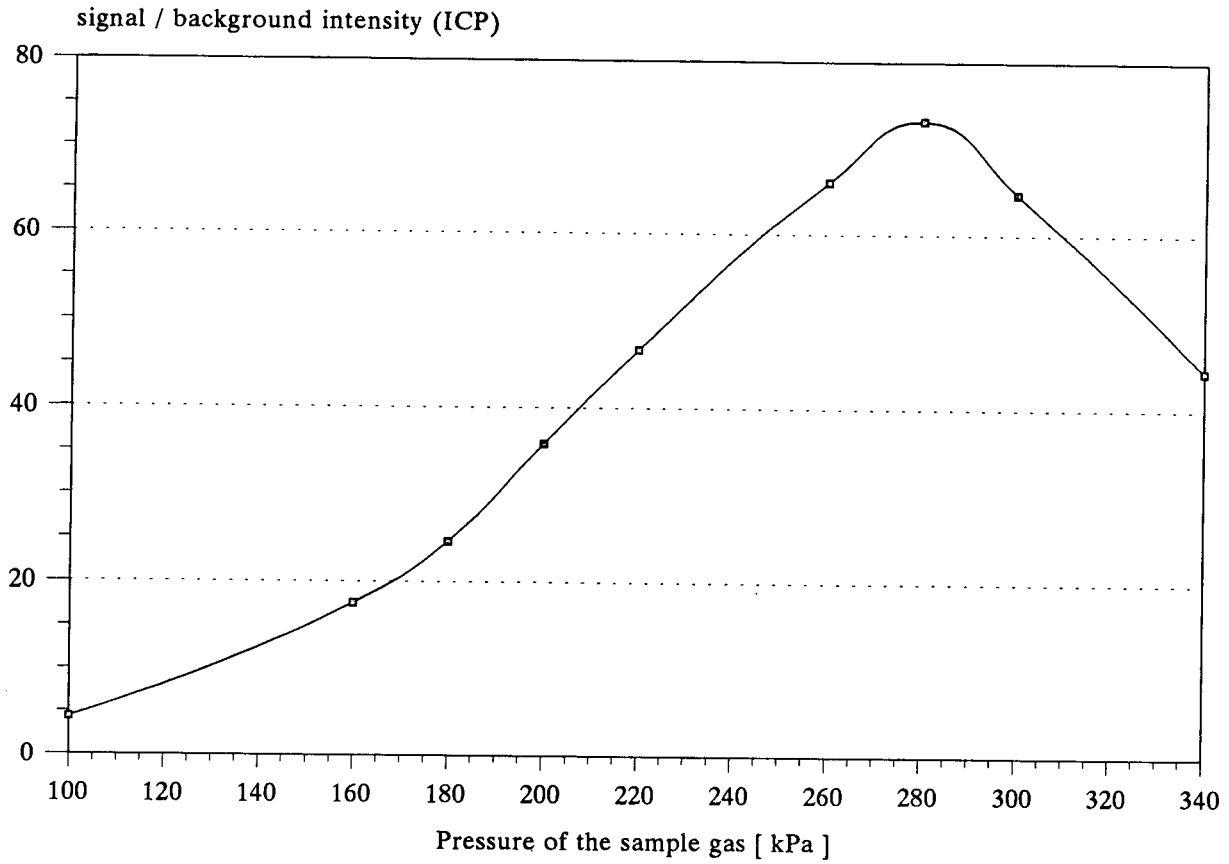

Fig. 2. Optimizing of the ICP-AES sample gas pressure. The test solution was 100 mg/kg Cr(III) solution. The optimal pressure is at the highest signal/bakground ratio.

genphthalate with 5 g/l ethylene glycol and 40 g/l 2-propanol) yielded a satisfactory result.

A second separation method was also studied. Two eluents and a stepped gradient were applied. The eluent changing was controlled with a gradient HPLC pump. Eluent A was distilled water. In the first step the chromium(III) went through the anion-exchange column without any adsorption and all chromium(VI) anions were retained in the column. After 36 s the pump changed eluent. Eluent B, 1 *M* HNO_3 removed all absorbed anions from the column (Fig. 4.). We obtained a peak only at 2 min because of the volume between the pump and the loop. After 2 min the pump changed back to eluent A. The detection limits (at 3σ) for chromium(III) are the same for the first and second methods, 0.25 μg/ml. However, there is a difference between the detection limits of chromium(VI) using methods I (1.0) and II (0.27 μg/ml). The reproducibilities of both methods were less than 2% R.S.D.

These methods are suitable for measuring the water-soluble chromium(III) and chromium(VI) content of contaminated soils, waste waters and sewage sludge.

The total amount of chromium (measured by ICP-AES) and the sum of the Cr(III) and Cr(VI) contents were compared as well. The differences were less than 3%.

The calibration curves were determined with BDH and Reanal standard solutions. For each separation method the calibration chromatograms are shown in Figs. 5–8. The calibration

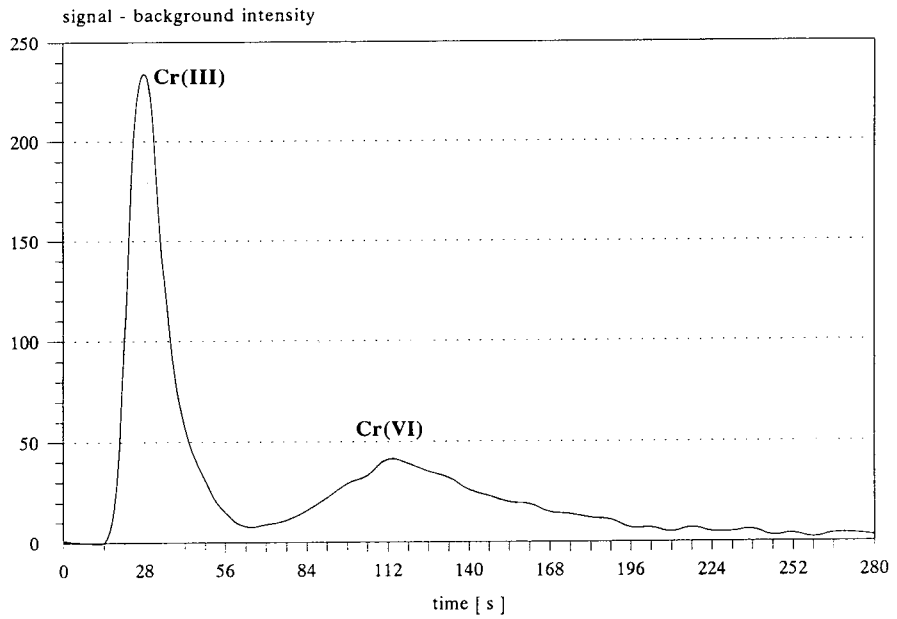

Fig. 3. Chromatogram of 10 μg/g chromium(III) and 10 μg/g chromium(VI) standard solution with method I. Eluent: 7.5 m*M* potassium hydrogenphthalate, flow-rate 4 ml/min, ICP-AES detection at 267.716 nm.

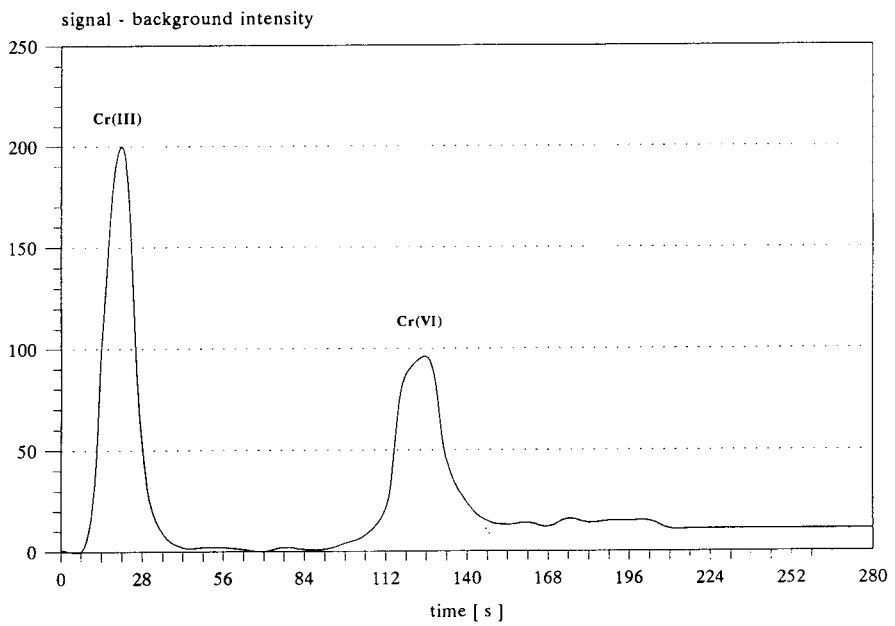

Fig. 4. Chromatogram of 10 μg/g chromium(III) and 10 μg/g chromium(VI) standard solution with method II. Gradient elution was applied. Eluent program 0–36 s water, 36–120 s 1 *M* HNO_3 followed by abrupt change to water after 120 s. Flow-rate 4 ml/min, ICP-AES detection at 267.716 nm.

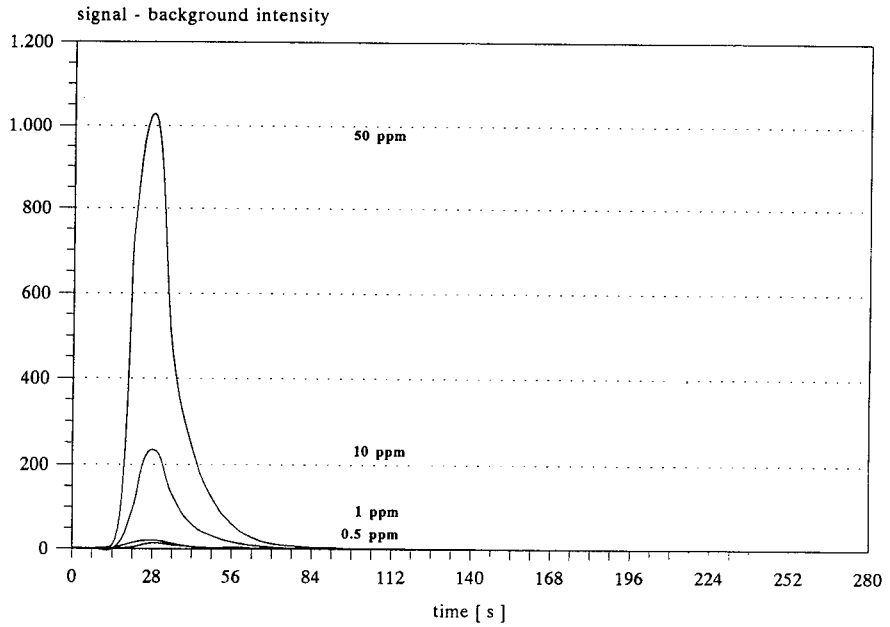

Fig. 5. Chromatograms of chromium(III) standard solutions for the calibration with method I (ppm = mg/kg). Conditions as in Fig. 3.

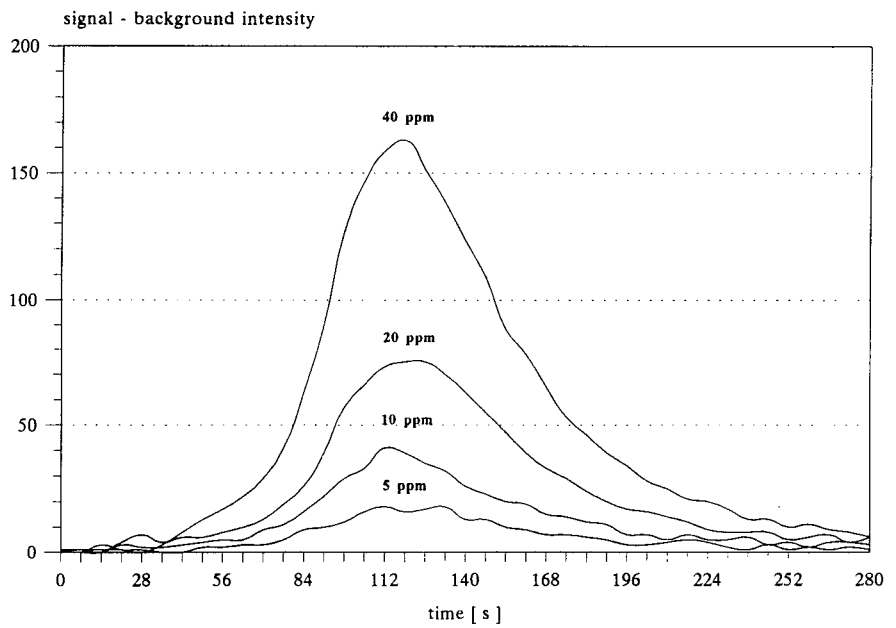

Fig. 6. Chromatograms of chromium(VI) standard solutions for the calibration with method I. Conditions as in Fig. 3.

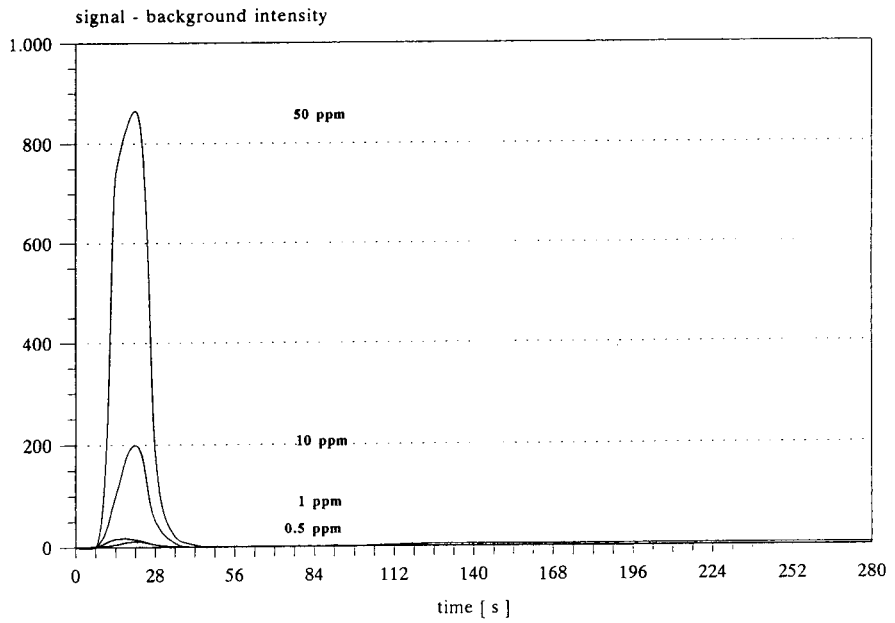

Fig. 7. Chromatograms of chromium(III) standard solutions with method II. Conditions as in Fig. 4.

equations are in Table 1 (based on the peak height). The calibration curves are linear in the 0–40 μg/ml concentration range for both chromium(III) and chromium(VI).

3.2. Long-term stability of the column

The Polispher IC AN column was used for a year only for the speciation of chromium with

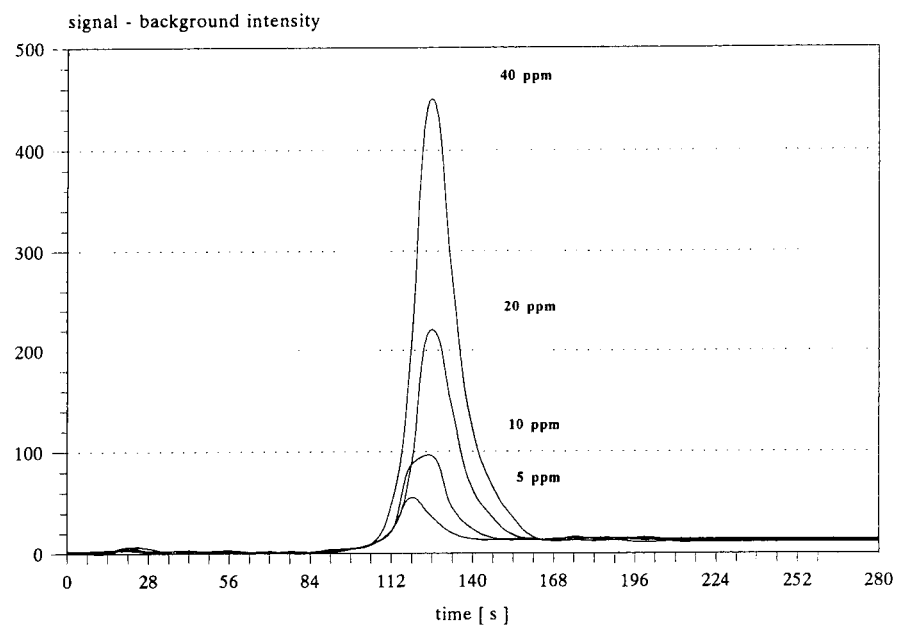

Fig. 8. Chromatograms of chromium(VI) standard solutions with method II. Conditions as in Fig. 4.

Table 1
Comparing the data of calibration curves $y = a + bx$

Ion	Method	a	b	r^2
Cr(III)	I	7.43	20.52	0.9992
Cr(III)	II	5.84	17.28	0.9990
Cr(VI)	I	0.00	4.36	0.9994
Cr(VI)	II	−4.65	11.07	0.9984

these two methods. We did not find any changes in the measurements of either chromium form. Changes in the theoretical plate number of the column were also estimated for the nitrate ion (with conductivity detection). It decreased to 70% of the original value by the end of the year. From this time onward the column was used only for chromium separation with method II, because decreases of the theoretical plate number have no effect on the efficiency of this method.

3.3. Data acquisition

The original ICP-AES software was used for data collection. The integration time was 5 s, with sufficiently low background noise ($\sigma = 1.12$)

3.4. Recovery from soil samples

Recovery of the entire amount of added chromium(VI) and chromium(III) from the soil samples is very difficult, because Cr(VI) oxidizes the organic matter in the soil and Cr(III) adsorbs at the surface of soil. The rate of oxidation depends on the pH and humus content. In the first few minutes the Cr(VI) content starts to decrease. The rate of this reaction varies for different soils. In our experiments 20 ml of a 100 μg/ml Cr(VI) solution was added to 20 g air dried soil samples. After 30 min shaking the samples were filtered and the Cr(VI) concentration was measured. Studying two soil types for 30 min after the chromium addition, the recoveries from neutral chernozem and sandy soil were 96.7 and 98.6%, respectively. When we added acidic (pH 3) Cr(VI) solution to these soils the recoveries from the chernozem and sandy soil were 42.9 and 77.0%, respectively. After 24 h shaking in the case of neutral Cr(VI) the concentrations of Cr(VI) in the filtered solution decreased to 70.9 and 88.5% for the chernozem and sandy soil respectively. When we used acidic Cr(VI) solution and it was shaken for 24 h, 9.74 and 32.8% recovery rates were obtained for the chernozem and sandy soil, respectively. This result shows that Cr(VI) can be measured exactly only in near-neutral soils by using a short shaking time.

References

[1] F. Borguet, R. Cornellis and N. Lameire, *Biol. Trace Elem. Res.*, 26 (1990) 449.
[2] H. Salem and S.A. Katz, *Sci. Total Environ.*, 86 (1989) 59.
[3] K.S. Subramanian, *Anal. Chem.*, 60 (1988) 11.
[4] H. Marchart, *Anal. Chim. Acta*, 30 (1964) 11.
[5] S. Arpadjan and V. Krivan, *Anal. Chem.*, 58 (1986) 2612.
[6] A.N. Araujo, J.L.F.C. Lima and A.O.S.S. Rangel, *Analyst*, 114 (1989) 1465.
[7] A.G. Cox, I.G. Cook and W. McLeod, *Analyst*, 110 (1985) 331.
[8] M. Sperling, X. Yin and B. Welz, *Analyst*, 117 (1992) 629.
[9] M. Sperling, S. Xu and B. Welz, *Anal. Chem.*, 64 (1992) 3101.
[10] A.G. Cox and C.W. McLeod, *Anal. Chim. Acta*, 179 (1986) 487.
[11] X. Yao, J. Liu, J. Cheng and Y. Zeng, *Chem. Res. Chin. Univ.*, 7 (1991) 37.
[12] J. Jen, G. Ou-Yang, C. Chen and S. Yang, *Analyst*, 118 (1993) 1281.
[13] T. Tande, J.E. Pettersen and T. Torgrimsen, *Chromatographia*, 13 (1980) 607.
[14] E. Eijarvi, H.J. Lajunen and M. Heikka, *Finn. Chem. Lett.*, (1985) 227.
[15] A.M. Bond and G.G. Wallace, *Anal. Chem.*, 54 (1982) 1706.
[16] A. Syty, R.G. Christensen and T.C. Rains, *J. Anal. At. Spectrom.*, 3 (1988) 193.
[17] I.S. Krull, K.W. Panaro and L.L. Gerschman, *J. Chromatogr. Sci.*, 21 (1983) 460.
[18] I.T. Urasa and S.H. Nam, *J. Chromatogr. Sci.*, 27 (1989) 30.
[19] I.S. Krull and D. Bushee, *Anal. Lett.*, 15 (1982) 267.
[20] R. Milacic, J. Stupar, N. Kozuh and J. Korosin, *Analyst*, 117 (1992) 125.

ELSEVIER

Journal of Chromatography A, 683 (1994) 261–267

JOURNAL OF CHROMATOGRAPHY A

Speciation of arsenic and selenium compounds by ion chromatography with inductively coupled plasma atomic emission spectrometry detection using the hydride technique

Dirk Schlegel, Jürgen Mattusch, Klaus Dittrich*

Department of Analytical Chemistry, Centre for Environmental Research, Permoserstrasse 15, D-04318 Leipzig, Germany

Abstract

Different forms (species) of arsenic and selenium play an important role in biological and environmental samples. For example, arsenic is widely dispersed in the environment by emission of about $32 \cdot 10^6$ kg/year as a result of anthropological inputs. The feasibility of species and multi-element determinations after ion chromatographic separation was investigated using inductively coupled plasma atomic emission spectrometry (ICP-AES) as an atomic spectrometric detection technique. After the separation of arsenic(III), arsenic(V), dimethylarsinic acid and selenium(IV) on an ion-exchange column PRP X-100 with a mobile phase of 1 m*M* *p*-hydroxybenzoate–0.4 m*M* benzoate at pH 8.5 the analyte ions were transferred to the hydride forms. The analyte gas was separated from the aquatic phase by a laboratory-made low-volume gas–liquid separation chamber. With optimized reagent concentrations of sodium borohydride and hydrochloric acid the efficiency of the hydride generation of the investigated compounds is in the range of 85 to 96%. Compared with the pneumatic nebulization, the sensitivity was increased by a factor of 50 using on-line post-column hydride formation. In addition, the parameters of the plasma, *e.g.* plasma power, argon gas flows and emission lines were optimized to achieve a high sensitivity of the ICP detection. The comparison of the sensitivities and reproducibilities shows the improvement by ICP-AES detection.

1. Introduction

Various arsenic species found in the environment have different toxicological properties in living organisms, ranging from relatively nontoxic to extremely toxic [1–3]. Therefore, evaluations of arsenic exposure to humans or plants should include chemical speciation [4–6], not only the total amounts of the elements. Due to the increasing demand for quantitative information of the form of trace metals in environmental and biological samples, chemical and instrumental techniques have been developed that allow selective detection of different species at very low levels [7–10], usually in the ng/ml range. Most of these techniques consist of couplings of two independent analytical systems ("hyphenated techniques") [11–13], which combine the ability for separation of similar compounds with a selective and sensitive detection mode. Couplings of liquid [HPLC, ion chromatography (IC)] or gas chromatography and atomic spectrometric methods [atomic absorption spectrometry (AAS), inductively coupled plasma (ICP) atomic emission spectrometry (AES), ICP-MS] are often used to achieve the efficient

* Corresponding author.

0021-9673/94/$07.00
SSDI 0021-9673(94)00327-6

separation and sensitive quantification of the species investigated [14–17]. The discontinuous monitoring normally used in AAS techniques in many cases does not correspond with the detection scheme of chromatographic methods. The two main reasons are: (1) the transfer of the sample from the column to the source of excitation leads to a drastical loss of sensitivity by low-efficient, high-volume nebulizers and (2) the data acquisition of the spectrometer does not allow the collection of data during the whole chromatographic run. To transfer elements that form volatile hydrides —As, Se, Bi, Pb, Sn, Te— into the plasma in a simple way, a on-line hydride generation (HG) by chemical reduction of the elements with higher oxidation states may be performed [18]. Rauret *et al.* [19] demonstrated the potential of coupling a HG system to ICP-AES for arsenic determination. A problem is the quick conversion of As(V) to the hydride because of the lower HG efficiency of this oxidation state. Nothing is reported about the improvement and how to reach nearly the same sensitivity as for As(III). The aim of this study was an evaluation and improvement of the hydride formation and of the gas–liquid separation to obtain high efficiencies for the determination of arsenic and selenium species.

2. Experimental

2.1. Instrumentation

For the IC separation a Perkin-Elmer HPLC system (LC 250 pump and ISS 200 autosampler) (Norwalk, CT, USA) equipped with a self-thermostating conductivity detector GAT 320 in series was applied. For separation of the ionic species two ion exchange columns Nucleosil SB 10, 125 × 3 mm and Hamilton PRP X-100, 125 × 4 mm (Bischoff, Leonberg, Germany) were used. The columns were thermostated to 25°C. The element-specific detection was performed by an ICP-atomic emission spectrometer Plasmaquant 100 (Carl Zeiss, Jena, Germany). The high optical resolution of this instrument results from the echelle polychromator with crossed lines. Twelve element lines are detectable simultaneously. Special software was developed to collect data with integration times of 0.1 to 2.0 s depending on the whole time of the chromatogram ranging from 20 to 400 min, respectively. The measured emission intensities of transient signals were saved as ASCII files and then converted to the graphic program Origin (Microcal Software, USA), so that the results could be presented graphically. The coupling unit was a miniaturized laboratory-made gas–liquid separator. The mixing of the hydride generation reagents and the mobile phase was realized with two-way splitters, polyether ether ketone (PEEK) tubes and a multichannel peristaltic pump with three different speeds (MLW, Germany). The diameters of the silicon tubes for pumping were varied to achieve different flow-rates. The scheme of the complete apparatus is shown in Fig. 1.

2.2. Chemicals

All reagents were of analytical-reagent grade. Double de-ionized water was used for the mobile phases and the standard solutions. Stock solutions (1000 μg/ml) of the species were prepared by dissolution: arsenite from As_2O_3 (Merck),

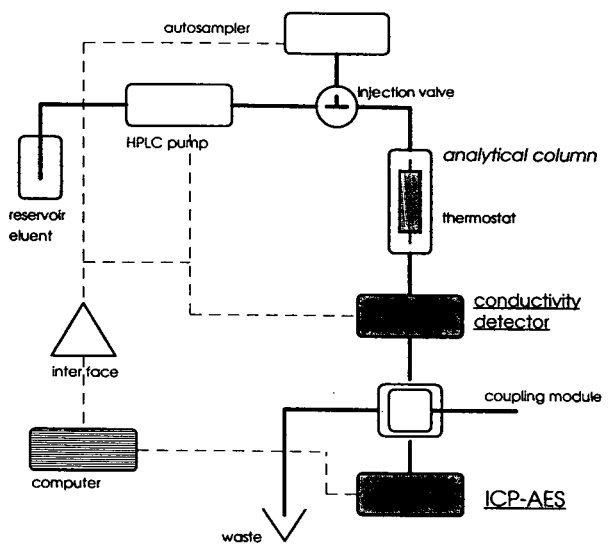

Fig. 1. Scheme of coupling IC with ICP-AES.

Table 1
Protonation constants of arsenic and selenium species [25]

Compound	pK_{a1}	pK_{a2}	pK_{a3}
Arsenic acid, As(V)	2.3	6.9	11.5
Arsenous acid, As(III)	9.2	13.5	–
Dimethylarsinic acid, DMA	1.3	6.2	–
Selenic acid, Se(VI)	−3.0	2.0	–
Selenous acid, Se(IV)	2.5	8.0	–

dimethylarsinate from cacodylic acid (Merck), selenite, selenate from Na_2SeO_3, Na_2SeO_4 (Alfa), respectively, and arsenate from a Titrisol solution (Merck). The working solutions were prepared daily by dilution of the stock solution to the required concentration in eluent. Sodium tetrahydroborate solutions were prepared by dissolution of $NaBH_4$ (Merck) and stabilized by 0.1 *M* NaOH. The mobile phases for the chromatographic separation consisted of phthalate or *p*-hydroxybenzoate, benzoate, methanol and NaOH to adjust the pH. The mobile phase was deaerated by helium and filtered (0.45 μm).

3. Results and discussion

3.1. Chromatographic separation

To determine the optimal conditions for an efficient IC separation of the species described above their protonation constants (pK_a) must be considered (Table 1). The difficulties getting uniform conditions for all components are caused by the quite different pK_a values and different electrochemical charges (Fig. 2).

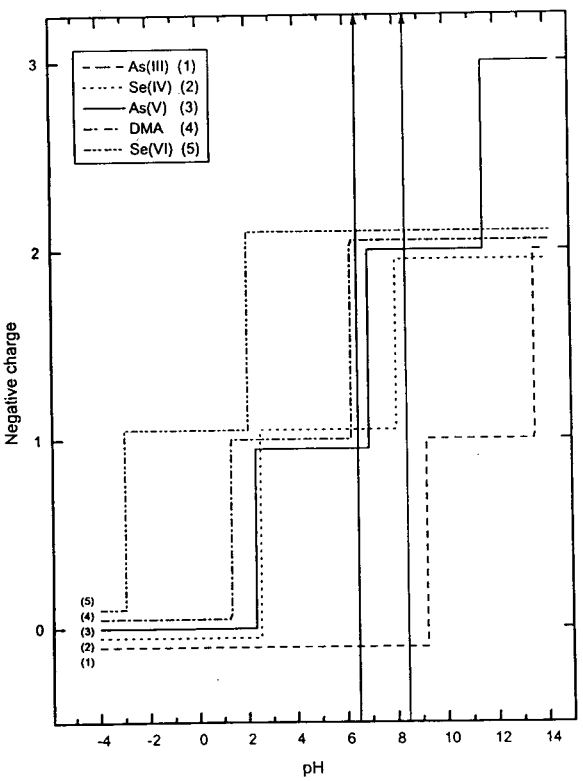

Fig. 2. Schematic dependence of the charge of selenium and arsenic compounds on pH value.

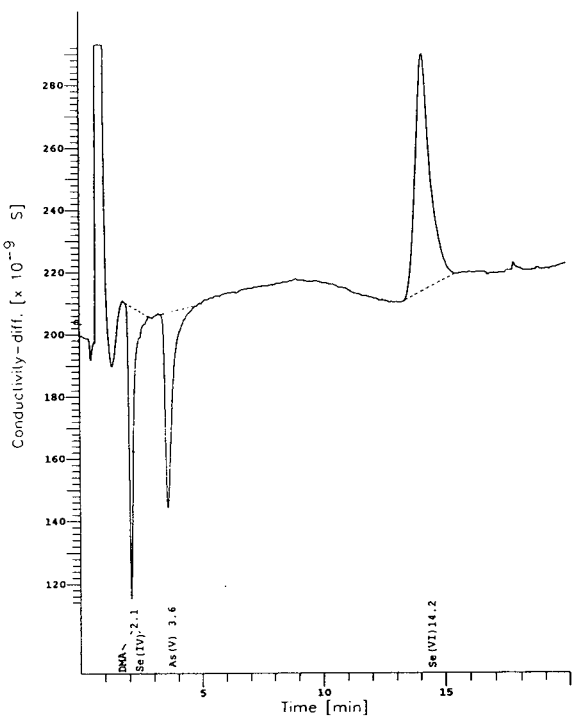

Fig. 3. Ion chromatogram of Se(IV), Se(VI), As(V), DMA with conductivity detection. Nucleosil SB 10; eluent: phthalate 2 m*M*, pH 6.5, 1 ml/min. Se(IV), Se(VI), As(V), DMA 100 mg/l.

Therefore, two different columns, Nucleosil SB 10 and Hamilton PRP X-100, were used in combination with eluents of different pH. In a weak acidic medium (pH 6.5) As(III) should not retain on the ion-exchange column Nucleosil, because of its non-ionic form. Otherwise, DMA and Se(VI) with a charge of −2 should interact very intensively with the stationary phase resulting in long retention times. As(V) and Se(IV) with a charge of −1 should show short retention times like chloride or nitrate. Fig. 3 and Table 2 show the separation and separation parameters, respectively, for a mixture of As(V), Se(IV) and Se(VI) in an identical sequence and a comparison with the traditional anions chloride, nitrate and sulphate. DMA has shown a diverging behaviour because of additional hydrophobic interaction with residual reversed-phase capacity and a pK_{a2} nearby the pH of the eluent. The existence of positive and negative peaks results from differences in conductivity compared with the conductivity of the eluent. In contrast, in a weak alkaline solution of pH 8.5 all species have a negative charge of −2 except As(III). Fig. 4 shows the separation of the five arsenic and selenium species during 30 min. The As(V) and Se(VI) signals were interfered by system peaks. The calibration plots show linear behaviour over two orders of magnitude and detection limits comparable to those of the other anions (Table 2).

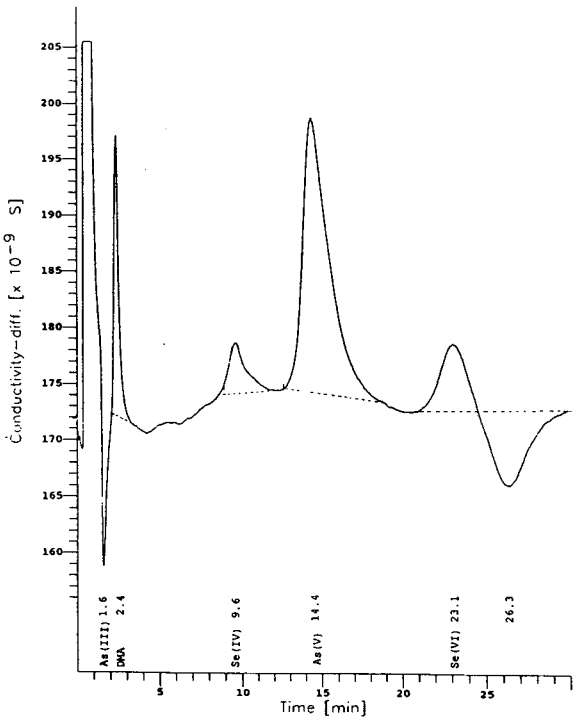

Fig. 4. Ion chromatogram of DMA, As(III), As(V), Se(IV), Se(VI) with conductivity detection. PRP X-100; eluent: 0.4 m*M* benzoic acid–1.0 m*M* *p*-hydroxybenzoic acid, methanol 2.5%, pH 8.5, 2 ml/min. DMA, As(III), As(V), Se(IV), Se(VI) 40 mg/l.

Table 2
Retention times and capacity factors of various anionic species, conductivity detection

Species	t'_R (min)	k'	Detection limit (mg/l)
$HSeO_3^-$	1.3	1.62	0.34
DMA^{2-}	1.3	1.62	0.90
$H_2AsO_4^-$	2.8	3.5	0.56
SeO_4^{2-}	13.4	16.7	0.40
Cl^-	1.9	2.4	0.08
HPO_4^{2-}	2.5	3.1	n.d.
NO_3^-	4.2	5.2	0.30
SO_4^{2-}	11.5	14.4	0.45

Conditions: Nucleosil SB 10, eluent phthalate 2.0 m*M*, pH 6.5. n.d. = Not determined.

3.2. ICP Detection

To overcome limitations of unspecific conductivity detection like unresolved or overlapping signals as well as system peaks, ICP-AES is a good choice. To enable this element-specific detection, the column eluate should be transferred to the plasma continuously. Many studies have been undertaken to enhance the poorer sensitivity if a Meinhardt or cross-flow nebulizer was used for sample introduction into the plasma [20]. With the formation of gaseous arsenic and selenium hydrides a more efficient technique was

applied. In comparison to the cross-flow nebulizer the introduction efficiency was nearly 100% with the hydride formation of As(III) and Se(IV). The optimization of the ICP-AES operating parameters such as gas flow-rates, radio frequency (rf) power and integration time was performed by continuously introducing a test solution. The best signal-to-background ratio (SBR) was chosen as the criterion for optimization. The three most sensitive analytical emission lines for arsenic —193.6, 197.1 and 228.8 nm— were tested. The observed SBR values determined the choice of the 228.8-nm line for further investigations. For selenium only the emission line of 196.0 nm was available. The argon gas streams were optimized with respect to additional hydrogen evaporation by HG. The carrier gas flow (Fig. 5) has shown a significant influence on the SBR with a maximum at 0.6 to 0.8 l/min similar to the selenium and arsenic species investigated. The optimized ICP-AES conditions are: rf power, 1.95 kW; view height, 7.5 mm; plasma gas flow, 11.5 l/min; auxilliary gas flow, 0.4 l/min; carrier gas flow, 0.75 l/min.

The transformation process to the hydrides strongly depends on the sodium borohydride concentration added to the eluent stream like a post-column derivatization. A continuous increase of the borohydride concentration yielded improved sensitivities for As(V) and DMA (Fig. 6). Concentrations higher than 4% were not suitable because the hydrogen production disturbed the plasma stability. The reduction efficiency, near 96% for the lower oxidation states, decreased from As(III) to As(V) or Se(IV) to Se(VI), so an additional reduction step by iodide [21,22] or cysteine [23,24] was recommended to accelerate the reaction, which is important considering the short period between mixing and gas–liquid separation. In this case the reduction of As(V) by iodide did not improve the sensitivity but decreased the signal intensity of Se(IV) by a factor of approximately 2 depending on the iodide concentration. Se(IV) is reduced to the

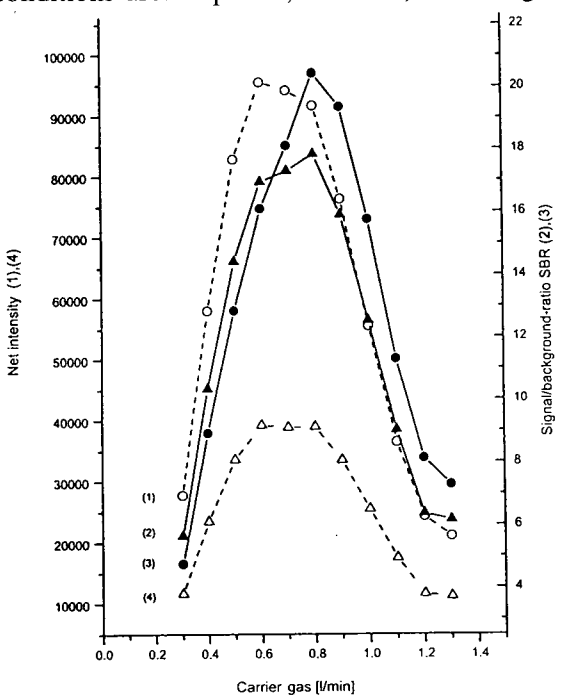

Fig. 5. Dependence of net intensity (○, △) and SBR (●, ▲) on carrier gas flow-rate. As(III) (○, ●) 5 mg/l, Se(IV) (△, ▲) 20 mg/l, power 1.95 kW, view height 7.5 mm.

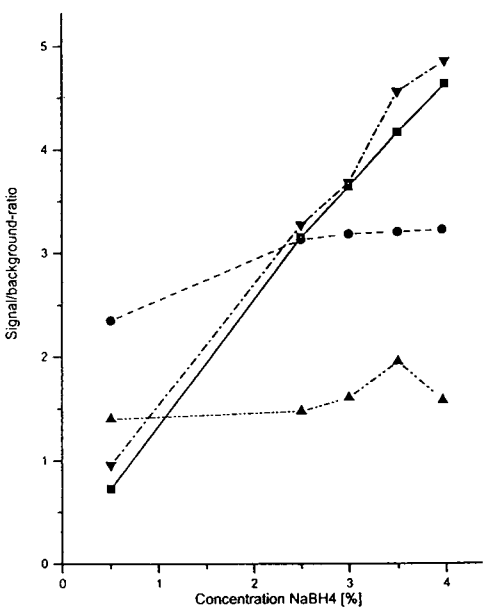

Fig. 6. Influence of $NaBH_4$ concentration on net intensity signals. DMA (▼) 10 mg/l, As(III) (●) 2 mg/l, As(V) (■) 10 mg/l, Se(IV) (▲) 8 mg/l, HCl 10%.

red elementary form, which is not converted to the hydride. The reduction of Se(VI) to the hydride form was not achieved. Here a combination of introduction techniques, *e.g.* hydride generation with an ultrasonic nebulizer, may increase the transfer for As(V) and Se(VI) by keeping the advantage of a complete introduction of the other species. Also, in this way the number of simultaneously detectable elements may be increased. An additional piece of software was used for the time-resolved ICP detection with different integration times and baseline correction. An example for a dual-channel monitoring of As and Se with overlapping signals is shown in Fig. 7, emphasizing the advantage of the element-specific detection mode. The calibration was performed under optimized conditions for the chromatographic system coupled to the ICP-AES detector: column, PRP X-100; *p*-hydroxybenzoate–benzoate, pH 8.5; HCl (added concentration), 10%; $NaBH_4$, 3.5%.

The calibration plots of arsenic and selenium species are illustrated in Fig. 8. The slopes of the

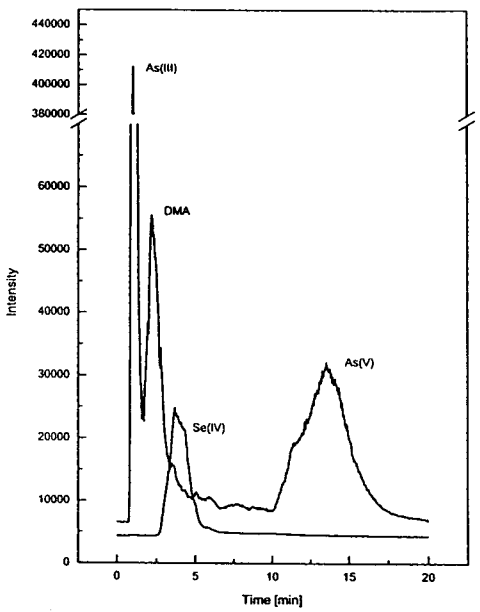

Fig. 7. Ion chromatogram of DMA, As(III), As(V), Se(IV); IC, HG, ICP-AES detection (rf power 1.95 kW, plasma gas 11.5 l/min, carrier gas 0.75 ml/min, HCl 10%, $NaBH_4$ = 3.5%, for chromatographic conditions see Fig. 4).

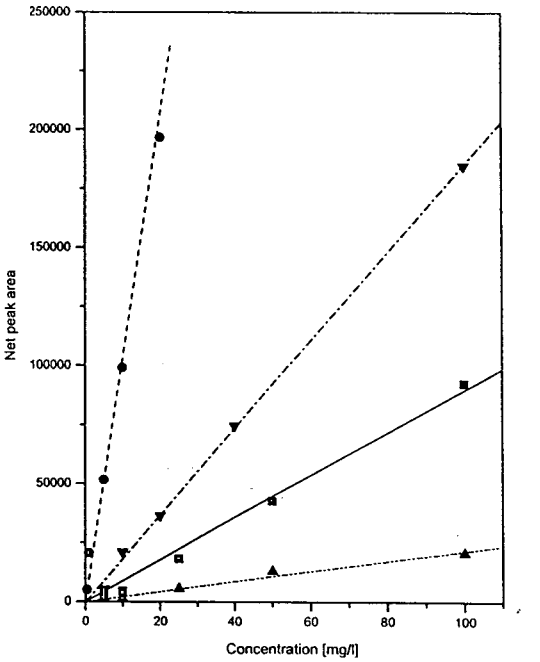

Fig. 8. Calibration plots for arsenic and selenium species (for conditions see Fig. 7). ○ = As(III); □ = As(V); ▽ = DMA; △ = Se(IV).

curves depend on the integration time, which varied from 0.2 to 2.0 s. Table 3 shows the analytical parameters of the calibration. The linearity of the method was determined for concentrations ranging over two orders of magnitude. Reproducibility was measured by five replicate injections of a test mixture of 1 mg/l as a relative standard deviation less than 5%. As(III) has the best limit of detection (17 μg/l), As(V) is the compound detected with the lowest sensitivity. This is due to the different kinetics of the reduction process.

The column eluate was always monitored with a conductivity cell in series (Fig. 1). In this way extra information about the anion content of the sample can be obtained concerning non-metallic ions like chloride, nitrate and sulphate, often present in natural materials and not normally detected by AES.

In the future this principle will be expanded to a variety of environmental samples and also include the ICP-MS technique.

Table 3
Calibration parameters IC–HG–ICP-AES

Species	Sensitivity (l/mg)		Detection limit	
	$t_{integr.} = 0.2$ s	$t_{integr.} = 2.0$ s	mg/l, $t_{integr.} = 2.0$ s	g, $t_{integr.} = 2.0$ s
As(III)	10620	10335	0.017	$1.7 \cdot 10^{-9}$
As(V)	811.5	890.2	0.64	$0.64 \cdot 10^{-7}$
Se(IV)	217.5	128.7	0.23	$2.3 \cdot 10^{-8}$
DMA	1217	187.9	0.10	$1.0 \cdot 10^{-8}$

Conditions: PRP X-100, eluent 1.0 m*M* *p*-hydroxybenzoate–0.4 m*M* benzoate, methanol 2.5%, pH 8.5, reagents HCl 10%, $NaBH_4$ 3.5%.

References

[1] W. Mertz (Editor), *Trace Elements in Human and Animal Nutrition*, Academic Press, San Diego, CA, 1987.
[2] W.R. Cullen and K.J. Reimer, *Chem. Rev.*, 89 (1989) 713.
[3] B.S. Chana and N.J. Smith, *Anal. Chim. Acta*, 197 (1987) 177.
[4] P. Quevauviller, O.F. Donard, E.A. Maier and E.A. Griepink, *Mikrochim. Acta*, 109 (1992) 169.
[5] L. Landner (Editor), *Speciation of Metals in Water, Sediment and Soil Systems —Lecture Notes in Earth Sciences, Workshop Proceedings (11)*, Springer, Berlin, 1987.
[6] J.C. van Loon and R.R. Barefoot, *Analyst*, 117 (1992) 563.
[7] F.T. Henry and T.M. Thorpe, *Anal. Chem.*, 52 (1980) 80.
[8] K. Dix, C. Cappon and T. Toribara, *J. Chromatogr. Sci.*, 25 (1987) 164.
[9] I.T. Urasa and F. Ferede, *Anal. Chem.*, 59 (1987) 1563.
[10] M. Burguera and J.L. Burguera, *J. Anal. At. Spectrom.*, 8 (1993) 229.
[11] B. Gercken and R.M. Barnes, *Anal. Chem.*, 63 (1991) 283.
[12] O.F.X. Donard and F.M. Martin, *Trends Anal. Chem.*, 11 (1992) 17.
[13] S.J. Hill, M.J. Bloxham and P.J. Worsfold, *J. Anal. At. Spectr.*, 8 (1993) 499.
[14] D. Heitkemper, J. Creed, J. Caruso and F.L. Fricke, *J. Anal. At. Spectrom.*, 4 (1989) 279.
[15] E.H. Larsen, *J. Anal. At. Spectrom.*, 6 (1991) 375.
[16] E. Hakala and L. Pyy, *J. Anal. At. Spectrom.*, 7 (1992) 191.
[17] N.P. Vela and J.A. Caruso, *J. Anal. At. Spectrom.*, 8 (1993) 787.
[18] T. Nakahara, *Prog. Anal. Atom. Spectrosc.*, 6 (1983) 163.
[19] G. Rauret, R. Rubio and A. Padrò, *Fresenius' J. Anal. Chem.*, 340 (1991) 157.
[20] R.F. Browner, *Trends Anal. Chem.*, 2 (1983) 121.
[21] B. Welz, *Atomabsorptionsspektrometrie*, VCH, Weinheim, 1983.
[22] J.F. Tyson, S.G. Offley, N.J. Seare, H.A. Kibble and C.S. Fellows, *J. Anal. At. Spectrom.*, 7 (1992) 315.
[23] H. Chen, I.D. Brindle and X.-C. Le, *Anal. Chem.*, 64 (1992) 667.
[24] F. Sperling, Y. He and B. Welz, in K. Dittrich and B. Welz (Editors), *CANAS '93, Colloquium Analytische Atomspektroskopie*, University of Leipzig, Leipzig, 1993, p. 989.
[25] E.-G. Jaeger, K. Schoene and G. Werner, *Elektrolytgleichgewichte und Elektrochemie*, DVG, Leipzig, 1989.

ELSEVIER

Journal of Chromatography A, 683 (1994) 269–276

JOURNAL OF CHROMATOGRAPHY A

Determination and speciation of organotin compounds by gas chromatography–microwave induced plasma atomic emission spectrometry

S. Tutschku*, S. Mothes, K. Dittrich

Department of Analytical Chemistry, Centre for Environmental Research, Permoserstrasse 15, 04318 Leipzig, Germany

Abstract

An optimized analytical method for the determination of organotin compounds in environmental samples is described. After derivatization the resulting compounds were measured with a hyphenated technique, gas chromatography coupled with element-selective detection by helium atmospheric pressure microwave induced plasma atomic emission spectrometry (GC–MIP-AES). The sensitivity of the most intensive emission lines in the range of 180–350 nm was investigated. The best results were obtained by using the 326.23 nm line. The influence of the reagent gases (H_2,O_2) on the signal intensity was determined. After the optimization of the source conditions a calibration was realized on the base of a multicomponent standard solution, prepared by pentylation of organotin salts. A detection limit of 0.8 pg Sn could be achieved. Measurements of the sensitivity on mixtures of organotin compounds with different alkylation showed a dependence of the grade of pentylation. This could be caused by plasma effects (formation of CO and OH molecular bands).

The proposed method was applied to the analysis of organotin compounds in a sediment of the Elbe river. Furthermore, a new arrangement of GC–MIP-AES was studied. It consists of a gas chromatograph, directly coupled to a newly designed MIP (without interface) and a quartz fibre optics to transmit the emitted light to the spectrometer.

Parameters, such as gas flow, power of the microwave generator, distance of the capillary column to the plasma, were optimized.

1. Introduction

During the last decade a fast development of species-selective analytical methods for organometallic compounds in environmental samples has been observed. Organotin compounds have been used in increasing large amounts in industry as stabilizing agents in poly(vinyl chloride) [1,2], as biocides in antifouling paints [3], etc. The increase in the industrial use of all these materials cause environmental pollution. Because of the great differences in toxicity of the various organotin compounds, depending on the structure, it is important to develop an analytical technique capable of speciation of various organotin compounds in environmental samples. The organotin compounds cannot be analyzed directly; a derivatization step is necessary. The resulting compounds can be measured by GC with a modified flame photometric detector [4–7], GC–MS [8] or GC–AAS [9,10]. A hyphenated technique for the separation and charac-

* Corresponding author.

0021-9673/94/$07.00
SSDI 0021-9673(94)00681-4

terization of such compounds is the use of GC coupled with helium atmospheric pressure microwave induced plasma atomic emission spectrometry (MIP-AES) [11–16].

This article describes an optimized analytical method for the determination of organotin compounds with GC–MIP-AES and first results of measurements to explain processes in the plasma interfering the determination of tin, such as the formation of two-atomic molecules.

2. Experimental

2.1. Instrumentation

GC–AES

An HP Model 5890 Series II gas chromatograph (Hewlett-Packard, Avondale, PA, USA) equipped with a split/splitless injection port interfaced to an HP Model 5921A atomic emission detector was used. Injections were made by means of an HP Model 7673A automatic sampler.

A new arrangement of GC–MIP-AES was investigated. It consists of a gas chromatograph HP 5890 II (Hewlett-Packard), microwave generator GMW 24-302 DR and a resonant cavity HMW 25-471 N-W (both AHF Analysentechnik, Tübingen, Germany), a monochromator SPM-2 (Carl-Zeiss-Jena, Jena, Germany) and a registration unit.

2.2. Reagents

The plasma gas and the carrier gas used for the GC-AES were helium, 99.9999%. Hydrogen, 99.999% and oxygen, 99.999%, were used for the determination of tin as reagent gases. All the gases were supplied by Linde (Leipzig, Germany).

The following organotin compounds were used. Tetrabutyltin, Bu_4Sn (98%), (Fluka, Neu-Ulm, Germany); tributyltin chloride, Bu_3SnCl (96%); dibutyltin dichloride, Bu_2SnCl_2 (95%); butyltin trichloride, $BuSnCl_3$ (95%); and *n*-pentylmagnesium bromide, PeMgBr (2.0 mol/l) in diethylether (all obtained from Aldrich, Steinheim, Germany).

Tetraethyltin, Et_4Sn and the used solvents *n*-hexane and *n*-octane, respectively, were purchased from E. Merck (Darmstadt, Germany).

Stock solutions were prepared by dissolving the appropriate amount of the organotin salt in hexane in order to yield a theoretical concentration of 500 μg/ml (as Sn) and the solutions were stored at 4°C in the dark.

Working standard solutions were prepared daily by a series of dilutions with *n*-octane–*n*-hexane from the stock solution.

Pentylated alkyltin standards were prepared by pentylation of organotin salts as described in Ref. [9].

2.3. Extraction procedure for the analysis of a sediment

Sediment (5 g) were acidified with 6 ml HCl (5%, v/v), then 20 ml of a 0.05% w/v solution of tropolone in hexane were added. This mixture was shaked for 30 min. The organic phase was separated and dried over $NaSO_4$. The Grignard reagent (pentylmagnesium bromide solution) was added to the hexane extract and stirred for 30 min. Carefully, 15 ml 0.5 *M* H_2SO_4 and 60 ml H_2O was added and the organic phase was separated and dried over Na_2SO_4.

2.4. GC–AES conditions

Working conditions for the gas chromatograph, injector, interface and atomic emission detector are summarized in Table 1.

3. Results and discussion

3.1. Optimization of GC–AES conditions for the determination of organotin compounds

On the base of conditions given in Ref. [11] the parameters emission lines and reagent gases concentration were optimized. A standard solution of 200 ng/ml tetrabutyltin in hexane was used.

Table 1
GC-AED Parameters

GC parameters	
Injection port	split/splitless
Injection port temperature	170°C
Injection volume	1 μl
Split ratio	splitless
Column	HP-1: 25 m × 320 μm × 0.17 μm I.D.
Oven program	
Initial temperature	110°C
Ramp rate	28°C
Final temperature	230°C (0.75 min)
Interface parameters	
Transfer line temperaure	250°C
AES parameters	
Helium make up flow	240 ml/min
Scavenger gases	
H_2 pressure	2.0 bar
O_2 pressure	2.0 bar
N_2 spectrometer purge flow	2 l/min
Solvent vent off time	1.5 min

Determination of the most intensive emission signals of Sn

In order to reach a higher sensitivity and an improvement of the detection level, measurements have been carried out using the following wavelengths: 189.98, 235.48, 242.17, 242.95 257.16, 270.65, 284.00, 286.33, 300.91, 303.41, 317.50 and 326.23 nm. Fig. 1 shows the comparison of signal intensities. For the measurements to follow the 326-nm wavelength was used.

Influence of the reagent gases on the signal intensity

As reagent gases either oxygen or hydrogen (or both) may be added to the gas flow in order to increase the sensitivity. For the analyses of organotin compounds the presence of oxygen is necessary to prevent the deposition of carbon at the discharge tube. The presence of oxygen leads, on the other side, to the formation of refractory oxides of tin inside the MIP interface. The tin oxides tend to accumulate on the inner wall of the quartz discharge tube changing the parameters of the MIP and resulting in a decrease of sensitivity, peak tailing, and subsequent memory effects. The negative effect of oxygen on the determination of tin can be compensated for by adding of some hydrogen to the plasma gas. Hydrogen seems to support tin excitation probably by forming very volatile hydrides which are easily atomized and excited [11].

The influence of the reagent gases on the signal intensity (for tetraethyltin in hexane) is shown in Fig. 2. It can be seen, that a maximum intensity is found using 2.4 bar hydrogen and that the intensity is minimal using oxygen.

3.2. Calibration

Using the optimized parameters a calibration for tin was made on the basis of tetrabutyltin in hexane. In all cases an excellent linearity for a concentration range over 3 orders of magnitude is realizable. An evaluation of the peak heights shows that the detection limits for the different Sn emission lines are in the range from 0.8 to 8.4 pg Sn, listed in Table 2. Looking at the signal intensities in Fig. 1 one should expect the 284.00 nm line is characterized by the best detection limit. The data given in Table 2 show, however, that the best detection limits are obtained at the 326.2 nm Sn emission line. This is caused by the high background using the 284.00 nm line and the fact that the detection limit is given by the 3σ criteria. The effect of background emission will be discussed in Section 3.3.

Investigations of mixtures of organotin compounds

First studies were done with butyltin species which play an important role in polluted aqueous systems. Because these organotin compounds, besides tetrabutyltin, can not be analyzed directly (the volatility of this cationic species is insufficient), a derivatization was realized (Grignard reagent). A multicomponent standard solution was prepared by pentylation of organotin salts. It consist of tetrabutyltin, tributylpentyltin, dibutyldipentyltin, and monobutyltripentyltin. Measurements of mixtures of organotin compounds were carried out in hexane (Fig. 3) and

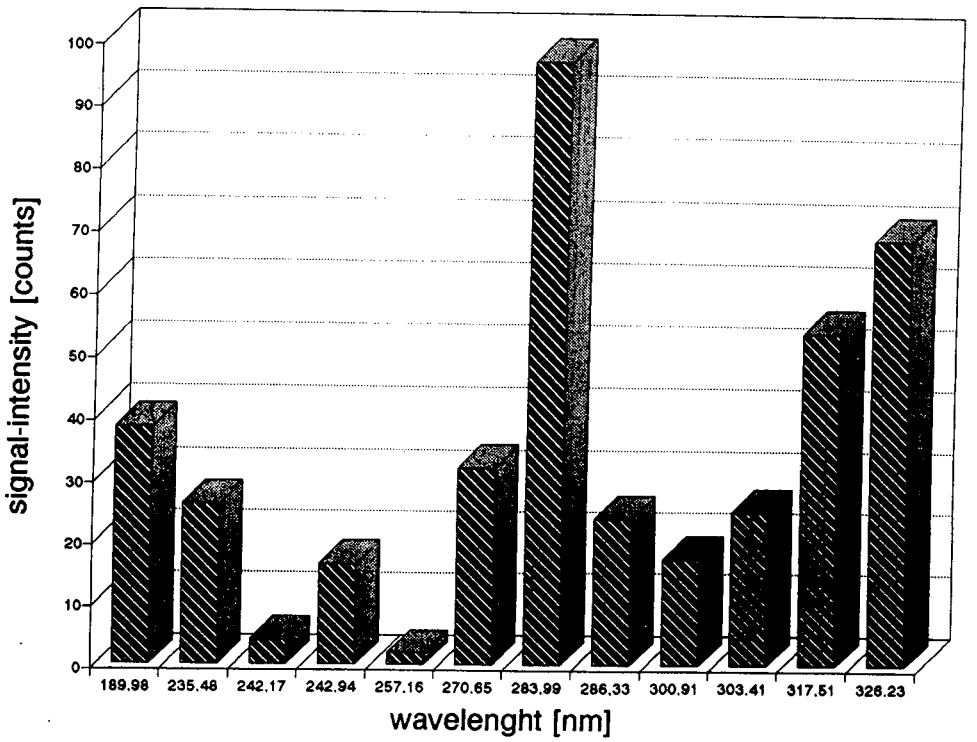

Fig. 1. Comparison of signal intensities of tin at the most sensitive emission lines, conditions are given in the Experimental section. A solution of tetrabutyltin in hexane with 500 ng/ml Sn was used.

octane, respectively. It was found, that there is no influence on the sensitivity of the used organotin compounds for both solvents. But it was found that with an increase of the degree of pentylation there is a remarkable decrease in sensitivity.

In order to exclude influences due to derivatization and extraction, tetraethyltin which

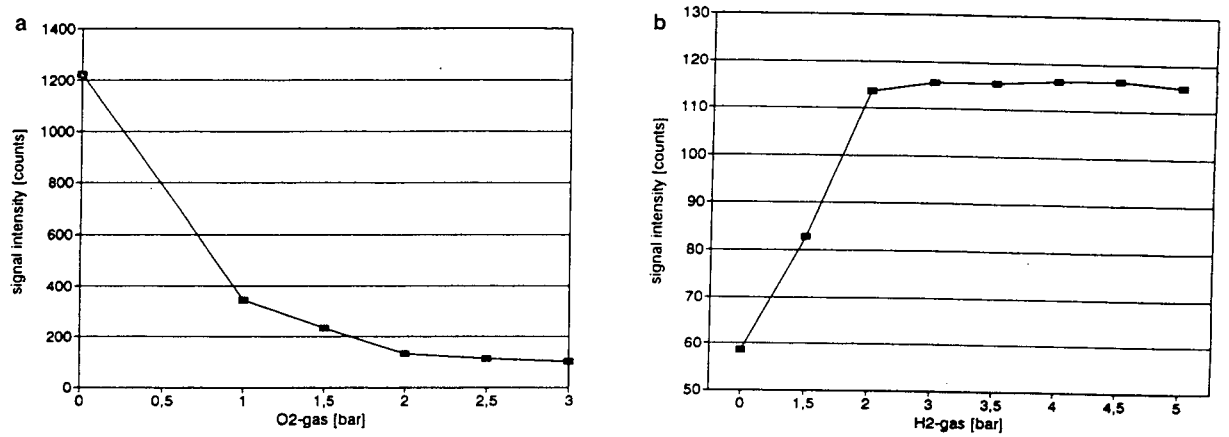

Fig. 2. Influence of the reagent gases on the signal intensity, using tetrabutyltin in hexane with 500 ng/ml Sn. (a) Influence of O_2 on the signal intensity; (b) influence of H_2 on the signal intensity.

Table 2
Detection limits for tin at the most intensive wavelengths

Wavelenght (nm)	Detection limit (pg Sn)
189.98	1.4
270.65	2.3
284.00	2.1
303.41	2.5
317.50	8.4
326.23	0.8

Table 3
Sensitivities and detection limits for the different compounds

Compound	Sensitivity (counts/pg Sn)	Detection limit (pg Sn)
Bu_4Sn	0.77	0.8
Bu_3SnPe	0.67	0.9
Bu_2SnPe2	0.45	1.4
$BuSnPe_3$	0.21	3.1
Et_4Sn	0.07	8.3

does not have to be derivatized was calibrated and compared with calibration of tetrabutyltin. Even here, a distinctly lower sensitivity of tetraethyltin in comparison with tetrabutyltin can be noticed. That means that the detection limit is depending on the binding of the element, in contrast of the claim of the manufacturer that the response factors for each element should be nearly the same for all compounds. In the literature [13,14,17] differences were also reported. Sensitivities and detection limits for the different compounds are listed in Table 3.

3.3. Plasma investigations

The device used in this study has the possibility to confirm the identity of a peak with a so-called snap shot . It takes an instantaneous spectrum of the wavelength range where the photodiode array (PDA) is positioned. The typical emission spectra with wavelengths ranging from 260 to 340 nm are shown in Fig. 4.

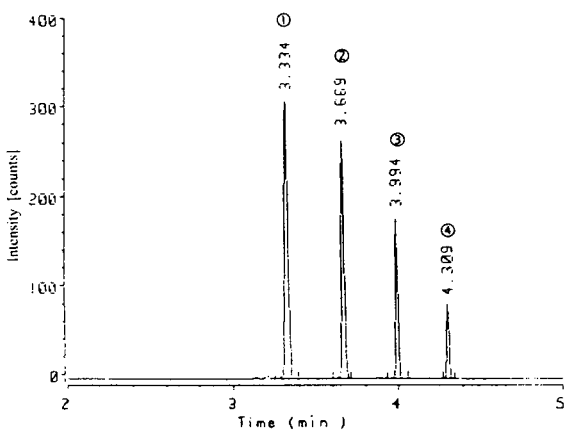

Fig. 3. Chromatogram of a mixture of Bu_4Sn, Bu_3PeSn, Bu_2Pe_2Sn and $BuPe_3Sn$ (containing 400 pg Sn each, in hexane, measured at the 326 nm Sn line, conditions listed in Table 1), 1 = Bu_4Sn; 2 = Bu_3PeSn; 3 = Bu_2Pe_2Sn; 4 = $BuPe_3Sn$.

An investigation of the background (Fig. 5) showed that the 284.00 nm line and the 317.50 nm line are superimposed by molecular bands. That is the reason for the worse detection limits at this wavelengths. The band at 317.50 nm is probably an OH molecular emission, the band at 284.00 nm turned out to be a CO-band. For verification a (CO) molecular emission during a run of a organotin compound was measured at a wavelength of 342.57 nm at the retention time of the organotin compound. The obtained signal is shown in Fig. 6.

The formation of molecules (CO, OH, SnO, SnH, SnOH) can be explained by the relatively low gas temperature within the MIP. The plasma temperatures are lower than for other plasmas such as ICP. (The intense spectral emission for many elements, including non-metals is giving by the high electron temperatures in the plasma.) Besides the presence of OH and CO confirmed by the bands of both species, the formation of SnO_2 in the MIP was tested. The inner surface of the discharge tube was analysed using the combination of ICP-MS and laser ablation. The semiquantitative analysis of an used discharge tube showed a high concentration of tin.

3.4. Analysis of an environmental sample

The potentials of the method described, were studied by the analysis of an environmental sample, a sediment from the river Elbe near

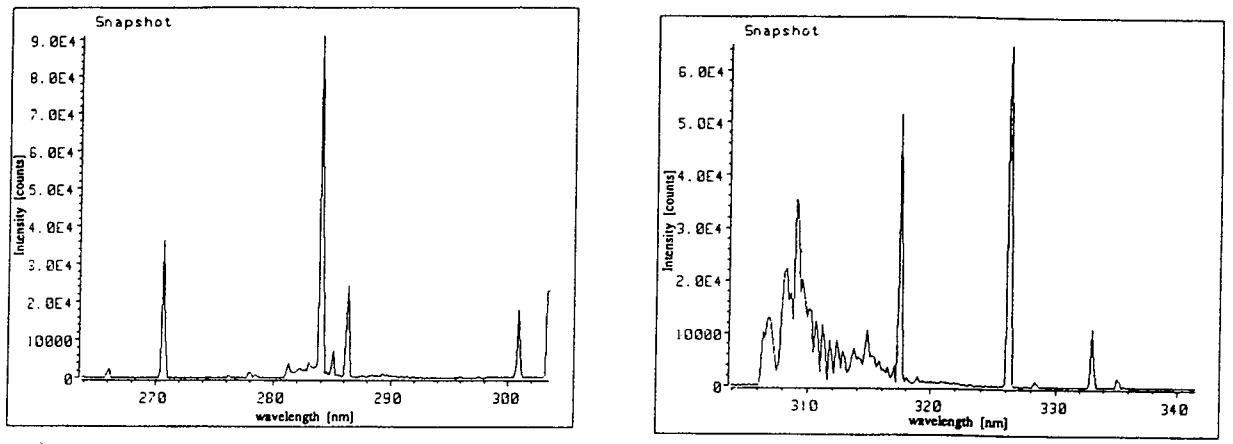

Fig. 4. Snap shot: atomic emission spectrum of tin in the range from 260 to 370 nm taken from the peak maximum of a tetrabutyltin peak (500 pg Sn).

Hamburg, harbour Teufelsbrück. For the preparation of this sample 5 g of sediment were extracted with a hexane–tropolone solution and the extract was derivatized using pentyl magnesium bromide [8]. The procedure is given in Section 2.3. A volume of 1 μl of the extract was injected into the GC–AED system. The chromatogram is shown in Fig. 7. The presence of tin was confirmed by snap shots in a preliminary qualitative analysis.

All peaks of the chromatogram on the Sn 326 nm line were identified as tin in organotin compounds by adding of a mixture of known tin organic compounds to the extract. It was impossible to quantify the results because of the insufficient degree of extraction of the organotin species from the sediment by the used technique.

3.5. Preliminary results with a laboratory-made arrangement of a GC–MIP-AES coupling

A new microwave induced He plasma sustained under atmospheric pressure was used in conjunction with a monochromator as an element-specific detector in capillary GC for the determination of tin. This arrangement (Fig. 8) is simple, cheap and was used for first measurements, to test the capability for the determination of tin compounds. It is planed to couple this MIP arrangement with an Echelle spec-

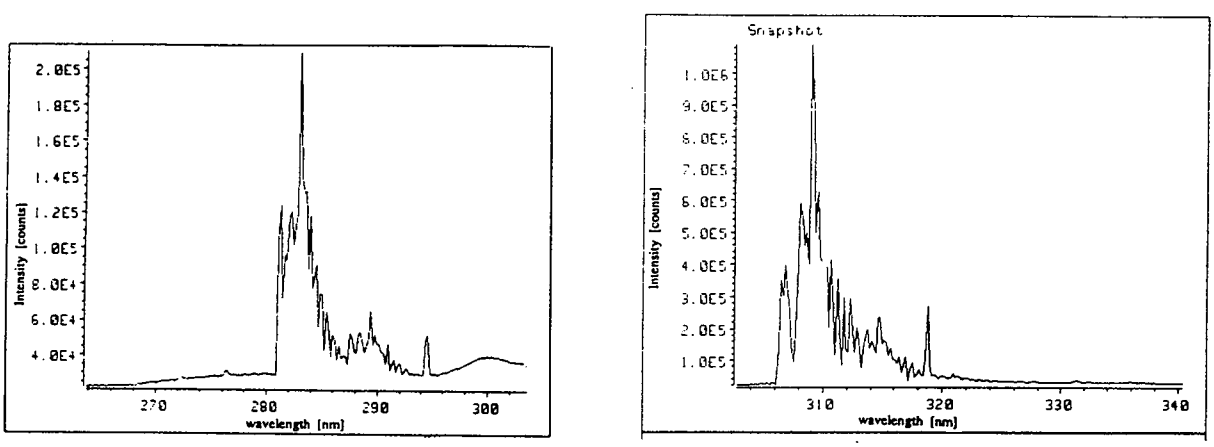

Fig. 5. Background in the range from 260 to 370 nm.

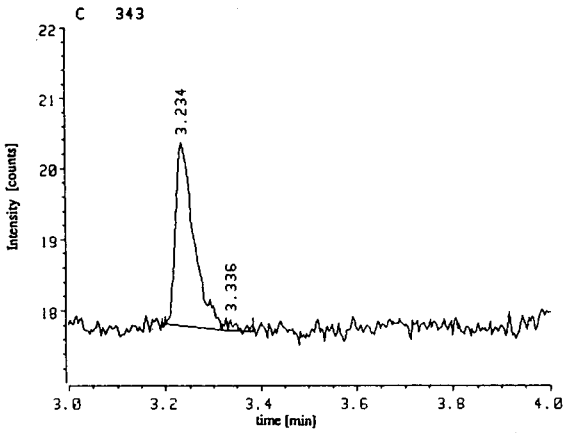

Fig. 6. Emission intensity of the CO band (342.57 nm), obtained during a run of tetrabutyltin in hexane (conditions listed in Table 1).

trometer to detect up to 12 elements simultaneously.

The specificity of this MIP is an concentric dual flow torch . This design (Fig. 9) utilizes two concentric alumina tubes and two plasma gas flows. The first gas flow passed between the two tubes while the second flow passed through the inner tube. This arrangement prevents the plasma interacting with the walls and makes it more spatially stable. Plasma centering in the discharge tube reduces interactions with the walls. The second make-up flow, passing through the

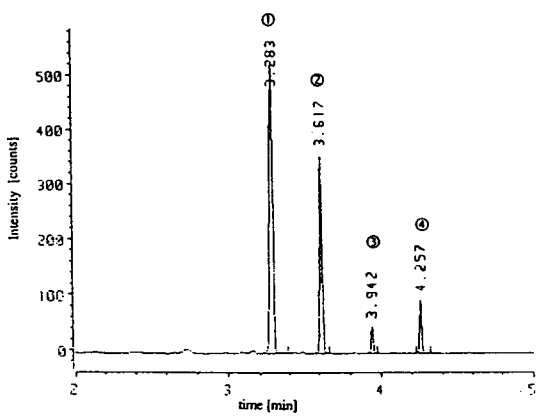

Fig. 7. Chromatogram of a sediment sample from the River Elbe after extraction and derivatization with Grignard reagent. 1 = Bu_4Sn; 2 = Bu_3PeSn; 3 = Bu_2Pe_2Sn; 4 = $BuPe_3Sn$ (conditions listed in Table 1).

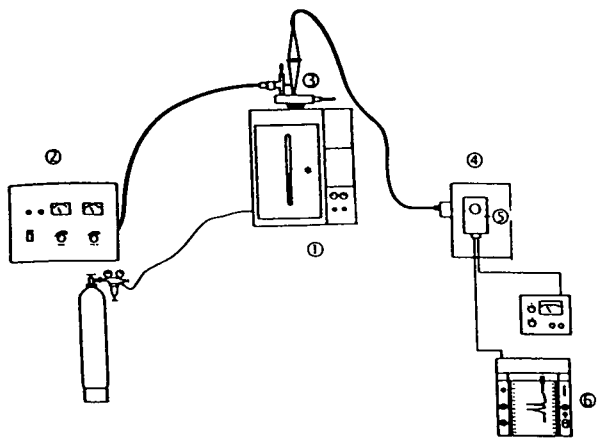

Fig. 8. The schematic diagram of the laboratory-made arrangement of the GC–MIP system. 1 = Chromatograph, 2 = microwave generator; 3 = cavity with plasma; 4 = spectrometer; 5 = photomultiplier tube; 6 = registration unit.

inner tube, is usually at a relatively low flow to sweep analyte into the plasma at a relatively low flow-rate, hence providing long residence times of analytes in the plasma. This has been described earlier in Ref. [18].

Working conditions

It was first necessary, to study the amount of solvent (hexane) which is acceptable for the

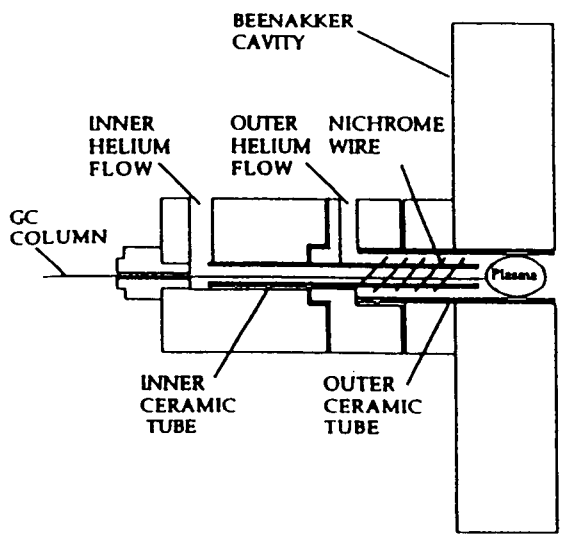

Fig. 9. Dual flow torch. From Ref. [18].

plasma. Using splitless injection and a column head pressure of 18 bar it was possible to inject 0.5–5 μl of hexane. The parameters inner flow, outer flow, power of the microwave generator, distance of the capillary column to the plasma were investigated for the analysis of tin organics. Optimum plasma conditions are: inner flow 20 ml/min, outer flow 120 ml/min and a power of 95 W. We found, there is no influence of the distance between the end of the capillary column and the plasma on the signal intensity.

The detection limit obtained in this preliminary studies was 4 ng Sn absolute. This detection limit is worse compared with that obtained with the commercially device. The reason for this is the optics and the data requisition of the very simple spectrometer used. Further investigations will be done with a polychromator.

4. Conclusions

The two methods using GC–MIP-AES were successfully applied for the determination of organotin compounds. The GC–AES (Hewlett-Packard) allows to achieve absolute detection limits in the range of a few pg (as Sn). A quantitative analysis of these compounds in polluted aqueous systems is realizable.

The signal intensity is influenced by several parameters of the MIP and GC system, such as added reagent gases and the Sn emisssion lines used. An investigation of the parameters showed that the analytical response depends on the kind of tin compounds itself. This behaviour could not be fully explained. First, studies reveal an incomplete destruction of all bondings in the organotin compounds and thus an incomplete atomization of Sn, which is also shown by the presence of molecules inside the plasma (CO, OH) and in the discharge tube (SnO_2). These processes can be explained by the relatively low gas temperature within the MIP.

References

[1] C.A. Krone, D.W. Brown, D.G. Burrows, R.G. Bogar, S.L. Chan and U. Varanasi, *Mar. Environ. Res.*, 27 (1989) 1.
[2] K. Fent, *Mar. Environ. Res.*, 28 (1989) 477.
[3] S.J. Blunden and A. Chapman, in P.J. Craig (Editor), *Organometallic Compounds in the Environment, Principles and Reactions*, Longman, Essex, 1986, p. 111.
[4] I.L. Comez-Ariza, E. Morales and M. Ruiz-Beritez, *Analyst*, 117 (1992) 641.
[5] M.J. Waldock, M.E. Waite, D. Miller, D.J. Smith and R.J. Law, *Aquatic Environment Protection: Analytical Methods*, MAFF, Lovestoft, 1989, p. 4.
[6] J. Tolosa, J.M. Bayona, J. Albaiges, L.F. Alencastro and J. Tarradellas, *Fresenius' Z. Anal. Chem.*, 339 (1991) 646.
[7] M.D. Müller, *Anal. Chem.*, 59 (1987) 617.
[8] E. Jantzen and R. Wilken, *Vom Wasser*, 76 (1991) 1–11.
[9] W.M.R. Dirx, W.E. van Mol, R.J.A. van Cleuvenbergen and F.C. Adams, *Fresenius' Z. Anal. Chem.*, 335 (1989) 796–774.
[10] Y.K. Chau, S. Zhang and R.J. Maguire, *Analyst*, 117 (1992) 1161.
[11] R. Lobinski, M.R. Dirkx, M. Ceulemans and F.C. Adams, *Anal. Chem.*, 64 (1992) 159–165.
[12] W. Besler and D. Laschka, *Umweltforschungsplan des Bundesministers für Umwelt, Naturschutz und Reaktorsicherheit, Wasser, Forschungsbericht 10205138*, Umweltbundesamt, Berlin, April, 1991.
[13] T. Gremm, *Dissertation*, Karlsruhe, 1992.
[14] B.F. Scott, Y.K. Chau and A. Rais-Firouz, *Appl. Organomet. Chem.*, 3 (1989) 105.
[15] S.A. Estes, P.C. Uden and R.M. Barnes, *Anal. Chem.*, 53 (1981) 1829.
[16] F. Davids and P. Sandra, *Analusis*, 20 (1992) 53.
[17] M.E. Birch, *Anal. Chim. Acta*, 282 (1993) 451-458.
[18] T.M. Dowling, J.A. Seeley, H. Feuerbacher and P.C. Uden, in P.C. Uden (Editor), *Element-specific Chromatographic Detection by Atomic Emission Spectroscopy*, American Chemical Society, Washington, DC, 1992, Ch. 5, pp. 91–103.

END OF SYMPOSIUM PAPERS

The Data Analysis Handbook

By **I.E. Frank** and **R. Todeschini**

Data Handling in Science and Technology Volume 14

Analyzing observed or measured data is an important step in applied sciences. The recent increase in computer capacity has resulted in a revolution both in data collection and data analysis. An increasing number of scientists, researchers and students are venturing into statistical data analysis; hence the need for more guidance in this field, which was previously dominated mainly by statisticians.

This handbook fills the gap in the range of textbooks on data analysis. Written in a dictionary format, it will serve as a comprehensive reference book in a rapidly growing field. However, this book is more structured than an ordinary dictionary, where each entry is a separate, self-contained entity. The authors provide not only definitions and short descriptions, but also offer an overview of the different topics. Therefore, the handbook can also be used as a companion to textbooks for undergraduate or graduate courses.

Approximately 1700 entries are given in alphabetical order grouped into 20 topics and each topic is organized in a hierarchical fashion. Additional specific entries on a topic can be easily found by following the cross-references in a top-down manner. Several figures and tables are provided to enhance the comprehension of the topics and a list of acronyms helps to locate the full terminologies. The bibliography offers suggestions for further reading.

©1994 386 pages Hardbound
Price: Dfl. 325.00 (US$185.50)
ISBN 0-444-81659-3

ELSEVIER
An imprint of Elsevier Science

ORDER INFORMATION

ELSEVIER SCIENCE B.V.
P.O. Box 330
1000 AH Amsterdam
The Netherlands
Fax: +31 (20) 5862 845

For USA and Canada:
P.O. Box 945
New York, NY 10159-0945
Fax: +1 (212) 633 3680

US$ prices are valid only for the USA & Canada and are subject to exchange rate fluctuations; in all other countries the Dutch guilder price (Dfl.) is definitive. Customers in the European Union should add the appropriate VAT rate applicable in their country to the price(s). Books are sent postfree if prepaid.

Flow-Through (Bio)Chemical Sensors

By **M. Valcárcel** and **M.D. Luque de Castro**, Department of Analytical Chemistry, University of Córdoba, 14004 Córdoba, Spain

Techniques and Instrumentation in Analytical Chemistry Volume 16

Flow-through sensors are more suitable than classical probe-type sensors for addressing real (non-academic) problems. The external shape and operation of flow-through (bio)chemical sensors are of great practical significance as they facilitate sample transport and conditioning, as well as calibration and sensor preparation, maintenance and regeneration, all of which result in enhanced analytical features and a wider scope of application.
This is a systematic presentation of flow-through chemical and biochemical sensors based on the permanent or transient immobilization of any of the ingredients of a (bio)chemical reaction (i.e. the analyte, reagent, catalyst or product) where detection is integrated with the analytical reaction, a separation process (dialysis, gas diffusion, sorption, etc.) or both.

The book deals critically with most types of flow-through sensors, discussing their possibilities and shortcomings to provide a realistic view of the state-of-the-art in the field. The large numbers of figures, the wealth of literature references and the extensive subject index complement the text.

© 1994 332 pages Hardbound
Price: Dfl. 355.00 (US$ 202.75)
ISBN 0-444-89866-2

ELSEVIER SCIENCE

ORDER INFORMATION
ELSEVIER SCIENCE B.V.
P.O. Box 330
1000 AH Amsterdam
The Netherlands
Fax: (+31-20) 5862 845
For USA and Canada
P.O. Box 945
Madison Square Station
New York, NY 10159-0945
Fax: (212) 633 3680
US$ prices are valid only for the USA & Canada and are subject to exchange rate fluctuations; in all other countries the Dutch guilder price (Dfl.) is definitive. Customers in the European Union should add the appropriate VAT rate applicable in their country to the price(s). Books are sent postfree if prepaid.

PUBLICATION SCHEDULE FOR THE 1995 SUBSCRIPTION

Journal of Chromatography A and *Journal of Chromatography B: Biomedical Applications*

MONTH	O 1994	N 1994	D 1994	
Journal of Chromatography A	683/1 683/2 684/1	684/2 685/1 685/2 686/1	686/2 687/1 687/2 688/1 + 2	The publication schedule for further issues will be published later.
Bibliography Section				
Journal of Chromatography B: Biomedical Applications				

INFORMATION FOR AUTHORS

(Detailed *Instructions to Authors* were published in *J. Chromatogr. A*, Vol. 657, pp. 463–469. A free reprint can be obtained by application to the publisher, Elsevier Science B.V., P.O. Box 330, 1000 AH Amsterdam, Netherlands.)

Types of Contributions. The following types of papers are published: Regular research papers (full-length papers), Review articles, Short Communications and Discussions. Short Communications are usually descriptions of short investigations, or they can report minor technical improvements of previously published procedures; they reflect the same quality of research as full-length papers, but should preferably not exceed five printed pages. Discussions (one or two pages) should explain, amplify, correct or otherwise comment substantively upon an article recently published in the journal. For Review articles, see inside front cover under Submission of Papers.

Submission. Every paper must be accompanied by a letter from the senior author, stating that he/she is submitting the paper for publication in the *Journal of Chromatography A* or *B*.

Manuscripts. Manuscripts should be typed in **double spacing** on consecutively numbered pages of uniform size. The manuscript should be preceded by a sheet of manuscript paper carrying the title of the paper and the name and full postal address of the person to whom the proofs are to be sent. As a rule, papers should be divided into sections, headed by a caption (*e.g.*, Abstract, Introduction, Experimental, Results, Discussion, etc.). All illustrations, photographs, tables, etc., should be on separate sheets.

Abstract. All articles should have an abstract of 50–100 words which clearly and briefly indicates what is new, different and significant. No references should be given.

Introduction. Every paper must have a concise introduction mentioning what has been done before on the topic described, and stating clearly what is new in the paper now submitted.

Experimental conditions should preferably be given on a *separate* sheet, headed "Conditions". These conditions will, if appropriate, be printed in a block, directly following the heading "Experimental".

Illustrations. The figures should be submitted in a form suitable for reproduction, drawn in Indian ink on drawing or tracing paper. Each illustration should have a caption, all the *captions* being typed (with double spacing) together on a *separate sheet*. If structures are given in the text, the original drawings should be provided. Coloured illustrations are reproduced at the author's expense, the cost being determined by the number of pages and by the number of colours needed. The written permission of the author and publisher must be obtained for the use of any figure already published. Its source must be indicated in the legend.

References. References should be numbered in the order in which they are cited in the text, and listed in numerical sequence on a separate sheet at the end of the article. Please check a recent issue for the layout of the reference list. Abbreviations for the titles of journals should follow the system used by *Chemical Abstracts*. Articles not yet published should be given as "in press" (journal should be specified), "submitted for publication" (journal should be specified), "in preparation" or "personal communication".

Vols. 1–651 of the *Journal of Chromatography*; *Journal of Chromatography, Biomedical Applications* and *Journal of Chromatography, Symposium Volumes* should be cited as *J. Chromatogr.* From Vol. 652 on, *Journal of Chromatography A* (incl. Symposium Volumes) should be cited as *J. Chromatogr. A* and *Journal of Chromatography B: Biomedical Applications* as *J. Chromatogr. B.*

Dispatch. Before sending the manuscript to the Editor please check that the envelope contains four copies of the paper complete with references, captions and figures. One of the sets of figures must be the originals suitable for direct reproduction. Please also ensure that permission to publish has been obtained from your institute.

Proofs. One set of proofs will be sent to the author to be carefully checked for printer's errors. Corrections must be restricted to instances in which the proof is at variance with the manuscript.

Reprints. Fifty reprints will be supplied free of charge. Additional reprints can be ordered by the authors. An order form containing price quotations will be sent to the authors together with the proofs of their article.

Ovomucoid Bonded Column for Direct Chiral Separation

ULTRON ES-OVM

Narrow-Bore Column (2.0 I.D. x 150 mm) for Trace Analyses
Analytical Column (4.6 I.D. , 6.0 I.D. x 150 mm) for Regular Analyses
Semi-Preparative Column (20.0 I.D. x 250 mm) for Preparative Separation

Analysis of Trace FLURBIPROFEN in Metabolite with NARROW-BORE COLUMN

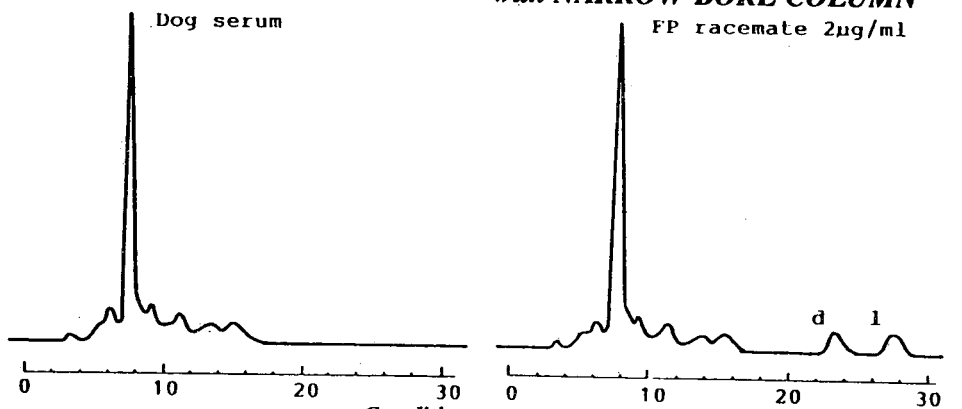

Conditions

Column: ULTRON ES-OVM(2.0I.D. x 150mm)
Mobile Phase: 20mMPhosphate Buffer(pH=3.0)/CH3CN =100/15
Flow Rate: 0.1ml/min
Temperature: 25°C
Injection: 5µl
Detection: UV- 247nm(0.05AUFS)

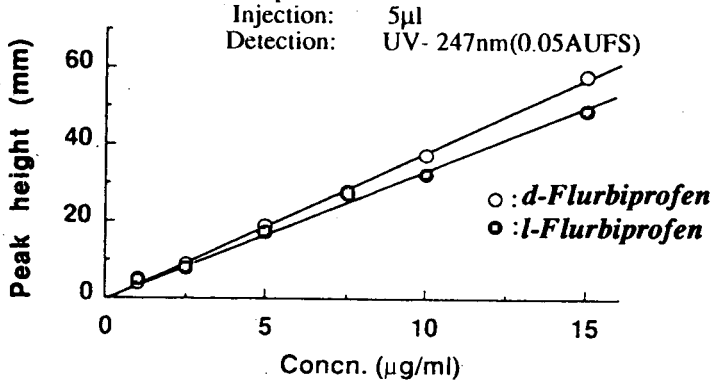

Calibration Curve for Each Enantiomer of Flurbiprofen

SHINWA CHEMICAL INDUSTRIES, LTD.

50 Kagekatsu-cho, Fushimi-ku, Kyoto 612, JAPAN
Phone:+81-75-621-2360 Fax:+81-75-602-2660

In the United States and Europe, please contact:

Rockland Technologies, Inc.

538 First State Boulevard, Newport, DE 19804, U.S.A.
Phone: 302-633-5880 Fax: 302-633-5893

This product is licenced by Eisai Co., Ltd.